INTERNATIONAL DOCTORAL
SCHOOL OF THE USC

Alejandro
Gutiérrez González

PhD Thesis

Orthogonal Metal Catalysis in Biological Systems

Santiago de Compostela, 2023

Doctoral Programme in Chemical Science and Technology

TESIS DE DOCTORADO

Orthogonal Metal Catalysis in Biological Systems

Alejandro Gutiérrez González

ESCUELA DE DOCTORADO INTERNACIONAL DE LA UNIVERSIDAD DE SANTIAGO DE COMPOSTELA

PROGRAMA DE DOCTORADO EN CIENCIA Y TECNOLOGÍA QUÍMICA

SANTIAGO DE COMPOSTELA / LUGO
AÑO 2023

D. **Alejandro Gutiérrez González**

Título de la tesis: **Orthogonal Metal Catalysis in Biological Systems**

Presento mi tesis, siguiendo el procedimiento adecuado al Reglamento y declaro que:

1) La tesis abarca los resultados de la elaboración de mi trabajo:
2) De ser el caso, en la tesis se hace referencia a las colaboraciones que tuvo este trabajo.
3) Confirmo que la tesis no incurre en ningún tipo de plagio de otros autores ni de trabajos presentados por mí parte para la obtención de otros títulos.
4) La tesis es la versión definitiva presentada para su defensa y coincide la versión impresa con la presentada en formato electrónico.

Y me comprometo a presentar el Compromiso Documental de Supervisión en el caso que el original no esté depositado en la Escuela

En Santiago de Compostela, a 28 de enero de 2023

AUTORIZACIÓN DEL DIRECTOR / TUTOR DE LA TESIS

Orthogonal Metal Catalysis in Biological Systems

D. José Luis Mascareñas Cid
D. Fernando López García

INFORMAN:

Que la presente tesis, se corresponde con el trabajo realizado por D. Alejandro Gutiérrez González, bajo mi dirección/tutorización, y autorizo su presentación, considerando que reúne los requisitos exigidos en el Reglamento de Estudios de Doctorado de la USC, y que como director de esta no incurre en las causas de abstención establecidas en la Ley 40/2015.

De acuerdo con lo indicado en el Reglamento de Estudios de Doctorado, declara también que la presente tesis doctoral es idónea para ser defendida en base a la modalidad de Monográfica con reproducción de publicaciones, en los que la participación del doctorando fue decisiva para su elaboración y las publicaciones se ajustan al Plan de Investigación.

En Santiago de Compostela, 28 de enero de 2023

Firmado José Luis Mascareñas Cid

Firmado Fernando López García

Acknowledgements

This PhD thesis has been funded by the Spanish Ministry of Universities through the "Formación de Profesorado Universitario" program (FPU17/00711).

This work has received financial support from Spanish grants (Grant PID2019-108624RB-I00 funded by MCIN/AEI/10.13039/501100011033), the Consellería de Cultura, Educación e Ordenación Universitaria (Grant ED431C 2017/19 and Grant ED431G 2019/03) and the European Union (ERC-2103-AdG 340055, European Regional Development Fund-ERDF corresponding to the multiannual financial framework 2014-2020).

Agradecimientos

En primer lugar me gustaría agradecer a mis directores, José Luis y a Fernando, por haberme dado la oportunidad de realizar la tesis en el grupo, así como por su guía durante estos casi 6 años. Me he sentido apoyado y escuchado durante este tiempo, y no me habéis pedido nada a cambio salvo ser riguroso en el laboratorio.

Si la química del grupo es interesante, lo es más el conjunto de personas que has conseguido aunar, José Luis. Tú mismo lo has venido diciendo en los últimos años "primero que sean buenas personas y ya luego que sean buenos". Gracias por estos años, por el grupo y por preocuparte siempre por nosotros (sobre todo por esto último).

Fernando, gracias por la guía y por estar siempre disponible. He crecido como químico gracias a tu dirección. Gracias.

Al profesor Fürstner y a Sebastian Peil, gracias por acogerme en Alemania, más aún en unos momentos complicados como fueron el principio del 2021. Aprendí un muchísimo y ha sido una de las experiencias que más confianza en mí mismo me ha otorgado. Gracias.

No sé si es la sensación que tiene todo el mundo al leer la tesis, pero creo que soy de los últimos de Filipinas, de los últimos de una generación. Al principio cuando llegué lo hice como "CiQUS maker" luego regresé como estudiante de máster para más tarde seguir con el doctorado. Entré en un grupo al que no pertenecía, pero al que no le costó acogerme y hacerme sentir a gusto. De aquellos primeros meses en 2017 no queda nadie ya (Cristian, Marc, Soraya, Paolo, Felipe…). No obstante, el recambio no ha quedado mal del todo al final ;) un malagueño, un asturiano, una cántabra, una italiana, un holandés, el madrileño, unos riquiños gallegos o un portugués que se dice gallego, por ejemplo.

A los de la *old school*, Soraya, José, Jaime, Marc, Felipe, Xandro, Borja, Cajiao, Paolo, Ronald y compañía. Cuando yo entré, el grupo erais vosotros y me acogisteis, me hicisteis hueco. Gracias.

A Tito, el catalán del laboratorio por antonomasia. La *boy band* no cuajo al final, holdeamos las cryptomonedas y se han quedado en nada, igual que los planes de independencia de Canarias aprovechando el conflicto catalán. Una de las cosas más difíciles es saber que en el siguiente capítulo no estaremos juntos, pero también supone una excusa para volver a vernos en Alemania como en el 2021. Sé que en Deutsche Länder brillarás como cual lampara Kessil Tuna Blue LED de 30 W.

Cristian, el valiente inorgánico catalán que también es asturianu. He de confesar que cuando dejaste el sagrado laboratorio en pos de las verdes praderas de Janssen fue uno de los momentos más duros de mi paso por este nuestro noble grupo. Siento que no has sido solo un amigo, sino un mentor. De ti he copiado muchas cosas, y creo que todas me han hecho mejor químico y mejor persona.

Don Atanes, deje las borilaciones, no queda nada en SR4 o en California a lo que no le haya intentado meter un borillo por el *o-*. Tienes una energía que no es normal, ojalá que no te abandone nunca. Mediante estos agradecimientos te cedo la corona de Pichi Di senior de P3L4, pero ya te aviso que, por propia experiencia, durará poco, disfrútala. Mientras dure tu reinado se indolente, gobierna con mano férrea, "*Make P3L4 great again*".

Destito, gracias por tu paciencia durante el máster. Estoy al final de la tesis y aun sigo queriendo ser tan buen químico como tú. Gracias.

Y de repente fue un malagueño. El *power ranger* amarillo. Saladito. Un paraguas amarillo a un andaluz pegado. No tenía otra cosa que hacer que dejar la soleada Málaga para venirse a una de las ciudades más lluviosas de España y de Europa. Como me identifico contigo. Sabes que puedes contar conmigo si me necesitas, tú eres Ron y yo Kim Possible (o al revés, como más gustes). Gracias por ser tú (salvo por lo del maldito cloruro de benzoilo, esa me la debes).

Sara, un cachito del corazón de todo el grupo se fue contigo a Madrid. Es increíble lo profundo que calaste en todos nosotros. Eres inteligente, graciosa y además buena persona, gracias a Dios que lo equilibras un poco con los laísmos y los leísmos. Gracias por tus consejos y por escuchar mis chapas vitales.

Cinzia, la mafiosa napoletana del laboratorio, tutti stanno attenti a te nel caso tu faccia loro delle scarpe di cemento (scherzo, ti vogliamo tutti bene). Avete una buona strada davanti a voi, continuate a essere metodici e allegri come lo siete già. Grazie per questi ultimi anni in cui ho potuto fidarmi di voi. Come per Sara, avete già un pezzetto del cuore dell'intero laboratorio.

Adrián, gracias por tu infinita paciencia, por tu trabajo y por hacernos la vida más fácil. Gracias.

Xuli, eres un intenso, tómate las cosas con calma, que quiero poder ver tu tesis. El sucesor natural del Dr. Joan Miguel Ávila. Te doy las gracias por poder haberte visto crecer en el lab, del chico tímido, al que lo rompe en congresos y seminarios. Gracias por hacer el laboratorio un poco más divertido.

Soraya, gracias haber sido eje vertebrador del grupo durante estos años y por acogernos a todos sin importar lo raro que seamos. Gracias Sori <3.

Fer / Bro. Me lo he pasado muy bien contigo. Tengo ganas de ver cómo te va. Eres puro amor (Y a ver si sacas los malditos vinilidenos).

Leo, Ale, habéis tenido que aguantarme más que los demás, espero que no os deje taras. Tened por seguro seguiré lo que hagáis con mucha atención. Los dos tenéis buenas manos y mejor mente. Por favor, no perdáis el contacto conmigo, si necesitáis cualquier cosa no dudéis en hablarme. Gracias por soportarme sin queja.

María, no me extraña que te llamen la mami del grupo, te preocupas por todo el mundo. Gracias por los proyectos que hemos compartido, por tu guía y tus consejos. Estas junto a Cristian en mi corazoncito.

Marc, tú también te mereces tu párrafo. Tenerte en el lab ha sido increíble, creo que me llevo un amigo (otro catalán como no) y momentos que atesorare. Gracias por hacer el P3L4 divertido y por ayudarme durante tu tiempo con nosotros.

Proteíno, te quiero, amigo. De las cosas que más me enorgullezco es de no haber dejado de lado nuestra amistad durante estos años. Gracias por ayudarme a mantener los pies en la Tierra (en la figurada y en la natal).

P3L3. Andy, Richi, Alex, Sergio, Pablo, Carlos... sabéis que el 3 es una zoo, a cada cual más loco que el anterior. Sin embargo, no me puedo imaginar los cafés sin vosotros, ni las patujadas de Richi. Hemos compartido muchas cosas, e igual que antes dije que la *old school*, era el grupo cuando yo llegué, vosotros sois parte del grupo que dejo atrás, seguid así, manteniendo el listón alto y acogiendo a la gente.

Edu y José Manuel, sois los siguientes. Lo siento. Entramos juntos al doctorado y ya nos toca nuestro momento. Sois unos crac y unos trabajadores incansables, les habéis puesto el listón muy alto a los que vienen detrás. Hagáis lo que hagáis al terminar, haced algo que os haga felices, y lo petareis.

Al P3L5, sois un cajón de sastre. Andrés, gracias echarme una mano cuando lo he necisato, no solo eres ingenioso sino que eres una gran persona. David gracias por estar siempre ahí cuando lo he necesito, y por acogerme en los primeros congresos a los que asistí cuando aún no estaba integrado. Lara, Ana, Axel … y a los que ya no están el P3L5, Jacobo y Sonia, gracias por el tiempo que hemos compartido y que habéis animado.

A Helena gracias desde lo más profundo de mi corazón. Has soportado mis chapas de química de forma estoica durante este tiempo. Sé que nuestro paso por Galicia no ha sido fácil, nos hemos enfrentado a cosas que, siendo sinceros, habríamos estado mejor sin afrontar (ej., el COVID). Pero aguantaste, seguiste conmigo, haciendo de nuestro 3ºB un hogar. Gracias por todo este tiempo juntos, y por querer seguir conmigo en nuestros siguientes pasos. Te amo.

A mis padre y a mi madre. Gracias por haberme apoyado durante este tiempo viviendo fuera. Gracias por haberme ayudado cuando lo he necesitado. Ojalá Canarias estuviese más cerca, para poder haberos visto más, para poder haberos abrazado más. Sin vosotros esta tesis no hubiese sido posible. Os quiero.

"Nothing is too wonderful to be true if it be consistent with the laws of nature and in such things as these, experiment is the best test of such consistency."

19th of March 1849

Michael Faraday's diary

Abbreviations and acronyms

4T1	mouse mammary carcinoma cells
A2780	Immortalized human ovarian adenocarcinomic cells
A549	adenocarcinomic human alveolar basal epithelial cells
AHA	azidohomoalanine
Alloc	allyl carbamate
ALP	Alkaline Phosphatase
CEF	Chicken embryo fibroblast cells
COD	1,5-Cyclooctadiene
CTCF	Corrected total cell fluorescence
CuAAC	Copper catalyzed azide alkyne cycloaddition
DCE	Dichloroethane
DMAP	4-dimethylaminopyridine
DMEM	Dulbecco's modified Eagle medium
DMEM*	DMEM + 10% FBS + 1% Antibiotics
DMF	*N,N*-Dimethyl formamide
DMSO	Dimethyl sulfoxide
E_a	Activation Energy
EDG	Electron Donating Group
Equiv	Equivalent
ESI-MS	Electrospray ionization mass spectrometry
ESIPT	excited-state intramolecular proton transfer
ET	Electron transfer
EWG	Electron Withdrawing group
FBS	Fetal Bovine Serum
FCC	Flash column chromatography
GSH	Glutathione
HBT	2-(2'-hydroxyphenyl) benzothiazole
HEK-293T	Immortalized human embryonic kidney cells
HeLa	Immortalized human cervical cancer cells
HPLC	High performance liquid chromatography
ICP-MS	Inductively coupled plasma mass spectrometry
ICT	Intramolecular Charge Transfer

IEDDA	Inverse Electron Demand Diels-Alders reaction
MAAC	Metal catalyzed Azide-Alkyne cycloaddition
MAO	Monoamine oxidase
NaAsc	Sodium ascorbate
NAD(P)+	Oxidized nicotinamide adenine dinucleotide (phosphate)
NAD(P)H	Reduced nicotinamide adenine dinucleotide (phosphate)
ncAAs	non canonical amino acids
NIR	Near Infrared
NMR	Nuclear Magnetic Resonance
PABA	*p*-aminobenzoic acid
PBS	Phosphate buffer solution
Proc	propargyl carbamate
ROMP	ring-opening metathesis polymerization
RuAAC	Ruthenium catalyzed Azide-Alkyne cycloaddition
RuAtAC	Ruthenium catalyzed Azide-thioAlkyne cycloaddition
SPAAC	Strain Promoted Azide Alkyne Cycloaddition
SPPS	solid phase peptide synthesis
THF	Tetrahydrofuran
TMS	Trimethyl silane
TOF	Turnover Frequency
TON	Turnover Number
tos	*p*-toluenesulfonate
Tris-HCl	tris(hydroxymethyl) aminomethane hydrochloride buffer
Vero	African green monkey kidney cells

Introduction

1 Catalysis

Catalysis is a word adapted from the ancient Greek, *kataluein* (*καταλύω)*. It is constituted by two parts *kata* (down or against) and *luein* (loosen) meaning "loosen" or "untie".[1] It is generally described as the acceleration of a reaction by the addition of a substance that is not consumed in the process.

Despite the term *catalysis* was coined by the Swedish chemist Jöns Jacob Berzelius, the concept was first described by Elizabeth Fume in 1794 in her book "*An Essay On Combustion with a View to a New Art of Dying and Painting, wherein the Phlogistic and Antiphlogistic Hypotheses are Proved Erroneous"*.[2] Among the experiments collected in this publication, it is described the reduction of metal salts in organic solvents (ethers and alcohols) by different reducing agents such as hydrogen gas, sulfur or phosphorus. One of the key discoveries of this work was that small quantities of water allowed the reduction of the metal salts to take place faster and at lower temperatures.[3] Even though it is not the first description of a substance that enhances the reaction rate of a transformation, it is the first generalization of the concept to a series of compounds.

Catalysis deals with changes in the route to the equilibrium. It is a kinetic process, where the general thermodynamics of the reaction remain unchanged.[4] In a system where **A** is transformed into **B**, the rate of interconversion is determined by the "height" of the barrier, activation energy (E_a). The addition of a third substance, a catalyst, **C**, decreases the activation energy, accelerating the process (**Figure 1**).[5]

[1] Concept: Catalysis V. Gold, Ed. , *The IUPAC Compendium of Chemical Terminology: The Gold Book*, International Union Of Pure And Applied Chemistry (IUPAC), Research Triangle Park, NC, **2019**.
[2] C. Jarvis, *Phys. Today* **2020**, *2020*, 0617a.
[3] D. A. Davenport, K. M. Ireland, *Bull. Hist. Chem.* **1989**, 6.
[4] G. Rothenberg, *Catalysis: Concepts and Green Applications*, Wiley-VCH, Weinheim, **2008**.
[5] P. W. Atkins, J. De Paula, *Atkins' Physical Chemistry*, Oxford University Press, Oxford ; New York, **2010**.

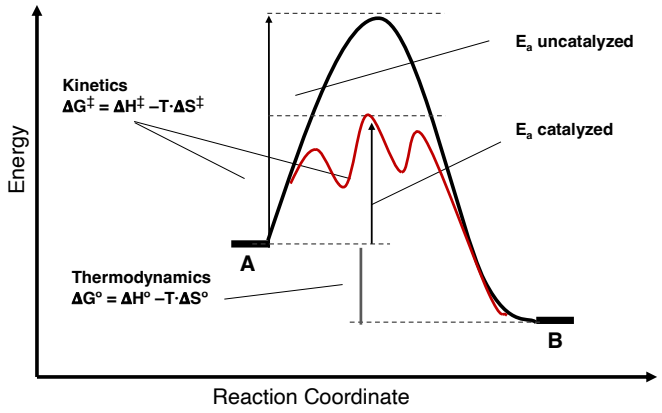

Figure 1. Reaction coordinate diagram.

1.1 Types of catalysis

There are several ways to classify the different catalytic processes, depending on the nature of the catalysts: organic (organocatalyst),[6,7,8] inorganic[9] or organometallic catalysts,[10] or the special case of enzymes and biocatalysts.[11] We can also classify them in terms of the mechanism of action: acid-base (Lewis[12] and Brønsted catalysts[13]); redox, where the catalyst is sequentially oxidized and reduced (usual for organometallic processes) or light promoted.

Furthermore, if the catalyst is in the same phase of the reaction mixture, we speak of homogenous catalysis, while it is heterogenous if they are in different phases. Although enzymes are homogeneous biological catalysts, they are often considered by their own within biocatalysis, albeit in this case the line is blurry. The mechanism and the process conditions may differ for each category, the principles of catalysis are general (**Figure 2**). Ideally, catalysts should not only lead to faster reactions but should also comply with selectivity issues, delivering high chemo-, regio- or/and stereoselectivities.

[6] D. W. C. MacMillan, *Nature* **2008**, *455*, 304–308.
[7] B. List, *Chem. Rev.* **2007**, *107*, 5413–5415.
[8] P. I. Dalko, Ed. , *Comprehensive Enantioselective Organocatalysis: Catalysts, Reactions, and Applications*, Wiley-VCH, Weinheim, **2013**.
[9] L. Liu, A. Corma, *Chem. Rev.* **2018**, *118*, 4981–5079.
[10] J. F. Hartwig, *Organotransition Metal Chemistry: From Bonding to Catalysis*, University Science Books, Sausalito, Calif, **2010**.
[11] E. L. Bell, W. Finnigan, S. P. France, A. P. Green, M. A. Hayes, L. J. Hepworth, S. L. Lovelock, H. Niikura, S. Osuna, E. Romero, K. S. Ryan, N. J. Turner, S. L. Flitsch, *Nat Rev Methods Primers* **2021**, *1*, 46.
[12] S. E. Denmark, G. L. Beutner, in *Lewis Base Catalysis in Organic Synthesis* (Eds.: E. Vedejs, S.E. Denmark), Wiley-VCH Verlag GmbH & Co. KGaA, Weinheim, Germany, **2016**, pp. 31–54.
[13] For a reviews on Brønsted catalysis see: J. Yu, F. Shi, L.-Z. Gong, *Acc. Chem. Res.* **2011**, *44*, 1156–1171.

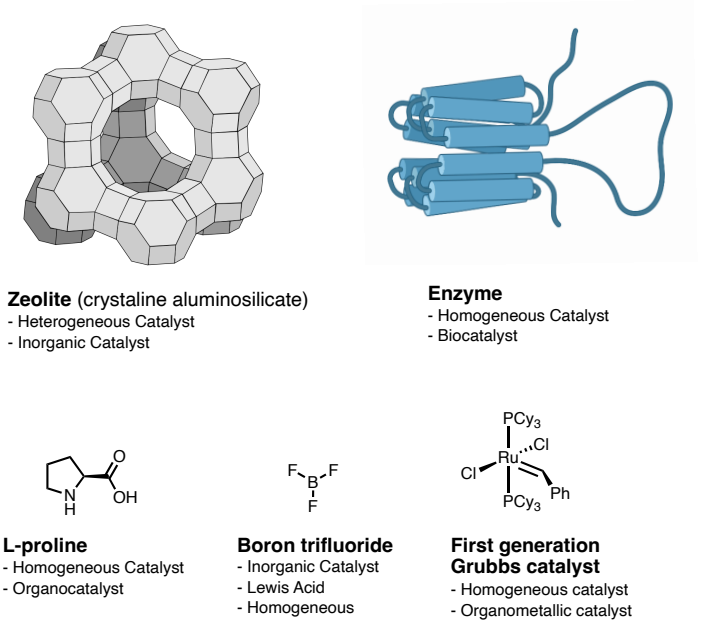

Figure 2. Examples of different catalysts.

2 Transition Metal Catalysis

2.1 Introduction

From the different types of catalysis, those based on the use of transition metal catalysts are especially attractive, owing to the versatility provided by the different metals and ligands. Transition metals have partially filled *d*-orbitals that can engage in bonding processes with organic moieties promoting their reactivity and, in many cases, they can easily engage in reversible redox cycles, facilitating turnover.[10]

Every catalytic cycle is composed by elementary organometallic steps such as *ligand exchange*, *oxidative addition, reductive elimination* or *nucleophilic* and *electrophilic attack on alkenes*, among many others. These elementary steps are the *monads* of a chemical reaction, simple building blocks with which we can describe the mechanism of a process. In the case of transition metal catalysis, we may distinguish between *inner-sphere* mechanisms, with the elementary steps taking place within the coordination sphere, and *outer-sphere,* when there is reaction with the ligand, but the reactant is not specifically linked to the metal (**Figure 3**).

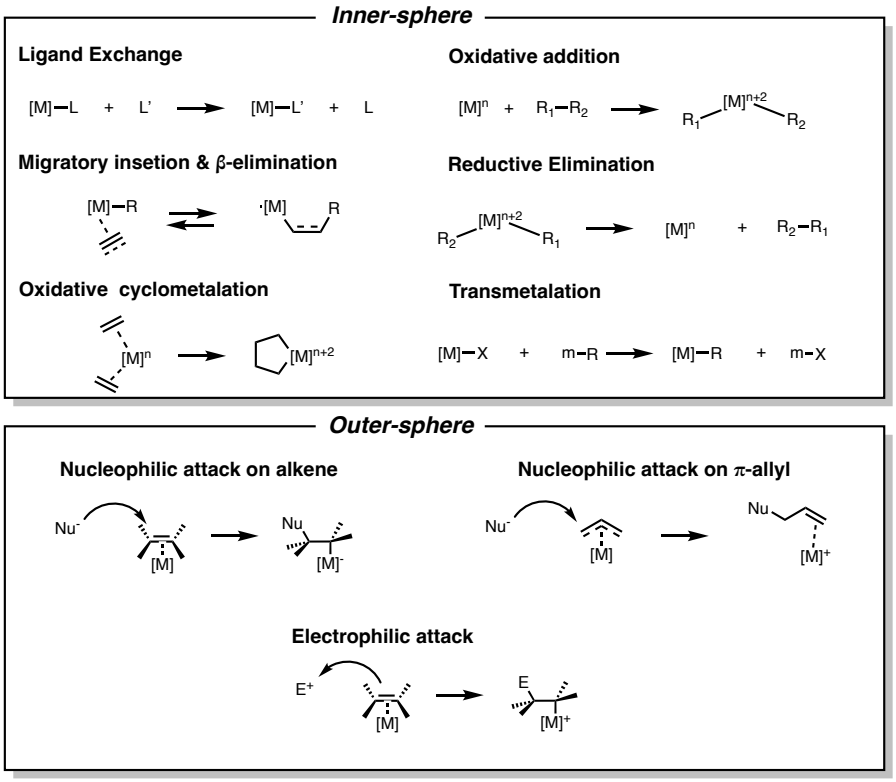

Figure 3. Elementary steps of organometallic reactions for inner- and outer-sphere mechanisms.

Since the early examples in the mid XIX century with organozinc reagents,[14] followed by organolithium and organomagnesium reagents,[15] synthetic chemists have been adding more and more transition metal-catalyzed processes to their arsenal, many of which have been used as key steps for streamlining synthetic processes.[16]

For example, the synthesis of cyclooctatetraene, a non-planar and non-aromatic fully conjugated carbocycle, was first achieved from tropinone in 13 steps, with an overall yield of 1-2%.[17] However, starting from acetylene and using a Nickel catalyst the cyclooctatetraene is accessible in just a single step with 90% yield (**Figure 4**).[18]

[14] A. D. Dilman, V. V. Levin, *Tetrahedron Letters* **2016**, *57*, 3986–3992.
[15] R. M. Peltzer, J. Gauss, O. Eisenstein, M. Cascella, *J. Am. Chem. Soc.* **2020**, *142*, 2984–2994.
[16] P. A. Wender, B. L. Miller, *Nature* **2009**, *460*, 197–201.
[17] R. Willstätter, E. Waser, *Ber. Dtsch. Chem. Ges.* **1911**, *44*, 3423–3445.
[18] W. Reppe, O. Schlichting, K. Klager, T. Toepel, *Justus Liebigs Ann. Chem.* **1948**, *560*, 1–92.

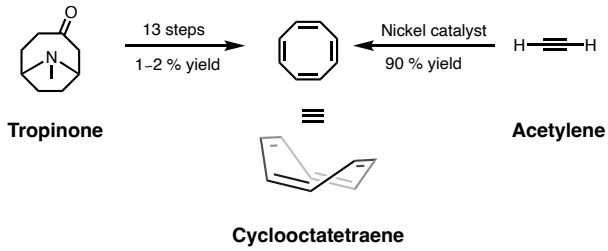

Figure 4. Different synthesis of cyclooctatetraene.

2.2 Representative examples

Within the myriad of transformations allowed by transition metals, bond-forming reactions such as cross-couplings, cycloadditions and allylic substitutions are particularly attractive.

2.2.1 C-C cross-couplings

Transition metal catalyzed carbon-carbon bond forming reactions are among the most powerful and versatile transformations in synthetic chemistry, and tend to be very robust and reproducible.[19] They have been extensively used in the synthesis of natural products,[20] the preparation of agrochemicals, and the assembly of pharmaceutical building blocks.[21,22] This huge impact was recognized in 2010 when the Nobel Prize in Chemistry was awarded to the pioneers who developed palladium-catalyzed cross-coupling reactions.[23]

In general, these reactions involve an organic electrophile (e.g., aryl halide, triflates or surrogates), a nucleophile (e.g., organoboron, magnesium, tin, or zinc reagent), and a transition metal catalyst.[10] Classical cross-coupling reactions have been named after their discoverers and based on the organic nucleophile used. *Stile reaction* for tin-containing nucleophiles, *Suzuki-Miyaura reaction* for boronates; *Negishi reaction* for zincates (also for aluminum and zirconium) or *Sonogashira* when copper acetylides are used.[24] Most cross-coupling reactions share a common mechanism consisting of **three elementary**

[19] L.-C. Campeau, N. Hazari, *Organometallics* **2019**, *38*, 3–35.
[20] K. C. Nicolaou, P. G. Bulger, D. Sarlah, *Angew. Chem. Int. Ed.* **2005**, *44*, 4442–4489.
[21] J. Magano, J. R. Dunetz, *Chem. Rev.* **2011**, *111*, 2177–2250.
[22] P. Devendar, R.-Y. Qu, W.-M. Kang, B. He, G.-F. Yang, *J. Agric. Food Chem.* **2018**, *66*, 8914–8934.
[23] R. F. Heck, E. Negishi, A. Suzuki. The Nobel Prize in Chemistry 2010.
[24] There are more types of cross couplings reactions and in many cases the whole name of the reaction is still on discussion based on the historical precedents. For a comprehensive review on the history of cross-coupling reactions see: C. C. C. Johansson Seechurn, M. O. Kitching, T. J. Colacot, V. Snieckus, *Angew. Chem. Int. Ed.* **2012**, *51*, 5062–5085.

steps. A low valent metal (e.g., Pd (0) or Ni (0)) reacts in first instance with an aryl halide by an **oxidative addition** to generate and aryl metal halide complex. In a second step, this intermediate reacts with the corresponding nucleophile by a **transmetalation** step, to yield a species containing two metal-carbon bonds. **Reductive elimination** yields the product bearing the new C-C bond and regenerating the active catalyst **(Figure 5**).

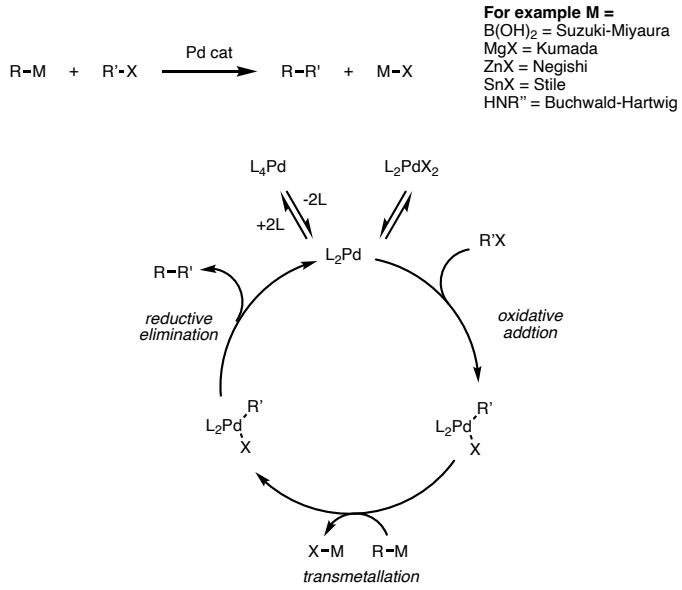

Figure 5. Generic mechanism proposal for cross-coupling reactions, and some examples of named reactions.

2.2.2 Cycloaddition Reactions

Cycloadditions are among the most important synthetic reactions to build *complexit*y, as they allow to build cyclic scaffold from acyclic compounds, usually with high levels of selectivity (chemo, region and stereoselectivity).[25] Classical cycloaddition reactions take place thermal or photochemically, following the Woodward-Hofmann rules. The most representative case is the Diels-Alder reaction, a thermal process that is electronically allowed [4π + 2π] where a diene reacts with a dienophile to form a cyclohexene (**Figure 6**).

[25] B. Dinda, *Essentials of Pericyclic and Photochemical Reactions,* Springer International Publishing, Cham, **2017**.

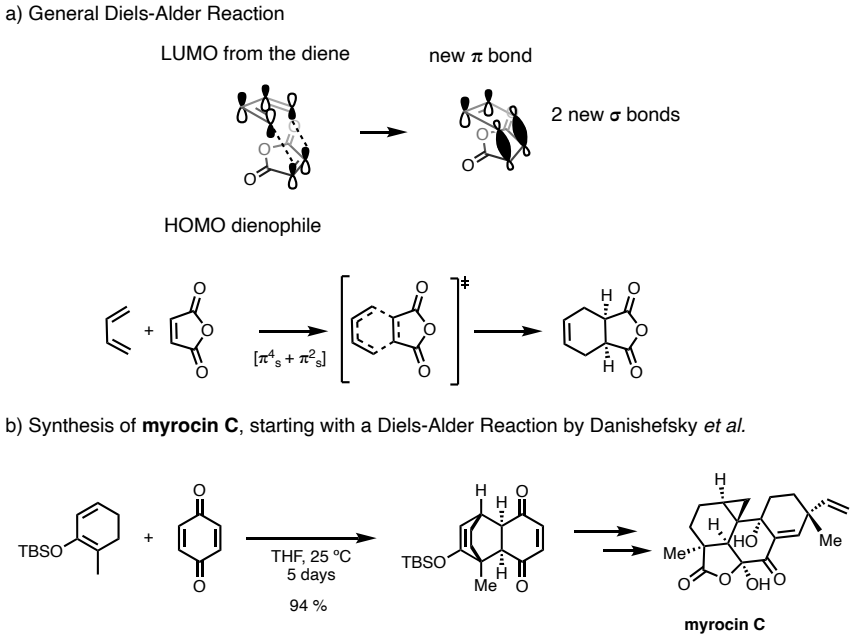

Figure 6. a) General scheme for a Diels-Alder reaction. B) Synthesis of natural product myrocin C, by Danishefsky *et al.*

Cycloaddition reactions are government by the orbital symmetry of the reactants. On the one hand, it gives an incredible control over the product skeleton (endo rule, Danishefsky dienes…) as can be seen in the application of the Diels-Alder reaction by Danishefsky in the total synthesis of **myrocin C** (**Figure 6b**).[26,27]

Another highly relevant class of classical annulations are 1,3-dipolar cycloadditions, usually called Huisgen cycloadditions. In these reactions, a 1,3-dipole and a dipolarophile react in a concerted fashion to deliver a five-member ring.[28] Like the Diels-Alder, these reactions involve $[\pi^4_s+\pi^2_s]$ electrons and therefore are allowed processes that follow the Woodward-Hoffman rules. There are several dipoles and dipholarophiles that can engage into this type of cycloadditions, like for example nitrones and alkenes (or alkynes) to yield isoxazolidines (**Figure 7**).

[26] M. Y. Chu-Moyer, S. J. Danishefsky, G. K. Schulte, *J. Am. Chem. Soc.* **1994**, *116*, 11213–11228.
[27] K. C. Nicolaou, S. A. Snyder, T. Montagnon, G. Vassilikogiannakis, *Angew. Chem. Int. Ed.* **2002**, *41*, 1668–1698.
[28] Rolf Huisgen was the main responsible of the investigation of the mechanism; therefore 1,3-dipolar cycloadditions usually are called Huisgen cycloadditions.

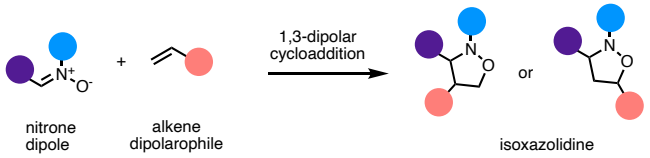

Figure 7. 1,3-dipolar cycloaddition between nitrones and alkenes to yield isoxazolidines.

A major limitation of these classical cycloadditions is the need of a good electronic match between the reaction partners, which impose the use of polarized bonds to reduce the HOMO-LUMO gap of the starting materials.

In this context, the use of transition metal catalysts that trigger new type of mechanisms can provide for many new types of formal annulations, that otherwise would not be possible. Transition metal complexes can coordinate to π-electrons of double and triple bonds, changing their electronic properties and enabling their annulation with other unsaturated partners. This can be illustrated by the case of the [2+2+2] cycloadditions shown in **Figure 8**, an electronically allowed processes that are entropically disfavored but, upon addition of the appropriate metal complex, they proceed to give access to aromatic rings [29]

A variety of formal cycloadditions catalyzed by transition metal complexes of Ir, Rh, Ru, Pd, Co and Ni have been developed.[29,30] Many of these reactions involve oxidative cyclometallations followed by migratory insertions and reductive elimination steps.

Importantly, metal-promoted cycloadditions are not restricted to carbon-carbon bond processes, and a great variety of heterocycloadditions have also been developed (see for instance in **Figure 8c**).

[29] M. Lautens, W. Klute, W. Tam, *Chem. Rev.* **1996**, *96*, 49–92.
[30] A. V. Gulevich, A. S. Dudnik, N. Chernyak, V. Gevorgyan, *Chem. Rev.* **2013**, *113*, 3084–3213.

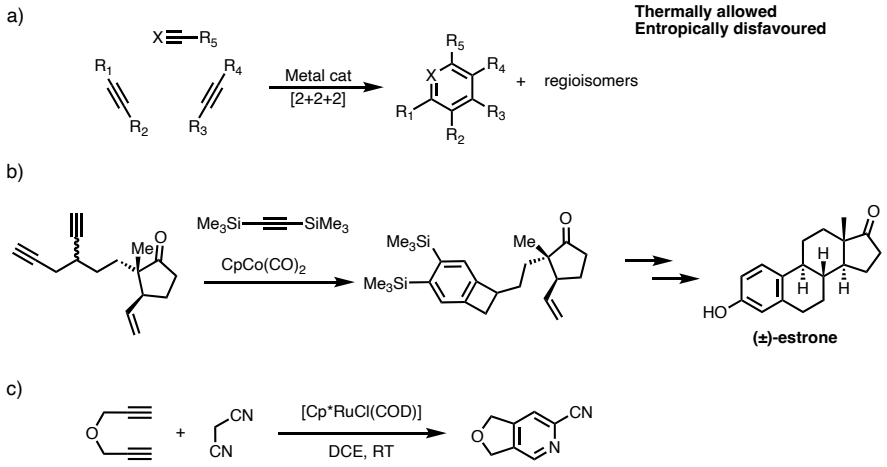

Figure 8. a) General Scheme for Transition Metal Catalyzed [2+2+2] cycloaddition. b) Application of the TM catalyzed [2+2+2] cycloaddition to the total synthesis of (±)-estrone.[31] c) Ruthenium catalyzed hetero [2+2+2] cycloaddition for the synthesis of pyridine derivatives.[32]

Metal catalysts can also be used to promote formal dipolar cycloadditions that otherwise are difficult to achieve. For instance, the reaction between an organic azide as 1,3-dipole and an alkyne as dipolarophile to give 1,2,3-triazoles usually requires high temperatures and give mixtures of regioisomers.[33] In a groundbreaking discovery over 20 years ago, Sharpless and Meldal independently demonstrated that adding a Cu(I) catalyst the reaction could be carried out at room temperature and regioselectively to yield 1,4-triazoles (**Figure 9**). [34,35]

[31] R. L. Funk, K. P. C. Vollhardt, *J. Am. Chem. Soc.* **1980**, *102*, 5253–5261.
[32] Y. Yamamoto, K. Kinpara, R. Ogawa, H. Nishiyama, K. Itoh, *Chem. Eur. J.* **2006**, *12*, 5618–5631.
[33] Himo, F.; Lovell, T.; Hilgraf, R.; Rostovtsev, V. V.; Noodleman, L.; Sharpless, K. B.; Fokin, V. V. *J. Am. Chem. Soc.* **2005**, *127*), 210–216.
[34] C. W. Tornøe, C. Christensen, M. Meldal, *J. Org. Chem.* **2002**, *67*, 3057–3064.
[35] V. V. Rostovtsev, L. G. Green, V. V. Fokin, K. B. Sharpless, *Angew. Chem. Int. Ed.* **2002**, *41*, 2596–2599.

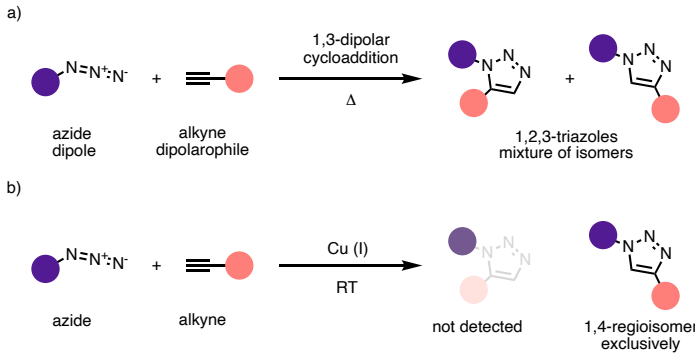

Figure 9. a) Thermal cycloaddition of azides and alkene. b) Copper catalyzed formal cycloaddition of azides and alkynes

2.2.3 Tsuji-Trost allylic substitution reaction

Another benchmarking transition metal catalyzed reaction is the allylic substitution, also known as Tsuji-Trost reaction. This reaction was originally reported with $PdCl_2$ by Tsuji in 1968,[36] and later extended and thoroughly studied by Trost.[37] Mechanistically the first step involves the coordination of the palladium complex to the allyl compound followed by oxidative addition to give a π-allyl complex; lastly an outer-sphere attack of a nucleophile closes the cycle to regenerate the catalyst and yield the product (**Figure 10**).

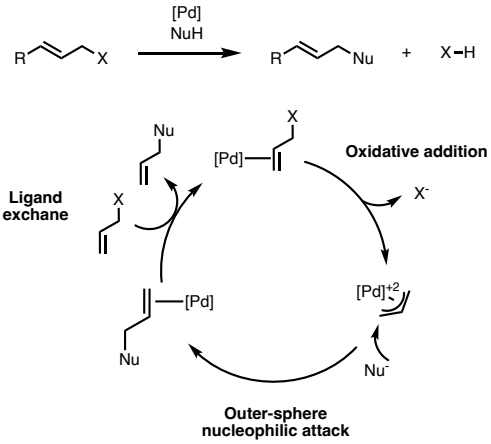

Figure 10. General scheme for the Tsuji-Trost substitution reaction and mechanism.

The use of phosphine ligands allowed to expand this transformation to a broad variety of oxygen and nitrogen nucleophiles and, furthermore, the use of chiral phosphines allowed

[36] T. Susuki, J. Tsuji, *BCSJ* **1968**, *41*, 1954–1958.
[37] B. M. Trost, T. J. Fullerton, *J. Am. Chem. Soc.* **1973**, *95*, 292–294.

to control the enantio- and/or diastereoselectivity of the process, expanding its synthetic applicability.[38]

The generality of this reaction and its robustness has allowed the development of allyl ethers as orthogonal protecting groups. For instance, allyl carbamoyl groups (alloc) are commonly used as orthogonal protecting group for lysine amino acids in solid phase peptide synthesis (SPPS). Treatment of the corresponding peptide in the solid phase with [$Pd(PPh_3)_4$] and phenyl silane as nucleophile allows to cleave the alloc group without touching any of the other protecting groups of the peptide (**Figure 11**).[39]

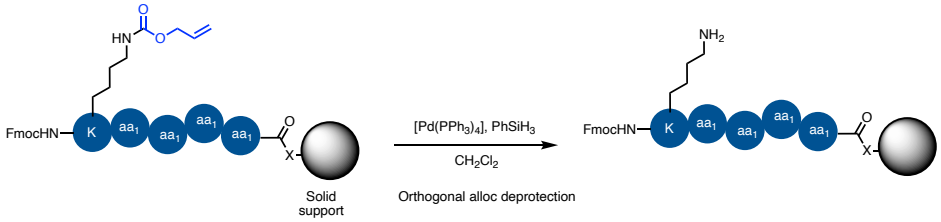

Figure 11. Palladium promoted removal of an alloc group in SPPS.

3 Transition Metal Catalysis in Water

Most catalytic reactions so far developed, including those involving transition metal reagents, have been carried out in organic solvents. Whereas these advances shaped the development of the world by supplying fertilizers, energy, medicines or new materials, the chemical processes behind these developments also has had a deep impact in our environment. Therefore, in recent decades there have been an intensive effort to develop processes that fit better with the principles of Green Chemistry,[40] and that lie on the use of safer solvents, especially water.

Water is the solvent of Nature and the most abundant liquid on Earth.[41] Biochemical transformations occur in aqueous environments or take advantage of water properties to work. For instance, hydrophobicity of long chain fatty acids promotes the formation of micelles, that allow for the compartmentalization required for biological processes.

[38] B. M. Trost, D. L. Van Vranken, *Chem. Rev.* **1996**, *96*, 395–422B. M. Trost, M. L. Crawley, *Chem. Rev.* **2003**, *103*, 2921–2944.
[39] N. Thieriet, J. Alsina, E. Giralt, F. Guibé, F. Albericio, *Tetrahedron Letters* **1997**, *38*, 7275–7278.
[40] P. T. Anastas, J. C. Warner, *Green Chemistry: Theory and Practice*, Oxford University Press, Oxford, **2000**.
[41] U. M. Lindström, Ed. , *Organic Reactions in Water: Principles, Strategies and Applications*, Blackwell Pub, Oxford ; Ames, Iowa, **2007**.

Unfortunately, translating organic reactions, especially organometallic processes, to water environments is extremely challenging, not only because of solubility problems, but also in terms of the compatibility of the reagents or catalysts with the aqueous media.[42] Indeed, organometallic reagents and catalysts have been classically considered incompatible with water, likely because of the historical use of polar organometallic reagents based on lithium and magnesium. However, with late transition metals the hydrolysis of carbon-metal bonds is kinetically disfavored. These metals have accessible *d*-orbitals that may prefer to interact with the π/π*-orbitals of unsaturated units than with "hard" nucleophiles.[42] At the same time, there was also an historical misconception that a compound "must" be dissolved to react, "*corpora non agunt nisi soluta*", which is not always the case. A slight solubility in water can be enough to trigger the reaction even better than in organic solvents.[42]

For instance, in 1988 Prof. Robert Grubbs showed that the $Ru(H_2O)_6(tos)_2$ (tos = *p*-toluenesulfonate) was an exceptional pre-catalyst for ring-opening metathesis polymerization (ROMP) in water. The reaction showed a 5000-fold acceleration in the initial rate, compared with the induction period that requires in organic solvents (**Figure 12a**).[43]

An alternative strategy to achieve catalysis in water is based on the *in situ* generation of micelles, where the interaction within hydrophobic catalysts and reactants can be favored. In this regard, amphiphiles developed by Lipshutz and coworkers (e.g., PTS and TPGS-750M) are particularly effective to promote organometallic reactions, as they form micelles that act as nano-reactors, mimicking the compartmentalization typical of biological systems. These micelles allow several palladium-catalyzed 'named' reactions to take place in water and at room temperature, whereas their analog processes carried out in organic solvents need longer reaction times and heating. (**Figure 12b**).[44]

[42] A. Chanda, V. V. Fokin, *Chem. Rev.* **2009**, *109*, 725–748.
[43] B. M. Novak, R. H. Grubbs, *J. Am. Chem. Soc.* **1988**, *110*, 7542–7543.
[44] B. H. Lipshutz, N. A. Isley, J. C. Fennewald, E. D. Slack, *Angew. Chem. Int. Ed.* **2013**, *52*, 10952–10958.

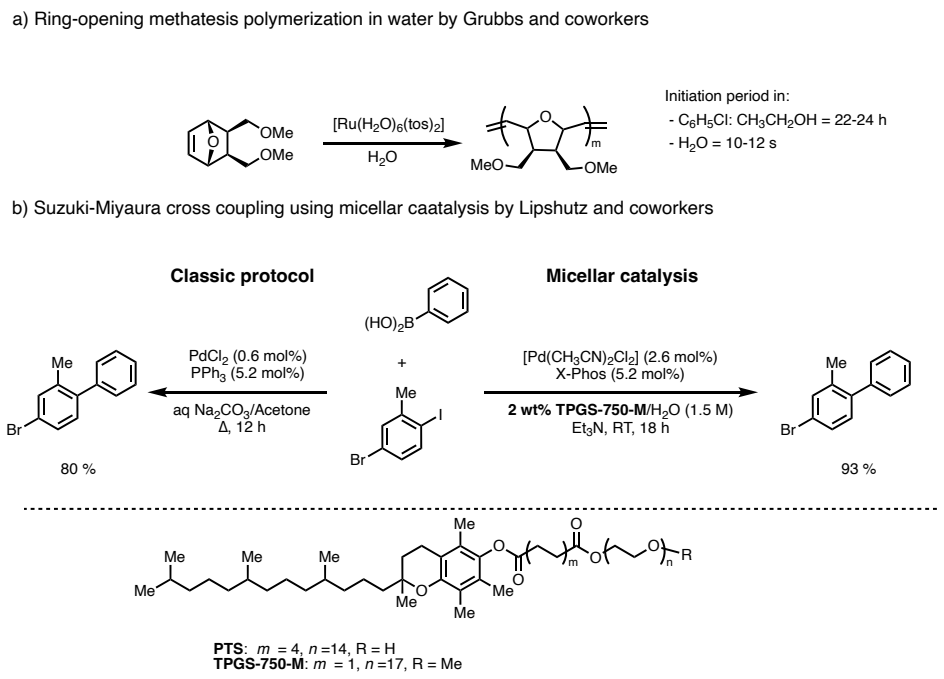

Figure 12. a) Ring-opening polymerization in water catalyzed by a ruthenium complex.[43] b) Suzuki-Miyaura cross-coupling reaction using micellar catalysis.[44]

One of the most impactful transition metal-catalyzed reaction that proceeds in aqueous solvents is the previously commented Copper Catalyzed Azide Alkyne Cycloaddition (CuAAC).[41,42] (**Figure 13**), considered as the benchmarking reaction of click chemistry.[45]

In addition to water compatibility, the CuAAC presents a broad scope, is robust and reliable, highly chemoselective and tolerant to other functional groups. Consequently, it rapidly spread and became one of the most reliable and used tools in chemistry, with a particular focus on chemical biology and medicinal chemistry,[46] as well as in material sciences.[47]

[45]This might be one of the most impactful pieces of word in the last two decades. Both original works had sum up over 19 000 citations: 6697 Meldal's article and 10.102 Sharpless' article at 2022/08/05.
[46] M. Yang, Y. Yang, P. R. Chen, *Top Curr Chem (Z)* **2016**, *374*, 2.
[47] S. Chassaing, V. Bénéteau, P. Pale, *Catal. Sci. Technol.* **2016**, *6*, 923–957.

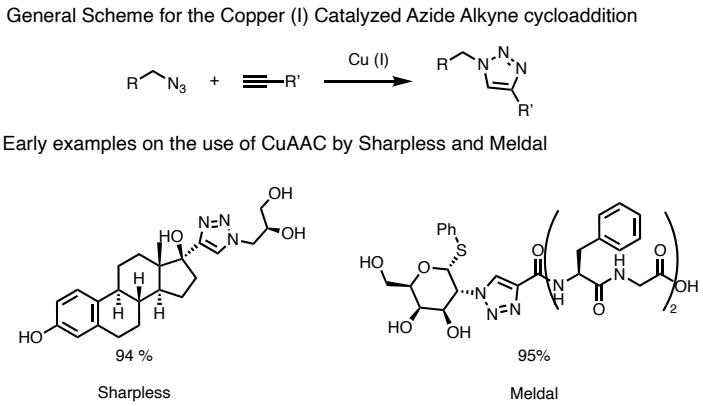

Figure 13. Copper Catalyzed Azide Cycloaddition and early examples by Sharpless and Meldal.

It is accepted that the reaction starts by formation of copper acetylides in water (with or without the addition of organic co-solvents) that cleanly and rapidly evolve to the triazole product, usually in very high yields. This reaction proved to be very robust and orthogonal to almost any other functional groups. The resulting triazoles, which are obtained with complete selectivity, are particularly interesting from a synthetic and biological point of view, due to their chemical inertness and structural similarity to the amide bonds.

Sharpless coined the concept "*click chemistry*" as that based on reactions with the above mentioned basic characteristics.[48] In the introduction of a *Chemical Reviews* special issue, commemorating the twentieth anniversary of the CuAAC, N. K. Devaraj and M. G. Finn stated that "*click chemistry was meant to convey the type of convenience and satisfaction one is afforded by snapping objects together with a luggage strap connector. It does not matter what the pieces are; if the two ends of the buckle can reach each other, the linkage is made."*[49]

4 Bioorthogonal Transformations

4.1 Bioorthogonal Chemistry. Metal-free reactions

Chemical Biology is a scientific discipline aimed at the development of chemical and synthetic tools for the study and manipulation of biological systems. Key for the development of the field is the development of **Bioorthogonal Chemistry**, which encompasses a class of chemical reactions that can take place in biological and living

[48] H. C. Kolb, M. G. Finn, K. B. Sharpless, *Angew. Chem. Int. Ed.* **2001**, *40*, 2004–2021.
[49] N. K. Devaraj, M. G. Finn, *Chem. Rev.* **2021**, *121*, 6697–6698.

environments in a selective and unharmful way. This term was first coined by Bertozzi in 2003, as part of their work for imaging glycans in live settings.[50]

Bioorthogonality or *bioorthogonal* summarizes all the conditions that a reaction must fulfill in order to be able to occur in living settings. In particular:

- *Chemoselectivity*. The reagents must yield the desired product without by-products and without reacting with other molecules of the biological media.
- *Compatible with physiological conditions*. Aqueous media, neutral pH, 37 ºC.
- *Fast rate*. The reaction must be fast enough to decrease the exposition time of the abiotic components, which might lead to unwanted processes. Moreover, since reactions are usually performed at the micro- to nanomolar concentration range, a fast rate is needed to overcome the dilution barrier.
- *Stability of reagents and products*. The reaction components should not be metabolized, unless intended.

Bioorthogonal chemistry was originally focused on the development of bioconjugation tools, namely reactions that modify specific biomolecules (DNA, proteins, etc.) by covalently attaching to them a desired label (i.e., fluorophore, pro-drug, etc.) or another biomolecule. In this regard, the most common strategy frequently involves two steps: firstly, a molecule bearing a tag (e.g., alkyne) is attached to a biological system (DNA, carbohydrate, protein... etc.) and, secondly, a reaction partner (e.g., azide) with a probe is added to selectively react with the tag in a bioorthogonal manner. Importantly, as the field evolved, bioorthogonal reactions have been used for different purposes, such as the controlled release of bioactive molecules,[51] or the selective synthesis of functional products (e.g., drugs, or fluorescence labels) from non-functional precursors (e.g., pro-drugs and pro-fluorophores).[52]

Early examples of what we can now call bioorthogonal chemistry can be traced back to the late 1980s, when Rideout and coworkers developed a bioconjugation technique based on the formation of hydrazones, which are more stable than the parent imines to hydrolysis.[53] In this seminal work, the authors developed a method for the *in cellulo*

[50] H. C. Hang, C. Yu, D. L. Kato, C. R. Bertozzi, *Proc. Natl. Acad. Sci. U.S.A.* **2003**, *100*, 14846–14851.
[51] X. Ji, Z. Pan, B. Yu, L. K. De La Cruz, Y. Zheng, B. Ke, B. Wang, *Chem. Soc. Rev.* **2019**, *48*, 1077–1094.
[52] B. Lozhkin, T. R. Ward, *Bioorganic & Medicinal Chemistry* **2021**, *45*, 116310.
[53] J. Kalia, R. T. Raines, *Angew. Chem. Int. Ed.* **2008**, *47*, 7523–7526.

synthesis of cell toxins from non-toxic starting materials (**Figure 14**).[54,55] The use of oxime ethers as bioconjugation tool was further developed by Bertozzi and coworkers to covalently modify cell membranes.[56,57]

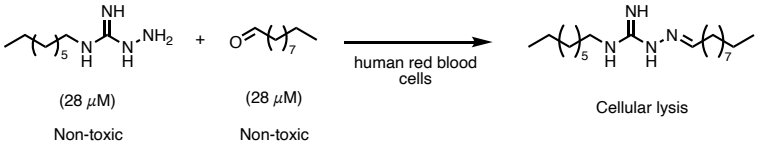

Figure 14. Formation of a hydrazone in the presence of human red blood cells.

A key transformation in the establishment of bioorthogonal chemistry has been the Staudinger reaction.[58,59] In the classical Staudinger, an organic azide reacts with a phosphine to form and aza-ylide intermediate, which is spontaneously hydrolyzed by water present in the media to deliver the phosphine oxide and the desired amine. The use of a designed phosphine bearing a methyl ester as electrophilic trap of the iminophosphorane intermediate, allowed to suppress the hydrolytic path, enabling the formation of a covalent amide bond. The simplicity of the reaction and the absence of phosphines and azides in biological environments made the Staudinger-Bertozzi reaction a promising candidate as bioconjugation reaction (**Figure 15**). However, despite its great selectivity, the poor kinetics of the process hampered its widespread application.[11]

[54] D. Rideout, *Science* **1986**, *233*, 561–563.
[55] D. Rideout, J. Jaworski, R. Dagnino, *Biochemical Pharmacology* **1988**, *37*, 4505–4512.
[56] L. K. Mahal, K. J. Yarema, C. R. Bertozzi, *Science* **1997**, *276*, 1125–1128.
[57] H. C. Hang, C. R. Bertozzi, *J. Am. Chem. Soc.* **2001**, *123*, 1242–1243.
[58] E. Saxon, C. R. Bertozzi, *Science* **2000**, *287*, 2007–2010.
[59] J. A. Prescher, D. H. Dube, C. R. Bertozzi, *Nature* **2004**, *430*, 873–877.

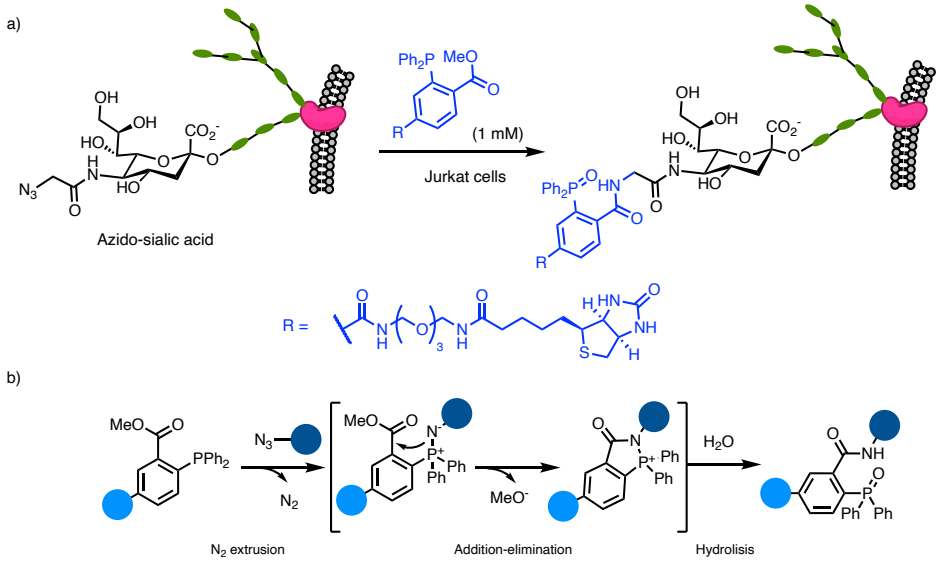

Figure 15. a) Modification of azido sugars in the surface of Jurkat cells by Staudinger- Bertozzi conjugation. b) Mechanism for the Staudinger- Bertozzi conjugation.

A cutting-edge turn in the field was the development of the strain-promoted 1,3-dipolar cycloadditions between azides and strained alkynes or alkenes,[60] and especially the more recent cycloaddition between tetrazines and *trans*-cyclooctenes, which is among the fastest of all bioorthogonal reactions (**Figure 16**).[61]

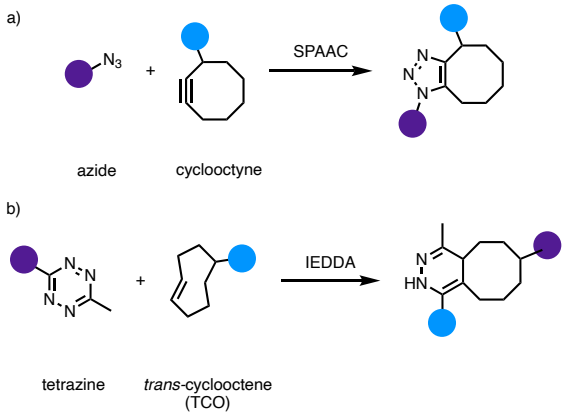

Figure 16. a) General scheme for the Strain-Promoted Azide Alkyne cycloaddition. b) General scheme for the Inverse Electron Demand Diels-Alder reaction.

[60] J. Dommerholt, F. P. J. T. Rutjes, F. L. van Delft, *Top Curr Chem (Z)* **2016**, *374*, 16.
[61] B. L. Oliveira, Z. Guo, G. J. L. Bernardes, *Chem. Soc. Rev.* **2017**, *46*, 4895–4950.

Although these reactions are impressive and have led to many useful applications, they rely on the use of classical organic reactivities with high reactive reactants that can lead to unwanted, secondary reactions, and usually require long and difficult synthesis. In this context, the development of bioorthogonal processes promoted by external catalytic reagents is very attractive, as the reactants would remain inert until finding the catalyst, so that much simpler materials could be a priori used.

Particularly attractive is the possibility of using transition metal complexes as catalysts, owing to the enormous breadth and scope of organometallic catalysis. Moreover, the possibility of tuning the physical and catalytic properties of the metal catalysts by modifying their ancillary ligands, represents a special bonus for this type of potential bioorthogonal tools. It is however true that translating transition metal catalysis to biological environments encompasses numerous challenges, including the compatibility of the reagents and organometallic intermediates with water and with the biological milieu, the potential deactivation of the active catalytic species, as well as the deleterious entropic factors derived from the use of an additional reaction component in catalytic amounts.

4.2 Transition Metal Catalyzed Bioorthogonal Reactions

The first examples of a transition metal catalyzed transformation in any kind of biological media can be traced back to the early 80's, when Csesplö and coworkers reported the use a water-soluble ruthenium catalyst ($RuCl_2L_2$, L = triphenylphosphine-3-sulfonic acid) to hydrogenate unsaturated fatty acids of the cell membranes of protoplasts.[62] The reduction of the unsaturated fatty acids changes the membrane fluidity as the percentage of unsaturation correlates with the microviscosity of the cell membranes. Even though the reaction induces the death of most the cells after 1.5-2 hours, it can be considered as a proof of concept, a pioneering example in the field (**Figure 17**).

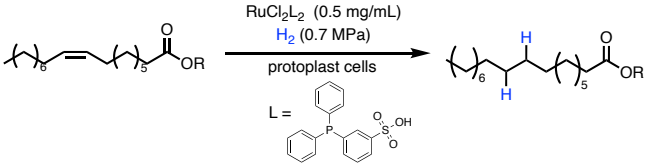

Figure 17. Ruthenium promoted hydrogenation of fatty acids in protoplast cells.

[62] L. Vigh, F. Joo, A. Cseplo, *Eur J Biochem* **1985**, *146*, 241–244.

The publication in 2001of the Copper Catalyzed Azide-Alkyne Cycloaddition (CuAAC), as previously described in **section 3**, represented a major driving force for the developments of the field of bioorthogonal metal catalysis.

The attributes of the CuAAC (and Click Chemistry) overlapped with those of **bioorthogonal reactions**. Both concepts reflect the same underlying chemical principles applied to different purposes, either to improve synthetic outcomes, or to perform reactions in biological media. On these bases and considering their huge impact in science, along the last two decades, it can not be seen as a surprise that the pioneers of both, Click and Bioorthogonal Chemistry, professors Bertozzi, Meldal and Sharpless, shared the Nobel Prize in Chemistry of 2022.[63]

During these years, there have been many attempts to translate the CuAAC ligation to biological and living environments. For instance, Tirrell and coworkers reported the modification of membrane proteins of bacteria by using the CuAAC as bioorthogonal tool.[64] In particular, they overexpressed a genetically engineered protein bearing azidohomoalanine (AHA), a non-natural amino acid, in the surface of *E. coli* and demonstrated that this azido protein could be conjugated to a biotin-alkyne derivative (**Figure 18a**) under copper catalysis, by means of the CuAAC.

Using a different approach, our group showed in 2018 that discrete and well-defined Cu (I) complexes can promote the CuAAC between propargyl alcohol and 9-antracenyl azide, in living A549 cells. The use of these particular discrete complexes allowed to circumvent the main drawback of the CuAAC, namely its low biocompatibility due to the cytotoxicity of Cu(I) ions and that of sodium ascorbate, which is an additive frequently used to warrant the presence of Cu(I) ions (**Figure 18b**).[65]

[63] C. R. Bertozi, M. P. Meldal, K. B.Sharpless. The Nobel Prize in Chemistry 2022.
[64] A. J. Link, D. A. Tirrell, *J. Am. Chem. Soc.* **2003**, *125*, 11164–11165.
[65] J. Miguel-Ávila, M. Tomás-Gamasa, A. Olmos, P. J. Pérez, J. L. Mascareñas, *Chem. Sci.* **2018**, *9*, 1947–1952.

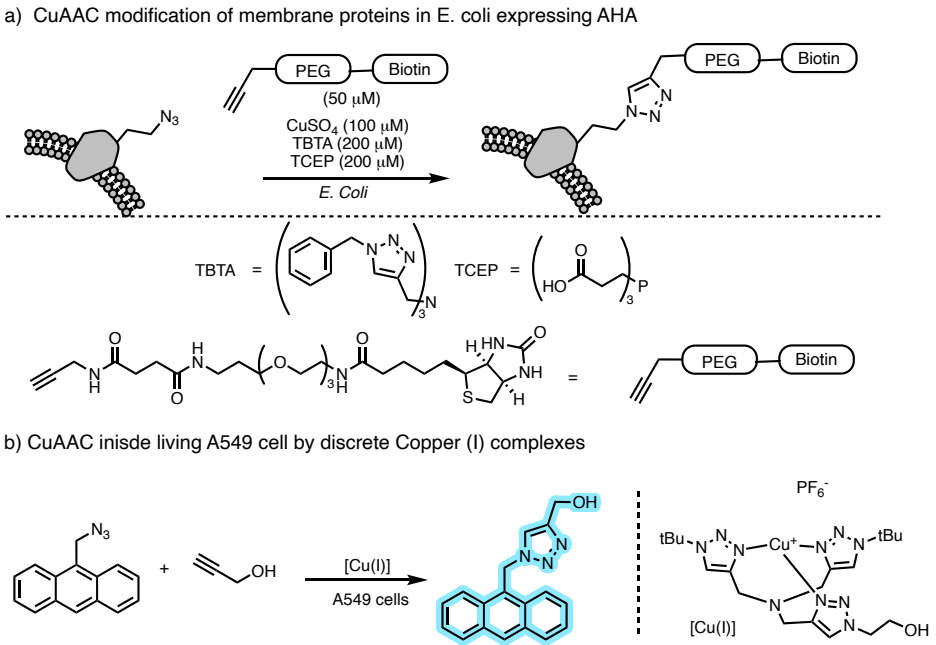

Figure 18. Biological application of the CuAAC: a) CuAAC on the cellular surface of fixed mammalian cells.[64] b) Intracellular formation of a fluorescent triazole by discrete Cu (I) complexes.[65]

Overall, the CuAAC has been extensively used for: cell-surface labelling,[64] proteomics through genetically encoded handles,[66] polymer modification, material science and even for *in cellulo* applications.[65]

Besides copper, other transition metals have been recently reported for promoting bioorthogonal cycloadditions between azides and alkynes, like Ru,[67] Ir [68],[69] or Rh[70]. Among these metals, the methods reported with ruthenium are the most versatile. For instance, our group reported the first azide alkyne cycloaddition catalyzed by ruthenium under aqueous and biocompatible conditions, using the complex [Cp*RuCl(COD)] and thioalkynes as reaction partners (**Figure 19**). Further details about this reaction (RuAAC) will be presented in Chapter 1.

[66] A. E. Speers, G. C. Adam, B. F. Cravatt, *J. Am. Chem. Soc.* **2003**, *125*, 4686–4687.
[67] P. Destito, J. R. Couceiro, H. Faustino, F. López, J. L. Mascareñas, *Angew. Chem. Int. Ed.* **2017**, *56*, 10766–10770.
[68] Y. Liao, Q. Lu, G. Chen, Y. Yu, C. Li, X. Huang, *ACS Catalysis* **2017**, *7*, 7529–7534.
[69] W. Song, N. Zheng, *Org. Lett.* **2017**, *19*, 6200–6203.
[70] W. Song, N. Zheng, M. Li, K. Ullah, Y. Zheng, *Adv. Synth. Catal.* **2018**, *360*, 2429–2434.

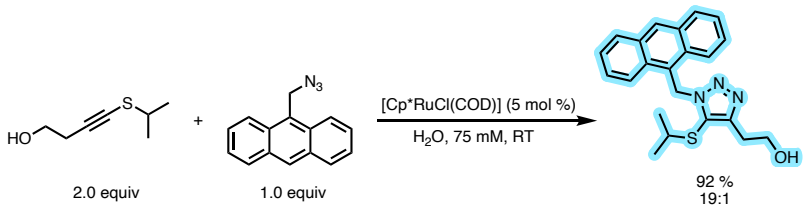

Figure 19. Representative example of the RuAtAC reaction.

Since the early introduction of the CuAAC, the development of bioorthogonal transition metal catalysis have progressed along two main lines involving 1) the development of uncaging methods based on the carbon-heteroatom bond breaking reactions and 2) the development of new C-C and C-heteroatom bond forming reactions that, alternatively, allow to increase the structural complexity of a biological system.

Among the different metals used, Pd and Ru are the most frequent, albeit others like Ir, Au, Cu, Os, and Fe have also been recently incorporated to the area.[71] In the following sections we describe some of more significant advances, with a special focus on Ru catalyzed processes, which constitute the core of this PhD work.

4.3 Metal-promoted uncaging processes

The use of transition metals for uncaging or deprotection reactions was soon reported after the first applications of the CuAAC. Namely, in 2006, Meggers and coworkers showed that the Ru(II) complex [Cp*Ru(COD)Cl] was able to promote the removal of allyl carbamate (i.e. alloc) protecting groups from a rhodamine-110 caged probe, not only *in vitro*, in aqueous buffers, but also in living HeLa cells.[72] The reaction, follows a Tsuji-Trost like mechanism: coordination of the ruthenium complex to the allyl compound followed by an oxidative addition to the metal center gives a π-allyl complex with the concomitant release of the unprotected molecule. In the case of carbamates, CO_2 is also released, leading to a primary amine. To close the catalytic cycle, an outer sphere attack of a sacrificial nucleophile is needed, so that the Ru (II) catalyst can be regenerated. In consonance with this mechanism, the supplementation of super-stochiometric quantities of an external nucleophile, such as thiophenol (PhSH), was required to achieve an efficient deprotection reaction (**Figure 20**).

[71] P. Destito, C. Vidal, F. López, J. L. Mascareñas, *Chem. Eur. J.* **2021**, *27*, 4789–4816.
[72] C. Streu, E. Meggers, *Angew. Chem. Int. Ed.* **2006**, *45*, 5645–5648.

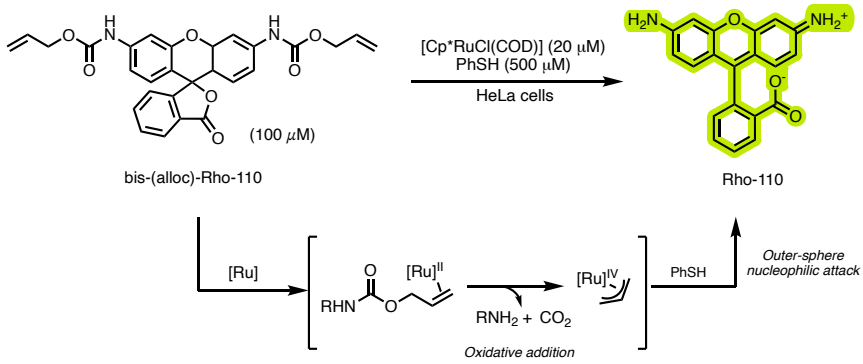

Figure 20. Tsuji-Trost mechanism for the deprotection of alloc-protected amines.

Later on, in 2014, Mascareñas and coworkers further demonstrated the bioorthogonal potential of this ruthenium catalyst, by using it for the uncaging of DNA-binding agents, such as DAPI or ethidium bromide, inside live mammalian cells.[73] In this work several binders were studied, like 4',6-diamidino-2-phenylindole (DAPI), a fluorescent molecule that binds DNA used as nuclei marker and also in cell membrane viability assays. The incubation of the deprotection of bis-(alloc)-DAPI was achieved in Chicken embryo fibroblast cells (CEF cells) and in African green monkey kidney cells (Vero cells) by [Cp*RuCl(COD)], again in the presence of thiophenol (**Figure 21**).

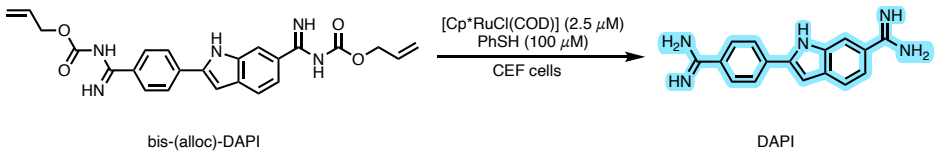

Figure 21. [Cp*RuCl(COD)] deprotection of bis-(alloc)-DAPI in CEF cells.

Importantly, Meggers developed several modifications of the original ruthenium deallylation catalyst, with improved performances. Thus, the second-generation catalyst, which is based on previous works by Kitamura, consisted of a Ru(IV) complex bearing the less electron donating cyclopentadienyl ligand (Cp) and a quinaldic acid derivative.[74] This catalyst provided turnover numbers (TON's) of up to 270 in the deallylation of water-soluble alloc-coumarins (500 μM), whereas the original Ru catalyst only afforded a TON of 4. Moreover, the second generation catalyst effectively works with glutathione

[73] M. I. Sánchez, C. Penas, M. E. Vázquez, J. L. Mascareñas, *Chem. Sci.* **2014**, *5*, 1901–1907.
[74] T. Völker, F. Dempwolff, P. L. Graumann, E. Meggers, *Angew. Chem. Int. Ed.* **2014**, *53*, 10536–10540.

(GSH) as nucleophile, instead of thiophenol, which significantly increases the biocompatibility of the method (**Figure 22**)

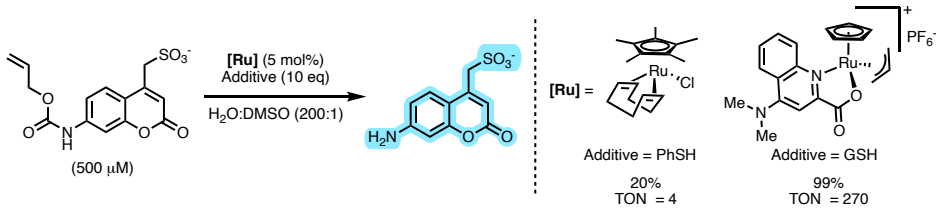

Figure 22. Deallylation of water soluble alloc-coumarin by a new Ru(IV) precatalyst.

The higher efficiency of this second-generation catalyst allowed for the *in situ* generation of doxorubicin inside HeLa cells. In particular, the authors treated the cells with a high concentration of N-alloc-doxorubicin (100 μM), which is significantly less toxic than doxorubicin. Upon treatment of the cells with 5 μM of the ruthenium catalyst, the alloc group is removed, and the biological effect of the drug is fully restored promoting cell death (**Figure 23**). This strategy highlights the potential of transition metals for therapeutic applications based on *in situ* activation of pro-drugs.

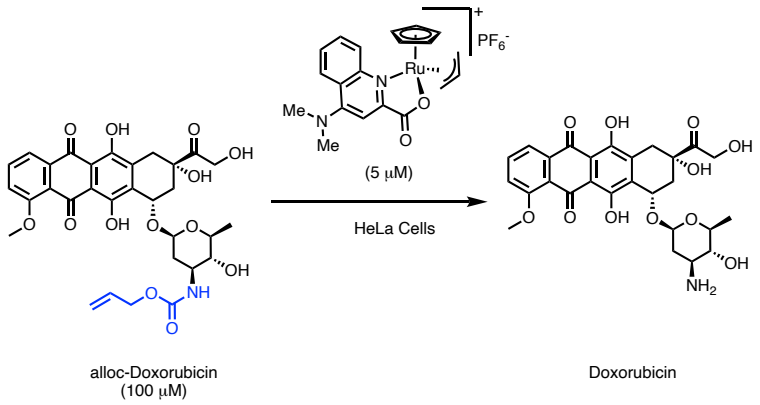

Figure 23. Activation of alloc-Doxorubicin by ruthenium catalyzed deallylation in HeLa cells.

In 2016 our group took advantage of the structural modularity of this second-generation Ru-catalysts and developed a family of novel ruthenium complexes with phosphonium moieties attached to the quinaldic acid ligand (**Figure 24**).[75] This lipophilic cationic groups exhibit a single positive charge resonance-stabilized over three phenyl groups and a large hydrophobic surface area. These features allow the ruthenium complex to be internalized and accumulated preferentially in the mitochondria, due to the membrane

[75] M. Tomás-Gamasa, M. Martínez-Calvo, J. R. Couceiro, J. L. Mascareñas, *Nat Commun* **2016**, *7*, 12538.

potential across the inner membrane. [76] Consequently, the authors showed that intracellular catalysis was feasible in specific organelles such as mitochondria.

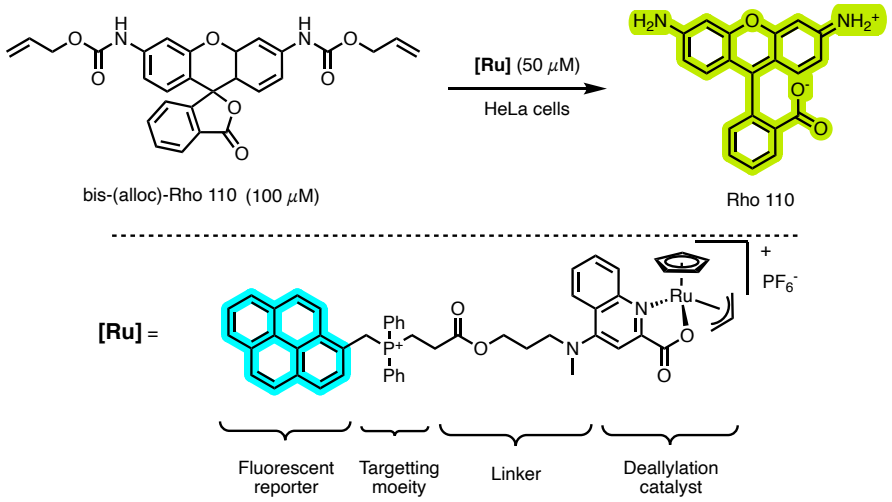

Figure 24. Deprotection of bis-(alloc)-Rho by a Ru catalyst with fluorescent reporter and mitochondrial targeting moiety.

In a new turn to improve catalytic efficiency, Meggers reported a third-generation catalyst, which incorporates an 8-hydroxyquinaldine instead of the quinaldic acid ligand, enabling the deallylation of the alloc-coumarins to proceed up to 30-times faster rates and with 5-times higher TON, compared to the second-generation catalyst (**Figure 25**).[77] Moreover, the new catalyst proved to be effective in undiluted blood serum.

[76] M. P. Murphy, *Biochimica et Biophysica Acta (BBA) - Bioenergetics* **2008**, *1777*, 1028–1031.
[77] T. Völker, E. Meggers, *ChemBioChem* **2017**, *18*, 1083–1086.

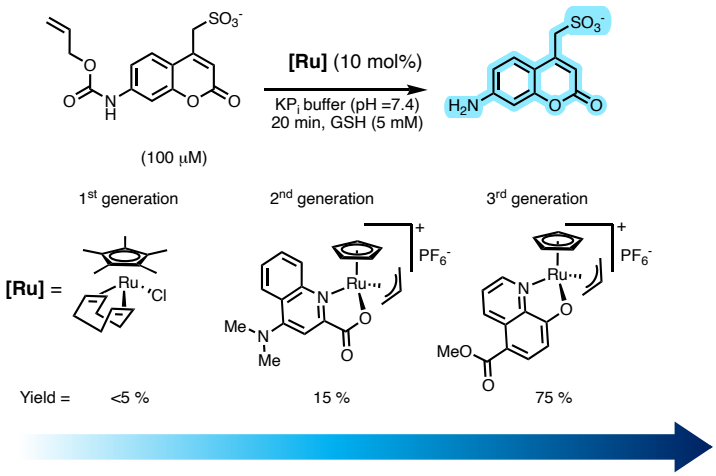

Figure 25. Deallylation of water soluble alloc-coumarin by different ruthenium catalyst at 100 μM.

Several other groups such as those of Balskus,[78] Rotello,[79,80] Mayer,[81] or Jessen-Trefzer[82] also reported significant contributions based on Ru-catalyzed deallylations to give bioactive compounds.

Importantly, ruthenium complexes have also been incorporated into protein scaffolds to form artificial metalloenzymes that can promote this type of bond cleavage reactions. In particular, Ward has worked extensively during the last decade to develop artificial metalloenzymes, in most cases based on a streptavidin-biotin binding strategy. In this context, this group reported in 2018 the use of a biotin containing ruthenium complex that, when bound to streptavidin, can promote the deallylation reaction of *N*-alloc containing substrates. The artificial metalloenzymes were structurally optimized by several rounds of directed evolution cycles. The optimal metalloenzyme was able to be uptaken by HEK-293T cells and to efficiently catalyze the deallylation of *N*-alloc-triiodothyronine (**Figure 26**). Remarkably, the released triiodothyronine hormone activates a gene switch that triggers the production of luciferase as redout, enabling the determination of the reaction efficiency.

[78] Y. Lee, A. Umeano, E. P. Balskus, *Angew. Chem. Int. Ed.* **2013**, *52*, 11800–11803.
[79] G. Y. Tonga, Y. Jeong, B. Duncan, T. Mizuhara, R. Mout, R. Das, S. T. Kim, Y.-C. Yeh, B. Yan, S. Hou, V. M. Rotello, *Nature Chem* **2015**, *7*, 597–603.
[80] R. Das, R. F. Landis, G. Y. Tonga, R. Cao-Milán, D. C. Luther, V. M. Rotello, *ACS Nano* **2019**, *13*, 229–235.
[81] R. Rubini, C. Mayer, *ACS Chem. Biol.* **2020**, *15*, 3093–3098.
[82] P. Lohner, M. Zmyslia, J. Thurn, J. K. Pape, R. Gerasimaitė, J. Keller-Findeisen, S. Groeer, B. Deuringer, R. Süss, A. Walther, S. W. Hell, G. Lukinavičius, T. Hugel, C. Jessen-Trefzer, *Angew. Chem. Int. Ed.* **2021**, *60*, 23835–23841.

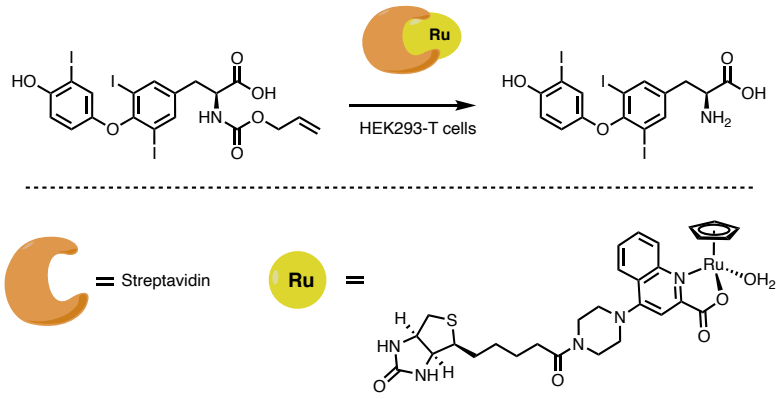

Figure 26. Streptavidin-Ru artificial metalloenzyme for the alloc deprotection of alloc-triiodothyronine in HEK293-T cells.

Besides ruthenium, palladium is undoubtedly the other metal of reference in bioorthogonal catalysis. Regarding uncaging processes, propargyl-protected amines and alcohols can be cleaved by palladium species. Thus, in 2014, P. R. Chen and coworkers reported the palladium based deprotection of *N*-allyl and *N*-propargyl carbamates (i.e., alloc and proc) for the activation of fluorescent probes and proteins in different cell lines.[83] In this work, this group screened several Pd(0), Pd(II) and Pd(IV) species for the uncaging of proc-Rhodamine 110. There was not a clear trend in the reactivity for the different complexes, being $Pd(dba)_2$ and $[PdCl(allyl)]_2$ the species with highest activity (**Figure 27a**). The same author also studied the intracellular palladium promoted activation of proteins that incorporate proc-lysine residues (ProcLys), finding that $[PdCl(allyl)]_2$ was a competent complex for the activation of a green fluorescent protein (GFP-N149-ProcLys) or the phospho-threoninelyase (OspF) (**Figure 27b**).

[83] J. Li, J. Yu, J. Zhao, J. Wang, S. Zheng, S. Lin, L. Chen, M. Yang, S. Jia, X. Zhang, P. R. Chen, *Nature Chem* **2014**, *6*, 352–361.

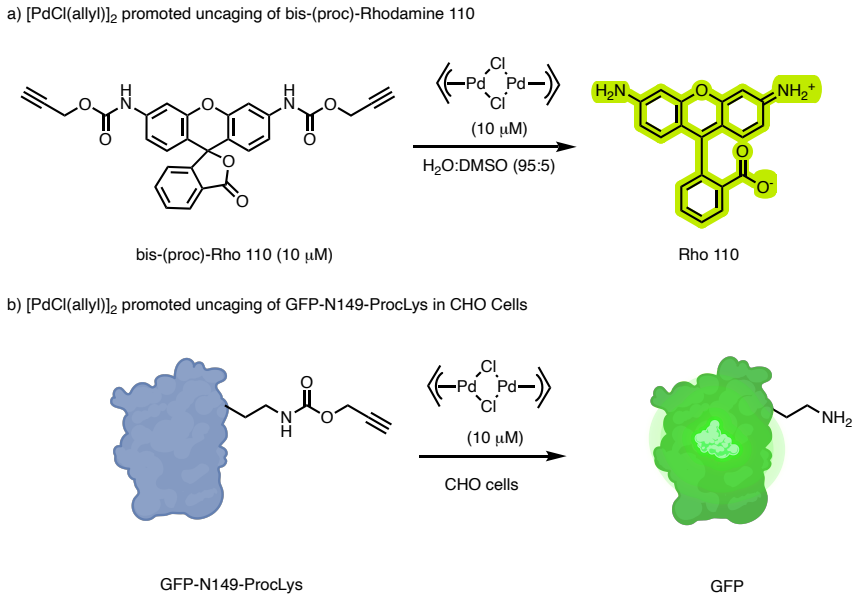

Figure 27. a) Palladium promoted depropargylation of bis-(proc)-Rho 110. b) Palladium promoted uncaging of GFP-N149-ProcLys.

However, it is important to notice that Pd(II) and Pd(IV) species show poor stability in aqueous and biological conditions, and the formation of palladium nanoparticles is quite usual. Therefore, the most studied approach for palladium-promoted deprotection reactions relays on the use of palladium nanoparticles or nano constructs. In this regard, Unciti-Broceta and Bradley reported the use of Pd(0)-containing microspheres for the extracellular activation of a pro-drug: *proc*-5-fluoro-uracil.[84] A similar strategy has been used by Unciti-Broceta and coworkers for the activation of different propargyl protected drugs such as vorinostat,[85] doxorubicin[86] or gemcitabine,[87] as depicted in **Figure 28**.

[84] J. T. Weiss, J. C. Dawson, K. G. Macleod, W. Rybski, C. Fraser, C. Torres-Sánchez, E. E. Patton, M. Bradley, N. O. Carragher, A. Unciti-Broceta, *Nat Commun* **2014**, *5*, 3277.
[85] B. Rubio-Ruiz, J. T. Weiss, A. Unciti-Broceta, *J. Med. Chem.* **2016**, *59*, 9974–9980.
[86] T. L. Bray, M. Salji, A. Brombin, A. M. Pérez-López, B. Rubio-Ruiz, L. C. A. Galbraith, E. E. Patton, H. Y. Leung, A. Unciti-Broceta, *Chem. Sci.* **2018**, *9*, 7354–7361.
[87] J. T. Weiss, J. C. Dawson, C. Fraser, W. Rybski, C. Torres-Sánchez, M. Bradley, E. E. Patton, N. O. Carragher, A. Unciti-Broceta, *J. Med. Chem.* **2014**, *57*, 5395–5404.

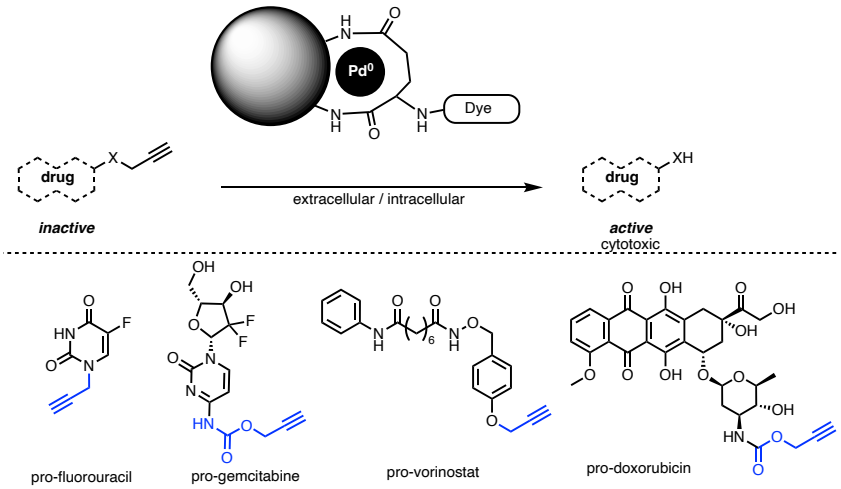

Figure 28. Pd(0) nanoparticles promoted uncaging of pro-drugs in biological milieus.

Rotello,[79] Unciti-Broceta, our group[88] and few others have exploited the use of palladium nanoparticles for the bioorthogonal activation of probes and pro-drugs. Discrete and well defined palladium complexes with improved stability have also been studied. In particular, our group showed in 2017 that engineered discrete palladium (II) η^3-allyl phosphine [Pd(allyl)PR_3] complexes show increased stability than $Pd(dba)_2$ and $[PdCl(allyl)]_2$ in biological media. These new complexes are able to promote different deallylation and depropargylation reactions in various cell lines. The modularity offered by the phosphine ligand allowed the introduction of organelle targeting moieties (i.e., phosphonium groups) as well as a fluorophore, for the intracellular tracking of the catalysts (**Figure 29a**).[89]

In an alternative strategy, our group reported the use of catalytic palladium minipeptides for the deprotection of propargyl ethers and carbamates, in living cells. The basic domain of bZIP transcription factor, mutated to include two histidine residues (position *i* and *i+4*), can react with palladium(II) sources to generate catalytically active stapled peptides. Importantly, whereas the mutated bZIP peptide is unable to be internalized by cells, the stapled palladium peptide undergoes efficient internalization and is able to promote the

[88] R. Martínez, C. Carrillo-Carrión, P. Destito, A. Alvarez, M. Tomás-Gamasa, B. Pelaz, F. Lopez, J. L. Mascareñas, P. del Pino, *Cell Reports Physical Science* **2020**, *1*, 100076.
[89] M. Martínez-Calvo, J. R. Couceiro, P. Destito, J. Rodríguez, J. Mosquera, J. L. Mascareñas, *ACS Catal.* **2018**, *8*, 6055–6061.

intracellular depropargylation of fluorescent probes with high efficiencies (**Figure 29b**).[90]

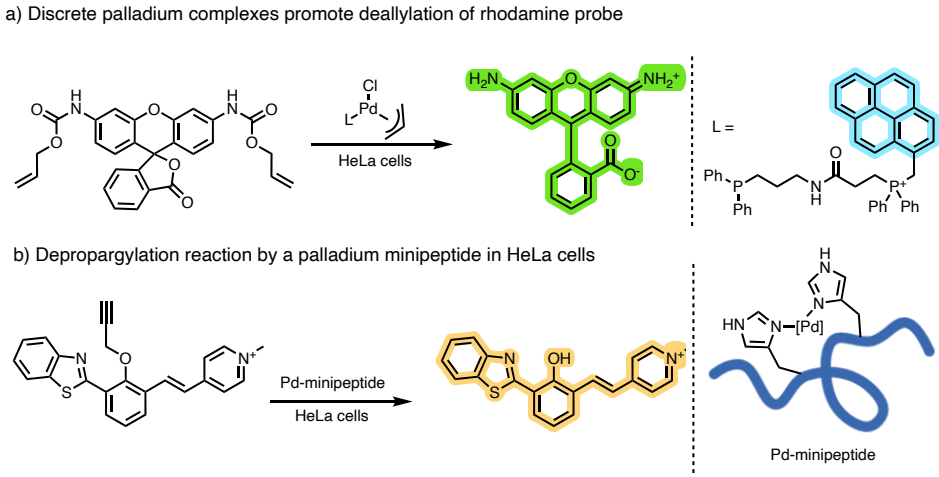

Figure 29. Application of uncaging reactions catalyzed by palladium a) Intracellular deprotection of an alloc-protected rhodamine inside living cells by a discrete palladium bearing a mitochondria targeting moiety (phosphonium). b) Palladium minipeptide for depropargylation inside living HeLa cells.

Besides Pd and Ru, other metal catalysts of copper[91] or gold[92] have also been proven successful for this type of uncaging reactions, although their effectiveness and applicability is far more limited.

4.4 Transition Metal Catalyzed Bond-forming Reactions

The development of bioorthogonal and biocompatible bond forming reactions promoted by transition metal catalysts is of high relevance because of their synthetic potential. The first examples in the area focused on the bioconjugation of exogenous markers to proteins, cell membranes, or cell structures. For instance, in 2009, Davis and coworkers developed a Suzuki coupling in aqueous media using the commercially available $Pd(OAc)_2$ and 2- aminopyrimidine-4-6-diol as ligand.[93] This system enabled the cross-coupling between different tyrosine halide derivatives and several boronic acids, at 37 ºC in buffer media. The phosphate buffer takes the role of the base, required for the Suzuki cross-couplings. This reaction was for instance applied to the selective modification of a

[90] S. Learte-Aymamí, C. Vidal, A. Gutiérrez-González, J. L. Mascareñas, *Angew. Chem. Int. Ed.* **2020**, *59*, 9149–9154.
[91] X. Wang, Y. Liu, X. Fan, J. Wang, W. S. C. Ngai, H. Zhang, J. Li, G. Zhang, J. Lin, P. R. Chen, *J. Am. Chem. Soc.* **2019**, *141*, 17133–17141.
[92] K. Vong, T. Yamamoto, T. Chang, K. Tanaka, *Chem. Sci.* **2020**, *11*, 10928–10933.
[93] J. M. Chalker, C. S. C. Wood, B. G. Davis, *J. Am. Chem. Soc.* **2009**, *131*, 16346–16347.

modified serine protease, SBL–156-ArI with several boronate counter parts (**Figure 30a**). Later in 2011, this was further applied to the cell-surface labeling of *E. coli* bacteria.[94] Several other examples of Suzuki cross-couplings have been published by Bradley,[95] Qu[96] and Mascareñas[97] using different types of palladium nanoparticles.

Lin's group reported a modified version of Davis' catalyst, using a *N,N*-dimethylamino pyrimidine ligand, $Pd(OAc)_2$ and sodium ascorbate, which is able to promote Sonogashira cross-couplings of ubiquitin proteins modified with homopropargyl glycine residues (HPG-Ub). In more recent reports, Lin was able to translate this methodology to label the cell surface of HEK-293 cells (**Figure 30b**).[98]

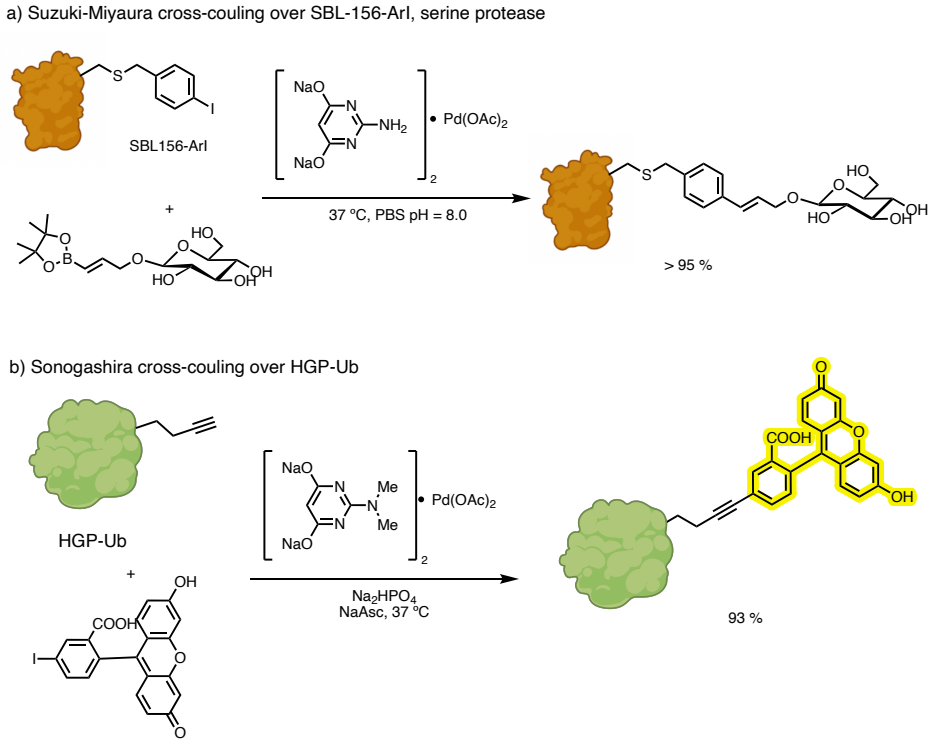

Figure 30. Suzuki-Miyaura cross-couplings. a) Cross-coupling over modified Serine Protease (SBL.156-ArI). b) Sonogashira cross-coupling over HGP-Ub protein.

[94] C. D. Spicer, T. Triemer, B. G. Davis, *J. Am. Chem. Soc.* **2012**, *134*, 800–803.
[95] R. M. Yusop, A. Unciti-Broceta, E. M. V. Johansson, R. M. Sánchez-Martín, M. Bradley, *Nature Chem* **2011**, *3*, 239–243.
[96] F. Wang, Y. Zhang, Z. Du, J. Ren, X. Qu, *Nat Commun* **2018**, *9*, 1209.
[97] P. Destito, A. Sousa-Castillo, J. R. Couceiro, F. López, M. A. Correa-Duarte, J. L. Mascareñas, *Chem. Sci.* **2019**, *10*, 2598–2603.
[98] N. Li, R. K. V. Lim, S. Edwardraja, Q. Lin, *J. Am. Chem. Soc.* **2011**, *133*, 15316–15319.

Ruthenium has also played a major role in the context of bioorthogonal transition metal bond forming reactions. Ruthenium-catalyzed alkene metathesis reactions can be considered among the most relevant transformations in the field of synthetic chemistry, as it has been extensively applied in industry for polymerization processes as well as in the synthesis of complex macrocyclic products, including some pharmaceutical drugs currently in the market.[99] Remarkably, the reaction can be carried out in water using soluble complexes such as $Ru(H_2O)_2(tos)_2$, used for promoting ring opening polymerization processes of cyclic alkenes (**Figure 31a**). [100] Another water-soluble ruthenium complex (based on the 2nd generation Hoveyda-Grubbs catalyst), which bears a polyethylene glycol In the *N*-heterocyclic carbene moiety, efficiently promotes ring closing metathesis processes under aqueous conditions (**Figure 31b**).[101]

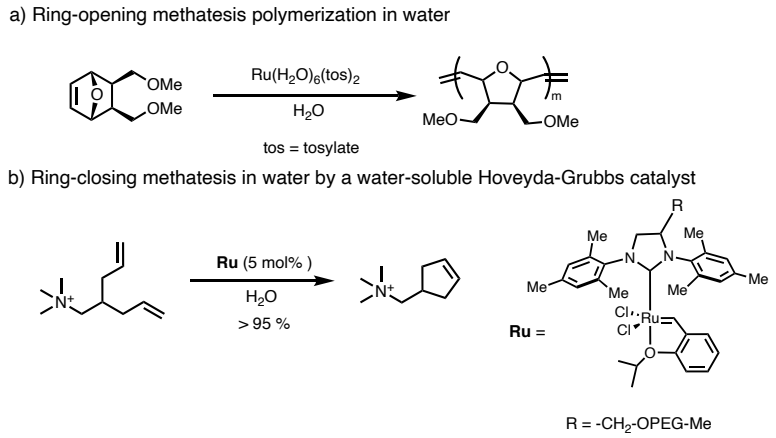

Figure 31. a) Ring opening polymerization in water by a water-soluble ruthenium catalyst. b) Ring closing metathesis by a water soluble 2nd Generation Hoveyda-Grubbs catalyst.

A very elegant application of a ring closing metathesis reaction in chemical biology has been recently described by Ward and coworkers, using the Hoveyda-Grubbs 2nd generation catalyst.[102] The authors demonstrated that the ring closing metathesis of *o*-allylphenyl allyl ethers, generates 1,4-dyhydronaphtalenes which, upon a spontaneous 1,4-elimination process, delivers a naphthalene unit and the oxygen-tethered cargo, which in the case shown in **Figure 32** is a fluorescent coumarin.

[99] Y. S. Tsantrizos, J.-M. Ferland, A. McClory, M. Poirier, V. Farina, N. K. Yee, X. Wang, N. Haddad, X. Wei, J. Xu, L. Zhang, *Journal of Organometallic Chemistry* **2006**, *691*, 5163–5171.
[100] B. M. Novak, R. H. Grubbs, *J. Am. Chem. Soc.* **1988**, *110*, 7542–7543.
[101] S. H. Hong, R. H. Grubbs, *J. Am. Chem. Soc.* **2006**, *128*, 3508–3509.
[102] V. Sabatino, J. G. Rebelein, T. R. Ward, *J. Am. Chem. Soc.* **2019**, *141*, 17048–17052.

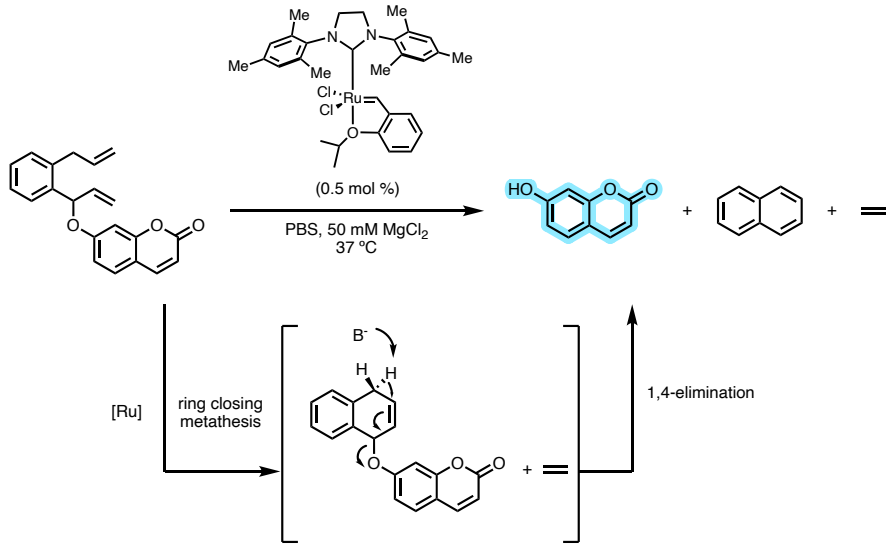

Figure 32. Ruthenium catalyzed ring closing metathesis of an *o*-allylphenyl allylether, followed by 1,4-elimination and release of the cargo.

A key element in the bioorthogonal success of Cu- or Ru-catalyzed reactions is the easy coordination of metal complex to unsaturated moieties of the substrates. Performing other type of metal-catalyzed bioorthogonal cycloadditions does not seem easy unless one could somewhat favor a pre-coordination of the metal to a desired partner in the presence of other biological components. This might be achieved by using bidentate type of coordination reagents, which could facilitate the trapping of the metal. This strategy was used by Teply and coworkers for the development of formal [2+2+2] cycloadditions of triyne, **I**, catalyzed by [Cp*RuCl(COD)]. The reaction, which generates the fluorescent [5] – helquat **II** shown in **Figure 33a** was found to proceed under aqueous conditions and even of bacteria lysates (E. Coli).[103]

Remarkably, our group demonstrated that it is possible to perform this type of annulations in a more challenging intermolecular scenario. Indeed, ruthenium complexes originally used for deallylation processes can promote the formal [2+2+2] cycloaddition of a diyne, **III**, and alkyne, **IV**, in aqueous mixtures and even in cell lysates (**Figure 33b**). More importantly, the annulation can even be performed in live mammalian cells, as demonstrated by the detection of the fluorescent anthraquinone product **IV** by microscopy. This product is an aggregation induced emission dye (AIEgen), which

[103] L. Adriaenssens, L. Severa, J. Vávra, T. Šálová, J. Hývl, M. Čížková, R. Pohl, D. Šaman, F. Teplý, *Collect. Czech. Chem. Commun.* **2009**, *74*, 1023–1034.

doesn't internalize into cells by itself because of its intrinsic tendency to self-aggregate. However, it can be efficiently generated inside cells using the aforementioned Ru-catalyzed bioorthogonal cycloaddition.[104]

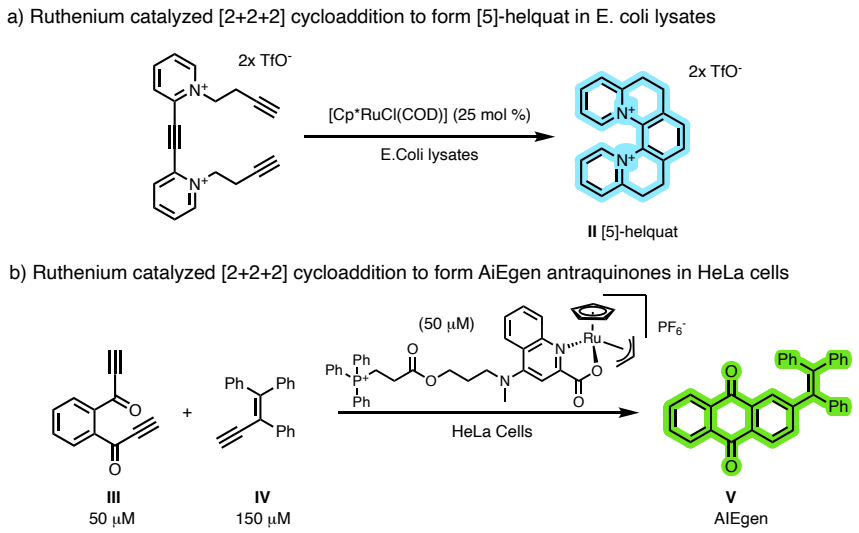

Figure 33. a) Ruthenium catalyzed intramolecular [2+2+2] cycloaddition to form [5]-helquat in E. coli lysates. b) Ruthenium catalyzed [2+2+2] intermolecular cycloaddition in HeLa cells to form an AIEgen anthraquinone.

Regarding C-X bond forming reactions promoted by ruthenium complexes, Spring and coworkers reported in 2017 a Ru-catalyzed bioorthogonal hydrosilylation of alkynes. Although the process delivers C-Si bonds rather than C-C bonds, it is particularly relevant because of its intermolecular nature and of the use of $[Cp^*Ru(MeCN)_3]PF_6$, a highly important catalyst in synthetic chemistry but poorly explored in a chemical biology context. [105] The reaction was especially efficient when arylsilanes and propargyl alkynes were employed. Moreover, the reaction can be used for the modification of peptides and even proteins, provided that they bear reactive alkyne moieties. However, in many cases it requires an excess of the catalyst (up to 15 equivalents with respect to the alkyne) and of the silane counterpart (up to 288 equivalents) in order to provide significant conversions. Nonetheless, it showcases the potential of the $[Cp^*Ru]^+$ fragment as catalyst for bioconjugation and bioorthogonal transformations (**Figure 34**).

[104] J. Miguel‐Ávila, M. Tomás‐Gamasa, J. L. Mascareñas, *Angew. Chem. Int. Ed.* **2020**, *59*, 17628–17633.

[105] T. T.-L. Kwan, O. Boutureira, E. C. Frye, S. J. Walsh, M. K. Gupta, S. Wallace, Y. Wu, F. Zhang, H. F. Sore, W. R. J. D. Galloway, J. W. Chin, M. Welch, G. J. L. Bernardes, D. R. Spring, *Chem. Sci.* **2017**, *8*, 3871–3878.

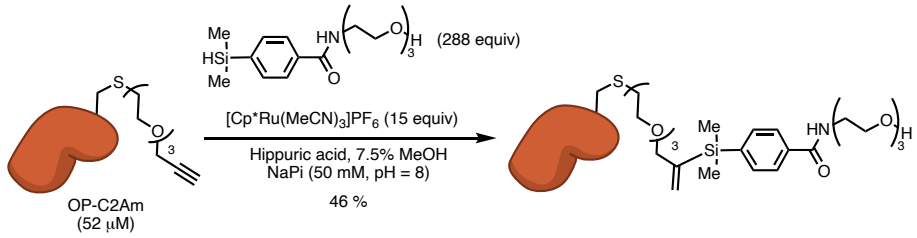

Figure 34. Peptide modification via Ruthenium promoted hydrosilylation

Other metals have also been used for bond forming reactions. Gold complexes, for instance, known to activate π-systems like those of alkynes, have been broadly adopted by the synthetic community. However, gold-catalyzed processes for bond-forming reactions in biological media have been scarcely investigated. In a pioneer example, Tanaka developed a glycoalbumin-gold (III) complex for *in vivo* (mice)organ specific propargyl ester amidation of nearby proteins.[106]

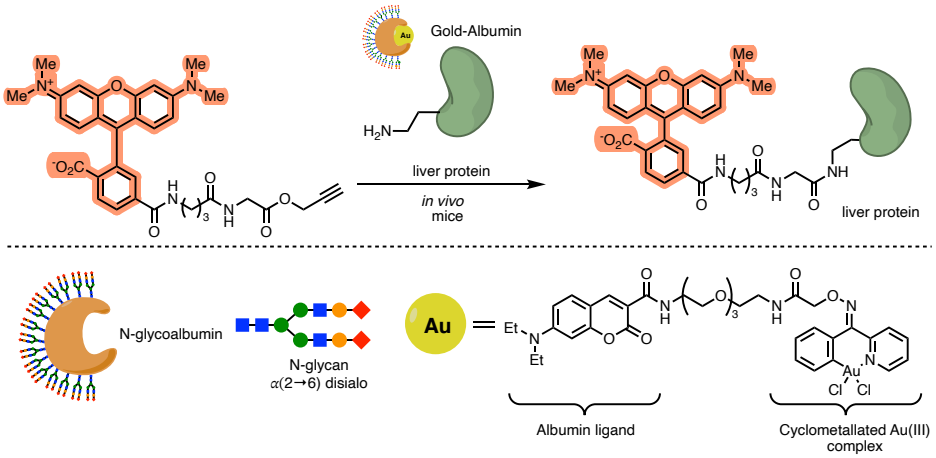

Figure 35. Glycoalbumin Gold complex for organ specific amidation of free amines.

On the other hand, in 2018, our group reported the gold(I)-promoted cycloisomerization of propargyl esters to yield coumarins inside HeLa cells. This reaction probed to be robust enough to be carried concurrently to a ruthenium catalyzed deallylation reaction, without observable cross reactivity or inhibition.[107]

[106] K. Tsubokura, K. K. H. Vong, A. R. Pradipta, A. Ogura, S. Urano, T. Tahara, S. Nozaki, H. Onoe, Y. Nakao, R. Sibgatullina, A. Kurbangalieva, Y. Watanabe, K. Tanaka, *Angew. Chem. Int. Ed.* **2017**, *56*, 3579–3584.

[107] C. Vidal, M. Tomás-Gamasa, P. Destito, F. López, J. L. Mascareñas, *Nat Commun* **2018**, *9*, 1913.

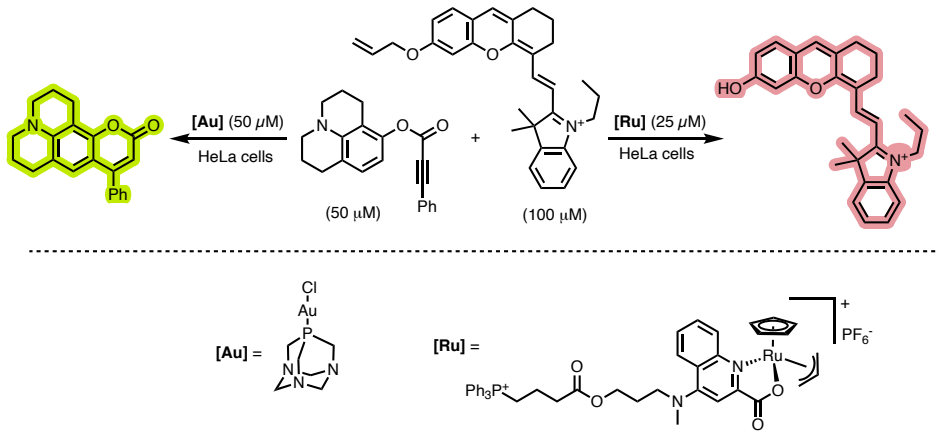

Figure 36. Orthogonal Gold-promoted hydroarylation and Ruthenium-promoted deallylation in HeLa cells.

General Objectives

Despite the significant advances in the area of bioorthogonal chemistry and on the use of transition metal catalysis in biological contexts, the field can still be considered in its infancy, and the toolbox of biocompatible, metal-promoted processes still very small. Therefore, the work of this doctoral thesis has been focused on the development of novel biocompatible transformations promoted by transition metal catalysts, with a specific emphasis on ruthenium. Ruthenium complexes are very attractive not only because of the coordination and redox properties of the metal, but also because they tend to present a very good balance between reactivity and stability in aqueous and biological environments.

Specifically, our work has been focused to the following topics:

1) **Second generation Ruthenium catalyzed Azide-ThioAlkyne cycloaddition**. As briefly commented in the introduction, the group has previously developed a ruthenium catalyzed azide-thioalkyne cycloaddition that works efficiently under aqueous and biocompatible conditions but requires relatively high concentration of the reactants for being efficient. In order the reaction can reach further it is necessary to develop more efficient catalysts.
2) **New bioorthogonal C-C bond-forming reactions based on a ruthenium catalyzed alkene-alkyne couplings**. Up to now, most bioorthogonal bond forming reactions involve functionalized reactants with a built-in reactivity (e.g., azides or halogenated substrates). Triggering the reactivity of more stable (less reactive) precursors is more challenging, but transition metals may offer different opportunities for this endeavor. Indeed, Ru catalysts can promote the formation of C-C bonds from relatively inert alkenes or alkynes via metathesis reactions, also in aqueous media. In chapter II, we describe our efforts to develop an alternative, bioorthogonal ruthenium mediated C-C bond forming reaction entailing an alkene-alkyne coupling.
3) **Ruthenium catalyzed isomerization of allylic alcohols in cellular environments**. Whereas a number of transition metal catalyzed isomerization reactions had been described, some even in presence of water media, they had never been investigated under biological conditions. In chapter III, we demonstrate that the isomerization of allylic alcohols to ketones catalyzed by ruthenium(IV) catalysts, a process that involves ruthenium hydride intermediates, can be translated to cellular environments, and even used for eliciting biological responses.

4) **I*n cellulo* concurrent and tandem transformations mediated by metals and/or enzymes**. Using the inspiration of natural metabolisms, in chapter IV we describe our efforts to build intracellular artificial reaction networks by combining different metal-promoted reactions or coupling them with enzymatic processes.

Chapter I: Ruthenium Catalyzed Azide-Thioalkyne Cycloadditions [108]

[108] This chapter includes work published in Angewandte Chemie International Edition as: Bioorthogonal Azide-Thioalkyne Cycloadditions Catalyzed by Photoactivatable Ru(II) Complexes A. Gutiérrez-González, P. Destito, J. R. Couceiro, C. Pérez-González, F. López, J. L. Mascareñas, *Angew. Chem. Int. Ed.* **2021**, *60*, 16059–16066.

1 Introduction

The 1,3-dipolar cycloaddition between azides and alkynes is a powerful method to build 1,2,3-triazoles, but tends to require high temperature and usually yields a mixture of regioisomeric products.[109] Therefore the discovery that this annulation can be carried out in a more efficient and regioselective manner by adding Cu(I) salts (CuAAC, see **sections 3** and **4.2**) represented a substantial contribution, even merely from the synthetic point of view.

1.1 Copper Catalyzed Azide Alkyne Cycloaddition (CuAAC)

As briefly commented in the introductory chapter, in 2001 Sharpless and Meldal independently reported the use of copper (I) salts (or copper (II) and a mild reducing agents) to catalyze the (3+2) formal cycloaddition between organic azides ($R\text{-}N_3$) and terminal alkynes.[34,35] This reaction proceeds in many cases quantitatively to deliver a 1,4-disubtituted triazole with complete regioselectivity, it can be performed in presence of many functional groups and, interestingly, it is also compatible with water, which not only does not inhibit the reaction, but it can even increase the reaction rate.

The copper-catalyzed reaction presents an organometallic mechanism initiated by formation of a dicopper acetylide intermediate and coordination of organic azide to one of the copper centers. A subsequent nucleophilic attack to the terminal nitrogen atom of the azide by the β-carbon of the acetylide delivers a six-member metallocycle. Reductive elimination and protonation yields the expected triazole (**Figure 37**).[110]

[109] F. Himo, T. Lovell, R. Hilgraf, V. V. Rostovtsev, L. Noodleman, K. B. Sharpless, V. V. Fokin, *J. Am. Chem. Soc.* **2005**, *127*, 210–216.
[110] B. T. Worrell, J. A. Malik, V. V. Fokin, *Science* **2013**, *340*, 457–460.

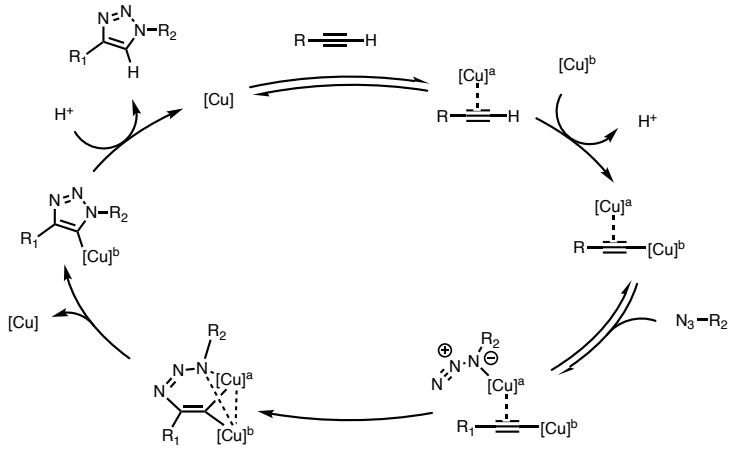

Figure 37. Accepted mechanism for the CuAAC.

Organic azides are highly stable to water and oxygen also in the presence of different types of other molecular components. Their synthesis usually requires the use of sodium azide, which is highly toxic (with similar IC_{50} levels to those of sodium cyanide), and therefore must be handled with care. Organic azides are ideal candidates for bioorthogonal chemistry because of their good stability and the fact that this functional group is new-to-nature.[111]

The original report by Sharpless and coworkers already included reactions in aqueous media at room temperature and, in the case of Meldal, the application was intended to "click" together peptidic fragments in solid phase. The reaction became soon a reference for Click chemistry and for performing bioorthogonal transformations because of its good rate and chemoselectivity. Therefore, it was soon used for instance by Tirrell coworkers for cell surface labeling (commented in the **section 4.2**),[64] and later on for *in cellulo* reactions.[65,66,67]

Despite its efficiency, and great scope and versatility, the CuAAC still presents important limitations. Because of the mechanistic requirement of forming copper acetylides, the reaction is restricted to terminal alkynes. The soft character of copper makes it incompatible with thiols. Additionally, to obtain high conversions under diluted biological conditions, the reaction is usually promoted by Cu(II) salts that are reduced *in situ* to Cu(I) by addition of sodium ascorbate, a non-innocent reductant in biological

[111] S. Bräse, C. Gil, K. Knepper, V. Zimmermann, *Angew. Chem. Int. Ed.* **2005**, *44*, 5188–5240.

settings. Moreover, as commented in the **section 4.2**, copper (I) salts tend to be cytotoxic.[112,113]

Even though some of these issues can be partially addressed by using copper-stabilizing ligands,[114] there has been a lot of interest in the development of related cycloadditions that could be promoted by other, less toxic, and more biocompatible transition metals.

1.2 Ruthenium Catalyzed Azide Alkyne Cycloaddition (RuAAC)

Ruthenium displays a rich chemistry related to the modification and transformation of alkynes,[115] thus, it is not surprising that this metal had also been tested as an alternative to copper for performing azide-alkyne cycloadditions.

Sharpless and Fokin showed that ruthenium complexes like [Cp*RuCl(PPh_3)$_2$] or [RuH_2(CO)(PPh_3)$_3$] can promote the cycloaddition between azides and terminal alkynes to afford 1,4 and 1,5- triazoles depending on the catalyst.[116] Contrary to the CuAAC, internal alkynes can also engage in the cycloaddition yielding fully substitutes triazoles, albeit with variable regioselectivity.

In general, the use of ruthenium (II) catalysts equipped with pentamethylcyclopentadienyl (Cp*) and chloride ligands are effective to promote the reaction and leads to the expected 1,5-triazoles regioselectively and with high yields, whereas complexes with the general formula [RuX(PPh_3)$_n$] afforded the 1,4-regioisomers, in moderate to low yields. Complexes bearing the cyclopentadienyl (Cp) ligand also gave the 1,5-triazole but with poorer regioselectivity than the more sterically crowded Cp* counterpart (**Figure 38**).[117]

[112] V. Hong, S. Presolski, C. Ma, M. G. Finn, *Angew. Chem. Int. Ed.* **2009**, *48*, 9879–9883.
[113] D. C. Kennedy, C. S. McKay, M. C. B. Legault, D. C. Danielson, J. A. Blake, A. F. Pegoraro, A. Stolow, Z. Mester, J. P. Pezacki, *J. Am. Chem. Soc.* **2011**, *133*, 17993–18001.
[114] V. O. Rodionov, S. I. Presolski, D. Díaz Díaz, V. V. Fokin, M. G. Finn, *J. Am. Chem. Soc.* **2007**, *129*, 12705–12712.
[115] See for instance the work by Fürstner in ruthenium catalyzed alkyne functionalization: A. Fürstner, *J. Am. Chem. Soc.* **2019**, *141*, 11–24.
[116] L. Zhang, X. Chen, P. Xue, H. H. Y. Sun, I. D. Williams, K. B. Sharpless, V. V. Fokin, G. Jia, *J. Am. Chem. Soc.* **2005**, *127*, 15998–15999.
[117] Boren, B. C.; Narayan, S.; Rasmussen, L. K.; Zhang, L.; Zhao, H.; Lin, Z.; Jia, G.; Fokin, V. V. *J. Am. Chem. Soc.* **2008**, *130* (44), 14900–14900.

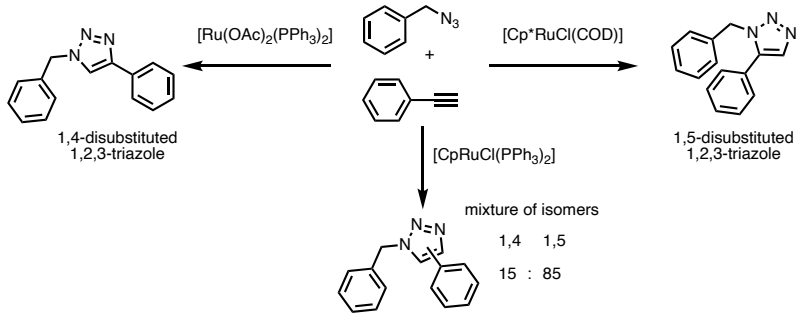

Figure 38. RuAAC reaction with different ruthenium pre-catalysts.

Fokin and coworkers performed different experiments to light up the reaction mechanism. They found that abstraction of the chloride ligand in [Cp*RuCl(COD)] (**Ru1**) with a Ag (I) scavenger affords a cationic ruthenium complex that is inactive in the RuAAC. This mechanistic observation for [Cp*Ru(COD)Cl] and considering that [Cp*RuCl(PPh_3)$_2$], [Cp*Ru(NBD)Cl] and [Cp*RuCl]$_4$ were all competent catalysts for the RuAAC, suggested that the neutral [Cp*RuCl] fragment was likely the catalytically active motif in all these cases. This also explains why when using the [Cp*RuCl(PPh_3)$_3$], the reaction requires temperatures between 60 to 80 ºC, likely to promote the phosphine dissociation; whereas with [Cp*RuCl(COD)] (**Ru1**), which bears a labile cyclooctadiene ligand, the reaction occurs at room temperature and with shorter reaction times (e.g., 30 min).

Originally, the reaction was carried with 5 mol% of catalyst loading, even though it can be reduced to 1 mol% in many cases, leading to similar yields. Either polar or apolar solvents can be used (e.g., benzene, 1,2-dichloroethane, DMSO, THF, among others), but protic solvents gave substantially lower yields (i.e., MeOH). Importantly, Fokin and coworkers highlighted that, despite the reaction can be carried out in solvents with traces of water, they should be degassed to avoid catalyst decomposition. Additionally, the order of addition was of special relevance, as the addition of the azide to a solution of the catalyst or *vice versa*, without the presence of the alkyne, could lead to the deactivation of the catalyst by formation of a highly stable ruthenium tetraazadiene complex (**Figure 39**).[116,118]

[118] J. R. Johansson, T. Beke-Somfai, A. Said Stålsmeden, N. Kann, *Chem. Rev.* **2016**, *116*, 14726–14768.

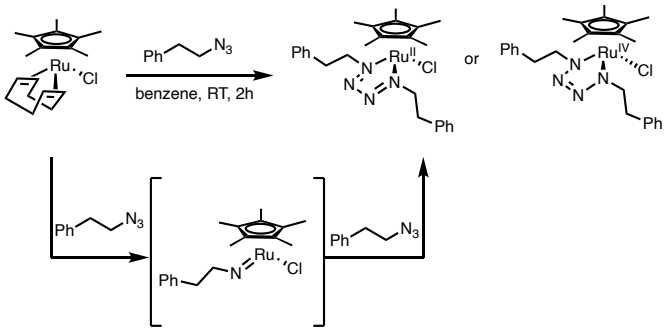

Figure 39. Formation of ruthenium tetraazadiene complex.

In contrast to that proposed for CuAAC, DFT calculations carried out by the authors discarded the formation of ruthenium acetylides.[116,117] This is also supported by two experimental evidences: firstly, no discrete ruthenium acetylides nor vinylidene complexes yielded triazoles under presence of an organic azide; secondly, the reaction allows the use of internal alkynes, which definitely suggests that the mechanism must be different than that of the CuAAC.

Indeed, the current accepted mechanism starts with the coordination of the azide by the α-nitrogen and the π-coordination of the alkyne (**I**). Then, oxidative coupling of the alkyne and the azide yields a ruthenacycle intermediate **II** which, upon reductive elimination (**III**) and ligand exchange, delivers the product and regenerates the [Cp*Ru] complex, that restarts the catalytic cycle (**IV**) (**Figure 40**).[117]

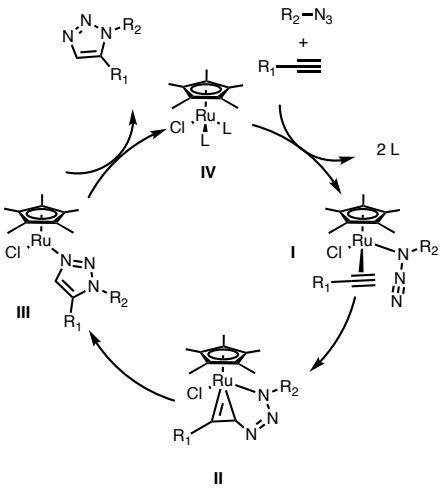

Figure 40. Mechanism of the RuAAC reaction.

The reaction is tolerant to a wide variety of functional groups, allowing the synthesis of relatively complex molecules. For instance, Fokin and Jia,[116] reported the RuAAC with substrates bearing boronic esters, polyalcohols, modified nucleotides or dipeptides (**Figure 40a**). Since then, it has been applied for the synthesis of peptidomimetics (**Figure 40b**),[119] to the macrocyclization of peptides[120,121] or to carbohydrate chemistry,[122,123] among several other applications. Importantly, reports of the RuAAC in the presence of aqueous media remained very scarce. In this regard, Lo described the use of a ruthenium azido trispyrazolylborate (Tp) complex [TpRu(N_3)(PPh_3)($EtNH_2$)] to promote a RuAAC in water, but it required heating at 80 ºC.[124]

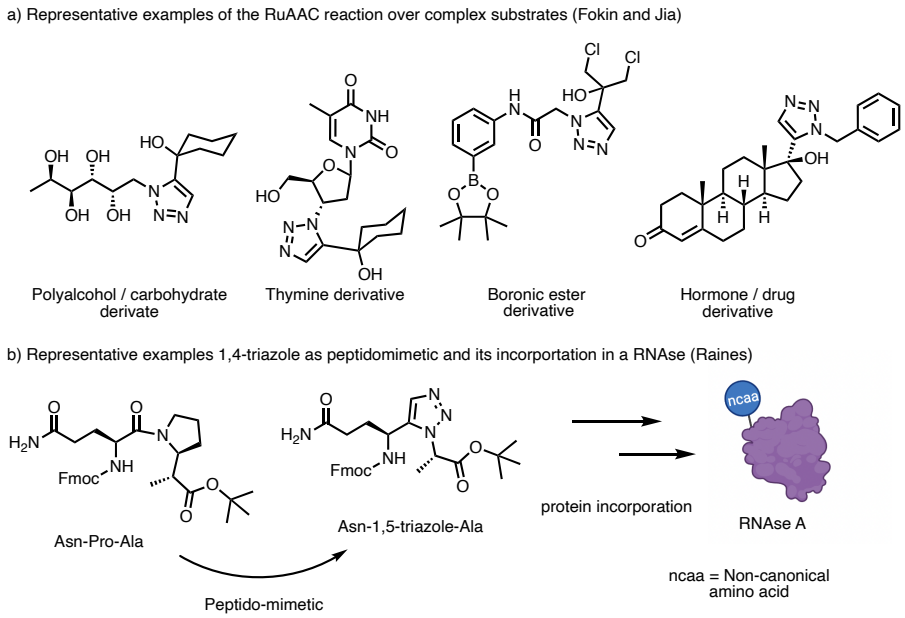

Figure 41. Application of the RuAAC for the synthesis of complex molecules.

Overall, despite the reaction is truly relevant, its restriction to organic solvents, the required exclusion of oxygen and the observation of mixture of regioisomeric products in

[119] J. R. Johansson, E. Hermansson, B. Nordén, N. Kann, T. Beke-Somfai, *Eur. J. Org. Chem.* **2014**, *2014*, 2703–2713.
[120] W. S. Horne, C. A. Olsen, J. M. Beierle, A. Montero, M. R. Ghadiri, *Angew. Chem. Int. Ed.* **2009**, *48*, 4718–4724.
[121] L. A. Marcaurelle, E. Comer, S. Dandapani, J. R. Duvall, B. Gerard, S. Kesavan, M. D. Lee, H. Liu, J. T. Lowe, J.-C. Marie, C. A. Mulrooney, B. A. Pandya, A. Rowley, T. D. Ryba, B.-C. Suh, J. Wei, D. W. Young, L. B. Akella, N. T. Ross, Y.-L. Zhang, D. M. Fass, S. A. Reis, W.-N. Zhao, S. J. Haggarty, M. Palmer, M. A. Foley, *J. Am. Chem. Soc.* **2010**, *132*, 16962–16976.
[122] D. Crich, F. Yang, *Angew. Chem. Int. Ed.* **2009**, *48*, 8896–8899.
[123] A. J. Cagnoni, O. Varela, M. L. Uhrig, J. Kovensky, *Eur. J. Org. Chem.* **2013**, *2013*, 972–983.
[124] T.-H. Wang, F.-L. Wu, G.-R. Chiang, S.-T. He, Y.-H. Lo, *J. Organomet. Chem.* **2014**, *774*, 57–60.

many cases, represent important limitations when considering its application for bioorthogonal chemistry.

Not surprisingly, the rapid expansion of the RuAAC prompted the development of other metal catalyzed azide-alkyne cycloadditions.[125] Iridium,[126,127] Rhodium,[128,129,130], or Nickel[131] complexes have been tested for promoting azide-alkyne formal cycloadditions. Among these cases, the report by Jia in 2014 describing Iridium catalyzed cycloadditions between azides and thioalkynes caught the attention of our group, since the process was efficient and fully regioselective at room temperature.[126] Moreover, although the solvent of choice was CH_2Cl_2, the report included an isolated example of the reaction with benzyl azide in neat water (**Figure 42**).[126]

Additionally, the same manuscript also included an example of the reaction in CH_2Cl_2 using the ruthenium complex [Cp*RuCl(COD)] as catalyst to give the expected product in good yield and moderate regioselectivity (4.5:1).

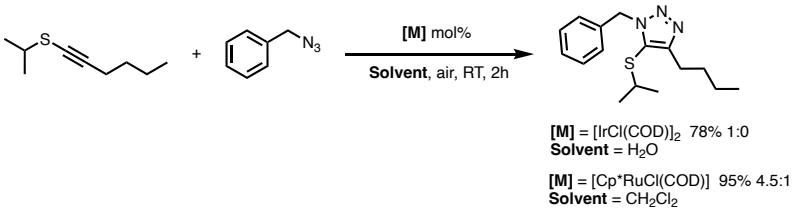

Figure 42. Precedent of the Iridium catalyzed azide thioalkyne cycloaddition under aqueous conditions and a Ruthenium catalyzed version in CH_2Cl_2.

1.3 Ruthenium Catalyzed Azide-Thioalkyne Cycloaddition (RuAtAC)

Based on these precedents and our own experience with Ru catalysis, our group investigated the feasibility of the RuAAC reaction in aqueous media using thioalkynes as key partners. Gratifyingly, the ruthenium complex [Cp*RuCl(COD)] (**Ru1**) was found to be particularly efficient promoting the reaction in water at room temperature, provided that a 2 to 1 ratio of alkyne and azide is used. Thus, the RuAtAC (**R**uthenium **A**zide-

[125] C. Wang, D. Ikhlef, S. Kahlal, J.-Y. Saillard, D. Astruc, *Coordination Chemistry Reviews* **2016**, *316*, 1–20.
[126] S. Ding, G. Jia, J. Sun, *Angew. Chem. Int. Ed.* **2014**, *53*, 1877–1880.
[127] E. Rasolofonjatovo, S. Theeramunkong, A. Bouriaud, S. Kolodych, M. Chaumontet, F. Taran, *Org. Lett.* **2013**, *15*, 4698–4701.
[128] Y. Liao, Q. Lu, G. Chen, Y. Yu, C. Li, X. Huang, *ACS Catalysis* **2017**, *7*, 7529–7534.
[129] W. Song, M. Li, K. Dong, Y. Zheng, *Adv. Synth. Catal.* **2019**, *361*, 5258–5263.
[130] W. Song, N. Zheng, M. Li, K. Dong, J. Li, K. Ullah, Y. Zheng, *Org. Lett.* **2018**, *20*, 6705–6709.
[131] W. G. Kim, M. E. Kang, J. B. Lee, M. H. Jeon, S. Lee, J. Lee, B. Choi, P. M. S. D. Cal, S. Kang, J.-M. Kee, G. J. L. Bernardes, J.-U. Rohde, W. Choe, S. Y. Hong, *J. Am. Chem. Soc.* **2017**, *139*, 12121–12124.

thioAlkyne **C**ycloaddition) provides an efficient access to fully substituted 1,2,3-triazoles with high regioselectivity (typically with a 1,5- to 1,4-regioisomer ratio of 20 to 1), and with a broad scope both of the thioalkyne and of the azide counterpart (**Figure 43**).[132]

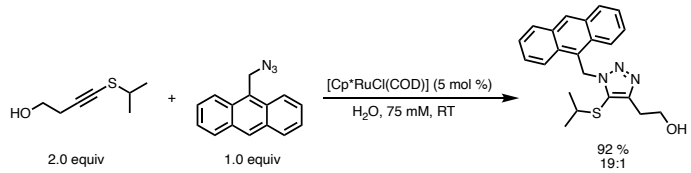

Figure 43. Representative example of the RuAtAC reaction. The reaction was benchmarked using an anthracenyl azide because it yields fluorescent products.

Regular alkynes such as but-1-yn-1-ylbenzene also reacted under the above conditions, but with much lower regioselectivities. Cross competition studies confirmed the much higher reactivity of thioalkynes (**Figure 44**).

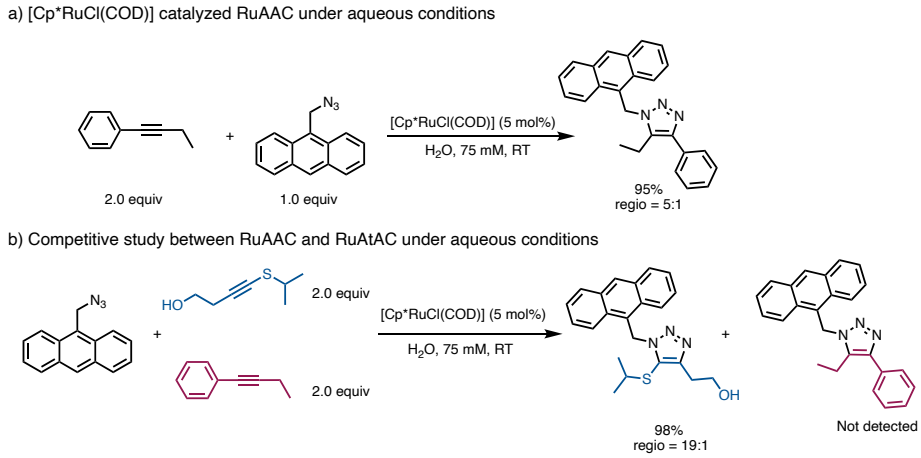

Figure 44. a) [Cp*RuCl(COD)] catalyzed RuAAC reaction in water with and internal alkyne. b) Competitive study between RuAAC and RuAtAC.

Interestingly, the RuAtAC reaction is also very efficient in CH_2Cl_2, but requires the use of anhydrous CH_2Cl_2 and an inert atmosphere. Overall, these results indicate that the use of water as solvent is somehow precluding the rapid deactivation of the catalyst, probably due to the lower solubility of oxygen in water, although water might also enhance the reaction.

The above water-compatible RuAtAC allowed the modification of dipeptides and protected sugars, and the generation of fluorescent products (**Figure 45a**). It can also be

[132] P. Destito, J. R. Couceiro, H. Faustino, F. López, J. L. Mascareñas, *Angew. Chem. Int. Ed.* **2017**, *56*, 10766–10770.

coupled with the CuAAC, in a sequential process involving the addition of the copper and the ruthenium regents (**Figure 45b**). The reaction also tolerates the presence of biomolecules such as glutathione (GSH) or free amino acids and can be carried out in DMEM culture media (Dulbecco's Modified Eagle Medium), in HeLa cell lysates and even in the presence of living bacteria (*E. coli*); therefore, it can be considered quite bioorthogonal.

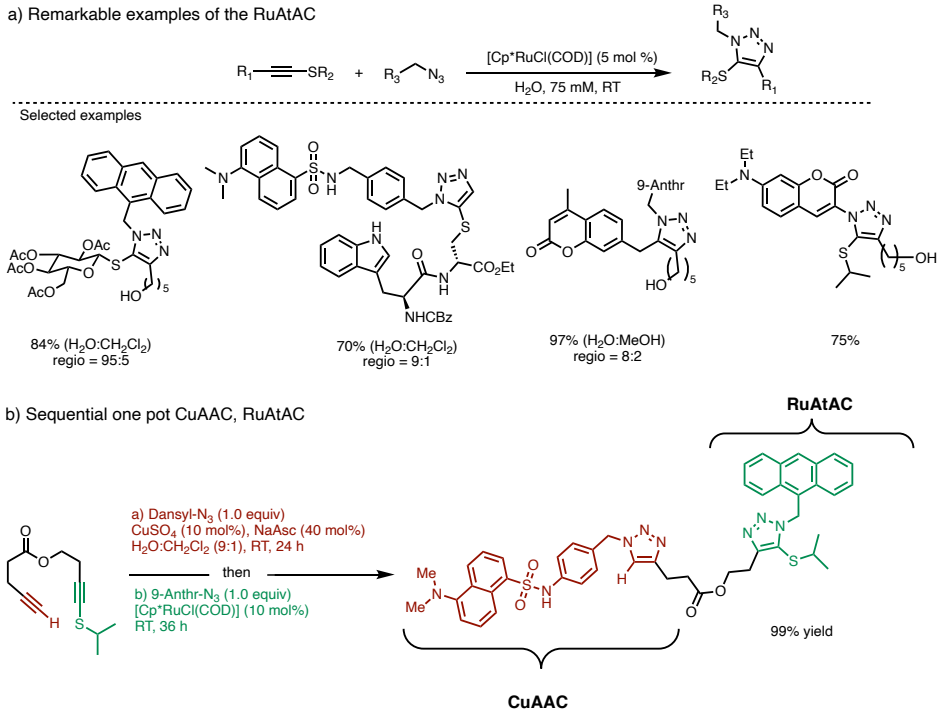

Figure 45. a) Remarkable 1,2,3-triazoles synthetized with the RuAtAC. b) Sequential one-pot CuAAC-RuAtAC reactions.

Unfortunately, there are also limitations that preclude the use of the RuAtAC in more complex settings. In particular, the reaction proved to be much less efficient at concentrations below 75 mM and does not proceed at micromolar concentrations (**Figure 46a**). Despite the standard catalyst **Ru1** leads to an excellent selectivity, discriminating internal alkynes and thioalkynes (see **Figure 44b**), there is cross-reactivity with terminal alkynes, so that the orthogonality of the CuAAC and RuAtAC is restricted to performing first the copper catalysis (**Figure 46b**).

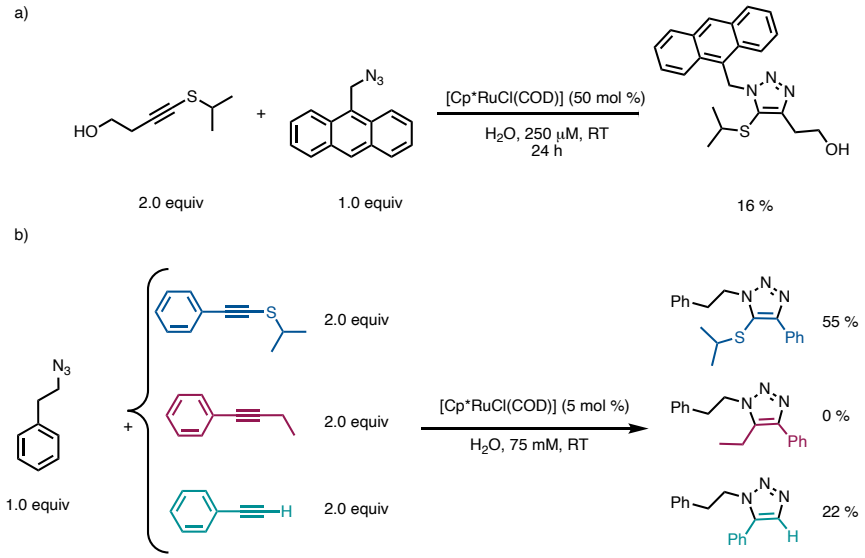

Figure 46. a) RuAtAC at 250 μM with 50 mol% of [Cp*RuCl(COD)]. b) Competition studies between a thioalkyne, an internal alkyne and a terminal alkyne.

After our publication describing this RuAtAC, other water compatible MAACs were reported, in particular with Iridium and Rhodium catalysts, using particularly activated alkynes such as ynamides,[133, 134] disulfanyl alkynes,[135] alkynyl phosphonates[136] or sulfonyl alkynes.[137] Curiously, these new MAACs required the use of a slight excess of the azide partner (1.5 equiv of azide), just the opposite than with the abovementioned RuAtAC, which work best when an excess of thioalkyne is used (**Figure 47**). Among the different reports, only those based on iridium catalysis have been preliminary explored for bioorthogonal chemistry. More importantly, none of these methods has been reported to be efficient under diluted conditions (all reported reactions are at concentrations ≥100 mM) and have not been applied either for bioconjugation nor for reactions *in cellulo.*

[133] Y. Liao, Q. Lu, G. Chen, Y. Yu, C. Li, X. Huang, *ACS Catalysis* **2017**, *7*, 7529–7534.
[134] W. Song, N. Zheng, *Org. Lett.* **2017**, *19*, 6200–6203.
[135] M. Li, N. Zheng, J. Li, Y. Zheng, W. Song, *Green Chem.* **2020**, *22*, 2394–2398.
[136] W. Song, N. Zheng, M. Li, K. Ullah, Y. Zheng, *Adv. Synth. Catal.* **2018**, *360*, 2429–2434.
[137] W. Song, N. Zheng, M. Li, K. Dong, J. Li, K. Ullah, Y. Zheng, *Org. Lett.* **2018**, *20*, 6705–6709.

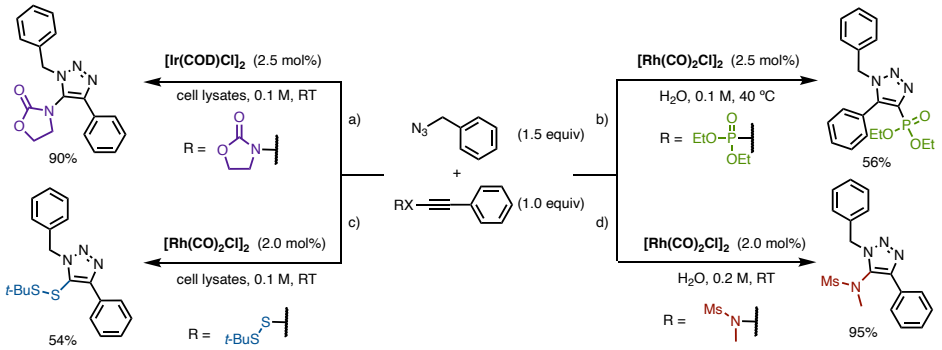

Figure 47. Different MAAC reported of iridium and rhodium reported to work under aqueous conditions with different functionalized alkynes.

2 Objectives

The RuAtAC is the first Ruthenium catalyzed Azide-Alkyne cycloaddition that worked in water, at room temperature, with excellent regioselectivity and with a good bioorthogonal profile. However, its further application for bioconjugation is precluded due to poor reactivity under diluted conditions, so that a faster biocompatible alternative would be needed. An additional challenge in this field has to do with the possibility to control the reactivity of the system using external stimuli, as this could open new opportunities for biological applications.

On these bases, our specific objectives in this chapter involve:

1) The development of more active ruthenium catalysts, and if possible, with better chemoselectivities with respect to terminal alkynes (used in CuAAC). To pursue this goal, we would explore other ruthenium catalysts with ligands different than the standard chloride and cyclooctadiene (COD).

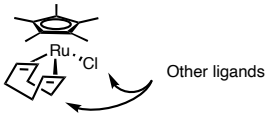

2) The development of light responsive catalysts, which could provide for spatiotemporal control of the activity. To achieve this goal, we will focus our attention on Ru sandwich complexes bearing ligands that can be labilized with light.

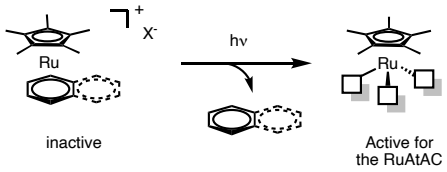

3 Results and Discussion[138]

3.1 Cationic ruthenium complexes as catalysts for the RuAtAC

As commented in the **section 1.3** of this chapter, the complex Cp*RuCl(COD) (**Ru1**) is a good catalyst for the RuAtAC reaction but holds limitations in terms of activity and chemoselectivity. Therefore, we aimed at identifying more active ruthenium catalysts that might overcome such limitations.

Previous reports by Fokin and Sharpless on structure-activity analysis of the RuAAC concluded that the Cp* and chloride ligands were both required for an efficient RuAAC. Furthermore, Sun and coworkers showed that cationic complexes like $[Cp^*Ru(MeCN)_3]PF_6$ or $[CpRu(MeCN)_3]PF_6$ failed to promote the cycloaddition of [hex-1-yn-1-yl(isopropyl)sulfane] and benzyl azide (**Figure 46**) in dichloromethane.[126]

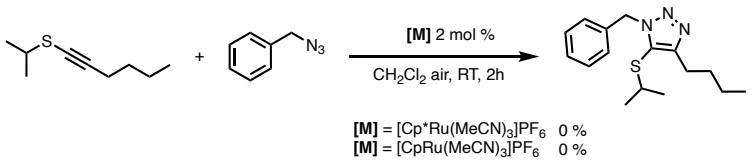

Figure 48. $[Cp^*Ru(MeCN)_3]PF_6$ or $[CpRu(MeCN)_3]PF_6$ performance on the cycloaddition of [hex-1-yn-1-yl(isopropyl)sulfane] and benzyl azide.

Despite these precedents and considering the dissimilar reactivity of **Ru1** in organic solvents and water, we decided to investigate the catalytic performance of $[Cp^*Ru(MeCN)_3]PF_6$ (**Ru2**) in water.[139] We envisioned that *in situ* treatment of **Ru2** with an external chloride source might afford a catalytically competent [Cp*RuCl] derivative.[140] Additionally, since several variants of **Ru2** had been previously reported bearing modified Cp*-type ligands,[141,142] we reasoned that the electronic and steric characteristics of these ligands could eventually influence the reactivity (**Figure 49**).

[138] The experimental work presented in this chapter was done in collaboration with PhD Paolo Destito.
[139] Indeed, complex **Ru2** has been proven to efficiently catalyze alkyne hydrosilation in aqueous media. See **section 4.4** of the introduction and the refence 105.
[140] J. A. Varela, S. G. Rubín, C. González-Rodríguez, L. Castedo, C. Saá, *J. Am. Chem. Soc.* **2006**, *128*, 9262–9263.
[141] H. Zhang, B. Demerseman, Z. Xi, C. Bruneau, *Eur. J. Inorg. Chem.* **2008**, *2008*, 3212–3217.
[142] T. Biberger, C. P. Gordon, M. Leutzsch, S. Peil, A. Guthertz, C. Copéret, A. Fürstner, *Angew. Chem. Int. Ed.* **2019**, *58*, 8845–8850.

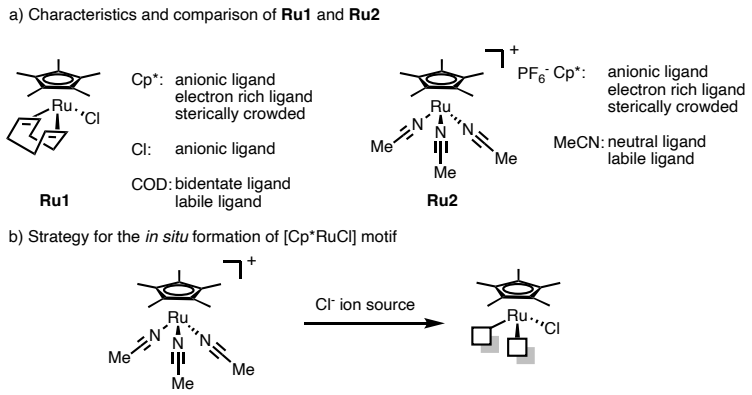

Figure 49. Analysis of **Ru1** and **Ru2** complexes and *in situ* formation of [Cp*RuCl]

The reaction was benchmarked using the anthracenyl azide probe **1a**, which delivers a fluorescent triazole after the cycloaddition with an alkyne. The reactions were carried out by mixing **1a** (1.0 equiv) and the thioalkyne **2a** (2.0 equiv),[143] in CH_2Cl_2 at 75 mM (azide), with the ruthenium catalysts, either [Cp*RuCl(COD)] (**Ru1**), or the cationic variant $[Cp^*Ru(MeCN)_3]PF_6$ (**Ru2**). The reaction with the neutral complex **Ru1** led to the fluorescent triazole **3aa** in 99% yield after 30 min. The cationic complex **Ru2** afforded the product **3aa** in only 15% yield after 1 h, reaching a 30% yield after 6 h (**Figure 50**). Electrospray Ionization Mass Spectra (ESI-MS) analysis of the reaction mixture promoted by **Ru2**, allowed the detection of a ruthenium species with m/z = 723.17, which could be assigned to an species with a Cp* ligand and three units of the thioalkyne **2a**.

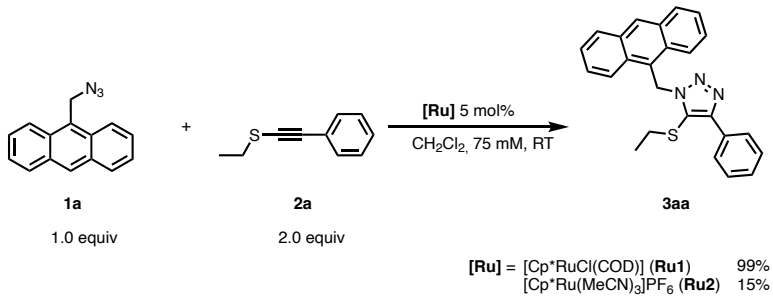

Figure 50. Performance of **Ru1** and **Ru2** in the RuAtAC in CH_2Cl_2

To fully determine the nature of this species, we tried to crystalize it. To our delight, slow diffusion of dry pentane at -28 ºC into a solution of **Ru2** and an excess of thioalkyne **2a** (4.0 equiv), in freshly distilled CH_2Cl_2, led to deep-orange crystalline needles which could be thoroughly analyzed. ESI-MS analysis allowed for the detection of the same molecular

[143] We selected a thioalkyne :azide ratio of 2 to 1, since in the previous work with **Ru1** afforded the best results.

ion with m/z = 723.17, previously detected in the reaction mixture. Moreover, X-ray crystallographic analysis of the crystals allowed to determine the structure of the complex **Ru2'** (**Figure 51a**). NMR spectra are in full agreement with such a structure.

These results confirm that, in CH_2Cl_2, **Ru2** promotes the trimerization of the thioalkyne **2a,** to give a non-productive complex exhibiting a bidentate fulvene ligand that coordinates the Ru center through its sulfur atoms. A tentative mechanism for its formation would involve an initial oxidative cyclization of **2a** to generate the ruthenacyclopentadiene species **I**. A subsequent migratory insertion of a third unit of thioalkyne yields a ruthenacycloheptatriene intermediate **II**, which can also be considered as a Fisher carbene ruthenium complex. Thus, a C-C reductive elimination will generate a cyclopentadienyl carbene intermediate **III** that might evolve to the final complex **Ru2'** via a 1,2-phenyl migration with concomitant elimination of the Cp*Ru moiety, **Figure 51b**. The highly coordinating character of the bidentate alkenyl thioethers would trap the highly unsaturated $[Cp^*Ru]^+$ center leading to this inactive complex.

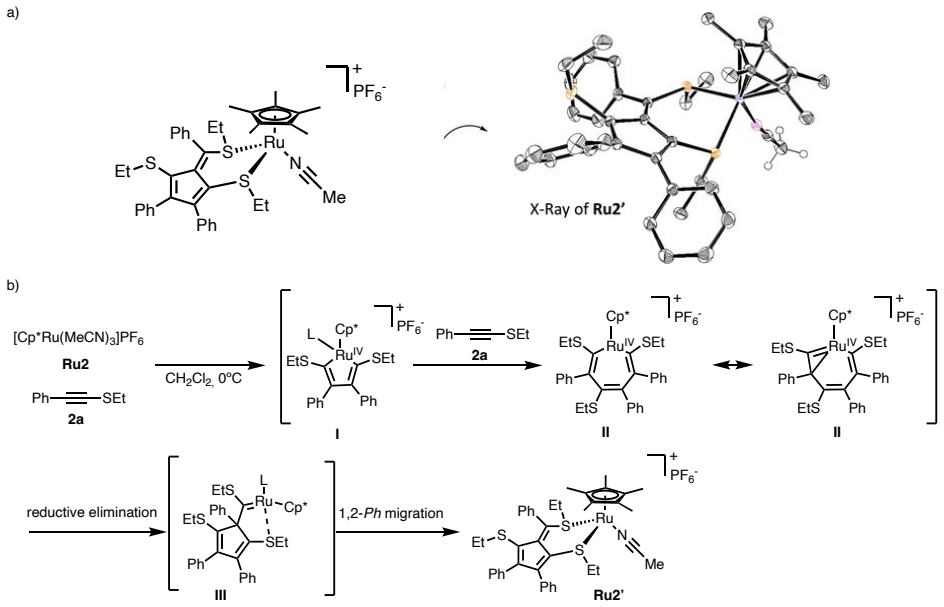

Figure 51. a) X-Ray structure of **Ru2'** and its schematic representation. b) Tentative mechanism for the trimerization of thioalkyne **2a** with **Ru2**; formation of **Ru2'**.

Interestingly, further experiments indicated that this non-productive pathway observed in CH_2Cl_2 can be partially suppressed by premixing **Ru2** with Et_4NCl, so that a 28% yield is obtained after 1 h reaction and a good 72% yield after 6 h. The presence of chloride

likely favors the *in situ* formation of a neutral Cp*–ruthenium(II) chloride species (**Table 1, entry 1**), which might hamper the thioalkyne-to-fulvene trimerization.

More importantly, we found that if **Ru2** is premixed with Et_4NCl in DMF and the resulting mixture added to aqueous media, the triazole **3aa** is obtained in an excellent 99% yield (**entry 2**). Moreover, further controls revealed that the use of Et_4NCl as an activator was indeed not needed if the reaction is carried out in water. Thus, contrary to what was initially expected, the cationic Ru complex **Ru2** can promote the RuAtAC between **1a** and **2a** in water, in a highly efficient manner (**Table 1**, **entries 1-4**).

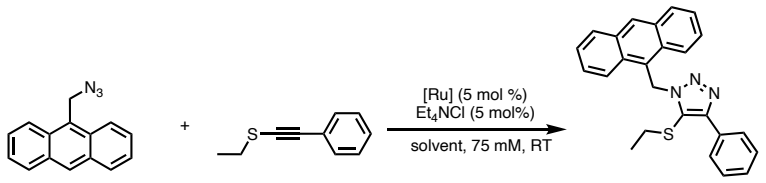

1a 1.0 equiv | **2a** 2.0 equiv | **3aa**

Entry	Solvent	Premixed in:	t [h]	Yield [%][a]
1	CH_2Cl_2	CH_2Cl_2	1	28 (72) [b]
2	H_2O	DMF	0.5	99
3	H_2O	H_2O	0.5	99
4[c]	H_2O	-	0.5	99

Table 1. Reaction conditions: **1a** (75 µmol), **2a** (150 µmol), solvent (1 mL) and **Ru2** (5 mol% + Et_4NCl 5 mol%) were added to a vial under air, and the mixture was stirred for the indicated time. [a] Yield determined by ^{1}H-NMR spectroscopy of the reaction crude mixture using 1,3,5-trimethoxybenzene as an internal standard. [b] The yield after 6h is indicates in parenthesis. [c] No Et_4NCl was used in this case

These results seemed striking at first, as in all previous reports either by Sharpless and Fokin or by Jia, cationic ruthenium complexes showed marginal reactivity. However, in both cases they used organic solvents, which we also found detrimental to the yield of the RuAtAC (**Table 1 entry 1** and **Figure 50**).

We hypothesized that the active catalytic species could be a ruthenium aquo complex, even though oxo or hydroxo species cannot be discarded. Speciation by ESI-MS of a solution of $[Cp^*Ru(MeCN)_3]PF_6$ in water and in a water/acetonitrile mixture, showed several ruthenium-oxygenated species: oxo species $[Cp^*Ru(O)]^+$, $[Cp^*Ru(O)(MeCN)_2]^+$,

and $[Cp^*Ru(O)_2(MeCN)_2]^+$; hydroxo species $[\{Cp^*Ru(O)\}_2(OH)]^+$(for a representative example on the speciation of **Ru2,** see **Figure 52**).[144]

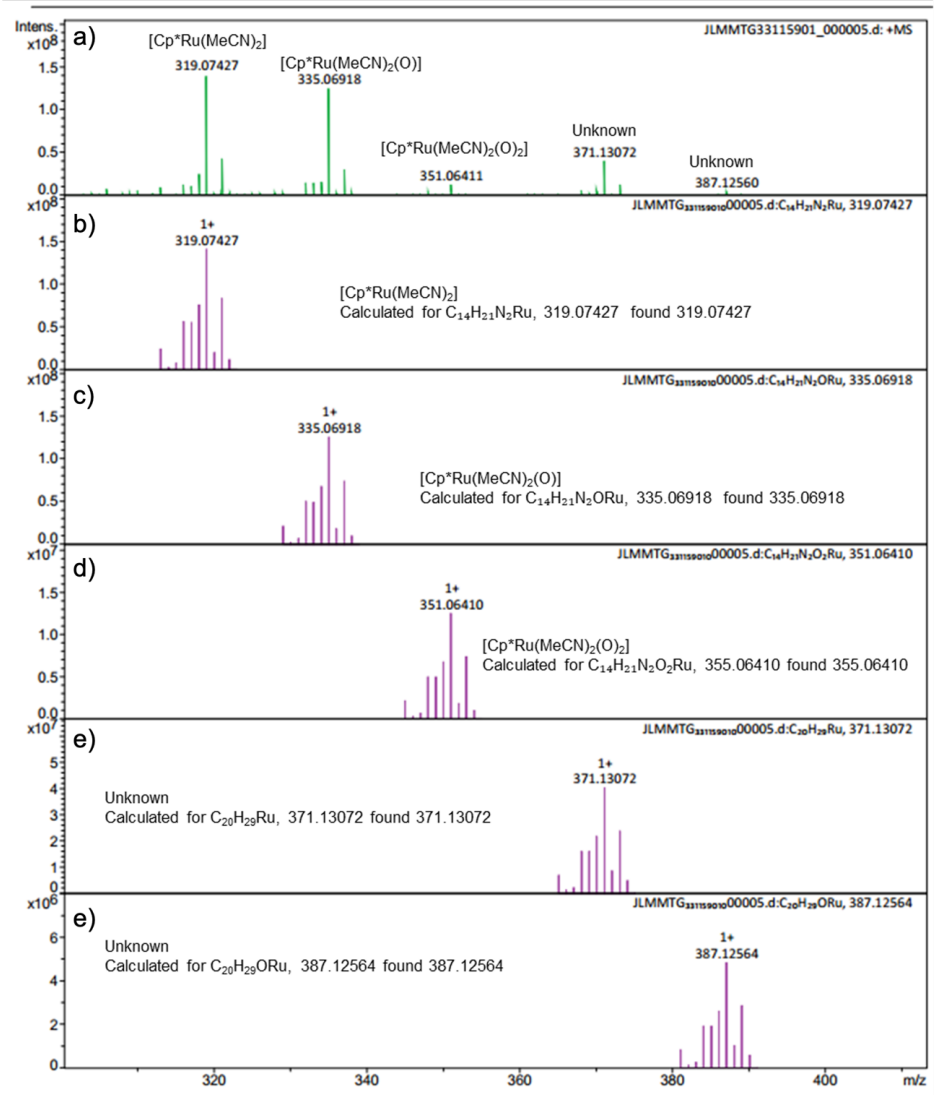

Figure 52. a) HRMS Speciation of $[Cp^*Ru(MeCN)_3]PF_6$, **Ru2**, in H_2O:MeCN (2:8). B) $[Cp^*Ru(MeCN)_2]^+$ m/z = 319, HRMS-ESI calculated for $C_{14}H_{21}N_2Ru$ 319.07427 found 319.07827. c) $[Cp^*Ru(MeCN)_2(O)]$ m/z = 335, HRMS-ESI calculated for $C_{14}H_{21}N_2Oru$ 335.06918 found 335.06918. d) Unknown m/z = 371, HRMS-ESI calculated for $C_{20}H_{29}N_2Ru$ 371.13072 found 371.13072. e) Unknown m/z = 387, HRMS-ESI calculated for $C_{20}H_{29}N_2Oru$ 387.12564 found 387.12560

We next evaluated the scope of the reaction using **Ru2**. Thioalkynes such as **2a**, bearing an ethyl group at the sulfur atom, were particularly reactive, but other groups such as

[144] See the experimental section for more details on the speciation experiments

aromatic substituents **2b,** benzyl **2c** and isopropyl **2d**, are also tolerated, and the respective products **3bb**, **3cc** and **3cd** were obtained in good to very good yields (**Figure 45**). In general, organic azides participate efficiently, regardless of the nature of their substituents; however when using azides that bear a phosphonium moiety, such as **1c** and **1d,** the addition of a 10%$_{(v/v)}$ of DMSO was needed to obtain good yields of the corresponding triazoles (**3ca** and **3da**), probably due to their poor solubility in water, at 75 mM (**Figure 53**).

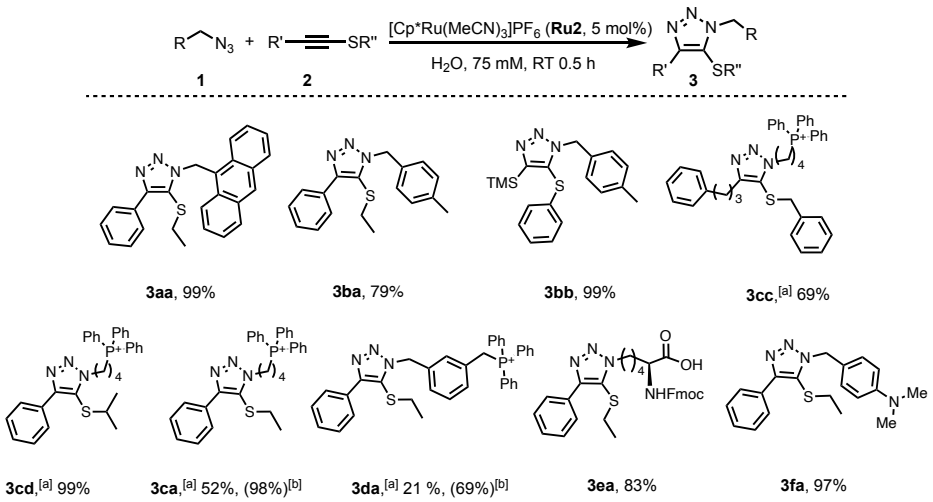

Figure 53. Scope of the annulation using the complex **Ru2**. Azide **1** (75 μmol, 1.0 equiv), thioalkyne **2** (150 μmol, 2.0 equiv) and **Ru2** (3.8 μmol, 0.05 equiv) [a] The counterion is probably bromide, as in the starting material.[b] Yield of the reaction carried out using a H_2O/DMSO (9:1) mixture is shown in parenthesis. Fmoc=fluorenyl-methoxycarbonyl.

We next explored the chemoselectivity of reaction with **Ru2** with respect to terminal alkynes. The reaction of phenyl acetylene **2e** with benzyl azide **1b** using **Ru1** as catalyst gave the corresponding triazole **3be** in 26% yield, whereas with **Ru2** we observed almost no conversion at the same reaction time (30 min). Similarly, when an internal alkyne such as **2f** was used, **Ru1** promoted the RuAAC to yield the triazole **3bf** in 95% yield (5:1 regioselectivity), whereas **Ru2** only delivered traces of **3bf**., under otherwise identical reaction conditions These results confirm that **Ru2** has a much better chemoselective profile than **Ru1.**

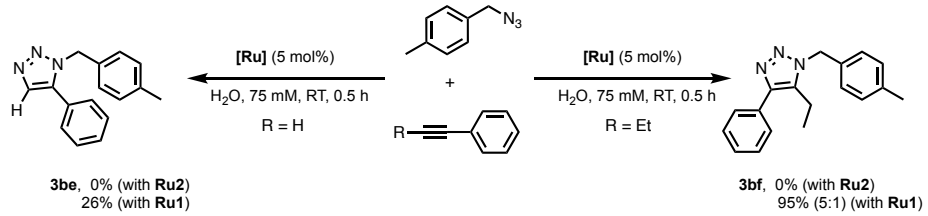

Figure 54. Orthogonality studies against therminal and internal alkyne with **Ru1** and **Ru2.**

3.2 RuAtAC and CuAAC orthogonality

Considering the high chemoselectivity observed with $[Cp^*Ru(MeCN)_3]PF_6$ (**Ru2**), we next explored the possibility of obtaining fully orthogonal RuAtAC and CuAAC reactions.

Gratifyingly, when a mixture of terminal alkyne **2g**, thioalkyne **2a**, and azide **1b** was treated under CuAAC conditions (5 mol% $CuSO_4$ and 10 mol% of NaAsc) only the triazole **3bg**, resulting from reaction of the terminal alkyne, was obtained (78% yield, **Table 2**, **entry 1**). Conversely, if the mixture is treated with **Ru2**, it is the thioether triazole **3ba** the one that is formed in 79% yield (**entry 3**). This opens the door for the orthogonal use of the CuAAC and the RuAtAC.

If we perform the CuAAC cycloaddition and, after its completion (2 h), we add another equivalent of the azide **1b** and the ruthenium catalyst **Ru2,** we obtained both triazoles with excellent yields (**entry 2**, 79% **3bg** and 78% **3ba**). Slightly better results are obtained if the RuAtAC is performed first and, after 2h, the azide **1b**, $CuSO_4 \cdot 5H_2O$, and NaAsc are added to the mixture (**entry 4**, 79% **3bg** and 95% **3ba**).[145] If both catalysts are present from the beginning, using only 1 equiv of azide **1b**, we obtained a 44% yield of CuAAC triazole **3bg** and a 50% of the RuAtAC triazole **3ba** (**entry 5**). This competition reaction suggests that the reaction rates of both the RuAtAC and the CuAAC, under these conditions, are quite similar.

Overall, this mutual selectivity opens the door to relevant applications, such as for the dual orthogonal tagging of biomolecules.

[145] The better results obtained when the CuAAC is performed after the RuAtAC might be due to partial inhibition of the of the copper catalyst when an excess of thioalkyne is present in the media (i.e. when the CuAAC is performed firstly).

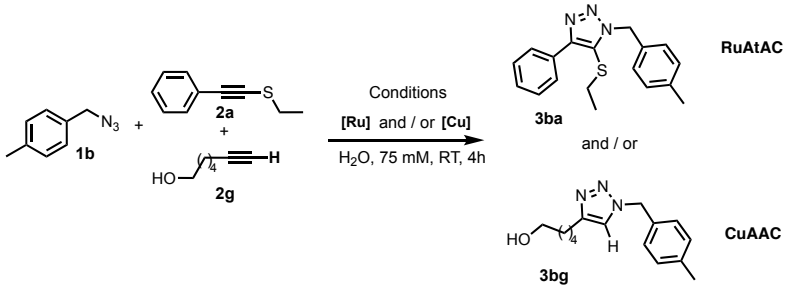

Entry	Catalyst (reaction time)	Yield [%][b]	
		3ba	**3bg**
1	**[Cu]** (2 h)	0	78
2[c]	**[Cu]** (2 h); then **[Ru]** (2 h)	79	78
3	**[Ru]** (2 h)	79	0
4[c]	**[Ru]** (2 h); then **[Cu]** (2 h)	78	95
5[d]	**[Ru]** and **[Cu]**(2 h)	44	55

Table 2. A solution of **2a** (2.0 equiv), **2g** (2.0 equiv), **1b** (1.0 equiv; 0.75 mmol·g^{-1}) in DMSO was added to water (500 µL, 75mM), followed by the corresponding catalyst, either **[Ru]** (accounts for **Ru2**, 5 mol%) or **[Cu]** (accounts for $CuSO_4 \cdot 5H_2O$, 5 mol%, NaAsc, 10 mol%), in a vial open to air. [b] Yield and conversion determined by ^{1}H-NMR using 1,3,5- trimethoxybenzene as internal standard. [c] After 2 h, a second equivalent of **1b** was added followed by the second catalyst. [d] Both catalysts, **[Ru]** and **[Cu]**, are present from the beginning of the reaction.

3.3 Development of stimuli responsive Ru catalysts for RuAtAC reactions

One of the objectives of this work was the development of stimuli responsive catalysts that could allow to introduce temporal control on the activity. Considering that the catalyst **Ru2**, which has been found highly active for RuAtAC, can be easily prepared by displacement of the arene ligand of precursors like [Cp*Ru(arene)]X, by UV irradiation in acetonitrile, we explored different ruthenium arene sandwich complexes as precatalysts for the reaction.[146,147] Thus, the active catalysts should be formed *in situ,* after irradiation of the precatalysts with light.

The mechanism proposed for this ligand displacement involves a change in hapticity of the arene ligand ($\eta^6 \rightleftarrows \eta^4$). This generates a coordination vacant that can be filled by the solvent, or any other ligand present in the media. The η^4-arene behave now as a labile ligand that can be easily exchange with the solvent.[146]

[146] A. M. McNair, K. R. Mann, *Inorg. Chem.***1986**, *25*, 2519–2527.
[147] E. P. Kündig, F. R. Monnier, *Adv. Synth. Catal.* **2004**, *346*, 901–904.

Among the family of ruthenium sandwich complexes, we focused our attention on those bearing polyaromatic rings like naphthalene and pyrene since their displacement might be easy as the recovery of the aromaticity of adjacent rings act as driving force. This can be illustrated by the fact that when benzene is used as ligand [Cp*Ru(C_6H_6)]PF_6], no displacement is observed at room temperature in acetonitrile, whereas the analog complexes with naphthalene or pyrene undergo ligand exchange under otherwise identical conditions. The exchange in these cases can be easily enhanced by irradiation with light.[146] In this regard, it is worth to note that a related strategy for light-promoted activation of ruthenium complexes has been previously reported by Meggers for promoting deallylation reactions.[148]

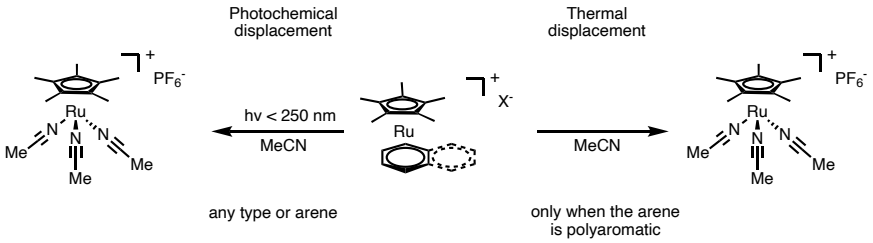

Figure 55. Activation of [Cp*Ru(arene)]X complex as function of the arene ligand.

3.3.1 Preliminary studies on the use of [Cp*Ru(arene)]x catalysts in the RuAtAC

To address the viability of using light to generate the active catalysts we synthetized the complex [Cp*Ru(pyrene)]PF_6 (**Ru3**, **Figure 56)**, following known synthetic protocols.[146]

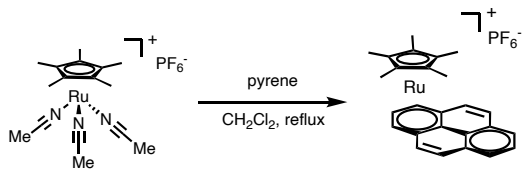

Figure 56. Synthesis of [Cp*Ru(pyrene)]PF_6, **Ru3**.

With this ruthenium complex in hand, we tested its performance in the reaction between the anthracenyl azide **1a** (1.0 equiv) and thioalkyne **2a** (2.0 equiv). Without irradiation, we observed no product after 2 h at room temperature, neither in water nor organic solvents (**Table 3**, **entries 1-3**). However, when the mixture (in water:acetone 1:1) was irradiated at 365 nm for 30 min, we observed high conversion of the azide **1a** (70%), and the formation of the desired triazole, **3aa**, although in a low 28% yield (**entry 4**). The high conversion of the anthracenyl azide **1a** is associated to its low photostability,

[148] P. K. Sasmal, S. Carregal-Romero, W. J. Parak, E. Meggers, *Organometallics* **2012**, *31*, 5968–5970.

therefore next experiments were carried out with the *p*-tolyl azide **1b**. Indeed, using this azide we obtained a 43% yield (53% conversion, **entry 6**) using as solvent a mixture of H_2O:MeOH (1:1) and 10 min of irradiation time. In H_2O:MeCN (1:1) mixtures, we obtained full conversion under light irradiation (**entry 8**), but curiously, the same reaction without irradiation also led to a non-negligible 28% yield. This activity, without irradiation, might be due to the coordinating ability of acetonitrile, which is able to displace the pyrene ruthenium ligand, likely helped by ambient light. Indeed, by covering the vial with aluminum foil (i.e., dark conditions), the yield of **3ba** could be reduced down to 5%, under otherwise identical reaction conditions. Moreover, decreasing the amount of MeCN also diminished the reaction yield under dark conditions. Thus, using $10\%_{(v/v)}$ of MeCN, full conversion to the product could be observed after just 10 min of irradiation time (**entry 11**), whereas a neglectable yield was obtained in the dark (**entry 12**).

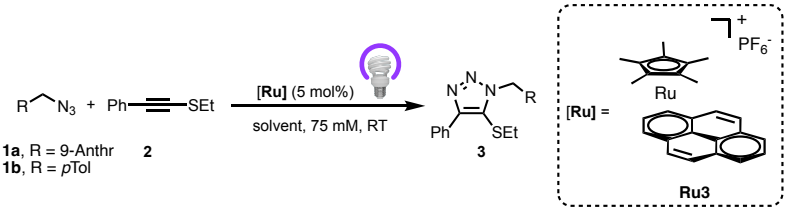

Entry	Azide	Time (h)	Solvent	hv (365nm) time	Conv (%)	Yield (%)[b]
1	**1a**	**2**	H_2O	0	7	0
2	**1a**	**2**	CH_2Cl_2	0	10	0
3	**1a**	**0.5**	MeCN	0	18	0
4	**1a**	**1**	H_2O:Acetone (1:1)	30 min	70	28
5[	**1a**	**1**	H_2O:Acetone (1:1)	0	10	0
6	**1b**	**2**	H_2O:MeOH (1:1)	10 min	53	43
7	**1b**	**2**	H_2O:MeOH (1:1)	0	5	0
8	**1b**	**2**	H_2O:MeCN (1:1)	10 min	99	99
9	**1b**	**2**	H_2O:MeCN (1:1)	0	30	24
10[c]	**1b**	**2**	H_2O:MeCN (1:1)	0	7	5
11	**1b**	**2**	H_2O:MeCN (9:1)	10 min	99	99
12[c]	**1b**	**2**	H_2O:MeCN (9:1)	-	1	0

Table 3. [a] Reaction conditions: **1a** (75 µmol), **2a** (150 µmol), solvent (1 mL) and the ruthenium complex (5 mol%) were added to a vial under air irradiated for the indicated time, and the mixture was stirred for 2h. [b] Yield determined by 1H-NMR spectroscopy of the reaction crude mixture using 1,3,5-trimethoxybenzene as an internal standard. [c] Dark conditions, vial covered with aluminum foil.

These good results with the stable complex [Cp*Ru(pyrene)]PF_6 led us to explore other arene ligands such as naphthalene (**Ru4**) and sodium 1-pyrenesulfonate (**Ru5**) by the treatment of the $[Cp^*RuCl_2]_2$ of the corresponding polyaromatic arene in methanol.

Additionally, we also explore the introduction of modifications into the Cp* ligand . In this regard when the $[Cp^*RuCl_2]_2$ dimer was bubbled with air in chloroform or dichloromethane, a new fulvene complex was formed. This fulvene derivative can react with nucleophiles like H_2O, alcohols or amines in the presence of an arene ligand to yield modified ruthenium complexes [Cp^iRu(arene)]X, **Figure 57**). [149][150] Following this procedure we synthetized several complexes bearing $Cp^‡$ modified ligands with an alcohol ($Cp^{‡OH}$) and with a methoxy group ($Cp^{‡OMe}$) and different arene ligands such as pyrene (**Ru6**) or naphthalene (**Ru7** and **Ru8**).

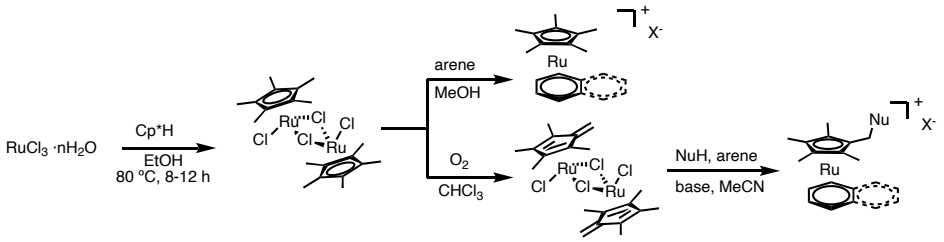

Figure 57. General scheme for the synthesis of [Cp*Ru(arene)]X and [Cp‡Ru(arene)]X from $RuCl_3 \cdot nH_2O$.

With the Ru complexes in hand, we tested their behavior under the optimized conditions (i.e., 10 min irradiation in a H_2O:MeCN (9:1) mixture, using 5 mol% of the Ru complex) in the model reaction between thioalkyne **2a** and azide **1b** (2:1 ratio). All ruthenium reagents with different arene ligands such as pyrene (**Ru3**), naphthalene (**Ru4**) and sodium 1-pyrenesulfonate (**Ru4**), gave excellent results (over 95% yield). The largest differences were observed when using the complexes that bear modified Cp* ligands. Thus, complex **Ru7,** which bears a $Cp^{‡OH}$ and a naphthalene ligand, provided lower yields than the analog with a regular Cp* (30% versus 99%).[151] Complexes bearing Cp* and $Cp^{‡OMe}$ either with naphthalene or pyrene provided quantitative yields. All of them required the irradiation with light to become active (yields without light irradiation are included under parenthesis), except for the complex **Ru8** [$Cp^{‡OMe}$Ru(naphthalene)]PF_6,

[149] R. M. Fairchild, K. T. Holman, *Organometallics* **2008**, *27*, 1823–1833.
[150] $Cp^‡$ stands for modified Cp* ligand
[151] The synthesis of the pyrene analog, [$Cp^{‡OH}$Ru(pyrene)]PF_6, was unsuccessful with very low yields, presumably due to the poor solubility of the pyrene ligand in water.

for which unexpectedly we also observed reaction without light irradiation (45% yield, **Figure 58**).

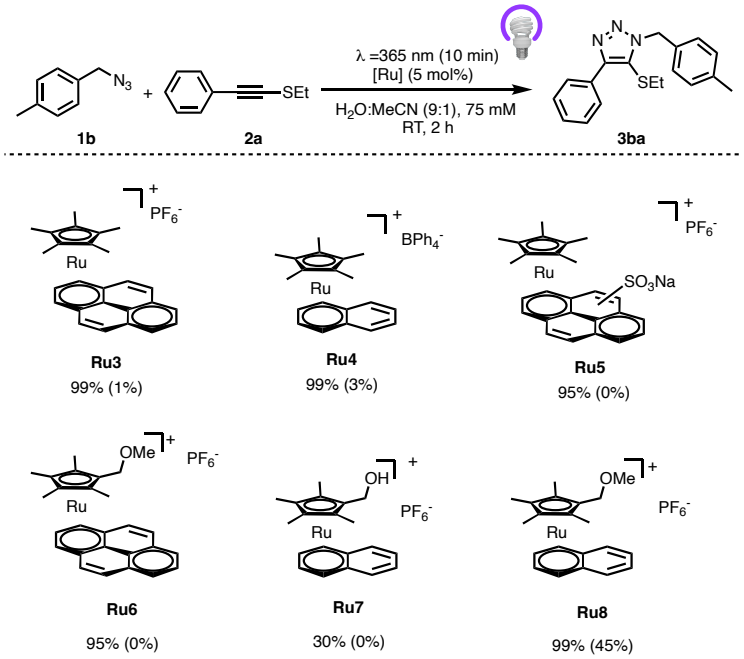

Figure 58. Performance of the different photoactivatable catalysts in the RuAtAC reaction. Yield under parenthesis corresponds to the non-irradiated reaction.

Interestingly, despite the complex [$Cp^{‡OH}$Ru(naphthalene)]PF_6 (**Ru7**) does not perform as well as its corresponding analogs with Cp* or $Cp^{‡OMe}$ ligands, it bears a reactive alcohol amenable for introducing different tags, such as fluorescent labels, organelle-targeting moieties, antibodies etc.

3.4 Efficiency of Ru catalysts Ru2, Ru3 and Ru5 under higher dilution

With these good results in hand, we next studied the behavior of the precatalysts **Ru2**, **Ru3** and **Ru5** under more diluted conditions, typically from 500 to 100 μM. To evaluate the performance of these complexes, we chose the triphenylphosphonium azide **1c** due to its good solubility in water and because the phosphonium tag might facilitate a precise monitoring of the reaction efficiency by LC–ESI-MS. In the case of the photoactivatable complexes **Ru3** and **Ru5,** the best results were obtained in water, without the addition of a co-solvent. Control experiments showed that the presence of acetonitrile was indeed detrimental, presumably due to its competitive coordination to the metal center. Therefore, the reactions were carried out in water at room temperature for 4 h, with

different concentrations of azide **1c** (from 1 mM to 100 µM), 50 mol% of ruthenium complex and, when using **Ru3** or **Ru5**, the reaction mixture was irradiated at 365 nm for 15 min.

To our delight, **Ru2**, **Ru3** and **Ru5** provided full conversions to the product at concentrations of azide of 1 mM and 500 µM, whereas the reference catalysts with the COD ligand, **Ru1,** provided low yields of 35% and 7%, respectively (no light used). At 250 µM, the pyrene-derived photoactivatable complex **Ru3** still afforded full conversion, whereas its sulphonated analog **Ru5**, and the tris-acetonitrile derivate, **Ru2,** provided yields of 67% and 86% respectively. Likewise, at 100 µM, the photoactivatable pyrene complex **Ru3** was the most efficient, affording **3ca** in 47% yield, with the tris-acetonitrile **Ru2** giving a 30% yield, whereas **Ru5** and the first-generation catalyst, **Ru1,** (no light used) provided less than a 5% (**Figure 59**).

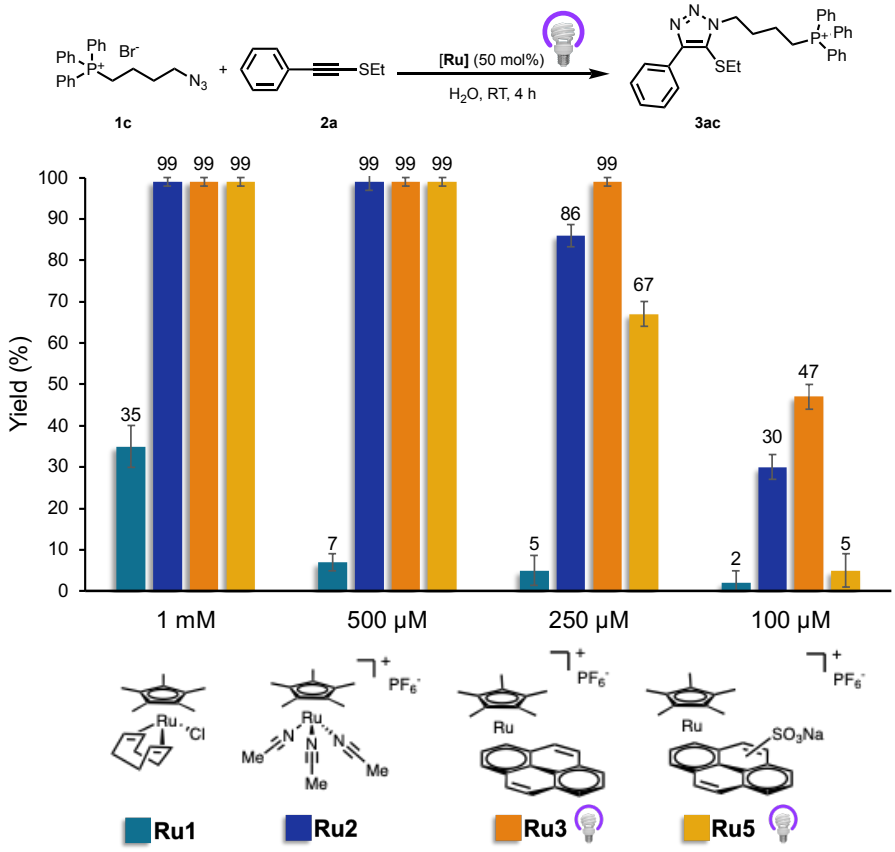

Figure 59. Catalyst performance in the micromolar range. Reactions were conducted in HPLC-vials equiped with a magnetic stirr bar. Yields were determined by UHPLC-MS using coumarin as internal

standart, by the average of three different reactions. Reactions carried out with **Ru3** and **Ru5** were irradiated for 15 min at 365 nm. Control experiments without irradiation for **Ru3** and **Ru5** provided yields <1%.

We further investigated the role of the catalyst loading for the most promising complexes, the precatalysts **Ru2** and **Ru4**. Thus, we found that the loading can be decreased down to 15 mol% without significantly affecting the yield (~10-15% lower yields, **Figure 60**)

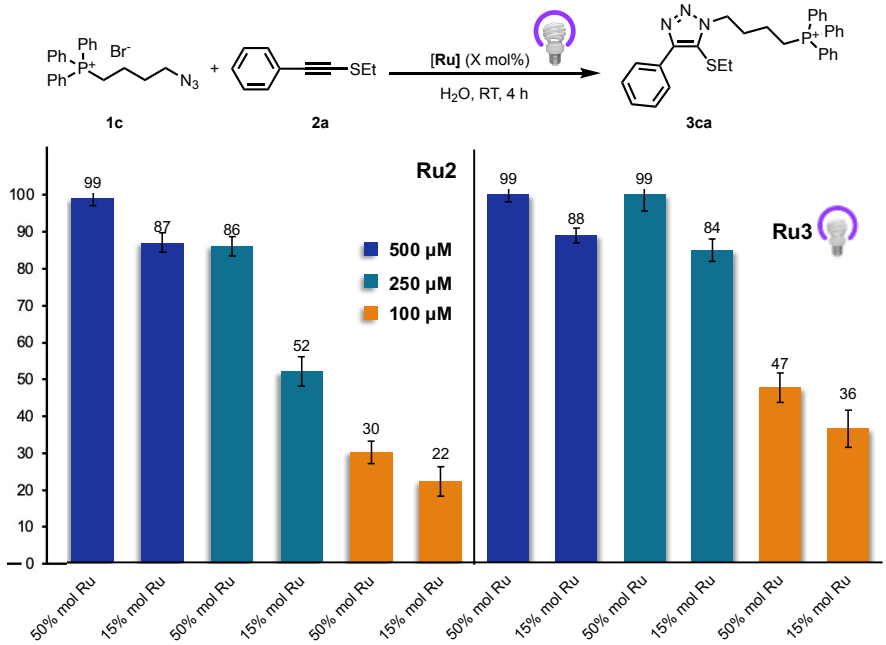

Figure 60. Effect of the catalyst loading with **Ru2** and **Ru3**. Reactions were conducted in HPLC-vials equiped with a magnetic stirr bar. Yields were determined by UHPLC-MS using coumarin as internal standart, by the average of three different reactions. Reaction mixtures of **Ru3** were irradiated for 15 min at 365 nm. Controls without irradiation for **Ru3** provided yields <1%

We also evaluate other azides and alkynes under diluted conditions (250 µM of azide). Thus, as can be seen in the **Figure 61,** the reaction between the thioalkyne **2c** and the azide **1c**, provided low yields with both **Ru2** (22% yield) and **Ru3** (15%yield), however, we were pleased to observe that other thioalkynes, bearing aromatic rings directly attached to the triple C-C bond, provided good yields of over 60% with **Ru2** and of 68% with **Ru3** (**Figure 61**).

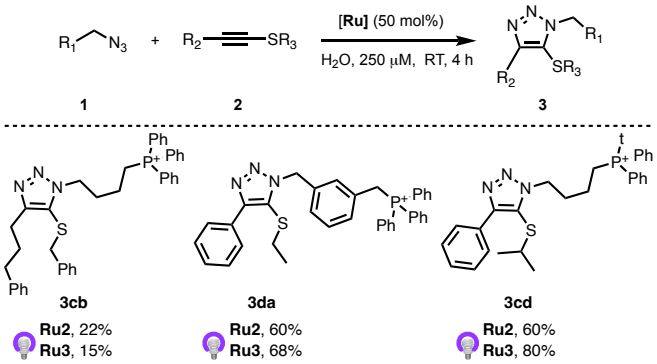

Figure 61. Scope under diluted conditions (**1**: 250 μM, **2**: 500 μM, **Ru**: 125 μM) with **Ru2** and **Ru3**. Reactions were conducted in HPLC-vials equiped with a magnetic stirr bar. Yields were determined by UHPLC-MS using coumarin as internal standart, by the average of three different reactions.

3.5 Bioorthogonality

At this point, we were in a position to assess the bioorthogonality of the reaction. We selected as model conditions an azide (**1c**) concentration of 500 μM and a ruthenium complex loading of 50 mol%. We tested different biological reaction media: phosphate buffer solution (PBS, pH = 7.2); Dulbecco's Modified Eagle Medium (DMEM), DMEM + 10% Fetal Bovine Serum + 1% Antibiotics (i.e., DMEM*);[152] DMEM without phenol-red and HEPES buffer (DMEM-HEPES) and HeLa Cell Lysates (4 mg/mL).

As can be deduced from **Figure 62**, **Ru2** had an outstanding performance providing quantitative yields of **3ca** regardless of the media, including cell lysates and DMEM*. **Ru3** also performed very well in PBS (99%). Remarkably, **Ru3** and **Ru5** precatalysts still provided good yields in DMEM (49 – 59% yield), while using other DMEM-based media, yields ranged from 50 to 70%, with the exception of **Ru5** in DMEM-HEPES, which provided a low 13% yield. Finally, **Ru3** and **Ru5** were almost as effective as **Ru2** in cell lysates, with yields above the 90% level (**Figure 62**).

[152] Fetal Bovine Serum is derived from the blood from bovine fetus. It contains albumin, hemoglobin, bilirubin, urea, creatinine, insulin, cortisol, testosterone among other biological components.

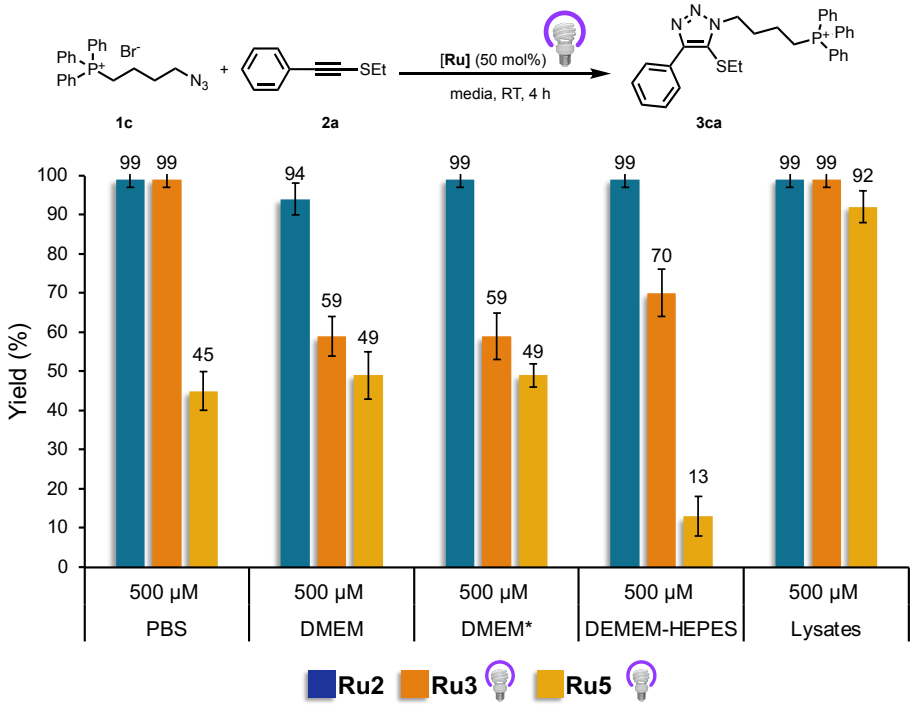

Figure 62. Reactions were conducted in HPLC-vials equiped with a magnetic stirr bar (**1**: 250 μM, **2**: 500 μM, **Ru**: 125 μM). Yields were determined by UHPLC-MS using coumarin as internal standart, by the average of three different reactions. Reaction mixtures of **Ru3** were irradiated for 15 min at 365 nm. Controls without irradiation for **Ru3** provided yields <1%.

3.6 RuAtAC vs IrAtAC vs RhAtAC

As commented at the end of the introduction of this chapter (**section 1.3**, page 53), after our publication of the RuAtAC, other reports on metal catalyzed alkyne azide cycloadditions using Iridium[153,154] and Rhodium catalysts were disclosed. [155,156] Among them, the work of Song on iridium-catalyzed cycloadditions between ynamides and azides is the only one that reported a bioorthogonality study with good results in cell lysates, although these studies were carried out at high concentration (>100 mM).

In order to further benchmark our results, we compared the performance of different metal-based catalysts in the reaction of azide **1c** and thioalkyne **2a**, as in the bioorthogonality studies. $[RhCl(CO)_2]_2$ (**Rh1**) and $[IrCl(COD)]_2$ (**Ir1**) were studied in water with concentrations of the limiting reagent of 250 and 100 µM, using the

[153] W. Song, N. Zheng, *Org. Lett.* **2017**, *19*, 6200–6203.
[154] M. Li, N. Zheng, J. Li, Y. Zheng, W. Song, *Green Chem.* **2020**, *22*, 2394–2398.
[155] W. Song, N. Zheng, M. Li, K. Dong, J. Li, K. Ullah, Y. Zheng, *Org. Lett.* **2018**, *20*, 6705–6709.
[156] W. Song, N. Zheng, M. Li, K. Ullah, Y. Zheng, *Adv. Synth. Catal.* **2018**, *360*, 2429–2434.

stoichiometric ratio reported in the abovementioned studies (azide : thioalkyne ratio = 1.5:1) as well as our optimal ratio of reactants (azide:thioalkyne ratio = 1:2). In all cases, we used a metal loading of 50 mol%.[157] As can be observed in **Figure 63**, both, **Ir1** and **Rh1** are quite sensitive to the azide:thioalkyne ratio. **Ir1** exhibited a moderate performance at 250 μM and at 100 μM when a 1.5:1 azide:thioalkyne ratio is used (46% and 23% respectively); however, if the ratio is changed to a 1:2 azide:thioalkyne proportion , the yield drops (<10%). Curiously, **Rh1** has an opposite behavior, and the best results were obtained with the 1:2 azide:thioalkyne stoichiometry. Nonetheless, yields are overall low, below the 30% level, even in this best-case scenario (1:2 azide:thioalkyne ratio, 250 μM: 24% yield; 100 μM: 29% yield).

These results for **Ir1** and **Rh1**, with maximum yields of 46% at 250μM and 29% at 100 μM, indicate a much poorer performance than our photoactivatable catalyst **Ru3** (99% and 53%, respectively).

[157] In all cases concentrations are referred to the limiting reagent

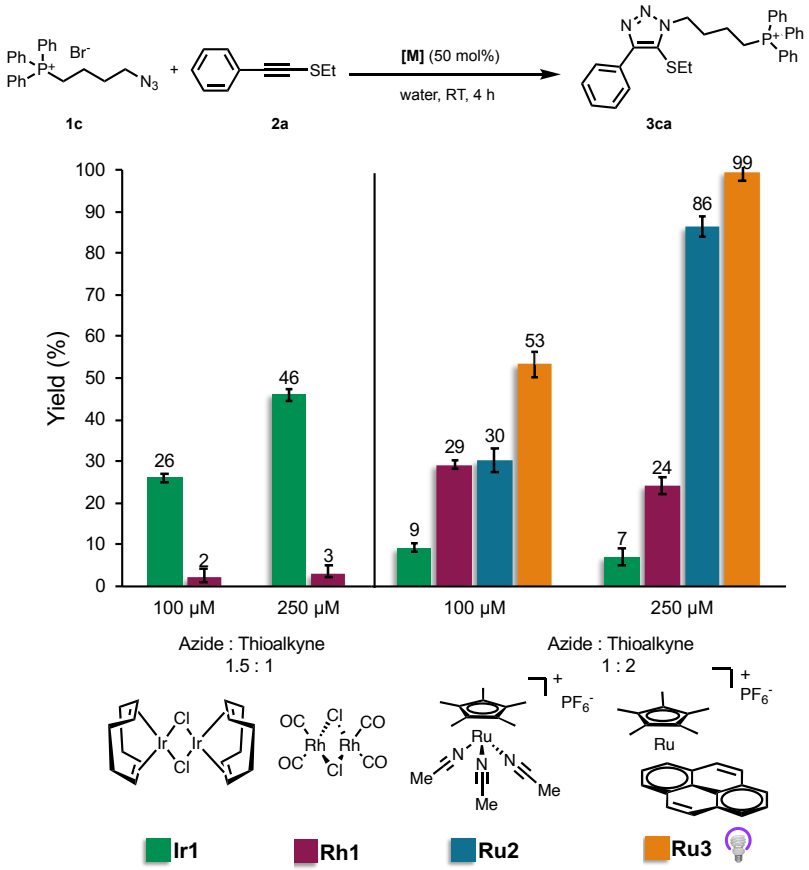

Figure 63. Comparison of different metal catalysts in the model reaction in water. In all examples, 50 mol% of metal was used. Reactions were conducted in HPLC-vials equiped with a magnetic stirr bar. Yields were determined by UHPLC-MS using coumarin as internal standart, by the average of three different reactions. Reaction mixtures of **Ru3** were irradiated for 15 min at 365 nm. Controls without irradiation for **Ru3** provided yields <1%.

We also checked the reactivity under biologically relevant conditions. Using the best azide: thioalkyne ratio for each metal. (1.5:1 for **Ir1** and 1:2 for **Rh1**) both complexes were tested in PBS, DMEM, DMEM* and cell lysates at 500 µM. In **Figure 64**, we collect the results in comparison with those of **Ru3** and **Ru5** (and light).

Under biologically relevant conditions, yields of **3ca** were lower than 10% for all cases except for **Ir1** in cell lysates which reached a 16% yield. In general, **Ir1** and **Rh1** performed much worse than any of the new cationic ruthenium precatalyst, and with extremely poor activity under biologically relevant conditions (**Figure 64**)

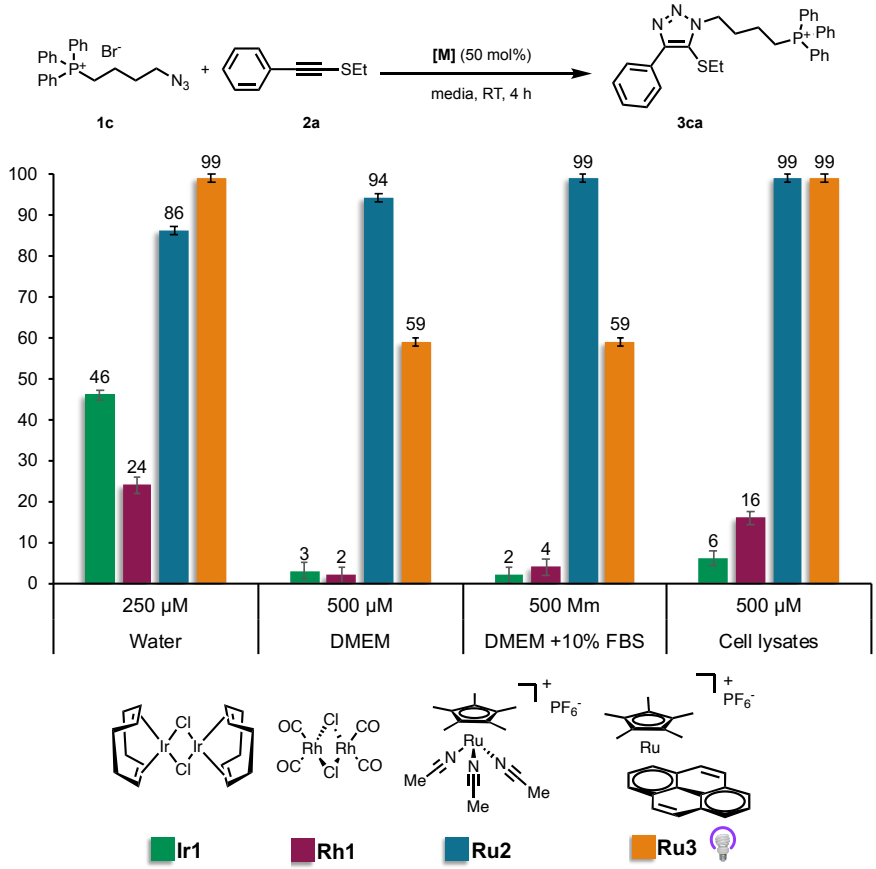

Figure 64. Comparison of different metal catalyst under bioorthogonal relevant conditions. In all examples, 50 mol% of metal were used. Reactions were performed using the optimal azide/thioalkyne ratios found for each metal catalyst (1.5:1 for **Ir1** and 1:2 for **Rh1**, **Ru2** and **Ru3** Reactions were conducted in HPLC-vials equiped with a magnetic stirr bar. Yields were determined by UHPLC-MS using coumarin as internal standart, by the average of three different reactions. Reaction mixtures of **Ru3** were irradiated for 15 min at 365 nm. Controls without irradiation for **Ru3** provided yields <1

Overall, we can conclude that **Ru2** and **Ru3** are robust catalysts that clearly outperform the previous generation ruthenium complexes, as well other catalysts based on Iridium or Rhodium.

3.7 Further applications

3.7.1 Modification of biopolymers[158]

A particularly appealing application of bioorthogonal reactions is related with the chemoselective modification of biopolymers. Indeed, the original report of the CuAAC by Meldal applied the copper-promoted cycloaddition to the modification of small peptides bearing alkynes (**Figure 65a**). Even though this original conjugation was carried out in solid phase, it was later applied to the modification of peptides in aqueous solutions and extended for other biopolymers. For instance, Finn and coworkers have also applied the CuAAC for labeling 21-mer siRNAs (**Figure 65b**).[159,160]

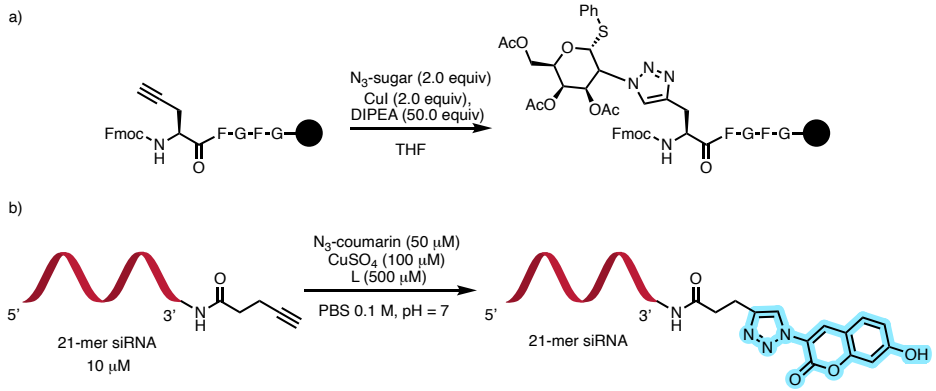

Figure 65. a) Original report by Meldal on the CuAAC peptide modification in the solid phase. b) Modification of 21-mer siRNA by CuAAC

On these basis, we analyzed whether our catalysts could also be used for chemoselective bioconjugation reactions of peptides and nucleic acids.

We first evaluated the reaction for the modification of an azide-containing peptide. The peptide was synthetized by solid phase peptide synthesis using Rink-amide ChemMatrix resin and fluorenylmethyloxycarbonyl (Fmoc) as amino protecting group. The azide moiety was introduced as lysine azide derivative. The peptide was cleaved from the resin by a deprotection cocktail and purified by preparative HPLC.

The modification was tested by treating a 500 μM solution of the azido-peptide in NH_4OAc (0.1 M) with 2.0 equiv of thioalkyne **2a** and 50 mol% of the corresponding

[158] Experiment in this section were performed in collaboration with PhD. Cibrán Pérez-González
[159] 21-mer RNAs are small interference RNAs with many pharmacological uses, like knockdown genes. S. D. Rose, *Nucleic Acids Research* **2005**, *33*, 4140–4156.
[160] V. Hong, S. Presolski, C. Ma, M. G. Finn, *Angew. Chem. Int. Ed.* **2009**, *48*, 9879–9883.

ruthenium precatalyst. The use if **Ru2** led to a moderate 55% yield of the desired peptide-triazole product and, to our delight, the photoactivatable **Ru3** gave a higher yield (84%) (**Figure 66**).

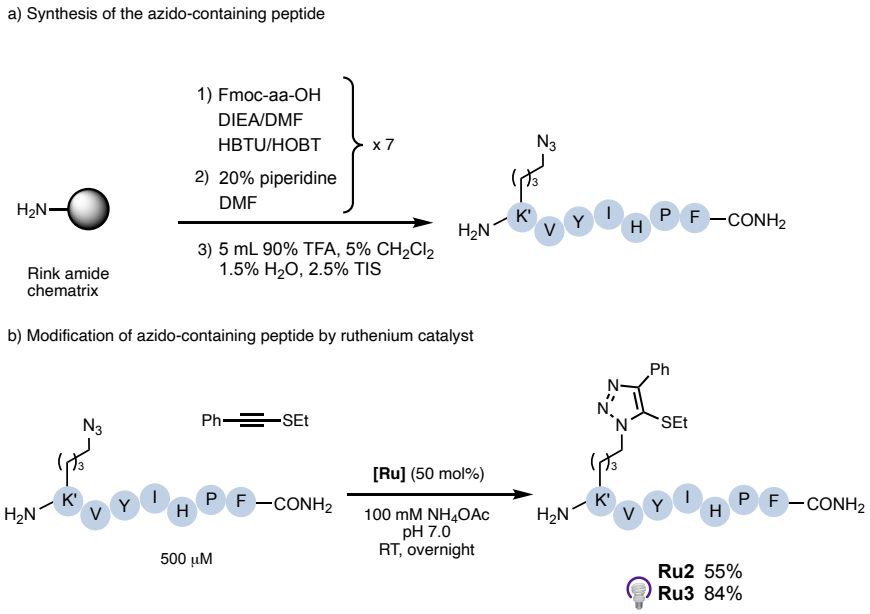

Figure 66. a) Synthesis of the azido-containing peptide b) Reaction scheme for the modification of the corresponding peptide.

Single strand DNA oligonucleotides (ss-DNA) with an azide modified adenosine in the 5'- terminus were purchased *biomers.net GmbH* and also tested in the RuAtAC reaction. ssDNA sequence = 5'- A(N_3)TA GAC GAG A-3'. Reactions were carried out at 200 μM concentration of the oligonucleotide in triethylamine: acetic acid buffer (TEAA, 100 mM, pH = 7.0). The thioalkyne used was the Rhodamine B derivative **2h**. The reaction was analyzed by Electrophoretic Mobility Shift Assay (EMSA) and quantified by HPLC. The cycloaddition reaction between the azido – oligonucleotide and the Rhodamine-thioalkyne **2h** proceeded in a moderate 55% yield with **Ru2** as catalyst. This result is in agreement with those at 250 μM performed before (see **Figure 59**). In a similar fashion, the best performance was observed with **Ru3** with a gratifyingly 72% yield of the oligonucleotide adduct (**Figure 67**).

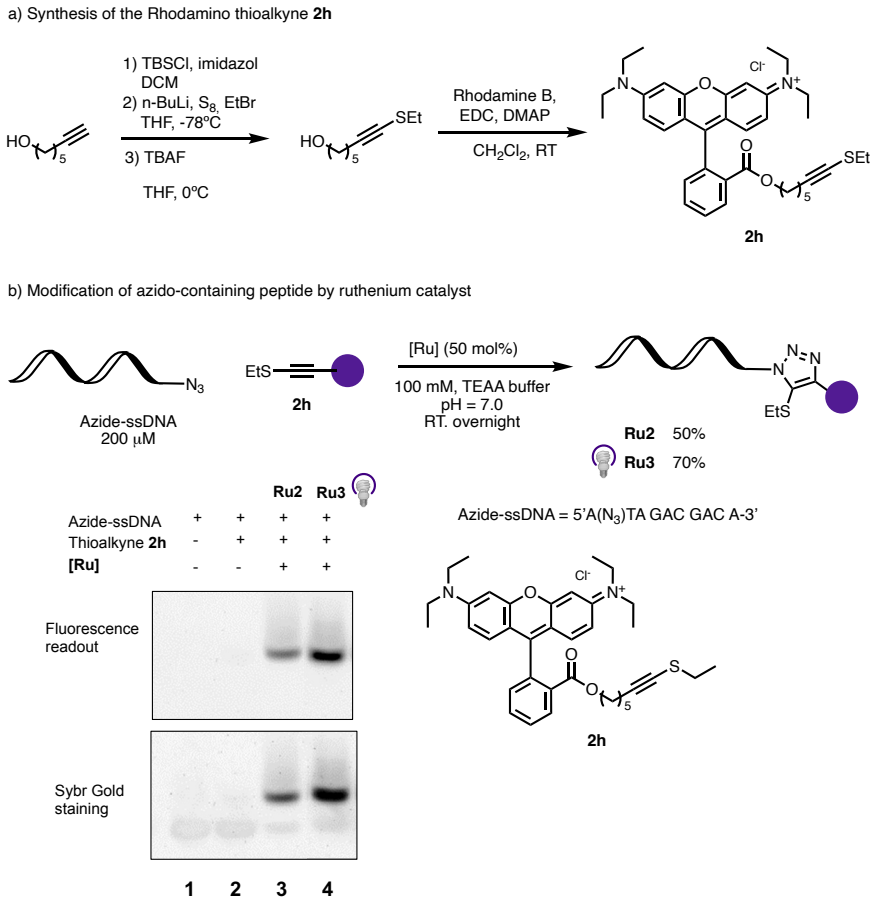

Figure 67. a) Synthesis of Rhodamine thioalkyne **2h**. b) Modification of the azide-ssDNA by RuAtAC.

3.7.2 Cellular experiments

Translating the RuAtAC to cellular conditions is a major challenge. To test the viability of the process we selected the anthracenyl azide reactants, as their conversion can be monitored by fluorescence. Electron transfer from the α-nitrogen from the azide to the anthracenyl ring in the excited state quenches the intrinsic fluorescence of the anthracenyl moiety (Off state). Upon the click reaction the lone pair electrons of the nitrogen become part of the aromatic ring of the triazole, with a weaker electron donor behavior and therefore the anthracenyl fluorescence is recovered (On state).[161]

[161] F. Xie, K. Sivakumar, Q. Zeng, M. A. Bruckman, B. Hodges, Q. Wang, *Tetrahedron* **2008**, *64*, 2906–2914.

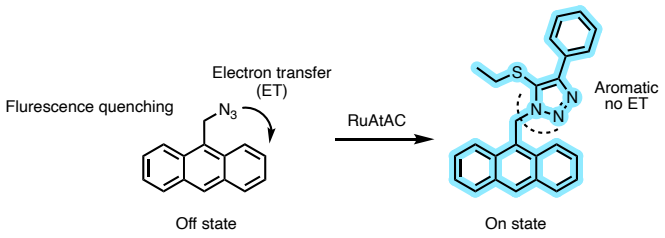

Figure 68. Off-On probe for the RuAtAC.

Unfortunately, *in vitro* control experiments irradiating the Ru complexes in the presence of the anthracenyl azide led to either the decomposition of the azide or photobleaching of the corresponding fluorescent triazole. Therefore, we moved to another azide which, equipped with a triphenyl phosphonium unit, could be monitored by MS.

Thus, we checked the viability of the cycloaddition between the phosphonium azide **1c** and the thioalkyne **2a** in the presence of cells (in suspension). The experiments were carried out by mixing the ruthenium catalyst, either **Ru2** or **Ru3**, the thioalkyne **2a** and azide **1c** in DMEM-HEPES containing HeLa cells (10^6 cells /mL). In the case of **Ru3**, the mixture was irradiated for 15 min at 365 nm. After 2h, the cells were centrifuged, the supernatant was collected, and the cell pellet extracted with MeOH 80%$_{(v/v)}$. The supernatant and the cellular content were analyzed by HPLC-MS.

We were delighted to find out that using either the **Ru2** or the photoactivatable catalyst **Ru3** (15 min of irradiation) we can the detect the expected triazole adduct **3ca**, both in the supernatant and in the extract of the cellular content. This methanolic extract was particularly rich in the triazole product **3ca**, whereas the supernatant contained lower amounts of it, which suggest an intracellular reaction, although this cannot be fully confirmed (**Figure 69**).

Overall, both catalysts, **Ru2** and **Ru3**, are capable to promote the [3+2] cycloaddition under highly diluted condition in the presence of HeLa cells.

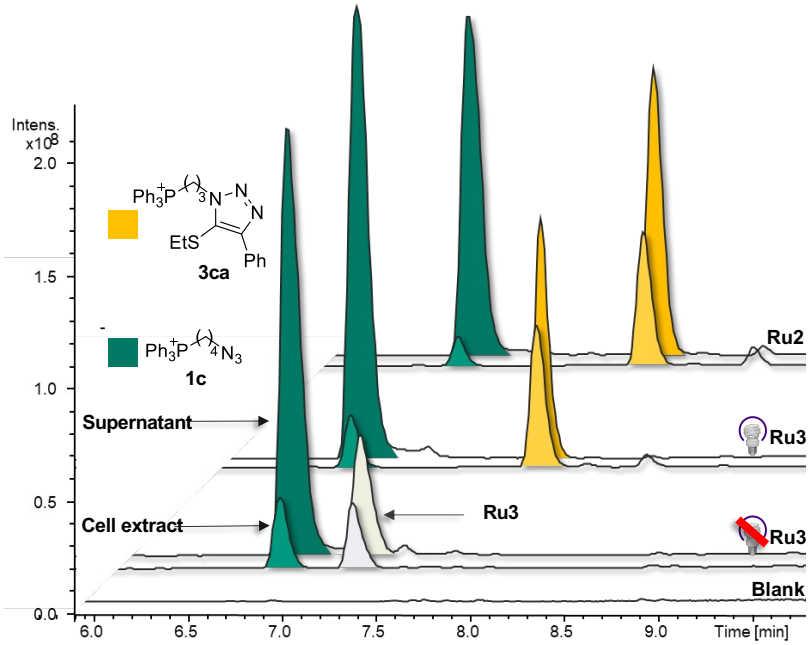

Figure 69. Reaction in the presence of HeLa cells suspended in DMEM-HEPES. HPLC traces: MS signal of the methanolic cell extract and supernatant for **Ru2** and **Ru3** (+ 15 min irradiation), **Ru3** (without irradiation) and a blank.

4 Conclusions

In conclusion, we have discovered that cationic ruthenium complexes are highly active in ruthenium catalyzed azide-thioalkyne cycloadditions under aqueous conditions. The reaction proved to be fully compatible and mutually orthogonal with the CuAAC.

Furthermore, we have developed a series of ruthenium arene sandwich complexes that act as photoactivatable precatalysts. This provides spatio-temporal control of the reactivity but also higher efficiencies probably due to the stability of the complex until activation. These precatalysts allow to carry out the cycloaddition under diluted and biocompatible conditions.

We have also demonstrated that this new generation of ruthenium catalysts are able to promote the modification of azide containing peptides and oligonucleotides, and that the RuAtAC reaction can be carried out in the presence of HeLa cells.

Chapter II: Ruthenium Catalyzed Bioorthogonal Alkene-Alkyne couplings

1 Introduction

Bioorthogonal reactions could be classified depending on whether they break or create new bonds. Among the latter, research has been mainly focused on reactions that build carbon-heteroatom bonds, and on the use of intrinsically reactive moieties like azides. This is the case of the above discussed CuAAC,[162] and the ruthenium variant RuAtAC[108,132] as well as of alternative metal-free variants such as the strain promoted azide-alkyne cycloadditions SPAAC,[163] or the inverse electron demanding Diels Alder IEDDA.[164]

In contrast, bioorthogonal reactions entailing the formation of C-C bonds, have lagged clearly behind. In the case of transition metal catalyzed processes several examples of aqueous-compatible and bioorthogonal C-C cross couplings based on Suzuki or Sonogashira type of reactions have been described.[165] Moreover, ruthenium catalyzed alkene metathesis have also been used in aqueous and biological media.[166] These organometallic reactions have been elegantly applied, for instance, to the radio labeling of proteins with boronic acid coupling agents containing Fluorine-18 (**Figure 70a**) as well as to the modification of allyl (seleno)cysteines by alkene-metathesis (**Figure 70b**).

[162] L. Li, Z. Zhang, *Molecules* **2016**, *21*, 1393.
[163] J. Dommerholt, F. P. J. T. Rutjes, F. L. van Delft, *Top Curr Chem (Z)* **2016**, *374*, 16.
[164] B. L. Oliveira, Z. Guo, G. J. L. Bernardes, *Chem. Soc. Rev.* **2017**, *46*, 4895–4950.
[165] J. M. Chalker, C. S. C. Wood, B. G. Davis, *J. Am. Chem. Soc.* **2009**, *131*, 16346–16347.
[166] B. Bhushan, Y. A. Lin, M. Bak, A. Phanumartwiwath, N. Yang, M. K. Bilyard, T. Tanaka, K. L. Hudson, L. Lercher, M. Stegmann, S. Mohammed, B. G. Davis, *J. Am. Chem. Soc.* **2018**, *140*, 14599–14603.

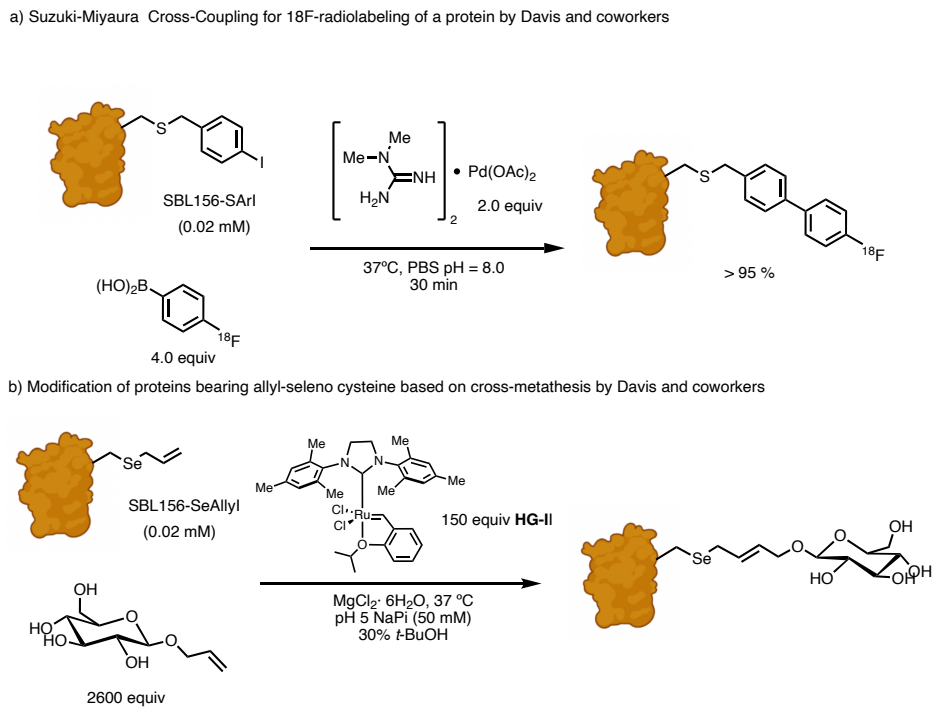

Figure 70. General scheme for bioorthogonal metal promoted C-C bond forming reactions.

The Sonogashira coupling has also been used for the modification of proteins bearing the non-canonical amino acid homopropargyl glycine and even for the modification of cell membranes of cells that expresses this ncAA.[98]

Our group has recently reported a highly efficient and bioorthogonal [2+2+2] cycloaddition promoted by cyclopentadienyl ruthenium (CpRu)-based catalysts.[167] As commented in **section 4.4** of the introduction, this annulation can be even carried out inside living mammalian cells to generate fluorescent anthraquinones. Very likely, the bioorthogonality of this annulation lies on the bidentate nature of the diyne, which favors the coordination to the metal to give the ruthenacyclopentadiene intermediate **I**, by means of an intramolecular oxidative cyclization (**Figure 71**). Once this intermediate is formed a migratory insertion of an external alkyne delivers a new ruthenacycle intermediate **II** that evolves to the product via a reductive elimination step.

[167] V. Sabatino, J. G. Rebelein, T. R. Ward, *J. Am. Chem. Soc.* **2019**, *141*, 17048–17052.

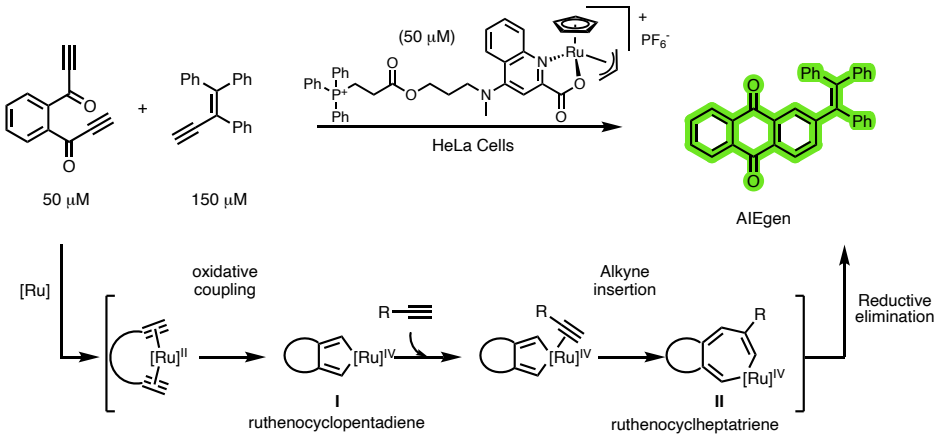

Figure 71. Ruthenium catalyzed [2+2+2] cycloaddition and mechanistic insights.

These results entailing C-C bond formations from alkynes and/or alkenes, without the need to introduce further functional groups that could trigger the metal catalyzed process, are quite exciting and raise the question of whether it would be possible to perform other type of bioorthogonal C-C cross-couplings just relying on the coordination ability and organometallic reactivity of C-C unsaturated precursors like alkynes or alkenes.

2 Objectives

The success of some cross-metathesis processes in water and in biological media, as well as our discovery Ru-promoted [2+2+2] cycloadditions in cells, led us to question whether it would be possible to export other type of C-C cross-couplings entailing unsaturated reactants to the bioorthogonal field.

In particular, we considered the Ru-catalyzed coupling between alkynes and alkenes, a reaction originally developed by Trost in organic solvents which requires the intermolecular generation of a ruthenacycle intermediate species. We reasoned that in a complex aqueous mixture, the alkyne and the alkene should be able to coordinate the ruthenium catalyst in an orthogonal manner. When both reactants are eventually linked to the ruthenium, they could react to give the corresponding ruthenacycle (oxidative cyclometallation), which might irreversibly evolve to a diene product by β-hydride elimination.

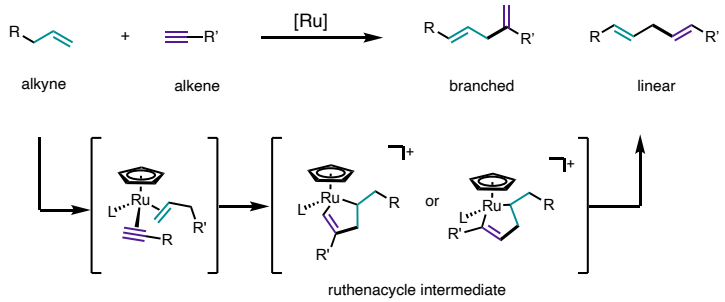

The development of such a process to expand the toolbox of bioorthogonal chemistry is challenging, but highly appealing from a chemical biology standpoint, due to the inertness of alkynes and alkenes in biological media, as well as considering the number of efficient methods that are available to introduce alkynes and alkene moieties in biomolecules (e.g., expansion of the genetic code, etc.).

3 Results and discussion

3.1 Precedents on the ruthenium-catalyzed coupling between alkenes and alkynes

The catalog of synthetic transformations that are promoted by Ru(II) catalysts in organic solvents is very broad, with many reactions developed by the group of Trost.[168] Among them, the ruthenium catalyzed coupling between alkenes and alkynes to provide 1,4-dienes is particularly attractive due to its perfect atom economy, which allows to cross-couple two molecules without the introduction of additional functional groups.[169]

This reaction was first developed using terminal alkenes and alkynes to give skipped 1,4-dienes, either branched (bearing a 1,1' disubstituted alkene) or linear (with a 1,2-disubstituted alkene, **Figure 72**). The coupling is tolerant to a broad variety of functional groups, take place at room temperature, in polar and protic solvent and tolerates water. The regioselectivity of the process is difficult to control but it can be adjusted by appropriately selecting the Ru catalyst and the degree of substitution, sterics and electronics of the reactants.[170]

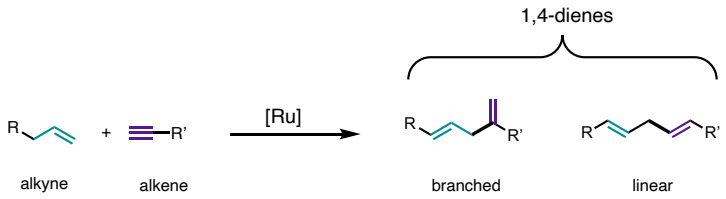

Figure 72. General scheme for the ruthenium catalyzed alkene-alkyne coupling.

The catalyst of choice is usually $[CpRu(MeCN)_3]PF_6$ (**Ru9**), even though CpRu(COD)Cl has also been used, however, it usually requires higher temperatures to work efficiently, possible due to the need to dissociate the chloride ligand from the Ru center. Complex $[Cp^*Ru(MeCN)_3]PF_6$ (**Ru2**) has been also reported to work, but the examples remain scarce.[171,172] The accepted mechanism involves the coordination of the alkene and alkyne to the ruthenium center (in a parallel or antiparallel fashion), followed by the oxidative cyclization to yield two possible regioisomer ruthenacycles **Int-3** and **Int-3'**.

[168] B. M. Trost, M. U. Frederiksen, M. T. Rudd, *Angew. Chem. Int. Ed.* **2005**, *44*, 6630–6666.
[169] B. M. Trost, A. F. Indolese, T. J. J. Mueller, B. Treptow, *J. Am. Chem. Soc.* **1995**, *117*, 615–623.
[170] B. M. Trost, *Acc. Chem. Res.* **2002**, *35*, 695–705.
[171] S. Murugesan, F. Jiang, M. Achard, C. Bruneau, S. Dérien, *Chem. Commun.* **2012**, *48*, 6589.
[172] S. M. Rummelt, G. Cheng, P. Gupta, W. Thiel, A. Fürstner, *Angew. Chem. Int. Ed.* **2017**, *56*, 3599–3604.

A β-hydride abstraction, followed by C-H reductive elimination eventually delivers the 1,4-diene, which can be obtained as a linear (from **Int-4'**) or branched isomer. According to the interpretation of the accumulated results obtained with [CpRu] catalyst **Ru9** by Trost, in the branched path, also call the thermodynamic path, the elemental step with the highest steric interactions is the C-C bond formation step (oxidative cyclization, **Int-2**). However, in the linear path the strongest steric interaction occurs in **Int-4'** within the $[CpRu]^+$ fragment and the substituent of the alkyne (**Figure 73**).

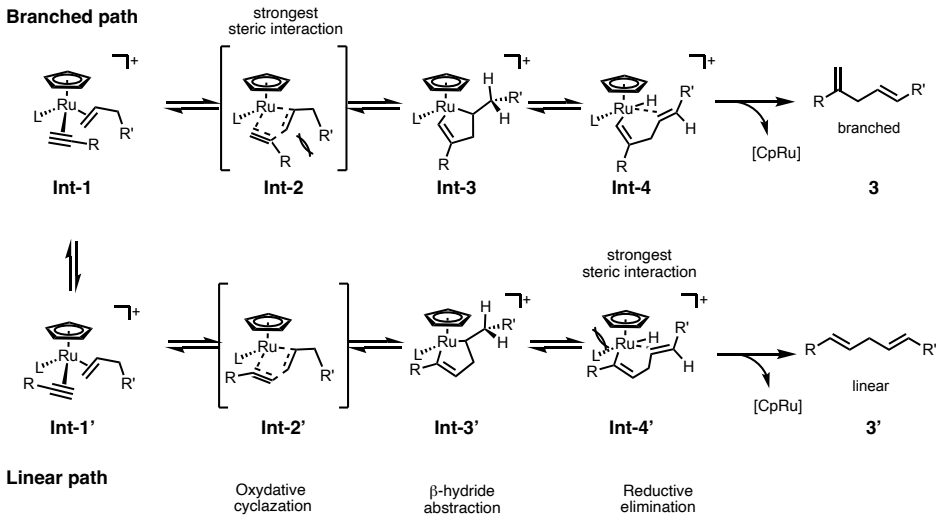

Figure 73. Mechanism for the formation of the branched and linear 1,4-diene.

The formation of the two possible ruthenacycles, **Int-1** and **Int-1'** is *a priori* reversible, so that it has been proposed that the relative barrier for the two possible β- hydride eliminations is what eventually determines the selectivity.[173] Therefore, using aliphatic linear alkenes and alkynes and the complex $[CpRu]^+$ as catalytic species, the branched diene is favored due to the increase in steric strain in the linear path. On the contrary, propargylic alcohols bearing quaternary C-centers at the propargylic position kinetically favor the linear diene by increasing the energy barrier for the formation of the ruthenocyclopentene of the branched path (Curtin-Hammett controlled).

When using the catalyst Cp*Ru (precatalyst **Ru2**), instead of the Cp-derivative (**Ru9**), there is an increase in the steric constrains in the β-hydride elimination of the linear

[173] It is assumed that the two possible C-H reductive eliminations, to deliver either the branched or linear adduct, would involve similar energy barriers

pathway, regardless of the sterics of the alkyne, leading to the branched diene as can be observed in the total synthesis of **Amphidinolide A** (**Figure 74**).[174]

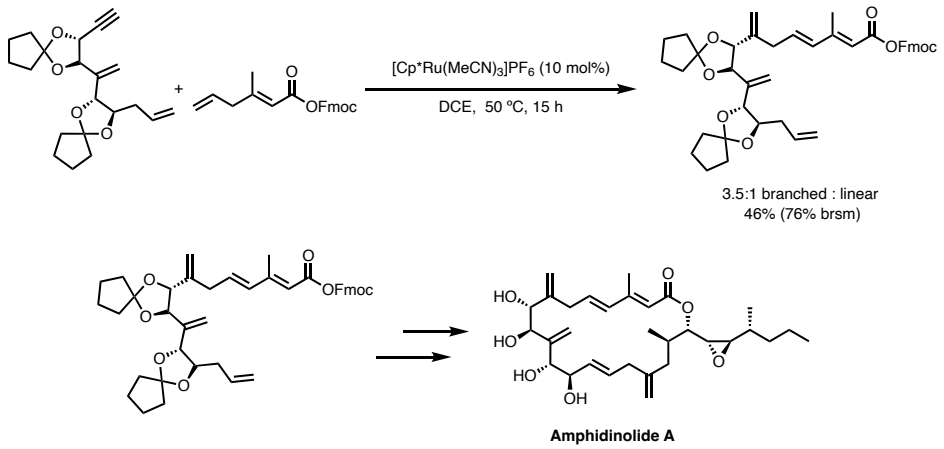

Figure 74. Application of the $[Cp^*Ru(MeCN)_3]PF_6$ in the total synthesis of Amphidinolide A.

This reaction has been thoroughly studied, mainly by Trost, who has extended the applicability to substituted alkenes and internal alkynes (**Figure 75**).[175,176]

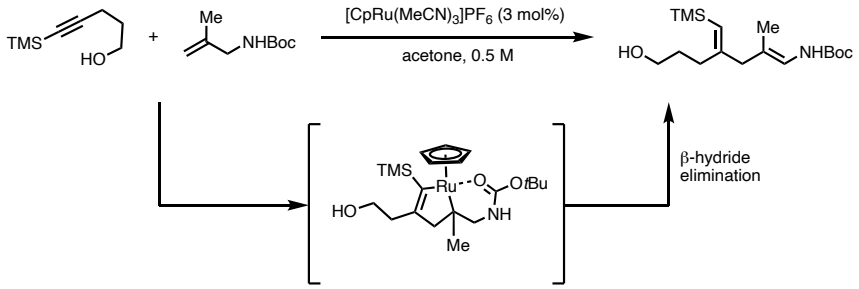

Figure 75. Ruthenium catalyzed alkene-alkyne coupling of internal alkynes and 1,1'-disubtituted alkenes.

During the development of this PhD work, Okuda and coworkers reported a preliminary exploration of the ruthenium catalyzed alkene-alkyne coupling in aqueous media. In particular, these authors developed an artificial metalloprotein that contains a $[Cp^*Ru]^+$ motif and evaluate its performance for the alkene-alkyne coupling (**Figure 76**).[177] The report is focused on synthetic aspects rather than on exploring the viability of adding this type of coupling to the armory of metal-catalyzed bioorthogonal reactions. They found that the artificial metalloenzyme allowed to increase the branched:linear ratio towards the

[174] B. M. Trost, J. D. Chisholm, S. T. Wrobleski, M. Jung, *J. Am. Chem. Soc.* **2002**, *124*, 12420–12421.
[175] B. M. Trost, A. Martos-Redruejo, *Org. Lett.* **2009**, *11*, 1071–1074.
[176] B. M. Trost, J. J. Cregg, *J. Am. Chem. Soc.* **2015**, *137*, 620–623.
[177] A. Thiel, D. F. Sauer, U. Markel, M. A. S. Mertens, T. Polen, U. Schwaneberg, J. Okuda, *Org. Biomol. Chem.* **2021**, *19*, 2912–2916.

linear product in the coupling of 3-butenol with 5-hexynenitrile, (1:1.6 branched:linear without the protein scaffold, and 1:16 with the protein). Importantly, the reactions do not proceed at temperatures below 60 ºC, limiting its applicability in chemical biology.

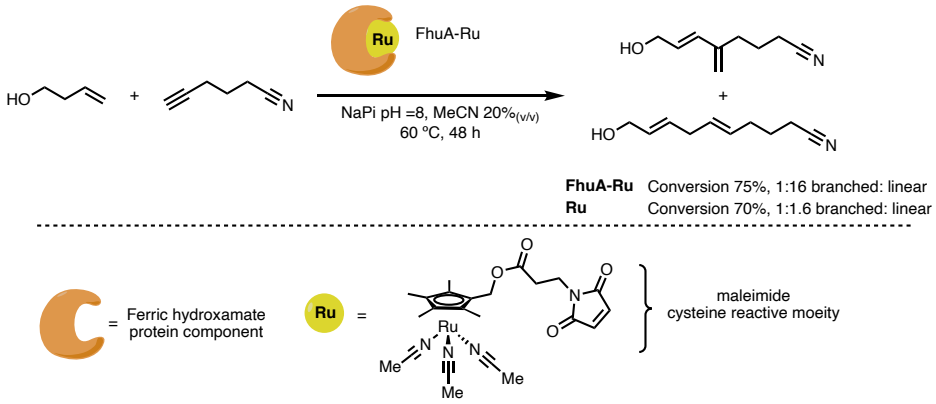

Figure 76. Schematic representation of the artificial metalloenzyme for the alkene-alkyne coupling.

3.2 Alkene-alkyne coupling in aqueous media. Optimization and scope

In other to assess the feasibility of an alkene-alkyne coupling in water, we selected as reactant the allyl ether **4a** (1.0 equiv) and the propargylic benzyl ether **5a** (1.0 equiv), and as catalyst the complex $[Cp^*Ru(MeCN)_3]PF_6$ (**Ru2**, 10 mol%). The reaction can be performed in organic solvent such as THF, acetone or CH_2Cl_2, albeit with modest NMR yields, from 30 to 40% of diene **6aa** in over 9:1 branched:linear ratio (**Table 4, entries 1-3**). Surprisingly, the use of water as the sole solvent led to comparable yields (36%) and regioselectivity (**entry 4**). Use of a $20\%_{(v/v)}$ of THF as cosolvent allowed to increase the yield up to a 71% (**entry 5**). In all cases we observed a high regioselectivity towards the branched isomer, obtained as *E*-isomer. The use of the more polar *N*-tosyl propargyl amide **5b** led to an excellent 99% yield of diene **6ab** and similar selectivity (**entry 7**). Lowering the amount of THF (**entry 8**) or performing the reaction in pure water (**entry 9**) was still possible delivering the corresponding diene in moderate to good yields. In both cases, with alkyne **5a** and **5b**, at this concentration using water or THF:water mixtures at 75 mM, we observed an heterogeneous mixture, whereas in pure THF, acetone or CH_2Cl_2 we have an homogeneous solution.

Interestingly, we can switch the regioselectivity of the process by using the related complex $[CpRu(MeCN)_3]PF_6$ (**Ru9**). In both cases, using either the benzyl ether **5a** or the tosyl amide **5b** we obtained moderate yield of the corresponding linear dienes with

slightly worse regioselectivities (1:6 and 1:7 branched:linear ratios, for **5a** and **5b** respectively).

From now on, we selected 10 mol% of catalyst loading, H_2O:THF (8:2), 1:1 alkene: alkyne ratio and 75 mM as optimal reaction conditions.

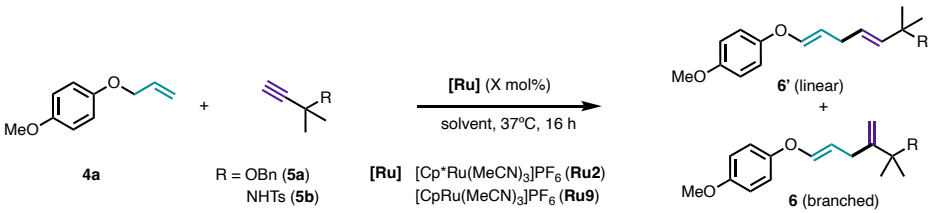

Entry	Alkyne	Solvent	Ru (X mol%)	Yield (%)[a]	6:6' ratio[b]
1	**5a** (OBn)	THF	**Ru2** (10)	32 (**6aa**)	>9:1
2	**5a** (OBn)	Acetone	**Ru2** (10)	30 (**6aa**)	>9:1
3	**5a** (OBn)	CH_2Cl_2	**Ru2** (10)	40 (**6aa**)	>9:1
4	**5a** (OBn)	H_2O	**Ru2** (10)	36 (**6aa**)	>9:1
5	**5a** (OBn)	H_2O:THF (8:2)	**Ru2** (10)	71 (**6aa**)	>9:1
6	**5a** (NHTs)	H_2O:THF (9:1)	**Ru2** (5)	56 (**6ab**)	>9:1
7	**5b** (NHTs)	H_2O:THF (8:2)	**Ru2** (5)	99 (**6ab**)	>9:1
8	**5b** (NHTs)	H_2O:THF (9:1)	**Ru2** (5)	68 (**6ab**)	>9:1
9	**5b** (NHTs)	H_2O	**Ru2** (10)	53 (**6ab**)	>9:1
10	**5b** (NHTs)	H_2O:THF (8:2)	**Ru9** (10)	78 (**6ab**)	1:7
11	**5a** (OBn)	H_2O:THF (8:2)	**Ru9** (10)	56 (**6aa**)	1:6

Table 4 Alkene **4a** (0.075 mmol), alkyne **5** (0.075 mmol), solvent (1.0 mL) and **Ru** (X mol%). a) NMR yield using DMSO (0.33 equiv) as Internal Standard. b) Branched (**6**) : linear (**6'**) ratios are shown under parenthesis, determined in the crude reaction mixtures by NMR.

The alkyne **5a** delivers the diene **6aa** in 9:1 branched:linear ratio. However, if we reduce the steric hindrance in the propargylic position, like in the propargyl benzyl ether **4c**, the yield is almost equal (68%), but the selectivity decreases to a branched to linear ratio of 2:1 (**Figure 77**).

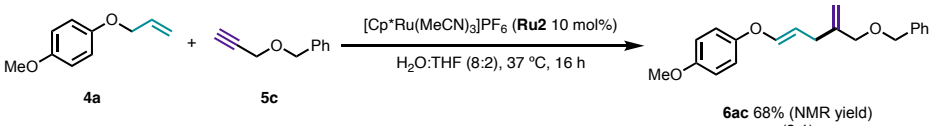

Figure 77. Alkene **4a** (0.075 mmol), alkyne **5c** (0.075 mmol), H_2O:THF (8:2, 1.0 mL) and **Ru2** (10 mol%). NMR yield using $DMSO_2$ (0.33 equiv) as Internal Standard. Branched (**6ac**) : linear (**6ac'**) ratios are shown under parenthesis, determined in the crude reaction mixtures by NMR.

If we suppress the propargylic oxygen but keep the quaternary center, like in **5d**, the selectivity towards the branched is restored to a 9 to 1 ratio (**Figure 78**).

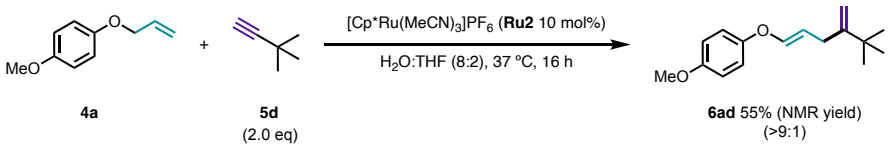

Figure 78. Alkene **4a** (0.075 mmol), alkyne **5d** (0.075 mmol), H_2O:THF (8:2, 1.0 mL) and **Ru2** (10 mol%). NMR yield using $DMSO_2$ (0.33 equiv) as Internal Standard. Branched (**6ad**) : linear (**6ad'**) ratios are shown under parenthesis, determined in the crude reaction mixtures by NMR.

This can be rationalized considering that with a catalysts containing the Cp* ligand, the selectivity relies on the relative stability of two possible ruthenacycles. In the branched path the bulky substituent of the alkyne is further from the metal center than in the linear path, where it is in proximity to the bulky Cp*ligand (**Figure 79**).

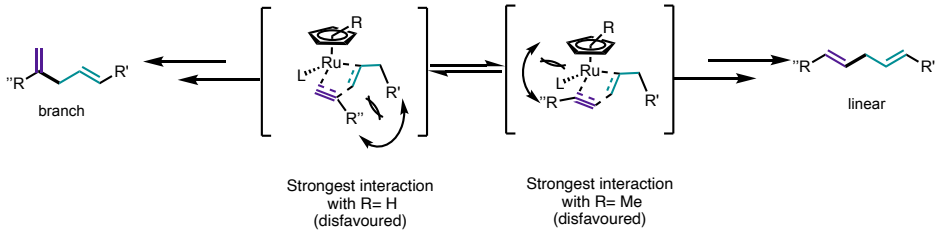

Figure 79. Branched: linear selectivity for Cp and Cp* ligands and as function of the bulkiness of the alkyne.

We next explored the scope of the reaction. The aliphatic diene **6be** can be obtained in 85% yield from the reaction between alkene **4b** and alkyne **5e.** The method is not limited to propargylic ethers and alcohols; thus, tosylpropargyl amides (**5b** and **5f**) are also excellent counterparts leading to full conversions and good selectivities towards their corresponding branched dienes (**6ab** and **6af**). Cyclic propargyl alcohols like **5h** and **5i** also yielded the desired dienes with good yields (90 and 83% isolated yield for **6ah** and **6ai** respectively) and selectivities > 9 :1. Phenyl rings are also tolerated at propargylic substituents, **5j**, so that the reaction of this alkyne with **4a** deliver the expected product (**6aj**) with good yield (76%). Even an internal alkyne, such as **5k**, does engage quite efficiently in the reaction with alkene **4a**, to deliver **6ak** in a moderate 46% yield.

The reaction is not restricted to allyl ethers like **4a**; indeed, different alkenes do undergo the coupling with moderate to good yield: aliphatic alkene **4b** (**6ba**, 59%), homoallylic ether **4c** (**6ca**, 55%),and homoallyl thioether **4d** (**6da**, 79%).

More interesting substrates, such as the *N*-tosyl glycine derivative **4l** (**6al**, 70%), the *o*-allyl tyrosine **4e** (**6eh**, 62%), the glucoside **4f** (**6fa**, 90%) or the commercially available drug mestranol **5m** (**6am**, 67%), do undergo the coupling with the alkene counterpart with good to excellent yields.

The reaction also works with non-propargylic substrates like the aliphatic alkyne **5n,** which upon reaction with **4a** delivers **6an** in 66% yield (3:1 branched : linear), the homopropargyl alcohol **6ao** (83%, 3:1 branched: linear) or even phenyl acetylene, **6ap** (83%, 1:1 branched: linear). However, in these cases, despite the yields are good, the selectivities are poorer than with propargyl alkynes, especially with phenylacetylene, **5p**, which delivers a equimolar mixture of the two regioisomers (**6ap: 6ap'** = 1:1) (**Figure 80**).

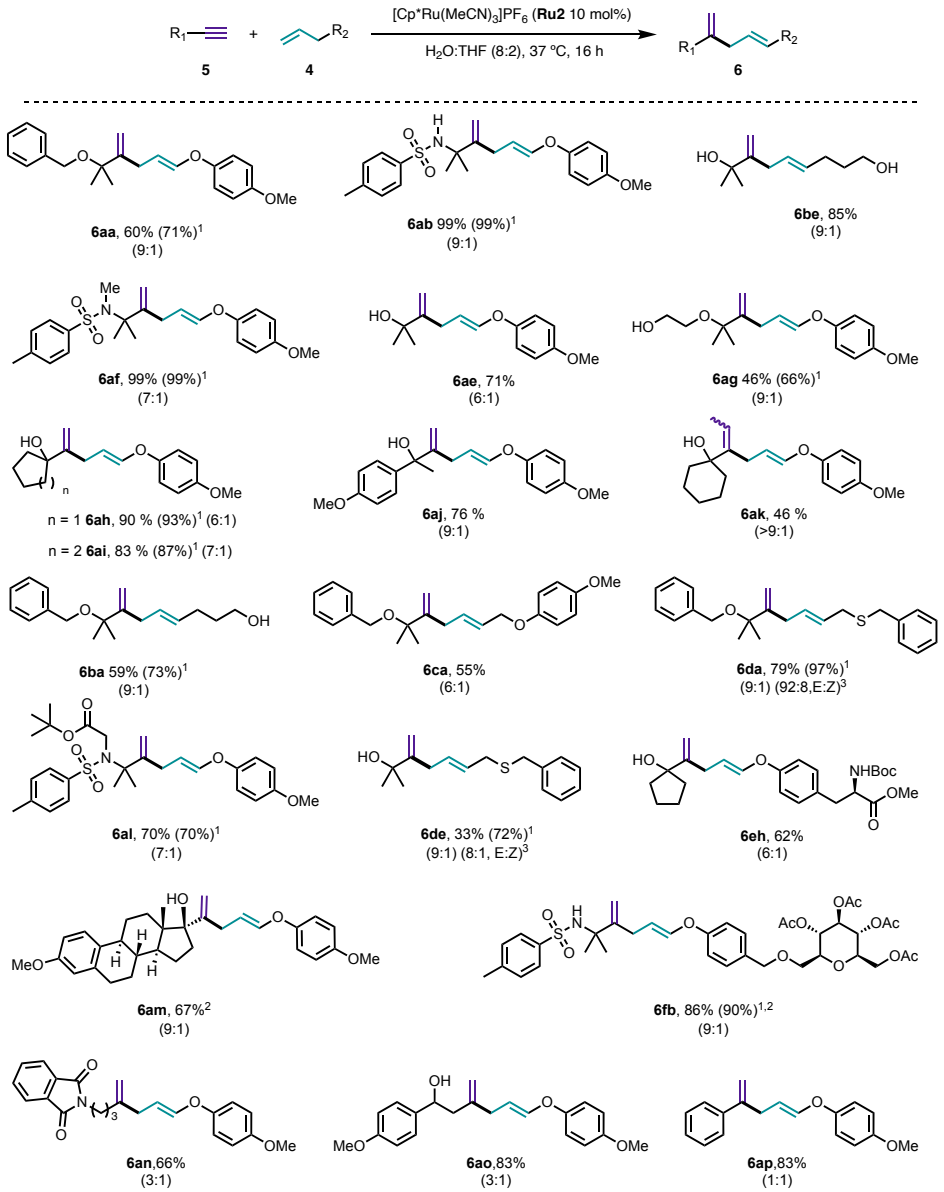

Figure 80. Alkene (**4**, 0.15 mmol), alkyne (**5**, 0.1 mmol), H_2O:THF (8:2, 2.0 mL) and **Ru2** (10 mol%). Only brached structure represented. Branched (**6**) : linear (**6'**) ratios are shown under parenthesis, determined in the crude reaction mixtures by NMR. 1) NMR yield of **6**/**6'** using $DMSO_2$ as internal standard. 2) 2.0 equiv of alkene (0.30 mmol). 3) E/Z ratio determined after purification.

At this point, we also tested the reaction with complex $[CpRu(MeCN)_3]PF_6$ (**Ru9**), containing a Cp instead the Cp* ligand, using the conditions optimized for alkene **4a**. We observed the expected inversion of the regioselectivity towards the linear 1,4-dienes. Thus, with the propargyl ether **5a**, we mainly obtained the linear 1,4-diene in 56% yield

(1:6 branched:linear ratio). With the propargylamide **5b** we got comparable results (78% yield, 1:6 ratio), and even the commercially available mestranol (**5m**) yields the linear product with reasonable selectivity. With alkynes that gave mixtures of regioisomers with **Ru2**, like **5p** and **5n**, we observed low yields, and also mixtures of products (**Figure 81**).

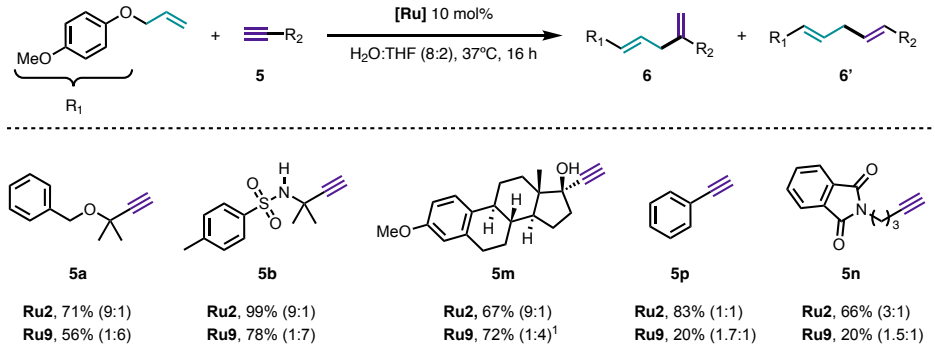

Figure 81. Alkene (0.075 mmol), alkyne (0.075 mmol), H_2O:THF (8:2, 1.0 mL) and **Ru2** or **Ru9** (10 mol%). NMR yield using $DMSO_2$ (0.33 equiv) as Internal Standard. Branched (**6**) : linear (**6'**) ratios are shown under parenthesis, determined in the crude reaction mixtures by NMR. 1) Isolated yield.

3.3 Bioorthogonality

To assess the bioorthogonality of the process, we studied the tolerance of the reaction towards different biological media and additives, using propargyl tosyl amide **5b** and the allyl ether **4a** as model reactants. When the reaction was performed in PBS (phosphate buffer solution 1X. pH =7.4), the corresponding 1,4-diene **6ab** was obtained in a 42% yield. On the contrary, the use of DMEM as solvent did not significantly affect the efficiency of the reaction, so that **6ab** was obtained in an excellent 90% yield. On the other hand, when the reaction was carried out in a more challenging cell culture media, such as DMEM* (DMEM + 10% of Feta Bovine Serum + 1% of antibiotics) the product was still obtained in 30% yield. This result is particularly relevant because the Fetal Bovine Serum is a cocktail of hormones, lipids, binding and transferring proteins, which makes the 30% yield a rather good result.

In relation to additives, we tested different biomolecules using 0.1 equiv and 1.0 equiv, with respect to the starting materials. Thiol-containing compounds such as cysteine or GSH exerted a similar effect, regardless of using either 0.1 or 1.0 equiv, affording the 1,4-diene **6ab** with yields around the 60% level. The addition of 0.1 equiv of an amino acid like Tyrosine, for instance, did not significantly affect the effectiveness of the process, leading to **6ab** in an excellent 87% yield. Increasing ten times the amount of

tyrosine to 1.0 equiv only had a marginal effect, so the product could still be obtained in a good 68% yield. Other additives, such as glucose, do not affect the yield when using 0.1 equiv or 1 equiv. Likewise, the use of 0.1 equiv of Riboflavin, a complex molecule which is part of the flavin mononucleotide (FMN) and flavin adenine dinucleotide (FAD) cofactors, did not affect the reactions (99% yield of **6ba**), while the use of 1.0 equiv was still compatible with the alkene-alkyne coupling (46% yield) (**Figure 82**).

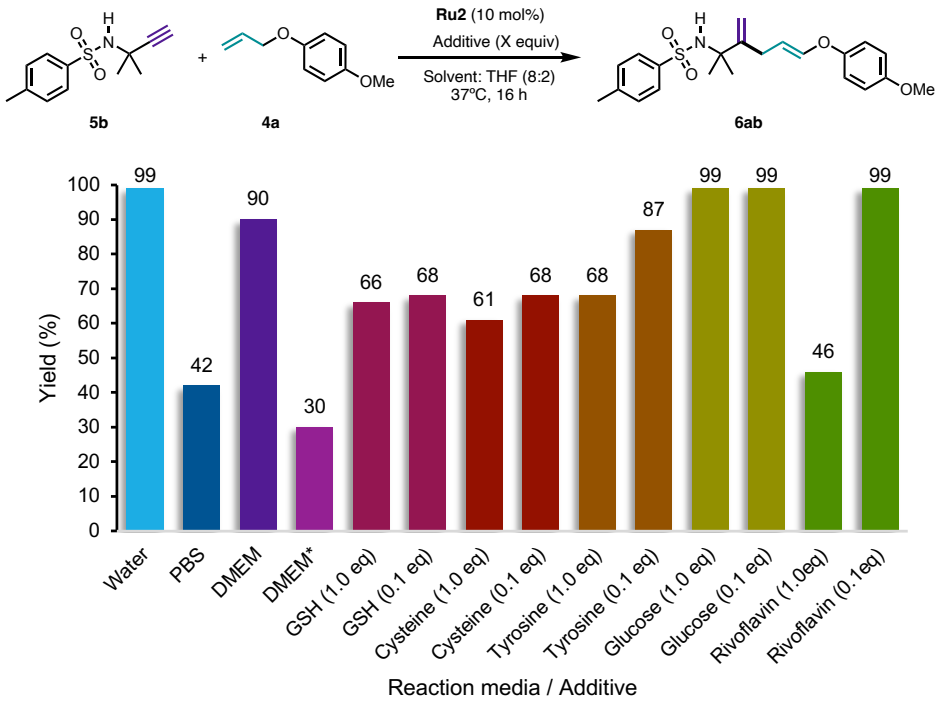

Figure 82. Alkene (**4**, 0.075 mmol), alkyne (**5**, 0.075 mmol), solvent:THF (8:2, 1.0 mL) and **Ru2** (10 mol%). DMEM = Dulbecco's Modified Eagle Medium; DMEM* = DMEM + 10 Fetal Bovine Serum + 1% Antibiotics. NMR yield using $DMSO_2$ (0.33 equiv) as Internal Standard

Overall, to put into perspective the observed bioorthogonality, it is important to consider that in these experiments the concentration of the additive ranged from 7.5 mM to 75 mM, concentration levels much higher than those typically encountered in a biological media, under physiological conditions. On the other hand, the amount of additive with respect to the catalyst varied from 1 to 10 equivalents. Thus, despite the potential ability of many of these additives to coordinate a cationic and highly unsaturated complex like **Ru2**, good efficiencies with yields that ranged from 40% to 90% were obtained. Therefore, taking into account these data and those of other biocompatible Ru-catalyzed

reactions, we can consider the present process to be amongst the ruthenium-catalyzed processes with the highest levels of bioorthogonality.

3.4 Modification of amino acids and peptides

With such good bioorthogonality profiles, we then wondered whether the alkene-alkyne cross coupling could be employed to modify aminoacids and short peptides equipped with appropriate alkene or alkyne handles. Therefore, we first synthetized the two di-peptides indicated in **Figure 83**, one with the alkyne in the side chain (**7a**) and the other with this unit at the *N*-terminus (**7b**, **Figure 83**).

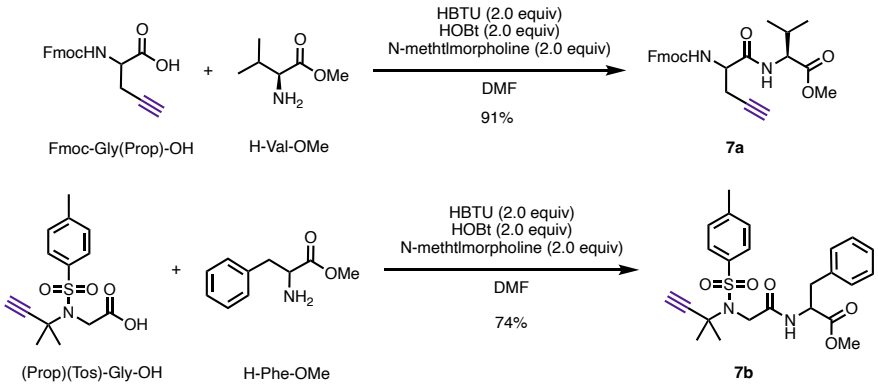

Figure 83. Reaction scheme for the synthesis of the corresponding dipeptides.

We studied the alkene-alkyne coupling of dipeptide **7a** at 75 mM, ith alkene **4a** and, gratifyingly, we could obtained the product **8aa** in 90% yield (3:1 branched:linear ratio). The coupling between peptide **7b** and allyl ether **4a** gave the diene **8ab** in a moderate 40% yield and with a good 9:1 branched:linear ratio (**Figure 83**).

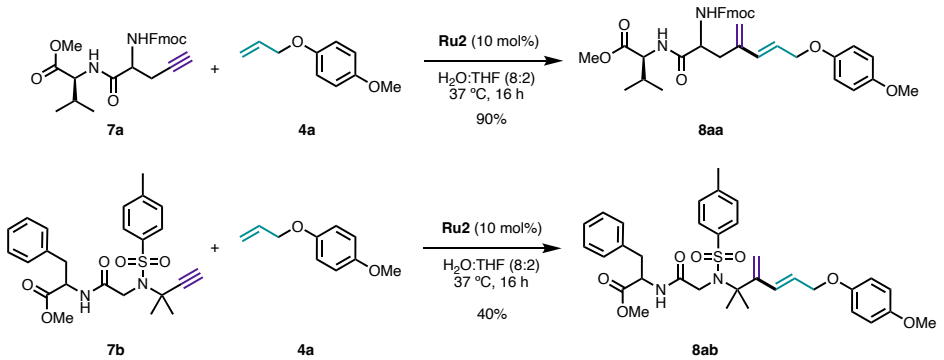

Figure 84. Alkene (0.15 mmol), alkyne (0.15 mmol), H_2O:THF (8:2, 2.0 mL) and **Ru2** (10 mol%).

We then moved to more complex peptides such as **7c**, which was assembled by solid phase peptide synthesis on a rink-amide resin (**Figure 85**).

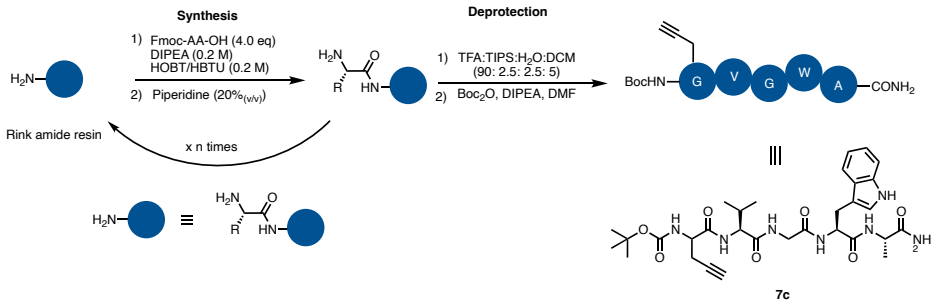

Figure 85. General scheme for the synthesis of peptide **7c**.

For our initial conjugation experiments, we used more diluted solutions of the peptide **7c**, below the previously optimized 75 mM conditions, in particular ranging from 1 to 20 mM. We also tested different equivalents of the allylether **4a** (from 1.0 to 10 equiv) and several amounts of **Ru2** (from 10 to 100 mol%). Reactions were analyzed by HPLC-MS.

Unfortunately, we could not detect appreciable amounts of the desired product. We observed the deallylation of allylether **4a**, to yield the free *p*-methoxyphenol.[178] Probably, as the alkene-alkyne coupling involve the concomitant participation of three species (alkyne, alkene and Ru complex), it is disfavored at high dilution compared to the deallylation reaction, which just involves two species.

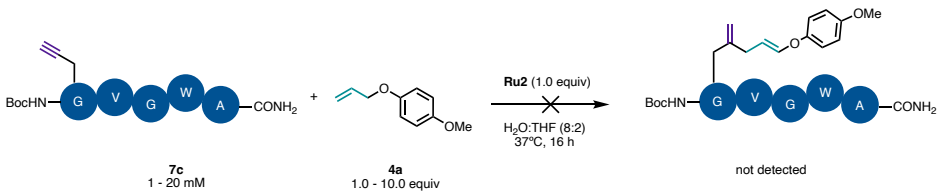

Figure 86. Reaction scheme for the peptide **7c** modification.

By ESI-MS we could detect a molecular ion which might correspond to a putative ruthenium arene sandwich complexes bearing the allyl ether **4a**, as well as other complex wherein the [Cp*Ru]$^+$ unit is coordinated to the deallylated product, *p*-methoxyphenol (**Figure 87**). The coordination of ruthenium to arene rings is well known, and it has been also reported the formation of complexes with phenylalanine and tyrosine residues in small peptides under aqueous conditions.[179,180]

[178] H. Saburi, S. Tanaka, M. Kitamura, *Angew. Chem. Int. Ed.* **2005**, *44*, 1730–1732.
[179] D. S. Perekalin, A. R. Kudinov, *Coordination Chemistry Reviews* **2014**, *276*, 153–173.
[180] D. S. Perekalin, E. E. Karslyan, P. V. Petrovskii, Y. V. Nelyubina, K. A. Lyssenko, A. S. Kononikhin, E. N. Nikolaev, A. R. Kudinov, *Chem. Eur. J.* **2010**, *16*, 8466–8470.

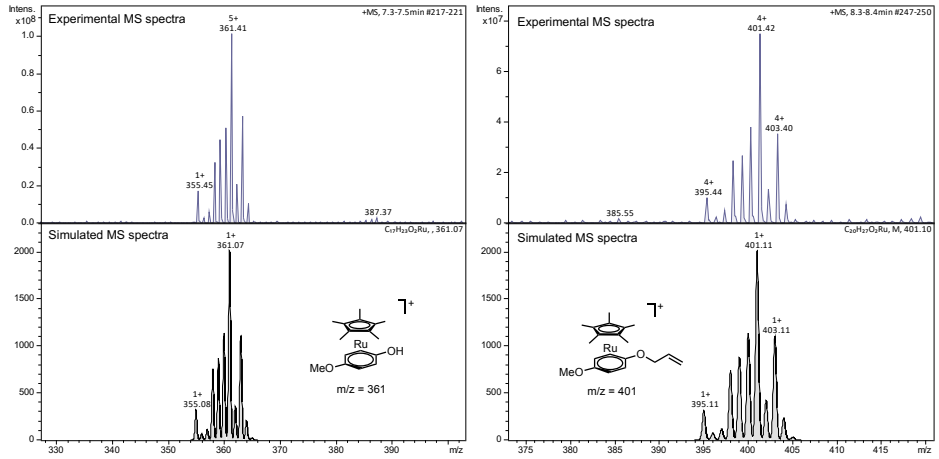

Figure 87. Experimental and simulated MS spectra for a) [Cp*Ru(*p*-methoxyphenol)]+ and b) [Cp*Ru(1-(allyloxy)-4-methoxybenzene)]$^{+}$.

The failing of this peptide-alkene coupling led us to apply concepts of Design of Experiments (statistical optimization of multivariable systems) to try to optimize the reaction. We selected peptide **7c** and the homoallyl thioether **4d,** that gives good yields (see scope in **page 100**) and does not bear a leaving group in the allylic position. We fixed the reaction media {H_2O:THF (8:2)}, the reaction time (24 h) and the temperature (37 ºC) and screened different combinations with regard to the concentration of peptide, the alkene and ruthenium catalyst, analyzing the efficiency of the process by HPLC-MS (**Table 5**).

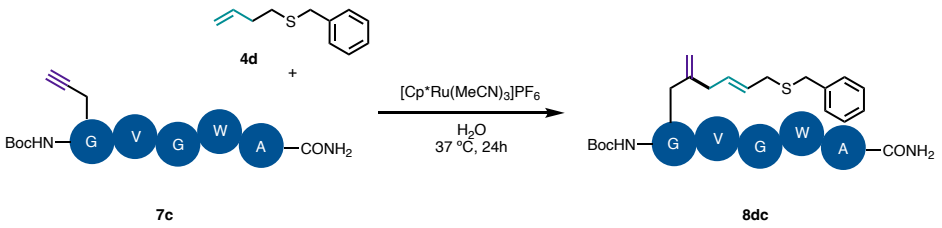

	Ru (mM)	*Peptide (mM)*	*Alkene (mM)*
-1	5.0	1.0	10
0	0.5	0.5	0.5
+1	0.05	0.1	0.1

Table 5. Optimization matrix for the alkene-alkyne coupling between peptide **7c**, and alkene **4d.**

Ideally, we should be able to calibrate a response towards these different conditions, and with that response determine the interaction between variables for a next round optimization. However, the process has multiple outcomes and it proved difficult to compute a response. Nonetheless, we did obtain some clues. The reaction using **Ru2** (0.05 mM), peptide **7c** (0.1 mM) and alkene **4d** (0.1 mM) led to a ~20% conversion of **7c** to the desired conjugate (**Figure 88**).

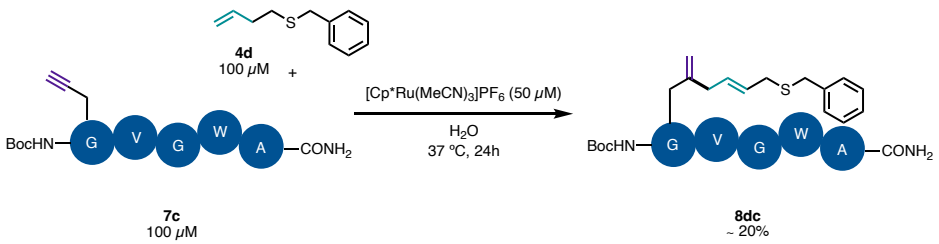

Figure 88. Modification of peptide **7c**

Using these micromolar concentrations we were able to rapidly screen for conditions. 200 µM of peptide **7c**, 5 equiv of homoallylthioether **4d** and 2 equiv of **Ru2** were found optimal for maximizing product formation. We had full conversion of starting peptide **7c**, gratifyingly we also detected the product and a small peak that corresponds to the complexation of the $[Cp^*Ru]^+$ fragment to this product (**Figure 89**). Based on the accumulated experience, we proposed this product to be the branched adduct.

HPLC MS data let us see that the excess of alkene works as a ruthenium scavenger, so that we detected different complexes that correspond to the coordination of **4d** to the Cp*Ru moiety, also including the mono and bis sulfur-oxidized species (possibly sulfoxides and sulphone), which might be formed in situ (**Figure 89**).

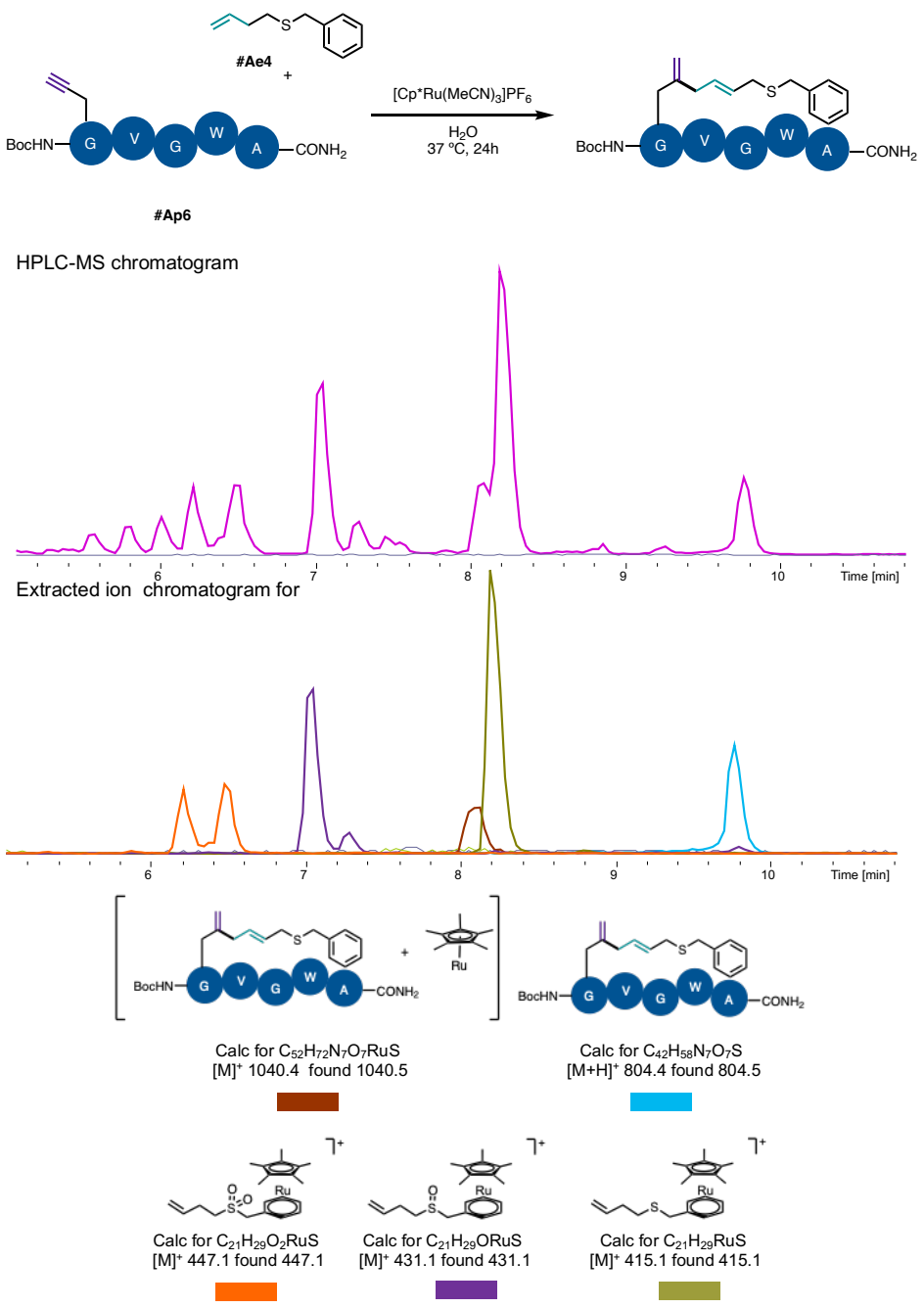

Figure 89. Alkene-alkyne coupling between **7c** and **4d**, and HPLC-MS analysis of the reaction.

More experiments regarding longer peptides and other alkene functionalities are planned to expand the scope of the peptide modification and to test the limits of this transformation.

4 Conclusions

We have demonstrated the viability of inducing intermolecular alkene-alkyne couplings under aqueous conditions at 37 ºC using $[Cp^*Ru(MeCN)_3]PF_6$ as catalyst. Alkynes bearing bulky groups in the propargylic position are especially selective toward the branched product, allowing to modify a broad variety of molecules including glucosides, amino acids and drugs with good selectivities.

The branched:linear selectivity can be switched towards the linear product changing the catalyst to $[CpRu(MeCN)_3]PF_6$ and using as substrate tertiary propargyl alcohols, ethers or amides.

The reaction is tolerant to a broad variety of biomolecular additives and reaction media, therefore presenting a very good bioorthogonality. We also present preliminary data that confirms that the reaction allows for the selective modification of amino acids, and small peptides under aqueous conditions, even at concentrations of100 μM.

Chapter III: Isomerization of allylic alcohols in biological settings[181]

[181] This chapter includes work published Journal of the American Chemical Society as: Ruthenium-Catalyzed Redox Isomerizations inside Living Cells. C. Vidal, M. Tomás-Gamasa, A. Gutiérrez-González, J. L. Mascareñas, *J. Am. Chem. Soc.* **2019**, *141*, 5125–5129.

1 Introduction

Ruthenium catalysis is not limited to bond forming and bond-cleaving reactions, such as those described in the first two first chapters. Ruthenium-based catalysts have also been shown to promote isomerization reactions, which are of high interest in synthetic chemistry. Isomerization reactions are also common in Nature and promoted by different type of biocatalysts.

1.1 Isomerization processes in nature. Isomerases

Isomerization reactions include a broad spectrum of processes wherein a molecule is transformed into another one of same molecular formula. If the molecule has a different connectivity between the atoms, the isomers are called constitutional isomers (e.g., regioisomers, tautomers and skeletal isomers), whereas if they have the same connectivity but differ on the three dimensional disposition of one or more of their atoms in the space are called stereoisomers. These latter include diastereoisomers, *cis-trans* isomers, and enantiomers, in the particular case in which the two isomers are non-superposable mirror images.

In nature, isomerization reactions play a fundamental role in metabolism, as isomers usually differ in their biological activity, as in the infamous example of the thalidomide enantiomers (**Figure 90a**).[182] Enzymes that catalyze the interconversion of species with the same molecular formula belong to the family of *isomerases*, a relatively small class of enzymes which catalyze unimolecular reactions that range from simple epimerizations to more complex skeletal rearrangements between constitutional isomers.[183,184]

Despite representing only a 4% of the total enzymes, they play a central role in biology.[185] For instance, glutamate-racemase (MurI) epimerizes L-glutamate, one of the 20 natural amino acids, into D- glutamate, which is involved in cell wall formation in bacteria. Prostaglandins- D synthase is involved in the biosynthesis of prostaglandin D_2 by the regioselective aperture of the 1,2-dioxalane ring of the epi-dioxyprostraglanding-D_2 (**Figure 90b**).

[182] J. H. Kim, A. R. Scialli, *Toxicological Sciences* **2011**, *122*, 1–6.
[183] Y. Asano, K. Hölsch, in *Enzyme Catalysis in Organic Synthesis* (Eds.: K. Drauz, H. Gröger, O. May), Wiley, **2012**, pp. 1607–1684.
[184] S. Martínez Cuesta, S. A. Rahman, J. M. Thornton, *Proc. Natl. Acad. Sci. U.S.A.* **2016**, *113*, 1796–1801.
[185] According to The Enzyme Database, there are 310 isomerases described in literature, of a total of 6674 different enzymes A. G. McDonald, S. Boyce, K. F. Tipton, *Nucleic Acids Research* **2009**, *37*, D593–D597.

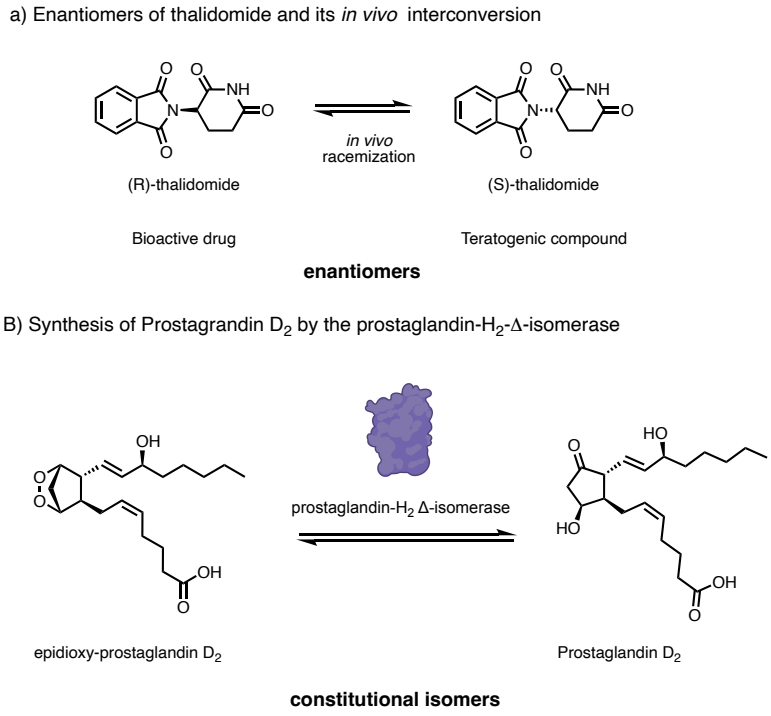

Figure 90.a) R and S thalidomide. b) Prostaglandins- D synthase catalyzed the synthesis of Prostaglandin D_2

1.2 Metal-catalyzed isomerizations. The case of allylic alcohols

A variety of late transition metal complexes can promote different type of isomerizations in substrates bearing unsaturated moieties. A number of mechanistic possibilities have also been disclosed. [186] The metal-catalyzed isomerization of allylic alcohols to the corresponding saturated ketones is especially appealing, as it represents an atom economical shortcut over the two-step process involving oxidation and reduction reactions (**Figure 91**).

[186] F. Scalambra, P. Lorenzo-Luis, I. de los Rios, A. Romerosa, *Coord. Chem. Rev.* **2019**, *393*, 118–148.

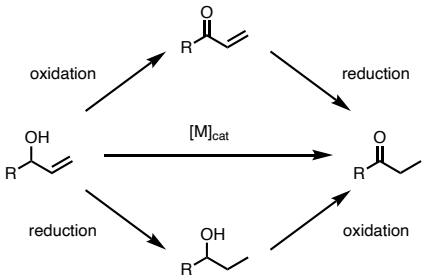

Figure 91. General scheme for the catalytic isomerization of allylic alcohols and for the stepwise oxidation / reduction process.

Several late transition metals have been used to promote the isomerization of allylic alcohols, with Ru,[187] Rh[187] and Ir[188] being the most representative. The reaction is typically performed in organic solvents, or under biphasic conditions with organometallic catalysts containing water-soluble ligands (**Figure 92**).

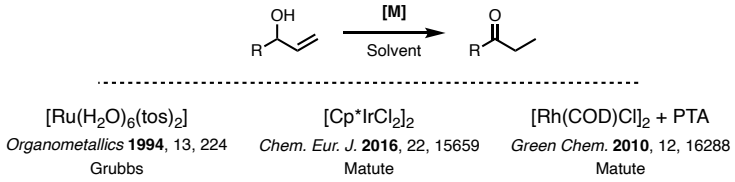

Figure 92. Examples of transition metal catalyzed isomerization of allylic alcohols

From a mechanistic perspective, there are three different proposals: **a**) starting with a metal hydride complex ([M]-H), a metal-alkyl complex is formed after migratory insertion of the double bond into the M-H bond, which is followed by a regioisomeric β-hydride elimination to regenerate the metal-hydride catalyst while delivering an enol intermediate that eventually tautomerizes to the ketone; **b**) the metal complex coordinates to the double bond and there is an allylic C-H activation to form a metal-hydride π-allyl complex which, upon reductive elimination, yields the enol intermediate, and **c**) the metal reacts with the hydroxy group to give an alkoxo-metal complex; there is now a β-hydride elimination / insertion sequence to yield an π-oxo-allyl complex, that after protonation releases the enol and the regeneration of the catalyst.[189]

[187] N. Ahlsten, H. Lundberg, B. Martín-Matute, *Green Chem.* **2010**, *12*, 1628.
[188] E. Erbing, A. Vázquez-Romero, A. Bermejo Gómez, A. E. Platero-Prats, F. Carson, X. Zou, P. Tolstoy, B. Martín-Matute, *Chem. Eur. J.* **2016**, *22*, 15659–15663.
[189] A. Varela-Álvarez, J. A. Sordo, E. Piedra, N. Nebra, V. Cadierno, J. Gimeno, *Chem. Eur. J.* **2011**, *17*, 10583–10599.

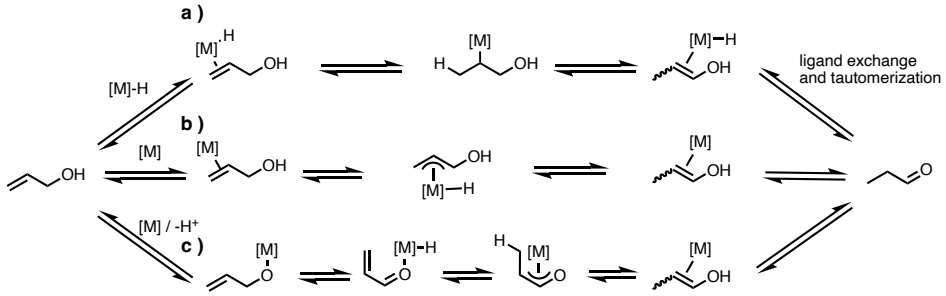

Figure 93. Main mechanisms described for the isomerization of allylic alcohols,

Whereas many isomerization processes have been described in organic solvents, in 1994 Grubbs and coworkers demonstrated that this reaction involving metal-hydrides intermediates was possible under fully aqueous conditions, using the ruthenium (II) complex $Ru(H_2O)_6(tos)_2$ (**Figure 94**). [190]

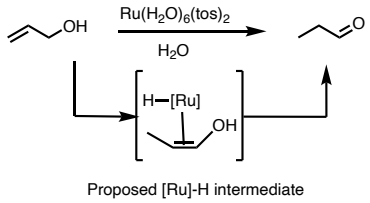

Figure 94. $Ru(H_2O)_6(tos)_2$ catalyzed isomerization of allylic alcohol in water

Other groups have further studied this type of isomerization reactions. For instance, in 2006 Gimeno and coworkers reported the use of ruthenium (IV) bis-allylic complexes for the isomerization of allylic alcohols in aqueous media, and that exhibits excellent Turnover Numbers (TONs) and Turnover Frequencies (TOF) (**Figure 95**).[191]

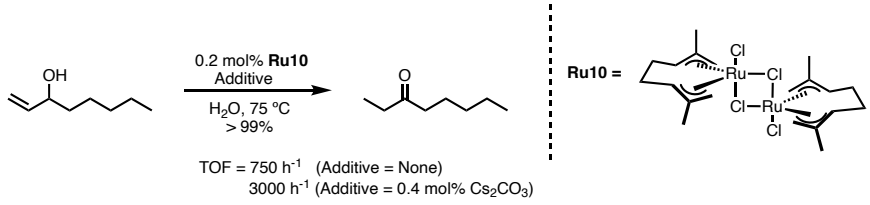

Figure 95. Isomerization of allylic alcohols by a ruthenium (IV) complex

Monomeric ruthenium complexes have also been demonstrated to promote the isomerization.[192] A remarkable example is the complex **Ru11**, that was applied for a

[190] D. V. McGrath, R. H. Grubbs, *Organometallics* **1994**, *13*, 224–235.
[191] V. Cadierno, S. E. García-Garrido, J. Gimeno, A. Varela-Álvarez, J. A. Sordo, *J. Am. Chem. Soc.* **2006**, *128*, 1360–1370.
[192] J. Gimeno, P. Crochet, S. Garcia-Garrido, V. Cadierno, *COC* **2006**, *10*, 165–183.

tandem ruthenium isomerization / enantioselective reduction process (using a ketoreductase).

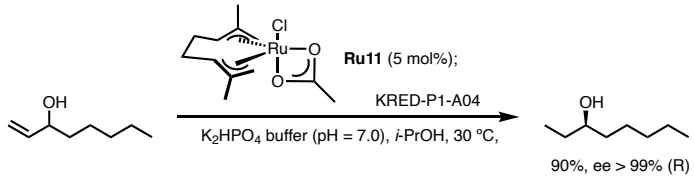

Figure 96. Tandem ruthenium catalyzed isomerization of allylic alcohols, ketoreductase enantioselective reduction.

Worth to note, related positional isomerizations of double bonds can also be performed in nature by specific isomerases, [193] but work through very different mechanisms relying on proton transfer processes (**Figure 97**).

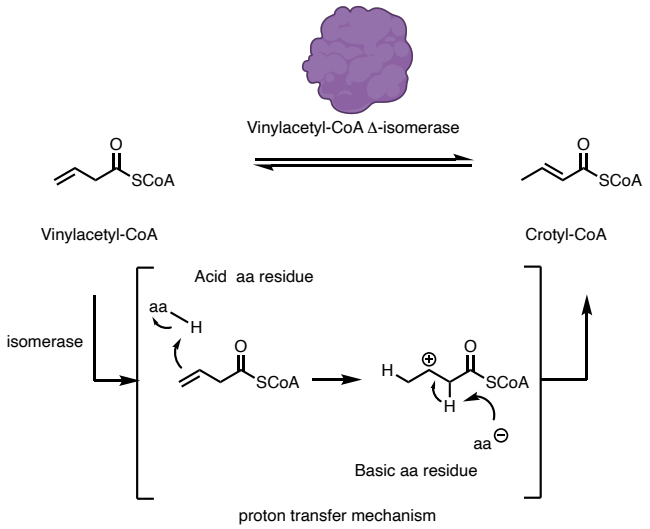

Figure 97. Positional double bond isomerization of Vinylacetyl-CoA to Crotyl-CoA by and isomerase.

Considering the synthetic and biological significance of this type of isomerizations, it is intriguing and though-provoking to know if metal-promoted processes could also be implemented in biological settings, as an artificial alternative to natural isomerases. Considering that metal hydrides have been sporadically used for biological applications, isomerization mechanisms involving metal hydrides might be viable.

[193] Isomerases enzyme with Enzyme Commission number EC 5.3.3.X are involved in double bond transposing activity. BRENDA enzyme database https://www.brenda-enzymes.org/

1.3 Metal-hydrides in bioorthogonal chemistry

Natural cofactors like nicotinamide adenine dinucleotide (NADH) and its phosphate variant (NADPH) can promote the reduction of carbonyl and imine substrates (ketoreductases) or in the reversed oxidation processes (e.g., dehydrogenases of alcohols and amines), in reactions that entail hydride transfer processes.[194,195]

In recent years there have been several reports aimed at mimicking this type of redox processes but using *in situ* generated metal hydrides. Pioneer examples by Sadler involved organometallic catalysts based on ruthenium {[(η^6-arene)Ru(en)]PF_6, en = ethylenediamine}, which were able to promote the reduction of the NAD+ nucleotide to its corresponding reduced derivative, NADH, using sodium formate as hydride source under physiological conditions (aqueous conditions, pH =7.2, 37 ºC).[196] Later, the same group translated this reaction to living cancer cells (A2780 cells) replacing the ethylenediamine ligand for N-tosyl ethylenediamine and with external supplementation of sodium formate to control the physiological levels of NAD+ and therefore, the reductive stress of the cell (**Figure 98a**).[197,198]

In 2018 Sadler reported a related example in which the hydride transfer takes place in an enantioselective fashion. In this case, the authors used a chiral osmium catalyst, instead of the putative ruthenium derivative, which allows to asymmetrically reduce pyruvate to D or L lactate, as function of the chirality of the metal complex, using sodium formate as hydride source in A2780 cells (**Figure 98b**). The process allows the modification of lactate in living cancer cells; however, it also causes the death of the cancer cells, due to reductive stress.[199] The use of formate allows to reduce the original complex to generate the metal-hydride (**Figure 98c**).

[194] J. Gębicki, A. Marcinek, J. Zielonka, *Acc. Chem. Res.* **2004**, *37*, 379–386.
[195] N. Archipowa, R. J. Kutta, D. J. Heyes, N. S. Scrutton, *Angew. Chem. Int. Ed.* **2018**, *57*, 2682–2686.
[196] Y. K. Yan, M. Melchart, A. Habtemariam, A. F. A. Peacock, P. J. Sadler, *J. Biol. Inorg. Chem.* **2006**, *11*, 483–488.
[197] S. Betanzos-Lara, Z. Liu, A. Habtemariam, A. M. Pizarro, B. Qamar, P. J. Sadler, *Angew. Chem. Int. Ed.* **2012**, *51*, 3897–3900.
[198] J. J. Soldevila-Barreda, I. Romero-Canelón, A. Habtemariam, P. J. Sadler, *Nat Commun* **2015**, *6*, 6582.
[199] J. P. C. Coverdale, I. Romero-Canelón, C. Sanchez-Cano, G. J. Clarkson, A. Habtemariam, M. Wills, P. J. Sadler, *Nature Chem* **2018**, *10*, 347–354.

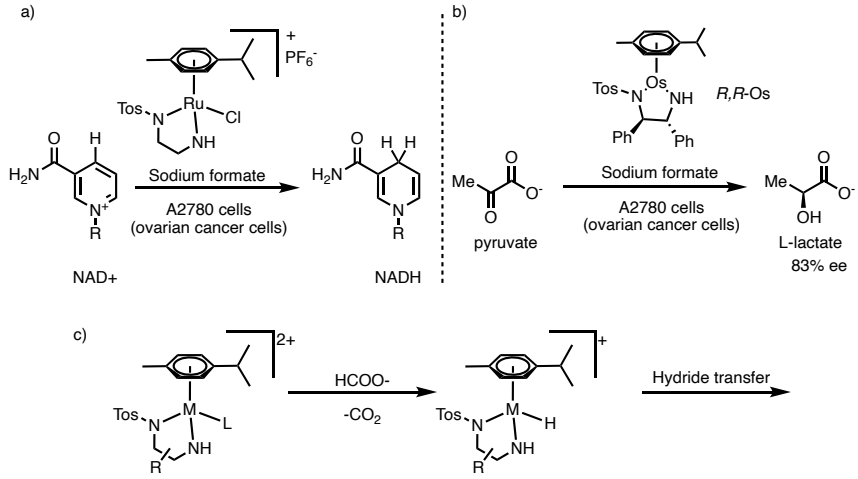

Figure 98. a) Reduction of NAD+ promoted by a ruthenium complex in A2780 cells. b) Osmium catalyzed enantioselective reduction of pyruvate in A2780 cells. c) Proposed metal-hydride intermediate for the reduction of carbonyls in biological environments

In 2017, Do reported an iridium promoted reduction of aldehydes inside living mouse embryo fibroblast cells (NIH-3T3 cells).[200] In this case, the authors employed a Cp* iridium complex {[Cp*IrCl(L)], L = N-phenylpicolamide} which in presence of the natural levels of NADH of these fibroblast cells is reduced to the active iridium hydride species of type **II** (**Figure 99**). The reduction of a BODIPY-derived aldehyde was claimed to be accomplished with the iridium catalyst inside living cells. However, the efficiency of the reaction seems to be low, obtaining just 1.6-fold increase in the fluorescence for the process against the controls, whereas in the original report, the reduced probe is five times more fluorescent that the aldehyde.

These examples showcase the potential of metal complexes to promote reactions that involve highly reactive metal-hydrides. However, they also suffer from the need of high amounts of external reductants (usually over 10 equiv), low yield under *in cellulo* conditions if no external reductant is used, and cell death by reductive stress.

[200] S. Bose, A. H. Ngo, L. H. Do, *J. Am. Chem. Soc.* **2017**, *139*, 8792–8795.

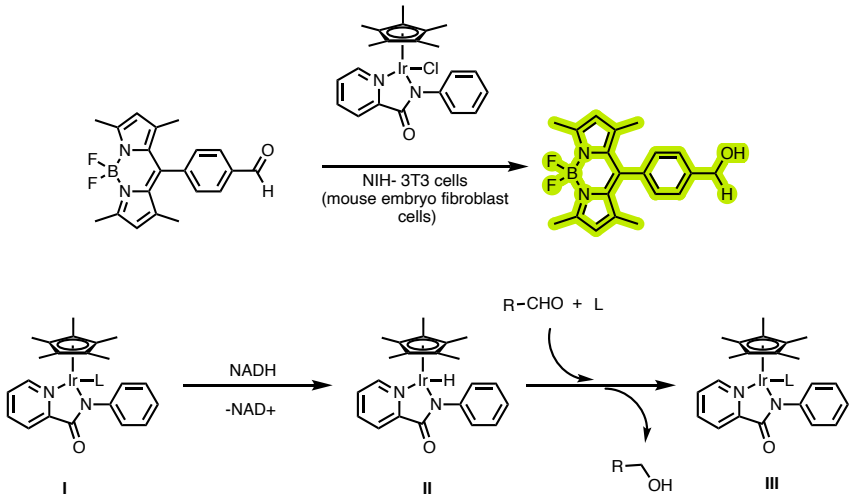

Figure 99. Reduction of a BODIPY aldehyde probe by a Iridium (I) complex in NIH-3T3 cells by Do and coworkers

2 Objectives

Considering the precedents on the ruthenium-promoted isomerization reactions, especially of allylic alcohols, and their excellent TONs and water compatibility, we reasoned that the reaction could fulfil the requirements of bioorthogonality. Additionally, and based the precedents on the use of metal hydrides in biological settings and even in cells, it seemed reasonable to us to predict that the isomerization process could be translated to living cells. From the perspective of developing a biocompatible process, a hypothetical isomerization of allylic alcohols would not deplete natural occurring reducing agents of cells, such as NAD+ and NADP+, [198,199] owing to its redox neutral characteristics.

On this grounds, we set as objective the development of a bioorthogonal Ru-catalyzed isomerization of allylic alcohols to their corresponding ketones and its translation to different biological media and live mammalian cells.

3 Results and Discussion

3.1 Viability in Biorelevant Media and Bioorthogonality[201]

Among the different ruthenium catalysts used for promoting the isomerization of allylic alcohols, we selected the complex [Ru(η^3:η^3-bis-allyl)(OAc)Cl] (bis-allyl = 2,7-dimethylocta-2,6-diene-1,8-diyl, **Ru11**) as it has already been reported to be very efficient in the isomerization of allylic alcohols in aqueous buffers. [202] Moreover, this Ru complex is easily accessible in two steps from $RuCl_3 \cdot nH_2O$.[203] $RuCl_3 \cdot nH_2O$ was heated to 60 ºC in 2-methoxyethanol with excess of isoprene (30 equiv, sealed tube for 3 days), yielding a pink solid identified as the bis-allyl ruthenium dimer **Ru10**. This complex was then treated with silver acetate in acetone to directly yield the desired complex **Ru11** in 60% yield (**Figure 100**).

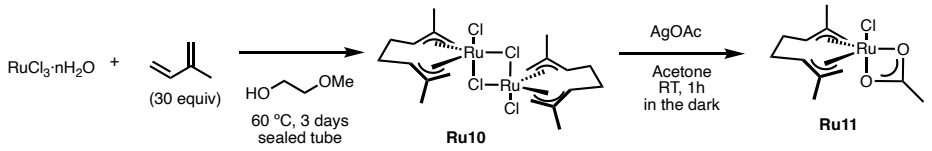

Figure 100 Synthesis of [Ru(η^3:η^3-bis-allyl)(OAc)Cl], **Ru11.**

The viability of the isomerization was first explored using 1-phenylprop-2-en-1-ol (**9a**) as substrate. The reaction is very efficient in water and PBS at physiological temperatures (37 °C), using just 2 mol% of **Ru11**, to give the propiophenone **10a** in 99% yield after 2 h (**Table 6, entry 1**). The reaction is also efficient in DMEM, although it required to slightly increase the amount of catalyst up to 4 mol (87% yield, after 4h, **entry 2**). Importantly, the use of a DMEM* (DMEM* +10% Fetal Bovine Serum + 1% antibiotics) as reaction media, or even Hela cell lysates, was not detrimental for the reaction. Indeed, we could obtain yields over 85% (**entries 3** and **4**)

[201] The experiments in this section were carried out in collaboration with Dr. Cristian Vidal Vides
[202] N. Ríos-Lombardía, C. Vidal, M. Cocina, F. Morís, J. García-Álvarez, J. González-Sabín, *Chem. Commun.* **2015**, *51*, 10937–10940.
[203] B. Kavanagh, J. W. Steed, D. A. Tocher, *J. Chem. Soc., Dalton Trans.* **1993**, 327.

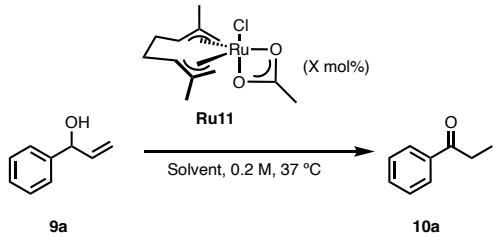

Entry	**Ru11** X mol%	Time (h)	Solvent	Yield (%)
1	2 mol%	2	PBS	99
2	5 mol%	4	DMEM	85
3	5 mol%	6	DMEM*	86
4	5 mol%	4	HeLa lysates	86

Table 6. Allylic alchol **9a** (0.2 mmol), milieu (1.0 mL) and **Ru11** (X mol%). DMEM = Dulbecco's Modified Eagle Medium; DMEM* = DMEM + 10 Fetal Bovine Serum + 1% Antibiotics; HeLa lystes 7 mg/mL.

Therefore, the bis-allylic ruthenium complex **Ru11** proved to be as a very good candidate to further study the viability of the reaction in biologically relevant media and particularly in cellular settings.

3.2 Comparison with other reported isomerization catalysts [204]

To check whether the ruthenium complex **Ru11** was the most active catalyst for the isomerization of allylic alcohols such as **9a**, we compared its performance with that of other related ruthenium and iridium complexes previously used in related isomerization reactions in water and in organic solvents. The comparison was carried out in in PBS, as well as in cell lysates, to validate their capabilities under biologically relevant conditions.

$[RuCl_2(p\text{-cymene})]_2$ (**Ru12**) provided a neglectable yield in PBS after 2h but, curiously, a modest 36% yield in cell lysates after 24h (**Table 7**, **entries 3**, **4**). The use of $[Cp^*Ru(MeCN)_3]PF_6$ (**Ru2**), which proved to be very efficient for the reactions studied in the first two chapters, led to moderate yields in both reaction media (62% in PBS and 56% in Lysates, **entries 5, 6**). Its neutral counterpart, [Cp*RuCl(COD], does not work efficiently under PBS (7%, **entry 7**) and with moderate yield under cell lysates (40% yield (**entry 8**). The iridium catalyst used by Do for the reduction of carbonyls, bearing a *N*-phenylpicolinamide ligand, **Ir2,** does not work in PBS, neither under our conditions or under those reported in the original article for the reduction reaction (**entries 8 and 9**).

[204] The experiments in this section were carried out in collaboration with Dr. Cristian Vidal Vides

The dimer [Cp*IrCl]$_2$ (**Ir3**) reported by Martín Matute as efficient complex for isomerizations under aqueous conditions (**entry 10**) did show some activity, but the desired ketone was obtained in low yields (8% in PBS and 3% in cell lysates) (**entries 11 and 12**). Therefore, we can conclude that ruthenium complexes are by far the most active for this process and in particular, the bis-allylic ruthenium complex **Ru11** is the one that provides better yields in our model reaction.

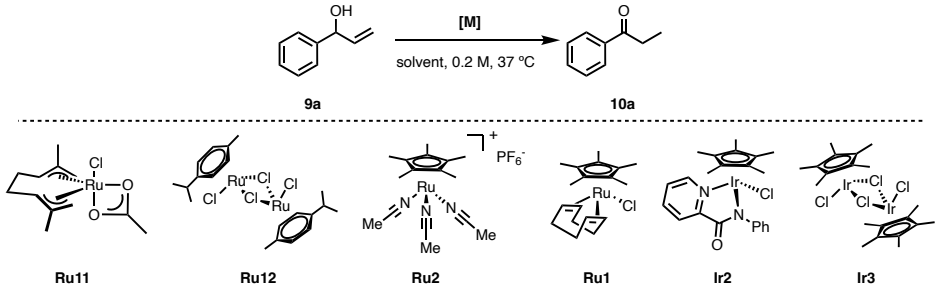

Entry	[M] (X mol%)	*Solvent*	Time (h)	*Yield*[d] *(%)*
1	[Ru(η^3:η^3-bis-allyl)(OAc)Cl], **Ru11** (2 mol%)	PBS	2	99
2	[Ru(η^3:η^3-bis-allyl)(OAc)Cl], **Ru11** (5 mol%)	Lysates[b]	4	86
3	[RuCl$_2$(*p*-cymene)]$_2$, **Ru12** (1 mol%)	PBS	2	0
4	[RuCl$_2$(*p*-cymene)]$_2$, **Ru12** (1 mol%)	Lysates[b]	24	36
5	[Cp*Ru(MeCN)$_3$]PF$_6$, **Ru2** (2 mol%)	PBS	6	62
6	[Cp*Ru(MeCN)$_3$]PF$_6$, **Ru2** (10 mol%)	Lysates[b]	24	56
7	[Cp*RuCl(COD)], **Ru1** (2 mol%)	PBS	2	7
8	[Cp*Ru(COD)], **Ru1** (10 mol%)	Lysates[b]	24	40
9	[Cp*IrCl(L)],[c] **Ir2**, (2 mol%)	*t*-BuOH:PBS (2:8)	16	0
10	[Cp*IrCl(L)],[c] **Ir2**, (5 mol%)	PBS	16	0
11	[Cp*IrCl$_2$]$_2$, **Ir3**, (1 mol%)	DMEM	16	8
12	[Cp*IrCl$_2$]$_2$, **Ir3**, (2.5 mol%)	Lysates[b]	16	8

Table 7. a) Allylic alcohol **9a** (0.2 mmol), milieu (1.0 mL) and **[M]** (X mol%). b) HeLa lystes 7 mg / mL. c) L = *N*- phenylpicolinamide. d) Yields determined by ^{1}H-NMR using CH_2Br_2 as internal standard.

3.3 Scope[205]

Several allylic alcohols were synthetized to further test the scope of the reaction under biologically relevant conditions. The substrates were easily made by addition of vinyl magnesium bromide to commercially available aldehydes (**Figure 101**).

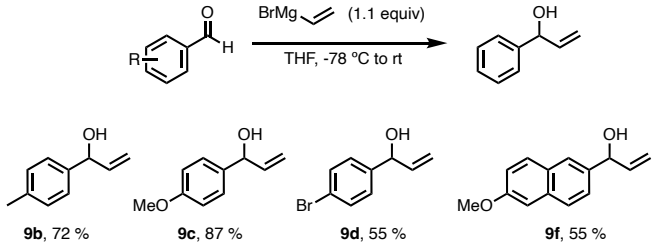

Figure 101. Synthesis of allyl alcohols.

We tested the isomerization of the different allylic alcohols under PBS, DMEM and cell lysates. As can be deduced from **Figure 102**, both substrates with *p*-methyl- (**9b**) *p*-methoxy-(9**c**) and *p*-bromo- (**9d**) groups in the aromatic rings proceed with very good yields (79%- 91%) independently of the reaction media used.

The commercially available 1-octen-3-ol (**9e**) also performed remarkably well with low reaction times to deliver the expected ketone in high yields. Alcohol **9f** bearing a naphthalene ring required 20%$_{(v/v)}$ of THF due to its low solubility at the working concentration, but the reaction gave good yields (**10f**, 79%) (**Figure 102**).

[205] The experiments in this section were carried out in collaboration with Dr. Cristian Vidal Vides

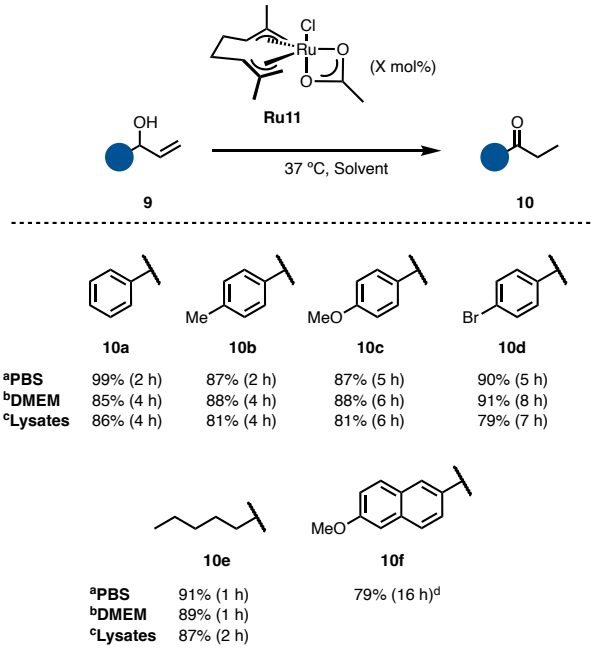

Figure 102. a) Allylic alchol (0.2 mmol), milieu (1.0 mL) and **Ru11** (2 mol%). b) **Ru11** (5 mol%) c) **Ru11** (5 mol%), HeLa lysates (7 mg / mL). d) reaction media with 20%$_{(v/v)}$ of THF.

3.4 Mechanistic insights[206]

To further understand the mechanism and therefore to confirm that a metal-hydride intermediate is involved, we carried out isotopic labeling experiments with deuterium. Firstly, we synthetized the corresponding deuterated allylic alcohol **9a-*d*** by reduction of the phenylvinyl ketone with $NaBD_4$. The desired product was obtained with a 99% deuteration incorporation (**Figure 103**).

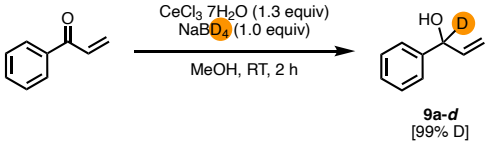

Figure 103. Synthesis of deuterated allylic alcohol **9a-*d***.

When the deuterated substrate **9a-*d*** was subjected to the isomerization conditions with **Ru11**, the corresponding ketone was obtained with full deuteration at its β-position (**10a-β*d***), both in PBS and DMEM (**Figure 104a**). Considering the complexity of these

[206] The experiments in this section were carried out in collaboration with Dr. Cristian Vidal Vides

reaction media, especially in the case of DMEM, the complete retention of the deuteration is a clear sign of selectivity in the hydride transfer and of its intramolecular nature.

No deuteration is observed if the propiophenone product **10a** is treated with the ruthenium catalyst **Ru11** in deuterated water (**Figure 104b**), confirming that the solvent does not participate in the hydride transfer, also in agreement with an intramolecular redox process.

On the other hand, no deuterium scrambling was observed in a cross-reactivity experiment between the deuterated alcohol **9a-*d*** and the non-deuterated alcohols **9c** (**Figure 104c**). These results further confirms the intramolecular mature of the hydride transfer and discards a hydrogen borrowing mechanism.

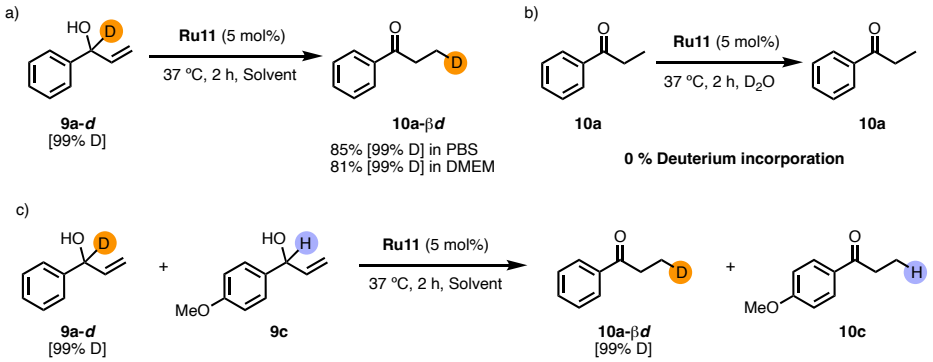

Figure 104. a) Isomerization of **9a-*d*** in PBS and DMEM. b) Stability of ketone **10a** under catalysis conditions in deuterated D_2O c) Cross-over experiments with **9a-*d*** and **9c**.

3.5 Fluorogenic probes to monitor the reaction

The catalytic and bioorthogonal properties of the reaction augured well for its transference to living settings. In order to monitor the reaction in cells, we designed a molecular probe that would allow us to obtain a read-out signal and, therefore, determine the efficiency of the isomerization. We prepared a derivate of Acedan (6-dimethylamino-2-acetyl-naphthalene), a type of push-pull 2,6-disubtituted naphthalene-derived fluorophore that bears an electron-donating dimethylamino moiety and an electron-withdrawing acetyl group, in conjugated positions.[207] These polar fluorophores allow for intramolecular charge transfer (ICT) through the π electron cloud, increasing the lifetime of the excited state and, therefore, the quantum yield of the process. Reducing either the

[207] S. Singha, D. Kim, B. Roy, S. Sambasivan, H. Moon, A. S. Rao, J. Y. Kim, T. Joo, J. W. Park, Y. M. Rhee, T. Wang, K. H. Kim, Y. H. Shin, J. Jung, K. H. Ahn, *Chem. Sci.* **2015**, *6*, 4335–4342.

donor or acceptor ability of the EDG and EWG groups produces a significant reduction in the fluorescence.[208] This property makes this core perfect for monitoring the isomerization process, since an electron withdrawing ketone moiety could be obtained as a result of the ruthenium catalyzed isomerization of an electronically neutral allylic alcohol substituent (see **Figure 105a**), which should exhibit a significantly reduced fluorescence.

Regarding the electron donating group of the fluorophore, we decided to change the most frequently used dimethylamine group for a pyrrolidine ring, as it has been shown that it exhibits a lower H-bonding capacity in protic solvents, avoiding the suppression of the ICT and the presence of non-radiative decays.[207] Moreover, its lower allylic strain, compared to the NMe_2 derivative, further enhances the ICT event.

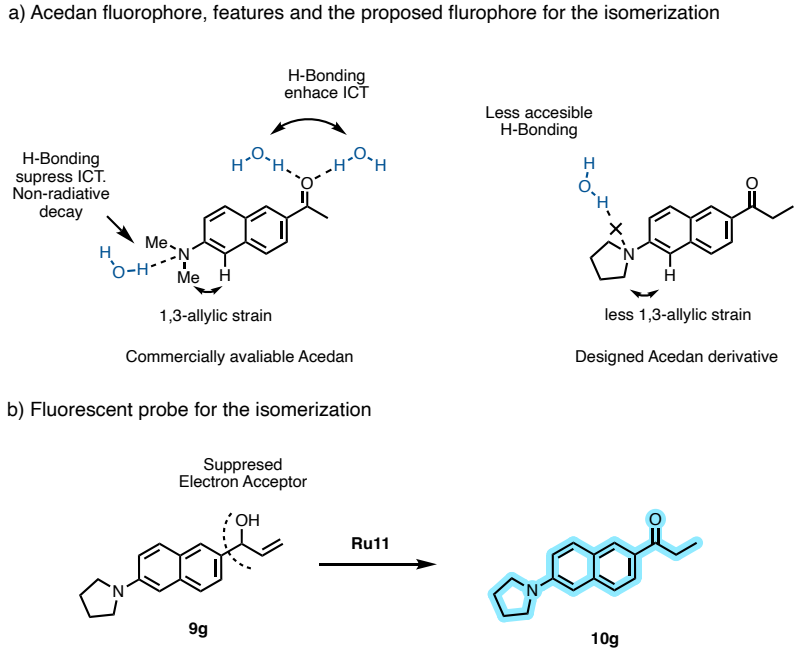

Figure 105. Design of molecular probe for the isomerization of allylic alcohols.

The synthesis of the probe **9g** was achieved in three steps from the commercially available 6-bromo-2-naphthol. In a first step the hydroxyl group of the naphthol is exchange for the pyrrolidine through a Bucherer reaction (95% yield). The intermediate **I** was converted to the corresponding aldehyde by lithium-halogen exchange with *n*-BuLi, followed by DMF addition and hydrolysis of the resulting hemiaminal. Finally, the addition of allyl

[208] A. S. Rao, D. Kim, T. Wang, K. H. Kim, S. Hwang, K. H. Ahn, *Org. Lett.* **2012**, *14*, 2598–2601.

magnesium bromide over the aldehyde **II** furnished the corresponding probe **9g** in 71% yield. The corresponding fluorophore is accessible by isomerization of the probe with **Ru11** in PBS with a 20% $_{(v/v)}$ of THF, with a 96% yield (**Figure 106**)

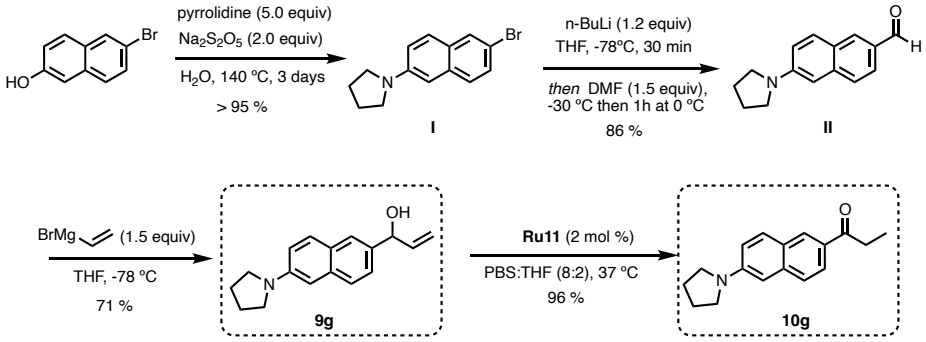

Figure 106. Reaction scheme for the synthesis of the allylic alcohol probe **9g** and the fluorophore **10g**.

The probe and the fluorophore were characterized spectroscopically. The UV-Vis absorbance spectra of the allylic alcohol **9g** is significantly different from the spectra of the fluorophore **10g** with lower absorption in the 320-450 nm range (**Figure 107**).

Regarding the fluorescence spectra it is worth to highlight that there is a different emission shift between the alcohol and the ketone, around 100 nm. Moreover, the ketone exhibits a high Stokes shift of 175 nm. These two differences make this probe a great system for monitoring the transformation, as the use of filters of 520 nm can cut-off any emission from the allylic alcohol and record just the emission of the ketone probe.

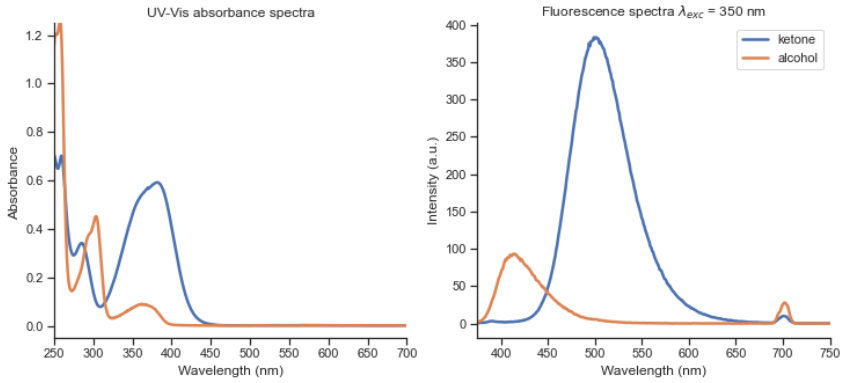

Figure 107. Absorption and emission spectra for **9g** and **10g** at 1 μM in MeOH.

3.6 Isomerization in live mammalian cells[209]

The intracellular isomerization was explored with two human cell lines: adenocarcinomic human alveolar basal epithelial cells (A549), and cervical cancer cells (HeLa) as well as with one animal line, monkey kidney epithelial cells (Vero).

In all cases, cells were incubated with 10 μM of **Ru11** for 30 minutes, followed by two washing steps with DMEM, and incubation of 100 μM of the allylic probe **9g**, and a final washing with DMEM. A considerable intracellular increase of fluorescence was observed in all cell lines, with mainly cytosolic staining (**Figure 108**). This increased fluorescence can be measured by the corrected total cell fluorescence (CTCF),[210] yielding up to a 38 - fold increase against control cells incubated just with the probe. Control experiments confirmed that the intracellular fluorescence was the result of the product formation.

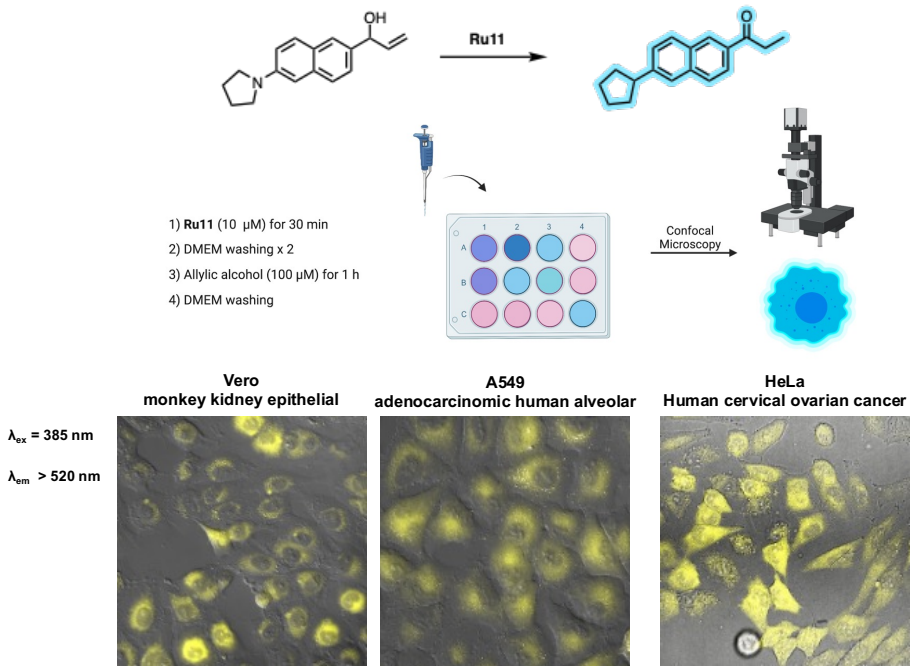

Figure 108. Intracellular isomerization of **9g** by **Ru11** in Vero, A549 and HeLa cells.

The intracellular formation of the product (**10g**) was further confirmed by HPLC-MS analysis. The incubated cells were extracted with methanol after running the reaction for 30 minutes and 6 hours. The different washes with DMEM and PBS were also analyzed

[209] The experiments in this section were carried out by Dr. María Tomás Gamasa
[210] The corrected total cell fluorescence takes into account the density of cells to give a comparable measurement independently of the total number of cells

founding low concentrations of product. To our delight the cell extracts contained a significant amount of ketone, that upon calibration allowed for the quantification of the product. This analysis showed that formation of product increases over time, with small quantities after 30 min and ~2.5x times more product after 6 h. This is a great evidence of the robustness of catalyst **Ru11**, that is able to remain active in the stringent conditions of the cellular environment for long periods of time.

The intracellular content of ruthenium was determined by inductively coupled plasma mass spectrometry (ICP-MS) analysis. Cells were incubated using two different concentrations of **Ru11**, 10 μM and 25 μM, yielding values of 3.7 ng of Ru·10^{-6} cells, and 11 ng of Ru·10^{-6} cells respectively.

Having both results in hand, the intracellular content of ruthenium and product, we were able to estimate the intracellular TON for the isomerization process. Assuming that all the intracellular ruthenium content comes from the complex **Ru11** supplementation, and that all the ruthenium is catalytically competent, we can estimate a lower limit for the TON. Thus when 25 μM concentration of **Ru11** was used, we calculated a TON of 9 ± 5, gratifyingly when the **Ru11** loading is decreased to 10 μM, the obtained TON is even higher, 22 ± 8 (**Figure 109**).

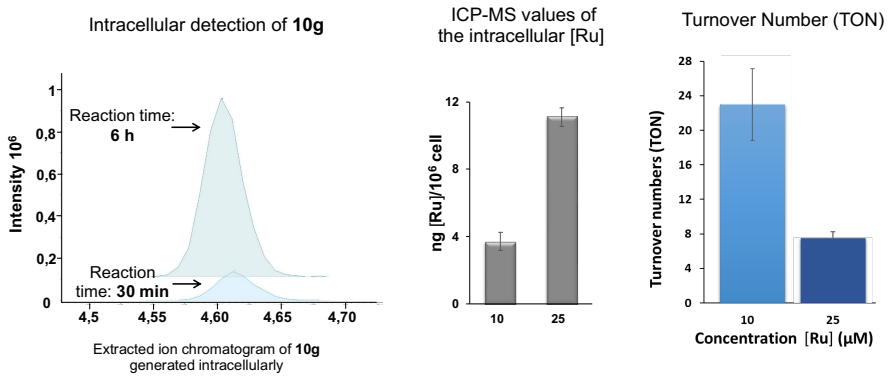

Figure 109. a) Extracted ion chromatogram for the intracellular generation of **10g**. b) ICP-MS values for the intracellular concentration of ruthenium. c) Turnover Number quantification as function of the concentration.

This result confirms that the intracellular isomerization of the allylic alcohol **9g** is occurring in a catalytical manner.

Using standard MTT techniques, we confirmed that using concentrations up to 100 μM, neither the ruthenium complex nor the substrate **9g** or product **10g** presented noticeable

toxicities after 6 h. However, after 24 h, we observed toxicity in the case of the product (32% of cell death). [211]

3.7 Interference with the natural metabolism of the cell[212]

Having developed an optimal protocol for the *in cellulo* ruthenium promoted isomerization of allylic alcohols, we envisioned that the isomerization of a non-symmetric bis-allylic alcohol could generate a reactive α,β-unsaturated ketone that could eventually act as a Michael acceptor in the presence of suitable biological nucleophiles. In particular, thiols are particularly efficient nucleophiles in Michael additions so that we foresaw that the intracellular generation of this α,β-unsaturated ketones in cells could modify the natural metabolism of the cells by acting as GSH depletors (**Figure 110**).

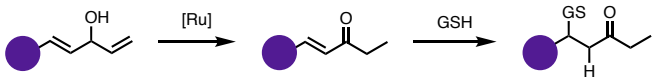

Figure 110. Conceptual generation of α,β-unsaturated ketones by ruthenium isomerization

To our knowledge there was no precedents of the synthesis of α,β-unsaturated ketones by the isomerization of bis-allylic alcohols, neither in organic solvents nor in water. Therefore, we first studied the viability of such isomerization process in aqueous media. To do so, we first synthetized three different bis-allylic alcohols by addition of vinyl magnesium bromide to the corresponding α,β-unsaturated aldehydes (**Figure 111**).

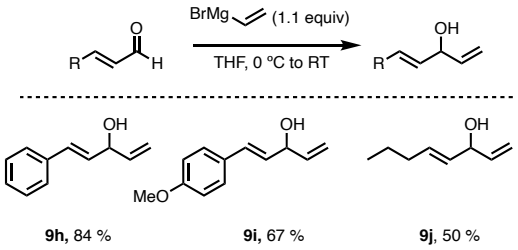

Figure 111. Reaction scheme for the synthesis of bis-allylic alcohols

Treatment of this allylic alcohols under our previously developed optimized conditions (2 mol% **Ru11**, 37 ºC, 2 h) in PBS led in all cases (**9h-j**) to full conversions towards the ketone products resulting from the isomerization of the less substituted alkene.

[211] For further information see the Experimental Section
[212] The experiments in this section were carried out in collaboration with Dr. Cristian Vidal Vides and Dr. María Tomás Gamasa

Gratifyingly, the reactions could also be performed in cell lysates, providing in the three cases 85% yield of the products (**Figure 112**).

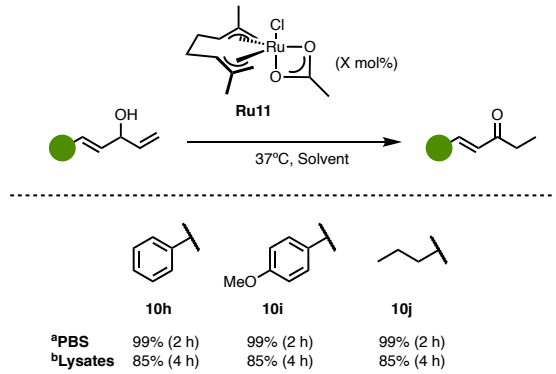

Figure 112. a) Allylic alchol (0.2 mmol), milieu (1.0 mL) and **Ru11** (2 mol%). b) **Ru11** (5 mol%), HeLa lysates 7 mg / mL.

With these results in hand, we then conducted the isomerization reaction of **9i** in cellulo. To analyze the effectiveness of the process, we measured the levels of glutathione in its reduced (GSH) or oxidized form (GSSG), using a commercial kit (GSH/GSSG Ratio Detection Assay Kit-Abcam). For the ruthenium catalyzed isomerization, cells were incubated with the catalyst **Ru11** for 30 min, followed by two washing steps with DMEM, and incubation of the substrate, **9i**, for 6 and 24h. Finally, we measured the GSH/GSSG levels with the commercial glutathione detection kit.

Similar protocol was followed to measure the levels of glutathione for untreated cells, cells incubated with the substrate, **9i,** and cells incubated with the product **10i**.

We observed neglectable differences between untreated cells and those treated with the bis-allylic alcohol **9i**. Cells treated with α,β-unsaturated ketone **10i** do present lower levels of reduced glutathione, around a 20%, however, to our delight, the intracellular generation of the **10i** exerted a much higher effect on the GSH levels, (around a 40% of GSH depletion) than its solo supplementation. We hypothesize that the intracellular formation of the of the unsaturated ketone **10i** prevents Michael additions during the internalization process, which could eventually lower the effect of **10i** on GSH levels, even though differences in the internalization of alcohol **9i** and ketone **10i** can not be discarded.

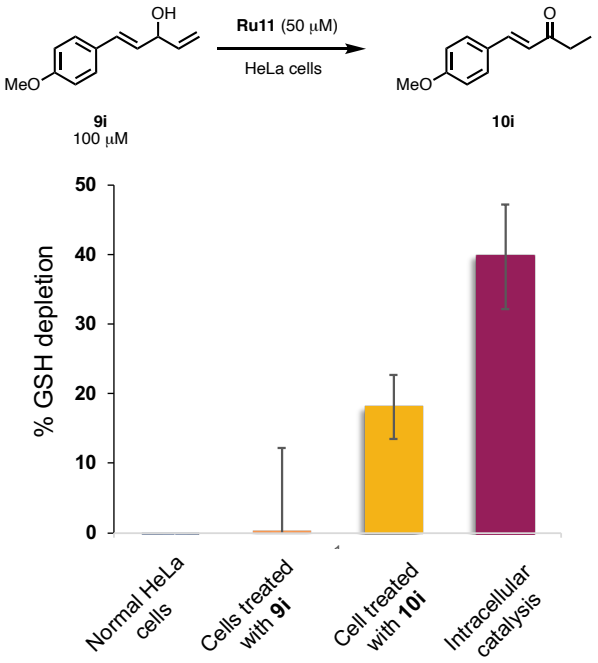

Figure 113. a) Reaction scheme for the isomerization of **9i** in HeLa cells. b) GSH depletion for: untreated cells, cells treated with **9i**; cells treated with **10i**; intracellular generation of **10i**.

This example shows the potential of the isomerization of allylic alcohol as a bioorthogonal transformation for the in situ formation of bioactive compounds

4 Conclusions

We have demonstrated that the ruthenium-catalyzed isomerization of allylic alcohols is an excellent reaction in terms of biological compatibility and bioorthogonality. It is compatible with complex biological media such as DMEM, cell lysates and even living mammalian cells. The ruthenium complex is not toxic and survives inside living cells for a relatively long period of time. Importantly, we demonstrated that the intracellular reaction takes place with a TON of over 22 ± 8, which confirms the existence of catalytic cycles.

Finally, we have also shown that the reaction can be used for the in situ generation of Michaels acceptors that effectively work as GSH depleting agents inside cells.

Chapter IV: Tandem Reactions in Cellulo

1 Introduction

1.1 Tandem catalysis

Tandem catalytic processes are usually referred to reactions that happen sequentially in the same reaction vessel, without the need of isolating intermediates. It is also sometimes referred as "relay catalysis" to distinguish it from cooperative catalysis, wherein two or more catalysts/catalytic cycles work in a concerted manner, sharing common intermediates, to deliver a single product (**Figure 114**).[213,214,215]

The development of tandem catalytic systems requires to address challenges such as the compatibility of reagents and catalysts and the need to find suitable conditions for all reactions in place. However, they present significant advantages, beyond the reduction of waste and time: in many cases they allow the access to products that otherwise are difficult to make, by capturing intermediates that might be unstable or difficult to isolate.

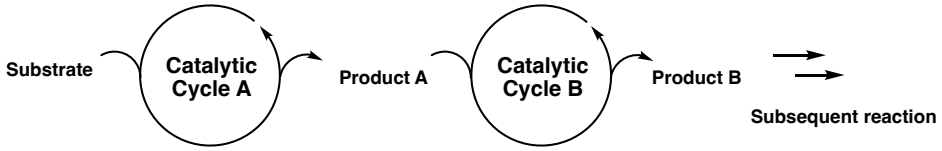

Figure 114. Conceptual scheme for a tandem catalyzed process.

For instance, Hartwig and coworkers reported the tandem rhodium catalyzed hydroformylation / iridium catalyzed reductive amination of aliphatic alkenes.[216] The tandem process allows to use milder conditions than alternative protocols (**Figure 115**)[217]

[213] S. Martínez, L. Veth, B. Lainer, P. Dydio, *ACS Catal.* **2021**, *11*, 3891–3915.
[214] T. L. Lohr, T. J. Marks, *Nature Chem* **2015**, *7*, 477–482.
[215] D. E. Fogg, E. N. dos Santos, *Coordination Chemistry Reviews* **2004**, *248*, 2365–2379.
[216] S. Hanna, J. C. Holder, J. F. Hartwig, *Angew. Chem. Int. Ed.* **2019**, *58*, 3368–3372.
[217] The previously reported rhodium catalyzed-tandem catalysis was reported at 140 ºC and 40 bar. M. Ahmed, A. M. Seayad, R. Jackstell, M. Beller, *J. Am. Chem. Soc.* **2003**, *125*, 10311–10318.

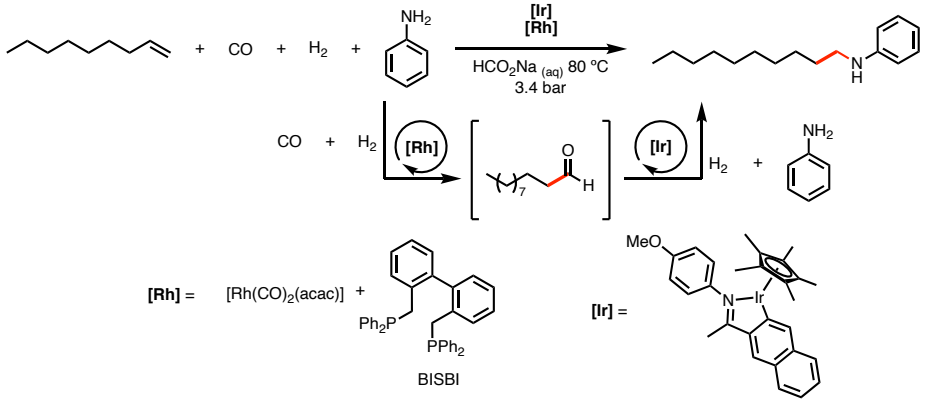

Figure 115. Tandem Rh-hydroformylation, Ir-reductive amination.

In the abovementioned case, the two catalysts are organometallic entities; however, tandem catalysis might also involve two different types of catalysts, rendering the compatibility issues even more challenging. Especially interesting is the combination of organometallic catalysts with a biocatalysts, although finding compatible conditions is truly challenging. Nonetheless, a crescent number of examples have been reported during the last decade showcasing the great potential of combining the breadth and power of transition metal catalysis with the exquisite selectivity of enzymes. [218,219,220]

Toste, for instance, reported the combination of a gold catalyst with natural enzymes, like the Amano lipase PS, but they had to use a supramolecular cage to encapsulate the metal catalyst, to protect it from the reaction media. The tandem reaction consists of an enzymatic kinetic resolution of a chiral racemic allenyl acetate prior to the gold-catalyzed intramolecular cyclization of the resulting enantiopure allenol. Although the diastereomeric excess of the product is low, the enantiomeric excess of the recovered allenyl acetate was of 89% (**Figure 116**).[221]

[218] H. C. Hailes, P. A. Dalby, J. M. Woodley, *J. Chem. Technol. Biotechnol.* **2007**, *82*, 1063–1066.
[219] X. Huang, M. Cao, H. Zhao, *Curr. Op. Chem. Bio* **2020**, *55*, 161–170.
[220] M. Cortes-Clerget, N. Akporji, J. Zhou, F. Gao, P. Guo, M. Parmentier, F. Gallou, J.-Y. Berthon, B. H. Lipshutz, *Nat Commun* **2019**, *10*, 2169.
[221] Z. J. Wang, K. N. Clary, R. G. Bergman, K. N. Raymond, F. D. Toste, *Nature Chem* **2013**, *5*, 100–103.

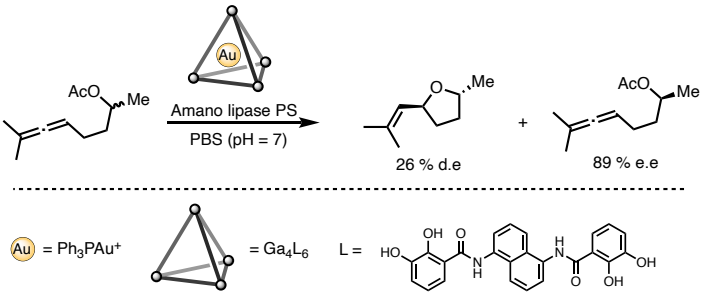

Figure 116. Tandem kinetic resolution of allenes by Amano lipase ester hydrolysis, gold (I) hydroxyalkoxylation of allenes under aqueous conditions.

There are many other nice examples that showcase the potential of combining the reactivity of transition metal catalysts with that of enzymes, all of them focused to synthetic purposes.[222,223,224] Metabolic networks involve many type of tandem enzymatic processes, critical for the functioning of the cells.

Considering the progress in translating transition metal catalysts to biological media and to live settings, the possibility of coupling these catalysts with natural enzymes to carry out new-to-nature transformations in biological habitats is intriguing.

1.2 Tandem catalysis in chemical biology: Combining transition metals with enzymes

We can go back to an early report in the 1980's by Mountfort and coworkers showing that is possible to decouple the metabolic functions of two obligated syntrophs, [225] *Syntrophomonas wolfei* and *Methanospirillum hungatei*, with a metal catalyzed process, namely Pd-catalyzed hydrogenation of ethylene. Thus, by using a non-biological metal catalyst, they interfere with the biological equilibria of this living system. *S. wolfei* generates H_2 by butyrate oxidation and depends metabolically on its consumption by the syntroph *M. hungatei*. Using the Pd catalyst, Pd-BaSO4, Mountfort demonstrated a Pd-catalyzed hydrogenation of ethylene with the *in situ* generated H_2 by *S. wolfei*, that can take up the role of *M. hungatei,* allowing *S. wolfei* to avoid acetogenesis

[222] P. Schaaf, T. Bayer, M. Koley, M. Schnürch, U. T. Bornscheuer, F. Rudroff, M. D. Mihovilovic, *Chem. Commun.* **2018**, *54*, 12978–12981.
[223] C. A. Denard, H. Huang, M. J. Bartlett, L. Lu, Y. Tan, H. Zhao, J. F. Hartwig, *Angew. Chem. Int. Ed.* **2014**, *53*, 465–469.
[224] C. Adamson, M. Kanai, *Org. Biomol. Chem.* **2021**, *19*, 37–45.
[225] Syntrophy is the phenomenon of one species feeding metabolic product to another specie in order to survive.

and continue the butyrate oxidation and the hydrogen production without the need of its syntroph. Therefore, the Pd catalysts take up the role of *M. hungatei.* (**Figure 117**).[226]

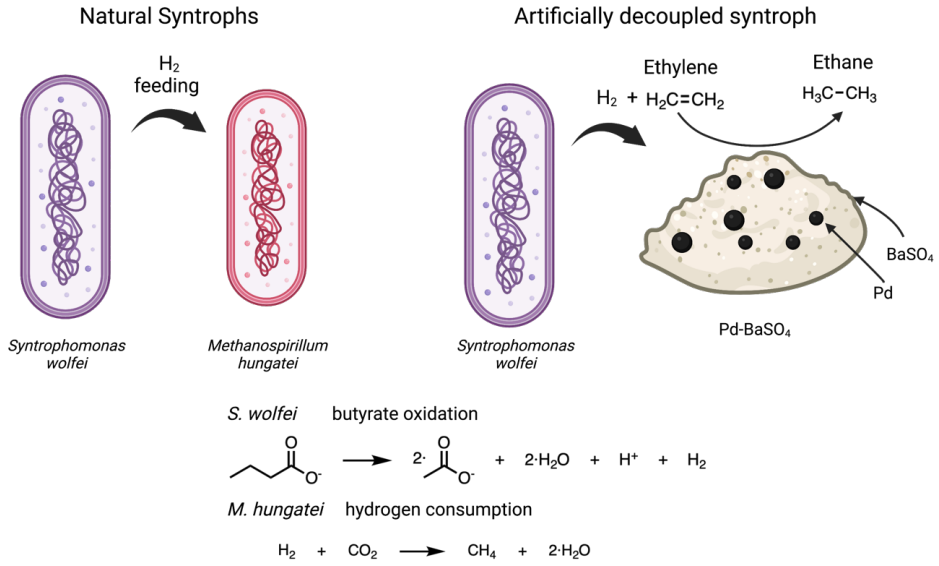

Figure 117. General scheme for the artificial metabolic decoupling of *S. wolfei* and *M. hungatei* by Pd catalyzed ethylene hydrogenation.

In 2013, Balskus reported an elegant example in which they used a ruthenium-promoted deprotection of *N*-alloc-*p*-aminobenzoic acid (N-alloc-PABA) to deliver *p*-aminobenzoic acid (PABA), a nutrient that is key for the growth and survival of PABA-auxotroph organisms. Accordingly, Balskus used three different *E. coli* mutants that lack the ability to produce PABA to demonstrate that, only when the *N*-alloc-PABA and the ruthenium catalyst [Cp*RuCl(COD)] were added to a PABA-free culture media, the survival and growth of these E. coli auxotroph mutants could be recovered at normal levels (**Figure 118**).[227]

[226] H. F. Kaspar, A. J. Holland, D. O. Mountfort, *Arch. Microbiol.* **1987**, *147*, 334–339.
[227] Y. Lee, A. Umeano, E. P. Balskus, *Angew. Chem. Int. Ed.* **2013**, *52*, 11800–11803.

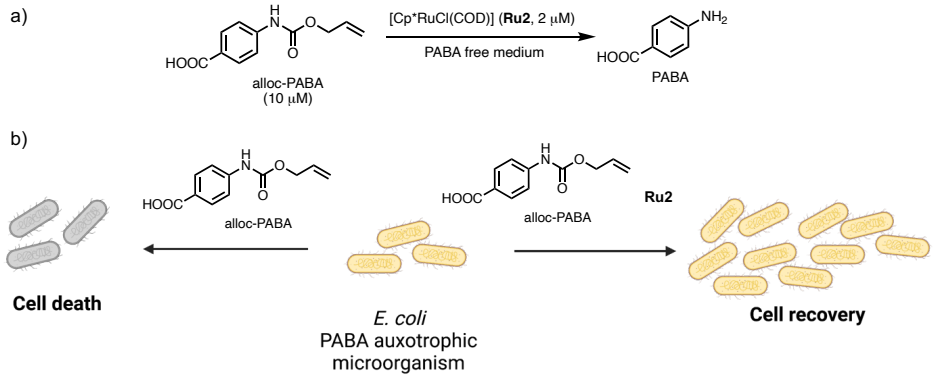

Figure 118. Dependence of *E. coli* mutant on ncAA and ruthenium deallylation catalysis.

A similar report by Mayer was published in 2020, in which they used the second generation deallylation catalyst {[CpRu(Qty)(allyl)]PF_6, Qty = 4-methoxyquinaldic acid} for the uncaging of an alloc protected essential non-canonical amino acid (alloc-ncAA), also in *E. coli*. They showed that the in situ synthesis of the ncAAs by transition metal catalysis was a promising strategy to achieve bacterial survival dependent on this new-to nature reaction (**Figure 119**).[228]

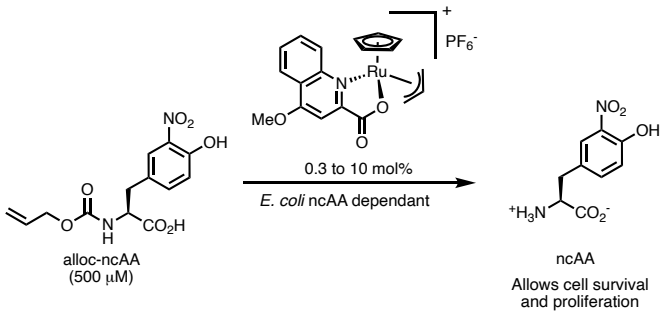

Figure 119. Ruthenium catalyzed deprotection of alloc-ncAA for the survival of artificial *E. coli* auxotroph.

Several other reports have used new-to-nature reactions to interfere in the metabolism of bacteria[229] or to produce fine chemicals.[230] However, precedents on tandem or concurrent catalysis taking place in **live mammalian cells** are scarce and limited to very specific conditions.

[228] R. Rubini, C. Mayer, *ACS Chem. Biol.* **2020**, *15*, 3093–3098.
[229] S. Wallace, E. E. Schultz, E. P. Balskus, *Curr. Opin. Chem. Biol.* **2015**, *25*, 71–79.
[230] S. Wallace, E. P. Balskus, *Curr. Opin. Biotech.* **2014**, *30*, 1–8.

Wender reported in 2016 the use of a ruthenium complex for the deprotection of an *N*-alloc-luciferin derivative in mouse carcinoma cell line (4T1 cells).[231] After the deallylation, the free luciferin reacts with luciferase to emit bioluminescence (**Figure 120**). The authors had to engineer the cells in order to express the luciferase protein, and the aim of the work was not to build or interfere with metabolic networks, but to have a biochemical method to determine the turn-over number (TON) of a reaction through photon counting.

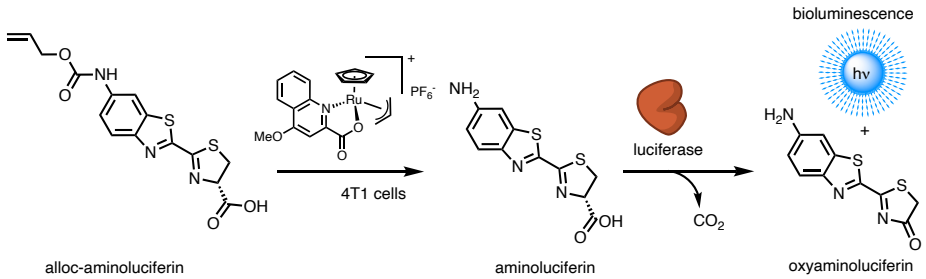

Figure 120. Tandem deprotection of aminoluciferin and its oxidation of to oxyaminoluciferin plus bioluminescence.

Another example developed by Sadler, already commented in the previous chapter, consists of a hydrogenation of pyruvate with sodium formate by an osmium catalysts to deliver L-lactate (**Figure 121**). The conversion of pyruvate, the starting material for the Krebs cycle, into L-lactate interferes with the redox equilibria of cells.[232]

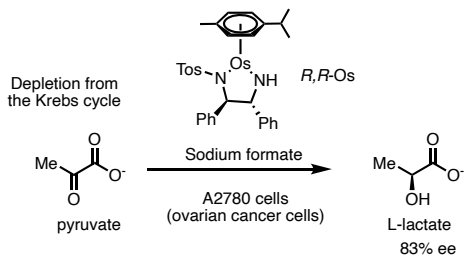

Figure 121. Osmium promoted enantioselective reduction of pyruvate to lactate in A2780 cells.

These two examples combined the use of a metal catalyst with enzyme-catalyzed processes. However, tandem reactions combining two organometallic catalysts should also be possible, *a priori*. Although tandem catalytic processes have not been yet reported,

[231] H.-T. Hsu, B. M. Trantow, R. M. Waymouth, P. A. Wender, *Bioconjugate Chem.* **2016**, *27*, 376–382.
[232] J. P. C. Coverdale, I. Romero-Canelón, C. Sanchez-Cano, G. J. Clarkson, A. Habtemariam, M. Wills, P. J. Sadler, *Nature Chem* **2018**, *10*, 347–354.

a related case described by our group shows how two different transition metal processes, namely a gold-catalyzed hydroarylation and a ruthenium-catalyzed deallylation can be performed in an orthogonal and concurrent manner inside living mammalian cells (HeLa cells). Thus, the Au-catalyzed process is able to generate a coumarin from an alkynyl ester, whereas the Ru-catalyzed deallylation concurrently generates a NIR-fluorophore, from the corresponding allylated counterpart (**Figure 122**).[107]

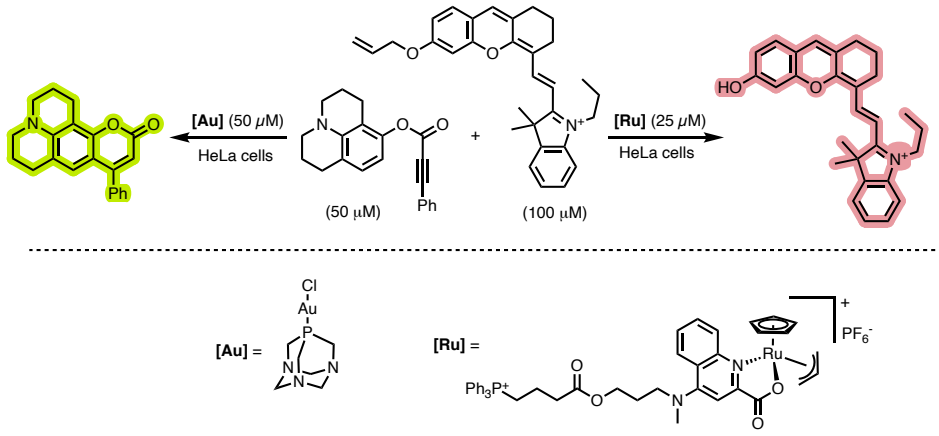

Figure 122. Concurrent and orthogonal ruthenium promoted deallylation and gold promoted hydroarylation in HeLa cells.

2 Objectives

The development of artificial tandem processes in biological media and living systems, in particular those involving a transition metal catalyzed event, might allow to devise new strategies to interfere with biology as well as to create artificial metabolic networks. Considering the versatility and high bioorthogonality of ruthenium catalysts,[77,182] in this last chapter of the PhD thesis we aimed at the following objectives:

- Develop a concurrent catalytic processes that combine two ruthenium catalyzed bioorthogonal processes (dual metal concurrent catalysis). In particular, we focused our attention on the highly versatile Ru-catalyzed deallylation processes and the newly developed Ru-catalyzed isomerizations of allylic alcohols.

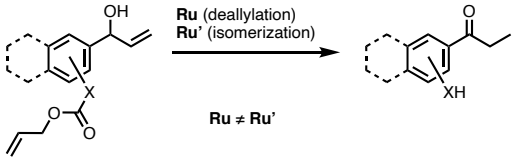

- Develop tandem reactions that combine one of this metal-catalyzed processes with a second biocatalytic event, promoted by an enzyme. In particular, we proposed the combination of the Ru-deallylation reaction with Alkaline Phosphatases (ALP)s for the hydrolysis of phosphate ester and Monoamine Oxidases (MAOs) for the oxidation of monoamines.

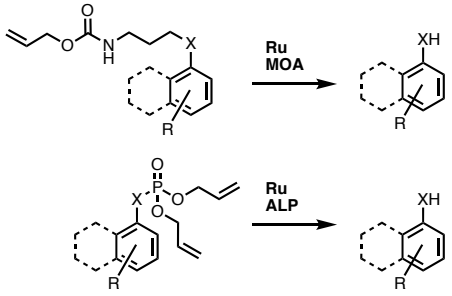

3 Results and discussion

3.1 Dual metal concurrent catalysis

3.1.1 Preliminary studies[233]

Considering the concurrent Au- and Ru-catalyzed processes developed by our group in the past,[107] we proposed to develop a substrate that could allow to couple in tandem two different metal promoted reactions, a ruthenium catalyzed isomerization and a ruthenium catalyzed deallylation.

To design the probe, we must take into account that it has to undergo two different metal catalyzed processes to be finally converted into a read-out signaling product, ideally, a fluorescent compound. Our initial design was inspired in the 2-(2'-hydroxyphenyl) benzothiazole probe (HBT) **11** as this polar fluorophore exhibits intramolecular charge transfer (ICT) in the excited state as well as excited-state intramolecular proton transfer (ESIPT), with both phenomena providing for high fluorescence (**Figure 123**).[234,235]

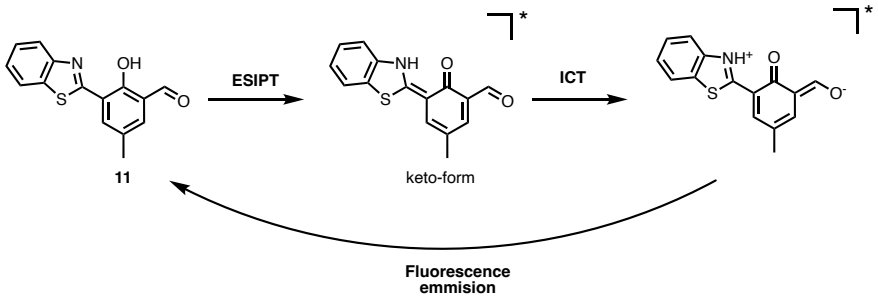

Figure 123. Mechanism of fluorescence for **11.**

We reasoned that the phenol moiety could be protected as an allyl ether, as a reactive moiety for Ru-deallylation catalysis, and its ortho-carbonyl moiety could be masked as an allylic alcohol (probe **12**), so that a Ru-catalyzed isomerization (developed in Chapter III) could deliver a related ketone (**Figure 124**). We hypothesized that having this alkyl ketone, **13**, instead of the original aldehyde of HBT, should not drastically influenced its fluorescence properties. According to this design, since both reactive handles are not connected, the overall process would be concurrent rather than tandem, but both reactions

[233] The experiments on this section were carried out in collaboration with PhD. Cristian Vidal Vides
[234] T. Chen, T. Wei, Z. Zhang, Y. Chen, J. Qiang, F. Wang, X. Chen, *Dyes and Pigments* **2017**, *140*, 392–398.
[235] A. C. Sedgwick, L. Wu, H.-H. Han, S. D. Bull, X.-P. He, T. D. James, J. L. Sessler, B. Z. Tang, H. Tian, J. Yoon, *Chem. Soc. Rev.* **2018**, *47*, 8842–8880.

would occur on the same substrate. Either the isomerization or the deallylation process could *a priori* take place as first step, generating two possible intermediates (**14** and **15**).

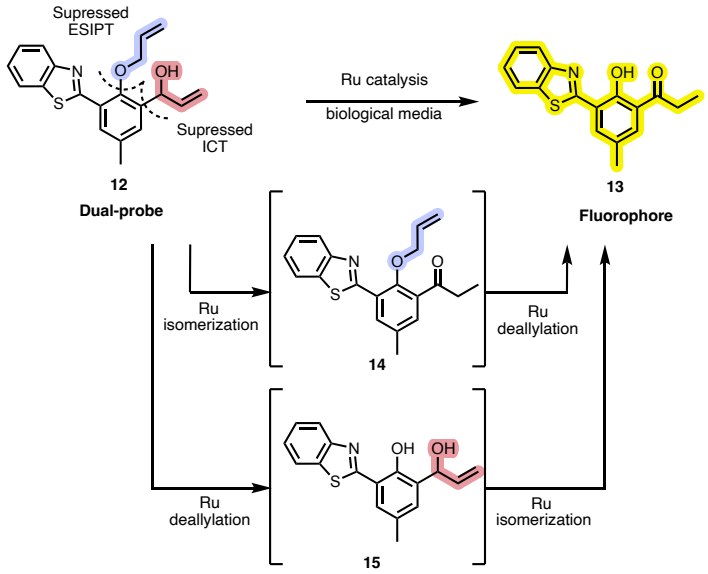

Figure 124. Design of dual metal probe **12.**

The synthesis of the fluorophore **11** was carried out in two steps from the commercially available materials, following reported procedures.[236] Condensation of 2-hydroxy-5-methylbenzaldehyde and 2-aminothiphenol in DMF (110 ºC) led to the benzothiazole intermediate **16** in 74% yield. Formylation with a hexamethyltretaamine in trifluoracetic acid at 110 ºC in a Duff-reaction, yielded the fluorophore **11** (97% yield). To synthetize the dual probe, alkylation of the phenol with allyl bromide in the presence of K_2CO_3, under refluxing acetonitrile yielded the intermediate **17** in 55% yield. Finally, addition of magnesium vinyl bromide at -78 ºC to the aldehyde **17**, delivered the desired probe **12**, in 88% yield (**Figure 125**).

[236] T. Chen, T. Wei, Z. Zhang, Y. Chen, J. Qiang, F. Wang, X. Chen, *Dyes Pigm.* **2017**, *140*, 392–398.

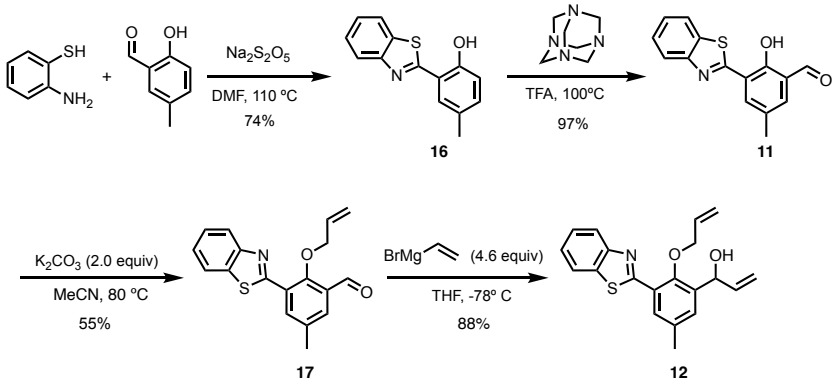

Figure 125. Reaction scheme for the synthesis of dual-probe **12**.

Figure 126 depicts the absorbance and fluorescence spectra for **12** and **11**. As expected, **12** did not have significant fluorescence compared with **11** as both mechanisms of fluorescence are suppressed. Ideally, we would need the photophysical characterization of the intermediates **14**, **15**, and the corresponding fluorophore **13**, to be able to perform all the required control experiments; however, as all the intermediates should be accessible by the stepwise isomerization / deallylation processes, we first evaluated those reactions.

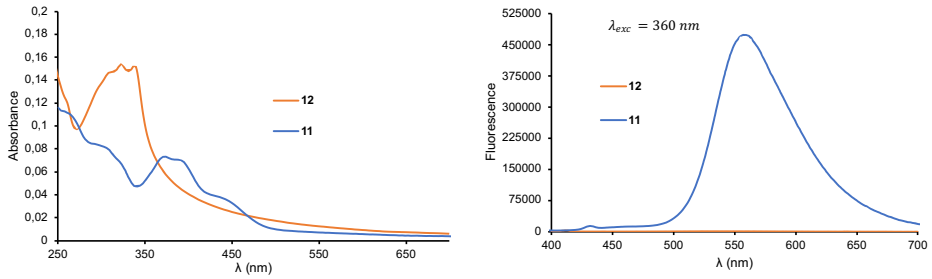

Figure 126. Absorbance and fluorescence of **12** and **11**.

We initially tested the individual steps of the process, namely the ruthenium catalyzed deallylation of **12** (using 50 mol% of **Ru13** + 33 equiv of GSH) and the ruthenium catalyzed isomerization of the allylic alcohol moiety of **12** (using 50 mol% of **Ru11**), both processes in PBS, using a concentration of the probe of 500 µM.

Analysis of the reactions by HPLC-MS led us to conclude that the protected probe **12** undergoes an efficient deallylation using the catalyst **Ru13** to yield the intermediate **15** quantitatively. However, when the same probe **12** was subjected to **Ru11**, the isomerization did not take place. On the other hand, when we performed the deallylation

reaction first, to generate the intermediate **15** and, after 4h, the isomerization catalyst **Ru11** was added, we did not observe the formation of the desired product (**13**), but a complex mixture instead. We considered the possibility of GSH poisoning the isomerization catalyst **Ru11**, so we performed the same experiments in the absence of GSH, but, unfortunately, we obtained similar complex mixtures (**Figure 127a**).

At this point we focused our attention towards the isomerization process. We studied the reactivity of intermediate **15** at 75 mM, using the 10 mol% of **Ru11** and longer reaction times (>16 h) in PBS. Unfortunately, we recovered the starting material. The addition 20%$_{(v/v)}$ THF as co-solvent or 1 equiv of base (K_2CO_3), which have been proven to be beneficial for isomerization reactions in water,[191] did not improve the conversion. Finally, we tried the isomerization in THF with 1.0 equiv of Cs_2CO_3, under reflux, but again, we obtained again similar unsatisfactory results (**Figure 127b**). In any case, we did not observe the desired ketone. Although the reasons for this failure are not evident, we hypothesize that the benzothiazole scaffold might be acting as a strong ligand, coordinating the ruthenium center of **Ru11** and, therefore, inhibiting the catalytic isomerization.

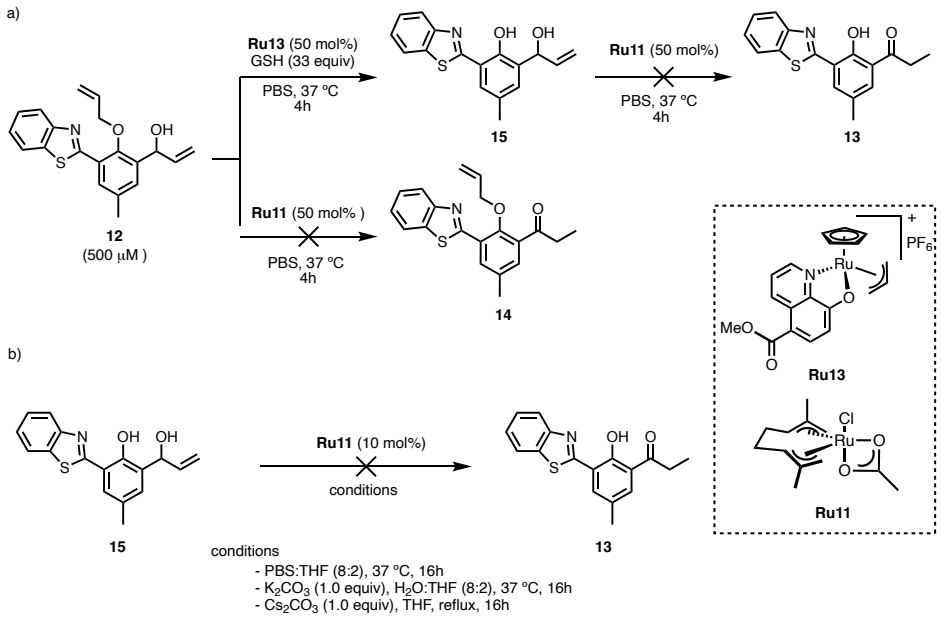

Figure 127. *In vitro* studies for the concurrent ruthenium isomerization-deallylation

3.1.2 Design and preparation of a dual Acedan-based probe

Considering the failure of the HBT-based probed in the isomerization reaction, we focused our attention on an alternative design which would not involve a strongly coordinating ligand. In particular, we selected the Acedan core, previously used in the previous chapter as a fluorescent reporter for the ruthenium catalyzed isomerization of allylic alcohols. It is also a polar fluorophore that exhibits intramolecular charge transfer (ICT) in the excited state. To design the probe, we considered reducing either the electron donor or acceptor ability of its electron donor and electro drawing groups to decrease the fluorescence. For that reason, we selected methyl amine as the electron donating moiety, as its protection with an allyl carbamate would reduce its electron-donating abilities. Regarding the electron withdrawing group (or acceptor group), we selected an ethyl ketone since this moiety can be directly obtained from the Ru-catalyzed isomerization of an electron-neutral allylic alcohol precursor, such as that of **18**.

Again, since the orthogonal groups are not connected, rather than a tandem process, we would be developing a concurrent catalytic processes, where either the isomerization or the deallylation step could take place first, generating two possible intermediates, **20** and **21** (**Figure 128**).

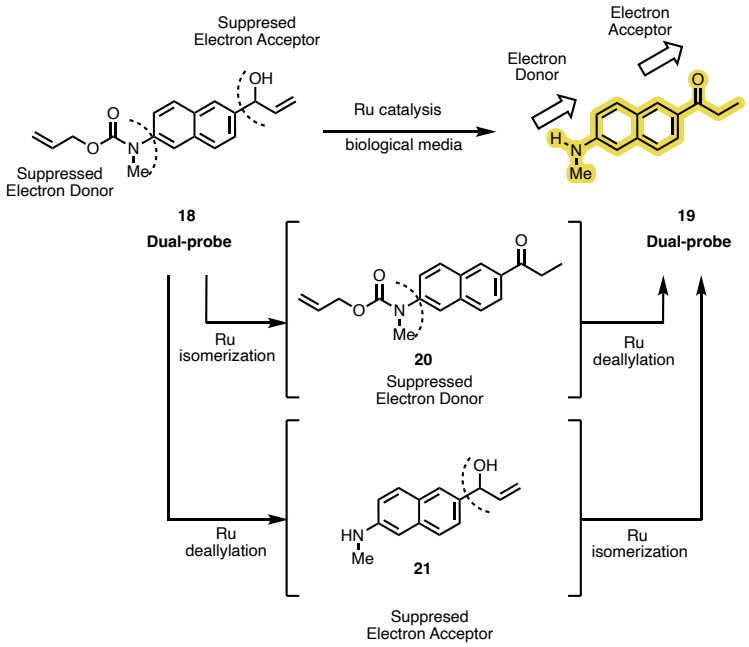

Figure 128. Design of a dual probe based on Acedan.

The synthesis of the probe, **18**, intermediates **20**, and **21** and the fluorophore **19** was achieved in a divergent fashion starting from the commercially available 6-bromo-2-naphtol Introduction of the methyl amine into the naphthalene core was carried out using a Bucherer reaction with aqueous methyl amine to yield **22** (95% yield). Deprotonation of the N-H bond of intermediate **22** with *n*-BuLi, followed by halogen-lithium exchange with *t*-BuLi in THF at -78 ºC and treatment with DMF, afforded the aldehyde **23** in 99% yield. Protection of the secondary amine of **23** with allyl chloroformate leads to the intermediate **20** in quantitative yield. Finally, treatment of aldehyde **20** with vinyl magnesium bromide afforded the desired probe **18** (70% yield, **Figure 129a**).

The fluorophore **19** was easily accessible from the intermediate **22**, following a similar protocol as for aldehyde **23**. Sequential deprotonation with *n*-BuLi, halogen-lithium exchange with *t*-BuLi and addition of the Weinreb amide afforded the fluorophore **19** in 99% yield. Treatment of the fluorophore **19** with allyl chloroformate in CH_2Cl_2 affords the intermediate **20** in 99% yield (**Figure 129b**).

Finally, treatment of aldehyde **23** with vinyl magnesium bromide gave the corresponding allylic alcohol **21** in 40% yield (**Figure 129c**).

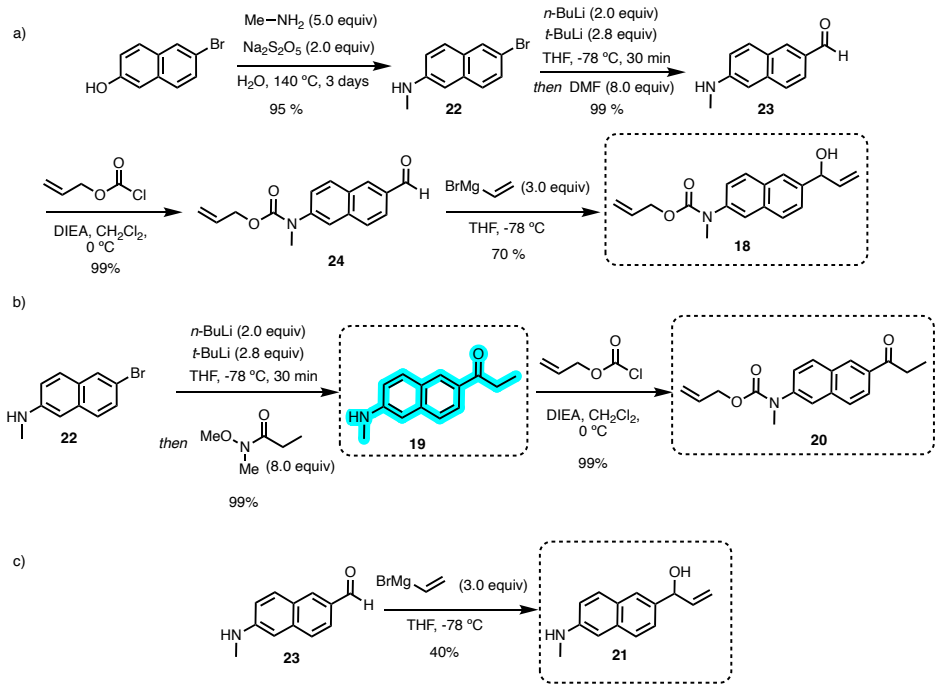

Figure 129. Synthesis of a) **18** b) **19** and **20** c) **21**.

3.1.3 Spectroscopic characterization of the Acedan probe

The probe **18**, intermediates **20**, and **21** and the fluorophore **19** were characterized spectroscopically. The UV-Vis absorbance spectra shows a significant difference between the fluorophore **19** and the probe **18** and intermediates (**20**, **21**). The fluorophore presents a maximum at 360 nm, with a large absorption up to 400 nm, whereas neither the probe **18** nor the intermediates **20** and **21** have a significant absorption (**Figure 130**).

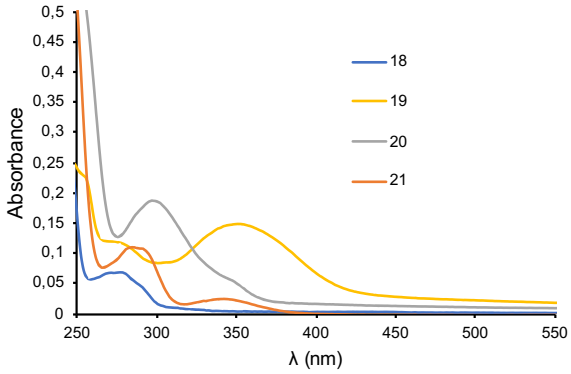

Figure 130. Absorbance spectra of **18, 19**, **20** and **21** at 10 μM in PBS 1X, pH = 7.4.

Regarding the fluorescence of the different compounds, we faced two different situations. When we irradiate at 360 nm, we have a strong emission from the ketone-containing fluorophore **19** as expected, and we can also observe some fluorescence for the intermediates **20** and **21** and neglectable fluorescence for the substrate **18**. In contrast, if we irradiate at 390 nm,[237] only **19** is significantly fluorescent, in particular, it is up to 350-fold more fluorescent than the probe **18**, and between 70 and 170-fold than the intermediates **20** and **21**, respectively (**Figure 131**).

[237] 390 nm is the wavelength typically used in confocal microscopy.

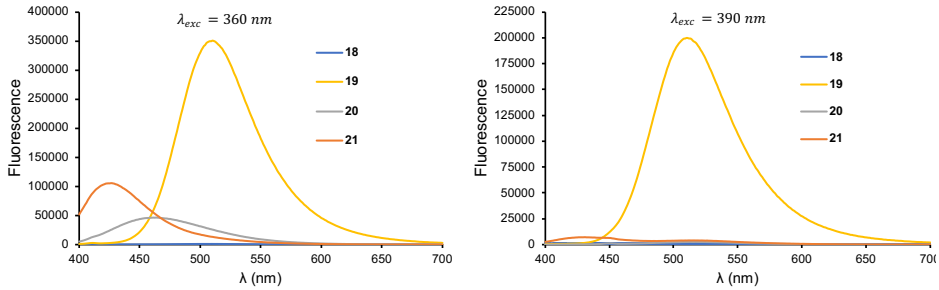

Figure 131. Fluorescence spectra for **18**, **19**, **20** and **21** at 5 μM in PBS 1X, pH = 7.4 irradiating at 360 (left) and 390 nm (right)

3.1.4 In vitro reactivity studies

We studied the viability of the concurrent deallylation/isomerization process using concentrations of 1 mM in H_2O:THF (8:2), with different loadings of the ruthenium catalysts, **Ru11** and **Ru13** and in presence of GSH. We were delighted to observe an intense fluorescent signal of the product, but only when both catalysts are present, even with loadings of 25 mol% (**Figure 132**).

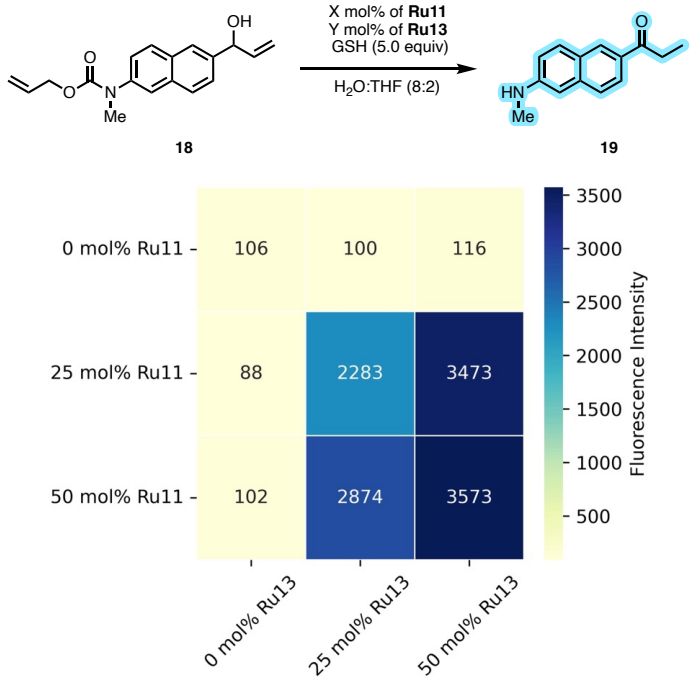

Figure 132. Fluorescent heat-map for the concurrent Ru-deallylation Ru-isomerization (λ_{exc} = 390 nm, λ_{em} = 515 nm).

3.1.5 In cellulo studies

At the moment, *in cellulo* experiments are pending. However, based on the *in vitro* experiments and the precedents on the isomerization and deallylation reaction, we are confident that this is a promising probe for dual metal catalysis *in cellulo*.

3.2 Tandem catalysis combining transition metal complexes and enzymes

To develop this type of tandem processes, we selected the ruthenium-catalyzed deallylation reaction and two different enzymatic reactions catalyzed by the enzymes Alkaline Phosphatases (ALP) or Monoamine Oxidases (MAO-A and MAO-B).

Alkaline Phosphatases (ALPs) catalyze the hydrolysis and transphosphorylation of mono phosphates (**Figure 133**). ALP can be found in different types of organisms, from prokaryotes to eukaryotes. In humans there are four isoforms: three of them tissue specific (intestinal, placental and germ cell) and one non-specific (mainly expressed in liver, bones and kidneys). The presence of ALP in blood, in clinically abnormal levels, can be an indicator for diseases like hepatitis, metabolic syndrome, or hepatic and pancreatic cancer.[238]

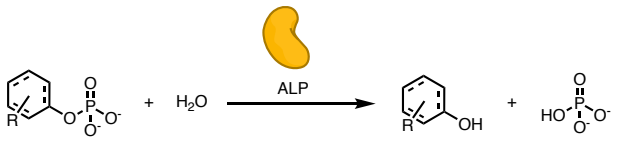

Figure 133. Hydrolysis of phosphate monoester by ALP.

On the other hand, monoamine oxidases (MAO) are localized in the outer membrane of mitochondria and catalyze the aerobic oxidation of primary, secondary and tertiary amines, like serotonin, dopamine, noradrenaline and adrenaline. MAO proteins use flavin adenine dinucleotide (FAD) as redox cofactor for the oxidation, with O_2 as stoichiometric oxidant (**Figure 134**).[239,240] MAO exists in two isoforms, MAO-A and MAO-B. They have a quite different tissue distribution since MAO-A is mainly found in liver, pulmonary vascular endothelium, placenta and gastrointestinal tract, whereas MAO-B is present in blood platelets. From a biochemical perspective, MAO enzymes are involved in the metabolism of neurotransmitters and its malfunction is related to different neurological problems (depression, schizophrenia, attention deficit disorder…).

[238] U. Sharma, D. Pal, R. Prasad, *Ind J Clin Biochem* **2014**, *29*, 269–278.
[239] S. Manzoor, N. Hoda, *Eur. J. Med. Chem.* **2020**, *206*, 112787.
[240] X. Wu, W. Shi, X. Li, H. Ma, *Acc. Chem. Res.* **2019**, *52*, 1892–1904.

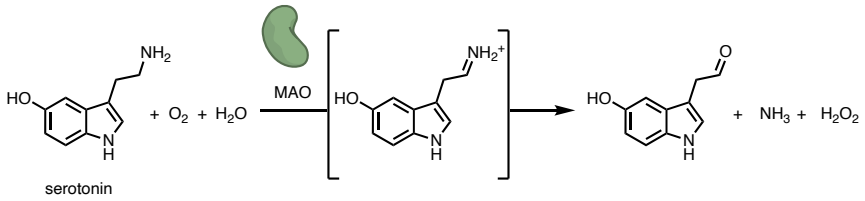

Figure 134. Oxidation of serotonin by MAO.

Monoamine Oxidases A and B (MAO-A/B), along with Alkaline Phosphatase (ALP) have been thoroughly studied and have been found to be relatively promiscuous, able to promote reactions on relatively different types of precursors, in comparison with other more substrate-specific enzymes. There have been several designs of chemical probes for the determination of the activity of these two types of enzymes both *in vitro* and *in cellulo* (Vero, HeLa or A549).[240] For instance, in the case of the ALP, a number of phosphoric esters probes have been described. As an example, Kim and coworkers developed the phosphate ester **I**, that upon hydrolysis by the ALP generates a free phenol that cyclize to the fluorescent iminocumarine **II**, allowing to measure the activity of ALP in living cells (**Figure 135a**).[241]

In the case of the MAO enzymes, Wood and coworkers published in 2006 the use of 3-hydroxypropylamine as recognition moiety for MAO. This moiety acts also as linker and, upon oxidation, is cleft by β-elimination to deliver the cargo. In this case, the authors applied this methodology for the activation of luciferin derivatives (**Figure 135b**).[242] The propylamine moiety can be recognized for both MAO-A and MAO-B, however, it may display different specificities depending on the overall structure of the molecule, so neither isoform can be discarded *a priori*.[239]

[241] T.-I. Kim, H. Kim, Y. Choi, Y. Kim, *Chem. Commun.* **2011**, *47*, 9825.
[242] W. Zhou, M. P. Valley, J. Shultz, E. M. Hawkins, L. Bernad, T. Good, D. Good, T. L. Riss, D. H. Klaubert, K. V. Wood, *J. Am. Chem. Soc.* **2006**, *128*, 3122–3123.

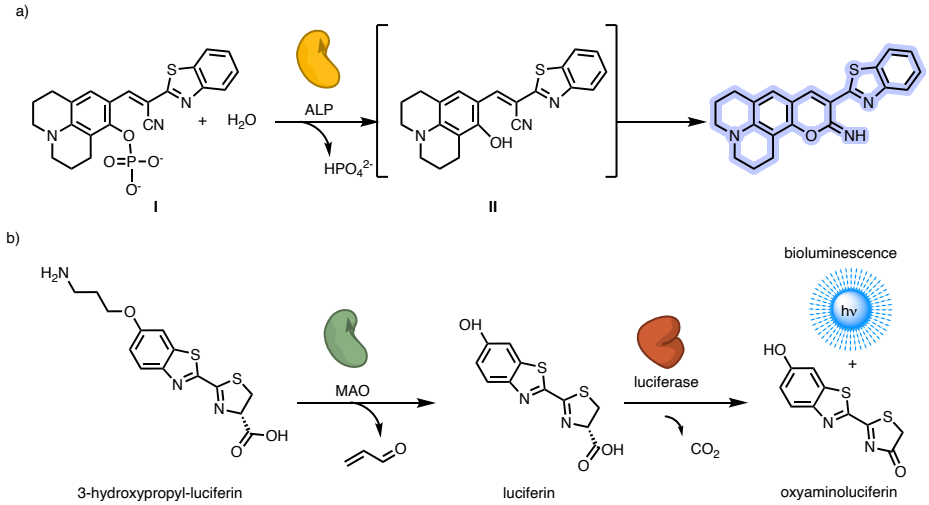

Figure 135. ALP and MAO-luciferase probes.

We selected two different scaffolds for the design of the probes, the first one is the HBT **11** as commented in the first section of this chapter, a fluorophore that exhibit ESIP and ICT.[234,235] The second scaffold is a BODIPY, which also exhibits ICT as well as emission in the Near-Infrared (NIR) region.[243] In both cases, the modification of the phenol decreases the fluorescence of the molecules (**Figure 136**).

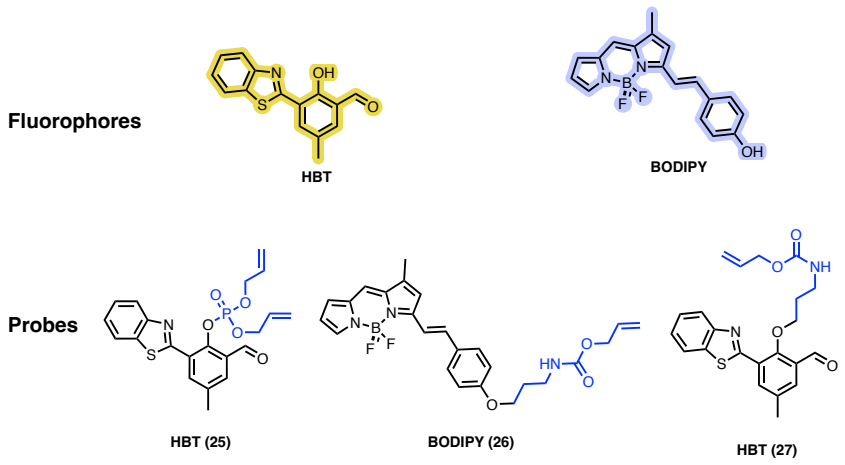

Figure 136. Fluorophores selected and designed probes.

[243] J.-S. Lee, N. Kang, Y. K. Kim, A. Samanta, S. Feng, H. K. Kim, M. Vendrell, J. H. Park, Y.-T. Chang, *J. Am. Chem. Soc.* **2009**, *131*, 10077–10082.

3.2.1 Tandem process involving a ruthenium catalyzed deallylation and alkaline phosphatase hydrolysis

*3.2.1.1 Synthesis of HBT probe **25*** [244]

The synthesis of the dual probe **25** for deallylation-ALP tandem process was accomplished in one step from **11** by oxidative phosphate formation with triallyl phosphite, DMAP and iodine as oxidant. The intermediate phosphoric acid **28** was easily accessible via deallylation promoted by the ruthenium catalysis ($[CpRu(MeCN)_3]PF_6$ + quinaldic acid) in methanol followed purification by reverse phase HPLC (**Figure 137**).

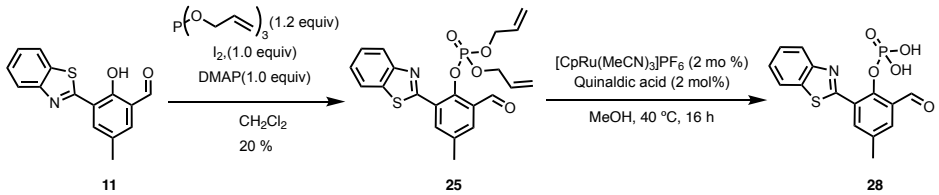

Figure 137. Synthesis of **25** and **28**.

As expected, the suppression of the ESIPT phenomena in both, **25** and **28**, decreases the fluorescence significantly in comparison with fully deprotected product **11**, which is 37-fold more fluorescent than the corresponding precursors (**Figure 138**).

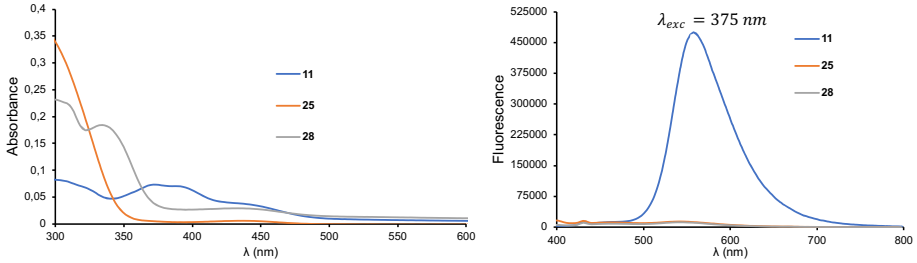

Figure 138. a) Absorbance spectra for **11**, **25** and **28** at 20 μM in PBS. b) Fluorescence of **11**, **25** and **28** at 10 μM in PBS.

3.2.1.2 Reactivity studies in vitro

We studied the tandem activation of the probe **25** (100 µM) by monitoring the fluorescence corresponding to the fluorophore **11**. We tested the tandem process by using 50 mol% of **Ru13** in Tris-HCl buffer (pH = 7.4, 10 mM), using different concentrations

[244] The experiments in this section were carried out in collaboration with Alejandra Vale Gómez

of GSH (0, 0.1, 0.2, 0.5 and 5.0 mM) as well as of the commercially available ALP enzyme (0, 0.1, 1.0, 10.0 and 100.0 U/mL).[245]

We found that the highest fluorescence intensity was achieved when using 10 U/mL of ALP and 0.5 mM of GSH. Higher concentrations of GSH (over 0.5 mM) does not improve the reaction, probably due to the change in the pH and the consequent interference in the ALP activity. Control experiments without ALP or without Ru catalyst, under otherwise identical reaction conditions confirmed that these two catalyst are required for the appearance of fluorescence (**Figure 139**).

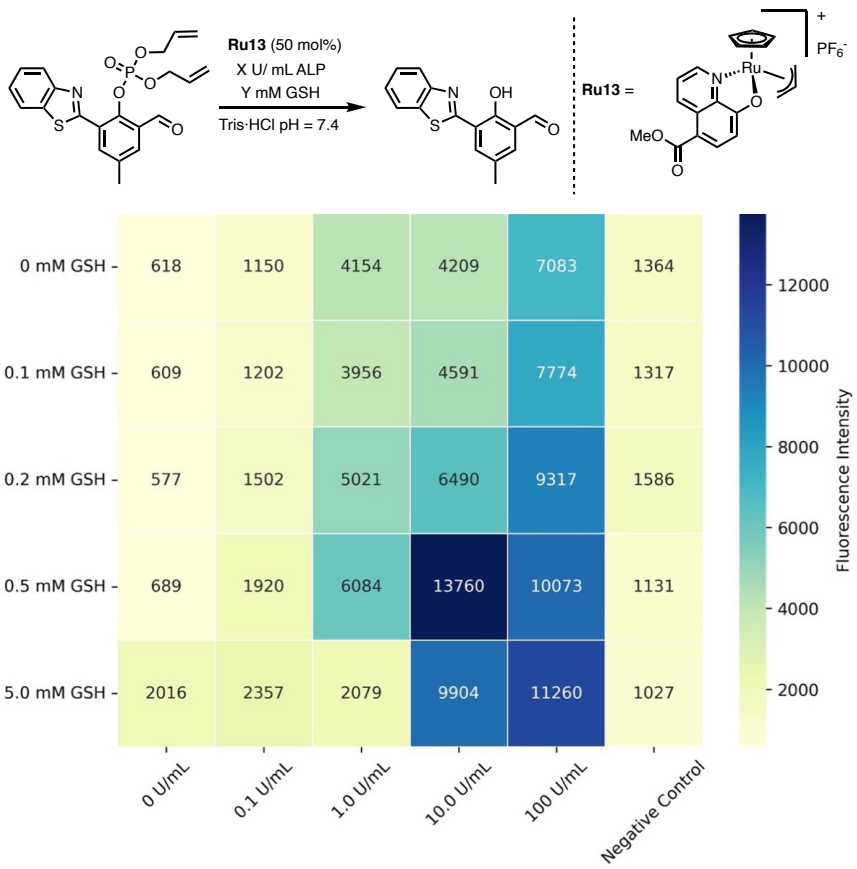

Figure 139. Fluorescent heat-map for the tandem ruthenium promoted-deallylation ALP hydrolysis, with variable loadings of GSH and ALP.

[245] U/mL = Enzymatic Units per Milliliter. 1 U (μmol/min) is defined as the amount of the enzyme that catalyzes the conversion of one micromole of substrate per minute under the specified conditions of the assay method

3.2.1.3 In cellulo experiments.[246]

In cellulo experiments were carried out in HEK-293 cells with native levels of ALP and with overexpressed levels of ALP (HEK-293 transfected with a plasmid for Secreted Embryonic ALP)[247]. The overall protocol is depicted in the **Figure 140.**

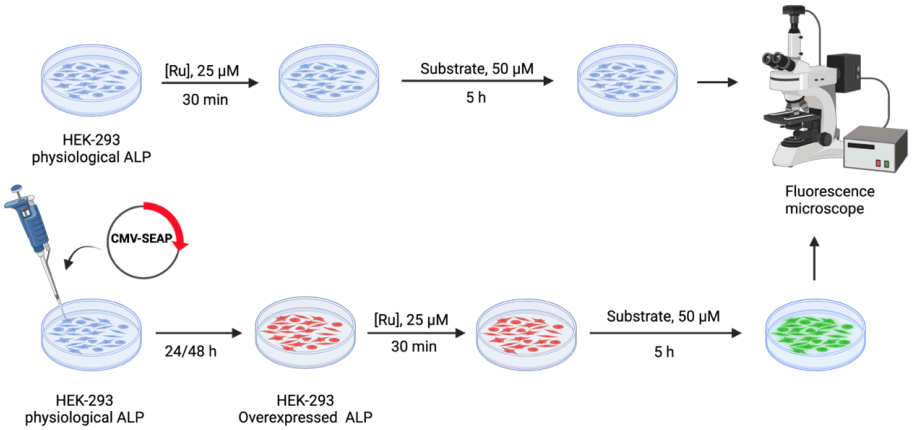

Figure 140. Experimental procedure for the cell experiments.

The level of overexpression of ALP were measured using a colorimetric commercial kit for the specific detection of ALP (NBT/BCIP).[248] Showing 2-fold increase in the levels of ALP after 24h and 5-10 fold after 48h.

Cellular experiments were carried out by incubation with ruthenium catalyst (either **Ru14** or **Ru15** at 25 μM) for 30 min followed by two washing steps with fresh media (DMEM) to avoid extracellular reactivity, and finally addition of the probe **25** (50 μM dissolved in DMEM) for 5 h. After the indicated time, cells were analyzed by fluorescence microscopy.

In cells with native levels of ALP that were treated with **Ru15**, we were delighted to observe an increment of cytoplasmatic levels of fluorescence that corresponds to the formation of the product **12** (**Figure 141, micrography C**). These results agree with the *in vitro* experiments for the tandem process.

[246] The experiments in this section were carried out by Alejandra Vale Gómez and PhD. María Tomás Gamasa

[247] Cells were transfected with the plasmid p-BLUESCRIPT CMV-SEAP (Secreted Embryonic ALP) using PEI as transfected agent.

[248] The levels of transfection were measure at 24 and 48 with a colorimetric commercial kit. NBT/BCIP Stock Solution from Merck. 11681451001.

Cells with overexpressed levels of ALP showed a significant increase in the fluorescence levels with a much higher intensity than that detected in the above experiments (**Figure 141**, **micrographies E,F**), showing that the reaction outcome correlates both, with the presence of artificial ruthenium catalyst and the natural enzyme.

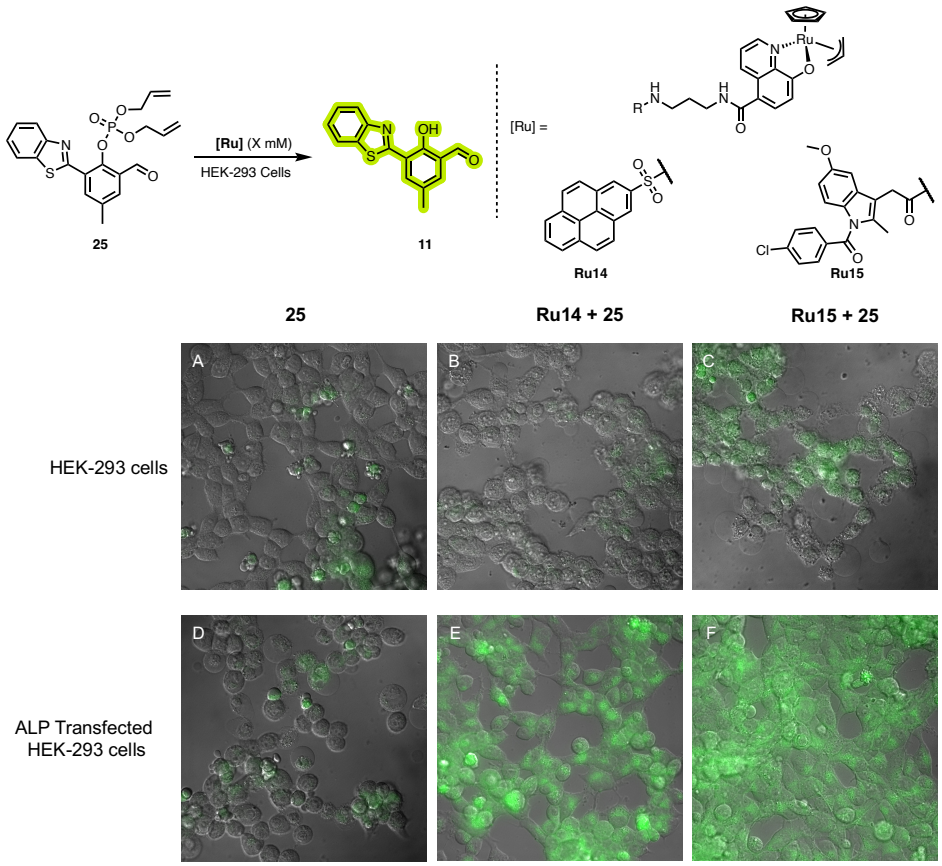

Figure 141. Intracellular tandem Ruthenium promoted deallylation ALP dephosphorilation. Fluorescence micrographies of HEK-293 cells (brightfield) after incubation with: A,D) probe **25**; B,E) **Ru14**, washed, and treated with **25**; C,F) **Ru15**, washed and trated with **25**. Conditions: cells were incubated with **Ru14** or **Ru15** (25 µM) for 30 min, followed by two washings with DMEM, and treatment with **25** (50 µM).A,B,C) HEK-293 cell with native levels of ALP. D,E,F) HEK-293 cells with overexpressed levels of ALP after 48 h after transfection.

Further controls incubating the cells with the intermediate **28** and the free phosphate, are planned. However, taking into consideration that probe **25** and the intermediate **28** have neglectable fluorescence compared to the fluorophore **11**, we are confident about the tandem nature of the process.

3.2.2 Tandem Ruthenium catalyzed deallylation – Monoamine Oxidase oxidation

3.2.2.1 BODIPY probe: synthesis and characterization[249]

The core of the BODIPY **29**, was synthetized by a Knoevenagel reaction followed by *in situ* complexation of the resulting bis-pyrrole with $BF_3 \cdot Et_2O$ (42% yield). A second Knoevenagel reaction either with *p*-hydroxybenzaldehyde in the presence of acetic acid and piperidine in toluene at 130 ºC (sealed tube) yielded the fluorophore **30** (60% yield). The same reaction but using the aldehyde **31** instead of *p*-hydroxybenzaldehyde, yielded the probe **26** in 20% yield. To access the intermediate **32**, deprotection of the probe under ruthenium catalysis ($[CpRu(MeCN)_3]PF_6$ + quinaldic acid), using triflic acid as additive in methanol afforded the free amine **32**, isolated after preparative HPLC (**Figure 142**).[250]

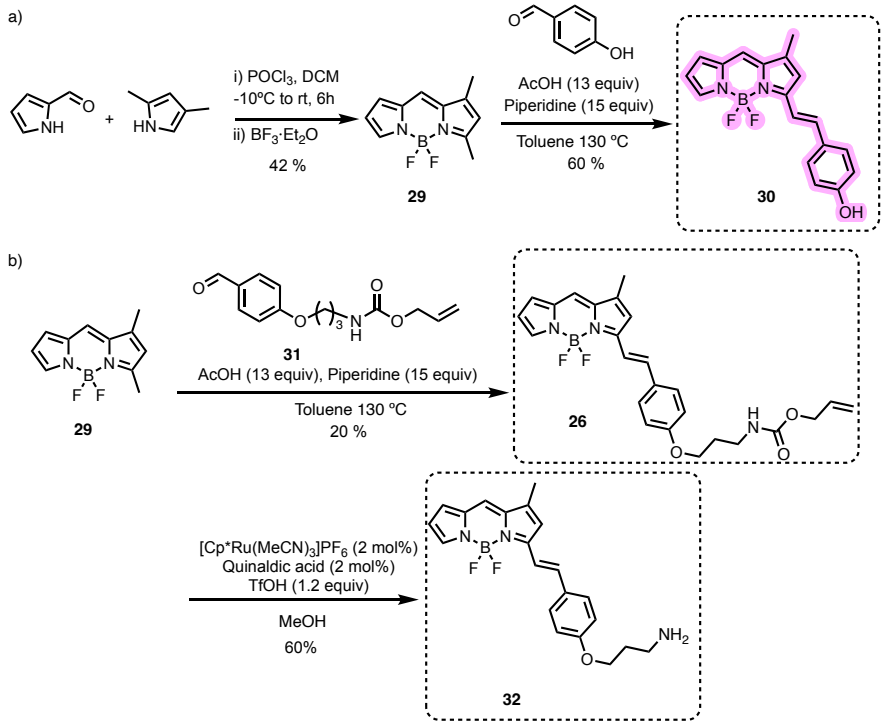

Figure 142. Synthesis of a) **30** and b) **26** and **32**.

The alkylation of the phenol ring from the BODIPY, allows to suppress the ICT fluorescence, even though the free amine **32** shows a higher fluorescence levels than the alloc counterpart (**26**) (**Figure 143**)

[249] The experiments in this section were carried out in collaboration with Leonard G. Cool
[250] S. Tanaka, Y. Suzuki, H. Saburi, M. Kitamura, *Tetrahedron* **2015**, *71*, 6559–6568.

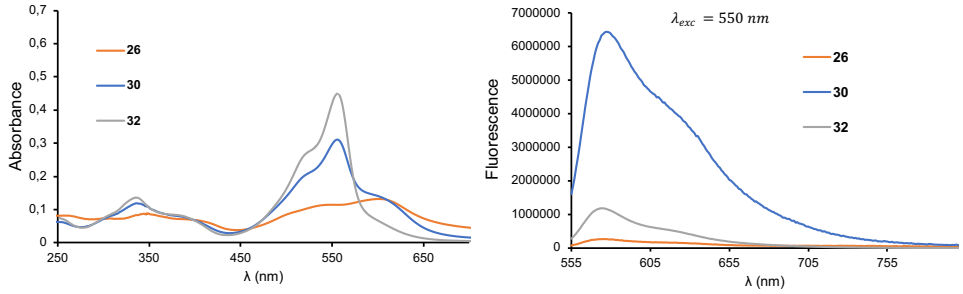

Figure 143. a) Absorbance spectra for **26**, **30** and **32** at 20 μM in PBS. b) Fluorescence of **26**, **30** and **32** at 10 μM in PBS.

*3.2.2.2 Cellular experiments for the tandem catalysis Ru-deallylation – MAO oxidation. Protected Bodipy probe **26**.*[251]

Due to a shortage in the MAO enzyme availability we first carried out the *in cellulo* experiments. [252] We select HeLa cells for the cellular experiments as they present relatively high levels of MAO enzymes.[240]

Different ruthenium catalyst (50 µM) for the deprotection of the probe **26** (100 μM) were tested. Hela cells were incubated for 30 min with 50 µM of the corresponding catalyst, two washing steps with cellular culture media, followed by the addition of the probe **24** (100 μM dissolved in DMEM) was incubated for 1.5 h. Analogously, control experiments incubating only with the probe, **26**, and the fluorophore, **32**, were carried out, showing a clear fluorescence difference between starting material and product.

Among the different catalysts used, the ruthenium catalyst, **Ru18**, bearing a pyrene moiety, showed the best results. However, the combination of the **Ru18** and the probe at 50, and 100 μM seems to be slightly toxic. To our delight the concentration can be reduced down to 75 and 25 μM respectively, without affecting the cell viability nor compromising the reactivity.

[251] The experiments in this section were carried out in collaboration by Leonard G. Cool and Dr. María Tomás Gamasa

[252] In vitro experiments with the two isolated MAO isoforms, A and B, are planned and will be carried out as soon as commercial availability of these enzymes is restored.

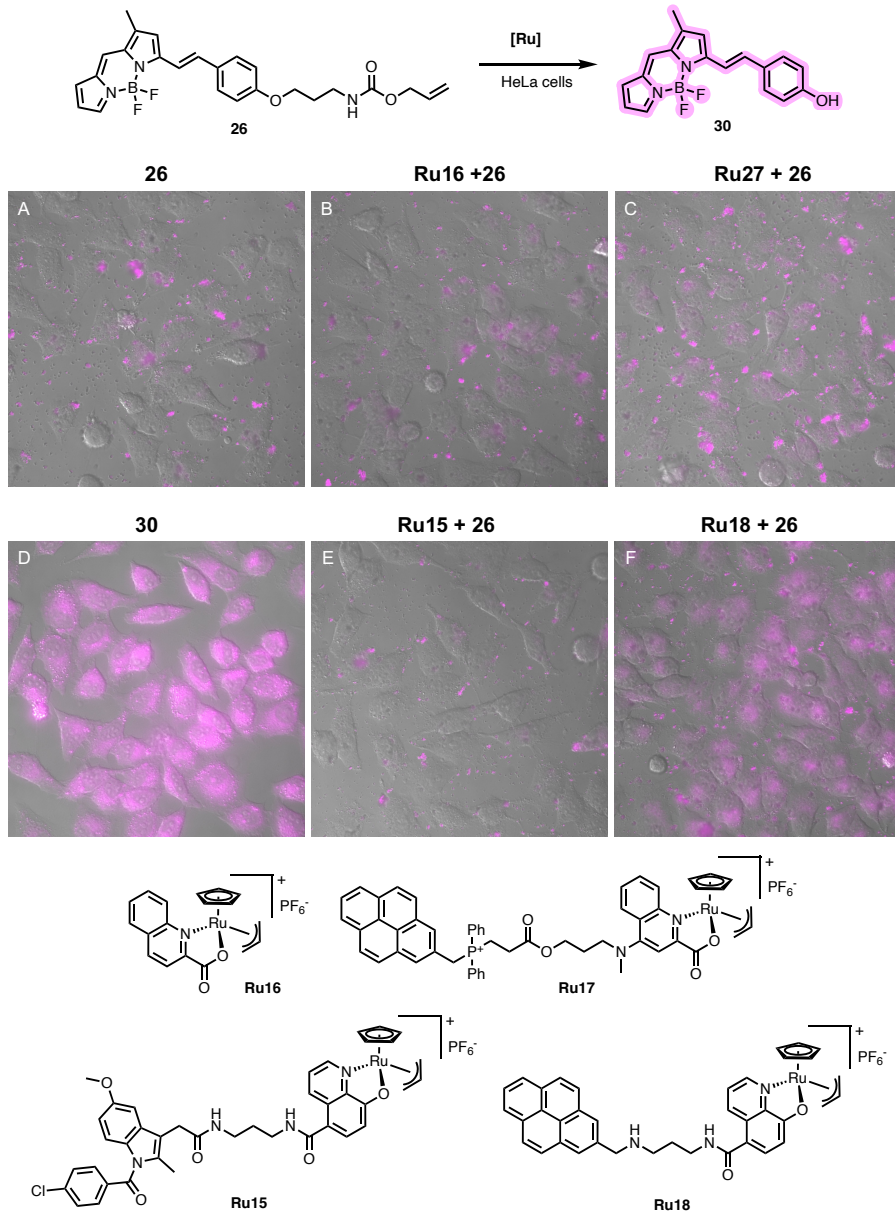

Figure 144. Intracellular tandem Ruthenium promoted deallylation MAO amine oxidation for **26**. Fluorescence micrographies of HeLa cells (brightfield) after incubation with: A) probe **26**; D) product **30**, B) **Ru16**; washed and treated with **26**; C) **Ru17**, washed and treated with **26**; E) **Ru15**; washed treated with **26**; F) **Ru18**, washed and treated with **26.** Conditions: cells were incubated with **Ru15, Ru16, Ru17** or **Ru18** (50 µM) for 30 min, followed by two washings with DMEM, and treatment with **26** (100 µM). Structure for **Ru15**, **Ru16**, **Ru17** and **Ru18** are shown in the bottom of the figure.

Incubation of the intermediate **32** (75 μM premixed in DMEM), showed similar results to those of the tandem process, with the progressive appearance of fluorescence upon the MAO oxidation. Controls with the probe **26** and the fluorophore **30** are in agreement with the MAO oxidation of the intermediate **32**.

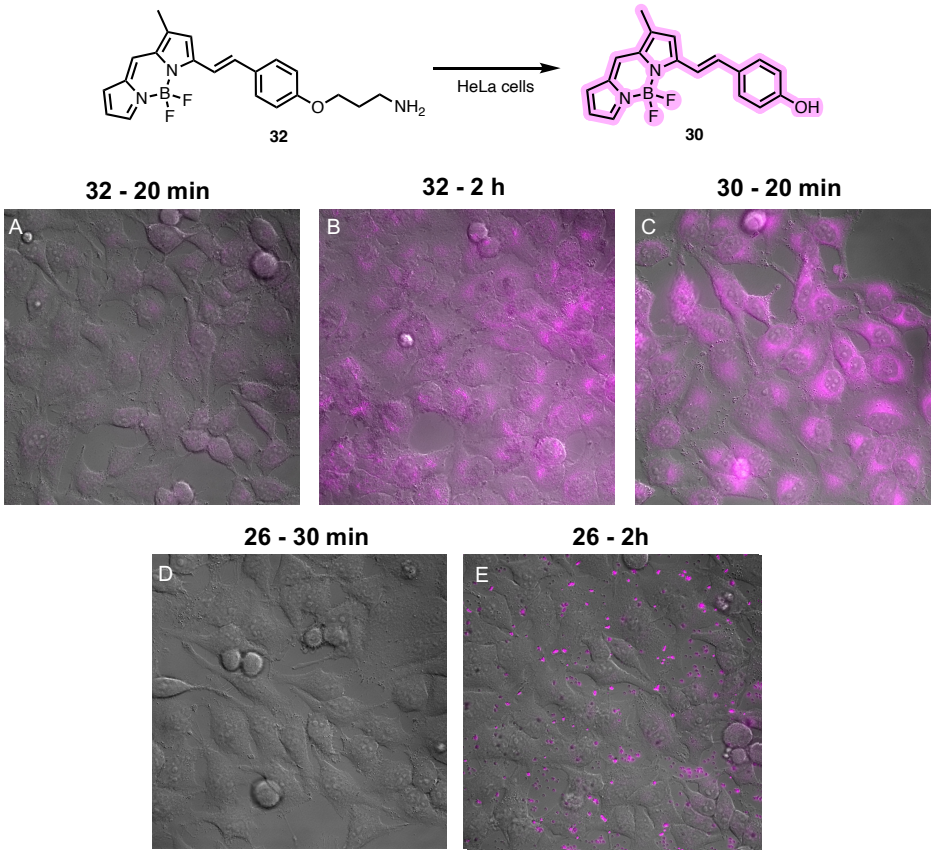

Figure 145. Intracellular MAO amine oxidation of **32**. Fluorescence micrographies of HeLa cells (brightfield) after incubation with: A) intermediate **32** for 20 min; B) intermediate **32** for 2 h; C) flurophore **30** for 20 min; D) probe **26** for 30 min; E) probe **26** for 2 h. Conditions: cells were incubated with **26**, **30** or **32** for the indicated time

3.2.2.3 HBT probe synthesis and characterization

The synthesis of the dual probe **27** for the deallylation-MAO tandem process was achieved in one step by alkylation of the phenol moiety of HBT, **11**, with the alkyl bromide derivative **33** in the presence of K_2CO_3, under refluxing conditions (70% yield).

The synthesis and isolation of the corresponding free amine **34**, as control for the MAO activity, was unsuccessful. Standard conditions for the ruthenium catalyzed uncaging of

alloc protected amines alloc amines (1 mol% of $[CpRu(MeCN)_3]PF_6$ +1 mol% of quinaldic acid), using triflic acid as additive (1.0 equiv) in MeOH,[250] did not provided the free amine **34**; instead, we observed the formation of the hemiaminal **36** quantitively. On the other hand, when thiophenol was used instead of the triflic acid and the reaction is performed in CH_2Cl_2, the imine **35** was isolated as main product (quantitavely). Substitution of the N-alloc group for a N-Boc group and its subsequent deprotection under acid conditions (TFA:CH_2Cl_2 1:1) neither provided the desired product, **34**, but the imine **35** (**Figure 146**).

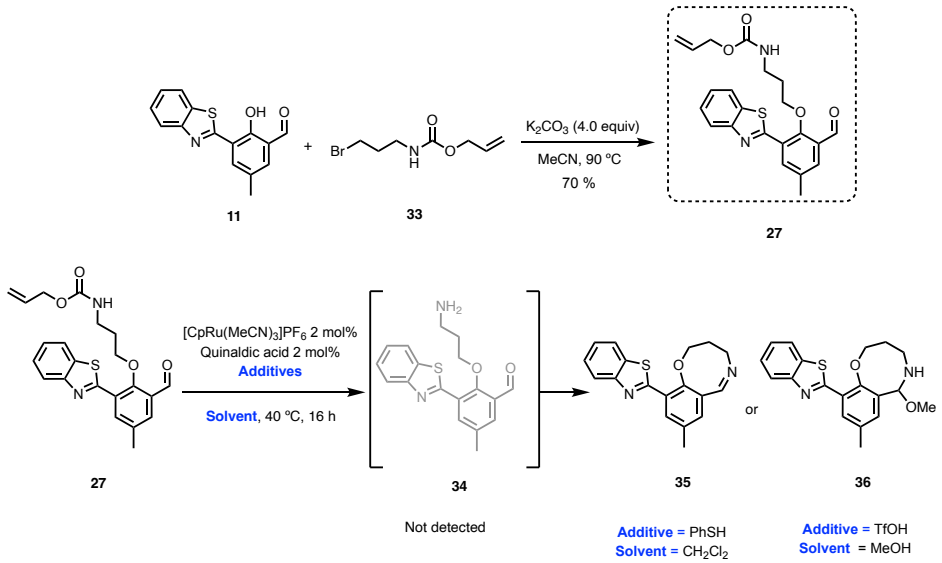

Figure 146. Synthesis scheme for the probe **27**, **35** and **36**.

As in the previous case, the alkylation of the phenol of the HBT core suppressed the ESIPT mechanism in the probe **27** and the imine derivative **35** (**Figure 147**).

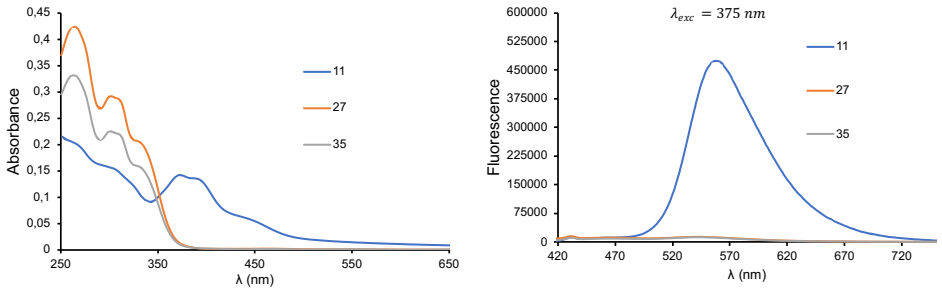

Figure 147. a) Absorbance spectra for **11**, **27** and **35** at 20 μM in H_2O:*i*PrOH (1:1).
b) Fluorescence of **11**, **27** and **35** at 10 μM in PBS.

3.2.2.4 Cellular experiments.[253]

Despite the failure in the preparation of the intermediate probe, **34**, we decided to carry on and perform preliminary experiments of the tandem catalysis in HeLa cells.

We selected started with the optimized conditions found for the BODIPY probe **26**: incubation of **Ru18** (25 μM) for 30 min, two washing steps with DMEM and incubation with the probe (75 μM dissolved in DMEM) for 2h. Analogously, control experiments were carried out with incubation of just the imine, **35**, the probe, **27**, and the fluorophore, showing a clear fluorescence difference between the starting materials and product.

When cells are treated with the probe **27** and the ruthenium catalyst **Ru18** we can observe the appearance of fluorescence, a clear signal that the tandem process is taking place. No fluorescence is observed when cells are treated with the cyclic imine **35**. This results suggest that the transient species (**34**), bearing a primary amine, might be generated in the cell and gratifyingly, it appears to has been metabolized by MAO before its conversion to the otherwise non-productive cyclic imine **35**. This results clearly highlights the influence of the cell environment on the chemoselectivity of a transformation and, moreover, it also showcase one of the main features of tandem catalysis, the trapping of short live intermediates that otherwise are not viable.

[253] The experiments in this section were carried out by Dr. María Tomás Gamasa

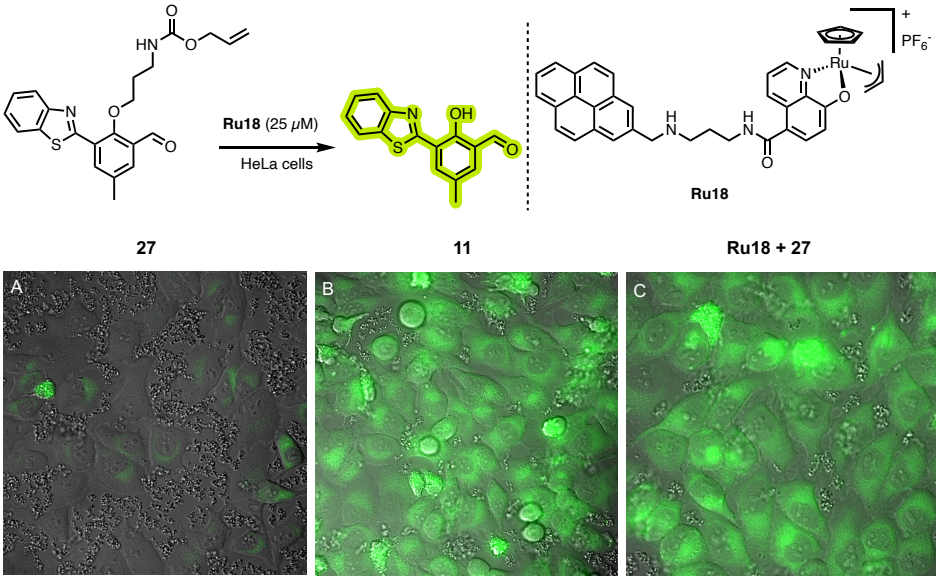

Figure 148. Intracellular tandem Ruthenium promoted deallylation MAO amine oxidation for **27**. Fluorescence micrographies of HeLa cells (brightfield) after incubation with: A) probe **27**; B) product **11**, C) **Ru18**; washed and treated with **27**; Conditions: cells were incubated with **Ru18** (25 μM) for 30 min, followed by two washings with DMEM, and treatment with **26** (75 μM).

Although further controls using inhibitors of MAO enzyme and additional efforts to try to detect the formation of the probe **11** by LC-MS techniques are required and will be done in due course, we can confidently propose that the gathered data is only compatible with the designed tandem process, involving a ruthenium catalyzed alloc deprotection followed by an oxygenase digestion.

ANNEX

Development of a cell selective deallylation catalyst [254]

All the above mentioned results on transition metal catalyzed processes in cells are based on the ability of these low molecular metal catalysts to cross the cell membrane and thus being internalized without becoming deactivated. Although this strategy proved to be successful, we reasoned that a finer control of the catalytic events could be achieved if we could design catalysts that could only work with specific cell types that enable their internalization.

On these bases, and to try to eventually achieve more selective and efficient tandem processes, we devised the development of novel ruthenium catalysts that could be exclusively active in specific types of cells, which precisely recognize and allow their internalization.

Peptides that exhibit the RGD motif are involved in the cell adhesion by its recognition with integrins, however, this motif has also been used for cell recognition and drug delivery. Thus, we hypothesize that introduction of the peptidic motif RGD in a deallylation ruthenium catalyst will add this new level of selectivity, by allowing the differentiation between different cell types and therefore confining the process to cells bearing integrin receptors.

In particular, we designed the ruthenium complex **Ru-RGD**. It consists on the RGD motif bearing a terminal L-lysine from which a fluorescent reporter, 5-carboxytetramethylrhodamine (Tmr) is linked to the N-terminus and the 8-hydroxyquinoline ligand for the Ru complex is attached through an amide bond to the amino group of the side chain (**Figure 149**).

[254] The experiments in this section were carried out in collaboration with Alejandra Vale Gómez

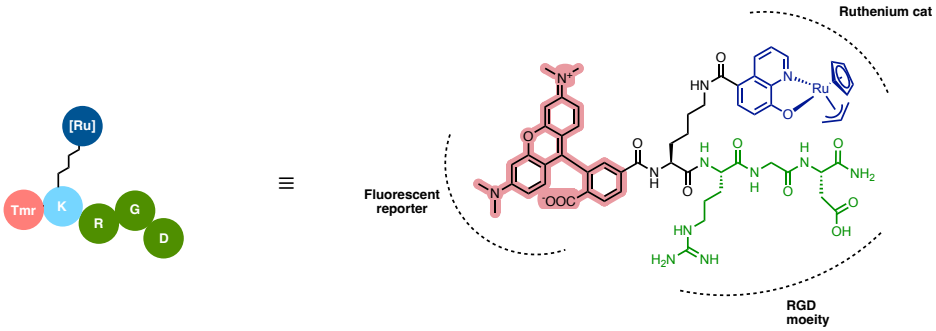

Figure 149. Design of the **Ru-RGD**

The Fmoc-K(alloc)RGD peptide was assembled by solid phase peptide synthesis. For the introduction of the 8-hydroxyquinaline, the side chain of the lysine was orthogonally deprotected by a palladium promoted Tsuji-Trost deallylation to yield the Fmoc-K(NH_2)RGD. The free amine from the lysine was then coupled with the *N*-succinimidyl ester from the 8-(allyloxy)quinoline-5- carboxylic acid ligand (Qti-NHS).

Deprotection of the *N*-terminus of the peptide with piperidine and coupling of the activated *N*-succinimidyl ester of the 5-tetramethylrhodamine (5-NHS-Tmr), followed by cleavage from the resin with a deprotection cocktail, afforded the crude peptide (**RGD-ligand**). The ligand was purified by reverse phase preparative HPLC.

To synthetize the complex, the **RGD-ligand** was dissolved in a 1:1 degassed mixture of H_2O:CH_2Cl_2 followed he by addition an equimolar amount of $[CpRu(MeCN)_3]PF_6$ (**Ru9**). The reaction was followed by ESI-MS, upon completion the sample was freeze-dried to afford the desired metal complex **Ru-RGD**. The ESI-MS spectra of the complex is in agreement with the simulated spectra.

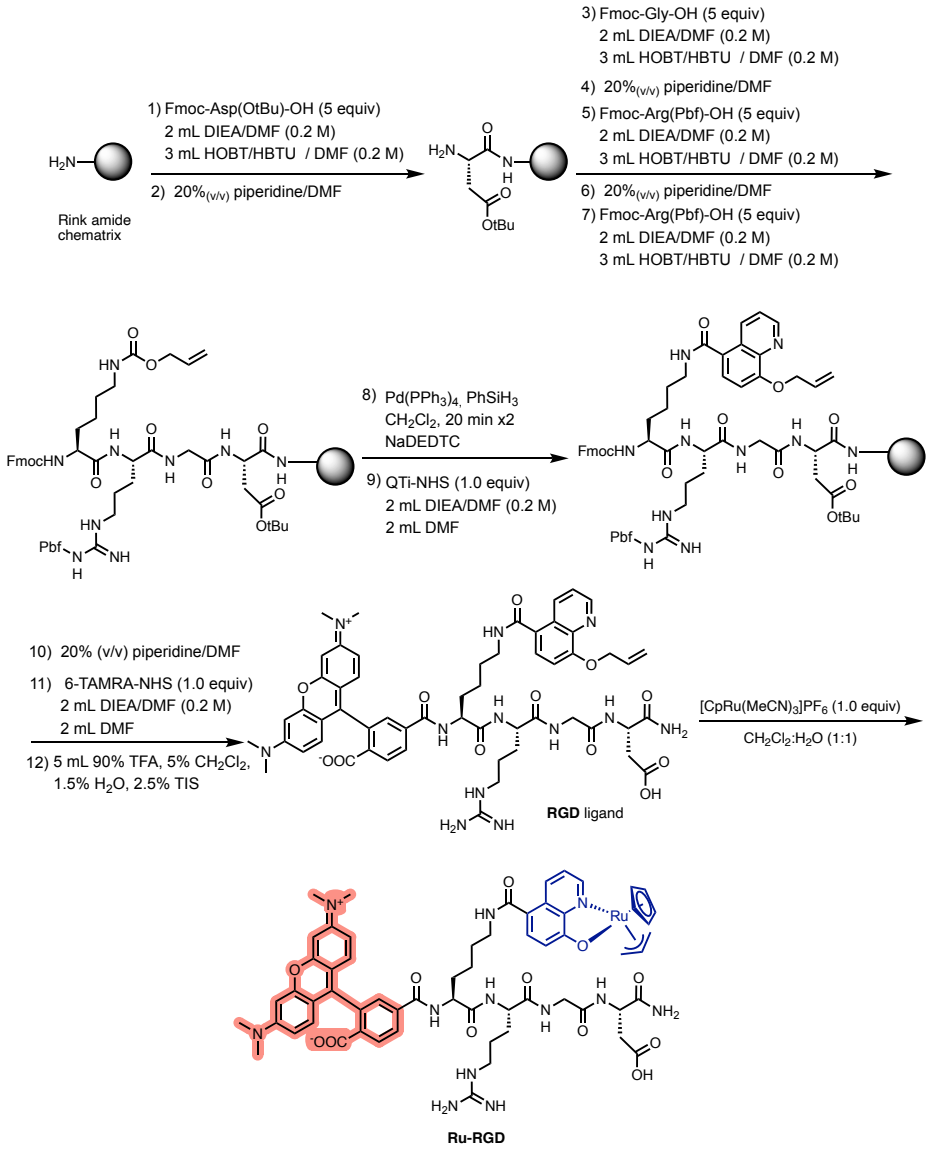

Figure 150. General synthesis scheme for the synthesis of **Ru-RGD**

In vitro activity testing

We studied the catalytic activity of **Ru-RGD** on the deallylation reaction of the HBT-based probe **17**. We tested the deallylation at a probe concetration of 150 μM, with increasing catalytic loadings of **Ru-RGD** (0, 37.5 and 75 μM), with and without GSH (0, 500 μM).

We can observe that upon increase of the catalyst loading the band corresponding to the starting material **17** disappears and the fluorescence band corresponding to the product **11**, appears. The highest fluorescence was observed when using 75 μM of **Ru-RGD** in combination with a 500 μM concentration of GSH. These results confirm that the **Ru-RGD** is catalytically active and can promote deallylation reactions under highly diluted conditions (**Figure 151**).

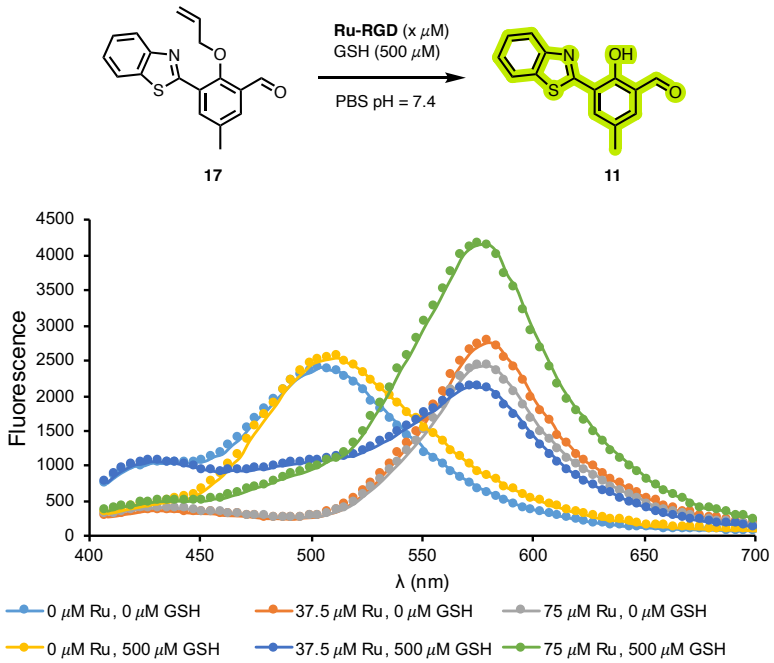

Figure 151. Deallylation of **17** (150 μM) with **Ru-RGD**

Cellular experiments

We first used two different cell lines for the *in cellulo* studies, HEK-293 (already employed in the deallylation-ALP tandem), which holds good levels of integrins, the receptor required for the internalization, and MCF7 cells (human breast adenocarcinomic cells) which displays low levels of integrins.

Then both cell lines were incubated with 15 μM of the **Ru-RGD** complex for 1.5 h, and subsequentially washed with cell culture media. In the case of MCF7 cells we did not observed any red-fluorescent signal, meaning that there was a poor internalization. However, in the case HEK-293 cells, to our delight, we detected a clear intracellular

signal from the **Ru-RDG**, meaning that cellular differentiation strategy for internalization works (**Figure 152**).

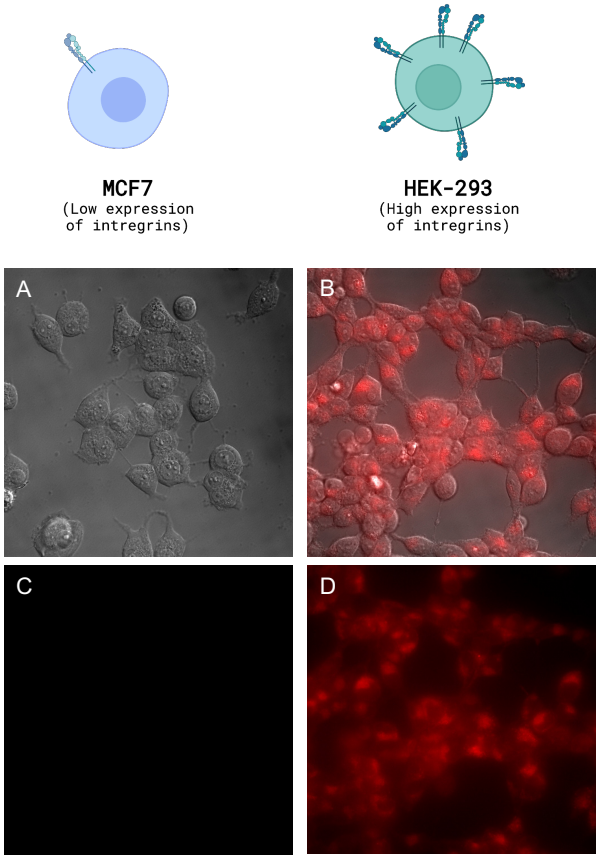

Figure 152. Celullar differenciation between MCF7 and HEK-293 cells by **RuRGD**. Fluorescence micrographies of A) MCF7 (brigthfield) incubated with **RuRGD**; B) HEK-293 (brigthfield) incubated with **RuRGD**, C) MCF7 (brifgfield +Red Chanel) incubated with **RuRGD**; D) HEK-293 (brifgfield +Red Chanel) incubated with **RuRGD** Conditions: cells were incubated with RuRGD (15 μM) for 1.5 h followed by two washes with DMEM. λ_{exc} = 550 nm y λ_{em} = 570-590 nm.

Studies regarding the catalytic activity of the **Ru-RGD** *in cellulo* are required. However, these good results allow us to envision its use for the tandem process in co-cultures of different cell types and selectively promoting the tandem process selectively in the target cell line.

4 Conclusions

We have designed, synthetized and characterized a dual metal probe for ruthenium promoted isomerization of allylic alcohol and ruthenium promoted deallylation. The *in vitro* results are good and cell experiments are pending.

We have designed, synthetized and characterized three probes for metal-enzyme tandem process: one for ALP and two for MAO enzyme. We have accomplished the tandem process both *in vitro* and *in cellulo* for the ALP enzyme and the *in cellulo* experiment for the MAO. These results show the potential of bioorthogonal transition metal catalyst to interfere in enzyme promoted processes, and therefore either building artificial metabolic networks or interfere in the host metabolism.

Lastly, we have designed and tested a RDG ruthenium deallylation catalyst capable of differentiate between cells with high and low integrins levels. The complex is active *in vitro* and can differentiate between HE-293 and MCF7 cell lines.

Overall conclusions

This PhD work has developed different ruthenium based transformation that can be carried out in aqueous and biological media, in some cases inside live mammalian cells and even in a tandem fashion with natural occurring enzymes.

General conclusion.

1) We studied the activity of several ruthenium complexed for the azide-thioalkyne cycloadditions finding that under aqueous conditions, cationic ruthenium complexes are highly active. Furthermore, we have developed a series of ruthenium photoactivatable precatalysts providing spatio-temporal control of the RuAtAC reaction. These precatalysts allowed to carry out the cycloaddition under diluted and biocompatible conditions and are able to promote RuAtAC using azide containing peptides and oligonucleotides. Moreover, these complexes allowed also allowed to carry out the reaction in the presence of HeLa cells.
2) We have translated the intermolecular alkene-alkyne couplings to aqueous conditions at 37 ºC using $[Cp^*Ru(MeCN)_3]PF_6$ as catalyst, allowing the modification of complex molecules such as glucosides, amino acids and drugs with good selectivities. We also demonstrated that the reaction is tolerant to a broad variety of biomolecular additives and reaction media, therefore presenting a very good bioorthogonality profile. And finally, we were able to selective modify amino acids, and small peptides under aqueous conditions, even at low concentrations of 100 μM.
3) We have presented the first metal catalyzed isomerization that can take place in live mammalian cells, using as key component allylic alcohols and a Ru(IV) precatalyst. We have shown that the key intermediates in the process are ruthenium-hydrides and that theses hydrides intermediates do not react with the environment but evolve to the product in a intramolecular manner. We have determined the TON of the intracellular process showing that the ruthenium catalyzed isomerization of allylic alcohols takes place catalytically. Furthermore, we were able to deplet the GSH levels of HeLa cells by synthetizing *in cellulo* Michael acceptors, by means of the ruthenium catalyzed isomerization of bis-allylic alcohols. This result showcases a potential use of bioorthogonal transition metal catalysis as a therapeutic tools.

4) We have extended the scope of transition metal catalyzed processes for concurrent dual metal catalysis and for tandem processes involving metal and enzyme catalysis. We have shown that two discrete transition metal complexes can independently work over one substrate to yield a fluorescent molecule under diluted aqueous conditions. Further experiments to extend this methodology to living cells are planned.

   We have also shown that organometallic reagents can work with existing natural enzymes to promote tandem processes that we might envision as an incipient artificial metabolic network. We have been able to translate this concept to live mammalian cells using different fluorogenic scaffolds and different enzymes showing that it is a concept that can be generalized. Further research to broaden the scope of artificial and biocompatible transformations is highly desirable as well as for expanding these networks beyond two consecutive reactions.

Resumo Da Tese Doutoral

A química biolóxica é a disciplina científica cuxo obxectivo é o desenvolvemento de novas ferramentas químicas para a manipulación de sistemas biolóxicos. Dentro deste campo inclúese a área da química bioortogonal, que engloba as reaccións químicas que poden ter lugar en ambientes biolóxicos e vivos de forma non nociva. A pesar do éxito desta modalidade, evidenciado coa concesión do Nobel de Química de 2022, o desenvolvemento de novas reaccións biocompatibles segue a ser un desafío debido aos requirimentos necesarios: quimio selectividade, compatibilidade coas condicións fisiolóxicas, biocompatibilidade dos reactivos e os produtos; cinética rápida; e estabilidade de reactivos e produtos.

Neste contexto, o desenvolvemento de procesos bioortogonais promovidos por axentes catalíticos externos resulta moi atractivo, xa que os reactivos permanecerían estables ata atopar o catalizador. Especialmente atractiva é a posibilidade de utilizar complexos de metais de transición como catalizadores, debido á enorme amplitude e alcance da catálise organometálica. Ademais, a posibilidade de afinar as propiedades físicas e catalíticas dos catalizadores metálicos modificando os seus ligandos, representa unha vantaxe adicional para este tipo de estratexia.

A introdución desta tese recolla unha breve introdución ás reaccións catalíticas facendo fincapé no desenvolvemento de procesos catalizados por metais de transición en condicións acuosas e biocompatibles. En primeiro lugar, fai unha descrición xeral dos procesos catalíticos e as diferentes formas de clasificación destes. Seguidamente centrámonos nos procesos clasificados como "catálise homoxénea", que fai referencia a todos aqueles procesos catalíticos nos que o catalizador e o substrato están na mesma fase, pero que normalmente está asociado ás reaccións catalizadas por compostos organometálicos. Neste apartado describense os pasos elementais dos procesos catalizados por metais de transición, así como a versatilidade destes. Describense as características xerais e mecanismos de dous tipos de transformacións relevantes para a presente tese, a saber, reaccións de acoplamento cruzado e cicloadicións.

Seguidamente fai unha breve introdución á catalisis mediada por metais de transición en condicións acuosas. Nesta sección destacase a importancia da auga como disolvente das reaccións biolóxicas, así como o seu papel como disolvente "verde" (non tóxico, renovable, alta constante dieléctrica... etc.). Así mesmo, aborda a idea errónea de que os compostos organometálicos son incompatibles con condicións acuosas, mediante unha descrición das propiedades coordinativas destes, así como exemplos relevantes de

reaccións catalizadas por complexos metálicos en condicións acuosas por Grubbs e por Lipshutz.

Despois desta breve introdución, dáse paso á cicloadición entre azidas e alquinos catalizada por cobre (I). Esta transformación, principal exemplo de "reacción click", foi independentemente descrita por Meldal e Sharpless en 2002, destaca polo seu alto rendemento, regioselectividade, robustez e xeralidade. Supón, ademais, un punto de unión entre as reaccións catalizadas por metais de transición e as reaccións bioortogonais, xa que é o primeiro exemplo da unión de ambas no contexto da química biolóxica.

A continuación, realízase un seguimento histórico do desenvolvemento de reaccións bioortogonais catalizadas por metais de transición. Dos diferentes exemplos descritos neste apartado, pódense extraer dúas conclusións: primeiro, que o Paladio e o Rutenio son os dous elementos predominantes neste campo cunha xenerosa cantidade de exemplos. E segundo, que, entre ambos metais, o Rutenio exhibe unha maior variedade de transformacións e os seus compostos discretos presentan unha maior estabilidade en ambientes biolóxicos.

As conclusións obtidas a partir desta introdución son que o desenvolvemento de reaccións bioortogonais catalizadas por metais de transición permite realizar transformacións imposibles mediante reactividades orgánicas clásicas e que, entre os diversos metais exemplificados, o rutenio destaca pola súa versatilidade e alcance.

No **capítulo I** recolle o desenvolvemento dunha segunda xeración para a cicloadición entre azidas e tioalquinos catalizada por complexos de rutenio (RuAtAC polas súas siglas en inglés). Neste apartado estúdase o uso de complexos catiónicos de rutenio(II) na RuAtAC, demostrando que estes complexos son capaces de superar a xeración anterior en actividade a baixa concentración. Así mesmo, desenvolveuse unha batería de compostos fotoactivables de rutenio que permiten o control da reactividade do sistema. Estudouse o perfil de bioortogonalidade en condicións de dilución observando unha gran actividade para todos os novos compostos e aplicouse estes para a modificación de biopolímeros, así como en reaccións en presencia de células.

Nun traballo previo informado polo grupo de investigación, desenvolveuse a primeira reacción de cicloadición entre azidas e alquinos catalizada por rutenio en condicións acuosas facendo uso como compoñentes clave tioalquinos e o complexo [Cp*RuCl(COD)]. Esta reacción demostrou ser robusta e xeral en canto ao alcance

refírese, así como con un bo perfil bioortogonal. Con todo, tamén presentaba limitacións en canto a actividade en condicións de dilución (micromolar) e á selectividade fronte a alquinos terminais, o que dificultaba a súa aplicación en química biolóxica e o seu uso conxunto á CuAAC, respectivamente.

Co obxectivo de desenvolver unha segunda xeración de catalizadores que abordara estes problemas, estudouse a actividade do complexo $[Cp^*Ru(MeCN)_3]PF_6$ na RuAtAC. Atopouse que, malia os informes anteriores da súa inactividade en disolventes orgánicos, é un catalizador competente en condicións acuosas para a reacción de cicloadición de azidas e tioalquinos. Así mesmo, estudouse o seu comportamento en disolventes orgánicos, atopando unha especie de rutenio non produtiva, a súa especiación en condicións acuosas e a súa selectividade fronte a alquinos terminais e internos. Neste último aspecto, atopouse que o complexo $[Cp^*Ru(MeCN)_3]PF_6$ é máis selectivo que o seu predecesor fronte a alquinos terminais, permitindo a súa aplicación secuencial coa CuAAC.

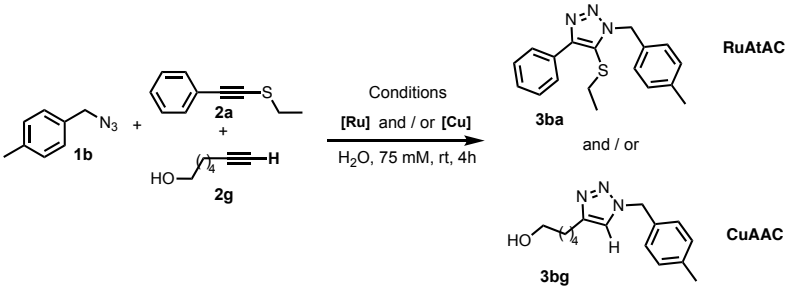

Figura 1. Ortogonal CuAAC e RuAtAC en condicións aquosas.

Estes bos resultados co complexo catiónico $[Cp^*Ru(MeCN)_3]PF_6$, permitiron o desenvolvemento e estudo de complexos tipo sándwich $[Cp^*Ru(arene)]X$ na RuAtAC. Atopamos que estes compostos son facilmente activables nas condicións de reacción mediante a aplicación dun feixe de luz en presenza de pequenas cantidades de acetonitrilo. A capacidade de activar selectivamente o catalizador mediante un estímulo externo supón un control espazo-temporal da reactividade, o que é de gran interese debido á súa aplicación biolóxica.

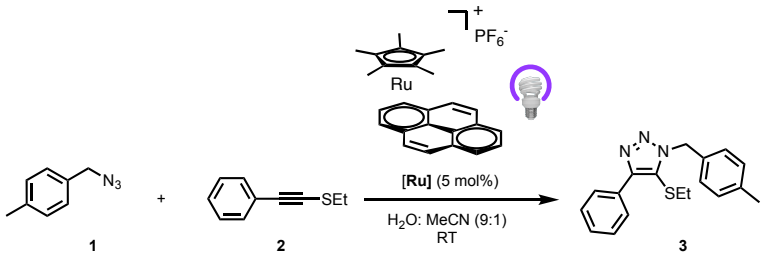

Figura 2. Uso de complexos de rutenio fotoactivables para a RuAtAC.

A continuación estudouse a actividade do $[Cp^*Ru(MeCN)_3]PF_6$ así como diversos compostos fotoactivables en condicións de alta dilución, atopando que tanto o $[Cp^*Ru(MeCN)_3]PF_6$ como o $[Cp^*Ru(pyrene)]PF_6$ presentan unha alta activade ata 100 μM. Así mesmo estudouse a bioortogonalidade destes compostos en diversos medios bioloxicamente relevantes como medio de cultivo celular ou lisados celulares, atopando que son capaces de promover a RuAtAC con altas eficiencias en ditos medios incluso en condicións de dilución.

Estes novos catalizadores foron posteriormente comparados con outros metais (Iridio e Rodio) que foron reportados como capaces de promover cicloadicións entre azidas e diversos tipos de alquinos en condicións acuosas, atopando que ningún deles iguala aos novos catalizadores de rutenio en condicións de dilución nin en condicións bioortogonais.

Finalmente, os novos catalizadores foron aplicados na unión de un péptido e un oligonucleótido (ambos modificados cunha azida) mediante a reacción de RuAtAC, en ambos os casos con bos rendementos, especialmente no caso dos compostos fotoactivables. E, por último, demostrouse que a reacción pode ter lugar en presenza de células de mamífero, realizando a reacción nunha suspensión de células HeLa.

No **capítulo II**, recollese a translación da reacción de acoplamento de alquenos e alquinos catalizada por rutenio e desenvolvida por Trost a condicións acuosas e biocompatibles.

No contexto de reaccións de formación de ligazóns carbono-carbono bioortogonais, existen poucos precedentes, algúns poucos acoplamentos cruzados catalizados por paladios (Sonogashira e Suzuki, principalmente) así como a reacción de metatese de alquenos catalizadas por rutenio. En xeral, todos estes procesos fan uso de alquenos e alquinos como grupos bioortogonais, debido á súa estabilidade cinética e a súa fácil activación mediante metais de transición.

Dentro das reaccións clásicas de formación de enlaces? carbono-carbono, Trost desenvolveu un acoplamento entre alquinos e alquenos catalizado por complexos catiónicos de rutenio. Este acoplamento pode ter lugar a temperatura ambiente e tolera pequenas cantidades de auga, polo que, en base aos bos resultados no capítulo anterior para a RuAtAC, decidimos explorar a translación desta reacción a medios acuosos e biolóxicos.

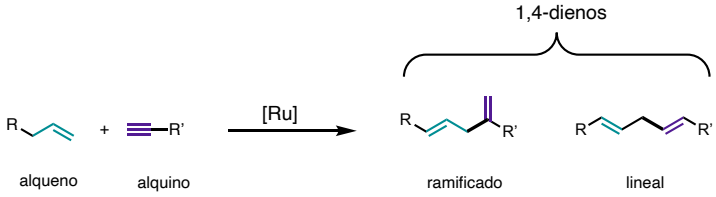

Figura 3. Esquema xeral da reacción de acoplamento de alquinos e alquenos.

Descubriuse que o complexo $[Cp^*Ru(MeCN)_3]PF_6$ é un catalizador competente para o acoplamento entre alquenos e alquinos para dar lugar a dienos 1,4 ramificados, con boas rexioselectividades. Este acoplamento funciona especialmente ben se o alquino de partida ten un heteroátomo na posición proparxílica e con altas rexioselectividades se o centro proparxílico é cuaternario. Así mesmo, descubrimos que se pode cambiar a selectividade do proceso de dienos 1,4 ramificados a dienos 1,4 lineais cambiando o ligando Cp* por o Cp. O alcance da reacción é bastante xeral permitindo o acoplamento de diferentes alquinos e alquenos. A reacción demostrou ser robusta e bioortogonal, tolerando unha ampla variedade de medios bioloxicamente complexos, así como diversos aditivos tales como aminoácidos ou vitaminas e cofactores enzimáticos.

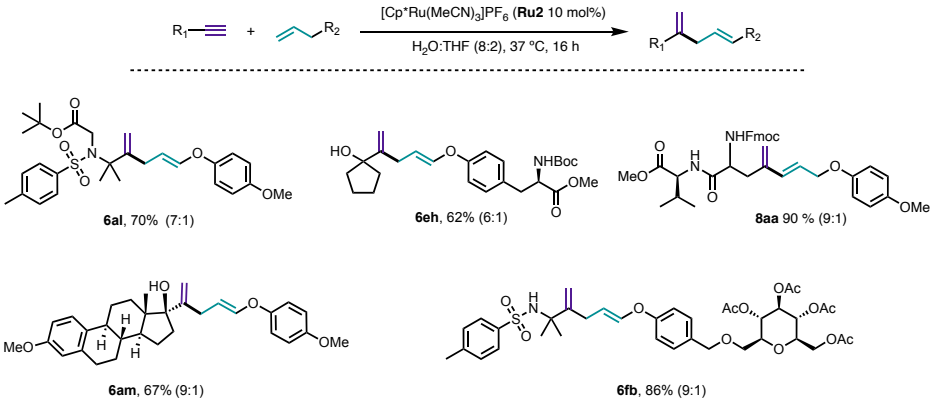

Figura 4. Selección de exemplos para a reacción de acoplamento de alquinos e alquenos catalisada por rutenio.

En base a estes bos resultados, estudamos a aplicabilidade do proceso para o acoplamento de dipéptidos con grupos alquinos e alquenos, atopando bos resultados. Finalmente puido aplicarse esta reacción a modificación de pequenos péptidos en condicións de alta dilución.

No **capítulo III** recóllese os nosos esforzos para a translación de reaccións de isomerización de alcoholes alílicos a entornos celulares catalizadas por complexos de rutenio.

Os procesos de isomerización, procesos nos que unha molécula se transforma noutra coa mesma fórmula molecular, son moi importantes na natureza xa que distintos isómeros presentan distinta actividade biolóxica. Dentro dos procesos catalizados por enzimas, existe un grupo de enzimas denominadas isomerasas que son as encargadas de catalizar este tipo de procesos.

No ámbito sintético, os procesos de isomerización de alcoholes alílicos a grupos carbonilo mediantes por metáis de transición son de especial interés. Este tipo de procesos son moi útiles sinteticamente xa que son un atallo para o acceso a cetóns sobre o proceso de dous pasos de oxidación / reducción. Así mesmo, un aspecto importante destes procesos é que todos os mecanismos descritos ata agora involucran a formación de intermedios metal-hidruro, un mecanismo non descrito para a isomerización de dobres enlaces mediante por isomerasas. Pese a que este tipo de procesos fai uso destes intermedios metal-hidruro altamente reactivos, existen moitos precedentes da isomerización de alcoholes alílicos en auga e incluso en presencia de presenza de proteínas como alcoholdeshidrogenasas.

Non hai precedentes deste tipo de isomerizaciones nun contexto bioortogonal, pero si de procesos que teñen como intermedios complexos metal-hidruro, concretamente para a redución de compostos carbonílicos. Este tipo de reaccións fan uso de complexos de iridio, rodio, rutenio ou osmio e redutores externos como formiato sódico ou dinucleótido de nicotinamida e adenina (NADH) como fontes de hidruro para a redución de compostos carbonílicos.

A reacción de isomerización de alcoholes alílicos é un proceso totalmente económico atómicamente, que a diferenza da redución de compostos carbonílicos non fai uso de redutores externos, con precedentes en condicións acuosas, todas estas condicións fan desta reacción unha altamente atractiva para ser trasladada a un contexto biolóxico.

Para o noso estudo escollemos un complexo de rutenio cun ligando bis-alilo que xa fora previamente estudado en condicións acuosas. Ao estar xa descrita a reacción en auga, estudamos directamente diferentes medios de reacción bioloxicamente complexos como buffers, medios de cultivo ou lisados celulares, con altos rendementos en todos eles. Realizouse unha comparativa con outros complexos previamente reportados para a isomerización de alcoholes alílicos, atopando que só o complexo de rutenio proposto era capaz de promover esta isomerización eficientemente.

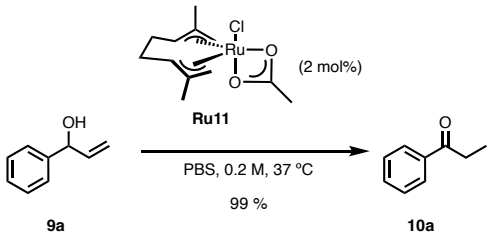

Figura 5. Exemplo de isomerización de alcohol alílico en PBS.

O alcance da reacción é bo, tolerando grupos electrón donante e electrón atraínte, incluíndo alcoholes alílicos alifáticos e poliaromáticos.

Estudamos mediante diversos experimentos de deuteración o mecanismo da reacción. Os resultados obtidos son compatíbeis cun proceso de transferencia de hidruro intramolecular, sen intercambio co medio nin "préstamo de hidróxeno".

Co obxectivo de trasladar esta transformación a condicións celulares, deseñamos unha sonda fluorescente que fose facilmente sintetizable mediante a reacción de isomerización. Neste caso escollemos un fluoróforo dipolar, o cal a cetona con función electrón atrayente podería ser enmascarada como un alcohol alílico. A sonda foi sintetizada e caracterizada espectroscopicamente.

A reacción ensaiouse en células HeLa, demostrando que pode ter lugar intracelularmente. Así mesmo realizouse unha cuantificación do contido intracelular de produto e de rutenio, permitindo a primeira determinación cuantitativa do TON dunha reacción intracelular.

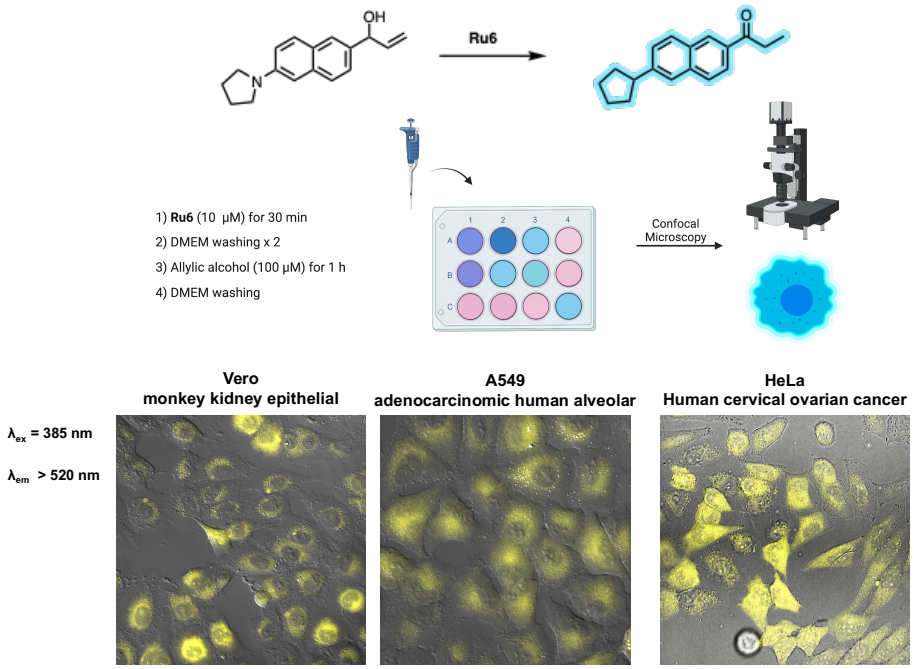

Figura 6. Isomerización intracelular dunha sonda fluoroxénica en diferentes liñas celulares.

Co obxectivo de desenvolver unha aplicación que permitise interferir co metabolismo intrínseco das células decidiuse estudar a isomerización de alcoholes bis alílicos. A isomerización de alcoholes bis-alílicos daría *a priori* cetonas α,β-insaturadas, que poderían actuar como aceptores de Michael reaccionando con nucleófilos celulares como o glutatión (GSH).

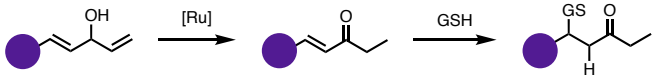

Figura 7. Esquema conceptual para a xeración de compoñentes bioactivos mediante a isomerización de alcoholes bis-alílicos.

Sintetizáronse unha batería de alcoholes bis alílicos e estudouse a súa isomerización en condicións bioloxicamente relevantes. Os resultados foron positivos, con altos rendementos independentemente do alcohol e do medio. Con estes resultados, pasouse aos estudos celulares usando un kit comercial para a determinación dos niveis de GHS e GSSG (glutatión reducido). Afortunadamente, atopamos que os niveis de GSH vense alterados pola produción intracelular dos compostos α,β-insaturados, inclusive con un maior efecto que a suplementación do produto por si só.

En conclusión, desenvolveuse unha metodoloxía que habilita a isomerización catalítica de alcoholes alílicos en condicións celulares, mediada por intermediario rutenio-hidruro. Demostrouse a natureza catalítica do proceso mediante a determinación cuantitativa do TON intracelular, e desenvolveuse un método para a modificación dos niveis de GSH a nivel celular mediante a xeración de aceptores de Michael.

No **capítulo IV** recóllense os nosos esforzos para o desenvolvemento de reaccións simultáneas mediadas por dous compostos discretos, e o desenvolvemento de procesos tándem catalizados por compostos organometálicos e enzimas.

As reaccións tándem son aquelas que teñen lugar de forma secuencial nun mesmo matraz de reacción. Presentan moitas vantaxes tales como a redución de pasos de aislamento e purificación, ou a posibilidade de acceder a produtos de outra forma imposibles debido a intermedios inestables.

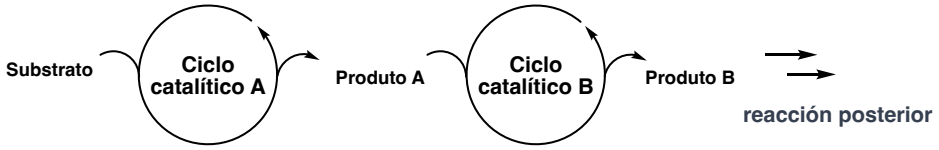

Figura 8. Esquema conceptual dos procesos catalíticos en serie (tándem).

Dende un punto de vista sintético esta aproximación está bastante establecida e afianzada, con exemplos representativos facendo uso de complexos organometálicos e incluso mediante a combinación destes últimos con enzimas.

No contexto da química biolóxica, hai exemplos do uso de compostos organometálicos para interferir no metabolismo de microorganismos, a saber, bacterias. Non obstante, exemplo deste tipo de procesos, ben sexan tándem ou concorrentes, en células de mamífero son limitados. Polo tanto, tendo en conta a experiencia adquirida no grupo e nos capítulos anteriores desta tese, plantexouse o desenvolvemento de reaccións concorrentes desenvolvidas por complexos discretos de rutenio en sistemas celulares, e o desenvolvemento de reaccións tándem catalizadas por complexos organometálicos e enzimas dentro de células de mamífero.

En primeiro lugar, comezamos co deseño dunha sonda baseada en hidroxibenzotiazol (HBT) cun mecanismo de fluorescencia ESIPT e ICT. No desenvolvemento da sonda, plantexouse que a supresión destes mecanismos mediante un grupo alilo, facilmente desprotexible por complexos para dealilación, e un alcohol alílico, facilmente

isomerizable á correspondente cetona, pola reacción de isomerización desenvolvida no capítulo anterior.

Despois da síntese e da caracterización espectroscópica, pasouse ao estudo *in vitro* do proceso. Neste punto atopáronse dificultades, xa que, a pesar de que a desprotección do grupo alilo se podía conseguir facilmente baixo condicións de alta dilución, a isomerización non tiña lugar. Mais estudos, entorno á isomerización do correspondente alcohol alílico, demostraron que o substrato non se pode isomerizar mediante o complexo modelo, posiblemente debido a problemas de inhibición.

Plantexouse un redeseño da sonda, tomando como punto de partida o esqueleto da sonda usada no capítulo anterior. Diseñose, sintetizou e caracterizou a nova sonda. Os estudos *in vitro* para a isomerización da sonda foron satisfactorios, podendo demostrar que son necesarios os dous catalizadores distintos para a aparición de fluorescencia. Os experimentos en células están pendentes.

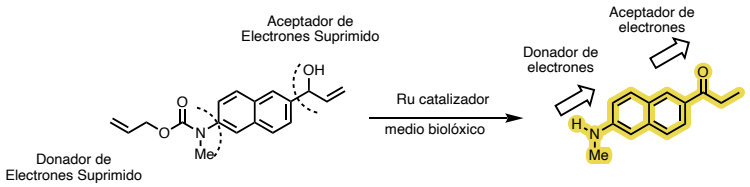

Figura 9. Deseño dunha sonda fluorescente dual.

Co obxectivo de desenvolver un proceso tándem catalizado por un complexo metálico e unha enzima, seleccionouse a reacción de dealilación catalizada por rutenio como a reacción modelo organometálica, e dúas enzimas, a fosfatasa alcalina (ALP, polas súas siglas en inglés) e a monoamino oxidasa (MAO) para o proceso enzimático.

Diseñáronse tres sondas distintas: unha sonda para a ALP baseada en HBT cun grupo alilfosfato; e dúas sondas para MAO unha baseada en HBT e outra cun núcleo tipo BODIPY, ambas con un grupo N-alloc-propilamina.

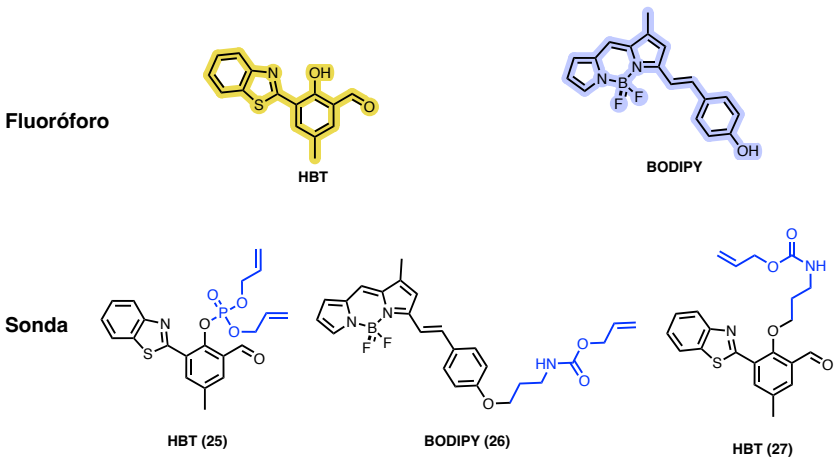

Figura 10. Fluoróforos seleccionados e sondas deseñadas.

No caso da sonda de ALP, a sonda foi sintetizada e caracterizada espectroscopicamente. así como do intermedio do proceso. Os experimentos *in vitro* coa enzima aislada e o complexo de rutenio para dealilación, foron altamente positivos, con altas actividades a condicións de baixo micromolar (150 µM), demostrando a natureza tándem do proceso *in vitro*.

Coas boas resultados *in vitro* pasouse aos experimentos celulares en células HEK-293. Para estes experimentos adicionalmente sobre-exprésase a enzima ALP mediante a transferencia cun plásmido, e comparouse a actividade das liñas con niveis naturais de ALP e niveis sobreexpresados. Os experimentos en células con niveis fisiolóxicos de ALP mostraron que a reacción tándem pode ter lugar, adicionalmente, o uso de células con niveis sobre expresados permitiu observar como o proceso tándem é dependente dos niveis de ALP en células xa que a maior nivel de ALP maior nivel de fluorescencia.

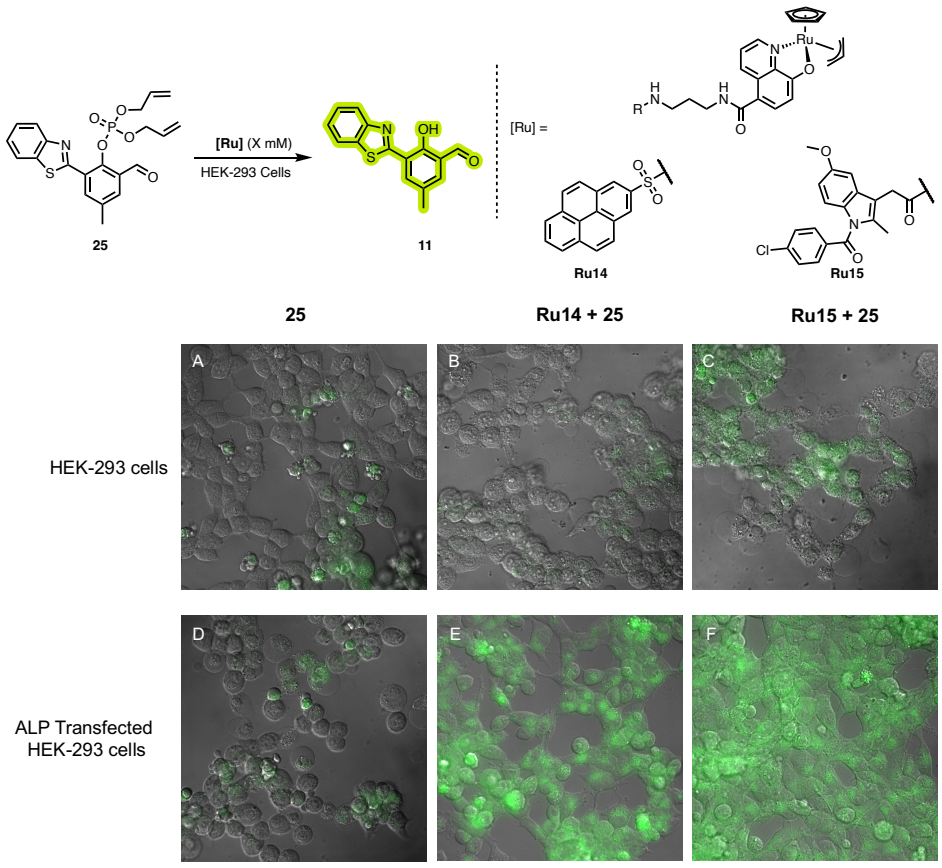

Figura 11: Micrografías correspondentes á dealilación catalizada por rutenio en proceso tándem, hidrólise catalizada pola ALP, en células HEK con niveis fisiolóxicos de ALP e en células con niveis sobreexpresados de ALP.

En relación á sonda BODIPY para MAO, sintetizouse e caracterizouse espectroscopicamente a sonda, así como do intermedio do proceso. Os experimentos i*n vitro* coa enzima aislada e o complexo de rutenio para dealilación, están pendentes, xa que non se dispuxo da enzima no momento de escribir este traballo doutoral.

Non obstante, ao dispor de todos os compoñentes, sonda e intermedio de reacción, realizáronse os experimentos celulares en células HeLa con niveis fisiolóxicos de MAO. Neste caso, realizouse un proceso de optimización con distintos catalizadores de rutenio, atopando condicións nas que o proceso tándem pode ter lugar. Os controis, co compoñente intermedio, así como na ausencia de catalizador de rutenio son fortes indicadores de que o proceso que está a ter lugar é o proceso tándem.

Por último, no caso da sonda de HBT para MAO, puidose acceder sinteticamente a mesma facilmente, non así ao correspondente intermedio do proceso tándem. Caracterizouse espectroscopicamente a sonda, e pese a non poder ter o correspondente control intermedio decidiuse proceder cos experimentos celulares.

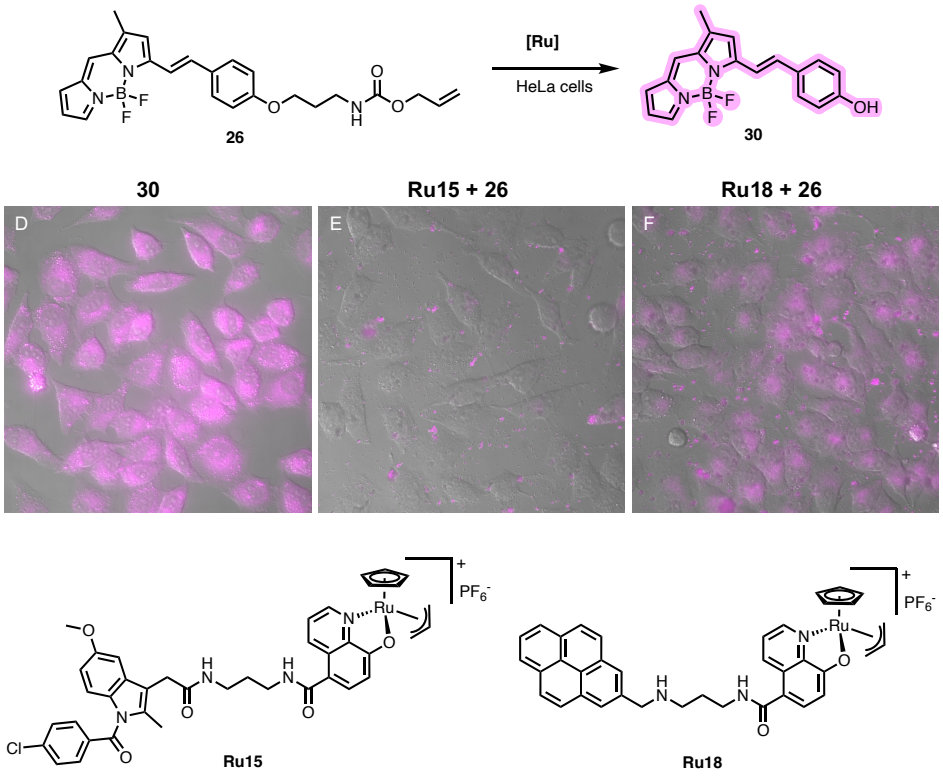

Figura 12. Micrografías correspondentes ao proceso tándem de dealilación catalizada por rutenio, oxidación amínica catalizada pola MAO, en células HeLa.

Tal como no caso da sonda BODIPY, foron utilizadas células HeLa con niveis fisiolóxicos de enzima MAO. Con satisfacción, puidemos observar a formación de fluorescencia só, cando as células estaban expostas aos catalizadores artificiais de rutenio, o que, xunto coa caracterización espectroscópica realizada con anterioridade, apuntan a que, a pesar de que o intermedio do proceso tándem non sexa accesible sinteticamente, este ten un tempo de vida suficiente para ser activado pola enzima MAO en condicións fisiolóxicas.

En conclusión, neste capítulo, desenvolveuse unha sonda para o proceso concorrente de isomerización e dealilación que está agardando os experimentos en condicións celulares.

Así mesmo, foron deseñados, sintetizados, caracterizados e trasladados a cultivos celulares para procesos tándem de dealilación e ben hidrólise por parte da ALP

Conclusion xeral

Como conclusión xeral, esta tese doutoral describe 4 tipos de transformacións catalizadas por rutenio en condicións bioortogonais. A primeira é o desenvolvemento dunha segunda xeración de catalizadores para a cicloadición de azidas e tioalquinos por complexos catiónicos de rutenio, incluíndo o desenvolvemento de complexos sándwich fotoactivables. En segundo lugar, trasladouse a reacción de acoplamento de alquenos e alquinos catalizada por complexos catiónicos de rutenio a condicións acuosas e biocompatibles. En terceiro lugar, trasladouse a reacción de isomerización de alcoholes alílicos a células vivas, determinando o TON da reacción e xerando aceptores de Michael como parte do proceso de isomerización. E, por último, o coñecemento adquirido aplicouse ao desenvolvemento de reaccións concorrentes catalizadas por dous complexos discretos de rutenio e ao desenvolvemento de reaccións tándem catalizadas por complexos discretos de rutenio e enzimas como ALP ou MAO, sendo o primeiro proceso tándem descrito en células

.

Experimental section

Experimental section

General information for Synthesis Experiments

Procedures for the synthesis of precursors and complexes were performed under an atmosphere of dry nitrogen using vacuum-line and standard Schlenk techniques. Dry solvents were directly purchased from Sigma Aldrich or Acros Organics and used without further purification. Water used in the catalytic reactions was fresh Mili-Q grade. The abbreviation "rt" correspond to approximately 23 ºC. All reactions were stirred using Teflon-coated magnetic stirring bars. Flash chromatography was carried out on Merck Geduran Si 60 (40 – 63 μm) silica gel (normal phase) or by reversed-phase high-performance liquid chromatography (RP-HPLC) otherwise stated. Na_2SO_4 or $MgSO_4$ were used as drying agents. Reactions carried out with temperature control were performed using either Thermo watch-controlled silicone oil baths for heating or the corresponding bath for cooling (water-ice for 0 ºC or acetone-dry ice for -78 ºC).

^{1}H, ^{13}C,^{19}F and ^{31}P NMR spectra were collected on a 300 MHz (Varian), 400 MHz (Varian) or 500 MHz (Bruker and Varian) in $CDCl_3$, CD_2Cl_2, CD_3OD, DMSO-d_6 or DMF-d_7. Carbon types and structure assignments were determined from DEPT-NMR. NMR spectra were analyzed using MestreNova© NMR data processing software (www.mestrelab.com). Abbreviations to denote the multiplicity of the signals are s (singlet), d (doublet), t (triplet), q (quartet), quint (quintet), sex (sextet), m (multiplet) and their corresponding combinations.

UV measurements were performed using a Jasco V-670 spectrometer.

Fluorescence measurements were performed using a Horiba FluoroMaxR-3 Spectrophotometer with the following settings: increment 1.0 nm, averaging time 0.2 s, excitation slit width 2.0 nm, emission slit width 5 nm, using 1 cm quartz cells.

All peptide synthesis reagents and amino acid derivatives were purchased from Sigma Aldrich and Iris Biotech; amino acids were purchased as protected Fmoc amino acids with the standard side chain protecting scheme: Fmoc-Lys(N_3)-OH, Fmoc-Phe-OH, Fmoc-Ile-OH, FmocTyr-OH, Fmoc-Pro-OH Fmoc-His(Trt)-OH, Fmoc-Val-OH, Fmoc-propargylGly-OH, Boc-propargylGly-OH. All other chemicals were purchased from Aldrich or Fluka. All solvents were dry and synthesis grade, unless specifically noted. Peptides were synthesized using an automatic peptide synthesizer CEM Liberty Lite, following the recommended procedures by the manufacturer: Peptide syntheses was

performed using Fmoc strategy on a Rink-amide-ChemMatrix (0.5 mmol/g) using DIC as activator, oxyma (ethyl(hydroxyimino)cyanoacetate) as base, and DMF as solvent. The removal of the temporal Fmoc protecting group was performed by treating the resin with 20% piperidine in DMF. Cleavage/deprotection step was performed by treatment of the resin-bound peptide for 2h with the following cleavage cocktail: 900 µL TFA, 50 µL CH_2Cl_2, 25 µL H_2O and 25 µL triisopropylsilane (1 mL of cocktail / 40 mg resin). The resin was filtered, and the cocktail was added onto ice-cold Et_2O. After 10 - 30 min, the precipitate was centrifuged and washed again with of ice-cold ether. The solid residue was dried under nitrogen and re-dissolved in water

Chapter I

Reaction that required activation of the [Cp*Ru(arene)]X complexes irradiated at 365 nm with a UV-B LED (Custom apparatus by ThorLabs) for the indicated time.

Front view Upper view

Figure S1 Irradiation set up. Two UV-led, 365 nm and 455 nm. Custom apparatus by ThorLabs

Oligonucleotides were purchased from *biomers.net GmbH*. Dry DNA pellets were dissolved in Milli-Q H_2O to a concentration of 1 mM and stored at -20°C. The exact concentration was then calculated by UV absorption at 260 nm using a *Thermo Scientific Nanodrop 1000*

General Information for the Biological Experiments

All steps were performed on a sterile clean bench Tesltar AV-100 at room temperature. Solutions stored in a fridge were warmed beforehand in a water bath (37 °C). Unless otherwise specified, all incubations were performed in DMEM.

Cell Culture: All cell lines were cultured in DMEM (Dulbecco´s modified Eagle´s medium), 5 mM glutamine, penicillin (100 units/mL) and streptomycin (100 units/mL)

(all from Invitrogen). Proliferating cultures were maintained in a 5% CO_2 humidified incubator at 37 °C.

For all the experiments, cells were seeded in the corresponding well at the indicated concentration two days before treatment.

Fluorescence microscopy: All images were obtained with an Andor Zyla mounted on a Nikon TiE. Confocal images were acquired in an Andor Dragonfly High Speed Confocal Platform. Images were further processed with Image J or NIS software (Nikon).

Microscopy settings: The filter sets for the observation of the fluorescence of the products were as follows:

Widefield: LED λ excitation: 385 nm. Filter cube DAPI-1160B-000 (Semrock): BP 387/11-25 nm, LP 447/60-25 nm and DM 409 nm. Confocal: Laser excitation: 405 nm. LP 450/50 and DM 418 nm.
Widefield: LED λ excitation: 385 nm. Filter cube: BP 375/28x nm, LP 515lp nm and DM 415 nm. Confocal: Laser excitation: 405 nm. LP 525/50 and DM 501 nm.
Widefield: LED λ excitation: 470 nm. Filter cube FITC-3540C-000 (Semrock): BP 482/35 nm, LP 536/40 nm and DM 506 nm. Confocal: Laser excitation: 488 nm. LP 525/50 and DM 501 nm.
TMRE (tetramethylrhodamine, ethyl ester) LED λ excitation: 550 nm. Filter cube TRITC-B-000 (Semrock): BP 543/22-25 nm, LP 593/40-25 nm and DM 562 nm. Confocal: Laser excitation: 561 nm. LP 620/60 and DM 567 nm.

Experimental Section:

Chapter I: Ruthenium Catalyzed Azide-Thioalkyne-Cycloadditions

Synthesis

Ruthenium complexes

η^5-(Pentamethyl-cyclopentadienyl)-η^6-(pyrene) ruthenium(II) hexafluorophosphate (Ru3):

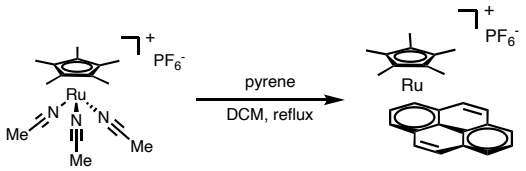

The synthesis of **[**Cp*Ru(pyrene)]PF_6 (**Ru3**) was carried out according to a reported procedure:[1]

In an oven dried Schlenk filled with nitrogen [Cp*Ru(MeCN)$_3$]PF_6 (100 mg, 0.19 mmol, 1.0 equiv) was added a solution of pyrene (40.6 mg, 0.20 mmol, 1.05 equiv) in degassed 1,2-dichloroethane (5 mL). The mixture was gently heated (just below the refluxing temperature) for 20 h, the solvent was removed, and the product was chromatographed on neutral alumina using Et_2O as eluent, collecting the yellow fractions. The solvent was removed under vacuum to give **[Cp*Ru(pyrene)]PF_6** (**Ru3**) as bright yellow needles (40 mg, 36% yield). The NMR data is in accordance with that previously reported.[1] **^{1}H NMR** (300 MHz, CD_2Cl_2) δ 8.26 – 8.05 (m, 5H), 7.55 (dd, J = 9.3, 4.2 Hz, 2H), 6.41 (d, J = 6.0 Hz, 2H), 6.12 (t, J = 6.0 Hz, 1H), 1.32 (s, 15H).

η^5-(Pentamethylcyclopentadienyl)-η^6-(pyrene-1-sulfonate) ruthenium (II) sodium hexafluorophosphate (Ru5).

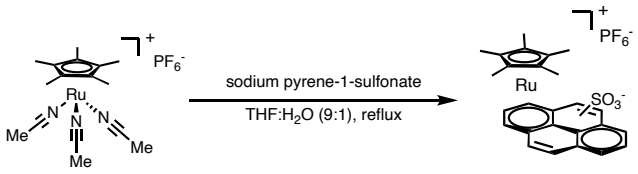

The synthesis of (**Ru5**) was carried out adapting the previous procedure:

Sodium pyrene-1-sulfonate (60.6 mg, 0.2 mmol) was suspended in degassed THF:H_2O (9:1) mixture and [Cp*Ru(MeCN)$_3$]PF_6 (100 mg, 0.2 mmol) was added. The reaction

[1] A. M. McNair, K. R. Mann, *Inorganic Chemistry* **1986**, *25*, 2519–2527.

mixture was refluxed for 14 h, cooled down to rt and the resulting precipitate was filtered and washed with CH_2Cl_2 and Et_2O.

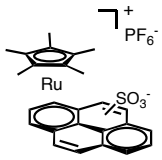

[Cp*Ru(1-NaSO$_3$pyrene)]PF$_6$ (Ru5). If needed, **Ru5** can be purified by recrystallization in MeOH:CH_2Cl_2 and slow diffusion of Et_2O. Isolated as pale green powder (41.1 mg 30% yield). Mixture of positional isomers, approximately 1:1. **^{1}H NMR** (300 MHz, Methanol-d_4) δ 9.13 (d, J = 9.7 Hz, 1H), 8.62 (t, J = 8.7 Hz, 2H), 8.30 – 8.02 (m, 7H), 7.61 (d, J = 9.7 Hz, 1H), 7.51 (dd, J = 9.3, 7.2 Hz, 2H), 6.77 (d, J = 6.2 Hz, 1H), 6.58 (d, J = 6.2 Hz, 1H), 6.47 (dd, J = 14.0, 6.0 Hz, 2H), 6.14 (t, J = 6.0 Hz, 1H), 1.28 (m, 30H). **^{13}C NMR** (75 MHz, Methanol-d_4) δ 143.5, 133.9, 133.6, 133.0, 132.7, 132.0, 130.3, 129.7, 129.1, 128.7, 126.6, 126.5, 126.2, 125.6, 125.3, 125.1, 124.8, 94.7, 94.6, 94.1, 93.9, 90.9, 88.8, 87.9, 86.6, 86.4, 85.3, 9.0, 8.7. **HRMS-ESI** calculated for $C_{26}H_{25}O_3S^+$ 519.0562 found 519.0562.

η^5 - (Pentamethyl-cyclopentadienyl) - η^6 - (naphthalene) ruthenium(II) tetraphenylborate (Ru4)

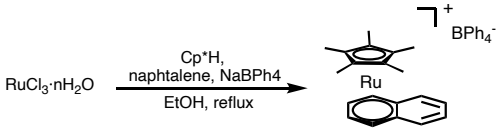

The synthesis of [Cp*Ru(naphthalene)]BPh$_4$ (**Ru4**) was carried out according to a reported procedure:[2]

In an oven dried Schlenk filled with nitrogen, $RuCl_3 \cdot nH_2O$ (100 mg, 0.482 mmol, 1 equiv) was suspended in EtOH (5 mL). The mixture was refluxed until all the starting material had dissolved. Then, Cp*H (151 µL, 0.946 mmol, 2 equiv) and naphthalene (123 mg, 0.946 mmol, 2 equiv) were added to the reaction vessel and the resulting solution was refluxed overnight. The solvent was concentrated under vacuum and the residue was dissolved in a water/Et_2O mixture (5 mL each one). The aqueous portion was retained and washed with Et_2O (3x5 mL). The aqueous layer was mixed slowly with 5 mL of a 0.30 M aqueous solution of NaBPh$_4$**.** The resulting precipitated was filtered and washed with Et_2O.

[2] B. T. Loughrey, B. V. Cunning, P. C. Healy, C. L. Brown, P. G. Parsons, M. L. Williams, *Chemistry - An Asian Journal* **2012**, *7*, 112–121.

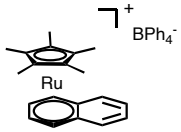

[Cp*Ru(naphthalene)]BPh$_4$ (Ru4). If necessary, **Ru4** can be purified through a short column of neutral alumina using acetone as eluent. Yellow- mustard-colored fractions were collected. Isolated as yellow needles. (Yield 94%). The NMR data is in accordance with that previously reported.[2] **^{1}H NMR** (300 MHz, DMSO-d_6) δ 7.73 – 7.61 (m, 4H), 7.22 – 7.11 (m, 8H), 6.92 (t, J = 7.3 Hz, 8H), 6.78 (t, J = 7.1 Hz, 4H), 6.71 (dd, J = 4.3, 2.4 Hz, 2H), 6.15 (dd, J = 4.3, 2.4 Hz, 2H), 1.61 (s, 15H).

η^5 - (1-methoxymethyl-2,3,4,5-tetramethylcyclopentadiene) – η^6 - (naphthalene) ruthenium(II) hexafluorophosphate (Ru8)

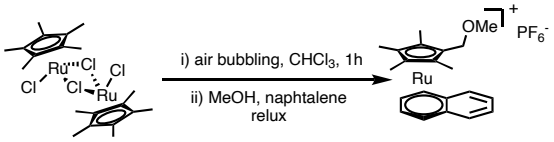

The synthesis of [Cp^{‡OMe}Ru(naphthalene)]PF$_6$ (**Ru8**) was carried out according to a reported procedure:[3]

Dichloro(pentamethylcyclopentadienyl) ruthenium dimer (100 mg, 0.16 mmol, 1.0 equiv) was dissolved in CH_2Cl_2 (20 mL) and air was bubbled into the solution for 1h for the formation of the fulvene complex. After the indicated time the solvent was removed under reduced pressure, and the flask air-purged and filled with nitrogen. Naphthalene (29 mg, 0.48 mmol, 3.0 equiv) was added followed by methanol (15mL), and the resulting suspension was refluxed for 5h. After the indicated time the solvent was removed under reduced pressure and the residue redissolved in water followed by a solution of KPF_6 (10-fold excess, 294 mg, 1.6 mmol) was added slowly. The resulting orange precipitated was collected by filtration. If further purification is needed, it can be purified through a short neutral alumina column using acetone as eluent collecting the yellow- mustard-coloured fractions.

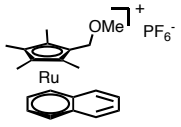

[Cp^{‡OMe}Ru(naphthalene)]PF$_6$ (Ru8). If necessary, **Ru8** can be purified through a short column of neutral alumina using acetone as eluent. Yellow- mustard-colored fractions were collected. Isolated as yellow needles. (Yield 30%). The NMR data is in accordance with that previously reported.[3] **^{1}H NMR** (300 MHz, $CDCl_3$) δ 7.66 (dd, J = 7.1, 2.9 Hz, 2H), 7.57 – 7.47 (m,

[3] R. M. Fairchild, K. T. Holman, *Organometallics* **2008**, *27*, 1823–1833.

2H), 6.57 (t, *J* = 3.3 Hz, 2H), 6.08 (dd, *J* = 4.5, 2.4 Hz, 2H), 3.93 (s, 2H), 3.39 (s, 3H), 1.70 – 1.54 (m, 13H).

η^5 - (1-methoxymethyl-2,3,4,5-tetramethylcyclopentadiene) – η^6 - (pyrene) ruthenium(II) hexafluorophosphate (Ru6)

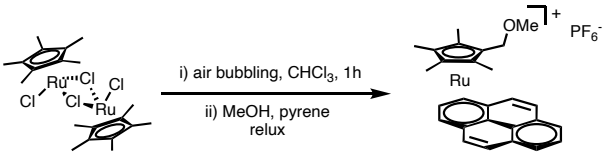

The synthesis of [Cp^{‡OMe}Ru(pyrene)]PF_6 (**Ru6**) was carried out according to the previous protocol using pyrene instead of naphthalene

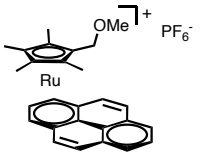

[Cp^{‡OMe}Ru(pyrene)]BPh_4 (Ru6). If necessary, **Ru6** can be purified through a short column of neutral alumina using acetone as eluent. Yellow- mustard-colored fractions were collected. Isolated as yellow needles. (Yield 32%). The NMR data is in accordance with that previously reported.[3] **^{1}H NMR** (400 MHz, Acetone-d_6) δ 8.26 (d, *J* = 9.0 Hz, 4H), 8.14 – 8.09 (m, 1H), 7.73 (d, *J* = 9.3 Hz, 2H), 6.79 (d, *J* = 6.0 Hz, 2H), 6.42 (t, *J* = 5.9 Hz, 1H), 3.73 (s, 2H), 3.18 (s, 3H), 1.41 (s, 6H), 1.19 (s, 5H).

η^5 - (1-hydroxymethyl-2,3,4,5-tetramethylcyclopentadiene) – η^6 - (naphthalene) ruthenium(II) tetraphenylborate (Ru7)

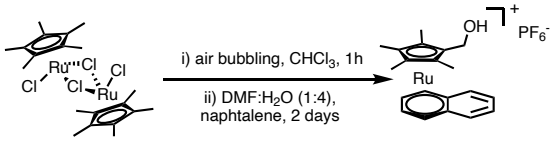

The synthesis of [Cp^{‡OH}Ru(naphthalene)]BPh_4 (**Ru7**) was carried out according to a reported procedure:[3]

Dichloro(pentamethylcyclopentadienyl) ruthenium dimer (100 mg, 0.16 mmol, 1.0 equiv) was dissolved in CH_2Cl_2 (20 mL) and air was bubbled into the solution for 1h for the formation of the fulvene complex. After the indicated time the solvent was removed under reduced pressure, and the flask air-purged and filled with nitrogen. Naphthalene (204 mg, 1.6 mmol, 10 equiv) was added followed by a mixture of water and DMF (4:1) the resulting suspension was stirrer for 2 days. After the indicated time the mixture was filtered and extracted with diethyl ether to remove the remaining arene in solution. The

aqueous layer was treated with an aqueous solution of $NaBPh_4$ (10 equiv) and the resulting precipitated collected by filtration.

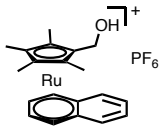

[Cp^{‡OH}Ru(naphthalene)]BPh$_4$ (**Ru7**). If necessary, **Ru7** can be purified through a short column of neutral alumina using acetone as eluent. Yellow- mustard-colored fractions were collected. Isolated as yellow needles. (36% yield). ^{1}H NMR (300 MHz, cdcl$_3$) δ 7.66 (dd, *J* = 7.1, 2.9 Hz, 2H), 7.57 – 7.47 (m, 2H), 6.57 (s, 2H), 6.12 – 6.04 (m, 2H), 3.93 (s, 2H), 1.70 – 1.54 (m, 13H).

Thiofulvene ruthenium complex Ru2'

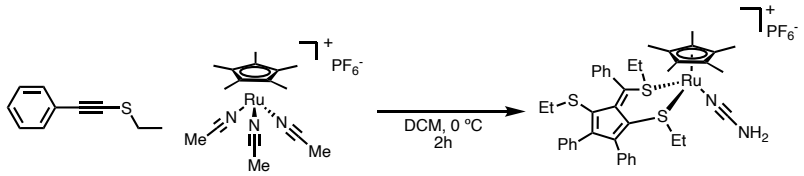

In a flame dried Schlenk, under nitrogen atmosphere the complex **Ru2** (15 mg, 31.7 µmol) was dissolved in freshly distilled, degassed CH_2Cl_2 (1 mL) and stirred at 0 ºC for 15 min (pale-orange solution). After the indicated time, the thioalkyne **2a** (21 µL, 20.6 mg, 127 µmol) was added via syringe to yield a dark green solution. The mixture was stirred at 0 ºC for 2 h resulting in a dark orange-brown solution. To this solution 6 mL of dried, degassed pentane were added slowly, in order to avoid mixing, and the mixture was kept at -28 ºC for 3 days to yield the entitled compound as deep-orange- crystalline needles (quant).

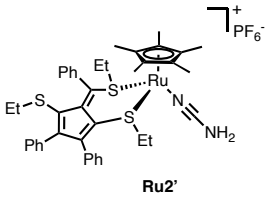

Ru2'

Ruthenium complex Ru2'. ^{1}H NMR (300 MHz, CD_2Cl_2) δ 7.90 – 7.82 (m, 1H), 7.71 (q, *J* = 4.7 Hz, 1H), 7.64 – 7.56 (m, 2H), 7.54 – 7.05 (m, 11H), 2.96 – 2.80 (m, 2H), 2.61 – 2.44 (m, 2H), 2.40 (d, *J* = 1.7 Hz, 3H), 1.72 (s, 15H), 1.70 – 1.61 (m, 3H), 1.17 (t, *J* = 7.4 Hz, 3H), 0.84 (t, *J* = 7.4 Hz, 4H), 0.59 (t, *J* = 7.2 Hz, 3H).**^{13}C NMR** (75 MHz, CD_2Cl_2) δ 156.1, 151.1, 149.6, 147.1, 140.9, 136.7, 136.2, 135.5, 133.2, 132.2, 131.7, 131.2, 131.0, 130.0, 129.7, 129.6, 129.5, 129.1, 89.6, 38.2, 37.2, 31.3, 15.9, 14.8, 14.4, 11.0, 10.5, 10.4, 5.8 (CH_3). **HRMS-ESI** calculated for $C_{40}H_{45}RuS_3^+$ 723.1730 found 723.1727

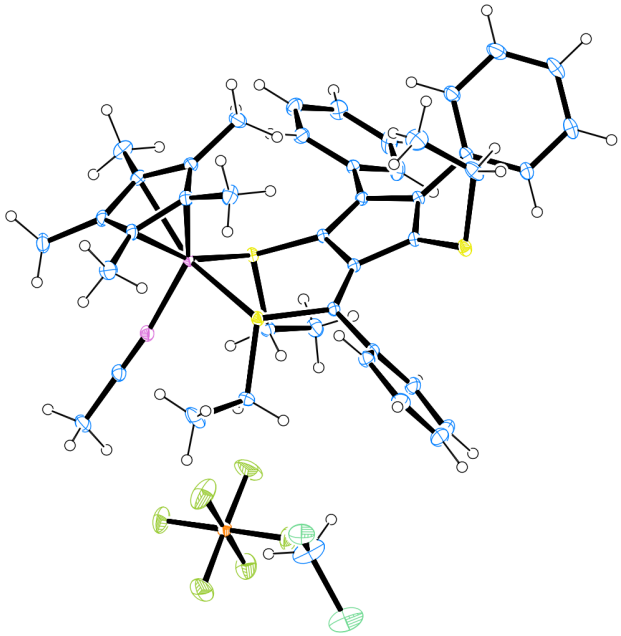

Figure S 2. Structure of **Ru2'** in the solid state; PF_6 and CH_2Cl_2 units are distorted within the crystalline structure, only one of the mayor contributions is shown for clarity

X-ray Crystal Structure Analysis of Compound Ru2': $C_{43}H_{50}Cl_2F_6NPRuS_3$, *MW*= 994.00 g/mol, orange-needles, crystal size 0.039 mm x 0.055 mm x 0.341 mm, monoclinic, space group $P2_{1/n}$, a = 19.4000(7) Å, b = 9.9869(4) Å, c = 23.9334(9) Å, β = 107.4067(14)°, V = 4424.6(3) Å^3, T = 100 K, Z = 4, D_{calc} = 1.492 g/cm^3, λ = 0.71073 Å, Gaussian absorption correction (T_{mn} = 0.89, T_{max} = 0.97) Bruker D8 VENTURE PHOTON-III C14 κ-geometry diffractometer, 4.400° < 2θ < 57.40°, 166840 measured reflections, 14775 independent reflections 10854 reflections with $I > 2\sigma(I)$, R_{int} = 0.087.

The structure was solved by direct methods and refined by full-matrix least-squares against F^2 to $R[F^2 > 2\sigma(F^2)]$ = 0.038, $wR(F^2)$= 0.095, 614 parameters. The H atoms were inferred from neighboring sites, H-atom parameters constrained, $w = 1/[\sigma^2(F_o^2) + (0.033P)^2 + 4.3237P]$ where $P = (F_o^2 + 2F_c^2)/3$, $(\Delta/\sigma)_{max}$ = 0.001, $\Delta\rho_{max}$ = 0.52 e Å^{-3} $\Delta\rho_{min}$ = −0.82 e Å^{-3}

Synthesis of organic azides

Azides **1a**,[4] **1b**[5], **1c**[6], **1f**[7] are known compounds and were prepared according to reported procedures. Azide **1e** (Fmoc-K(N3)-OH) is commercial and was used without further purification.

(3-(Azidomethyl)benzyl) triphenylphosphonium bromide (1d)

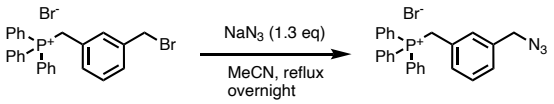

NaN_3 (241 mg, 3.70 mmol, 1.3 equiv) was added portion wise to a solution of (3-(bromomethyl) benzyl) triphenylphosphonium bromide[8] (1.50 g, 2.85 mmol, 1.0 equiv) in MeCN (30 mL) and DMF (5 mL), and the mixture was stirred under reflux overnight. Then, the solvent was removed under reduced pressure.

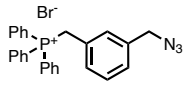

1d

(3-(Azidomethyl)benzyl) triphenylphosphonium bromide (1d). **FCC** in CH_2Cl_2:MeOH (95:5). Isolated as a light yellow powder (1.067 g, 77% yield). **^{1}H NMR** (300 MHz, $CDCl_3$) δ 8.18 (d, J = 7.1 Hz, 2H), 7.75 – 7.53 (m, 15H), 7.43 (m, 3H), 7.15 (mf, 3H), 7.01 (bs, 1H), 5.47 - 5.42 (m, 4H), 2.52 (q, J = 7.4 Hz, 2H), 1.01 (t, J = 7.4 Hz, 3H). **^{13}C NMR** (75 MHz, $CDCl_3$) δ 148.57, 135.96 (d, *J* = 3.2 Hz), 135.08, 134.20 (d, *J* = 9.8 Hz), 131.63 (d, *J* = 5.4 Hz), 130.17 (d, *J* = 12.6 Hz), 129.46, 129.42, 128.62, 128.51, 128.19 (d, *J* = 8.5 Hz), 127.84 (d, *J* = 3.5 Hz), 126.60, 125.36, 117.99, 116.86, 51.18, 30.93, 30.20, 14.57 (CH_3). **HRMS-ESI** Calculated for $C_{36}H_{33}N_3PS^+$ 570.2127 found 570.2129.

[4] K.-C. Chang, I.-H. Su, A. Senthilvelan, W.-S. Chung, *Org. Lett.* **2007**, *9*, 3363–3366.
[5] R. M. Pinto, R. I. Olariu, J. Lameiras, F. T. Martins, A. A. Dias, G. J. Langley, P. Rodrigues, C. D. Maycock, J. P. Santos, M. F. Duarte, M. T. Fernandez, M. L. Costa, *Journal of Molecular Structure* **2010**, *980*, 163–171.
[6] X.-L. Liu, L.-Y. Niu, Y.-Z. Chen, M.-L. Zheng, Y. Yang, Q.-Z. Yang, *Organic & Biomolecular Chemistry* **2017**, *15*, 1072–1075.
[7] D. González-Calderón, M. A. Morales-Reza, E. Díaz-Torres, A. Fuentes-Benítes, C. González-Romero, *RSC Adv.* **2016**, *6*, 83547–83550.
[8] Naghipour, A.; Ghasemi, Z. H.; Morales-Morales, D.; Serrano-Becerra, J. M.; Jensen, C. M. *Polyhedron* **2008**, *27* (8), 1947–1952.

Synthesis of thioalkynes

Thioalkynes **2a**,[9] **2b**[10] y **2d**[11] are known compounds and were prepared according to reported procedures.

Benzyl(5-phenylpent-1-yn-1-yl)sulfane (2c)

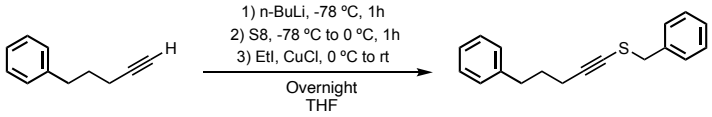

In an oven dried two neck round bottom flask was added the pent-4-yn-1-ylbenzene (1.6 mL, 10.2 mmol, 1.0 equiv) followed by freshly distilled THF (30 mL) and the mixture was cooled to -78 ºC in an acetone/dry-ice bath. Once cool, *n*-BuLi (4.3 mL 2.5 M in hexane, 10.7 mmol, 1.05 equiv) was added dropwise and the reaction was allowed to warm up to 0 ºC (water/ice bath) and stirred for 30 min. After the indicated time, elemental sulphur (0.327g, 1.27 mmol, 0.125 equiv) was added in one-portion, turning from yellow to deep red and stirred for further 1h. Catalytic CuCl (50 mg, 5 mol%) was added followed by benzylbromide (1.74 g, 1.2 mL, 1.0 equiv) and the solution was allowed to warm to rt and stirred overnight. The reaction was quenched by addition of saturated aqueous solution of NH_4Cl and extracted with Et_2O (2x30 mL), dried over $MgSO_4$ and the solvent removed under reduced pressure.

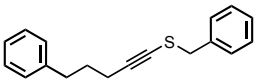

2c

benzyl(5-phenylpent-1-yn-1-yl)sulfane (**2c**). **FCC** in Hex. Isolated as a colorless oil (1.01 g, 3.8 mmol, 50% yield). **^{1}H NMR** (300 MHz, $CDCl_3$) δ 7.52 – 6.87 (m, 10 H), 3.87 (s, 2 H), 2.84 – 2.40 (t, J = 6.9 Hz, 2H), 2.25 (t, J = 6.9 Hz, 2H), 1.75 (p, J = 7.0 Hz, 2H). **^{13}C NMR** (75 MHz, $CDCl_3$) δ 141.68, 137.11, 129.14, 128.64, 128.46, 127.72, 126.01, 95.58, 68.81, 40.31, 34.79, 30.33, 19.65. **HRMS-ESI** Calculated for $C_{18}H_{19}S$ 267.1202 found 267.1203

[9] N. Riddell, W. Tam, *J. Org. Chem.* **2006**, *71*, 1934–1937.
[10] C. Eller, G. Kehr, C. G. Daniliuc, R. Fröhlich, G. Erker, *Organometallics* **2013**, *32*, 384–386.
[11] W. Zheng, F. Zheng, Y. Hong, L. Hu, *Heteroat. Chem.* **2012**, *23*, 105–110.

N-(6-(Diethylamino)-9-(2-(((7-(ethylthio)hept-6-yn-1-yl)oxy) carbonyl)phenyl)- 3H-xanthen-3-ylidene)-N-ethylethanaminium chloride. (2i)

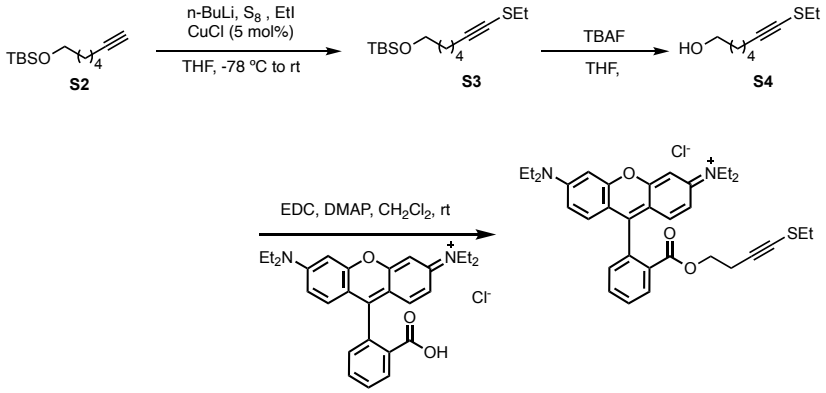

1. **Tert-butyl((7-(ethylthio)hept-6-yn-1-yl)oxy)dimethylsilane** (**S3)** was prepared according to the previously described procedure for 2c.

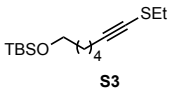
S3

Isolated as colorless oil (1.76 g, 70% yield). **^{1}H NMR** (300 MHz, $CDCl_3$) δ 3.57 (t, *J* = 6.2 Hz, 2H), 2.63 (q, *J* = 7.3 Hz, 2H), 2.27 (t, *J* = 6.8 Hz, 2H), 1.58 – 1.38 (m, 6H), 1.33 (t, *J* = 7.3 Hz, 3H), 0.86 (s, 9H), 0.01 (s, 6H).**^{13}C NMR** (75 MHz, $CDCl_3$) δ 94.6, 68.1, 63.1, 32.4, 29.5, 28.7, 26.0, 25.2, 20.2, 18.4, 14.7, -5.2 . **HRMS-ESI** Calculated for $C_{15}H_{31}OSSi$ 287.1859 found 287.1859.

2. Tert-butyl((7-(ethylthio)hept-6-yn-1-yl)oxy)dimethylsilane, **S3** (1.70 g, 5.93 mmol),was dissolved in THF (10 mL) at 0 ºC and TBAF solution (6.23 mL, 1.0 M, 6.23 mmol, 1.05 equiv) was added and the mixture stirred at 0 ºC for 15 min. Then, the reaction was allowed to warm to rt and stirred until full conversion was observed by TLC. Upon completion the mixture was poured into NH_4Cl (sat) (50 mL) and extracted with Et_2O. The organic phase was dried over $MgSO_4$ and the solvent removed under reduced pressure.

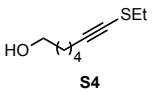
S4

7-(ethylthio)hept-6-yn-1-ol (**S4**). **FCC** in Hex:EtOAc (from 1:0 to 8:2). Isolated as colorless oil. 789 mg,4.68 mmol, 79% yield).**^{1}H NMR** (300 MHz, $CDCl_3$) δ 3.65 (t, *J* = 6.4 Hz, 2H), 2.68 (q, *J* = 7.3 Hz, 2H), 2.33 (t, *J* = 6.7 Hz, 2H), 1.63 – 1.31 (m, 10H). **^{13}C NMR** (75 MHz, $CDCl_3$) δ 94.6, 68.2, 62.7, 32.2, 29.6, 28.6, 25.0, 20.1, 14.7 **HRMS-ESI** Calculated for $C_9H_{17}OS$ 173.0995 found 173.0994

3. Rhodamine B (400 mg, 0.835 mmol, 1.0 equiv), EDC (176.1 mg, 0.919 mmol, 1.1 equiv), DMAP (25.5mg, 0.209, 0.25 equiv) and the thioalkyne 7 - (ethylthio)hept-6-yn-1-ol, **S4** (158 mg, 0.919 mmol, 1.1 equiv) were added to a dried round bottom flask containing CH_2Cl_2 (8.3 mL) at 0 ºC. The mixture was stirred at rt overnight, poured in of HCl 1N, extracted with CH_2Cl_2 (3 x 10 mL), washed with saturated $NaHCO_3$ (sat) and brine. The organic phase was dried over $MgSO_4$ and the solvent removed under reduced pressure.

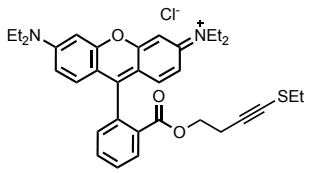

N-(6-(diethylamino)-9-(2-(((7-(ethylthio)hept-6-yn-1-yl)oxy)carbonyl)phenyl)-3H-xanthen-3-ylidene)-N-ethylethanaminium chloride (**2i**). **FCC** in CH_2Cl_2:MeOH (95:5). **2i** isolated as sticky solid (318 mg, 60% yield)..**^{1}H NMR** (500 MHz, $CDCl_3$) δ 8.26 (d, *J* = 7.82, 1H), 7.79 (td, *J* = 7.5, 1.4 Hz, 1H), 7.72 (td, *J* = 7.7, 1.3 Hz, 1H), 7.28 (dd, *J* = 7.6, 0.9 Hz, 1H), 7.06 (d, *J* = 9.5 Hz, 2H), 6.91 – 6.85 (m, 2H), 6.81 (d, *J* = 2.5 Hz, 2H), 4.00 (t, *J* = 6.5 Hz, 2H), 3.62 (q, *J* = 7.1 Hz, 8H), 2.63 (q, *J* = 7.3 Hz, 2H), 2.20 (m, 4H), 1.41 (m, 4H), 1.31 (t, *J* = 7.3 Hz, 12H), 1.27 – 1.16 (m, 3H). **^{13}C NMR** (75 MHz, $CDCl_3$) δ 148.57, 135.96 (d, *J* = 3.2 Hz), 135.08, 134.20 (d, *J* = 9.8 Hz), 131.63 (d, *J* = 5.4 Hz),130.17 (d, *J* = 12.6 Hz), 129.46, 129.42, 128.62, 128.5, 128.19 (d, *J* = 8.5 Hz), 127.84 (d, *J* = 3.5 Hz), 126.60, 125.36, 117.99, 116.86, 51.18, 30.93, 30.20, 14.57 (CH_3). **HRMS-ESI** Calculated for $C_{37}H_{45}N_2O_3S^+$ 597.3145 found 597.3145.

General Procedure for the RuAtAC under Millimolar Conditions

RuAtAC promoted by Ru2 in organic solvent

Exemplified for the cycloaddition of **1a** and **2a** in CH_2Cl_2.

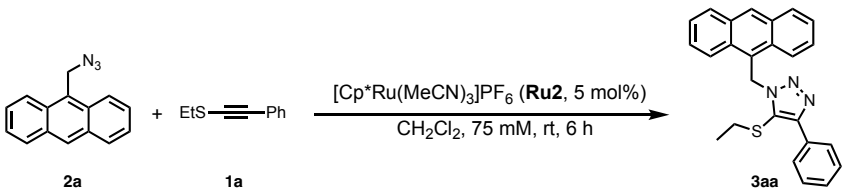

Ru2 (1.9 mg, 3.8 µmol) thioalkyne **2a** (24.3 mg 150 µmol), CH_2Cl_2 (1 mL), and azide **1a** (17.5 mg, 75 µmol), were sequentially added to a dry vial under argon at rt. The mixture was stirred for 6 h, after the indicated time the reaction mixture was filtered through a florisil plug, concentrated and analyzed by NMR using trimethoxybenzene as internal

standard. The resulting product, "**3aa**" was obtained in 30% yield. Its NMR data is in agreement with that previously reported.[12]

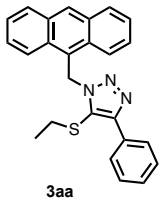

3aa

1-(anthracen-9-ylmethyl)-5-(ethylthio)-4-phenyl-1*H*-1,2,3-triazole (3aa). **^{1}H NMR** (500 MHz, $CDCl_3$) δ 8.54 (d, *J* = 8.1 Hz, 3H), 8.14 (d, *J* = 7.3 Hz, 2H), 8.04 (d, *J* = 7.7 Hz, 2H), 7.62 – 7.54 (m, 2H), 7.53 – 7.45 (m, 2H), 7.45 – 7.38 (m, 2H), 7.41 – 7.30 (m, 1H), 6.58 (s, 2H), 2.36 (q, *J* = 7.5 Hz, 2H), 0.94 (t, *J* = 7.4 Hz, 3H).

RuAtAC promoted by Ru2 in water

Exemplified for the cycloaddition of **1a** and **2a**

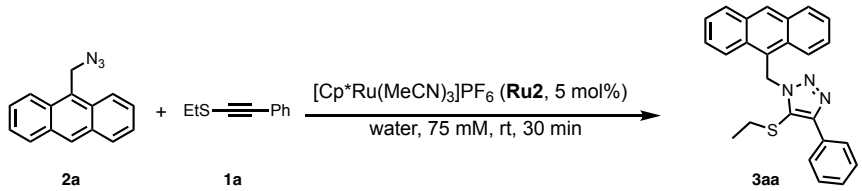

2a 1a 3aa

Ru2 (1.9 mg, 3.8 μmol) thioalkyne **2a** (24.3 mg, 150 μmol), H_2O (1 mL), and azide **1b** (11.0 mg, 75 μmol), were sequentially added under air to a vial. The mixture was irradiated at 365 nm for 10 min and stirred for 2 h. After the indicated time the reaction mixture was extracted with CH_2Cl_2 filtered through a florisil plug, concentrated, and analyzed by NMR using trimethoxybenzene as internal standard. The resulting product, "**3aa**" was obtained in 99% yield.

5-(Ethylthio)-4-phenyl-1-(p-methylbenzyl)-1H-1,2,3-triazole (3ba)

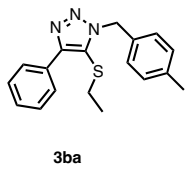

3ba

Yield = 79% (22.2 mg) **Rf** = 0.35 in 60:40 (Hexanes:Et_2O); flash column chromatography in Hexanesanes:Et_2O (from 80:20 to 30:70). **^{1}H NMR** (300 MHz, Chloroform-*d*) δ 8.18 (d, *J* = 7.6 Hz, 2H), 7.44 (t, *J* = 7.5 Hz, 2H), 7.37 (q, *J* = 7.3 Hz, 1H), 7.25 (d, *J* = 7.5 Hz, 2H), 7.14 (d, *J* = 7.8 Hz, 2H), 5.65 (s, 3H), 2.44 (q, *J* = 7.4 Hz, 2H), 2.32 (s, 4H), 0.97 (t, *J* = 7.4 Hz, 3H). **^{13}C NMR** (75 MHz, Chloroform-*d*) δ 149.07, 138.10, 132.37, 130.85, 129.48, 128.54, 128.34, 127.81, 126.84, 125.28, 30.05, 21.16, 14.40 (CH_3). **HRMS-ESI** Calculated for $C_{18}H_{19}N_3S^+$ 310.1373 found 310.1372.

[12] P. Destito, J. R. Couceiro, H. Faustino, F. López, J. L. Mascareñas, *Angew. Chem. Int. Ed.* **2017**, *56*, 10766–10770.

(4-(5-(Ethylthio)-4-phenyl-1H-1,2,3-triazol-1-yl)butyl)triphenylphosphonium bromide (3ca)

In this case a 9:1 Water: DMSO mixture is required

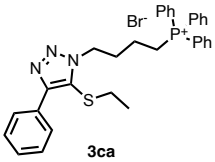

3ca

FCC in CH_2Cl_2:MeOH (from 98:2 to 90:10) as eluent. Isolated as cream solid (42.5 mg, 98% yield). **Rf** = 0.39 in CH_2Cl_2:MeOH (90:10). **^{1}H NMR** (500 MHz, $CDCl_3$) δ 8.09 (d, *J* = 7.2 Hz, 2H), 7.38 (t, *J* = 7.6 Hz, 2H), 7.30 (t, *J* = 7.4 Hz, 1H), 4.57 (t, *J* = 6.8 Hz, 2H), 3.64 (t, *J* = 5.9 Hz, 2H), 2.63 (q, *J* = 7.4 Hz, 2H), 2.15 – 2.08 (m, 3H), 1.05 (t, *J* = 7.4 Hz, 3H). **^{13}C NMR** (75 MHz, $CDCl_3$) δ 148.61, 134.92, 133.72, 130.34, 128.54, 126.69 (CH) 125.24, 118.67, 117.53, 46.76, 30.32, 29.70, 21.30, 19.19, 14.60. **HRMS-ESI** Calculated for $C_{32}H_{33}N_3PS^+$ 522.2127 found 522.2125.

(3-((5-(Ethylthio)-4-phenyl-1H-1,2,3-triazol-1-yl) methyl)benzyl) triphenyl-phosphonium bromide (3da)

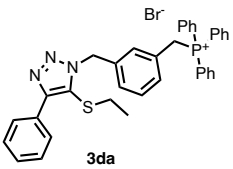

3da

FCC in CH_2Cl_2:MeOH (from 100:0 to 95:5) as eluent. Isolated as cream solid (33.6, 69%). **Rf** = 0.24 in CH_2Cl_2:MeOH (95:5). **^{1}H NMR** (300 MHz, $CDCl_3$) δ 8.18 (d, *J* = 7.1 Hz, 2H), 7.75 – 7.53 (m, 15H), 7.43 (m, 3H), 7.15 (mf, 3H), 7.01 (bs, 1H), 5.47 - 5.42 (m, 4H), 2.52 (q, *J* = 7.4 Hz, 2H), 1.01 (t, *J* = 7.4 Hz, 3H). **^{13}C NMR** (75 MHz, $CDCl_3$) δ 148.57, 135.96 (d, *J* = 3.2 Hz), 135.08, 134.20 (d, *J* = 9.8 Hz), 131.63 (d, *J* = 5.4 Hz), 130.17 (d, *J* = 12.6 Hz), 129.46, 129.42, 128.62, 128.51, 128.19 (d, *J* = 8.5 Hz), 127.84 (d, *J* = 3.5 Hz), 126.60, 125.36, 117.99, 116.86, 51.18, 30.93, 30.20, 14.57 . **HRMS-ESI** Calculated for $C_{36}H_{33}N_3PS^+$ 570.2127 found 570.2129.

(4-(5-(Isopropylthio)-4-phenyl-1H-1,2,3-triazol-1-yl)butyl)triphenyl phosphonium bromide (3cd)

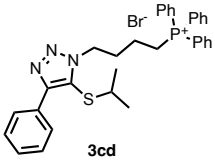

3cd

FCC CH_2Cl_2:MeOH (from 98:2 to 92:8). **Rf** = 0.58 in CH_2Cl_2:MeOH (90:10). Isolated as solid (46.0 mg, 99%). **^{1}H NMR** (300 MHz, $CDCl_3$) δ 8.04 (d, *J* = 7.2 Hz, 2H), 7.85 – 7.48 (m, 15H), 7.40-7.24 (m, 3H), 4.58 (t, *J* = 5.9 Hz, 2H), 3.91 (t, *J* = 14.5 Hz, 2H), 3.18 – 2.92 (m, 1H), 2.40-2.26 (m, 2H), 1.62-1.48 (m, 2H), 1.02 (d, *J* = 6.7 Hz, 6H). **^{13}C NMR** (75 MHz, $CDCl_3$) δ 148.88, 134.92 (d, *J* = 2.8 Hz, CH), 133.56 (d, *J* = 10.1 Hz, CH), 130.70, 130.38 (d, *J* = 12.6 Hz, CH), 128.41, 128.29, 126.70, 125.13, 118.49,

117.35, 46.65, 40.91, 29.54 (d, *J* =16.98), 22.88, 21.87, 21.19, 19.13(d, *J* = 3.5 Hz). **HRMS-ESI** Calculated for $C_{33}H_{35}N_3PS^+$ 536.2284 found 536.2284

1-(4-Methylbenzyl)-5-(phenylthio)-4-(trimethylsilyl)-1H-1,2,3-triazole (3bb)

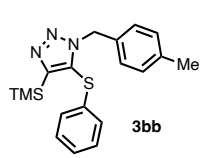

FCC in Hex:EtOAc (80:20) as eluent **Rf** = 0.21 in Hex:EtOAc (80:20 (26.5 mg, 99%). **^{1}H NMR** (300 MHz, $CDCl_3$) δ 7.19 – 7.04 (m, 4H), 6.99 (d, *J* = 7.9 Hz, 2H), 6.84 – 6.71 (m, 2H), 5.46 (s, 2H), 2.26 (s, 3H), 0.30 (s, 9H). **^{13}C NMR** (75 MHz $CDCl_3$) δ 153.09, 137.96, 134.83, 131.74, 131.52, 129.29, 128.25, 126.33, 126.24, 51.54, 21.16, -1.20. **HRMS-ESI** Calculated for $C_{19}H_{24}N_3SSi^+$ 354.1455 found 354.1457.

(4-(5-(Benzylthio)-4-(3-phenylpropyl)-1H-1,2,3-triazol-1-yl)butyl)triphenyl phosphonium bromide (3cc)

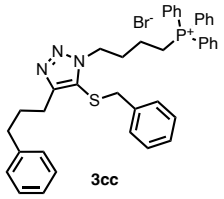

FCC in CH_2Cl_2:MeOH (from 98:2 to 92:8) Isolated as cream powder (65mg, 65% yield). **Rf** = 0.26 in CH_2Cl_2:MeOH (90:10**)** **^{1}H NMR** (500 MHz, $CDCl_3$) δ 7.72 (dd, *J* = 12.6, 7.4 Hz, 6H), 7.67 – 7.61 (m, 3H), 7.57 (td, *J* = 7.6, 3.4 Hz, 6H), 7.21 (d, *J* = 7.1 Hz, 2H), 7.11 (m, 6H), 6.83 (m, 2H), 4.09 (t, *J* = 6.2Hz, 2pH), 3.89 (tt, *J* = 13.5, 6.7 Hz, 2H), 3.65 (s, 2H), 2.53 (t, *J* = 7.7 Hz, 2H), 2.42 – 2.36 (t, *J* = 7.5,f Hz, 2H), 2.14 (dt, *J* = 13.1, 6.9 Hz, 2H), 1.81 (p, *J* = 7.8 Hz, 2H), 1.39 (td, *J* = 12.7, 10.2, 5.0 Hz, 2H). **^{13}C NMR** (126 MHz, $CDCl_3$) δ 152.52, 141.96, 136.55, 134.95, 133.74 (d, *J* = 10.0 Hz, CH), 130.45 (d, *J* = 12.6 Hz, CH), 128.80 (d, *J* = 9.6 Hz, CH), 128.51, 128.34, 127.78, 125.87, 124.77, 118.55, 117.87, 46.53, 40.92, 35.58, 30.72, 29.54, 29.41, 24.74, 21.50 (d, *J* = 50.9 Hz CH_2), 19.34 (CH_2). **HRMS-ESI** Calculated for $C_{40}H_{41}N_3PS,^+$ 626.2753 found 626.2756

(S)-2-((((9H-Fluoren-9-yl)methoxy)carbonyl) amino)-6-(5-(ethylthio)-4-phenyl-1H-1,2,3-triazol-1-yl)hexanoic acid (3ea)

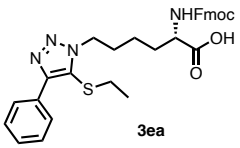

FCC CH_2Cl_2:MeOH (from 100:0 to 90:10). Isolated as a white powder (34 mg, 83%). **Rf** = 0.22 in CH_2Cl_2:MeOH (95:5). **^{1}H NMR** (500 MHz, $CDCl_3$) δ 8.04 (d, *J* = 7.4 Hz, 2H), 7.65 (d, *J* = 7.5 Hz, 2H), 7.54 – 7.41 (m, 2H), 7.35 (t, *J* = 7.5 Hz, 2H), 7.28 (t, *J* = 6.6 Hz, 3H), 7.20 (dt, *J* = 9.8, 5.1 Hz, 2fH), 5.57 (d, *J* = 7.7 Hz, 2H), 4.44 – 4.23 (m, 5H), 4.12 (t, *J* = 6.9 Hz, 1H), 2.56 (q, *J* = 7.4 Hz, 2H), 2.04 – 1.81 (m, 2H), 1.75 (s, 1H), 1.18 (s, 1H), 0.99 (t, *J* = 7.4 Hz, 3H). **^{13}C NMR** (126 MHz, $CDCl_3$) δ 175.25,

156.14, 148.66, 143.89, 143.74, 141.30, 130.41, 128.64 (CH) 128.56, 127.72, 127.10, 127.01, 125.47, 125.16, 119.98, 67.11, 53.55, 47.94, 47.15, 31.75, 30.20, 29.69, 22.10, 14.66. **HRMS-ESI** Calculated for $C_{31}H_{33}N_4O_4S$ 557.2217 found 557.2216

4-((5-(Ethylthio)-4-phenyl-1H-1,2,3-triazol-1-yl)methyl)-N,N-dimethylaniline (3fa)

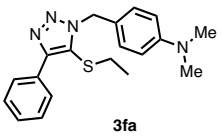

3fa

FCC in Hex:AcOEt (80:20). Isolated as white powder (22.8 mg, 90%). **Rf** = 0.25 in Hex:AcOEt (80:20). **^{1}H NMR** (300 MHz, $CDCl_3$) δ 8.20 (d, *J* = 7.4 Hz, 2H), 7.49 – 7.24 (m, 5H), 6.69 (d, *J* = 8.2 Hz, 2H), 5.60 (s, 2H), 2.94 (s, 6H), 2.47 (q, *J* = 7.2 Hz, 2H), 1.01 (t, *J* = 7.3 Hz, 3H). **^{13}C NMR** (75 MHz, $CDCl_3$) δ 150.4, 149.0, 131.0, 129.2, 128.5, 128.3, 126.9, 125.1, 122.8, 112.4, 51.8, 40.5, 30.1, 14.4. **HRMS-ESI** Calculated for $C_{19}H_{23}N_4S$ 339.1638 found339.1642

Orthogonality of RuAtAC and CuAAC annulations

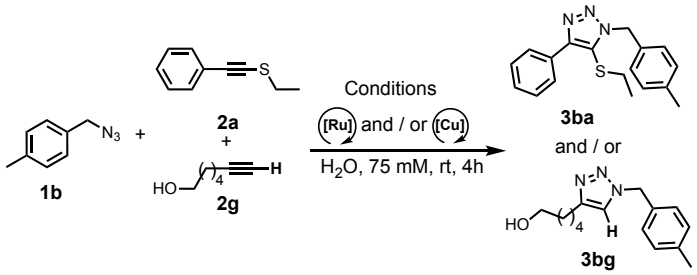

RuAtAC

In a 5 mL vial was added 50 mg of a solution of azide **1b** (5.5 mg, 37.5 µmol), thioalkyne **2a** (12.2 mg, 75 µmol) and alkyne **2h** (8.4 mg, 75 µmol) in DMSO (23.9 mg) followed by 400 µL of water and the precatalyst **Ru2** (1.1 mg, 1.9 µmol), the mixture was stirred for 2h After the indicated time the mixture was treated with 1 mL of a solution of EDTA-Na_2 (0.1M in water with 0.3 mL of aqueous ammonia/10 mL) for 5 min, extracted with CH_2Cl_2, filtered through a florisil plug, dried under vacuo and analyzed by NMR, using 1,3,5-trimethozybenzene as IS. 79% yield of **3ba**, 0% yield of **3bg.**

CuAAC

In a 5 mL vial was added 50 mg of a solution of azide **1b** (5.5 mg, 37.5 µmol), thioalkyne **2a** (12.2 mg, 75 µmol) and alkyne **2h** (8.4 mg, 75 µmol) in DMSO (23.9 mg) followed by 400 µL of water and 25 µL of a solution of sodium ascorbate (150 mM in water) and 25 µL of a solution of $CuSO_4 \cdot 5H_2O$ (75 mM in water) the mixture was stirred for 2h

followed. After the indicated time the mixture was treated with 1 mL of a solution of EDTA-Na_2 (0.1 M in water with 0.3 mL of aqueous NH_3/10 mL) for 5 min, extracted with CH_2Cl_2 and filtered through a florisil plug, dried under vacuo and analyzed by NMR, using 1,3,5-trimethozybenzene as IS. 0% yield of **3ba**, 78% yield of **3bg.**

RuAtAC first, CuAAC second

In a 5 mL vial was added 50 mg of a solution of azide **1b** (5.5 mg, 37.5 µmol), thioalkyne **2a** (12.2 mg, 75 µmol) and alkyne **2g** (8.4 mg, 75 µmol) in DMSO (23.9 mg) followed by 400 µL of water and the precatalyst **Ru2** (1.1 mg, 1.9 µmol), the mixture was stirred for 2h followed by the addition of another equivalent of azide **1b** (5.5 mg, 37.5 µmol), 25 µL of a solution of sodium ascorbate (150 mM in water) and 25 µL of a solution of $CuSO_4 \cdot 5H_2O$ (75 mM in water) and stirred for another 2h. After the indicated time the mixture was treated with 1 mL of a solution of EDTA-Na_2 (0.1M in water with 0.3 mL of aqueous ammonia/10 mL) for 5 min, extracted with CH_2Cl_2, filtered through a florisil plug, dried under vacuo and analyzed by NMR, using 1,3,5-trimethozybenzene as IS. 78% yield of **3ba**, 95% yield of **3bg.**

CuAAC first, RuAtAC second

In a 5 mL vial was added 50 mg of a solution of azide **1b** (5.5 mg, 37.5 µmol), thioalkyne **2a** (12.2 mg, 75 µmol) and alkyne **2g** (8.4 mg, 75 µmol) in DMSO (23.9 mg) followed by 400 µL of water and 25 µL of a solution of sodium ascorbate (150 mM in water) and 25 µL of a solution of $CuSO_4 \cdot 5H_2O$ (75 mM in water) the mixture was stirred for 2h followed by the addition of another equivalent of azide **1b** (5.5 mg, 37.5 µmol) the precatalyst **Ru2** (1.1 mg, 1.9 µmol) and stirred for another 2h. After the indicated time the mixture was treated with 1 mL of a solution of EDTA-Na_2 (0.1 M in water with 0.3 mL of aqueous NH_3/10 mL) for 5 min, extracted with $CH_2Cl_2$and filtered through a florisil plug, dried under vacuo and analyzed by NMR, using 1,3,5-trimethozybenzene as IS. 79% yield of **3ba**, 78% yield of **3bg.**

RuAtAC and CuAAC simultaneously

In a 5 mL vial was added 50 mg of a solution of azide **1b** (5.5 mg, 37.5 µmol), thioalkyne **2a** (12.2 mg, 75 µmol) and alkyne **2g** (8.4 mg, 75 µmol) in DMSO (23.9 mg) followed by 425 µL of water, 25 µL of a solution of sodium ascorbate (150 mM in water) and simultaneously the precatalyst **Ru2** (1.1 mg, 1.9 µmol) and the $CuSO_4 \cdot 5H_2O$ (0.5 mg, 1.9 µmol), and stirred for 2h. After the indicated time the mixture was treated with 1 mL of a

solution of EDTA-Na_2 (0.1 M in water with 0.3 mL of aqueous NH_3/10 mL) for 5 min, extracted with DCM and filtered through a florisil plug, dried under vacuo and analyzed by NMR, using 1,3,5-trimethozybenzene as IS. 50% yield of **3ba**, 44% yield of **3bg.**

5-(1-(4-methylbenzyl)-1H-1,2,3-triazol-4-yl)pentan-1-ol (3bh)

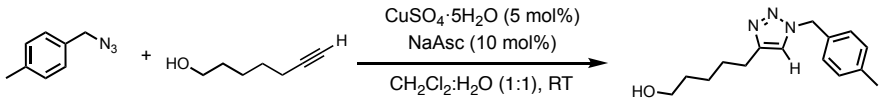

1b **2g** **3bg**

In a round bottom flask, under nitrogen atmosphere were added $CuSO_4$ 5·H_2O (3.7 mg, 15 µmol, 0.05 equiv), sodium ascorbate (6.0 mg, 30 µmol, 0.1 equiv), the solvent 4 mL (CH_2Cl_2:H_2O, 1:1) the alkyne, 6-heptyn-1-ol, **2g**, (33,7mg, 0.3 mmol, 1.0 equiv) and finally the azide **1b** (88.3 mg, 0.37 mmol, 2.0 equiv). Reaction concentration 75 mM referred to azide. The mixture was stirred at rt and followed by TLC. Crude was extracted with CH_2Cl_2, filtered through a florisil plug, concentrated, and purified by flash column chromatography (flash column chromatography).

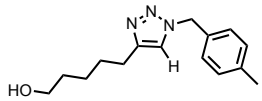

3bg

5-(1-(4-methylbenzyl)-1H-1,2,3-triazol-4-yl)pentan-1-ol. (3bg) FCC in Hex:AcOEt (70:30). Isolated as white solid (54 mg, 70%). **Rf** = 0.17 in Hex:AcOEt (70:30). **Yield** = **^{1}H NMR** (300 MHz, $CDCl_3$) δ 7.32 – 7.03 (m, 5H), 5.42 (s, 2H), 3.61 (t, *J* = 6.5 Hz, 2H), 2.74 (bs, 1H), 2.67 (t, *J* = 7.6 Hz, 2H), 2.33 (s, 3H), 1.84 – 1.52 (m, 4H), 1.48 – 1.27 (m, 2H). **^{13}C NMR** (75 MHz, $CDCl_3$) δ 148.5, 138.5, 131.9, 129.7, 128.1, 120.6, 62.5, 53.8, 32.4, 29.1, 25.6, 25.4, 21.2 (CH_3). **HRMS-ESI** Calculated for $C_{15}H_{22}N_3O$ 260.1757 found 260.1753

RuAtAC promoted by ruthenium (II) sandwich complexes in water

Exemplified for the cycloaddition of **1b** and **2a** with **Ru3.**

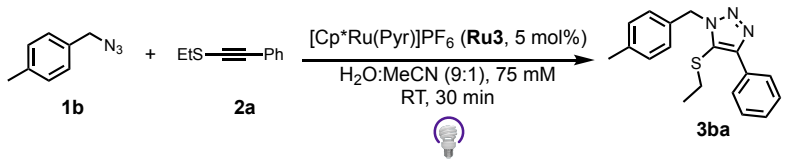

1b **2a** **3ba**

Ru3 (1.9 mg, 3.8 µmol), thioalkyne **2a** (24.3 mg, 150 µmol), H_2O:MeCN (9:1, 1 mL), and azide **1b** (11.0 mg, 75 µmol) were sequentially added to a dry vial under air to a vial. The mixture was stirred for 0.5 h, after the indicated time the reaction mixture was

extracted with CH_2Cl_2 filtered through a plug florisil, concentrated, and analyzed by NMR using trimethoxybenzene as internal standard. The resulting product, "**3ab**" was obtained in 99% yield.

General Procedure for the RuAtAC under Micromolar Conditions

RuAtAC promoted by Ru2 in water

Exemplified for the cycloaddition of **1c** and **2a** at 500 µM

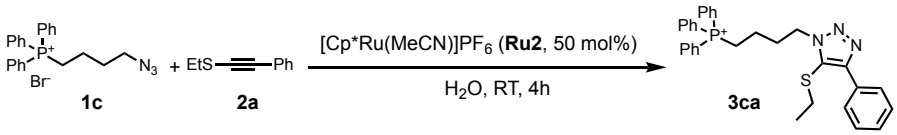

Thioalkyne **2a** (5 µL, from a stock solution 100 mM in DMSO, 2.0 equiv), azide **1c** (5 µL, from a stock solution 50 mM in DMSO, 1.0 equiv), water (500 µL) and **Ru2** (5 µL, from a stock solution 25 mM in DMSO, 0.5 equiv) were sequentially added to a HPLC vial equipped with a magnetic stir bar. The mixture was stirred for 4 h, diluted with MeOH (500 µL), 200 µL of the resulting solution were taken and diluted again with methanol (300 µL) to afford a 100 µM theoretical concentration of the expected triazole product **3ca**, coumarin (IS, 2.5 µL of a stock solution 20Mm in DMSO) was added as internal standard (final concentration of 100 µM) and analyzed by HPLC-MS, which allowed to determine a 99% yield of **3ca**.

RuAtAC promoted by ruthenium (II) sandwich complexes in water

Exemplified for the cycloaddition of **1c** and **2a** with **Ru3**

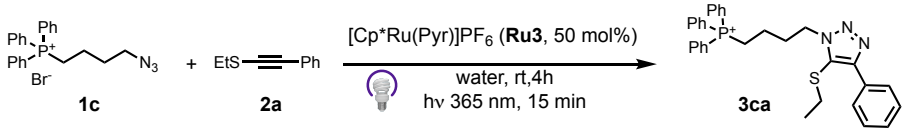

Thioalkyne **2a** (5 µL from a stock solution 100 mM in DMSO, 2.0 equiv), azide **1c** (5 µL, from a stock solution 50 mM in DMSO, 1.0 equiv), water (500 µL) and **Ru3** (5 µL, from a stock solution 25 mM in DMSO, 0.5 equiv) were sequentially added to a HPLC vial equipped with a magnetic stir bar. The mixture was irradiated for 15 min, stirred for 4 h, diluted with MeOH (500 µL), 200 µL of the resulting solution were taken and diluted again with methanol (300 µL) to afford a 100 µM theoretical concentration of the expected triazole product **3ca**, coumarin (IS, 2.5 µL of a stock solution 20Mm in DMSO)

was added as internal standard (final concentration of 100 μM) and analyzed by HPLC-MS, which allowed to determine a 99% yield of **3ca** (see Figure S3).

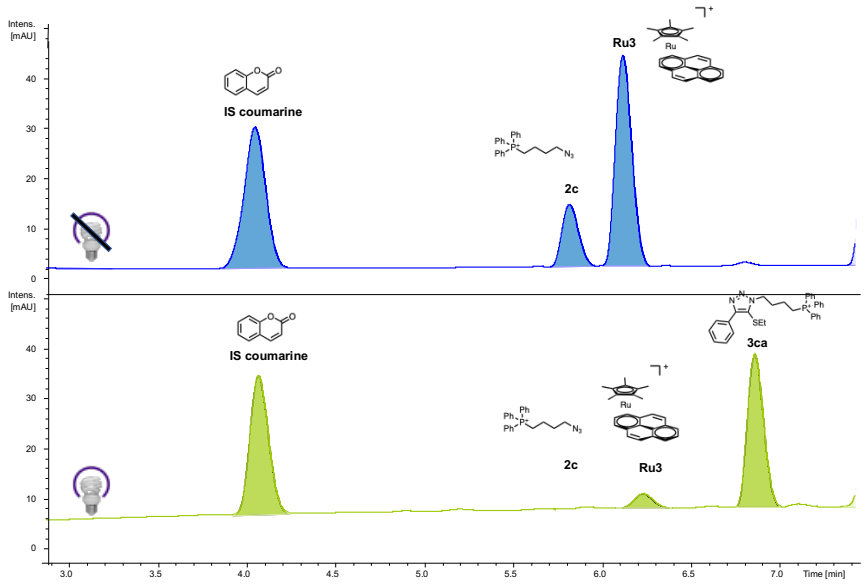

Figure S3. Yield determination for the reaction between thioalkyne **2a**, azide **1a,** and the precatalyst **Ru3** yields by UHPLC-MS. Internal standard coumarin. Upper chromatogram reaction control using **Ru3** without irradiation. Lower chromatogram reaction using **Ru3** with irradiation 15 min at 365 nm.

Calibration curves for yield determinations by HPLC

HPLC calibration curves were made by addition of a fixed quantity of and internal standard (coumarin, final concentration 100 μM) to the stock solutions of the corresponding compound. Curves are the result of the division of the area of the corresponding compound against the internal standard (absorption area recorded at 270 nm) plotted against the concentration of the sample.

HPLC calibration curve triazole 3ca

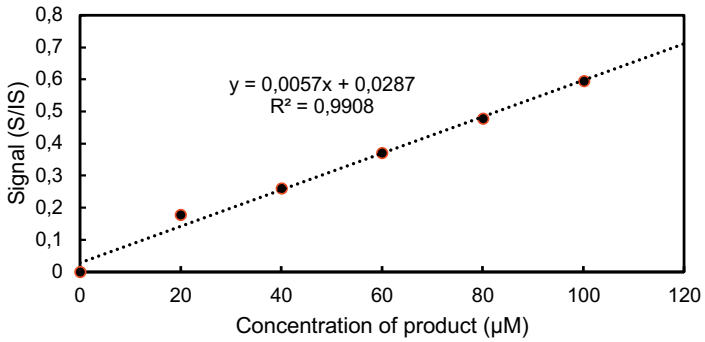

HPLC calibration curve azide 2c

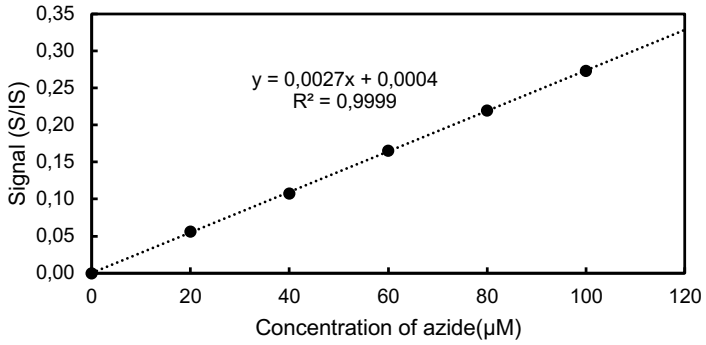

HPLC calibration curve triazole 3da

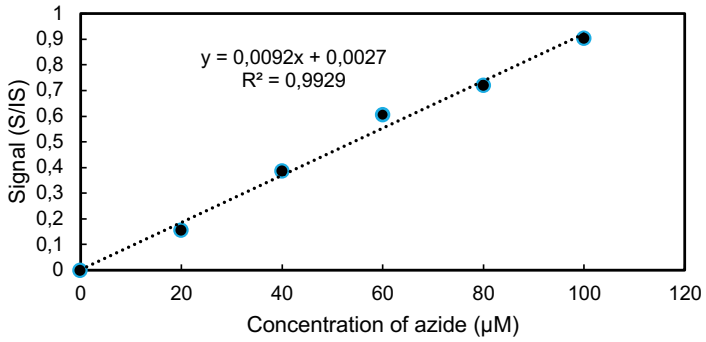

Biomolecule Modification

Oligonucleotides

HPLC assays for DNA quantification were performed in an *Agilent 1100* Series HPLC System using a Phenomenex Luna-C18(2) column 100 Å (250 x 4.6 mm, 5 µM), 1 mL/min, gradient 6 min isocratic at 0% B and then 0-73% over 40 min. (A: 95:5 H_2O:ACN containing 100mM TEAA pH 7.0, B: 70:30 ACN:H_2O containing 100 mM TEAA pH 7.0). Determination of the reaction yield was achieved by integration of the peaks recorded at 260 nm, with correction for the contribution of the rhodamine dye at this wavelength

Triethylammonium acetate buffer (TEAA pH 7.0, 1 M) was prepared from acetic acid and triethylamine following standard procedures.

EMSA experiments were performed using a *Bio-Rad Mini Protean* gel system powered by an electrophoresis power supplier *PowerPac Basic* model at a constant voltage of 120 V.

The products were resolved by PAGE using a 15% non-denaturing polyacrylamide gel and 0.5X TBE buffer for 40 min at 20 ºC. Gels were visualized by fluorescence, first after illumination of the rhodamine-labelled band and then by staining with SybrGold (Molecular Probes: 5 µL in 50 mL in 0.5X TBE) for 10 min to visualize the remanent unlabelled ssDNA.

Oligonucleotide modification with Ru2

In a HPLC vial the Azide-ssDNA (40 nmol, 1.0 equiv) was diluted with TEAA buffer (pH = 7, 0.1 M) up to a final volume of 200 µL, then the thioalkyne **2i** (80 nmol, 2 equiv), and finally the precatalyst **Ru2** (20 nmol, 0.5 equiv) were added and the mixture was stirred overnight, diluted to 100 µM and analyzed by HPLC.

Oligonucleotide modification with **Ru3**

In a HPLC vial the Azide-ssDNA (40 nmol, 1.0 equiv) was diluted with TEAA buffer (pH = 7, 0.1 M) up to a final volume of 200 µL, then the thioalkyne **2i** (80 nmol, 2 equiv), and finally the precatalyst **Ru3** (20 nmol, 0.5 equiv) were added, the reaction mixture was irradiated for 15 min the mixture was stirred overnight, diluted to 100 µM and analyzed by HPLC.

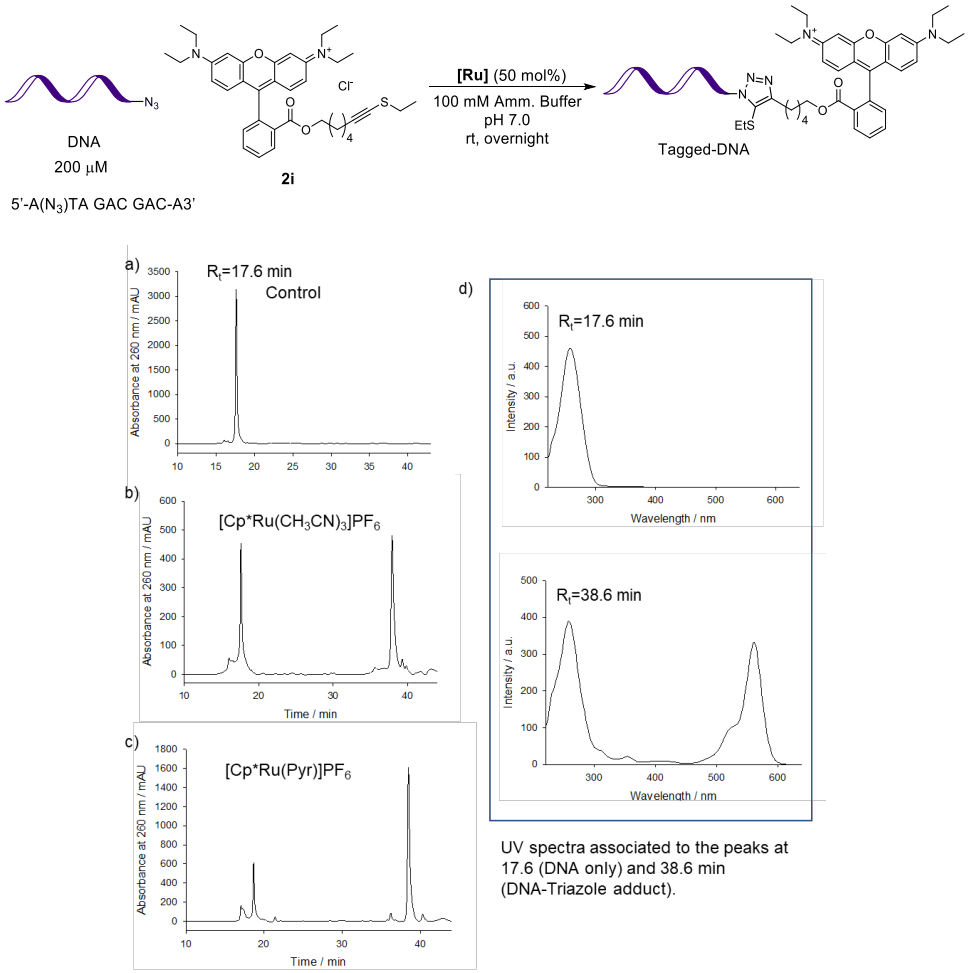

Figure S4. Reaction chromatograms a) Control, Azide-ssDNA without catalyst b) Reaction of the Azide-ssDNA in the presence of Ru2 c) Reaction of the Azide-ssDNA in the presence of Ru3 d) Absorption spectra of the ssDNA (Rt = 17.6 min) and triazole product (Rt = 38.6 min).

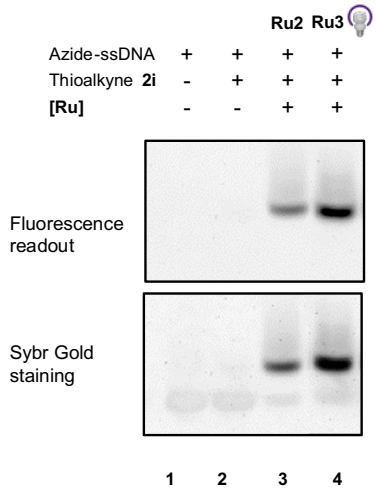

Figure S5. Comparative EMSA experiment for the labelling the Azide-ssDNA with different metal **Ru2** and **Ru3**. 100pmol DNA were loaded on each well. Lane 2 contains the thioalkyne 2i but no catalyst was added.

Peptides

Name **NH_2-K(N_3)-V-Y-I-H-P-F-$CONH_2$**

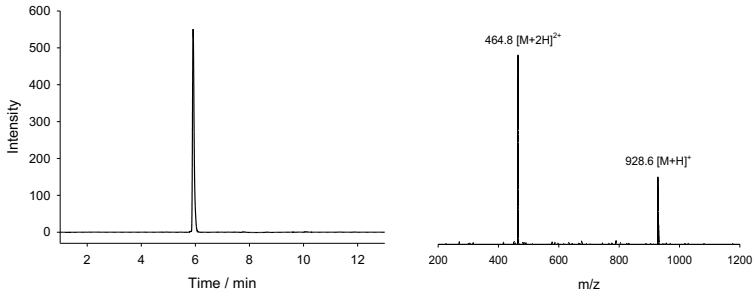

Figure S6. MS profile of A NH_2-K(N_3)-V-Y-I-H-P-F-$CONH_2$ Calculated mass for $C_{46}H_{65}N_{13}O_8$: 927.5. Found: 928.6 $[M+H]^+$; 464.8 $[M+2H]^{2+}$.

Name **NH_2-K(triazole)-V-Y-I-H-P-F-$CONH_2$**

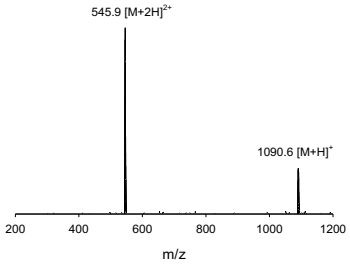

Figure S 7. MS profile NH_2-K(triazole)-V-Y-I-H-P-F-$CONH_2$. Calculated mass for $C_{56}H_{75}N_{13}O_8S$: 1089.6. Found: 1090.6 $[M+H]^+$; 545.9 $[M+2H]^{2+}$.

HPLC calibration curve azide-peptide (NH_2-K(N_3)-V-Y-I-H-P-F-$CONH_2$)

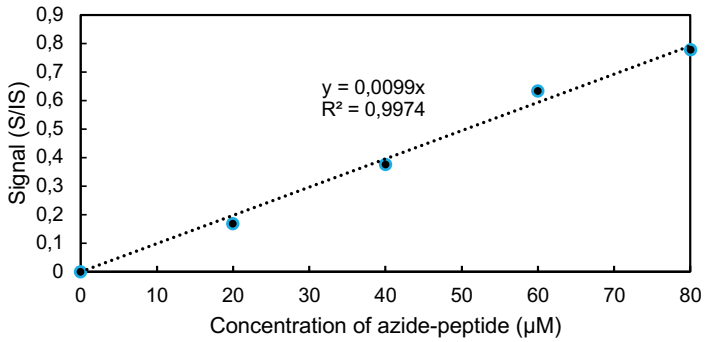

Peptide modification:

Determination of the reaction yield was achieved by conversion of the azide-peptide (N_3-K-V-Y-I-H-P-F-$CONH_2$) integrating the peaks recorded at 220 nm divided against the area of the internal standard (IS: coumarin). The yields are the average of three reactions.

Peptide modification with **Ru2**

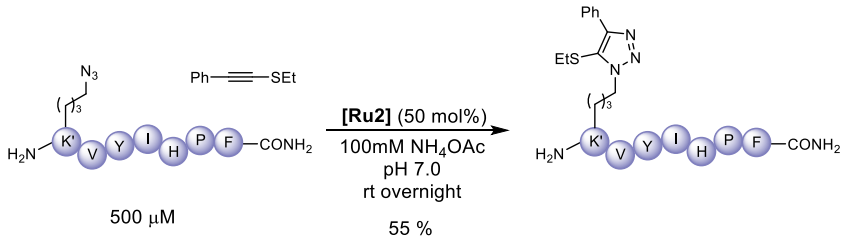

In a HPLC vial the NH_2-K(N_3)-V-Y-I-H-P-F-$CONH_2$ (250 nmol, 1.0 equiv) was diluted in a NH_4OAc solution (0.1 M) up to a final volume of 500 µL, then the thioalkyne **2a**

(500 nmol, 2 equiv), and finally the precatalyst **Ru2** (125 nmol, 0.5 equiv) were added dissolved in DMSO and the mixture was stirred overnight, diluted to 100 µM, internal standard addition (100 µM) and analyzed by HPLC.

Peptide modification with Ru3

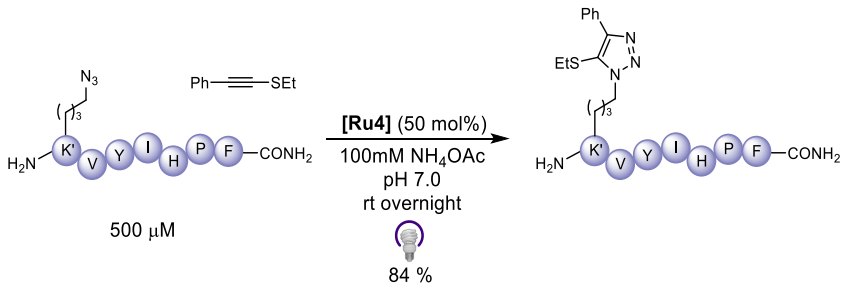

In a HPLC vial the NH_2-K(N_3)-V-Y-I-H-P-F-$CONH_2$ (250 nmol, 1.0 equiv) was diluted in a NH_4OAc solution (0.1 M) up to a final volume of 500 µL, then the thioalkyne **2a** (500 nmol, 2 equiv), and finally the precatalyst **Ru3** (125 nmol, 0.5 equiv) were added dissolved in DMSO the reaction mixture was irradiated for 15 min, then the mixture was stirred overnight, diluted to 100 µM, internal standard addition (100 µM) and analyzed by HPLC.

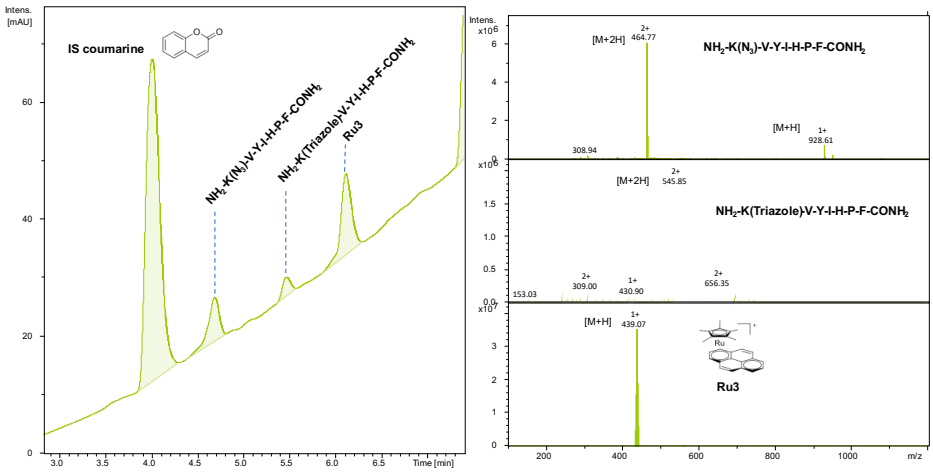

Figure S8. HPLC analysis for the ruthenium promoted azide-alkyne coupling with the peptide

Experiments in the Presence of Cells

Cell Culture: HeLa cells were cultured in DMEM (Dulbecco´s modified Eagle´s medium), 5 mM glutamine, penicillin (100 units/mL) and streptomycin (100 units/mL) (all from Invitrogen). Proliferating cultures were maintained in a 5% CO2 humidified incubator at 37 °C. For all the experiments, cells were suspended in DMEM-HEPES without Phenol Red) at 10^6 cells/mL.

RuAtAC between 1c and 2a promoted by Ru2, in the presence of cells

500 µL of a HeLa cell suspension (10^6 cells / mL) in DMEM-HEPES (without phenol-red) were transferred to a HPLC vial followed by sequential addition of the thioalkyne **2a** (10 µL, from a stock solution 40 mM in DMSO, 8.0 equiv), azide **1c** (2.5 µL, from a stock solution 20 mM in DMSO, 1.0equiv) and **Ru2** (2.5 µL, from a stock solution 10 mM in DMSO, 0.5 equiv).The resulting suspension was kept at 37 ºC and stirred for 2 h at 80 rpm. After the indicated time 400 µL of the suspension were taken to Eppendorf vial and centrifuged at 10 000 rpm for 4 min.

The supernatant was transferred to a HPLC vial diluted with 400 µL of MeOH (80%$_{v/v}$), coumarin was added as IS (4 µL of a stock solution 20 mM in DMSO) and analyzed by HPLC-MS.

The remaining cell pellet was treated with 200 µL of MeOH (80% $_{v/v}$) and shaked at 1000 rpm for 5 min, followed by centrifugation at 10 000 rpm for 5 min. The resulting extract was transferred to a HPLC vial diluted with 200 µL of MeOH (80% $_{v/v}$), coumarin was added as IS (2 µL of a stock solution 20 mM in DMSO) and analyzed by HPLC-MS.

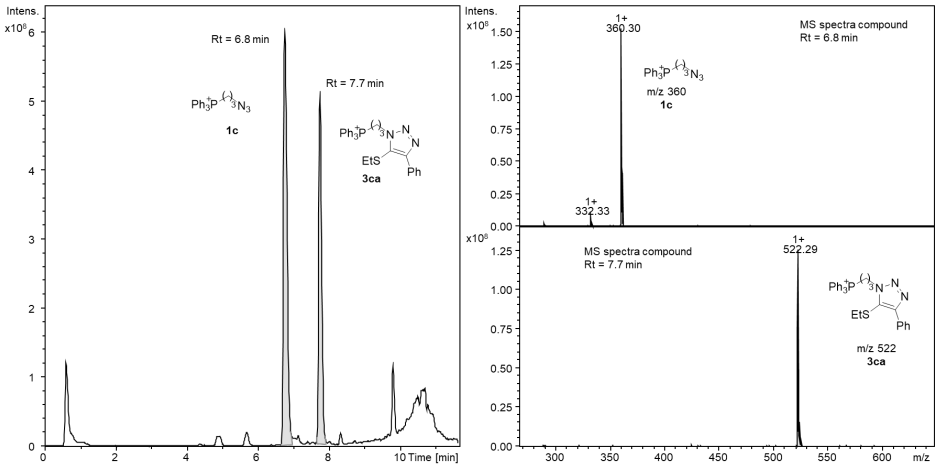

Figure S9. MS-chromatogram and MS-spectra for the indicated peaks in the supernatant

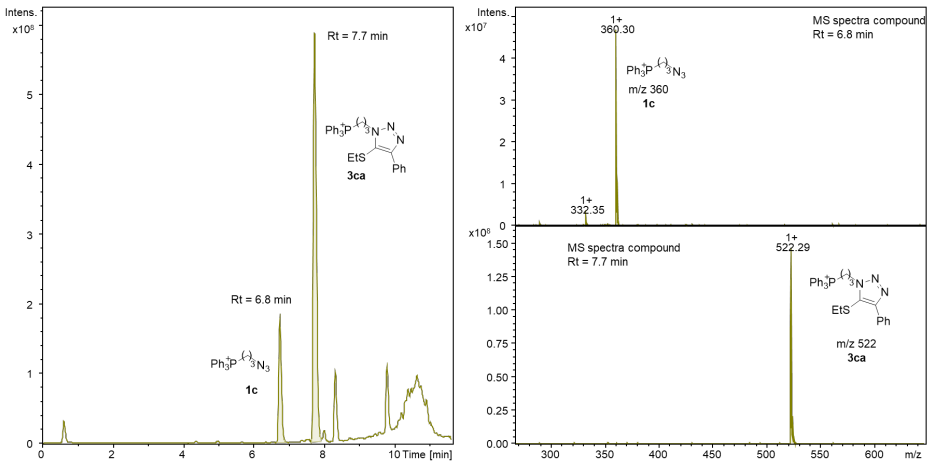

Figure S10. MS-chromatogram and MS-spectra for the indicated peaks in the methanolic extract.

RuAtAC between 1c and 2a promoted by Ru3, in the presence of cells

500 µL of a HeLa cell suspension (10^6 cells / mL) in DMEM-HEPES (without phenol-red) were transferred to a HPLC vial followed by sequential addition of the thioalkyne **2a** (10 µL, from a stock solution 40 mM in DMSO, 8.0 equiv), azide **1c** (2.5 µL, from a stock solution 20 mM in DMSO, 1.0equiv) and **Ru3** (2.5 µL, from a stock solution 10 mM in DMSO, 0.5 equiv).The resulting suspension was irradiated at 365 nm for 10 min, then kept at 37 ºC and stirred for 2 h at 80 rpm. After the indicated time 400 µL of the suspension were taken to Eppendorf vial and centrifuged at 10 000 rpm for 4 min.

The supernatant was transferred to a HPLC vial diluted with 400 µL of MeOH (80%$_{v/v}$), coumarin was added as IS (4 µL of a stock solution 20 mM in DMSO) and analyzed by HPLC-MS.

The remaining cell pellet was treated with 200 µL of MeOH (80% $_{v/v}$) and shaked at 1000 rpm for 5 min, followed by centrifugation at 10 000 rpm for 5 min. The resulting extract was transferred to a HPLC vial diluted with 200 µL of MeOH (80% $_{v/v}$), coumarin was added as IS (2 µL of a stock solution 20 mM in DMSO) and analyzed by HPLC-MS.

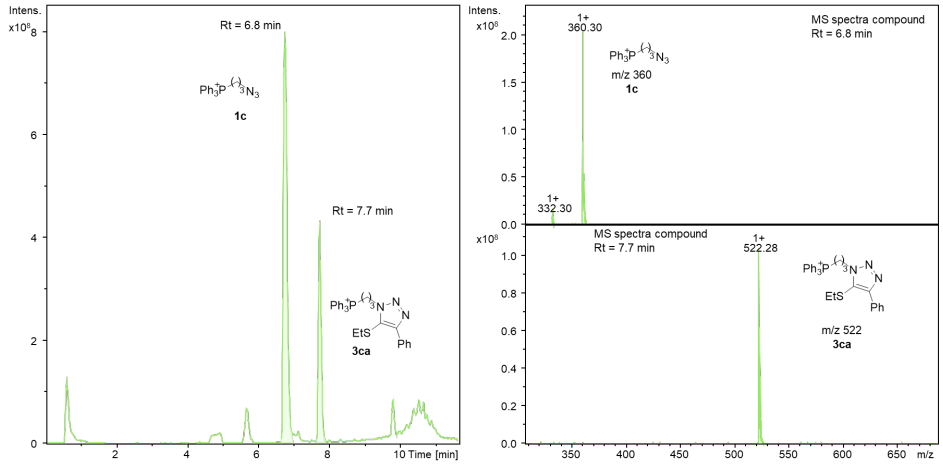

Figure S11. MS-chromatogram and MS-spectra for the indicated peaks in the supernatant

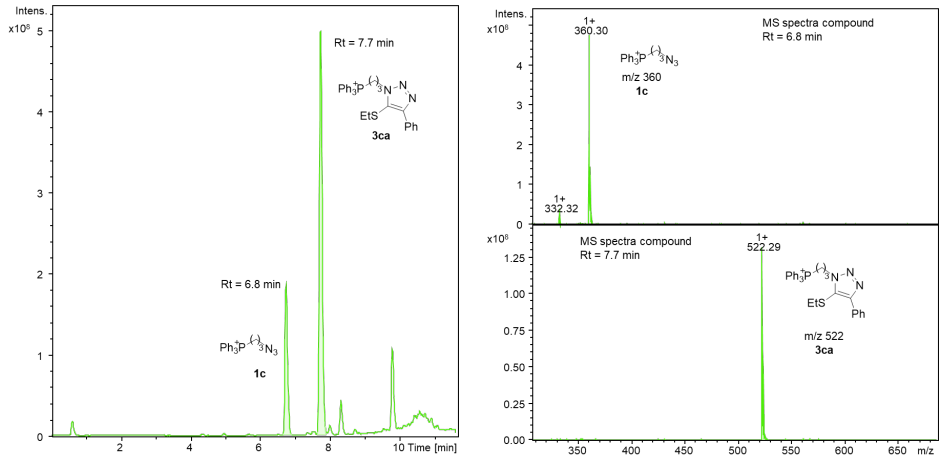

Figure S12. MS-chromatogram and MS-spectra for the indicated peaks in the supernatant

Controls

Blank

500 µL of a HeLa cell suspension (10^6 cells / mL) in DMEM-HEPES (without phenol-red) were transferred to a HPLC and kept at 37 ºC and stirred for 2 h at 80 rpm. After the indicated time 400 µL of the suspension were taken to Eppendorf vial and centrifuged at 10 000 rpm for 4 min.

The supernatant was transferred to a HPLC vial diluted with 400 µL of MeOH (80%$_{v/v}$), coumarin was added as IS (4 µL of a stock solution 20 mM in DMSO) and analyzed by HPLC-MS.

The remaining cell pellet was treated with 200 µL of MeOH (80% $_{v/v}$) and shaked at 1000 rpm for 5 min, followed by centrifugation at 10 000 rpm for 5 min. The resulting extract was transferred to a HPLC vial diluted with 200 µL of MeOH (80% $_{v/v}$), coumarin was added as IS (2 µL of a stock solution 20 mM in DMSO) and analyzed by HPLC-MS.

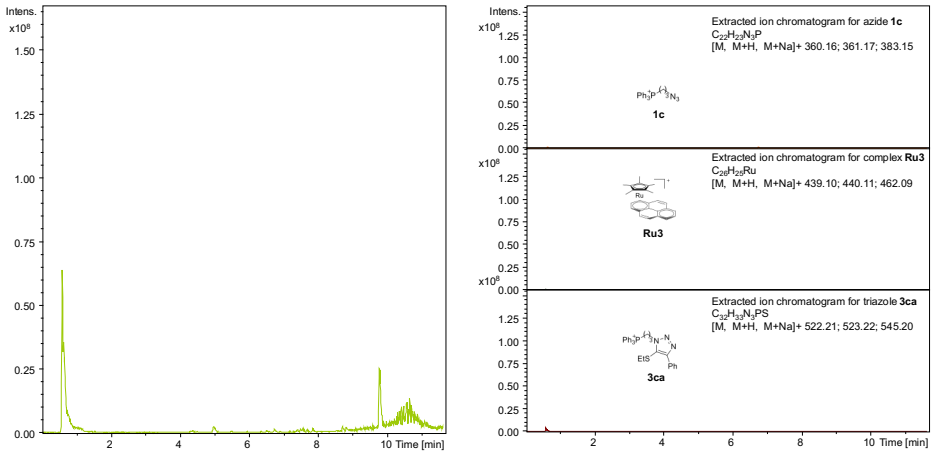

Figure S13. Blank MS-chromatogram of the supernatant. Extracted ion chromatograms for triazole **3ca**, azide 1c and ruthenium complex Ru3 for the supernatant of the blank.

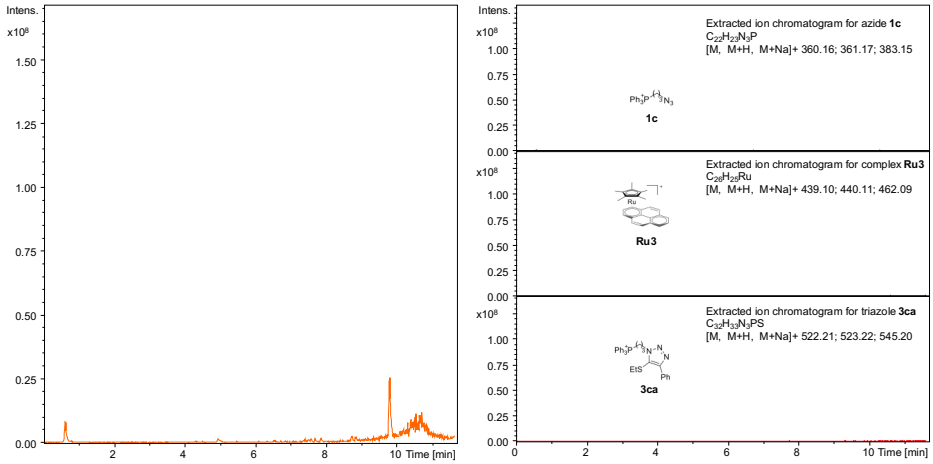

Blank MS-chromatogram of the supernatant. Extracted ion chromatograms for triazole **3ca**, azide **1c** and ruthenium complex **Ru3** for the methanolic extract of the blank.

Control for Ru3. No irradiation

500 µL of a HeLa cell suspension (10^6 cells / mL) in DMEM-HEPES (without phenol-red) were transferred to a HPLC vial followed by sequential addition of the thioalkyne **2a** (10 µL, from a stock solution 40 mM in DMSO, 8.0 equiv), azide **1c** (2.5 µL, from a stock solution 20 mM in DMSO, 1.0equiv) and **Ru3** (2.5 µL, from a stock solution 10 mM in DMSO, 0.5 equiv).The resulting suspension was kept at 37 ºC and stirred for 2 h at 80 rpm. After the indicated time 400 µL of the suspension were taken to Eppendorf vial and centrifuged at 10 000 rpm for 4 min.

The supernatant was transferred to a HPLC vial diluted with 400 µL of MeOH (80%$_{v/v}$), coumarin was added as IS (4 µL of a stock solution 20 mM in DMSO) and analyzed by HPLC-MS.

The remaining cell pellet was treated with 200 µL of MeOH (80% $_{v/v}$) and shaked at 1000 rpm for 5 min, followed by centrifugation at 10 000 rpm for 5 min. The resulting extract was transferred to a HPLC vial diluted with 200 µL of MeOH (80% $_{v/v}$), coumarin was added as IS (2 µL of a stock solution 20 mM in DMSO) and analyzed by HPLC-MS.

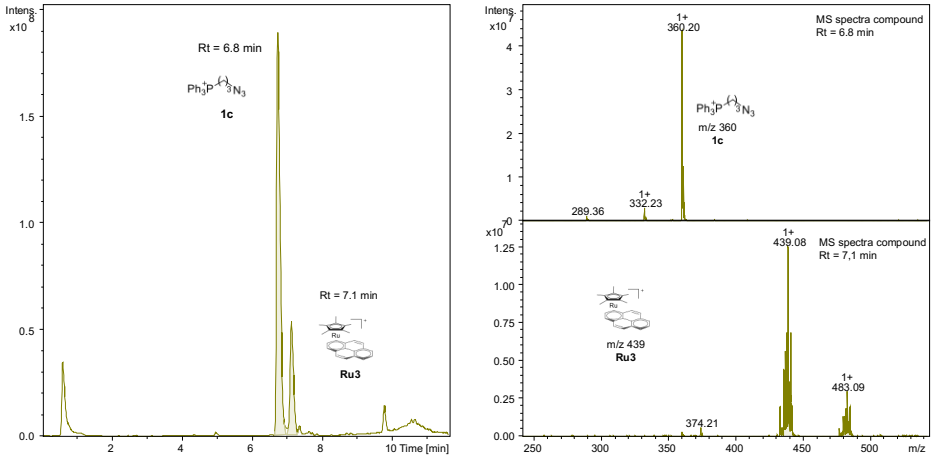

Figure S14. MS-chromatogram and MS-spectra for the indicated peaks in the supernatant

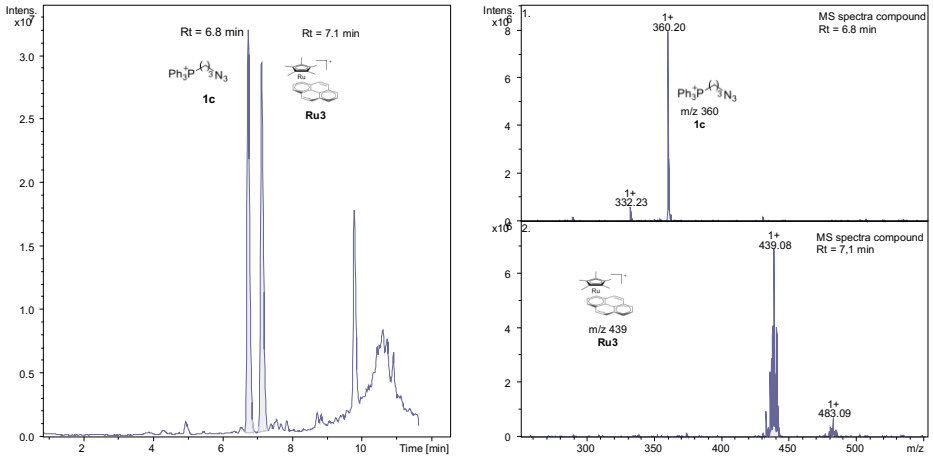

Figure S15. MS-chromatogram and MS-spectra for the indicated peaks in the methanolic extract

Control. No Ru No hv

500 µL of a HeLa cell suspension (10^6 cells / mL) in DMEM-HEPES (without phenol-red) were transferred to a HPLC vial followed by sequential addition of the thioalkyne **2a** (10 µL, from a stock solution 40 mM in DMSO, 8.0 eq) and azide **1c** (2.5 µL, from a stock solution 20 mM in DMSO, 1.0 equiv) The resulting suspension was kept at 37 ºC and stirred for 2 h at 80 rpm. After the indicated time 400 µL of the suspension were taken to Eppendorf vial and centrifuged at 10 000 rpm for 4 min.

The supernatant was transferred to a HPLC vial diluted with 400 µL of MeOH (80%$_{v/v}$), coumarin was added as IS (4 µL of a stock solution 20 mM in DMSO) and analyzed by HPLC-MS.

The remaining cell pellet was treated with 200 µL of MeOH (80% v/v) and shaked at 1000 rpm for 5 min, followed by centrifugation at 10 000 rpm for 5 min. The resulting extract was transferred to a HPLC vial diluted with 200 µL of MeOH (80% v/v), coumarin was added as IS (2 µL of a stock solution 20 mM in DMSO) and analyzed by HPLC-MS.

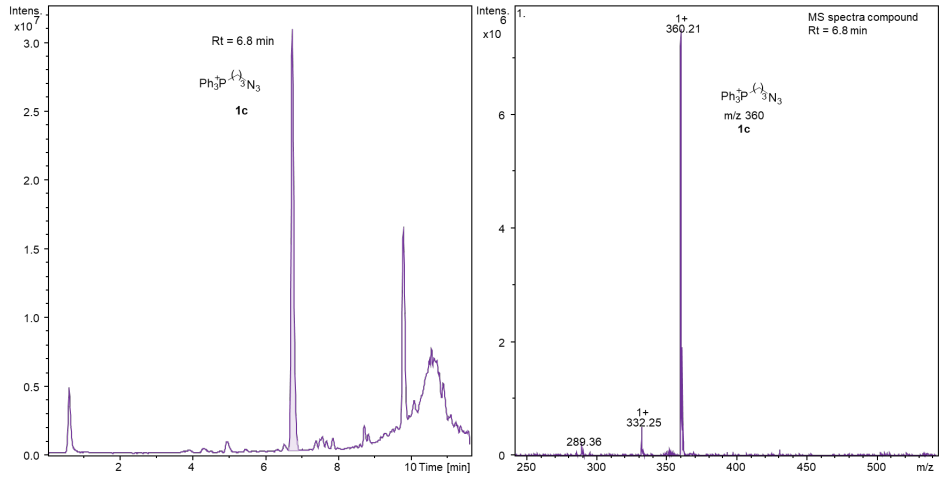

Figure S16. MS-chromatogram and MS-spectra for the indicated peaks in the supernatant

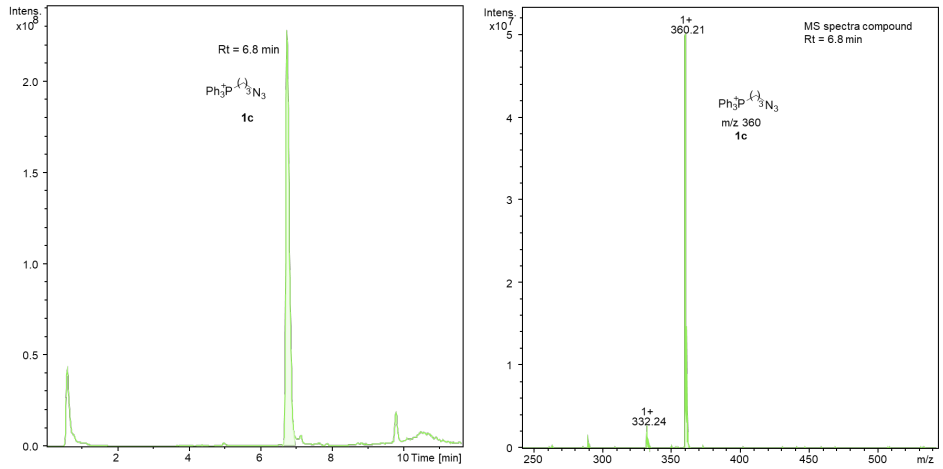

Figure S17. MS-chromatogram and MS-spectra for the indicated peaks in the methanolic extract

Control No Ru and with irradiation

500 µL of a HeLa cell suspension (10^6 cells / mL) in DMEM-HEPES (without phenol-red) were transferred to a HPLC vial followed by sequential addition of the thioalkyne **2a** (10 µL, from a stock solution 40 mM in DMSO, 8.0 equiv) and azide **1c** (2.5 µL, from a stock solution 20 mM in DMSO, 1.0equiv) The resulting suspension was irradiated at 365 nm for 10 min, then kept at 37 ºC and stirred for 2 h at 80 rpm. After the indicated time 400 µL of the suspension were taken to Eppendorf vial and centrifuged at 10 000 rpm for 4 min.

The supernatant was transferred to a HPLC vial diluted with 400 µL of MeOH (80%$_{v/v}$), coumarin was added as IS (4 µL of a stock solution 20 mM in DMSO) and analyzed by HPLC-MS.

The remaining cell pellet was treated with 200 µL of MeOH (80% $_{v/v}$) and shaked at 1000 rpm for 5 min, followed by centrifugation at 10 000 rpm for 5 min. The resulting extract was transferred to a HPLC vial diluted with 200 µL of MeOH (80% $_{v/v}$), coumarin was added as IS (2 µL of a stock solution 20 mM in DMSO) and analyzed by HPLC-MS.

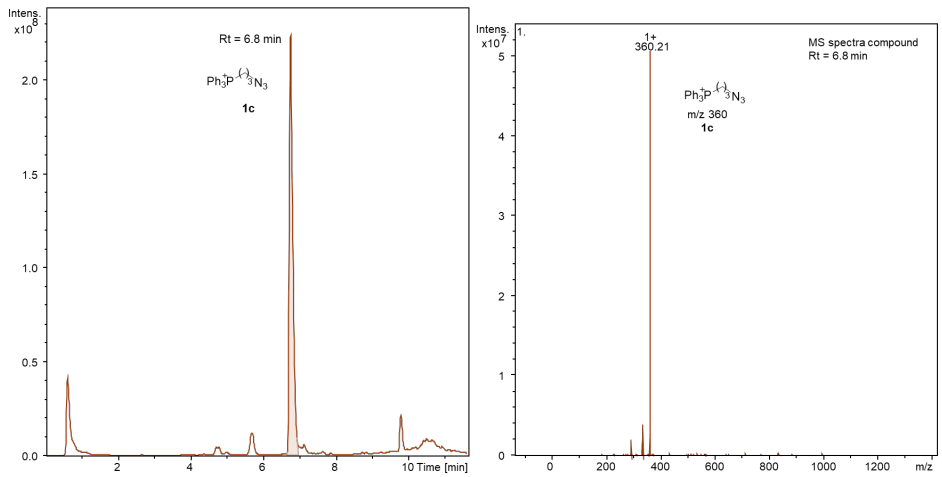

Figure S18. MS-chromatogram and MS-spectra for the indicated peaks in the supernatant

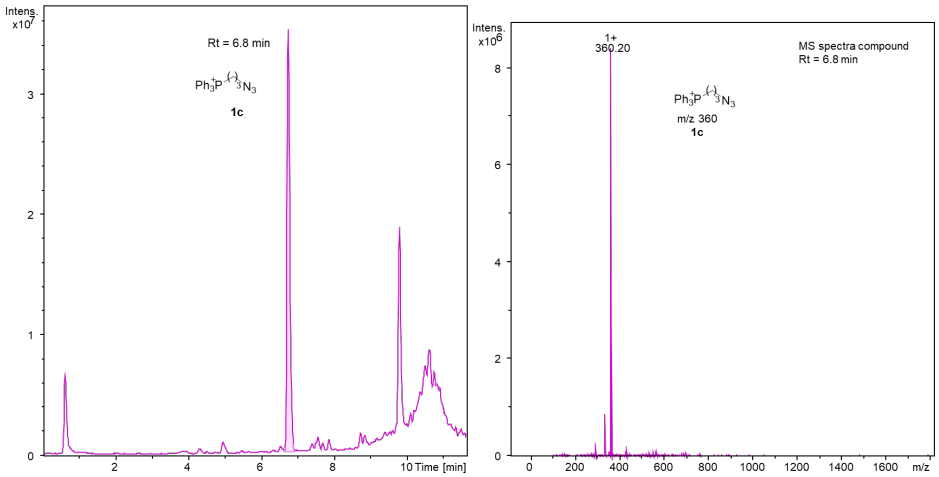

Figure S19. MS-chromatogram and MS-spectra for the indicated peaks in the methanolic extract

Control with the product

500 µL of a HeLa cell suspension (10^6 cells / mL) in DMEM-HEPES (without phenol-red) were transferred to a HPLC vial followed addition of the triazole **3ca** (2.5 µL, from a stock solution 20 mM in DMSO, 8.0 equiv) The resulting suspension was kept at 37 ºC and stirred for 2 h at 80 rpm. After the indicated time 400 µL of the suspension were taken to Eppendorf vial and centrifuged at 10 000 rpm for 4 min.

The supernatant was transferred to a HPLC vial diluted with 400 µL of MeOH (80%$_{v/v}$), coumarin was added as IS (4 µL of a stock solution 20 mM in DMSO) and analyzed by HPLC-MS.

The remaining cell pellet was treated with 200 µL of MeOH (80% $_{v/v}$) and shaked at 1000 rpm for 5 min, followed by centrifugation at 10 000 rpm for 5 min. The resulting extract was transferred to a HPLC vial diluted with 200 µL of MeOH (80% $_{v/v}$), coumarin was added as IS (2 µL of a stock solution 20 mM in DMSO) and analyzed by HPLC-MS.

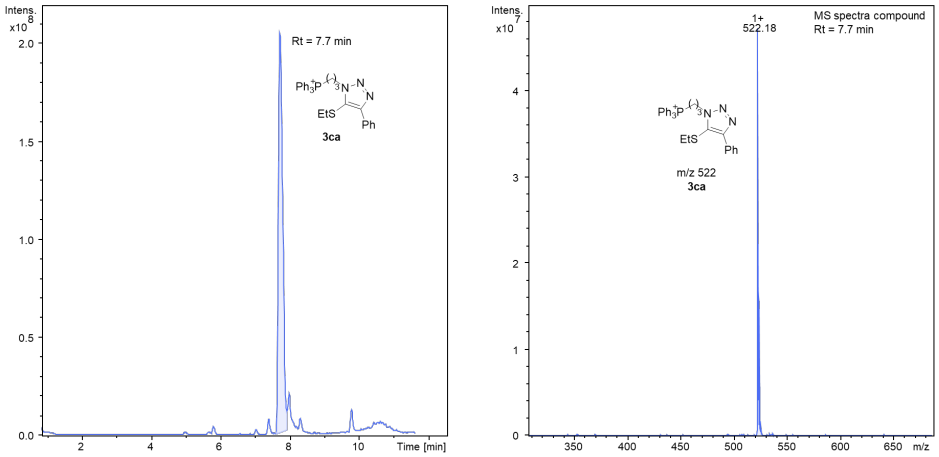

Figure S20. MS-chromatogram and MS-spectra for the indicated peaks in the supernatant

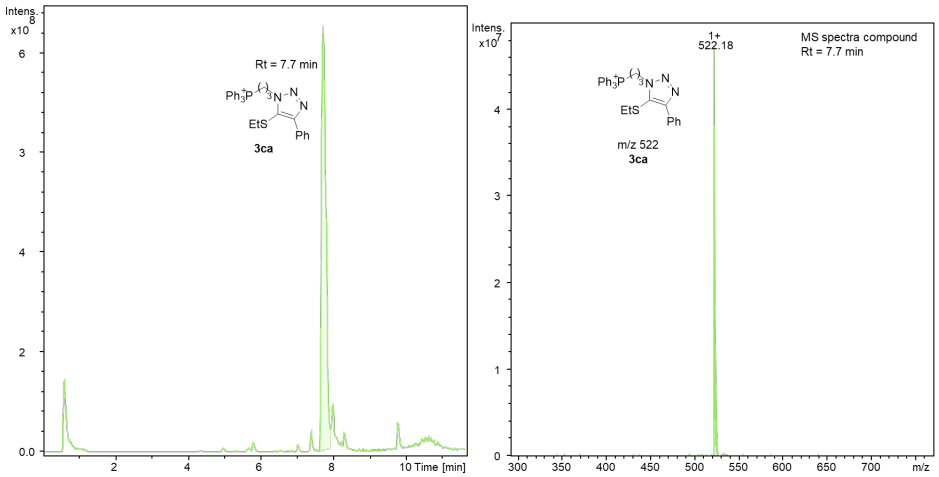

Figure S21. MS-chromatogram and MS-spectra for the indicated peaks in the methanolic extract.

Selected NMR Spectra

η5-(Pentamethylcyclopentadienyl)-η6-(pyrene-1-sulfonate) ruthenium(II) sodium hexafluorophosphate (Ru5)

^{1}H NMR (300 MHz, CD_3OD)

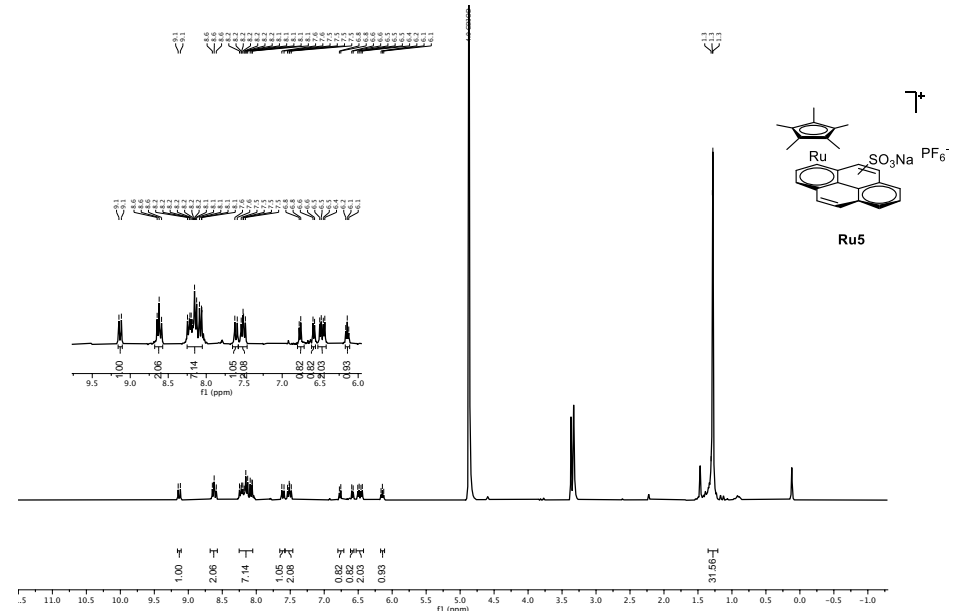

^{13}C NMR (75 MHz, CD_3OD)

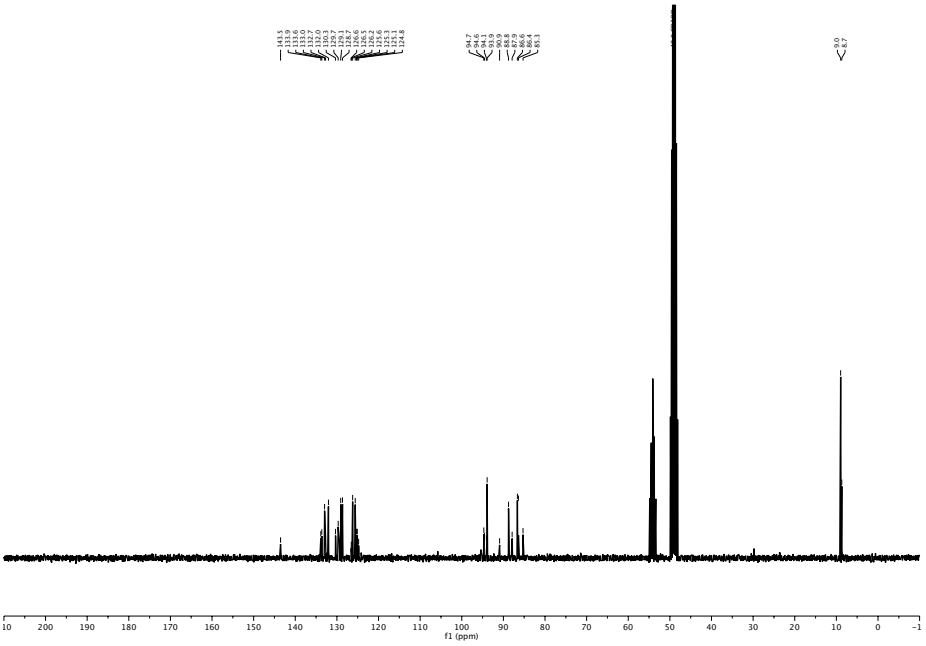

Thioalkynes

benzyl(5-phenylpent-1-yn-1-yl)sulfane (2c)

^{1}H NMR (300 MHz, $CDCl_3$)

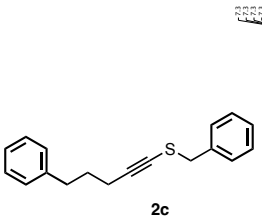

2c

^{13}C NMR (75 MHz, $CDCl_3$)

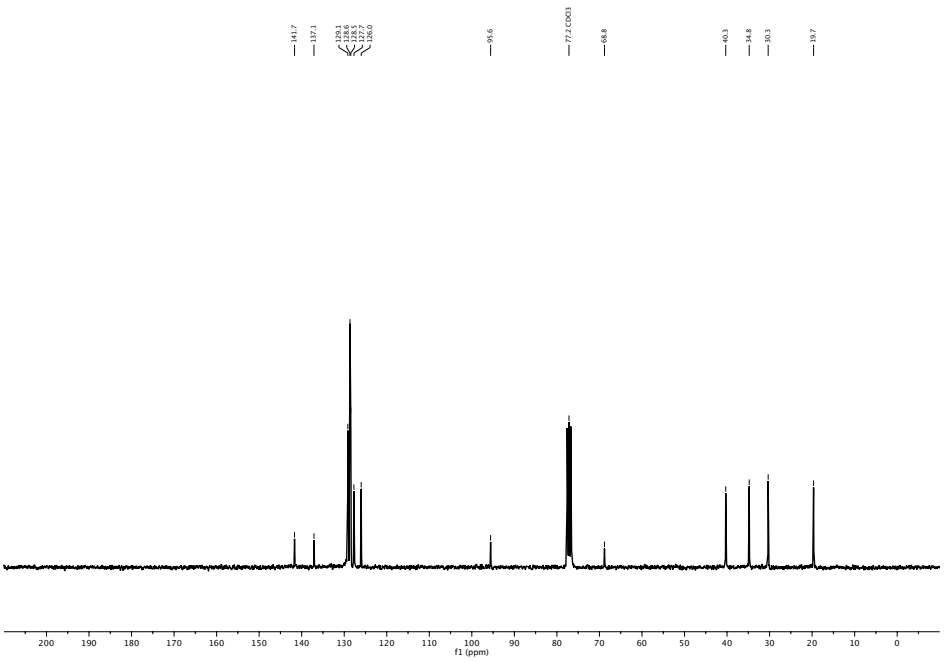

N-(6-(Diethylamino)-9-(2-(((7-(ethylthio)hept-6-yn-1-yl)oxy) carbonyl)phenyl)- 3H-xanthen-3-ylidene)-N-ethylethanaminium chloride. (2i)

^{1}H NMR (500 MHz, $CDCl_3$)

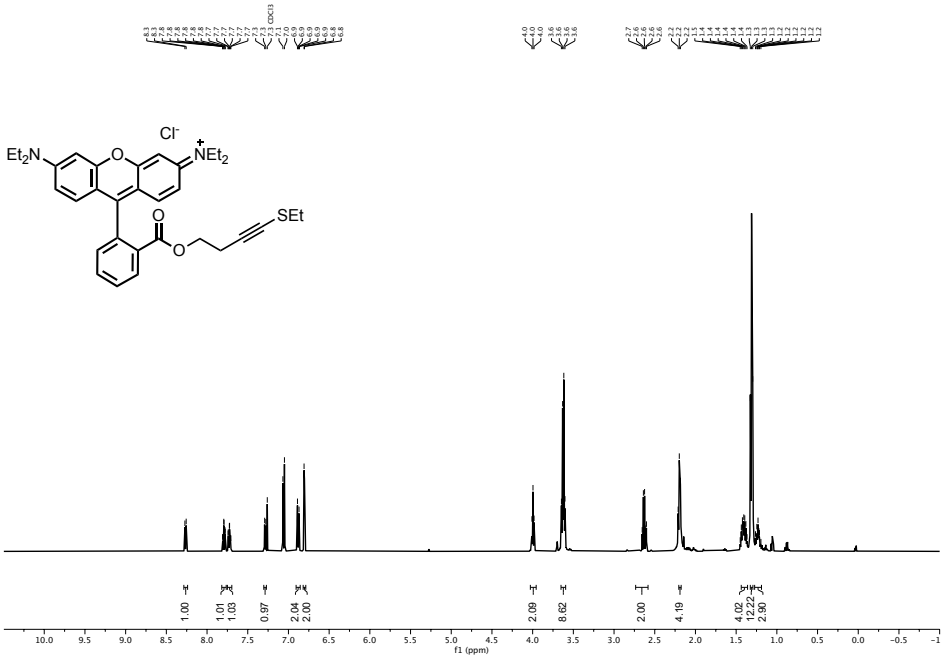

^{13}C NMR (75 MHz, $CDCl_3$)

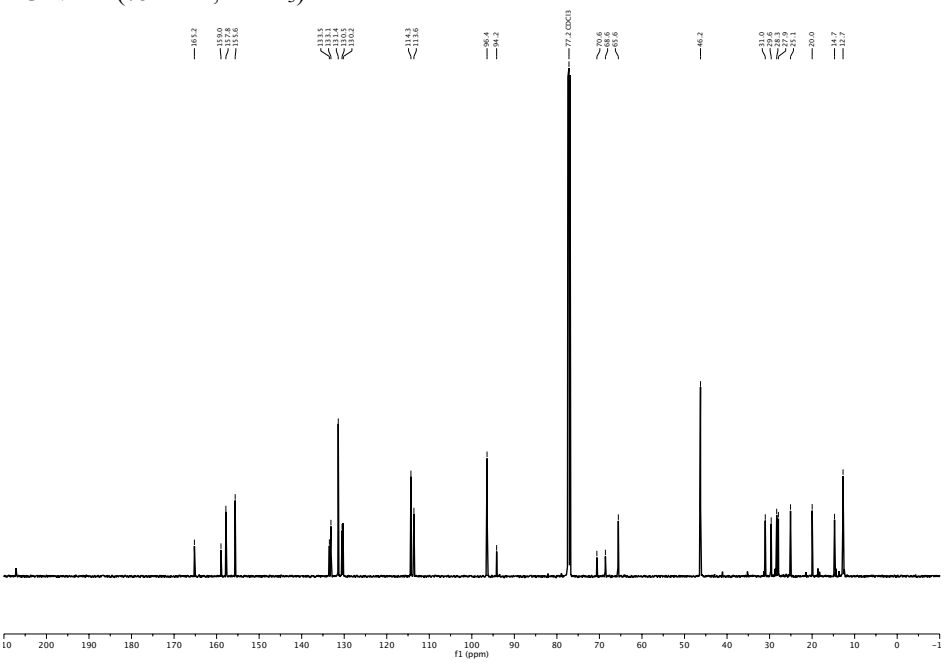

Triazoles

5-(Ethylthio)-4-phenyl-1-(p-methylbenzyl)-1H-1,2,3-triazole (3ba)

^{1}H NMR (300 MHz, $CDCl_3$)

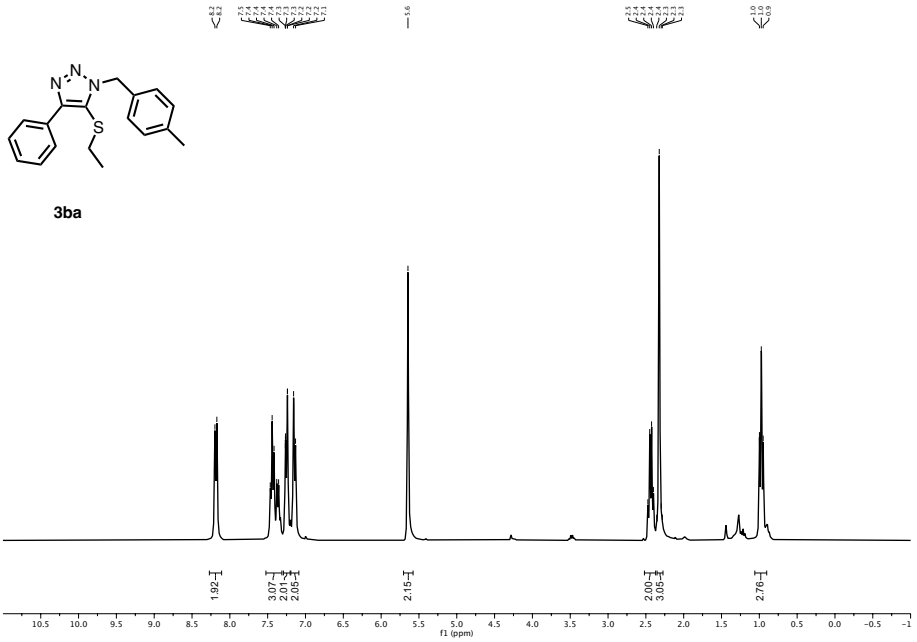

^{13}C NMR (75 MHz, $CDCl_3$)

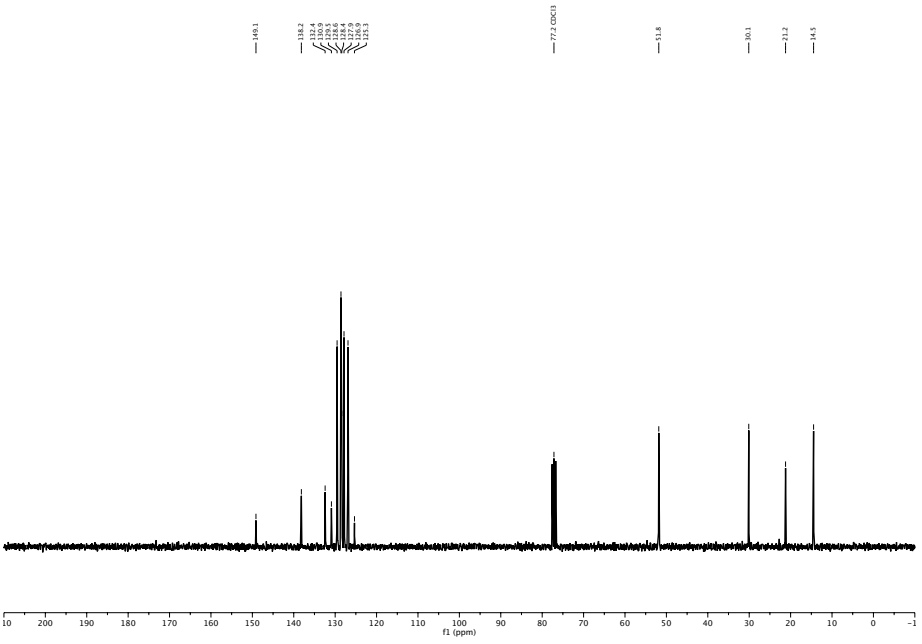

(4-(5-(ethylthio)-4-phenyl-1H-1,2,3-triazol-1-yl)butyl)triphenylphosphonium bromide (3ca)

^{1}H NMR (500 MHz, $CDCl_3$)

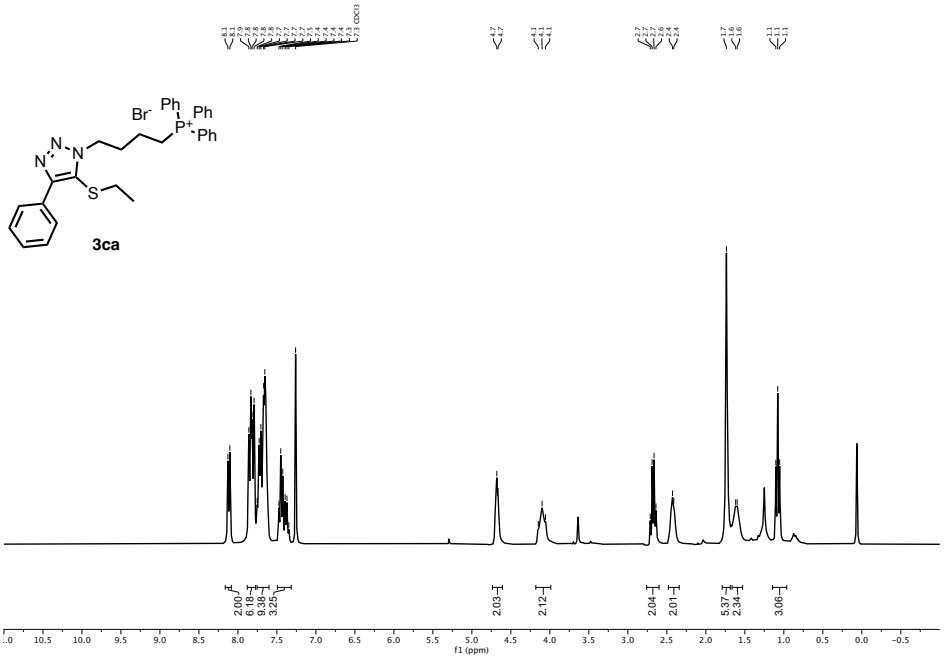

^{13}C NMR (75 MHz, $CDCl_3$)

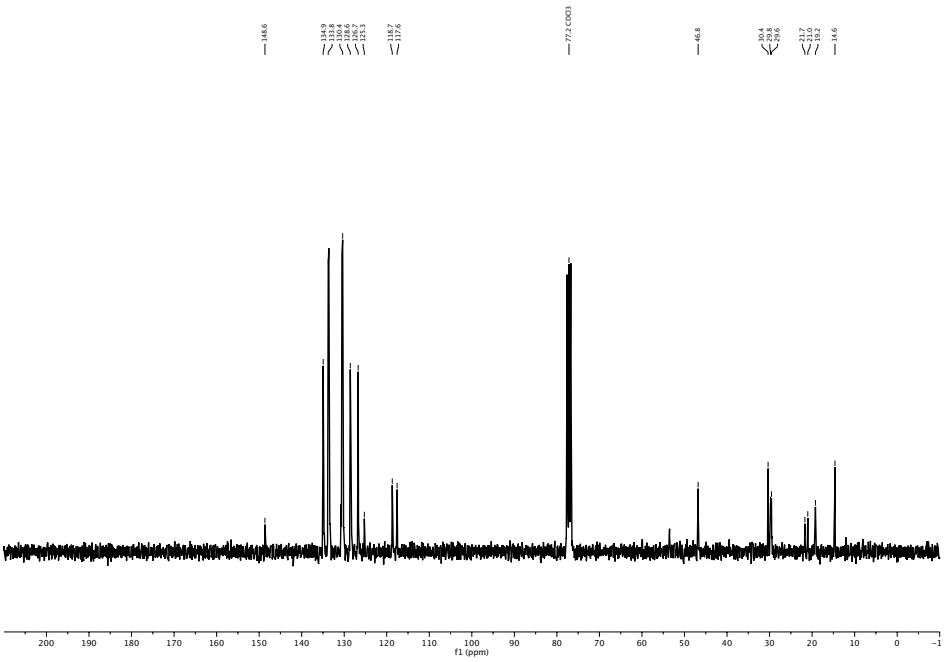

(S)-2-((((9H-Fluoren-9-yl)methoxy)carbonyl) amino)-6-(5-(ethylthio)-4-phenyl-1H-1,2,3-triazol-1-yl)hexanoic acid (3ea)

^{1}H NMR (500 MHz, $CDCl_3$)

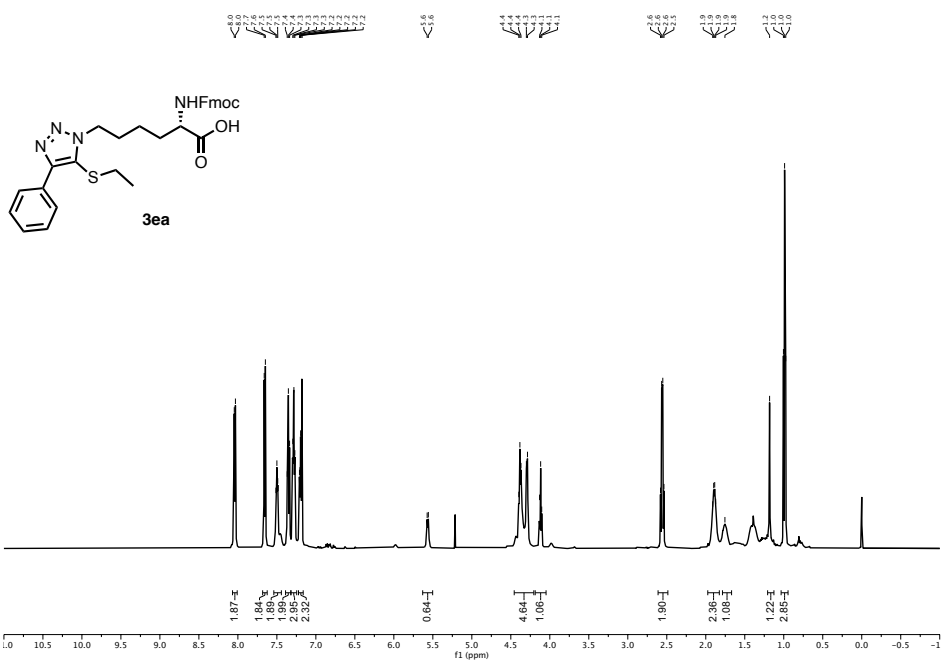

^{13}C NMR (126 MHz, $CDCl_3$)

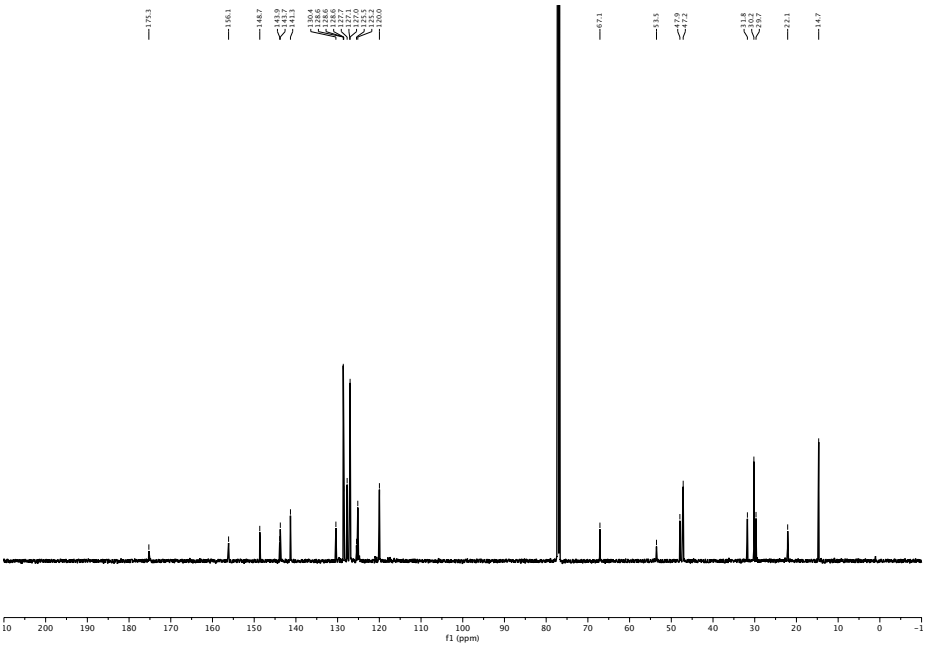

5-(1-(4-methylbenzyl)-1H-1,2,3-triazol-4-yl)pentan-1-ol. (3bg)

H NMR (300 MHz, $CDCl_3$)

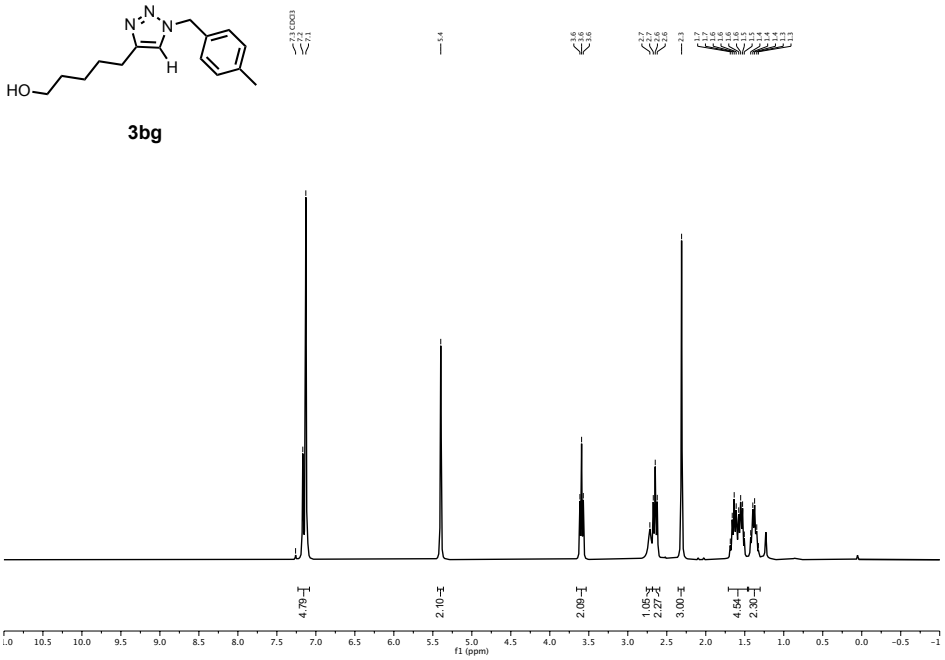

^{13}C NMR (75 MHz, $CDCl_3$)

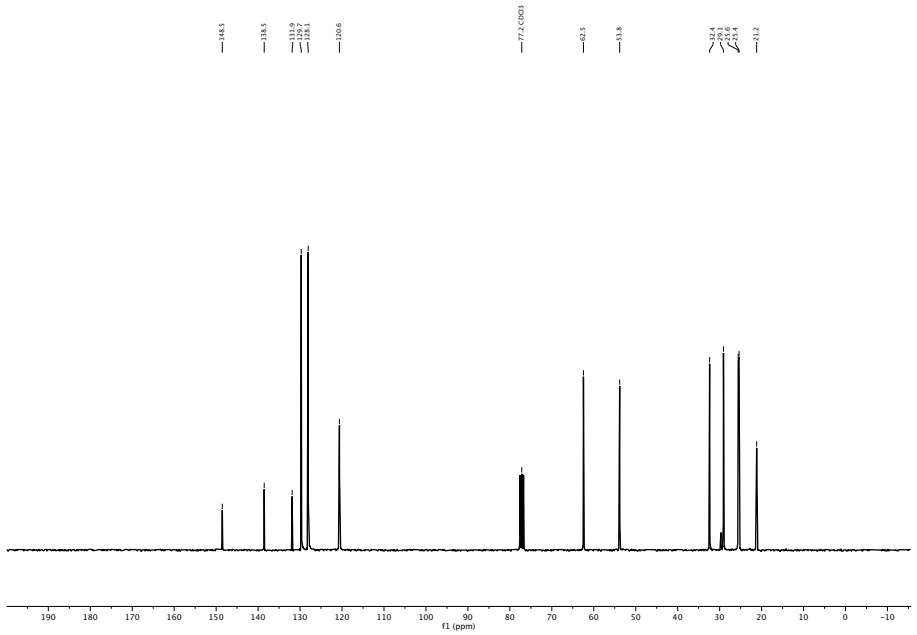

Experimental Section:

Chapter II: Ruthenium Catalyzed Alkene-Alkyne coupling

Synthesis

Alkynes

Alkynes **5b**, **5c**, **5d**, **5e**, **5h, 5i, 5k, 5m, 5n, 5p,** are commercially available and were used without further purification

(((2-methylbut-3-yn-2-yl)oxy)methyl)benzene (5a)

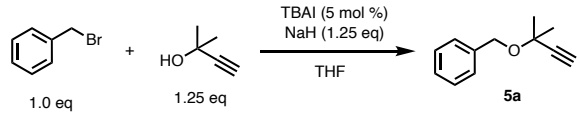

The synthesis of **5a** was carried out according to a reported procedure:[1]

In a flame dried 150 mL round bottom flask under nitrogen atmosphere 2-Methyl-3-butyn-2-ol (1.2 mL, 11.8 mmol, 1.0 equiv) was added to an heterogeneous mixture of NaH (60% in mineral oil, 0.594 g, 14.9 mmol, 1.25 equiv) in anhydrous THF (80.0 mL). After stirring the mixture for 1 at room temperature, tetrabutylammonium iodide (TBAI) (0.220 g, 0.6 mmol, 0.050 equiv) followed by benzyl bromide (1.8 mL, 14.9 mmol, 1.25 equiv) were added to the above alkoxide mixture. The mixture was stirred for 18 hours After which, the reaction was diluted with diethyl ether (100 mL), washed with water (20 mL), brine (20 mL), dried over $MgSO_4$, filtered and concentrated under reduced pressure.

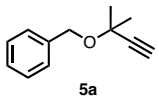

(((2-methylbut-3-yn-2-yl)oxy)methyl)benzene (5a). FCC in Hex: Et_2O (98:2). Isolated a colorless oil (1.490 g, 8.56 mmol, 72% yield). The NMR data is in accordance with that previously reported. **^{1}H NMR** (300 MHz, $CDCl_3$) δ 7.5 – 7.1 (m, 5H), 4.7 (s, 2H), 2.5 (s, 1H), 1.6 (s, 6H).

N-(1,1-dimethylprop-2-ynyl)-*p*-toluenesulfonamide (5b)

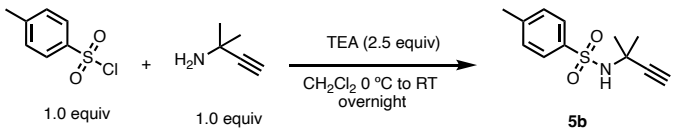

The synthesis of **5b** was carried out according to a reported procedure:[2]

In a flame dried two neck 100 mL round bottom flask under nitrogen atmosphere were added 36 mL of dry CH_2Cl_2, 2-methylbut-3-yn-2-amine (1.9 mL, 18.0 mmol, 1.0 equiv)

[1] Y.-S. Feng, C.-Q. Xie, W.-L. Qiao, H.-J. Xu, *Org. Lett.* **2013**, *15*, 936–939.
[2] S. Kim, Y. K. Chung, *Org. Lett.* **2014**, *16*, 4352–4355.

and the triethylamine (6.3 mL, 45.1 mmol, 2.5 equiv). The mixture was cooldown in an ice-water bath for 15min. After the indicated time the p-tosyl chloride (3.44 g, 18.0 mmol, 1.0 equiv) was added in one portion. The mixture was allowed to warm to room temperature and stirred overnight. The reaction was quenched by the addition of 15 mL of HCl 1M, the aqueous phase was extracted with CH_2Cl_2(2x10 mL). The organic phase wash then washed with 10% aqueous $NaHCO_3$ (15 mL), brine (15 mL) dried over $MgSO_4$ and concentrated under reduced pressure. No further purification required.

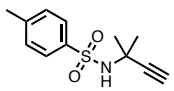

5b

N-(1,1-dimethylprop-2-ynyl)-*p*-toluenesulfonamide (5b). Isolated as white off powder (3.22g, 13.5 mmol, 75% yield). The NMR data is in accordance with that previously reported **^{1}H NMR** (300 MHz, $CDCl_3$) δ 7.8 (d, J = 8.3 Hz, 2H), 7.4 – 7.2 (m, 2H), 4.8 – 4.7 (m, 1H), 2.4 (s, 3H), 2.1 (s, 1H), 1.6 (s, 6H).

N-methyl-N-(1,1-dimethylprop-2-ynyl)-p-toluenesulfonamide (5f)

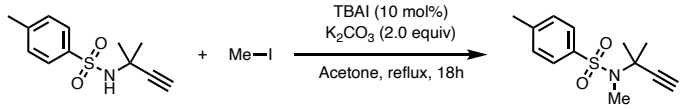

The synthesis of **5f** was carried out according to a reported procedure:[3]

In a flame dried 50 mL Schleck under nitrogen atmosphere, N-(1,1-dimethylprop-2-ynyl)-*p*-toluenesulfonamide, **5b**, (474 mg, 2.0 mmol, 1.0 equiv) was dissolved in acetone (10 mL). K2CO3 (567 mg, 4.0 mmol, 2.0 equiv), tetrabutylammonium iodide (TBAI) (74 mg, 0.2 mmol, 0.10 equiv) followed by methyl iodide (250 μL, 4.0 mmol, 2.0 equiv) were added to the above mixture. The mixture was refluxed for 18 h. After the indicated time, the solvent was removed under reduced pressure. The residue was redissolved in EtOAc (15 mL) and wash with water (10 mL), brine and dried over $MgSO_4$, filtered and concentrated under reduced pressure.

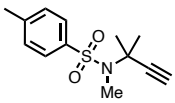

5f

N-methyl-N-(1,1-dimethylprop-2-ynyl)-p-toluenesulfonamide (5f). FCC in Hex: EtOAc (8:2). Isolated as a white off solid (410 mg, 1.6 mmol, 82% yield). The NMR data is in accordance with that

[3] R. Liu, Z. Ni, L. Giordano, A. Tenaglia, *Org. Lett.* **2016**, *18*, 4040–4043.

previously reported. **^{1}H NMR** (300 MHz, $CDCl_3$) δ 7.72 (d, *J* = 8.3 Hz, 2H), 7.27 (d, *J* = 8.5 Hz, 2H), 3.08 (s, 3H), 2.41 (s, 3H), 2.23 (s, 1H), 1.67 (s, 6H).

2-((2-methylbut-3-yn-2-yl)oxy)ethan-1-ol (5g)

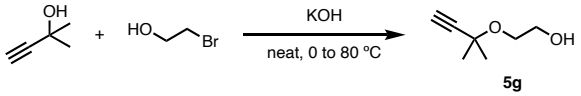

5g

The synthesis of 5g was carried out according to a reported procedure:[4]

In a 10 mL round bottom flask, crushed KOH pellets (2.7g, 47.5 mmol, 2.0 equiv) and 2-methylbut-3-yn-2-ol (2.0 g, 23.7 mmol, 1.0 equiv) were mixed for 15 min After the indicated time 2-bromoethanol (1.7 mL, 23.7 mmol, 1.0 equiv) was added to the reaction mixture and the reaction mixture was heated to 80 ºC overnight. The resulting mixture was cooled down, the mixture diluted with Et_2O, filtered through a celite plug and the solvent removed under reduced pressure.

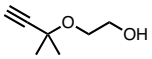

#Ay5

2-((2-methylbut-3-yn-2-yl)oxy)ethan-1-ol (**5g**) **FCC** in Pentane: Et_2O (6:4). Isolated as clear oil (450 mg, 3.50 mmol, 15% yield). The NMR data is in accordance with that previously reported. **^{1}H NMR** (300 MHz, $CDCl_3$) δ 3.80 – 3.59 (m, 4H), 2.47 – 2.39 (m, 1H), 1.54 – 1.51 (m, 3H), 1.48 (t, *J* = 0.9 Hz, 3H).

***p*-(4-methoxyphenyl)but-3-yn-2-ol (5j)**

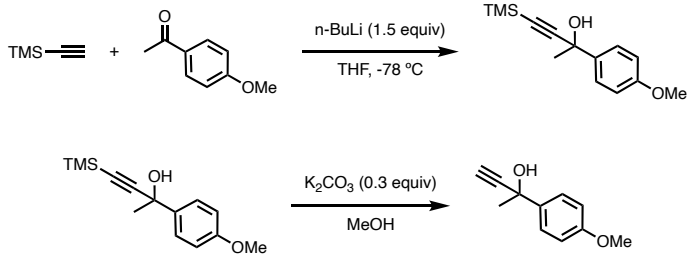

5j

The synthesis of 5j was carried out according to a reported procedure:[5]

i) In a flame dried 250 mL two neck round bottom flask under nitrogen atmosphere trimethylsilylacetylene (4.0 mL, 28.2 mmol, 1.6 equiv) was

[4] A. Semioshkin, A. Ilinova, I. Lobanova, V. Bregadze, E. Paradowska, M. Studzińska, A. Jabłońska, Z. J. Lesnikowski, *Tetrahedron* **2013**, *69*, 8034–8041.

[5] L. Mao, R. Bertermann, K. Emmert, K. J. Szabó, T. B. Marder, *Org. Lett.* **2017**, *19*, 6586–6589.

dissolved in 80 mL dry THF and cooled to -78 °C. After 15 minutes, a solution of *n*-BuLi (10.6 mL, 2.5 M in hexanes, 1.5 equiv) was added dropwise and the reaction allowed to stir at -78 ºC for an additional 15 minutes. A solution of 2-acetophenone (3.0 g, 17.6 mmol), in 10 mL THF was then added dropwise, the reaction mixture stirred at -78 °C for 15 minutes and then allowed to warm to room temperature. When TLC indicated complete consumption of starting material, a saturated $NaHCO_3$ (aq) solution of was added and diluted with EtOAc (100 mL). The aqueous phase was extracted (2 x 50 mL) with EtOAc and the combined organic layers were washed with brine (40 mL), dried over anhydrous Mg_2SO_4 and concentrated under reduced pressure.

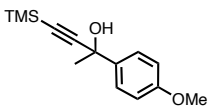

2-(4-methoxyphenyl)-4-(trimethylsilyl)but-3-yn-2-ol. FCC in Hex: EtOAc (8:2) Isolated as a colorless oil (5.6 g, 22.5 mmol, 90% yield). The NMR data is in accordance with that previously reported. **^{1}H NMR** (300 MHz, $CDCl_3$) δ 7.6 (d, *J* = 8.9 Hz, 2H), 6.9 (d, *J* = 8.2 Hz, 2H), 3.8 (s, 3H), 1.7 (s, 3H), 0.2 (s, 9H).

ii) In a 25 mL round bottom flask under nitrogen atmosphere the trimethylsilyl protected alkyne (1.0 g, 4.0 mmol, 1.0 equiv) was dissolved in MeOH (8.0 mL) followed by the addition of K_2CO_3 (167.0 mg, 1.21 mmol, 0.3 equiv). The mixture was stirred at RT until TLC indicated complete consumption of starting material. The solvent was then evaporated under low pressure. The mixture was resuspended in NH_4Cl(sat) (15 mL) and diethyl ether (15 mL). The phases were separated, and the aqueous phase extracted with diethyl ether (2 x 10 mL). The combined organic phases were washed with water (10 mL), brine (10 mL) and dried over $MgSO_4$ and the solvent removed under reduced pressure.

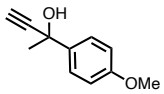

5j

***p*-(4-methoxyphenyl)but-3-yn-2-ol (5j)** FCC in Hex: EtOAc (8:2). Isolated as a colorless oil (210 mg, 1.2 mmol, 30% yield). The NMR data is in accordance with that previously reported. **^{1}H NMR** (300 MHz, $CDCl_3$) δ 7.6 (d, *J* = 8.4 Hz, 2H), 6.9 (d, *J* = 8.2 Hz, 2H), 3.8 (s, 3H), 2.7 (s, 1H), 1.8 (s, 3H).

tert-butyl N-(2-methylbut-3-yn-2-yl)-N-tosylglycinate (5l)

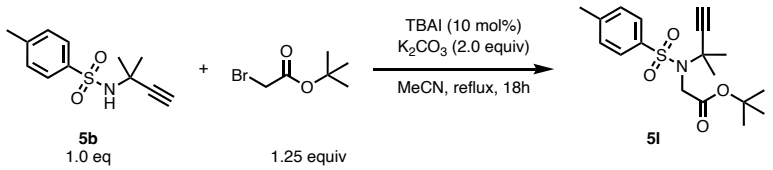

In a flame dried 50 mL Schleck under nitrogen atmosphere, N-(1,1-dimethylprop-2-ynyl)-*p*-toluenesulfonamide (1.0 g, 4.2 mmol, 1.0 equiv) was dissolved in acetonitrile (13.3 mL). K_2CO_3 (1.2g, 8.4 mmol, 2.0 equiv), tetrabutylammonium iodide (TBAI) (155 mg, 0.42 mmol, 0.10 equiv) followed by *tert*-butyl 2-bromoacetate (780 μL, 5.3 mmol, 1.25 equiv) were added to the above mixture. The mixture was refluxed for 18 h.

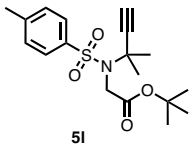

After the indicated time, mixture was filtered through a celite plug, and the solvent removed under reduced pressure.

tert-butyl N-(2-methylbut-3-yn-2-yl)-N-tosylglycinate (5l) FCC in Hex: EtOAc (7:3). Isolated as a white off solid (1.4 g, 4.0 mmol, 96% yield). **^{1}H NMR** (300 MHz, $CDCl_3$) δ 7.9 (d, *J* = 7.6 Hz, 2H), 7.3 (d, *J* = 8.1 Hz, 2H), 4.3 (s, 2H), 2.4 (s, 3H), 2.3 (s, 1H), 1.7 (s, 6H), 1.5 (s, 9H).

1-(4-methoxyphenyl)but-3-yn-1-ol (5o)

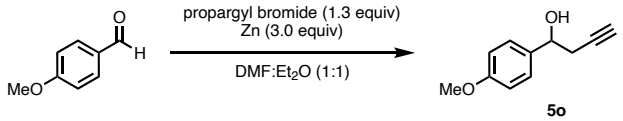

The synthesis of 5o was carried out according to a reported procedure:[6]

To a 250 mL round-bottom flask connected to a reflux condenser, p-anisaldehyde (1.2 mL, 10 mmol, 1.0 equiv) and propargyl bromide (80% in toluene, 1.4 mL, 13 mmol, 1.3 equiv) were dissolved in Et_2O:DMF (1:1, 100 mL). Freshly activated zinc (2.0 g, 30 mmol, 3.0 equiv) was added over the period of 10 min. The reaction mixture was stirred at room temperature for 18h. After the indicated time the reaction was quenched by slow addition of saturated ammonium chloride solution. The resulting mixture was transfer to a separatory funnel and extracted with diethyl ether (3 x 30 mL) and the

[6] A. M. Sherwood, S. E. Williamson, S. N. Johnson, A. Yilmaz, V. W. Day, T. E. Prisinzano, *J. Org. Chem.* **2018**, *83*, 980–992.

combined organic fractions were collected and washed with brine (3 x 50 mL), dried over $MgSO_4$ and the solvent removed under reduced pressure.

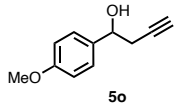

5o

1-(4-methoxyphenyl)but-3-yn-1-ol (5o) FCC in Hex: EtOAc (8:2) Isolated as a colorless oil (1.1 g, 6.2 mmol, 62% yield). The NMR data is in accordance with that previously reported **^{1}H NMR** (300 MHz, $CDCl_3$) δ 7.37 – 7.26 (m, 2H), 6.94 – 6.84 (m, 2H), 4.83 (td, *J* = 6.5, 3.4 Hz, 1H), 3.80 (s, 3H), 2.98 – 2.84 (m, 3H), 2.67 – 2.58 (m, 2H).

Alkenes

Alkenes **4b**, are commercially available and were used without further purification.

1-(allyloxy)-4-methoxybenzene (4a)

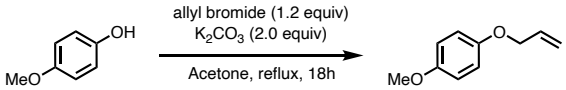

4a

The synthesis of **4a** was carried out according to a reported procedure:[7]

In a flame dried 100 mL round bottom flask under nitrogen atmosphere 4-methoxyphenol (2.0 mL, 16.1 mmol, 1.0 equiv) was dissolved in acetone (40 mL). K_2CO_3 (4.4 g, 32.2 mmol, 2.0 equiv) and allyl bromide (1.7 mL, 19.3 mmol, 1.2 equiv) were added to the reaction mixture. The mixture was refluxed for 18 h. After the indicated time the mixture was filtered through a celite plug and the solvent remove under reduced pressure.

1-(allyloxy)-4-methoxybenzene (4a). FCC in Hex: EtOAc (9:1) provided the product as colorless oil (2.5 g, 15.2 mmol, 94% yield). The NMR data is in accordance with that previously reported. **^{1}H NMR** (300 MHz, $CDCl_3$) δ 6.91 – 6.78 (m, 4H), 6.05 (ddt, *J* = 15.9, 10.5, 5.3 Hz, 1H), 5.40 (d, *J* = 17.2 Hz, 1H), 5.27 (d, *J* = 10.4 Hz, 1H), 4.49 (d, *J* = 5.1 Hz, 2H), 3.77 (s, 3H).

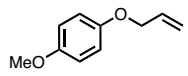

4a

1-(but-3-en-1-yloxy)-4-methoxybenzene (4c)

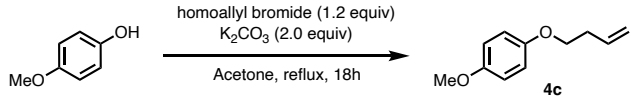

4c

[7] D. R. Vutukuri, P. Bharathi, Z. Yu, K. Rajasekaran, M.-H. Tran, S. Thayumanavan, *J. Org. Chem.* **2003**, *68*, 1146–1149.

The synthesis of **4c** was carried out according to a reported procedure:[8]

In a flame dried 100 mL round bottom flask under nitrogen atmosphere 4-methoxyphenol (2.0 g, 16.1 mmol, 1.0 equiv) was dissolved in acetone (40 mL). K_2CO_3 (4.4 g, 32.2 mmol, 2.0 equiv) and homoallyl bromide (2.0 mL, 19.3 mmol, 1.2 equiv) were added to the reaction mixture. The mixture was refluxed for 18 h. After the indicated time the mixture was filtered through a celite plug and the solvent removed under reduced pressure.

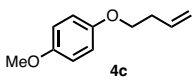

4c

1-(but-3-en-1-yloxy)-4-methoxybenzene (4c) FCC in Hex: EtOAc (9:1) Isolated as colorless oil (1.7 g, 10.0 mmol, 62% yield). The NMR data is in accordance with that previously reported.[1] **^{1}H NMR** (300 MHz, $CDCl_3$) δ 6.89 – 6.76 (m, 4H), 5.91 (ddt, *J* = 13.4, 10.1, 6.7 Hz, 1H), 5.25 – 4.98 (m, 2H), 3.97 (t, *J* = 6.7 Hz, 2H), 3.77 (s, 3H), 2.52 (q, *J* = 6.5 Hz, 2H).

benzyl(but-3-en-1-yl)sulfane (4d)

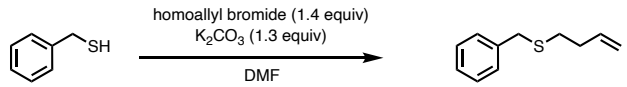

4d

The synthesis of **4d** was carried out according to a reported procedure:[9]

In a flame dried 100 mL round bottom flask under nitrogen atmosphere benzyl mercaptan (2.0 mL, 17.1 mmol, 1.0 equiv) was dissolved in DMF (40 mL). K_2CO_3 (3.0 g, 22.1 mmol, 1.3 equiv) and homoallyl bromide (1.3 mL, 23.9 mmol, 1.4 equiv) were added to the reaction mixture. The mixture was stirred for 18 h. After the indicated time the reaction mixture was poured into 200 mL of water and extracted with Et_2O (2x15 mL). The combined organic layers were washed with H_2O (100 mL), brine (100 mL), dried over $MgSO_4$, filtered and the solvent removed under reduced pressure.

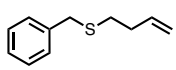

4d

benzyl(but-3-en-1-yl)sulfane (4d) FCC in Hex: EtOAc (98:2) Isolated as colorless oil (2.1 g, 12.0 mmol, 70% yield). The NMR data is in accordance with that previously reported. **^{1}H NMR** (300 MHz, $CDCl_3$) δ 7.30 (d, *J* = 15.8 Hz, 5H), 5.82 (ddt, *J* = 16.9, 10.3, 6.6 Hz, 1H), 5.19 – 4.91 (m, 2H), 3.75 (s, 2H), 2.51 (t, *J* = 7.3 Hz, 2H), 2.33 (q, *J* = 7.2 Hz, 2H).

[8] B. H. Lipshutz, S. Ghorai, W. W. Y. Leong, *J. Org. Chem.* **2009**, *74*, 2854–2857.
[9] Y. A. Lin, J. M. Chalker, N. Floyd, G. J. L. Bernardes, B. G. Davis, *J. Am. Chem. Soc.* **2008**, *130*, 9642–9643.

Methyl (*S*)-3-(4-(allyloxy)phenyl)-2-((*tert*-butoxycarbonyl)amino)propanoate. Boc- Tyr(Allyl)-OMe. (4e)

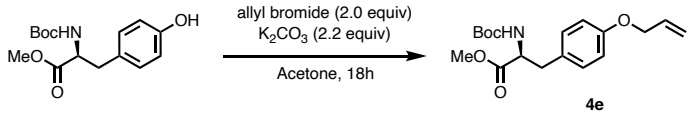

4e

The synthesis of **4e** was carried out according to a reported procedure:[10]

In a flame dried 100 mL round bottom flask under nitrogen atmosphere Boc-Tyr(OH)- OMe (500 mg, 1.7 mmol, 1.0 equiv) was dissolved in acetone (25 mL). K_2CO_3 (515 g, 3.7 mmol, 2.2 equiv) and allyl bromide (300 μL, 3.4 mmol, 2.0 equiv) were added to the reaction mixture. The mixture was stirred for 18 h. After the indicated time, the solvent was removed under reduced pressure. The residue was redissolved in EtOAc (15 mL) and wash with water (10 mL), brine and dried over $MgSO_4$, filtered and the solvent removed under reduced pressure. No further purification was required.

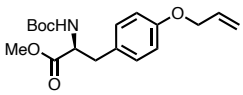

#Ae5

Methyl (*S*)-3-(4-(allyloxy)phenyl)-2-((*tert*-butoxycarbonyl)amino)propanoate. Boc- Tyr(Allyl)-OMe. (4e) White off powder (566 mg, 1.7 mmol, 99%). The NMR data is in accordance with that previously reported. **^{1}H NMR** (300 MHz, $CDCl_3$) δ 7.04 (d, *J* = 7.7 Hz, 2H), 6.91 – 6.81 (m, 2H), 6.14 – 5.96 (m, 1H), 5.54 – 5.39 (m, 1H), 5.30 (dd, *J* = 10.4, 2.2 Hz, 1H), 4.97 (d, *J* = 8.3 Hz, 1H), 4.60 – 4.48 (m, 2H), 3.76 – 3.69 (m, 3H), 3.05 (d, *J* = 6.1 Hz, 2H), 1.44 (s, 9H).

(2*R*,3*R*,4*S*,5*R*,6*R*)-2-(acetoxymethyl)-6-((4-(allyloxy)benzyl)oxy)tetrahydro-2*H*-pyran-3,4,5-triyl triacetate (4f)

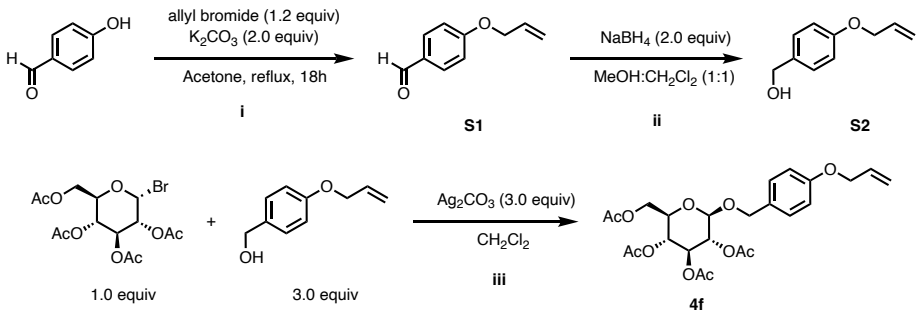

[10] J. Wang, Y. Wang, G. Ding, X. Wu, L. Yang, S. Fan, Z. Zhang, X. Xie, *Tetrahedron Letters* **2021**, *81*, 153341.

i) In a flame dried 100 mL round bottom flask under nitrogen atmosphere 4-hydroxybenzaldehyde (1.9 g, 16.1 mmol, 1.0 equiv) was dissolved in acetone (40 mL). K_2CO_3 (4.4 g, 32.2 mmol, 2.0 equiv) and allyl bromide (1.7 mL, 19.3 mmol, 1.2 equiv) were added to the reaction mixture. The mixture was refluxed for 18 h. After the indicated time the mixture was filtered through a celite plug and the solvent removed under reduced pressure.

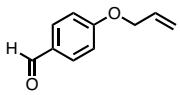

S1

4-(allyloxy)benzaldehyde (**S1**) FCC in Hex: EtOAc (95:5) Isolated as colorless oil (2.24 g, 13.8 mmol, 85% yield). **^{1}H NMR** (300 MHz, $CDCl_3$) δ 9.89 (d, *J* = 1.9 Hz, 1H), 7.07 – 6.96 (m, 2H), 6.15 – 5.96 (m, 1H), 5.50 – 5.37 (m, 1H), 4.67 – 4.58 (m, 3H).

ii) In a flame dried 100 mL Schleck **4-(allyloxy)benzaldehyde** (**S1**) (1.0 g, 6.2 mmol, 1.0 equiv) was dissolved in CH_2Cl_2:MeOH (1:1, 60 mL). The mixture was cooled to 0 ºC in an ice-water bath for 15 min. After the indicated time $NaBH_4$ (467 mg, 12.3 mmol, 2.0 equiv) was added portion wise. After 30 min the reaction was allowed to warm to rt and stirred overnight. After the indicated time the mixture was quenched by addition of aqueous HCl 1.0 M (10 mL) and the organic solvent removed under reduced pressure. The resulting aqueous solution was extracted with CH_2Cl_2 (2x20 mL), the combined organic fractions were washed with brine, dried over $MgSO_4$ and the solvent removed under reduced pressure.

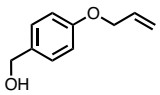

S2

(4-(allyloxy)phenyl)methanol (**S2**) FCC in Hex: EtOAc (8:2). Isolated as colorless oil (732 mg, 4.46 mmol, 72% yield). **^{1}H NMR** (300 MHz, $CDCl_3$) δ 7.36 – 7.22 (m, 2H), 6.98 – 6.87 (m, 2H), 6.08 (ddt, *J* = 17.2, 10.5, 5.3 Hz, 1H), 5.43 (dq, *J* = 17.3, 1.6 Hz, 1H), 5.31 (dq, *J* = 10.5, 1.4 Hz, 1H), 4.64 (s, 2H), 4.57 (dt, *J* = 5.3, 1.5 Hz, 2H).

iii)In a flame dried 10 mL Schleck **(4-(allyloxy)phenyl)methanol** (**S2**) (150 mg, 0.36 mmol, 1.0 equiv) was dissolved in dry CH_2Cl_2 (2.0 mL) over 4 A MS. Ag_2CO_3 (302 mg, 1.1 mmol, 3.0 equiv) and a crystal of iodine were added to the solution and stirred for 15 min. After the indicated time a solution of the bromo-sugar ((2*R*,3*R*,4*S*,5*R*,6*S*)-2-(acetoxymethyl)-6-(bromomethyl)tetrahydro-2*H*-pyran-3,4,5-triyl triacetate) (180 mg, 1.1 mmol, 3.0 equiv in 1.5 mL of CH_2Cl_2) was added to the reaction mixture, shielded from light and stirred overnight. After the indicated time, the reaction mixture was diluted with EtOAc and filtered through a celite plug and the solvent removed under reduced pressure.

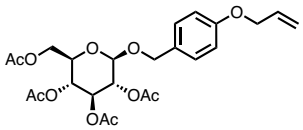

4f

(2*R*,3*R*,4*S*,5*R*,6*R*)-2-(acetoxymethyl)-6-((4-(allyloxy)benzyl)oxy)tetrahydro-2*H*-pyran-3,4,5-triyl triacetate (4f). FCC in Hex: EtOAc from (7:3 to 1:1) Isolated as colorless sticky oil (120 mg, 0.24 mmol, 66% yield). **^{1}H NMR** (300 MHz, $CDCl_3$) δ 7.24 – 7.12 (m, 2H), 6.94 – 6.81 (m, 2H), 6.03 (ddt, *J* = 17.1, 10.5, 5.2 Hz, 1H), 5.46 – 5.32 (m, 1H), 5.27 (dt, *J* = 10.4, 1.5 Hz, 1H), 5.21 – 4.95 (m, 3H), 4.79 (d, *J* = 11.9 Hz, 1H), 4.58 – 4.43 (m, 4H), 4.25 (dd, *J* = 12.3, 4.7 Hz, 1H), 4.14 (dd, *J* = 12.3, 2.5 Hz, 1H), 3.64 (m, 1H), 2.08 (s, 3H), 1.98 (d, *J* = 6.8 Hz, 9H). **^{13}C NMR** (75 MHz, $CDCl_3$) δ 170.7, 170.3, 169.5, 169.4, 158.6, 133.2, 129.6, 128.8, 117.8, 114.8, 99.0, 72.9, 71.9, 71.4, 70.5, 68.9, 68.5, 62.1, 20.8, 20.7, 20.7.

Dipeptides

methyl Fmoc-L-2-propargylglycyl-*L*-valinate (7a)

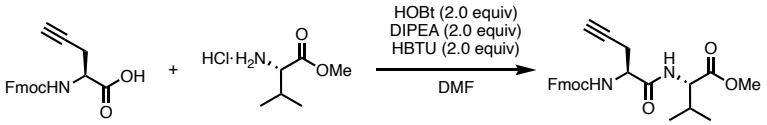

Fmoc-propargyl-Gly-Val-OMe
7a

In a 10 mL round bottom flask under nitrogen atmosphere Fmoc-propargyl-Gly-OH (75.8 mg, 0.36 mmol, 1.05 equiv), HBTU (217.4 mg, 0.68 mmol, 2.0 equiv), HOBt (103.7 mg, 0.68 mmol, 2.0 equiv) and the base, DIPEA (118 μL, 0.68 mmol, 2.0 equiv) were mixed in DMF (3.4 mL) and cooled to 0 ºC for 10 min. After the indicated time the amine was methyl L-valinate hydrochloride (61.5 mg, 0.34 mmol, 1.0 equiv) was added, the mixture was allowed to warm to rt and stirred overnight. The solvent was removed by vacuum distillation, the residue was redissolved in CH_2Cl_2(10 mL) and washed with aqueous 10% $NaHCO_3$ (10 mL) and brine (10 mL), dried over $MgSO_4$ and the solvent removed under reduced pressure.

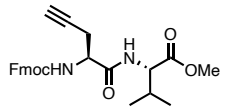

Fmoc-propargyl-Gly-Val-OMe
7a

methyl Fmoc-L-2-propargylglycyl-*L*-valinate (7a). FCC in CH_2Cl_2:*i*-PrOH (98:2). Isolated as colorless sticky oil (140 mg, 0.31 mmol, 92% yield). **^{1}H NMR** (300 MHz, $CDCl_3$) δ 7.76 (d, *J* = 8.0 Hz, 2H), 7.38 – 7.18 (m, 7H), 7.01 (d, *J* = 8.0 Hz, 1H), 4.87 (q, *J* = 6.6 Hz, 1H), 4.18 – 3.96 (m, 2H), 3.72 (s, 3H), 3.25 – 3.06 (m, 2H), 2.42 (s, 3H), 2.13 (s, 1H), 1.56 (s, 6H). **^{13}C NMR** (75 MHz, $CDCl_3$) δ 171.6, 169.4, 144.1, 137.1,

135.8, 129.7, 129.5, 128.8, 128.1, 127.3, 84.5, 72.6, 57.1, 53.2, 52.3, 51.7, 37.9, 30.6, 30.1, 21.6. **HRMS** (ESI+) for $C_{26}H_{29}N_2O_5$ $[M+H]^+$ 449.2071found 449.2070.

methyl *N*-(2-methylbut-3-yn-2-yl)-*N*-tosylglycylphenylalaninate (7b)

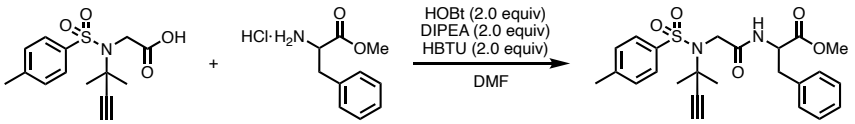

Tos-Prop-Gly-Phe-OMe
7b

In a 10 mL round bottom flask under nitrogen atmosphere *N*-(2-methylbut-3-yn-2-yl)-*N*-tosylglycine (100 mg, 0.36 mmol, 1.05 equiv), HBTU (217.4 mg, 0.68 mmol, 2.0 equiv), HOBt (103.7 mg, 0.68 mmol, 2.0 equiv) and the base, DIPEA (118 μL, 0.68 mmol, 2.0 equiv) were mixed in DMF (3.4 mL) and cooled to 0 ºC for 10 min. After the indicated time the amine was methyl D/L-phenylalaninate hydrochloride (76.7 mg, 0.34 mmol, 1.0 equiv) was added, the mixture was allowed to warm to rt and stirred overnight. The solvent was removed by vacuum distillation, the residue was redissolved in CH_2Cl_2(10 mL) and washed with aqueous 10% $NaHCO_3$ (10 mL) and brine (10 mL), dried over $MgSO_4$ and the solvent removed under reduced pressure.

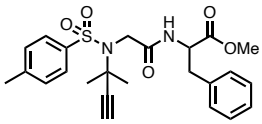

Tos-Prop-Gly-Phe-OMe
7b

methyl *N*-(2-methylbut-3-yn-2-yl)-*N*-tosylglycyl phenylalaninate (7b) FCC in CH_2Cl_2:*i*-PrOH (98:2). Isolated as colorless sticky oil (114 mg, 0.25 mmol, 74% yield). **^{1}H NMR** (300 MHz, $CDCl_3$) δ 7.77 (d, *J* = 7.5 Hz, 2H), 7.61 (d, *J* = 7.4 Hz, 2H), 7.41 (t, *J* = 7.5 Hz, 2H), 7.32 (t, *J* = 7.6 Hz, 2H), 6.94 (d, *J* = 8.7 Hz, 1H), 5.85 – 5.76 (m, 1H), 4.65 – 4.55 (m, 1H), 4.53 – 4.38 (m, 3H), 4.25 (t, *J* = 7.1 Hz, 1H), 3.73 (s, 3H), 2.82 (d, *J* = 17.1 Hz, 1H), 2.73 – 2.58 (m, 1H), 2.27 – 2.15 (m, 1H), 2.15 – 2.08 (m, 1H), 1.00 – 0.88 (m, 6H). **^{13}C NMR** (75 MHz, $CDCl_3$) δ 171.9, 169.9, 156.0, 143.8, 143.8, 141.4, 127.8, 127.2, 125.1, 120.1, 79.3, 72.0, 67.5, 57.5, 53.4, 52.2, 47.1, 31.3, 22.7, 19.0, 17.9. **HRMS** (ESI+) for $C_{24}H_{29}N_2O_5S$ $[M+H]^+$ 457.1786 found 457.1792.

Alkene-Alkyne coupling

Al crudes were analyzed by NMR using 0.33 equiv $DMSO_2$ (δ = 3.00 ppm, 6H) as internal standard. If NMR yield is not given is due to the overlapping of, either the IS with starting materials and/or product, or between starting materials and product. Unless otherwise stated all reaction were performed at 150 μmol scale suing 1.0 equiv of Alkene and Alkyne

Representative Procedure. Preparation of (E)-N-(7-(4-methoxyphenoxy)-2-methyl-3-methylenehept-5-en-2-yl)-4-methylbenzenesulfonamide (6ab).

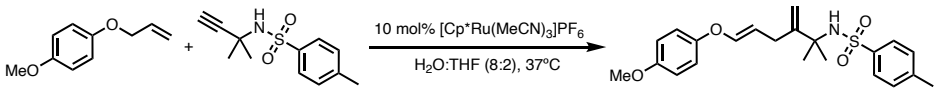

4a **5b** **6ab**

$[Cp^*Ru(MeCN)_3]PF_6$ (7.6 mg, 10 mol%) was added to a stirred solution of **4a** (24.6 mg, 150 μmol) and **5b** (37.7 mg, 150 μmol) in 2 mL of degassed H_2O:THF(8:2) under N2 atmosphere and stirred at 37 ºC. After 16 h, the mixture was extracted with CH_2Cl_2 (5 x 1 mL) and the extract was filtered through a florisil plug (in a 3 mL syringe) directly to a vial and the solvent removed under reduced pressure. 700 μL solution of $DMSO_2$ in $CDCl_3$ (4.4 mg of $DMSO_2$, 50 μmol, per 700 μL of $CDCl_3$) were added and the reaction analyzed by NMR.

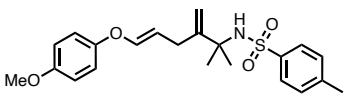

6ab

(E)-N-(7-(4-methoxyphenoxy)-2-methyl-3-methylenehept-5-en-2-yl)-4-methyl benzenesulfonamide (6ab) NMR Yield = 99% (9:1 branched : linear). **FCC** from Hex:EtOAc (87.5:12:5) to Hex:EtOAc (82.5:17:5). Isolated as a colorless oil (60.0 mg, 149 μmol, 99%). **^{1}H NMR** (300 MHz, $CDCl_3$) δ 7.81 – 7.69 (m, 2H), 7.36 – 7.25 (m, 2H), 7.00 – 6.82 (m, 4H), 6.38 (dt, J = 12.1, 1.3 Hz, 1H), 5.34 – 5.17 (m, 1H), 5.06 (s, 1H), 5.02 (s, 1H), 3.81 (s, 3H), 2.86 (s, 3H), 2.76 (dt, J = 7.7, 1.2 Hz, 2H), 2.44 (s, 3H), 1.43 (s, 6H). **^{13}C NMR** (75 MHz, cdcl$_3$) δ 155.4, 151.8, 151.2, 144.5, 143.1, 140.1, 129.5, 127.3, 118.0, 114.8, 111.8, 109.6, 59.6, 55.8, 28.9, 27.8, 21.6. **HRMS** (ESI+) for $C_{23}H_{30}NO_4S$ $[M+H]^+$ 418.1890 found 418.1885.

(E)-N-(7-(4-methoxyphenoxy)-2-methyl-3-methylenehept-5-en-2-yl)-N,4-dimethylbenzenesulfonamide (6af)

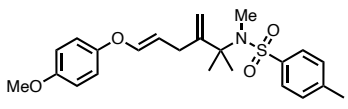

6af

Prepared according to the representative procedure with **4a** (24.6 mg, 150 μmol) and **5f** (37.7 mg, 150 μmol). **NMR Yield** = 99% (7:1 branched : linear). **FCC** from Hex:EtOAc (87.5:12:5) to Hex:EtOAc (82.5:17:5). Isolated as a colorless oil (47.0 mg, 112 μmol, 75%). **^{1}H NMR** (300 MHz, $CDCl_3$) δ 7.81 – 7.69 (m, 2H), 7.36 – 7.25 (m, 2H), 7.00 – 6.82 (m, 4H), 6.38 (dt, *J* = 12.1, 1.3 Hz, 1H), 5.34 – 5.17 (m, 1H), 5.06 (s, 1H), 5.02 (s, 1H), 3.81 (s, 3H), 2.86 (s, 3H), 2.76 (dt, *J* = 7.7, 1.2 Hz, 2H), 2.44 (s, 3H), 1.43 (s, 6H). **^{13}C NMR** (75 MHz, $CDCl_3$) δ 155.5, 153.8, 151.3, 144.4, 143.0, 139.9, 129.7, 127.2, 118.0, 114.8, 111.3, 109.8, 65.0, 55.8, 33.5, 28.5, 25.6, 21.6. **HRMS** (ESI+) for $C_{23}H_{30}NO_4S$ $[M+H]^+$ calc 418.1890 found 418.1885.

(*E*)-1-((4-((benzyloxy)methyl)penta-1,4-dien-1-yl)oxy)-4-methoxybenzene (6ac)

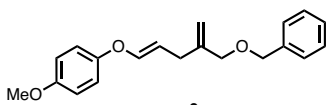

6ac

Prepared according to the representative procedure with **4a** (22.9 mg, 140 μmol) and **5c** (23 mg, 140 μmol). **NMR Yield** = 69% (2:1 branched : linear). **FCC** from Hex:EtOAC (95:5). Isolated as a colorless oil (30 mg, 90 μmol, 68%). Characterized as 2:1 mixture of isomers. **^{1}H NMR** (300 MHz, $CDCl_3$) δ 7.39 – 7.24 (m, 5H), 6.97 – 6.88 (m, 2H), 6.88 – 6.81 (m, 2H), 6.41 (ddt, *J* = 12.2, 5.6, 1.3 Hz, 1H), 5.72 (tdt, *J* = 15.4, 10.9, 5.7 Hz, 0.5H), 5.29 (dtd, *J* = 14.7, 7.5, 3.0 Hz, 1H), 5.11 (s, 0.5H), 5.03 (s, 0.5H), 4.52 (d, *J* = 1.4 Hz, 2H), 4.05 – 3.95 (m, 2H), 3.78 (s, 3H), 2.83 – 2.74 (m, 2H). **^{13}C NMR** (75 MHz, $CDCl_3$) δ 155.4, 151.2, 145.2, 144.5, 144.1, 138.4, 132.8, 128.5, 127.9, 127.8, 127.7, 127.3, 118.1, 118.0, 114.8, 112.9, 109.4, 108.8, 73.0, 72.2, 72.1, 70.8, 55.8, 31.2, 30.2. **HRMS** (ESI+): Calculated for $C_{20}H_{22}NaO_3$ $[M+Na]^+$, 333,1461 found 333,1461.

(*E*)-1-((5,5-dimethyl-4-methylenehex-1-en-1-yl)oxy)-4-methoxybenzene (6ad)

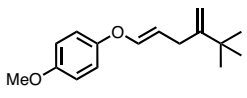

6ad

Prepared according to the representative procedure with **4a** (24.6 mg, 150 μmol) and **5d** (18.5 mg, 225 μmol). **NMR Yield** = 55% (>9:1 branched : linear). **FCC** from Hex:Et_2O (9:1) to Hex:EtOAc (82.5:17:5). Isolated as a colorless oil (14.5 mg, 60 μmol, 40%). **^{1}H NMR** (300 MHz, $CDCl_3$) δ 6.94 (d, *J* = 8.8 Hz, 2H), 6.88 – 6.81 (m, 2H), 6.37 (d, *J* = 12.1 Hz, 1H), 5.30 (dt, *J* = 12.3, 7.7 Hz, 1H), 4.92 (s, 1H), 4.79 (s, 1H), 3.78 (s, 3H), 2.76 (d, *J* =

7.6 Hz, 2H), 1.10 (s, 9H). **^{13}C NMR** (75 MHz, $CDCl_3$) δ 157.3, 155.4, 151.5, 143.8, 118.0, 115.9, 114.8, 111.1, 107.9, 55.8, 36.2, 29.9, 29.4. **HRMS** (ESI+): Calculated for $C_{16}H_{23}O_2$ $[M+H]^+$, 247.1693found 247.1686.

(*E*)-8-methyl-7-methylenenon-4-ene-1,8-diol (6be).

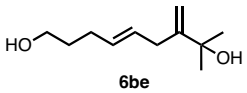

6be

Prepared according to the representative procedure with **5b** (15.0 mg, 150 μmol) and **4a** (12.6 mg, 150 μmol). No further purification needed after filtration through florisil (23.7 mg, 129 μmol, 86%, 9:1 branched : linear). **^{1}H NMR** (500 MHz, $CDCl_3$) δ 5.53 – 5.44 (m, 2H), 5.10 (d, J = 1.2 Hz, 1H), 4.77 (q, J = 1.4 Hz, 1H), 3.65 (t, J = 6.5 Hz, 2H), 2.81 (tt, J = 2.4, 1.1 Hz, 2H), 2.16 – 2.08 (m, 2H), 1.69 – 1.60 (m, 4H), 1.34 (s, 6H). **^{13}C NMR** (126 MHz, $CDCl_3$) δ 155.16, 131.66, 129.28, 108.68, 73.49, 62.58, 34.96, 32.46, 29.36, 29.03. **HRMS** (ESI+): Calculated for $C_{11}H_{20}NaO_2$ $[M+Na]^+$, 207.1356 found207.1356

(E)-6-(4-methoxyphenoxy)-2-methyl-3-methylenehex-5-en-2-ol (6ae).

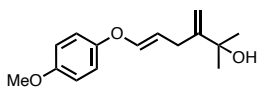

6ae

Prepared according to the representative procedure from $[Cp^*Ru(MeCN)_3]PF_6$ (9.0 mg, 5 mol%) **4a** (58.6 mg, 355 μmol) and **5e** (30.0 mg, 355 μmol) in 4.7 mL of degassed H_2O:THF (8:2). FCC in Hex:EtOAc (9:1), colorless oil (63.2 mg, 254 μmol, 71%, 6:1 branched : linear) **^{1}H NMR** (500 MHz, $CDCl_3$) δ 6.96 – 6.90 (m, 2H), 6.88 – 6.81 (m, 2H), 6.41 (dt, J = 12.1, 1.3 Hz, 1H), 5.30 (dt, J = 12.1, 7.6 Hz, 1H), 5.15 (q, J = 0.9 Hz, 1H), 4.88 (td, J = 1.5, 1.0 Hz, 1H), 3.78 (s, 3H), 2.83 (dtd, J = 7.6, 1.5, 1.0 Hz, 2H), 1.38 (s, 5H). **^{13}C NMR** (126 MHz, $CDCl_3$) δ 155.42, 155.21, 151.30, 144.28, 118.00, 114.82, 110.14, 108.89, 73.44, 55.82, 29.40, 29.34. **HRMS** (ESI+) for $C_{15}H_{20}NaO_3$ $[M+Na]^+$ calc 271.1305 found 271.1305.

(*E*)-1-((5-(benzyloxy)-5-methyl-4-methylenehex-1-en-1-yl)oxy)-4-methoxybenzene (6aa).

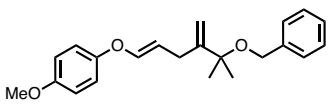

6aa

Prepared according to the representative procedure from **4a** (24.6 mg, 150 μmol) and **5a** (24.5 mg, 150 μmol). **NMR Yield** = 70% (9:1 branched : linear). **FCC** in Hex:EtOAc (95:5). Isolated as a colorless oil (30 mg, 88.5 μmol, 60%). **^{1}H NMR** (300 MHz, $CDCl_3$) δ 7.20 (dd, J = 23.1, 4.8 Hz, 5H), 6.88 – 6.69 (m, 4H), 6.29 (d, J = 12.1 Hz, 1H), 5.23 (dt, J = 12.1, 7.6 Hz, 1H), 5.08 (s, 1H), 5.02 (s, 1H), 4.19 (s, 2H), 3.69 (s, 3H), 2.76 (d, J = 7.7 Hz, 2H), 1.35 (s, 6H). **^{13}C NMR**

(75 MHz, $CDCl_3$) δ 155.50, 152.31, 151.46, 144.25, 139.64, 128.54, 127.52, 127.38, 117.98, 114.86, 112.40, 110.22, 64.93, 55.75, 28.08, 26.10. **HRMS** (ESI+) for $C_{22}H_{26}NaO_3$ $[M+Na]^+$ calc 361.1774 found 361.1777

(*E*)-6-(4-methoxyphenoxy)-2-(4-methoxyphenyl)-3-methylenehex-5-en-2-ol (6aj).

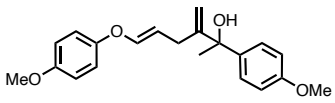

6aj

Prepared according to the representative procedure from **4a** (24.6 mg, 150 μmol) and **5j** (24.5 mg, 150 μmol) and $[Cp^*Ru(MeCN)_3]PF_6$ (7.6 mg, 10 mol%). **NMR Yield** = 70%. **FCC** in Hex:EtOAc (8:2). Isolated as a colorless oil (37mg, 114 μmol, 76%). **^{1}H NMR** (300 MHz, $CDCl_3$) δ 7.4 – 7.3 (m, 2H), 6.9 (ddt, *J* = 12.4, 9.1, 3.8 Hz, 6H), 6.3 (dd, *J* = 12.2, 1.4 Hz, 1H), 5.3 (s, 1H), 5.3 – 5.1 (m, 1H), 5.1 (s, 1H), 3.9 – 3.7 (m, 7H), 2.6 (qd, *J* = 16.8, 7.7 Hz, 2H), 1.8 – 1.7 (m, 3H). **^{13}C NMR** (75 MHz, $CDCl_3$) δ 158.7, 155.4, 153.9, 151.3, 144.2, 138.2, 129.4, 126.7, 118.0, 114.8, 113.7, 110.6, 109.9, 76.7, 55.8, 55.4, 32.5, 29.5, 29.3. **HRMS** (ESI+) for $C_{22}H_{28}NO_4S$ $[M+H]^+$ calc 402.1734 found 402.1734.

(*E*)-benzyl(6-(benzyloxy)-6-methyl-5-methylenehept-2-en-1-yl)sulfane (6da).

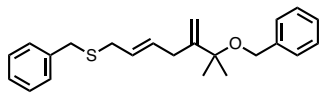

6da

Prepared according to the representative procedure from **4d** (25.1 mg, 140 μmol) **5a** (24.5 mg, 140 μmol) and $[Cp^*Ru(MeCN)_3]PF_6$ (7.1 mg, 10 mol%). **NMR Yield** = 97% (9:1 E/Z). **FCC** in Hex:EtOAc (95:5). Isolated as a colorless oil (39.1 mg, 111 μmol, 79%). Signals reported for the E isomer **^{1}H NMR** (750 MHz, $CDCl_3$) δ 7.39 – 7.31 (m, 8H), 7.31 – 7.25 (m, 2H), 6.16 (d, *J* = 11.7 Hz, 1H), 5.63 (ddd, *J* = 11.7, 7.7, 6.2 Hz, 1H), 5.31 (s, 1H), 5.07 (s, 1H), 4.34 (s, 2H), 3.74 (s, 2H), 2.54 (dtd, *J* = 8.6, 6.9, 1.7 Hz, 2H), 2.51 – 2.46 (m, 2H), 1.43 (s, 6H). **^{13}C NMR** (189 MHz, $CDCl_3$) δ 148.68, 139.52, 138.54, 131.08, 129.05, 128.94, 128.60, 128.39, 127.55, 127.27, 127.06, 114.33, 77.33, 77.16, 76.99, 64.98, 36.44, 31.48, 28.68, 26.35. **HRMS** (ESI+) for C23H28NaOS [M+Na]+ calc 375.1753 found 375.1750

(*E*)-1-((6-(benzyloxy)-6-methyl-5-methylenehept-2-en-1-yl)oxy)-4-methoxybenzene (6ca)

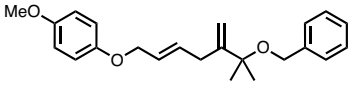

6ca

Prepared according to the representative procedure from **4c** (26.7 mg, 150 μmol) **5a** (26.1 mg, 150 μmol) and $[Cp^*Ru(MeCN)_3]PF_6$ (7.6 mg, 10 mol%). **NMR Yield** = 77%.**FCC** in Hex:EtOAc (9:1). Isolated as a colorless oil (27.2 mg, 77

μmol, 55%). **^{1}H NMR** (300 MHz, $CDCl_3$) δ 7.39 – 7.22 (m, 5H), 6.91 – 6.80 (m, 4H), 5.88 (dt, *J* = 13.6, 6.6 Hz, 1H), 5.75 (dt, *J* = 15.4, 5.6 Hz, 1H), 5.17 (s, 1H), 5.02 (s, 1H), 4.48 (d, *J* = 5.7 Hz, 2H), 4.28 (s, 2H), 3.79 (s, 3H), 2.96 (d, *J* = 6.6 Hz, 2H), 1.43 (s, 6H). **^{13}C NMR** (75 MHz, $CDCl_3$) δ 153.96, 152.91, 151.31, 139.48, 133.21, 128.45, 128.40, 127.47, 127.31, 127.28, 115.92, 114.72, 112.64, 69.33, 64.96, 55.85, 33.48, 26.13. **HRMS** (ESI+) for $C_{23}H_{28}O_3Na$ [M+Na]+ calc 375.1931 found 375.1944.

(*E*)-7-(benzylthio)-2-methyl-3-methylenehept-5-en-2-ol (6de)

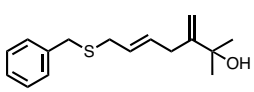

6db

Prepared according to the representative procedure from **4d** (26.7 mg, 150 μmol) **5e** (12.6 mg, 150 μmol) and $[Cp^*Ru(MeCN)_3]PF_6$ (7.6 mg, 10 mol%). **NMR Yield** = 72% (8:1 E/Z). **FCC** in Hex:EtOAc (9:1). Isolated as a colorless oil (13.0 mg, 55 μmol, 33%). Signals reported for the E isomer **^{1}H NMR** (500 MHz, $CDCl_3$) δ 7.2 (d, *J* = 4.4 Hz, 4H), 7.2 – 7.1 (m, 1H), 6.0 (d, J = 10.2 Hz, 1H), 5.6 – 5.5 (m, 1H), 5.2 (d, *J* = 1.6 Hz, 1H), 4.7 (t, *J* = 1.5 Hz, 1H), 3.6 (s, 2H), 2.4 – 2.4 (m, 4H), 1.3 (s, 6H). **^{13}C NMR** (126 MHz, $CDCl_3$) δ 151.7, 138.4, 131.4, 128.9, 128.9, 128.5, 127.0, 110.8, 72.8, 36.3, 31.3, 29.1, 28.1. **HRMS (ESI+):** for $C_{16}H_{22}NaOS$ $[M+Na]^+$ calc 285.1285 found 285.1284

(*E*)-8-(benzyloxy)-8-methyl-7-methylenenon-4-en-1-ol (6ba)

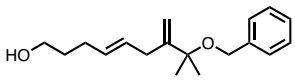

6ba

Prepared according to the representative procedure from **4b** (15 mg, 150 μmol), **5a** (26.1 mg, 150 μmol). **NMR Yield** = 66% (9:1 branched : linear). **FCC** from Hex:EtOAc (87.5:12:5) to Hex:EtOAc (82.5:17:5). Isolated as a colorless oil (22.6 mg, 82 μmol, 55%). Signals reported for the linear isomer **^{1}H NMR** (300 MHz, $CDCl_3$) δ 7.41 – 7.24 (m, 5H), 5.54 – 5.46 (m, 3H), 5.15 (s, 1H), 5.02 (s, 1H), 4.28 (s, 2H), 3.67 (t, *J* = 6.5 Hz, 2H), 2.86 (d, *J* = 4.6 Hz, 2H), 2.14 (q, *J* = 6.7 Hz, 2H), 1.74 – 1.60 (m, 2H), 1.43 (s, 6H). **^{13}C NMR** (126 MHz, $CDCl_3$) δ 151.0, 138.5, 130.5, 128.0, 127.3, 126.3, 126.1, 110.9, 76.6, 63.8, 61.5, 32.5, 31.4, 27.8, 25.0. **HRMS (ESI+)**: for $C_{18}H_{26}NaO_2$ $[M+Na]^+$ calc 297.1825 found 297.18.

(*E*)-2-((6-(4-methoxyphenoxy)-2-methyl-3-methylenehex-5-en-2-yl)oxy)ethan-1-ol (6ag)

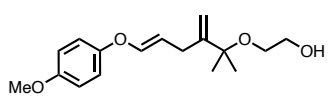

6ag

Prepared according to the representative procedure from **4a** (25.4mg, 150 μmol), **5g** (19.8 mg, 155 μmol) and $[Cp^*Ru(MeCN)_3]PF_6$ (7.8 mg, 10 mol%). **NMR Yield**

= 66% (9:1 branched : linear). **FCC** in Hex:EtOAc (8:2). Isolated as a colorless oil (21 mg, 72 μmol, 46%). **^{1}H NMR** (300 MHz, $CDCl_3$) δ 6.97 – 6.88 (m, 1H), 6.88 – 6.78 (m, 1H), 6.39 (d, *J* = 12.1 Hz, 1H), 5.28 (dt, *J* = 12.1, 7.6 Hz, 0H), 5.09 (s, 1H), 5.04 (s, 1H), 3.78 (s, 2H), 3.69 (p, *J* = 4.9 Hz, 1H), 3.30 (t, *J* = 4.7 Hz, 1H), 2.77 (d, *J* = 7.7 Hz, 1H), 1.35 (s, 3H).**^{13}C NMR** (126 MHz, $CDCl_3$) δ 155.37, 151.83, 151.30, 144.20, 117.94, 112.31, 110.01, 63.57, 62.45, 55.80, 31.04, 28.12, 26.02. **HRMS** (ESI+) for $C_{17}H_{24}NaO_4$ [M+Na]+ calc 315.1567 found 315.1567

(*E*)-1-(5-(4-methoxyphenoxy)penta-1,4-dien-2-yl)cyclopentan-1-ol (6ah)

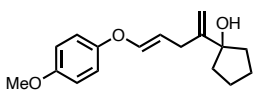

6ah

Prepared according to the representative procedure from **4a** (25.4 mg, 150 μmol), **5h** (17.1 mg, 155 mol) and [Cp*Ru(MeCN)$_3$]PF_6 (7.8 mg, 10 mol%). **NMR Yield** = 99% (9:1 branched: linear) **FCC** in Hex:EtOAc (9:1). Branched isomer isolated as a colorless oil (38.4 mg, 140 μmol, 90%). **^{1}H NMR** (300 MHz, $CDCl_3$) δ 7.01 – 6.89 (m, 2H), 6.92 – 6.82 (m, 2H), 6.43 (dq, *J* = 12.2, 1.4 Hz, 1H), 5.42 – 5.26 (m, 1H), 5.18 (dd, *J* = 1.9, 1.0 Hz, 1H), 4.93 (q, *J* = 1.4 Hz, 1H), 3.80 (s, 3H), 2.87 (dt, *J* = 7.6, 1.3 Hz, 2H), 1.99 – 1.63 (m, 8H). **^{13}C NMR** (75 MHz, $CDCl_3$) δ 155.5, 153.2, 151.4, 144.4, 118.1, 114.9, 110.2, 109.5, 84.6, 55.8, 38.8, 29.9, 23.5. **HRMS** (ESI+) for $C_{17}H_{22}NaO_3$ [M+Na]+ calc 297.1461 found 297.1461.

(*E*)-1-(5-(4-methoxyphenoxy)penta-1,4-dien-2-yl)cyclohexan-1-ol (6ai)

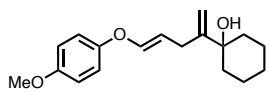

6ai

Prepared according to the representative procedure from **4a** (25.4 mg, 155 μmol), **5i** (19.2 mg, 155 mol) and [Cp*Ru(MeCN)$_3$]PF_6 (7.8 mg, 10 mol%). **NMR Yield** = 99% (9:1 branched: linear). **FCC** in Hex:EtOAc (9:1). Branched isomer isolated as a colorless oil (37.9 mg, 131 μmol, 85%). **^{1}H NMR** (300 MHz, $CDCl_3$) δ 6.93 (dd, *J* = 9.1, 2.0 Hz, 2H), 6.88 – 6.79 (m, 2H), 6.39 (d, *J* = 12.2 Hz, 1H), 5.30 (dtd, *J* = 12.0, 7.5, 1.9 Hz, 1H), 5.15 (s, 1H), 4.92 (s, 1H), 3.78 (s, 3H), 2.83 (d, *J* = 7.5 Hz, 2H), 1.64 (q, *J* = 8.0 Hz, 10H). **^{13}C NMR** (126 MHz, $CDCl_3$) δ 155.4, 151.3, 144.2, 118.0, 116.2, 114.8, 110.5, 109.7, 74.0, 55.8, 36.4, 31.1, 29.1, 25.8, 22.1. **HRMS** (ESI+) for $C_{18}H_{24}NaO_3$ [M+Na]+ calc 311.1618 found 311.1613.

***tert*-butyl (*E*)-*N*-(6-(4-methoxyphenoxy)-2-methyl-3-methylenehex-5-en-2-yl)-*N*-tosylglycinate (6al)**

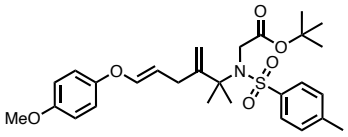

6al

Prepared according to the representative procedure from **4a** (23.8 mg, 145 μmol), **5l** (51.0 mg, 145 mol) and [Cp*Ru(MeCN)$_3$]PF$_6$ (7.3 mg, 10 mol%). **NMR Yield** = 70% (9:1 branched: linear). **FCC** in Hex:EtOAc (9:1). Branched isomer isolated as a colorless oil (37.9 mg, 131 μmol, 85%).**^{1}H NMR** (300 MHz, $CDCl_3$) δ 8.08 (d, *J* = 8.4 Hz, 2H), 7.44 – 7.20 (m, 4H), 7.02 – 6.78 (m, 4H), 6.33 (d, *J* = 12.1 Hz, 1H), 5.14 (s, 1H), 5.05 (s, 1H), 3.92 (s, 2H), 3.80 (s, 3H), 2.80 (d, *J* = 7.6 Hz, 2H), 2.51 – 2.33 (m, 6H), 1.50 (s, 9H). **^{13}C NMR** (75 MHz, $CDCl_3$) δ 169.5, 155.3, 153.4, 151.1, 144.4, 143.2, 140.7, 129.4, 129.3, 128.1, 127.8, 127.7, 118.2, 117.9, 114.8, 114.7, 112.4, 109.6, 81.5, 65.6, 55.7, 48.2, 29.6, 28.2, 28.1, 28.0, 28.0, 25.6, 21.5.

(*E*)-6-(4-methoxyphenoxy)-2-(4-methoxyphenyl)-3-methylenehex-5-en-2-ol (6aj)

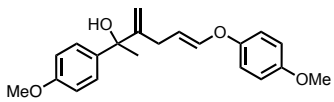

6aj

Prepared according to the representative procedure from **4a** (25.4 mg, 155 μmol), **5j** (19.2 mg, 155 mol) and [Cp*Ru(MeCN)$_3$]PF$_6$ (7.8 mg, 10 mol%). **NMR Yield** = 99% (9:1 branched: linear). **FCC** in Hex:EtOAc (9:1). Branched isomer isolated as a colorless oil (37.9 mg, 131 μmol, 85%). **^{1}H NMR** (300 MHz,CDCl3) δ 7.43 – 7.30 (m, 2H), 6.85 (ddt, *J* = 12.4, 9.1, 3.8 Hz, 6H), 6.26 (dd, *J* = 12.2, 1.4 Hz, 1H), 5.34 (s, 1H), 5.25 – 5.13 (m, 1H), 5.07 (s, 1H), 3.86 – 3.70 (m, 7H), 2.59 (qd, *J* = 16.8, 7.7 Hz, 2H), 1.77 – 1.66 (m, 3H). **^{13}C NMR** (75 MHz, $CDCl_3$) δ 158.7, 155.4, 153.9, 151.3, 144.2, 138.2, 129.4, 126.7, 118.0, 114.8, 113.7, 110.6, 109.9, 55.8, 55.4, 32.5, 29.5, 29.3. **HRMS (ESI+):** for $C_{21}H_{24}NaO_4$ calc 363.1567 $[M+Na]^+$ found 363.1562.

1-((5*E*)-6-(4-methoxyphenoxy)hexa-2,5-dien-3-yl)cyclohexan-1-ol (6ak)

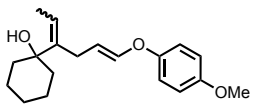

6ak

Prepared according to the representative procedure from **4a** (24.6 mg, 150 μmol), **5k** (20.7 mg, 155 mol) and [Cp*Ru(MeCN)$_3$]PF$_6$ (7.8 mg, 10 mol%). **FCC** in Hex:EtOAc (9:1). Isolated as colorless oil (25.7 mg, 85 µmol, 57%). **^{1}H NMR** (300 MHz, $CDCl_3$) δ 6.97 – 6.79 (m, 4H), 6.37 (d, *J* = 12.2 Hz, 1H), 5.36 (s, 1H), 5.32 – 5.16 (m, 1H), 3.77 (d, *J* = 1.5 Hz, 3H), 2.64 (d, *J* = 7.6 Hz, 2H), 1.90 (s, 3H), 1.62 (d, *J* = 7.2 Hz, 5H), 1.39 (d, *J* = 29.9 Hz, 5H). **^{13}C NMR** (75 MHz, $CDCl_3$) δ 155.4, 151.3, 144.1, 137.5, 131.9, 117.9,

114.8, 110.1, 71.9, 55.8, 40.3, 39.5, 38.8, 29.8, 25.6, 22.7, 17.6. **HRMS (ESI+):** for $C_{19}H_{26}NaO_3$ calc 325.1774 $[M+Na]^+$ found 325.1774.

(8*R*,9*S*,13*S*,14*S*,17*R*)-3-methoxy-17-((*E*)-5-(4-methoxyphenoxy)penta-1,4-dien-2-yl)-13-methyl-7,8,9, 11,12,13,14,15,16,17-decahydro-6*H*-cyclopenta[*a*]phenanthren-17-ol (6am)

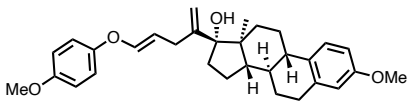

6am

Prepared according to the representative procedure from **4a** (24.6 mg, 150 μmol), **5m** (46.6 mg, 150 mol) and $[Cp^*Ru(MeCN)_3]PF_6$ (7.6 mg, 10 mol%). **NMR Yield** = 62%. **FCC** in fine silica (particle ⌀ = 25 – 40 µm) Hex:Et_2O (6:4). Isolated as a white off solid (43.2 mg, 91 μmol, 60%). **^{1}H NMR** (500 MHz, $CDCl_3$) δ 7.17 (d, *J* = 8.6 Hz, 1H), 6.97 – 6.91 (m, 2H), 6.89 – 6.82 (m, 2H), 6.70 (dd, *J* = 8.6, 2.6 Hz, 1H), 6.63 (d, *J* = 2.5 Hz, 1H), 6.42 (d, *J* = 12.1 Hz, 1H), 5.36 (ddd, *J* = 12.1, 8.4, 6.6 Hz, 1H), 5.17 (s, 1H), 4.88 (s, 1H), 3.81 – 3.72 (m, 6H), 3.01 – 2.94 (m, 1H), 2.90 – 2.79 (m, 3H), 2.29 – 2.16 (m, 2H), 2.11 (td, *J* = 11.5, 4.1 Hz, 1H), 1.96 – 1.85 (m, 2H), 1.80 – 1.64 (m, 3H), 1.63 – 1.54 (m, 2H), 1.53 – 1.40 (m, 3H), 1.39 – 1.17 (m, 3H), 0.98 (s, 3H). **^{13}C NMR** (126 MHz, $CDCl_3$) δ 157.57, 155.38, 153.64, 151.39, 144.12, 138.09, 132.80, 126.37, 117.93, 114.82, 113.93, 113.32, 111.57, 111.10, 87.85, 55.82, 55.33, 47.51, 47.30, 43.61, 39.66, 39.19, 33.81, 31.25, 29.99, 27.55, 26.64, 23.64, 14.52. **HRMS (ESI+):** for $C_{31}H_{38}NaO_4$ calc 497.2662 [M+Na]+ found 497.2658

Methyl (*S*,*E*)-2-((*tert*-butoxycarbonyl)amino)-3-(4-((4-(1-hydroxycyclopentyl)penta-1,4-dien-1-yl)oxy)phenyl)propanoate (6eh)

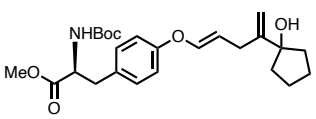

Prepared according to the representative procedure from **4e** (50 mg, 150 μmol), with excess of **5h** (24.5 mg, 234 μmol) and $[Cp^*Ru(MeCN)_3]PF_6$ (7.6 mg, 10 mol%). **FCC** in Hex:EtOAc (8:2). Isolated as a white off solid (41 mg, 93 μmol, 62%). **^{1}H NMR** (300 MHz, $CDCl_3$) δ 7.05 (d, *J* = 8.5 Hz, 2H), 6.96 – 6.83 (m, 2H), 6.50 – 6.38 (m, 1H), 5.41 (dt, *J* = 12.1, 7.6 Hz, 1H), 5.17 (s, 1H), 4.97 (d, *J* = 8.1 Hz, 1H), 4.91 (d, *J* = 1.5 Hz, 1H), 4.54 (d, *J* = 7.0 Hz, 1H), 3.71 (s, 3H), 3.06 (dt, *J* = 15.2, 6.9 Hz, 2H), 2.91 – 2.78 (m, 2H), 1.99 – 1.63 (m, 8H), 1.41 (s, 9H). **^{13}C NMR** (75 MHz, $CDCl_3$) δ 172.3, 156.4, 155.0, 152.8, 142.8, 130.4, 130.1, 116.5, 111.5, 109.4, 84.4, 80.0, 54.5, 52.2, 38.7, 37.6,

29.8, 28.3, 23.5. **HRMS (ESI+):** for $C_{25}H_{35}NNaO_6$ $[M+Na]^+$ calc 468.2357 found 468.2365.

(*E*)-7-(4-methoxyphenoxy)-1-(4-methoxyphenyl)-3-methylenehept-5-en-1-ol (6ao)

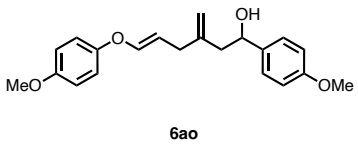

6ao

Prepared according to the representative procedure from **4a** (41.9 mg, 255 μmol), **5o** (45.0 mg, 255 mol) and $[Cp^*Ru(MeCN)_3]PF_6$ (12.9 mg, 10 mol%). **FCC** in Hex:EtOAc (85:15). Isolated as a colorless oil (57.1 mg, 116 μmol, 66%, 3:1 branched : linear mixture of isomers) Characterized as 3:1 mixture of isomers. **^{1}H NMR** (300 MHz, $CDCl_3$) δ 7.34 – 7.22 (m, 2H), 6.99 – 6.79 (m, 6H), 6.45 – 6.30 (m, 1H), 5.65 – 5.40 (m, 0.5 H), 5.33 – 5.17 (m, 1H), 5.00 (d, 0.75 H), 4.94 (s, 0.75 H), 4.79 (t, J = 6.7 Hz, 0.75H), 4.65 (t, J f= 6.5 Hz, 0.25H), 3.83 – 3.75 (m, 6H), 2.78 – 2.67 (m, 2H), 2.52 – 2.40 (m, 2H). **^{13}C NMR** (75 MHz, $CDCl_3$) δ 159.06, 155.34, 151.07, 145.35, 144.50, 143.67, 136.21, 132.48, 127.04, 126.78, 117.95, 117.87, 114.69, 113.82, 113.76, 113.67, 109.92, 108.81, 73.27, 71.59, 55.67, 55.27, 46.12, 42.50, 34.04, 30.33, 29.71. **HRMS (ESI+):** for $C_{21}H_{24}NO_4$ calc 363.1567 $[M+H]^+$ found 363.1559

(E)-2-(8-(4-methoxyphenoxy)-4-methyleneoct-6-en-1-yl)isoindoline-1,3-dione (6an)

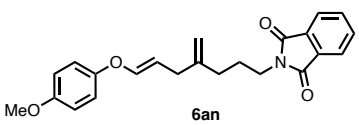

6an

Prepared according to the representative procedure from **4a** (19.1 mg, 116 μmol), **5n** (25.0 mg, 116 mol) and $[Cp^*Ru(MeCN)_3]PF_6$ (5.9 mg, 10 mol%). **FCC** in Hex:EtOAc (8:2). Isolated as a colorless oil (36.7 mg, 97 μmol, 83%, 3:1 branched : linear mixture of isomers). **^{1}H NMR** (300 MHz, $CDCl_3$) δ 7.83 (dd, J = 5.4, 3.1 Hz, 2H), 7.75 – 7.63 (m, 2H), 6.96 – 6.75 (m, 4H), 6.35 (m, 1H), 5.48 (m, 0.25H), 5.22 (m, 1H), 4.86 – 4.78 (m, 1.5H), 3.77 (m, 3H), 3.69 (m, 2H), 2.68 (m, 2H), 2.18 – 2.01 (m, 2H), 1.93 – 1.68 (m, 2H). **^{13}C NMR** (75 MHz, $CDCl_3$) δ 168.52, 155.38, 155.32, 151.35, 151.25, 147.35, 144.28, 143.58, 134.00, 132.27, 129.76, 129.54, 123.29, 117.98, 114.78, 110.58, 110.34, 109.33, 55.78, 37.86, 37.77, 34.08, 33.14, 30.34, 29.93, 28.22, 26.47. **HRMS (ESI+):** for $C_{23}H_{24}NO_4$ calc 378.1700 $[M+H]^+$ found 378.1696.

(2*R*,3*R*,4*S*,5*R*,6*R*)-2-(acetoxymethyl)-6-((4-(((*E*)-5-methyl-4-methylene-5-((4-methylphenyl)sulfonamido)hex-1-en-1-yl)oxy)benzyl)oxy)tetrahydro-2*H*-pyran-3,4,5-triyl triacetate (6fb).

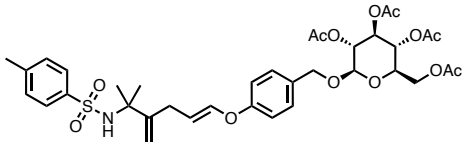

6fb

Prepared according to the representative procedure from **4f** (37.1 mg, 175 μmol), **5b** (17.8 mg, 75 μmol) and [Cp*Ru(MeCN)$_3$]PF$_6$ (3.8 mg, 10 mol%). **FCC** in Hex:EtOAc (1:1). Isolated as a white off solid (38.5 mg, 53 μmol, 70% isolated as 16: branched : linear). **^{1}H NMR** (300 MHz, $CDCl_3$) δ 7.75 (d, J = 7.7 Hz, 2H), 7.34 – 7.16 (m, 4H), 6.94 (d, J = 8.2 Hz, 2H), 6.46 – 6.28 (m, 1H), 5.26 – 4.97 (m, 5H), 4.99 – 4.59 (m, 2H), 4.64 – 4.47 (m, 3H), 4.33 – 4.05 (m, 3H), 3.66 (s, 1H), 2.72 (d, J = 7.6 Hz, 2H), 2.39 (s, 3H), 2.19 – 1.93 (m, 13H) 1.37 (s, 3H). **^{13}C NMR** (75 MHz, $CDCl_3$) δ 170.7, 170.3, 169.4, 169.3, 157.1, 151.5, 143.1, 142.9, 139.9, 130.7, 129.7, 129.4, 129.4, 127.2, 116.3, 115.3, 111.8, 111.3, 99.1, 72.8, 71.8, 71.3, 70.3, 68.4, 62.0, 59.6, 29.7, 28.8, 27.6, 21.5, 20.7, 20.7, 20.6.

(*E*)-1-methoxy-4-((4-phenylpenta-1,4-dien-1-yl)oxy)benzene & 1-methoxy-4-(((1*E*,3*E*)-4-phenylbuta-1,3-dien-1-yl)oxy)benzene (6ap)

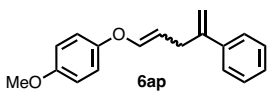

6ap

Prepared according to the representative procedure from **4a** (24.6 mg, 150 μmol), with excess of **5p** (23.0 mg, 225 μmol) and [Cp*Ru(MeCN)$_3$]PF$_6$ (7.6 mg, 10 mol%). **FCC** in Hex:EtOAc (97:3). Isolated as a yellow oil (32.8 mg, 123 μmol, 82%, 1.2 : 1 branched : linear mixture of isomers). **^{1}H NMR** (300 MHz, $CDCl_3$) δ 7.52 – 7.15 (m, 5H), 6.98 – 6.77 (m, 4H), 6.33-6.15 (m, 0.4H), 6.52 – 6.33 (m, 1.3H) 5.47 – 5.27 (m, 1.5H), 5.17 (m, 0.6H), 3.79 (m, 3H), 3.21 (dq, J = 7.3, 1.2 Hz, 1.2H), 2.94 (ddt, J = 7.6, 6.4, 1.4 Hz, 0.9H). **^{13}C NMR** (75 MHz, $CDCl_3$) δ 155.9, 155.8, 151.8, 151.8, 147.6, 145.1, 144.7, 141.6, 138.1, 131.1, 129.4, 129.1, 128.9, 128.1, 127.6, 126.6, 118.5, 118.3, 116.3, 115.3, 115.2, 113.6, 110.0, 110.0, 56.2, 33.6, 31.2, 1.6. **HRMS (ESI+):** $C_{18}H_{19}O_2$ $[M+H]^+$ calc 267.1380 found 267.1369

1-(((1E,4E)-6-(benzyloxy)-6-methylhepta-1,4-dien-1-yl)oxy)-4-methoxybenzene (6aa')

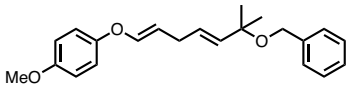

Prepared according to the representative procedure from **4a** (24.5 mg, 150 μmol), **5a** (26.1 mg, 234 μmol) and $[CpRu(MeCN)_3]PF_6$ (6.5 mg, 10 mol%). **NMR Yield** = 40% (1:6 branched: linear). **FCC** in fine silica (particle ⌀ = 25 – 40 µm) Hex:Et_2O (95:5). Isolated as a colorless oil (17 mg, 50 μmol, 33%, >1:9 branched : linear). **^{1}H NMR** (300 MHz, $CDCl_3$) δ 7.41 – 7.18 (m, 4H), 6.97 – 6.88 (m, 2H), 6.87 – 6.78 (m, 2H), 6.39 (d, *J* = 12.1 Hz, 1H), 5.75 – 5.55 (m, 2H), 5.29 (dt, *J* = 12.4, 7.3 Hz, 1H), 4.38 (s, 2H), 3.78 (s, 3H), 2.78 (t, *J* = 6.2 Hz, 2H), 1.37 (s, 6H). **^{13}C NMR** (75 MHz, $CDCl_3$) δ 155.5, 151.4, 143.9, 140.0, 136.8, 128.6, 128.5, 128.4, 127.5, 127.2, 118.0, 114.8, 110.0, 5.4, 65.0, 55.8, 30.3, 26.7, 1.2. **HRMS** (ESI+) for $C_{22}H_{26}NaO_3$ $[M+Na]^+$ calc 361.1774 found 361.1777

N-((3E,6E)-7-(4-methoxyphenoxy)-2-methylhepta-3,6-dien-2-yl)-4-methylbenzenesulfonamide (6ab')

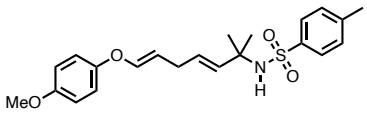

Prepared according to the representative procedure from **4a** (24.5 mg, 150 μmol), **5b** (35.6 mg, 234 μmol) and $[CpRu(MeCN)_3]PF_6$ (6.5 mg, 10 mol%). **NMR Yield** = 99% (1:7 branched: linear). **FCC** in fine silica (particle ⌀ = 25 – 40 µm) Hex:EtOAc (8:2). Isolated as a colorless oil (47 mg, 117 μmol, 78%, >1:9 branched : linear) **^{1}NMR** (300 MHz, $CDCl_3$) δ 7.78 – 7.67 (m, 2H), 7.24 (d, *J* = 8.1 Hz, 2H), 6.99 – 6.78 (m, 4H), 6.35 – 6.22 (m, 1H), 5.50 (dt, *J* = 15.7, 5.9 Hz, 1H), 5.40 – 5.26 (m, 1H), 5.13 – 4.93 (m, 1H), 4.88 (s, 1H), 3.77 (d, *J* = 0.9 Hz, 4H), 2.61 – 2.47 (m, 2H), 2.38 (s, 3H), 1.28 (s, 5H). **^{13}C NMR** (75 MHz, $CDCl_3$) δ 155.4, 151.2, 143.9, 142.9, 140.3, 136.0, 129.5, 127.5, 127.3, 117.9, 114.8, 109.3, 56.8, 55.8, 29.9, 28.5, 21.6. **HRMS** (ESI+) for $C_{23}H_{30}NO_4S$ $[M+H]^+$ 418.1890 found 418.1885.

(8*R*,9*S*,13*S*,14*S*,17*R*)-3-methoxy-17-((1*E*,4*E*)-5-(4-methoxyphenoxy)penta-1,4-dien-1-yl)-13-methyl-7,8,9,11,12,13,14,15,16,17-decahydro-6*H*-cyclopenta[*a*]phenanthren-17-ol (6am')

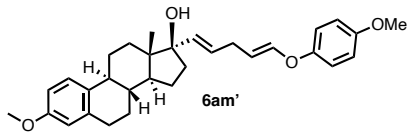

Prepared according to the representative procedure from **4a** (24.6 mg, 150 μmol), with excess of **5m** (46.6 mg, 150 μmol) and

[CpRu(MeCN)$_3$]PF$_6$ (6.5 mg, 10 mol%). **FCC** in fine silica (particle ⌀ = 25 – 40 μm) Hex:EtOAc (9:1). Isolated as a colorless oil (54.0 mg, 113 μmol, 75% isolated as a linear isomer). **^{1}H NMR** (300 MHz, $CDCl_3$) δ 7.20 (dd, J = 8.7, 1.1 Hz, 1H), 6.99 – 6.88 (m, 2H), 6.86 – 6.77 (m, 2H), 6.72 (dd, J = 8.6, 2.8 Hz, 1H), 6.64 (d, J = 2.8 Hz, 1H), 6.42 (dt, J = 12.2, 1.4 Hz, 1H), 5.79 (d, J = 15.6 Hz, 1H), 5.64 (dt, J = 15.5, 6.1 Hz, 1H), 5.32 (dt, J = 12.1, 7.0 Hz, 1H), 3.79 (s, 3H), 3.74 (d, J = 0.8 Hz, 3H), 2.94 – 2.74 (m, 4H), 2.37 – 2.22 (m, 1H), 2.20 – 1.97 (m, 2H), 1.89 (dq, J = 14.0, 6.3 Hz, 2H), 1.81 – 1.22 (m, 8H), 0.95 (s, 3H). **^{13}C NMR** (75 MHz, $CDCl_3$) δ 157.6, 155.5, 151.3, 144.0, 138.1, 135.9, 132.8, 126.9, 126.4, 118.0, 114.8, 114.0, 111.6, 110.2, 83.8, 55.8, 55.3, 49.2, 46.9, 43.9, 39.6, 36.7, 32.5, 30.3, 30.0, 27.6, 26.5, 23.3, 14.2. **HRMS (ESI+):** for $C_{31}H_{38}NaO_4$ calc 497.2662 [M+Na]+ found 497.2658.

methyl (*E*)-*N*-(6-(4-methoxyphenoxy)-2-methyl-3-methylenehex-4-en-2-yl)-*N*-tosylglycylphenylalaninate (8ab)

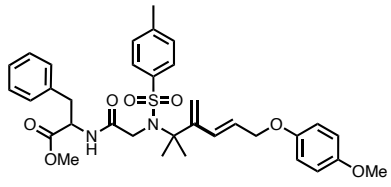

8ab

Prepared according to the representative procedure from **4a** (12.9 mg, 79 μmol), **7b** (36 mg, 79 μmol) and [Cp*Ru(MeCN)$_3$]PF$_6$ (4.0 mg, 10 mol%). **FCC** in fine silica (particle ⌀ = 25 – 40 μm) Hex:EtOAc (8:2 to 7:3). Isolated as a colorless oil (20 mg, 32 μmol, 40%, >9:1 branched : linear). **^{1}H NMR** (300 MHz, $CDCl_3$) δ 7.92 (d, J = 7.9 Hz, 2H), 7.37 – 7.14 (m, 7H), 6.97 – 6.80 (m, 4H), 6.72 (d, J = 7.9 Hz, 1H), 6.29 (d, J = 12.1 Hz, 1H), 5.16 (dt, J = 12.9, 7.5 Hz, 1H), 5.09 (s, 1H), 5.03 (s, 1H), 4.91 (q, J = 6.5 Hz, 1H), 3.92 (dd, J = 17.0, 13.0 Hz, 2H), 3.80 (s, 3H), 3.73 (s, 3H), 3.17 (d, J = 5.8 Hz, 2H), 2.79 – 2.56 (m, 2H), 2.43 (s, 3H), 1.37 (s, 6H). **^{13}C NMR** (75 MHz, $CDCl_3$) δ 171.6, 169.4, 155.3, 152.6, 151.2, 144.3, 143.7, 139.1, 135.7, 129.6, 129.6, 129.4, 128.7, 128.1, 127.2, 117.8, 114.7, 112.5, 109.7, 66.1, 55.7, 53.4, 52.3, 49.9, 37.9, 28.6, 26.3, 25.7, 21.5. . **HRMS** (ESI+) for $C_{34}H_{40}N_2NaO_7S$ $[M+Na]^+$ 643.2448found 643.2431

methyl ((*S*,*E*)-2-((((9*H*-fluoren-9-yl)methoxy)carbonyl)amino)-7-(4-methoxyphenoxy)-4-methylenehept-5-enoyl)-*L*-valinate.

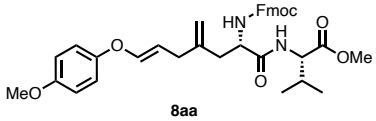

8aa

Prepared according to the representative procedure from **4a** (19.4 mg, 118 μmol), **7b** (35.4 mg, 79 μmol) and [Cp*Ru(MeCN)$_3$]PF$_6$ (4.0 mg, 10 mol%). **FCC** in fine silica (particle ⌀ =

25 – 40 µm) Hex:EtOAc (8:2). Isolated as a colorless oil (45 mg, 73 μmol, 93%, 3:1 branched : linear). A 20 mg fraction of the branched compound was isolated and characterized. **^{1}H NMR** (300 MHz, $CDCl_3$) δ 7.78 (d, *J* = 7.5 Hz, 2H), 7.59 (d, *J* = 7.4 Hz, 2H), 7.41 (t, *J* = 7.4 Hz, 2H), 7.32 (t, *J* = 7.6 Hz, 2H), 6.98 – 6.89 (m, 2H), 6.88 – 6.80 (m, 2H), 6.55 (d, *J* = 8.7 Hz, 1H), 6.46 (d, *J* = 12.2 Hz, 1H), 5.39 – 5.17 (m, 2H), 5.02 (s, 1H), 4.94 (s, 1H), 4.54 (dd, *J* = 8.7, 4.9 Hz, 1H), 4.42 (t, *J* = 7.4 Hz, 3H), 4.24 (t, *J* = 7.0 Hz, 1H), 3.77 (d, *J* = 1.6 Hz, 3H), 3.73 (s, 3H), 2.76 (s, 2H), 2.64 (dd, *J* = 14.6, 6.2 Hz, 1H), 2.48 (s, 1H), 2.17 (dp, *J* = 13.6, 6.9 Hz, 1H), 0.93 (t, *J* = 7.6 Hz, 6H). **^{13}C NMR** (75 MHz, $CDCl_3$) δ 171.2, 155.4, 151.1, 144.8, 143.9, 143.7, 141.3, 127.8, 127.1, 125.0, 120.0, 117.9, 114.7, 114.4, 108.3, 67.3, 57.3, 55.7, 53.3, 52.2, 47.1, 38.7, 33.6, 31.3, 18.9, 17.8. **HRMS** (ESI+) for $C_{36}H_{40}N2NaO_7$ $[M+Na]^+$ 635.2728 found 635.2726

Bioorthogonality

Bioorthogonality in different biological media

Reactions were carried out as the representative procedure of the previous section changing the aqueous media for the corresponding degassed biological milieu.

Bioorthogonality with the addition of different relevant biomolecules

Reactions were carried out as the representative procedure of the previous section adding the corresponding additive before the addition of the catalyst

Representative Procedure for (E)-N-(7-(4-methoxyphenoxy)-2-methyl-3-methylenehept-5-en-2-yl)-4-methylbenzenesulfonamide (6ab).

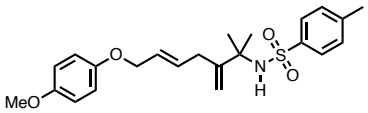

$[Cp^*Ru(MeCN)_3]PF_6$ (7.6 mg, 10 mol%) was added to a stirred solution of **4a** (24.6 mg, 150 μmol) and **5b** (37.7 mg, 150 μmol) in 2 mL of degassed H_2O:THF(8:2) under N_2 atmosphere and stirred at 37 ºC. After 16 h, the mixture was extracted with CH_2Cl_2 (5 x 1 mL) and the extract was filtered through a florisil plug (in a 3 mL syringe) directly to a vial and the solvent removed under reduced pressure. 700 μL solution of $DMSO_2$ in $CDCl_3$ (4.4 mg of $DMSO_2$, 50 μmol, per 700 μL of $CDCl_3$) were added and the reaction analyzed by NMR.

Peptides

Peptide 7c

Name **Boc-NH-G(Prop)-V-G-W-A-CONH$_2$ (7c)**

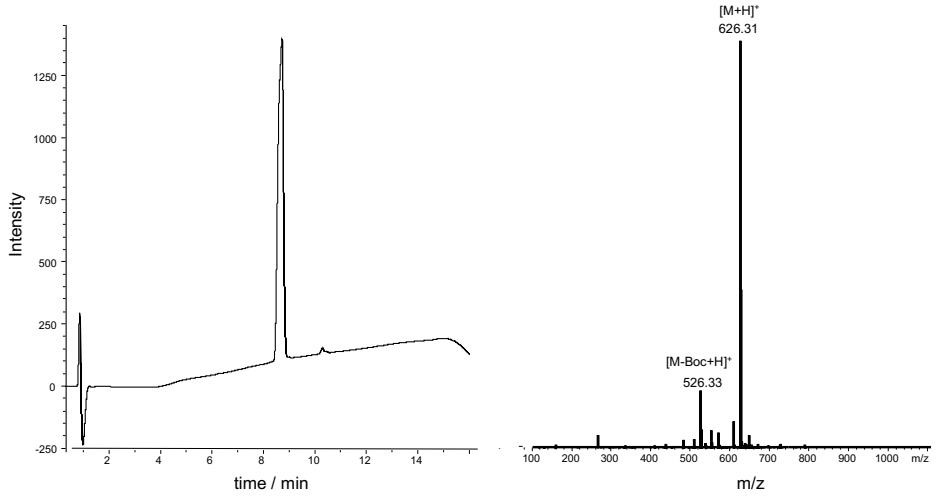

Figure S22 MS profile of A Boc-NH-G(Prop)-V-G-W-A-CONH$_2$ Calculated mass for $C_{31}H_{44}N_7O_7$: 626.3. Found: 626.3 $[M+H]^+$; 526.3 $[M\text{-}Boc+H]^+$.

Peptide modification

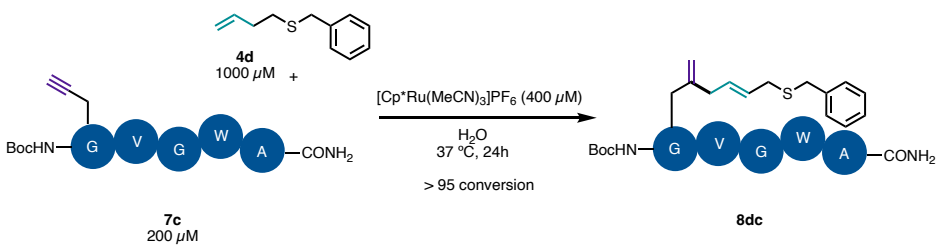

In a 100 µL Eppendorf vial were added 75 µL of water, followed by 5 µL of a solution of **7c** (4.0 mM in water), 15 µL of homoallylthioether **4d** (6.7 mM in THF) and finally 5 µL of **Ru2** (8.0 mM in DMSO), and the mixture was shaked at 700 rpm at 37 ºC for 24h. After the indicated time, the mixture was diluted with 100µL of MeOH and analyzed by HPLC-MS.

Full conversion of peptide **7c** was observed.

Just small quantities of adduct of product **8dc** and [Cp*Ru]+ were detected

Species detected

Product **7dc**:

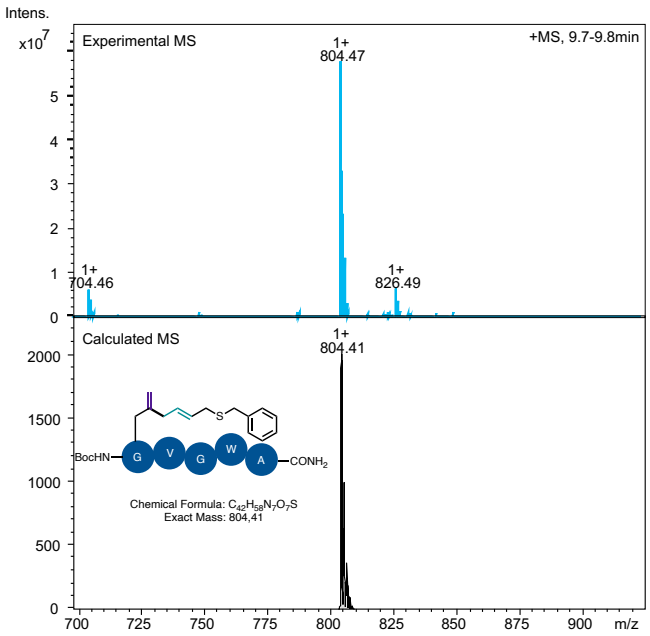

Figure S23. 7dc MS Calc for $C_{42}H_{58}N_7O_7S$ $[M+H]^+$ 804.4 found 804.7

Product [**7dc** +Cp*Ru]:

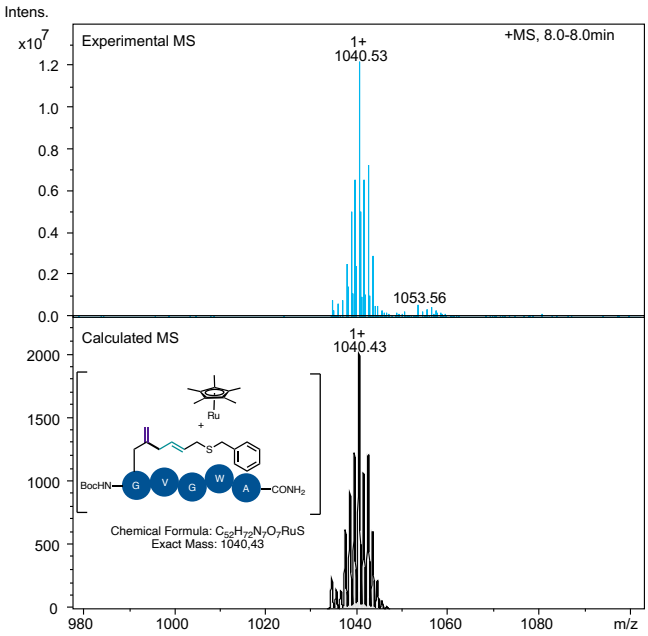

Figure S24. Calc for $C_{52}H_{72}N_7O_7RuS$ $[M+H]^+$ 1040.4 found 1040.5

[Cp*Ru+**4d**]:

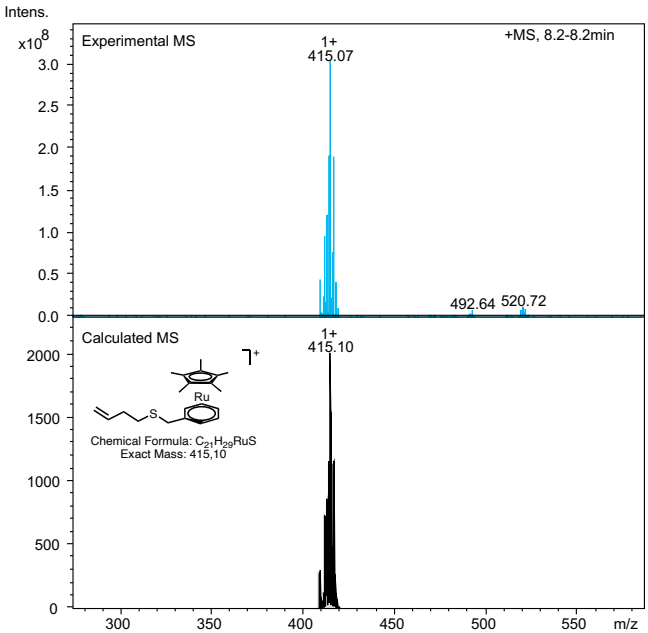

Figure S25. Calc $C_{21}H_{29}RuS$ for $[M+H]^+$ 415.1 found 415.1

[Cp*Ru+**4d**] Oxidized:

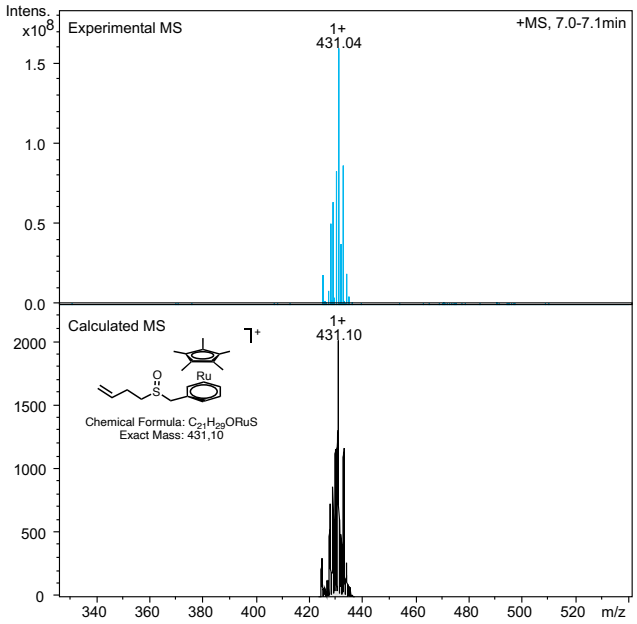

Figure S26. Calc $C_{21}H_{29}ORuS$ for $[M+H]^+$ 431.1 found 431.0

[Cp*Ru+**4d**] Oxidized:

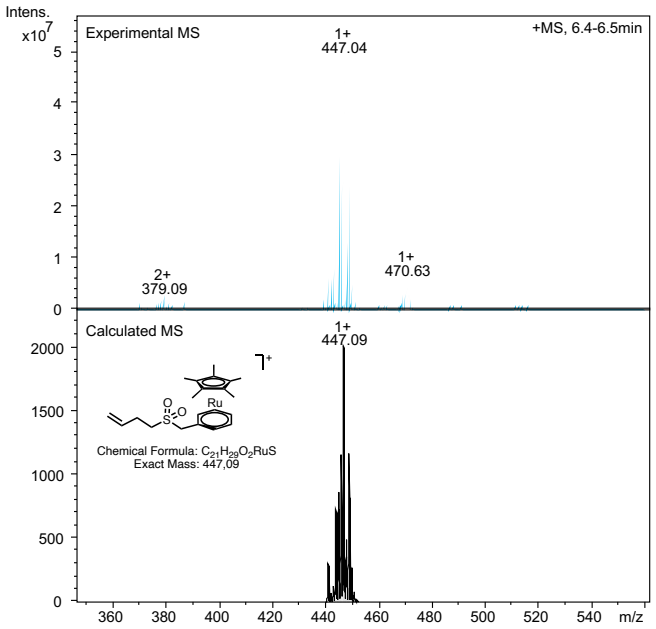

Figure S27. Calc $C_{21}H_{29}O_2RuS$ for $[M+H]^+$ 447.1 found 447.0

Selected NMR spectra

(*E*)-8-methyl-7-methylenenon-4-ene-1,8-diol (6be).

^{1}H-NMR (500 MHz, $CDCl_3$)

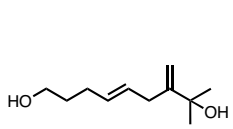

6be

^{13}C-NMR (126 MHz, $CDCl_3$)

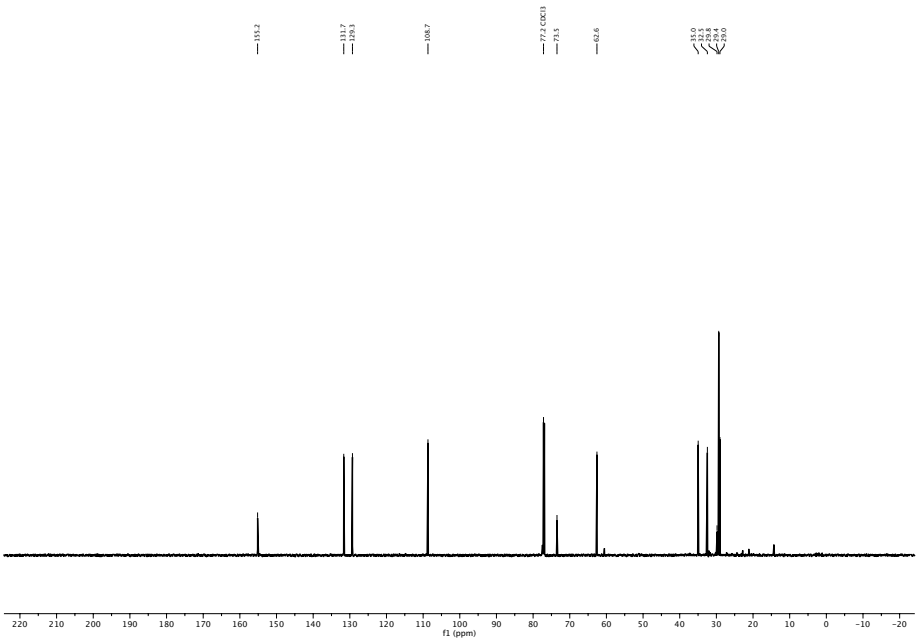

(*E*)-1-((5-(benzyloxy)-5-methyl-4-methylenehex-1-en-1-yl)oxy)-4-methoxybenzene (6aa).

^{1}H-NMR (300 MHz, $CDCl_3$)

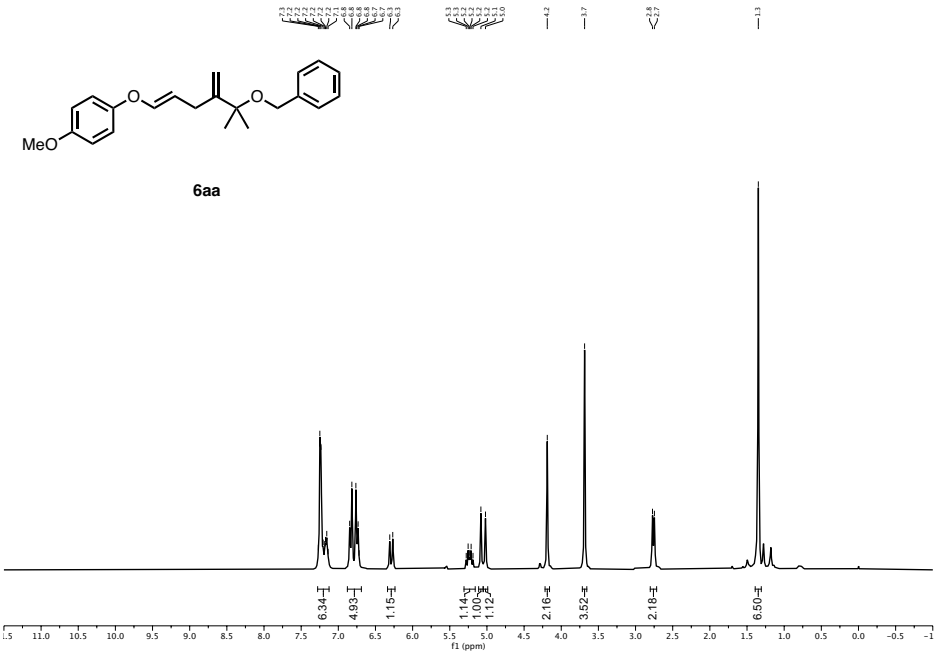

^{13}C-NMR (75 MHz, $CDCl_3$)

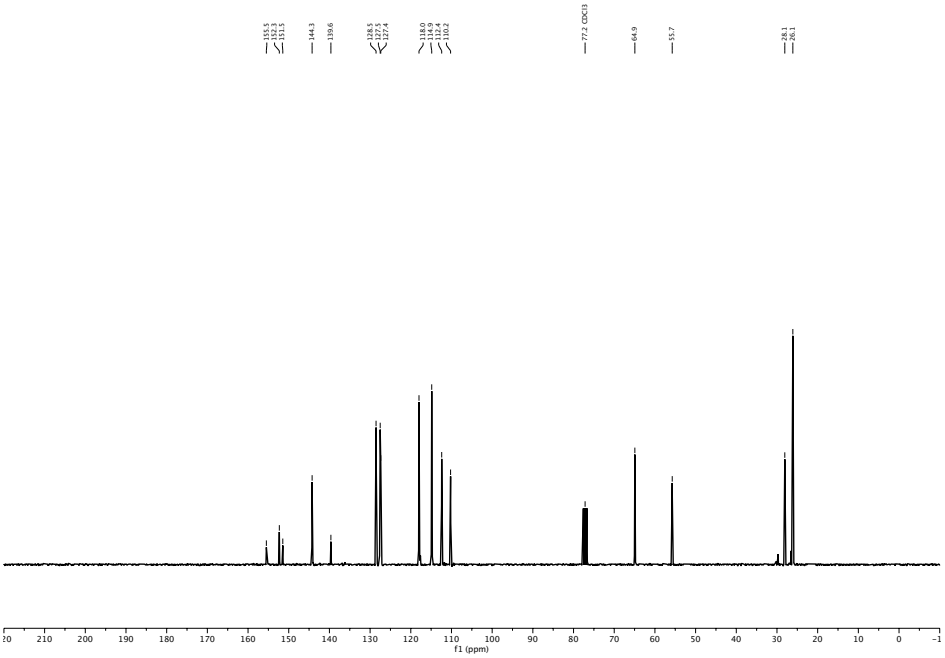

(E)-N-(7-(4-methoxyphenoxy)-2-methyl-3-methylenehept-5-en-2-yl)-4-methylbenzenesulfonamide (6ab).

^{1}H-NMR (300 MHz, $CDCl_3$)

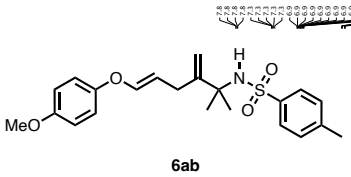

6ab

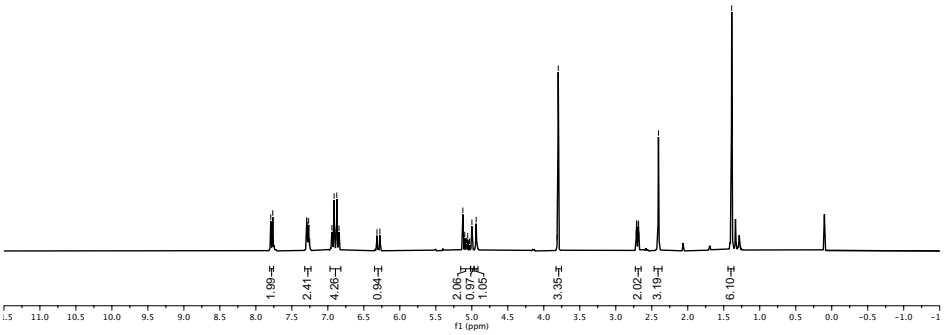

^{13}C-NMR (75 MHz, $CDCl_3$)

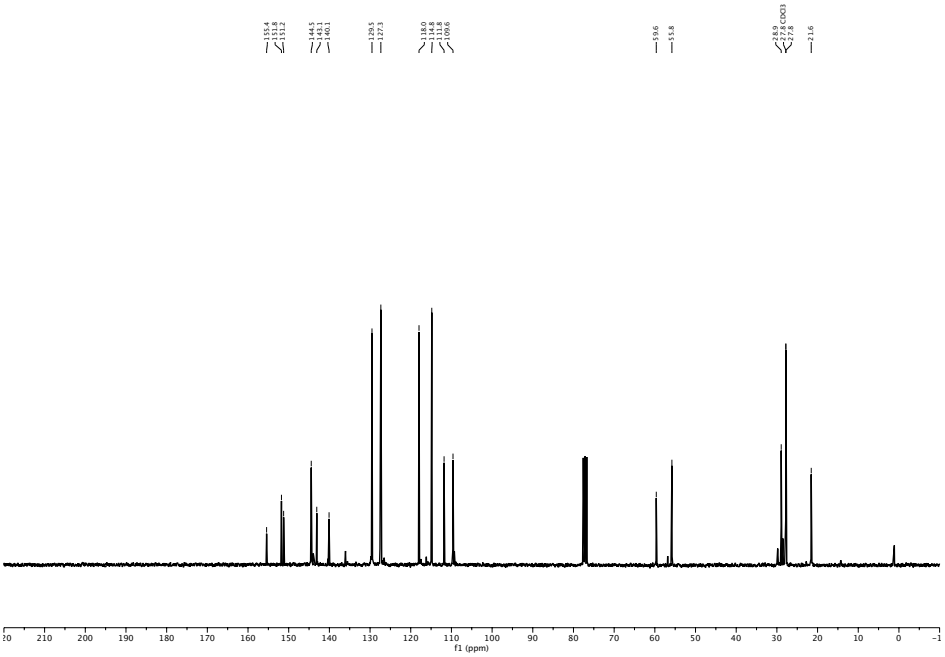

(*E*)-1-((4-((benzyloxy)methyl)penta-1,4-dien-1-yl)oxy)-4-methoxybenzene (6ac)

^{1}H NMR (300 MHz, $CDCl_3$)

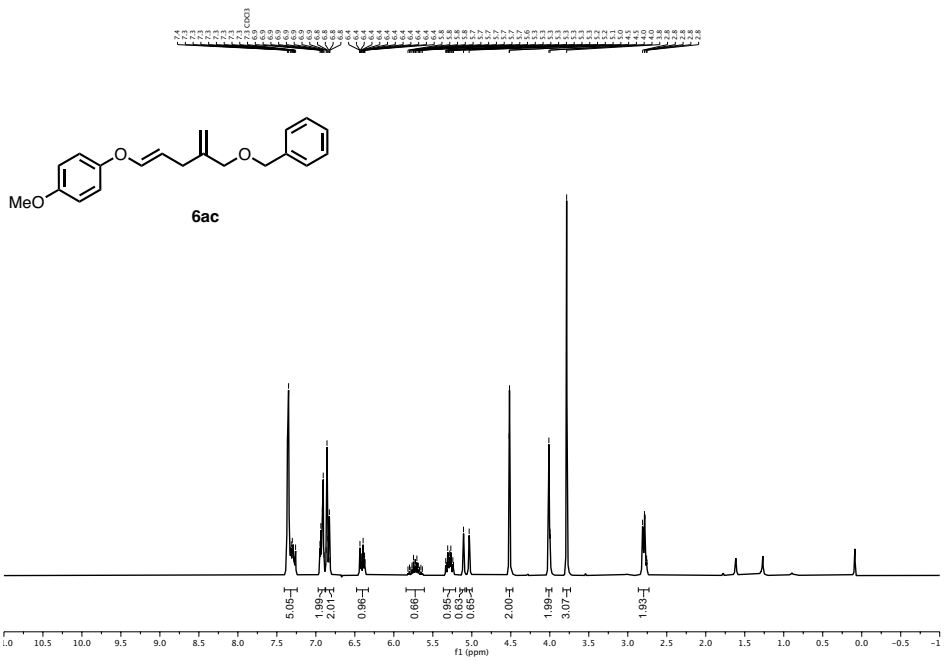

^{13}C NMR (75 MHz, $CDCl_3$)

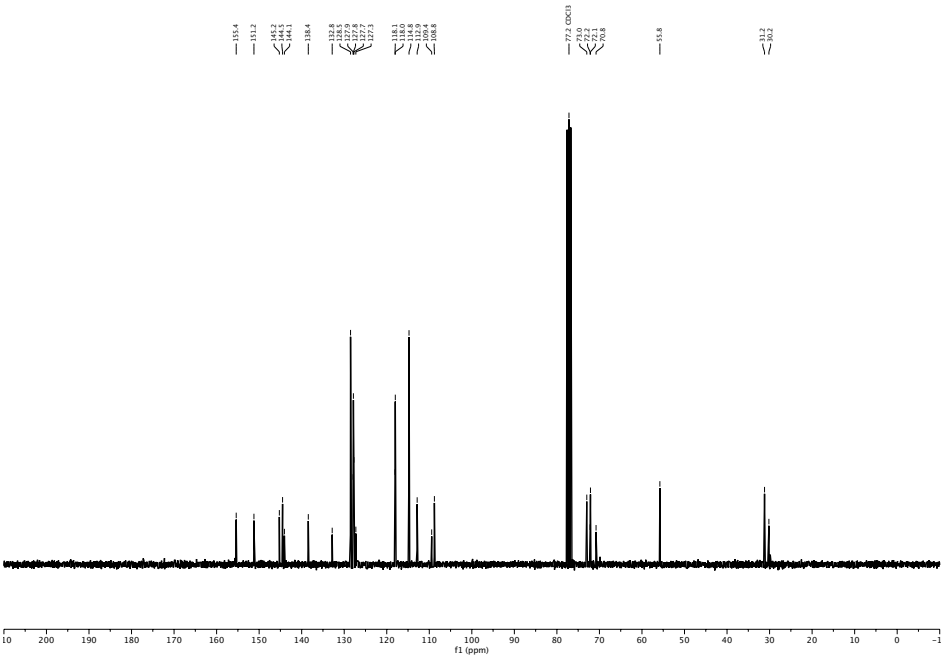

(*E*)-1-((5,5-dimethyl-4-methylenehex-1-en-1-yl)oxy)-4-methoxybenzene (6ad)

^{1}H NMR (300 MHz, $CDCl_3$)

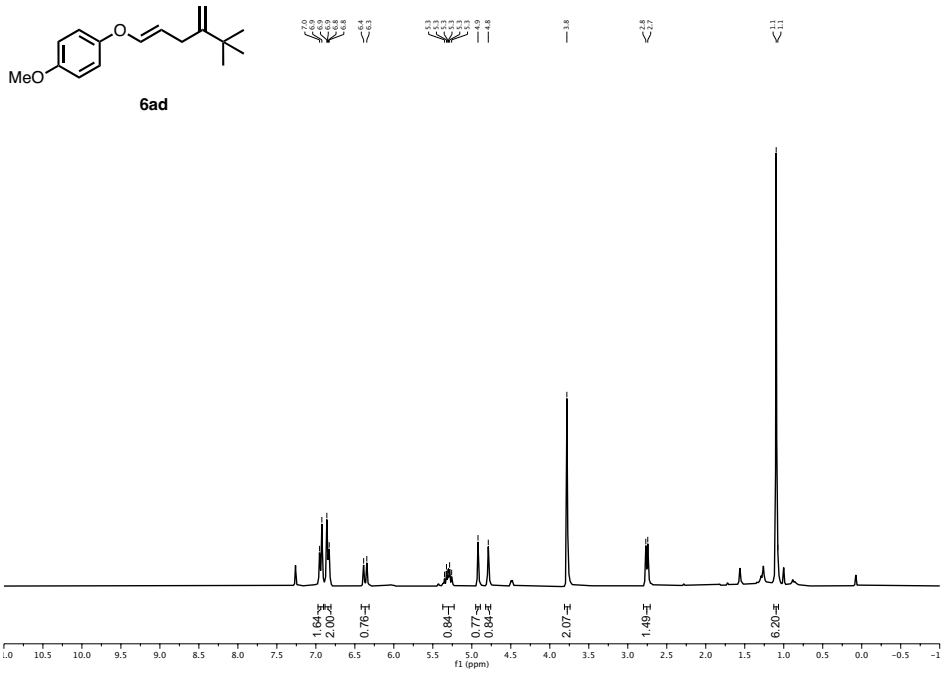

^{13}C NMR (75 MHz, $CDCl_3$)

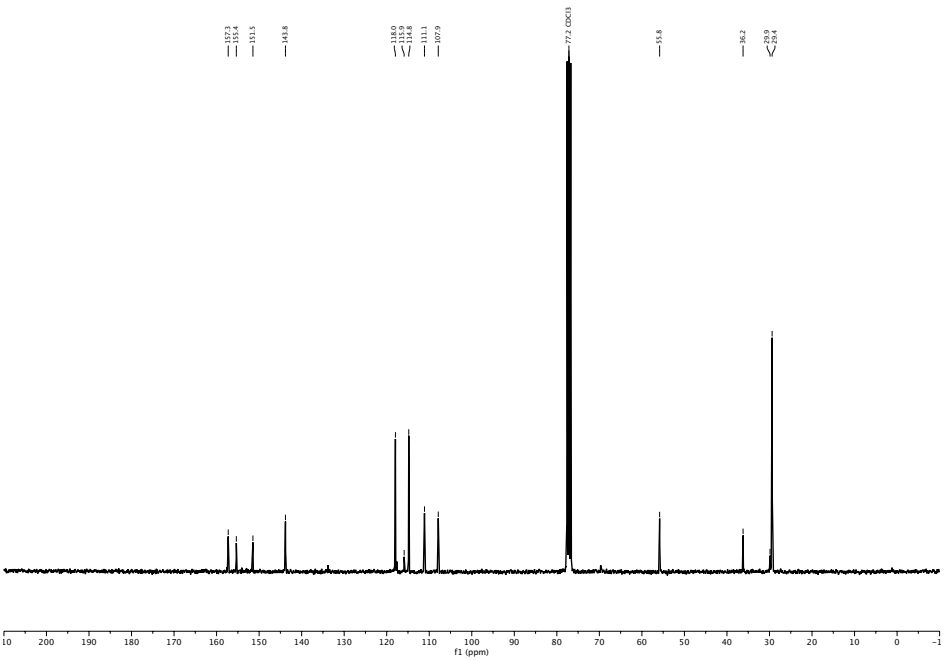

(8*R*,9*S*,13*S*,14*S*,17*R*)-3-methoxy-17-((*E*)-5-(4-methoxyphenoxy)penta-1,4-dien-2-yl)-13-methyl-7,8,9, 11,12,13,14,15,16,17-decahydro-6*H*-cyclopenta[*a*]phenanthren-17-ol (6am).

^{1}H NMR (500 MHz, $CDCl_3$)

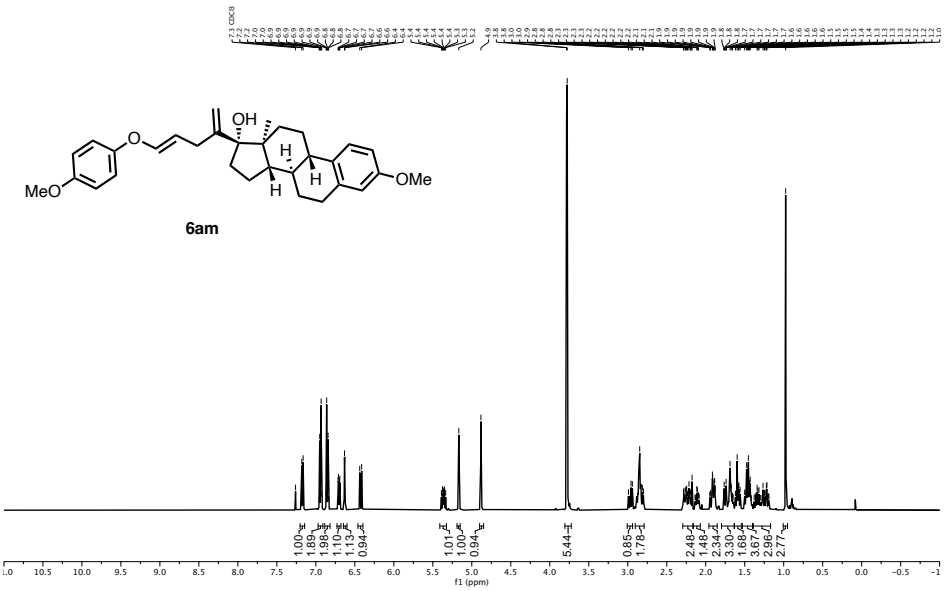

^{13}C NMR (126 MHz, $CDCl_3$)

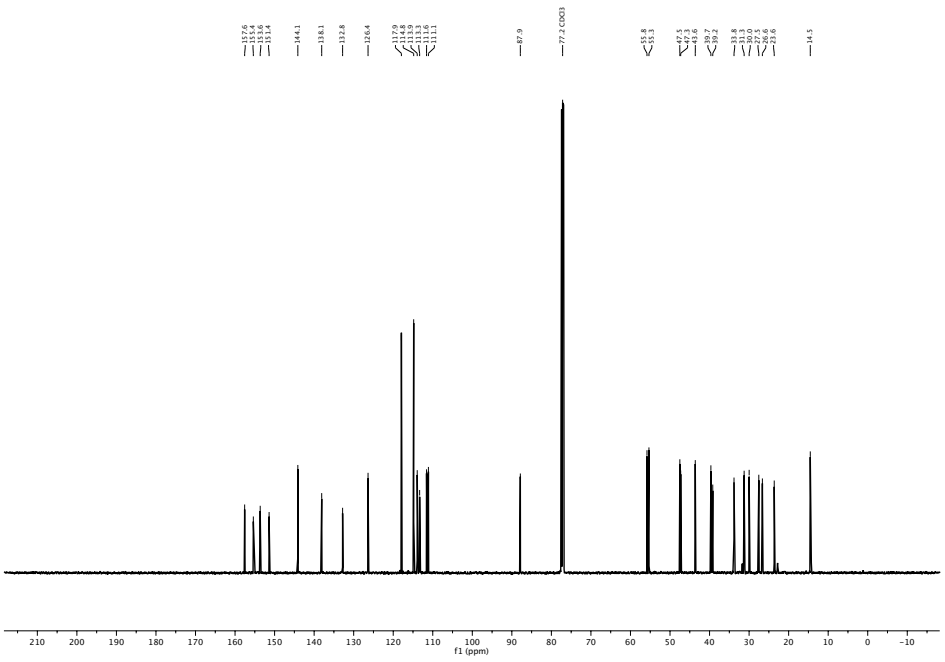

Methyl (*S*,*E*)-2-((*tert*-butoxycarbonyl)amino)-3-(4-((4-(1-hydroxycyclopentyl)penta-1,4-dien-1-yl)oxy)phenyl)propanoate (6eh).

^{1}H NMR (300 MHz, $CDCl_3$)

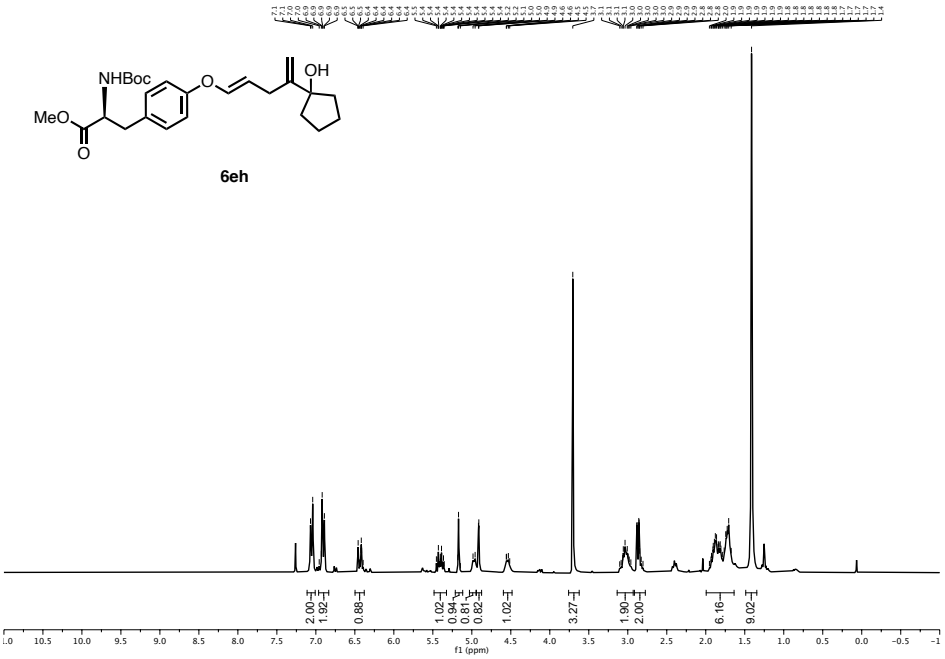

^{13}C NMR (75 MHz, $CDCl_3$)

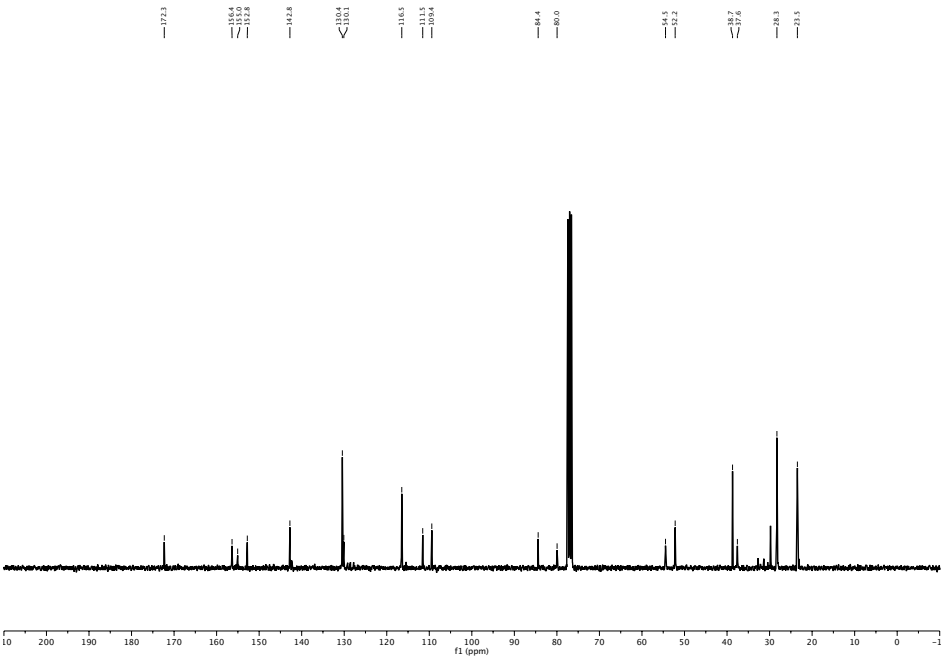

methyl (*E*)-*N*-(6-(4-methoxyphenoxy)-2-methyl-3-methylenehex-4-en-2-yl)-*N*-tosylglycylphenylalaninate (8ab)

^{1}H NMR (300 MHz, $CDCl_3$)

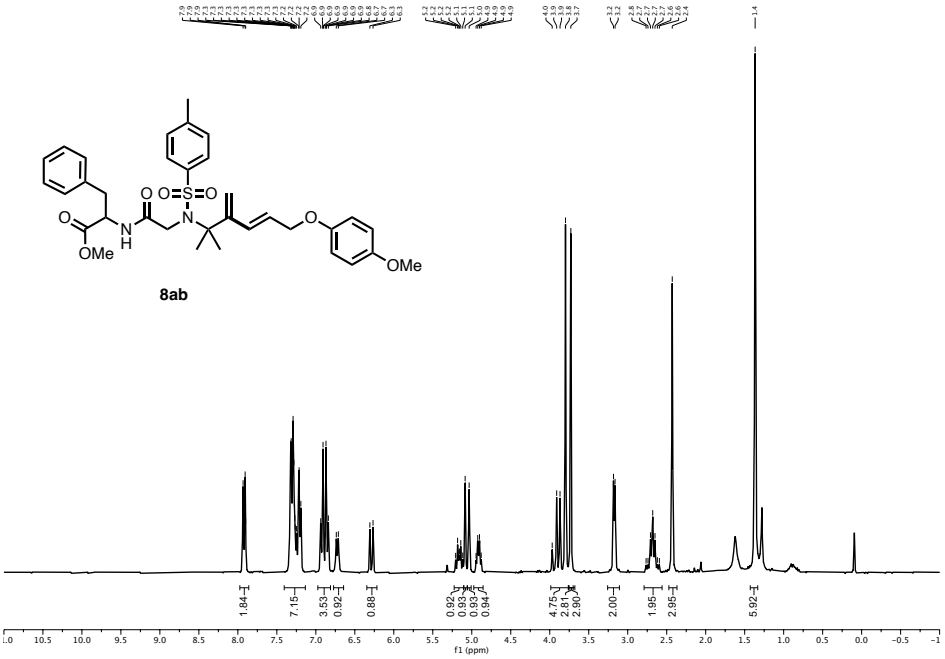

^{13}C NMR (75 MHz, $CDCl_3$)

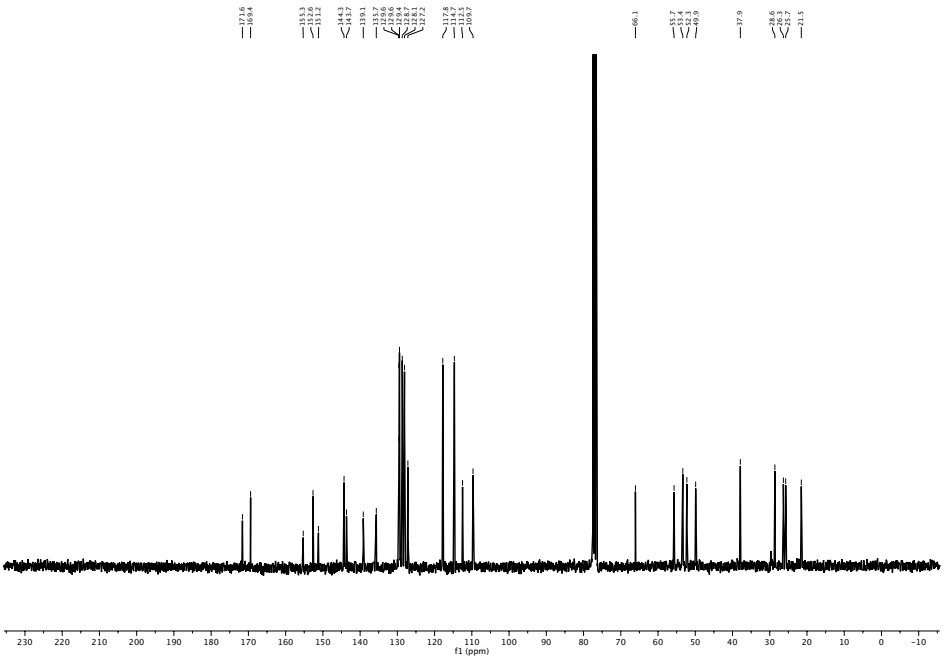

methyl ((*S*,*E*)-2-((((9*H*-fluoren-9-yl)methoxy)carbonyl)amino)-7-(4-methoxyphenoxy)-4-methylenehept-5-enoyl)-*L*-valinate.

^{1}H NMR (300 MHz, $CDCl_3$)

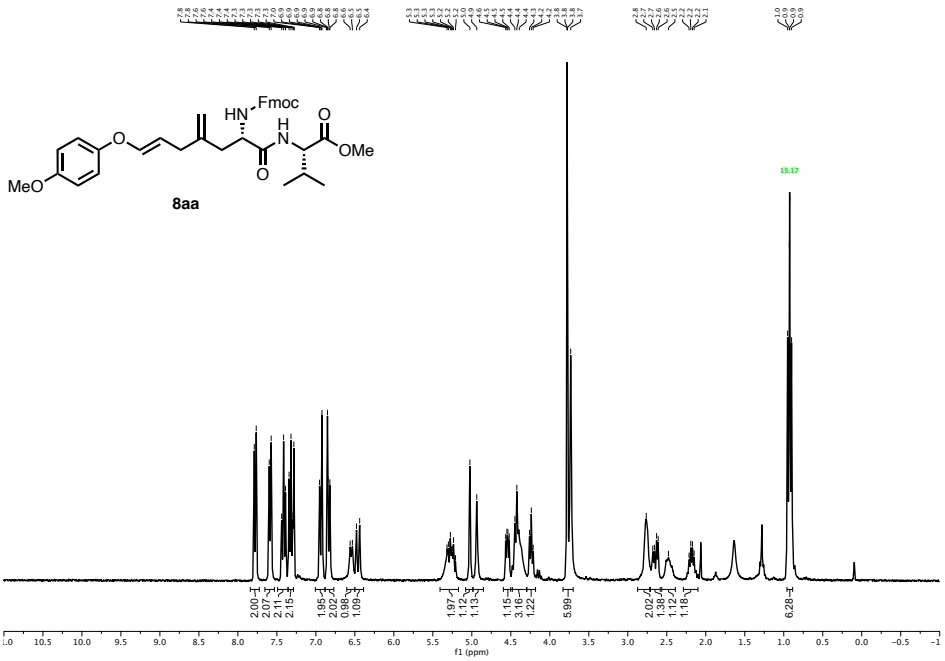

^{13}C NMR (75 MHz, $CDCl_3$)

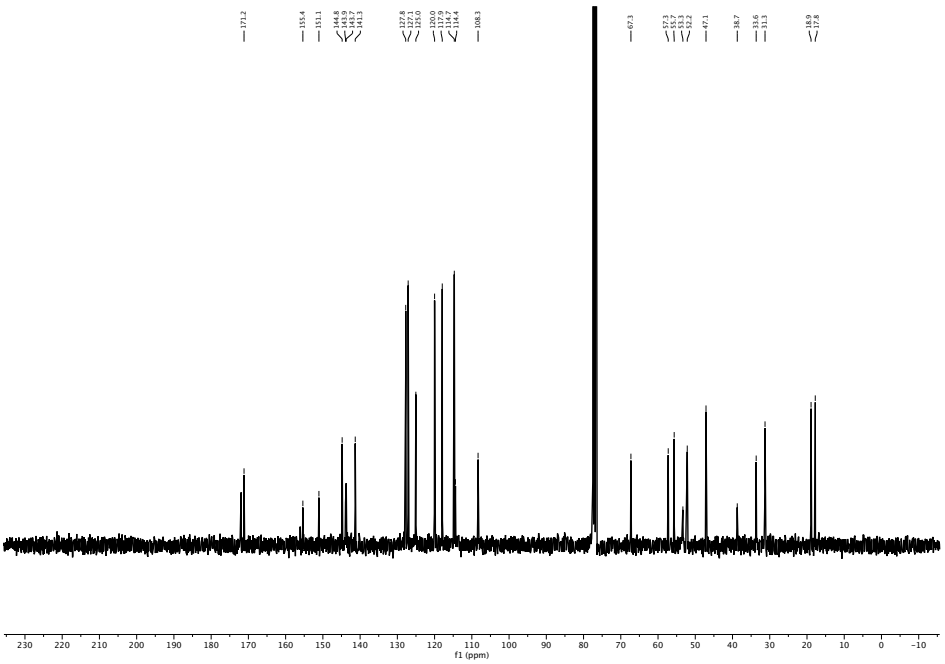

Experimental Section:

Chapter III: Isomerization of allylic alcohols in biological settings

Synthesis of complexes

[{Ru(η³ : η³ -$C_{10}H_{16}$)Cl(μ-Cl)}$_2$] (Ru10)

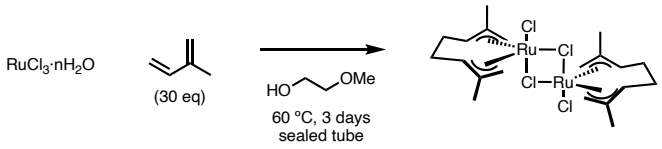

The synthesis of **[{Ru(η³ : η³ -$C_{10}H_{16}$)Cl(μ-Cl)}$_2$]** (**Ru10**) was carried out according to a reported procedure: [1]

$RuCl_3$·x H_2O (4.4 mmol, 1.00 g, 1.0 equiv) was added to a heat gun dried pressure Schlenk tube and then 2-methoxyethanol (13.0 mL, 0.34 M) and isoprene (139.9 mmol, 14.0 mL, 31.6 equiv) were added under nitrogen. The solution became dark and was stirred for 3 days at 60 °C. After this time, the reaction was cooled at room temperature and the solid was collected by filtration. The pink solid was washed with Et_2O (3 x 15.0 mL) and the solvent removed under reduced pressure

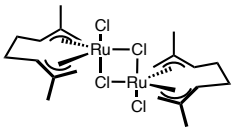

[{Ru(η³ : η³ -$C_{10}H_{16}$)Cl(μ-Cl)}$_2$] (**Ru10**) Isolated as a pink solid. Yield = 38%. The NMR data is in accordance with that previously reported. **^{1}H NMR** (300 MHz, $CDCl_3$): δ 6.09 (s, 1H), 5.72 (s, 1H), 5.40 (s, 1H), 5.22 (s, 1H), 5.07 (s, 1H), 4.87 (s, 1H), 4.74 (s, 1H), 4.73 (m, 1H), 4.65 (m, 1H), 4.49 (s, 1H), 4.48 (m, 1H), 4.45 (m, 1H), 2.7 - 2.4 (m, 2H), 2.47 (s, 3H), 2.38 (s, 3H), 2.28 (s, 3H), 2.24 (s, 3H). Resonances not specifically assigned to different diastereoisomers.

[{Ru(η³ : η³-$C_{10}H_{16}$)Cl (OAc)] (Ru11).

Ru6

The synthesis of **[{Ru(η³ : η³-$C_{10}H_{16}$)Cl (OAc)]** was carried out according to a reported procedure: [2]

The ruthenium complex [{Ru(η³ : η³-$C_{10}H_{16}$)Cl(μ-Cl)}$_2$] (0.3 mmol, 200.0 mg, 1.0 equiv) was suspended in acetone (25.0 mL, 0.01 M) in a heat gun dried Schlenk equipped with a stir bar. Then, AgOAc was added (0.7 mmol, 108.3 mg, 2.0 equiv) and the mixture was

[1] J. G. Toerien, P. H. Van Rooyen, *J. Chem. Soc., Dalton Trans.* **1991**, 1563–1568.
[2] B. Kavanagh, J. W. Steed, D. A. Tocher, *J. Chem. Soc., Dalton Trans.* **1993**, 327.

stirred at room temperature for 1 h in the absence of light. The resulting orange-red solution was then filtered over celite to remove the precipitate of AgCl and the solvent was removed under reduced pressure to give a pale brown solid.

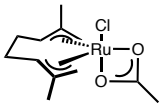

[{Ru(η^3 : η^3-$C_{10}H_{16}$)Cl (OAc)] (**Ru11**). Isolated as pale brown solid. Yield = 60%. The NMR data is in accordance with that previously reported. **^{1}H NMR** (300 MHz, $CDCl_3$): δ 5.51 (s, 1H), 4.65 (s, 1H), 4.63 (s, 1H), 4.20 (s, 1H), 3.56 (s, 1H), 3.49 (m, 1H), 2.53 (m, 4H), 2.29 (s, 3H), 2.12 (s, 3H), 1.85 (s, 3H).

Synthesis of [Cp* Ir (N-phenyl-2-pyridinecarbomidate)Cl] (Ir2).

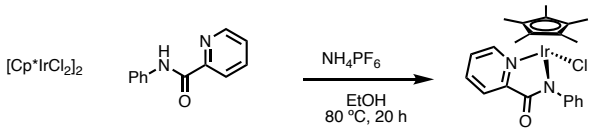

The synthesis of **[Cp*Ir(N-phenyl-2-pyridinecarbomidate)Cl]** (**Ir2**) was carried out according to a reported procedure:[3]

Pyridine-2-carboxylic acid phenylamide (75.0 µmol, 14.9 mg, 2.0 equiv) was added to a stirred suspension of $[Cp^*IrCl_2]_2$ (38 µmol, 30.0 mg, 1.0 equiv) in EtOH (9.4 mL, 4.0 µM) in a heat gun dried Schlenk equipped with a stir bar. The reaction mixture was stirred at 80 °C. After 15 min, $[NH_4][PF_6]$ (0.2 mmol, 28.8 mg, 4.7 equiv) was added and the mixture was stirred at 80 °C for 20 h. After that, the solvent was evaporated and the residue was dissolved in CH_2Cl_2 (30.0 mL), washed with water (2 x 10.0 mL), brine (10.0 mL), dried over $MgSO_4$ and evaporated to form an orange solid. The crude product was recrystallized by vapor diffusion using CH_2Cl_2 / pentane.

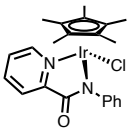

[Cp*Ir (N-phenyl-2-pyridinecarbomidate)Cl] (**Ir2**). Isolated as orange crystals (24 mg, 42 µmol, 57% yield). The NMR data is in accordance with that previously reported.[4] **^{1}H NMR** (300 MHz, $CDCl_3$): δ 8.57 (br d, J = 5.4 Hz, 1H), 8.17 (br d, J = 8.0 Hz, 1H), 7.92 (ddd, J = 7.7, 7.7, 1.4 Hz, 1H), 7.65 (br dd, J = 8.3, 1.1 Hz, 2H), 7.49 (ddd, J = 7.5, 5.6, 1.4 Hz, 1H), 7.32 (m, 2H), 7.09 (t, J = 7.1 Hz, 1H), 1.41 (s, 15H).

[3] Z. Almodares, S. J. Lucas, B. D. Crossley, A. M. Basri, C. M. Pask, A. J. Hebden, R. M. Phillips, P. C. McGowan, *Inorg. Chem.* **2014**, *53*, 727–736.
[4] S. Bose, A. H. Ngo, L. H. Do, *J. Am. Chem. Soc.* **2017**, *139*, 8792–8795.

Substrates

Allylic alcohol **9a** is commercial and was used without further purification,

General procedure for the preparation of aryl allylic alcohols (9)

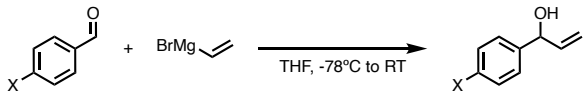

The synthesis of the different allylic alcohols (**9**) was carried out according to a reported procedure: [5]

In a flame dried round bottom flask, a 1.0 M solution of vinylmagnesium bromide in THF (11.0 mL, 11.0 mmol, 1.1 equiv) was added via syringe to a solution of aryl aldehyde (10.0 mmol) in dry THF (0.3 M) at -78 °C over 30 min. Upon complete addition, the reaction was allowed to reach room temperature and stirred overnight. Then, the reaction was quenched with saturated aqueous NH_4Cl (20.0 mL), stirred for 20 min, and extracted with EtOAc (3 x 25.0 mL). The combined organic phases were washed with brine (20.0 mL), dried, filtered, concentrated under reduced pressure and the crude purified by FCC.

1-(p-tolyl)prop-2-en-1-ol (9b).

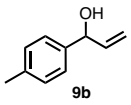

9b

Prepared according to the above representative procedure. Colorless liquid (1.07 g, 7.2 mmol, 72% yield). Rf = 0.6 (Hexane / EtOAc 80:20). Yield = 72%. The NMR data is in accordance with that previously reported. **^{1}H-NMR** (300 MHz, $CDCl_3$): δ 7.28 (d, *J* = 8.3 Hz, 2H), 7.20 (d, *J* = 8.3 Hz, 2H), 6.07 (dddd, *J* = 17.1, 10.3, 5.9, 0.4 Hz, 1H), 5.35 (dtd, *J* = 17.1, 1.4, 0.4 Hz, 1H), 5.21 (dtd, *J* = 10.3, 2.0, 0.8 Hz, 1H), 5.14 (d, *J* = 5.9 Hz, 1H), 2.40 (s, 3H).

1-(4-methoxyphenyl)prop-2-en-1-ol (9c).

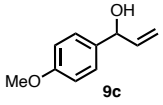

9c

Prepared according to the above representative procedure. Isolated as colorless liquid (1.43 g, 8.8 mmol, 87% yield). **Rf** = 0.6 (Hexane / EtOAc 80:20). The NMR data is in accordance with that previously reported **^{1}H-NMR** (300 MHz, $CDCl_3$): δ 7.28 (d, *J* = 8.0 Hz, 2H) 6.89 (d, *J* = 8.0, 2H), 6.08 - 5.98 (m, 1H), 5.32 (d, *J* = 18.4 Hz, 1H), 5.18 (d, *J* = 10.3, 1H), 5.13 (br s, 1H), 3.78 (s, 3H).

[5] P. Truong, C. S. Shanahan, M. P. Doyle, *Org. Lett.* **2012**, *14*, 3608–3611.

1-(4-bromophenyl)prop-2-en-1-ol (9d).

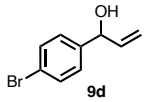

Prepared according to the above representative procedure. Isolated as colorless liquid (1.17 g, 5.5 mmol, 55% yield). Rf = 0.6 (Hexane / EtOAc 80:20). The NMR data is in accordance with that previously reported. **^{1}H-NMR** (300 MHz, $CDCl_3$): δ 7.48 (dd, *J* = 8.5, 3.0 Hz, 2H), 7.25 (dd, *J* = 8.5, 3.0 Hz, 2H), 6.04 - 5.97 (m, 1H), 5.34 (dd, *J* = 17.0, 1.5 Hz, 1H), 5.23 - 5.21 (m, 1H), 5.17 (br s, 1H), 2.01 (bs, 1H).

1-(6-methoxynaphthalen)prop-2-en-1-ol (9f).

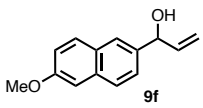

Prepared according to the above representative procedure. Isolated as white solid (1.62 g, 7.6 mmol, 76% yield). Rf = 0.17 (Hexane / EtOAc 90:10). The NMR data is in accordance with that previously reported.[6] **^{1}H-NMR** (300 MHz, $CDCl_3$) δ 7.76 - 7.66 (m, 3H), 7.44 (dd, *J* = 8.6, 1.7 Hz, 1H), 7.16 (dd, *J* = 8.8, 2.6 Hz, 1H), 7.12 (d, *J* = 2.5 Hz, 1H), 6.12 (ddd, *J* = 17.1, 10.3, 5.9 Hz, 1H), 5.39 (dt, *J* = 17.1, 1.5 Hz, 1H), 5.29 (d, *J* = 5.9 Hz, 1H), 5.22 (dt, *J* = 10.3, 1.4 Hz, 1H), 3.90 (s, 3H).

Synthesis of 1-(6-bromonaphthalen-2-yl)pyrrolidine (9g)

6-(pyrrolidin-1-yl)-2-naphthaldehyde

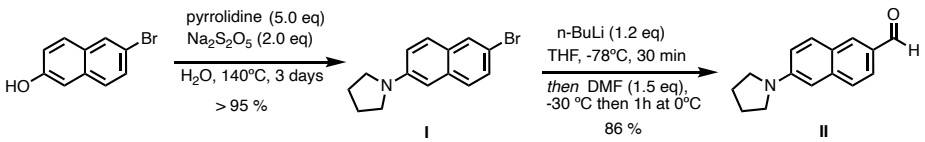

The synthesis of **6-(pyrrolidin-1-yl)-2-naphthaldehyde** (**II**). and related allylic alcohols was carried out according to a reported procedure:[7]

i) A mixture of pyrrolidine (43.5 mmol, 3.6 mL, 5.0 equiv), 6-bromo-2-naphtol (8.7 mmol, 2.0 g), $Na_2S_2O_5$ (17.4 mmol, 3.3 g, 2.0 equiv) and water (19.3 mL, 0.5 M) in a sealed tube was stirred at 145 °C for 48 h. After being cooled to room temperature the reaction mixture was diluted with 20.0 mL of water and the product was extracted with CH_2Cl_2 (2 x 30.0 mL). The organic phases were dried over $MgSO_4$ and the solvent removed under reduced pressure

[6] Y. Liu, Y. L. Tan, X. Zhang, G. Bhabha, D. C. Ekiert, J. C. Genereux, Y. Cho, Y. Kipnis, S. Bjelic, D. Baker, J. W. Kelly, *Proc. Natl. Acad. Sci. U.S.A.* **2014**, *111*, 4449–4454.
[7] S. Singha, Y. W. Jun, J. Bae, K. H. Ahn, *Anal. Chem.* **2017**, *89*, 3724–3731.

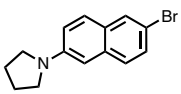

I

1-(6-bromonaphthalen-2-yl)pyrrolidine (I) FCC in hex:EtOAc (9:1 to 6:4) White solid. (1.84g, 8.3 mmol, 95% yield) Rf = 0.65 (Hex: EtOAc 90:10). The NMR data is in accordance with that previously reported. **^{1}H NMR** (300 MHz, $CDCl_3$): 7.81 (s, 1H), 7.61 (d, *J* = 8.7 Hz, 1H), 7.51 (d, *J* = 9.1 Hz, 1H), 7.39 (dd, *J* = 9.1, 2.1, 1H), 7.01 (m, 1H), 6.77 (bs, 1H), 3.41 (m, 4H), 2.07 (m, 4H).

ii) 1-(6-bromonaphthalen-2-yl)pyrrolidine (**I**) (3.0 mmol, 828.5 mg) was dissolved in anhydrous THF (7.5 mL, 0.4 M) in a heat gun dried round bottom flask, and the solution was cooled to -78 °C under nitrogen. Then, 2.5 M *n*-BuLi in hexane (4.5 mmol, 1.4 mL, 1.2 equiv) was added. The reaction was stirred at -30 °C for 1 h and then treated with anhydrous DMF (4.5 mmol, 0.4 mL, 1.5 equiv). It was allowed to attain 0 °C and after being stirred at that temperature for 1 h, the reaction mixture was quenched with sat. NH_4Cl (5.0 mL). The product was extracted with CH_2Cl_2 (2 x 30.0 mL). The organic phases were dried over $MgSO_4$ and the solvent removed under reduced pressure

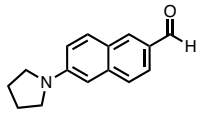

II

6-(pyrrolidin-1-yl)-2-naphthaldehyde (II). FCC in Hex: EtOAc (95:5 to 80:20), isolated as yellow solid (580 mg, 2.6 mmol, 86% yield). Rf = 0.16 (Hexane / EtOAc 95:5). Yield = 86%. The NMR data is in accordance with that previously reported. **^{1}H NMR** (300 MHz, $CDCl_3$): δ 9.99 (s, 1H), 8.13 (s, 1H), 7.90 (d, *J* = 9.6 Hz, 1H), 7.61 (d, *J* = 8.4 Hz, 1H), 7.00 (dd, *J* = 9.0, 2.4 Hz, 1H), 6.73 (d, *J* = 2.4 Hz, 1H), 3.43 (t, *J* = 6.6 Hz, 4H), 2.11 − 2.06 (m, 4H).

1-(6-(pyrrolidin-1-yl)naphthalen-2-yl)prop-2-en-1-ol (9g).

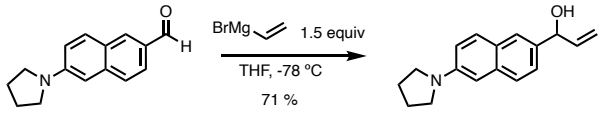

II 9g

6-(pyrrolidin-1-yl)-2-naphthaldehyde (**II**) (1.1 mmol, 250.0 mg) was dissolved in anhydrous THF (3.7 mL, 0.3 M) in a heat gun dried round bottom flask. The reaction was cooled to -78 °C and the 1.0 M vinyl magnesium bromide in hexane (1.7 mmol, 1.7 mL, 1.5 equiv) was added via syringe slowly. After that, the reaction was warmed to room temperature and followed by TLC. After 3 h, the reaction was quenched with sat. NH_4Cl

(5.0 mL). The product was extracted with CH_2Cl_2 (2 x 30.0 mL). The organic phases were dried over $MgSO_4$ and the solvent removed under reduced pressure.

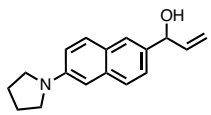

9g

1-(6-(pyrrolidin-1-yl)naphthalen-2-yl)prop-2-en-1-ol (9g). FCC in Hex:EtOAc (95:5 to 80:20) isolated ad yellow solid (197 mg, 0.78 mmol, 71% yield). Rf = 0.1 (Hexane / EtOAc 90:10). **^{1}H NMR** (300 MHz, $CDCl_3$): δ 7.70 – 7.62 (m, 3H), 7.35 (dd, *J* = 8.5, 1.3 Hz, 1H), 6.99 (dd, *J* = 8.9, 2.3 Hz, 1H), 6.74 (d, *J* = 1.8 Hz, 1H), 6.14 (ddd, J = 16.7, 10.3, 5.7 Hz, 1H), 5.39 (d, *J* = 17.2 Hz, 1H), 5.30 (t, *J* = 4.4 Hz, 1H), 5.22 (d, *J* = 10.4 Hz, 1H), 3.40 (t, *J* = 6.5 Hz, 4H), 2.10 - 2.00 (m, 4H). **^{13}C NMR** (126 MHz, $CDCl_3$): δ 146.1, 140.4, 135.2, 134.9, 128.9, 126.3, 125.9, 125.0, 124.9, 115.9, 114.7, 104.7, 75.5, 47.8, 25.5. **HRMS-ESI** Calculated for $C_{17}H_{20}NO$: 254.1539, found 254.1537.

General procedure for the preparation of (E)-1,4-dien-3-ols

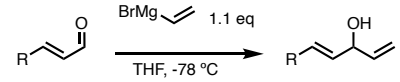

The synthesis of **9i** and related bis allylic alcohols was carried out according to a reported procedure:[8]

In a heat gun dried round bottom flask, a 1.0 M solution of vinylmagnesium bromide in THF (11.0 mL, 11.0 mmol, 1.1 equiv) was added via syringe to a solution of the corresponding aldehyde (10.0 mmol) in dry THF (0.3 M) at 0 °C over 10 min. Upon complete addition, the reaction was warmed at room temperature and follows by TLC using hexane / EtOAc (80:20) as eluents. Then the reaction was quenched with saturated aqueous NH_4Cl (20.0 mL), stirred for 20 min, and extracted with EtOAc (3 x 25.0 mL). The combined organic layer was washed with brine (20.0 mL), dried, filtered, and the solvent reduced under reduced pressure. FCC in Hex:EtOAc (from 90:10 to 70:30).

(E)-1-phenylpenta-1,4-dien-3-ol (9h)

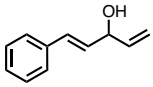

9h

Prepared according to the above representative procedure. Colorless liquid (1.3 g, 8.4 mmol, 84% yield). Rf = 0.43 (Hexane / EtOAc 80:20). The NMR data is in accordance with that previously reported. **^{1}H NMR**

[8] P. Radha Krishna, D. V. Ramana, *J. Org. Chem.* **2012**, *77*, 674–679.

(300 MHz, $CDCl_3$): δ 7.39 (dt, *J* = 2.8, 2.0 Hz, 2H), 7.36 - 7.29 (m, 2H), 7.29 - 7.21 (m, 1H), 6.64 (d, *J* = 16.1 Hz, 1H), 6.30 (d, *J* = 16.1 Hz, 1H), 6.06 (dd, *J* = 17.3, 10.6 Hz, 2H), 5.37 (dd, *J* = 17.3, 1.1 Hz, 2H), 5.23 (dd, *J* = 10.6, 1.1 Hz, 2H), 1.82 (d, *J* = 2.5 Hz, 1H).

(E)-1-(4-methoxyphenyl)penta-1,4-dien-3-ol (9i).

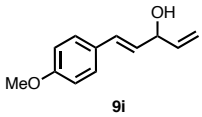

9i

Prepared according to the above representative procedure. Yellow syrup (1.27 g, 6.7 mmol, 67% yield). Rf = 0.41 (Hexane / EtOAc 70:30). The NMR data is in accordance with that previously reported.[15] **^{1}H-NMR** (300 MHz, $CDCl_3$): 7.43 - 7.30 (m, 2H), 6.96 - 6.82 (m, 2H), 6.66 - 6.51 (m, 1H), 6.12 (dd, *J* = 15.9, 6.6 Hz, 1H), 6.00 (ddd, *J* = 17.1, 10.3, 5.8 Hz, 1H), 5.35 (dt, *J* = 17.4, 1.4 Hz, 1H), 5.21 (dt, *J* = 10.4, 1.2 Hz, 1H), 4.81 (q, *J* = 5.5 Hz, 1H), 3.83 (s, 3H).

(E)-octa-1,4-dien-3-ol (9j).

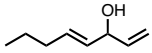

9j

Prepared according to the above representative procedure. Colorless liquid (630 mg, 5.0 mmol, 50% yield). Rf = 0.13 (Hexane / EtOAc 95:5). The NMR data is in accordance with that previously reported.[8] **^{1}H NMR** (300 MHz, $CDCl_3$): δ 6.02 - 5.82 (m, 1H), 5.78 - 5.63 (m, 1H), 5.58 - 5.44 (m, 1H), 5.25 (dq, *J* = 17.2, 1.6 Hz, 1H), 5.12 (dq, *J* = 10.4, 1.6 Hz, 1H), 4.69 - 4.46 (t, *J* = 5.8 Hz, 1H), 2.12 - 1.93 (m, 2H), 1.48 - 1.31 (m, 2H), 0.90 (td, *J* = 7.4, 1.4 Hz, 3H).

Synthesis of 1-phenylprop-2-en-1-*d*-1-ol (9a-*d*).

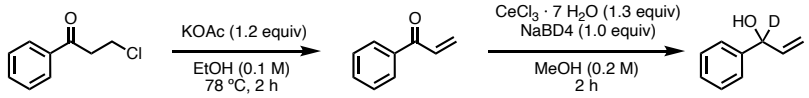

The synthesis of **9a-*d*** was carried out according to a reported procedure:[9]

i) A mixture of 3-chloro-1-phenyl-1-propanone (1.0 g, 5.8 mmol) and KOAc (684.0 mg, 6.9 mmol, 1.2 equiv) in EtOH (50.0 mL, 0.1 M) was stirred under reflux for 2.5 h. After cooling to room temperature the solvent was evaporated and the residue was dissolved in EtOAc (50.0 mL) and washed with H_2O (3 x 50.0 mL). The organic phases were dried over $MgSO_4$ and the solvent removed under reduced pressure.

[9] A. Bartoszewicz, M. Livendahl, B. Martín-Matute, *Chem. Eur. J.* **2008**, *14*, 10547–10550.

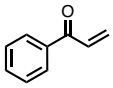

1-phenyl-2-en-1-one. FCC in Hex:EtOAc (100:1 to 95:5), isolated as a colorless oil (317 mg, 2.4 mmol, 50% yield). $\mathbf{R_f}$ = 0.29 (Hexane / EtOAc 95:5). The NMR data is in accordance with that previously reported. **^{1}H NMR** (300 MHz, $CDCl_3$): δ 7.97 - 7.93 (m, 2H), 7.58 (td, *J* = 7.5, 2.0 Hz, 1H), 7.51 - 7.45 (m, 2H), 7.16 (dd, *J* = 17.3, 10.6 Hz, 1H), 6.44 (dd, *J* = 17.3, 1.7 Hz, 1H), 5.94 (dd, *J* = 10.6, 1.7 Hz, 1H).

ii) $NaBD_4$ (110.9 mg, 2.6 mmol, 1.0 eq.), was added to a mixture of 1-phenylprop-2-en-1-one (350.0 mg, 2.6 mmol) and $CeCl_3 \cdot 7\ H_2O$ (1.3 g, 3.4 mmol, 1.3 eq.) in MeOH (14.0 mL, 0.2 M) over a period of 30 min. After 2 h, the solvent was evaporated and the residue was dissolved in Et_2O (30.0 mL) and washed with H_2O (3 x 25.0 mL). The organic phase was dried, filtered and concentrated. The residue was purified by silica gel column chromatography using hexane / EtOAc (90:10). The product **9a-*d*** was obtained as a colorless oil.

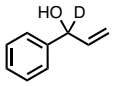

#X1A-*d*

1-phenylprop-2-en-1-d-1-ol (9a-*d*). FCC in hex:EtOAc (9:1), isolated as colorless oil (326 mg, 2.4 mmol, 93%). $\mathbf{R_f}$ = 0.15 (Hexane / EtOAc 90:10). The NMR data is in accordance with that previously reported. **^{1}H NMR** (300 MHz, $CDCl_3$): δ 7.40 - 7.25 (m, 5H), 6.06 (dd, *J* = 17.1, 10.4 Hz, 1H), 5.36 (dd, *J* = 17.1, 1.2 Hz, 1H), 5.21 (dd, *J* = 10.4, 1.2 Hz, 1H). **^{2}H NMR** (300 MHz, $CHCl_3$): δ 5.23 (s).

Catalytic reactions

Representative general procedure for the catalytic isomerization of allylic alcohols (9a-g) in different biological media.

Exemplified for the substrate **9a** using **Ru11** as catalyst and PBS as solvent

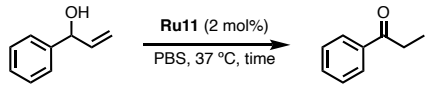

9a **10a**

Ru11 (4 µmol, 1.3 mg, 2.0 mol%) was added to a Schlenk tube containing a stir bar and PBS (phosphate buffer saline solution, 1.0 mL, 0.2 M), followed by the addition of substrate **9a** (0.2 mmol, 27 µL). The reaction mixture was stirred at 400 rpm and the Thermowatch-controlled heating block was fixed at 37 °C. The reaction was followed by TLC. After 2 h, the reaction mixture was extracted with CH_2Cl_2 (3 x 10.0 mL) and the combined organic fractions were dried, filtered and concentrated and analyzed by ^{1}H-NMR. The obtained yields for the different substrates using different biological media where those reported in the main manuscript, as well as the catalyst loading.

Propiophenone (10a).

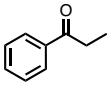

10a

Prepared according to the above representative procedure. Colorless oil. $\mathbf{R_f}$ = 0.42 (Hexane / EtOAc 80:20). The NMR data is in accordance with that previously reported. **^{1}H NMR** (300 MHz, $CDCl_3$): δ 7.99 - 7.96 (m, 2H), 7.58 - 7.53 (m, 1H), 7.49 - 7.43 (m, 2H), 3.02 (q, *J* = 7.2 Hz, 2H), 1.23 (t, *J* = 7.2 Hz, 3H).

1-(p-tolyl)propan-1-one (10b).

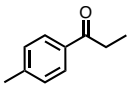

10b

Prepared according to the above representative procedure. Colorless oil. $\mathbf{R_f}$ = 0.45 (Hexane / EtOAc 80:20). The NMR data is in accordance with that previously reported.[10] **^{1}H NMR** (300 MHz, $CDCl_3$): δ 7.88 (d, *J* = 8.1 Hz, 2H), 7.26 (d, *J* = 8.0 Hz, 2H), 2.99 (q, *J* = 7.3 Hz, 2H), 2.42 (s, 3H), 1.22 (t, *J* = 7.3 Hz, 3H).

[10] Z. Zhang, M. G. Lindale, L. S. Liebeskind, *J. Am. Chem. Soc.* **2011**, *133*, 6403–6410.

1-(4-methoxyphenyl)propan-1-one (10c)

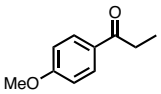

10c

Prepared according to the above representative procedure. Colorless oil. **R_f** = 0.45 (Hexane / EtOAc 80:20). The NMR data is in accordance with that previously reported.[11] **^{1}H NMR** (300 MHz, $CDCl_3$): δ 7.96 (d, *J* = 8.7 Hz, 2H), 6.94 (d, *J* = 8.7 Hz, 2H), 3.87 (s, 3H), 2.96 (q, *J* = 7.2 Hz, 2H), 1.22 (t, *J* = 7.2 Hz, 3H).

1-(4-bromophenyl)propan-1-one (10d).

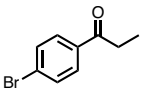

10d

Prepared according to the above representative procedure. Colorless oil. **R_f** = 0.45 (Hexane / EtOAc 80:20). The NMR data is in accordance with that previously reported.[12] **^{1}H NMR** (300 MHz, $CDCl_3$): δ 7.81 (d, *J* = 8.6 Hz, 2H), 7.58 (d, *J* = 8.7 Hz, 2H), 2.96 (q, *J* = 7.2 Hz, 2H), 1.20 (t, *J* = 7.2 Hz, 3H).

Octen-3-one (10e).

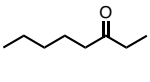

10e

Prepared according to the above representative procedure. Colorless oil. **R_f** = 0.60 (Hexane / EtOAc 80:10). The NMR data is in accordance with that previously reported.[13] **^{1}H NMR** (300 MHz, $CDCl_3$): δ 2.39 (t, *J* = 6.8 Hz, 2H), 2.36 (q, *J* = 6.9 Hz, 2H), 1.60 - 1.68 (m, 2H), 1.20 - 1.45 (m, 4H), 1.05 (t, *J* = 7.0 Hz, 3H), 0.94 (t, *J* = 7.1 Hz, 3H).

1-(6-methoxynaphthalen-2-yl)propan-1-one (10f).

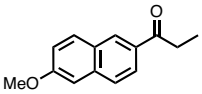

10f

Prepared according to the above representative procedure. White solid. **R_f** = 0.57 (Hexane / EtOAc 80:20). The NMR data is in accordance with that previously reported.[14] **^{1}H NMR** (300 MHz, $CDCl_3$): δ 8.73 (s, 1H), 8.35 (dd, *J* = 8.6, 1.8 Hz, 1H), 8.18 (d, *J* = 8.9 Hz, 1H), 8.09 (d, *J* = 8.6 Hz, 1H), 7.57 - 7.41 (m, 2H), 4.28 (s, 3H), 3.44 (q, *J* = 7.3 Hz, 2H), 1.62 (t, *J* = 7.3 Hz, 3H).

1-(6-(pyrrolidin-1-yl)naphthalen-2-yl)propan-1-one (10g).

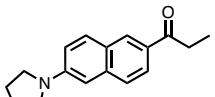

10g

Prepared according to the above representative procedure. Yellow solid. **R_f** = 0.60 (Hexane / EtOAc 80:20). **^{1}H NMR** (300 MHz,

[11] M. L. N. Rao, V. Venkatesh, D. Banerjee, *Tetrahedron* **2007**, *63*, 12917–12926.
[12] B. Scheiper, M. Bonnekessel, H. Krause, A. Fürstner, *J. Org. Chem.* **2004**, *69*, 3943–3949.
[13] P. N. Liu, K. D. Ju, C. P. Lau, *Adv. Synth. Catal.* **2011**, *353*, 275–280.
[14] T. Scheidt, H. Land, M. Anderson, Y. Chen, P. Berglund, D. Yi, W.-D. Fessner, *Adv. Synth. Catal.* **2015**, *357*, 1721–1731.

$CDCl_3$): δ 8.32 (d, *J* = 1.8 Hz, 1H), 7.92 (dd, *J* = 8.7, 1.8 Hz, 1H), 7.78 (d, *J* = 9.0 Hz, 1H), 7.61 (d, *J* = 8.7 Hz, 1H), 7.02 (dd, *J* = 9.0, 2.3 Hz, 1H), 6.74 (d, *J* = 2.4 Hz, 1H), 3.49 - 3.39 (m, 4H), 3.08 (q, *J* = 7.3 Hz, 2H), 2.15 - 2.02 (m, 4H), 1.27 (t, *J* = 7.3 Hz, 3H). **^{13}C NMR** (126 MHz, $CDCl_3$): δ 200.7, 148.0, 138.2, 131.2, 130.3, 130.4, 126.1, 125.1, 125.0, 116.6, 104.7, 48.1, 31.8, 25.9, 9.1. **LRMS** (*m/z,* ESI): 254.1 $[M-H]^+$. **HRMS-ESI** Calculated for $C_{17}H_{20}NO$: 254.1539, found 254.1539.

Representative general procedure for the catalytic isomerization of 1,4-dien-3-ols (9h-j) in different biological media

Exemplified for the substrate **9h** using **Ru11** as catalyst and PBS as solvent.

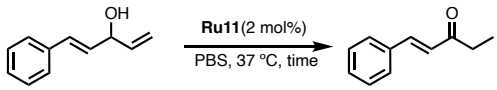

9h **10h**

Ru11 (0.01 mmol, 3.3 mg, 5.0 mol%) was added to a Schlenk tube containing a stir bar and PBS (phosphate buffer saline solution, 1.0 mL, 0.2 M), followed by the addition of substrate **9h** (0.2 mmol, 33 mg). The reaction mixture was stirred at 400 rpm and the Thermowatch-controlled heating block was fixed at 37 °C. After 12 h, the reaction mixture was extracted with CH_2Cl_2 (3 x 10.0 mL) and the combined organic fractions were dried, filtered and concentrated and analyzed by ^{1}H-NMR. The obtained yields for the different substrates using different biological media where those reported in the main manuscript.

(*E*)-1-phenylpent-1-en-3-one (10h).

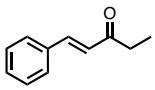

10h

Prepared according to the above representative procedure. White solid. **R_f** = 0.42 (Hexane / EtOAc 80:20). The NMR data is in accordance with that previously reported [15] **^{1}H NMR** (300 MHz, $CDCl_3$): δ 7.61 - 7.51 (m, 3H), 7.42 - 7.35 (m, 3H), 6.75 (d, *J* = 16.3 Hz, 1H), 2.70 (q, *J* = 7.5 Hz, 2H), 1.17 (t, *J* = 7.3 Hz, 3H).

(*E*)-1-(4-methoxyphenyl)pent-1-en-3-one (10i).

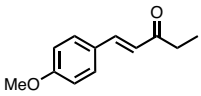

10i

Prepared according to the above representative procedure. Yellow solid. **R_f** = 0.43 (Hexane / EtOAc 90:10). The NMR data is in accordance with that previously reported.[15] **^{1}H NMR** (300 MHz,

[15] M. McConville, O. Saidi, J. Blacker, J. Xiao, *J. Org. Chem.* **2009**, *74*, 2692–2698.

$CDCl_3$): δ 7.58 - 7.45 (m, 3H), 6.95 - 6.84 (m, 2H), 6.63 (d, *J* = 16.1 Hz, 1H), 3.84 (s, 3H), 2.67 (q, *J* = 7.3 Hz, 2H), 1.16 (t, *J* = 7.3 Hz, 3H).

(*E*)-oct-4-en-3-one (10j).

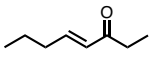

10j

Prepared according to the above representative procedure. Colorless oil. **R_f** = 0.64 (Hexane / EtOAc 80:20). The NMR data is in accordance with that previously reported.[13] **^{1}H NMR** (300 MHz, $CDCl_3$): δ 6.87 (dd, *J* = 15.0, 6.2 Hz, 1H), 6.10 (dt, *J* = 15.2, 0.9 Hz, 1H), 2.51 (q, *J* = 8.0, 2H), 2.27 - 2.20 (m), 1.57 - 1.45 (m, 2H), 1.08 (t, *J* = 7.2, 3H), 0.90 (t, *J* = 7.4, 3H).

General information for the biological experiments

All steps were performed on a sterile clean bench *Tesltar AV-100* at room temperature. Solutions stored in a fridge were warmed beforehand in a water bath (37 °C). Unless otherwise specified, all incubations were performed in DMEM.

Cell Culture: All cell lines were cultured in DMEM (Dulbecco´s modified Eagle´s medium), 5 mM glutamine, penicillin (100 units/mL) and streptomycin (100 units/mL) (all from *Invitrogen*). Proliferating cultures were maintained in a 5% CO_2 humidified incubator at 37 °C.

For all the experiments, cells were seeded in the corresponding well at the indicated concentration two days before treatment.

Protein quantification: For protein concentration measurements the Bio-Rad *DC* Protein Assay Kit was used (*Bio-Rad* 500-0114).

GSH detection: For glutathione concentration measurements the GSH/GSSG Ratio Detection Assay Kit from *Abcam* (ab138881) was used.

Fluorescence microscopy: All images were obtained with an *Andor Zyla* mounted on a *Nikon TiE*. Confocal images were acquired in an Andor Dragonfly High Speed Confocal Platform. Images were further processed with *Image J* or NIS software (Nikon).

Microscopy settings: The filter sets for the observation of the fluorescence of the products were as follows:

Widefield: LED λ excitation: 385 nm. Filter cube DAPI-1160B-000 (Semrock): BP 387/11-25 nm, LP 447/60-25 nm and DM 409 nm. Confocal: Laser excitation: 405 nm. LP 450/50 and DM 418 nm.

Widefield: LED λ excitation: 385 nm. Filter cube: BP 375/28x nm, LP 515lp nm and DM 415 nm. Confocal: Laser excitation: 405 nm. LP 525/50 and DM 501 nm.

Widefield: LED λ excitation: 470 nm. Filter cube FITC-3540C-000 (Semrock): BP 482/35 nm, LP 536/40 nm and DM 506 nm. Confocal: Laser excitation: 488 nm. LP 525/50 and DM 501 nm.

TMRE (tetramethylrhodamine, ethyl ester) LED λ excitation: 550 nm. Filter cube TRITC-B-000 (Semrock): BP 543/22-25 nm, LP 593/40-25 nm and DM 562 nm. Confocal: Laser excitation: 561 nm. LP 620/60 and DM 567 nm

Catalytic experiments in living cells.

A549, HeLa or Vero cells were seeded on glass coverslips two days before treatment. Then, they were incubated with catalyst **Ru11** (10 to 50 μM) for 30 min. Cells were then washed twice with DMEM and incubated with substrate **9g** (100 μM) for 30 min (HeLa cells) or 2 h (A549 and Vero cells). Prior to observation by fluorescence microscopy, the samples were washed twice with fresh DMEM. The coverslips were observed *in vivo* in a fluorescence microscope equipped with adequate filters. Digital pictures of the different samples were taken under identical conditions of gain and exposure.

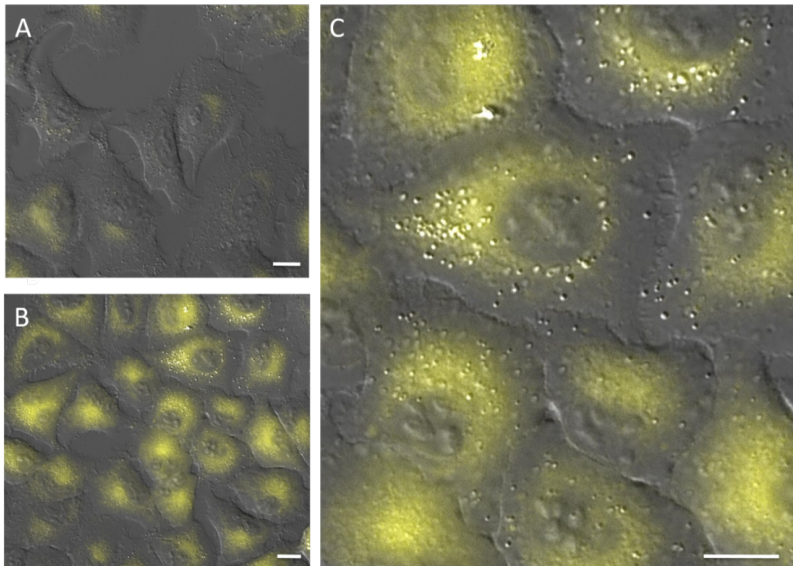

Figure S28. Fluorescence micrographies corresponding to intracellular transformations in A549 cells. (A) Cells incubated with substrate **9g** (Brightfield and green channel); (B) Cells incubated with **Ru11**, washed and treated with substrate **9g** (Brightfield and green channel); (C) Zoom of panel B. Reaction conditions: Cells were incubated with **Ru11** (50 μM) for 30 min, followed by two washings with DMEM and treatment with substrate **9g** (100 μM) for 2 h. λ_{ex} = 385 nm, λ_{em} = 520-700 nm. Scale bar: 12.5 μm.

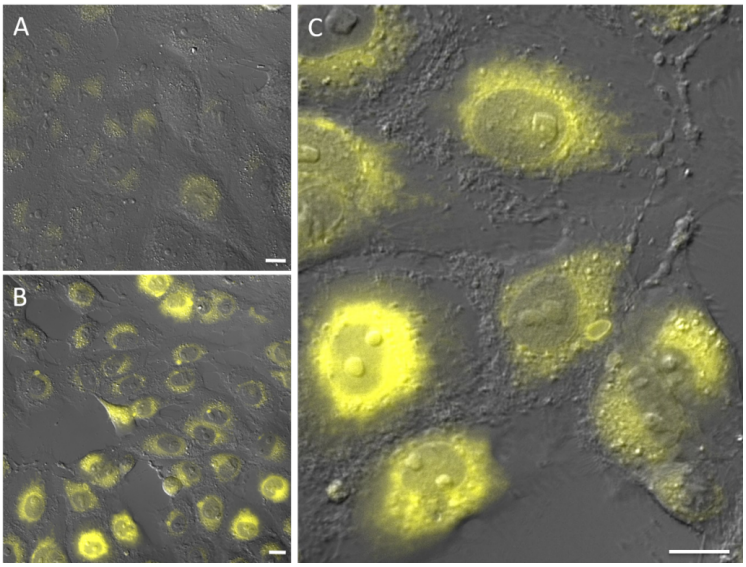

Figure S29. Fluorescence micrographies corresponding to intracellular transformations in Vero cells. (A) Cells incubated with substrate **9g** (Brightfield and green channel); (B) Cells incubated with **Ru11**, washed and treated with substrate **9g** (Brightfield and green channel); (C) Zoom of panel B. Reaction conditions: Cells were incubated with **Ru11** (50 μM) for 30 min, followed by two washings with DMEM and treatment with substrate **9g** (100 μM) for 2 h. λ_{ex} = 385 nm, λ_{em} = 520-700 nm. Scale bar: 12.5 μm.

GSH detection.

The experiments were performed in 6 well plates as follows: 100000 cells per well were seeded in 6 well plates two days before treatment.

For the ruthenium catalyzed isomerization of **9i** into **10i**, a total of 10^6 HeLa cells growing in 6 well plates were incubated with catalyst **Ru11** (50 μM) for 30 minutes followed by two washing steps with DMEM. Then, cells were incubated with substrate **9i** (100 μM) for 6 or 24 h. Afterwards, cells were washed with cold PBS. Finally, a commercial kit (GSH/GSSG Ratio Detection Assay Kit-Abcam) was used for the measurement of the glutathione in each well.

Untreated cells and cells incubated either with substrate **9i** or product **10i** (100 μM) for 6 or 24 h were subjected to the same protocol for the GSH detection.

The GSH levels of the samples were measured in a 96-well plate by recording changes in fluorescence at $E_x/_{Em}$ 490/520 nm in a microtiter plate reading spectrophotometer (*Tecan Infinite 200 PRO*).

The changes in fluorescence intensity with GSH concentration can be described as a linear regression:

Reduced GSH standard calibration curve.

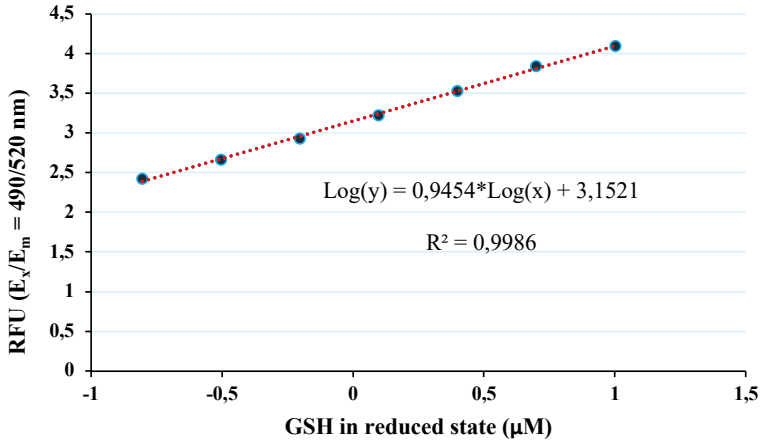

The results were normalized with respect to the amount of protein in each sample. The protein concentration was measured using the BIO-RAD *DC* Protein Assay.

ICP analysis

The experiments were performed in 6 well plates as follows: 100000 cells per well were seeded in 6 well plates two days before treatment.

For the ICP measurements, a total of 3 x 10^6 HeLa cells growing in 6 well plates were treated with different concentrations of **Ru11** and [Cp*RuCl(COD)] (**Ru1**) in DMEM for 1 h. Prior to digestion, the samples were washed with fresh DMEM and then twice with PBS. The obtained fractions were digested in duplicate in HNO_3/H_2O_2 by microwave heating and analyzed.

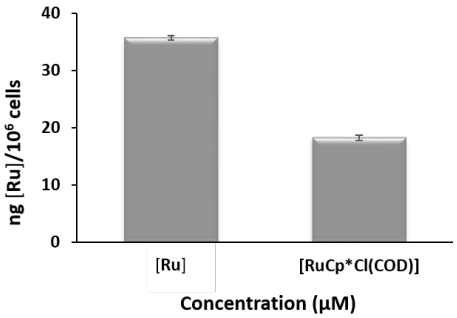

Figure S30 Representative figures of ICP analysis

ICP-MS measurements of ruthenium content in HeLa cells incubated with 50 μM of either **Ru11** or [Cp*RuCl(COD)] (**Ru1**) complexes, after washing and nitric treatment. The analysis reflects all ruthenium accumulated in the cell. Error bars represent the standard error of three independent experiments. ICP values: **Ru11** (50 μM, 1 h) = 35.76 ng/10^6 cells; [Cp*RuCl(COD)] (50 μM, 1 h) = 18.2 ng/10^6 cells.

Quantification studies using LC/MS.

For the quantification of the ruthenium catalyzed isomerization of **9g** into **10g** in HeLa cells, a total of 16 x 10^6 HeLa cells growing in 8 plates of 100 mm were used.

The experiments were performed in plates of 100 mm as follows: 100000 cells per well were seeded in 100 mm plated two days before treatment. For each measurement, eight plates were used. Cells were incubated with catalyst **Ru11** (10-25 µM) for 50 minutes followed by two washing steps with DMEM. Then, cells were incubated with substrate **9g** (100 µM) for 30 min or 6 h. Afterwards, the reaction media was collected for analysis in a 50 mL Falcon. Prior to extraction, cells were washed with 3 mL of DMEM, followed by 3 mL of PBS and the washings were also collected separately in two 50 mL Falcons. Then the cell monolayer was treated with 500 µL of MeOH. After 5 min and pipetting up this solution was transferred to a 15 mL Falcon. Finally, we obtained 4 mL of methanolic extracts from the eight plates employed. All the samples were lyophilized for 3 days and dissolved in MeCN until reach a theoretical concentration of 250 µM.

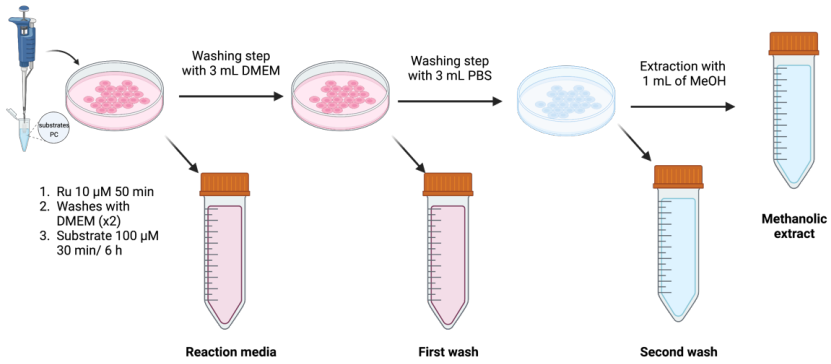

Figure S31. Schematic representation of the protocol for the quantification of the Ruthenium catalyzed intracellular reaction.

For the quantification of the product, the obtained samples (250 µM in MeCN) were centrifuged at 13500 rpm for 15 minutes and the supernatant was collected. In the case of the methanolic extract, it was diluted 1:4 using MeCN/H_2O 6:4. However, in the case of the samples of the reaction media, first and second washing, no dilution was required.

Each sample was injected in a *Bruker Elute* coupled with *timsTOF* using a column Zorba eclipse BXD-C18 2.1 x 10 mm 1.8 µm and a flow rate of 0.4 mL/min at room temperature. For the solvent system, initial conditions H_2O/MeCN (40:60) were used for 1 min and followed by a gradual change over 4 min to MeCN (100), maintained during 1 min and

followed by a gradual change over 20 secs to H_2O/MeCN (40:60) and maintained for 1 min 40 secs.

It's important to mention that in all the cases we have detected significant amounts of substrate **10g**

.Results obtained after 30 min of reaction in HeLa cells using 10 µM of Ru11.

A 10 mM standard solution in MeCN of product **10g** was prepared for the calibration curve. The following dilutions were prepared using a mixture of MeCN/H_2O 6:4. For the calibration curve, we represented the intensity obtained in the MS spectra vs the concentration using an internal standard.

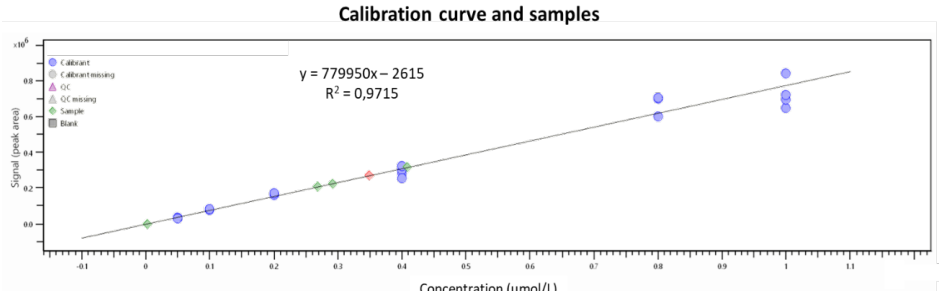

Calibration curve of the product **10g**. Circle: point for calibration; diamond: injected samples.

Table S2. Values for the product content detected in the methanolic extracts after 30 min of reaction in HeLa cells. **Important, we didn't observe the formation of product in the reaction media and in the two washings steps.**

Sample	Concentration (µM)	Original concentration (µM) (dilution factor of 4)
Methanolic extraction	0.292	
Methanolic extraction	0.349	
Methanolic extraction	0.408	
Methanolic extraction	0.268	
Average	0.329 ± 0.062	**1.316 ± 0.250**

Taking into account the number of cells used in these experiments (16 x 10^6 cells), we obtained a 0.082 ± 0.016 µM 10^6 $cells^{-1}$ of product.

ICP value: 3.54 ± 1.29 ng of Ru 10^6 $cells^{-1}$ which means 0.009 ± 0.003 µM of Ru 10^6 $cells^{-1}$

Estimated TON = mol product / mol Ru = 0.082 ± 0.016 / 0.009 ± 0.003 = **9.1 ± 4.8**

Results obtained after 6 h of reaction in HeLa cells using 10 µM of Ru11.

A 10 mM standard solution in MeCN of product **10g** was prepared for the calibration curve. The following dilutions were prepared using a mixture of MeCN/H_2O 6:4. For the calibration curve, we represented the intensity obtained in the MS spectra vs the concentration using an internal standard.

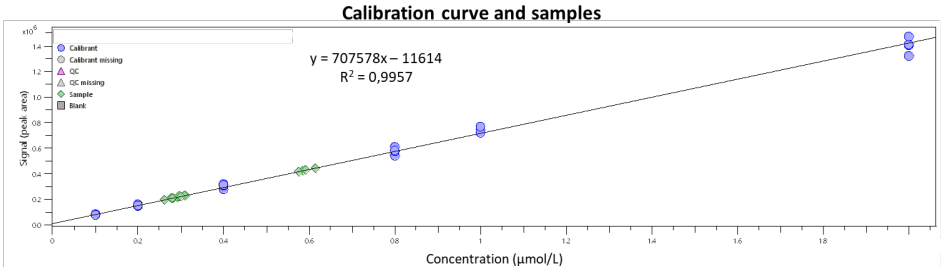

Calibration curve of the product **10g**. Circle: point for calibration; diamond: injected samples.

Table S3. Values for the product content detected in the methanolic extracts, the reaction media and the washings steps.

Sample	Value	Original concentration (µM) (dilution factor of 4)
Methanolic extraction	0.586	
Methanolic extraction	0.592	
Methanolic extraction	0.576	
Methanolic extraction	0.614	
Average	0.592 ± 0.016	**2.368 ± 0.064**
Reaction media	0.281	
Reaction media	0.310	
Reaction media	0.293	
Reaction media	0.282	
Average	0.292 ± 0.013	**0.292 ± 0.013**
First washing	0.310	
First washing	0.292	
First washing	0.295	
First washing	0.301	
Average	0.299 ± 0.007	**0.299 ± 0.007**
Second washing	0.294	

Second washing	0.278	
Second washing	0.260	
Second washing	0.280	
Average	0.278 ± 0.014	**0.278 ± 0.014**
Total Value		**3.237 ± 0.098**

Taking into account that all the amount of the product detected in all the fractions analyzed was generated inside the cells, we used the value 3.237 ± 0.098 µM as total concentration of intracellular generated product.

Taking into account the number of cells used in these experiments (16 x 10^6 cells), we obtained a 0.202 ± 0.006 µM 10^6 $cells^{-1}$ of product.

ICP value: 3.54 ± 1.29 ng of Ru 10^6 $cells^{-1}$ which means 0.009 ± 0.003 µM of Ru 10^6 $cells^{-1}$

Estimated TON = mol product / mol Ru = 0.202 ± 0.006/ 0.009 ± 0.003 = **22.4 ± 8.1**

Results obtained after 6 h of reaction in HeLa cells using 25 µM of Ru11.

A 10 mM standard solution in MeCN of product **10g** was prepared for the calibration curve. The following dilutions were prepared using a mixture of MeCN/H_2O 6:4. For the calibration curve, we represented the intensity obtained in the MS spectra vs the concentration using an internal standard.

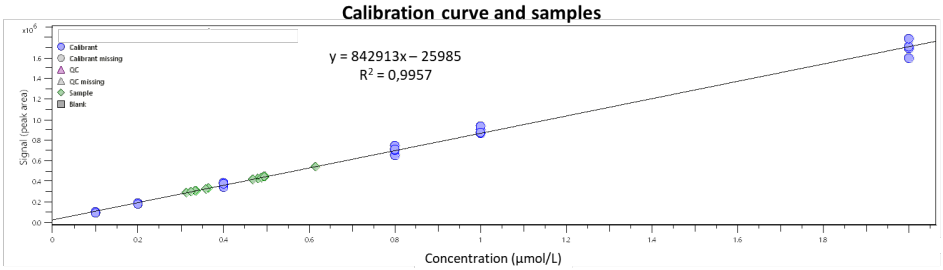

Calibration curve of the product **10g**. Circle: point for calibration; diamond: injected samples.

Table S4. Values for product content detected in the methanolic extracts, the reaction media and the washings steps.

Sample	Value	Original concentration (µM) (dilution factor of 4)
Methanolic extraction	0.477	
Methanolic extraction	0.493	
Methanolic extraction	0.488	
Methanolic extraction	0.603	
Average	0.515 ± 0.059	**2.061 ± 0.236**
Reaction media	0.510	
Reaction media	0.509	
Reaction media	0.494	
Reaction media	0.482	
Average	0.358 ± 0.014	**0.358 ± 0.014**
First washing	0.351	
First washing	0.378	
First washing	0.353	
First washing	0.349	
Average	0.499 ± 0.013	**0.499 ± 0.013**
Second washing	0.329	

Second washing	0.326	
Second washing	0.338	
Second washing	0.379	
Average	0.343 ± 0.025	**0.343 ± 0.025**
Total Value		**3.261 ± 0.287**

Taking into account that the amount of product detected in all the fractions analyzed was generated inside the cells, we used the value 3.261 ± 0.287 μM as total concentration of intracellular generated product.

Taking into account the number of cells used in these experiments (16 x 10^6 cells), we obtained a 0.204 ± 0.018 μM 10^6 $cells^{-1}$ of product.

ICP value: 11.1 ± 1.3 ng of Ru 10^6 $cells^{-1}$ which means 0.028 ± 0.003 μM of Ru 10^6 $cells^{-1}$

***Estimated TON* = mol product / mol Ru = 0.204 ± 0.017 / 0.028 ± 0.003 = 7.34 ± 1.5**

NMR spectra

1-(6-(pyrrolidin-1-yl)naphthalen-2-yl)prop-2-en-1-ol (9g).

^{1}H-NMR (300 MHz, $CDCl_3$)

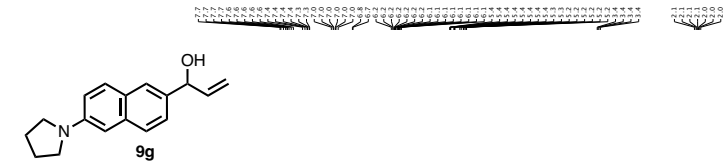

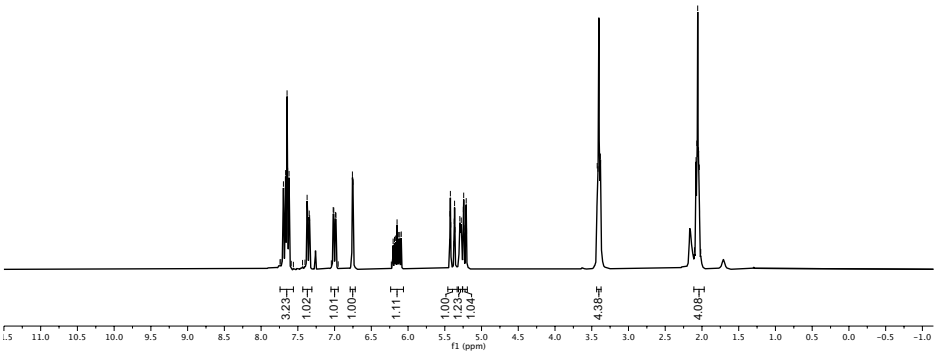

^{13}C-NMR (75 MHz, $CDCl_3$)

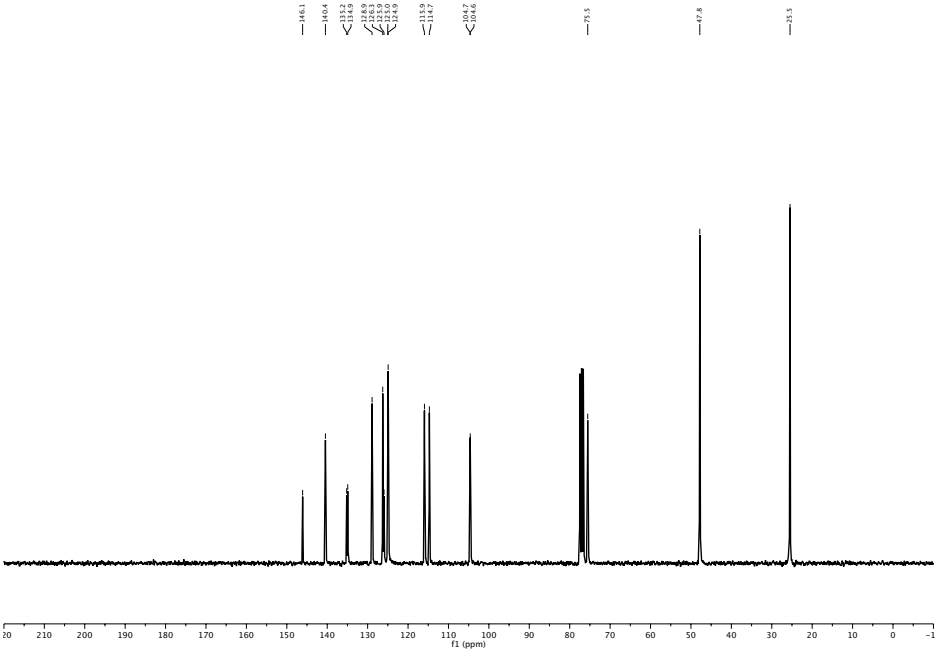

1-(6-(pyrrolidin-1-yl)naphthalen-2-yl)propan-1-one (10g).

^{1}H-NMR (300 MHz, $CDCl_3$)

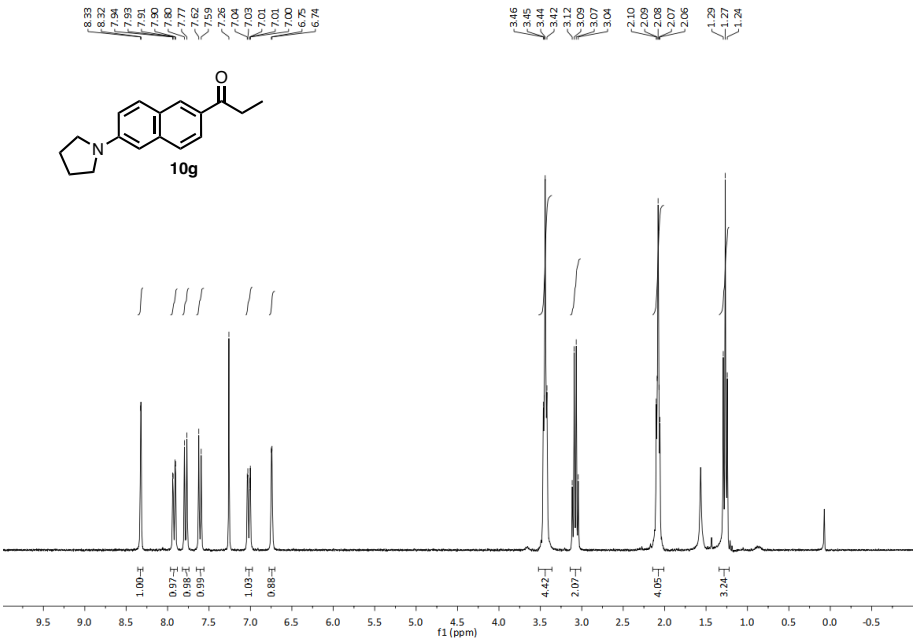

^{13}C-NMR (125 MHz, $CDCl_3$)

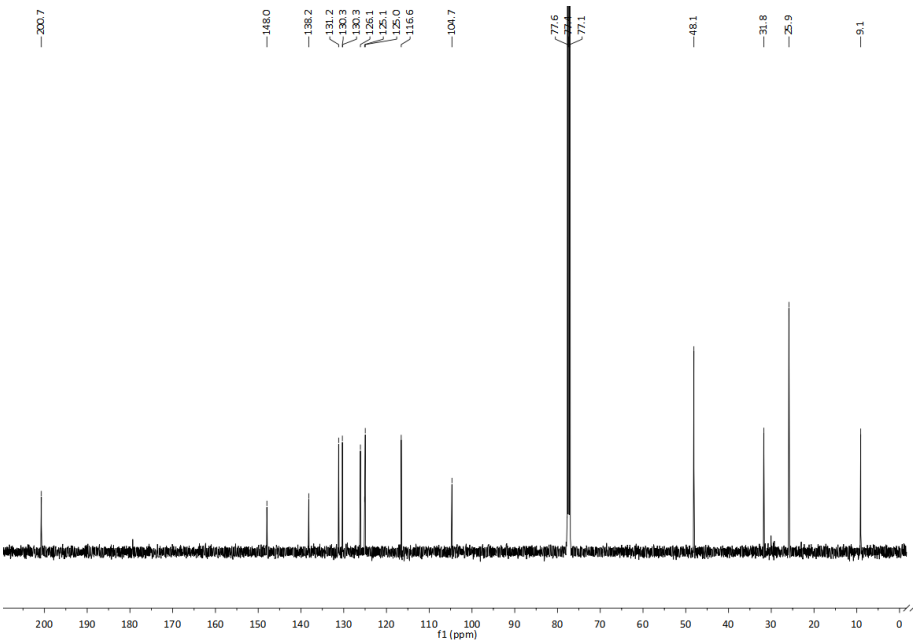

Experimental Section:

Chapter IV: Tandem Reactions in Cellulo

Synthesis of HBT fluorophore

3-(benzo[d]thiazol-2-yl)-2-hydroxy-5-methyl benzaldehyde (11)

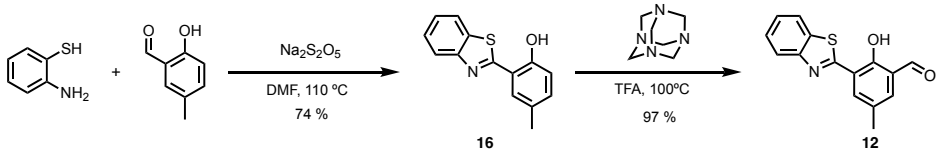

The synthesis of **11** was carried out according to a reported procedure:[1]

i) 2-hydroxy-5-methylenzaldehyde (1.50 g, 11.0 mmol, 1.0 equiv), 2-aminothiphenol (1.38 g, 11.0 mmol, 1.0 equiv) and sodium metabisulfite (1.8 g, 9.5 mmol, 0.86 equiv) were dissolved in DMF (16 mL) in a round bottom flask. The reaction was stirred at 110 ºC for 3 h. After the indicated time, the reaction was cooled to room temperature and the solid was precipitated out on addition of deionized water (5 mL) to the solution. The solid was filtered, washed with Mili-Q grade water for 5 times. The solid was dissolved in CH_2Cl_2 (50 mL), dried over $MgSO_4$, filtered and the solvent removed under reduced pressure to afford 11.

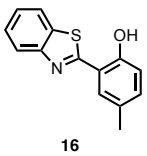

16

2-(benzo[*d*]thiazol-2-yl)-4-methylphenol (**16**) White solid (1.96 g, 8.1 mmol, 74%). **^{1}H NMR** (300 MHz, $CDCl_3$) δ 12.30 (s, 1H), 7.96 (d, *J* = 8.8 Hz, 1H), 7.88 (d, *J* = 8.0 Hz, 1H), 7.55 – 7.43 (m, 2H), 7.38 (ddd, *J* = 8.3, 7.3, 1.2 Hz, 1H), 7.18 (dd, *J* = 8.4, 2.1 Hz, 1H), 7.01 (d, *J* = 8.4 Hz, 1H), 2.35 (s, 3H).

ii) 2-(benzo[d]thiazol-2-yl)-4-methylphenol (**16**, 1.96 g, 8.1 mmol, 1.0 equiv) was dissolved in TFA (12.0 mL). Hexamethylentretramine was added in one portion and the solution was heat under reflux for 6 h. After the indicated time, the solution was cooled to room temperature, HCl 4M (20 mL) was added to the solution and extracted with CH_2Cl_2 (2 x 30 mL). The organic phase was dried over $MgSO_4$, and the solvent removed under reduced pressure.

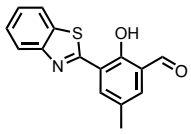

12

3-(benzo[*d*]thiazol-2-yl)-2-hydroxy-5-methylbenzaldehyde (11). FCC in Hex:EtOAc (8:2). Isolated as yellow powder (2.1 g, 7.9 mmol, 97% yield). **^{1}H NMR** (300 MHz, $CDCl_3$) δ 10.50 (s, 1H), 8.04 (d, *J* = 8.2 Hz, 1H), 7.99 – 7.88 (m, 2H), 7.72 (s, 1H), 7.55 (t, *J* = 7.7 Hz, 1H), 7.45 (t, *J* = 7.6 Hz, 1H), 2.42 (s, 3H).

[1] T. Chen, T. Wei, Z. Zhang, Y. Chen, J. Qiang, F. Wang, X. Chen, *Dyes Pigm.* **2017**, *140*, 392–398.

Synthesis of allyl-HBT.

2-(allyloxy)-3-(benzo[*d*]thiazol-2-yl)-5-methylbenzaldehyde (17)

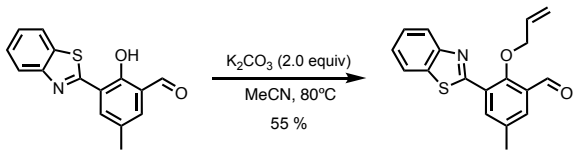

(benzo[d]thiazol-2-yl)-2-hydroxy-5-methylbenzaldehyde (**11**) (600 mg, 2.23 mmol, 1.0 equiv) was dissolved in DMF in a round bottom flask, followed by addition of K_2CO_3 (675 mg, 4.46 mmol, 2.0 eq) dissolved in the minimum quantity of H_2O. The reaction mixture was stirred at room temperature for 20 min. Allyl bromide (490 µL, 4.46 mmol, 2.0 equiv) was added to the reaction mixture was stirred overnight at 80 ºC. After the indicated period, the reaction was allowed to cool to room temperature, water was added and the reaction mixture was extracted with EtOAc (2x15mL), washed with water, brine, dried with over $MgSO_4$, filtered and the solvent removed under reduced pressure.

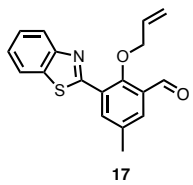

Synthesis of allyl-HBT. 2-(allyloxy)-3-(benzo[*d*]thiazol-2-yl)-5-methylbenzaldehyde (17) FCC using CH_2Cl_2:iPrOH (100:0.2) as eluent and coarse silica (particle ⌀ = 63 - 200µm) as solid support. Isolated as white solid (377 mg, 1.22 mmol, 55% yield). **^{1}H NMR** (300 MHz, $CDCl_3$) δ 10.42 (s, 1H), 8.53 – 8.45 (m, 1H), 8.14 (d, *J* = 7.9 Hz, 1H), 7.98 (d, *J* = 7.2 Hz, 1H), 7.81 (dd, *J* = 2.4, 0.8 Hz, 1H), 7.61 – 7.50 (m, 1H), 7.50 – 7.40 (m, 1H), 6.15 (ddt, *J* = 17.2, 10.4, 5.8 Hz, 1H), 5.47 (dq, *J* = 17.1, 1.5 Hz, 1H), 5.36 (dq, *J* = 10.4, 1.2 Hz, 1H), 4.55 (dt, *J* = 5.8, 1.3 Hz, 2H), 2.49 (s, 4H).

Synthesis of the dual metal probe HBT.

1-(2-(allyloxy)-3-(benzo[*d*]thiazol-2-yl)-5-methylphenyl)prop-2-en-1-ol (12)

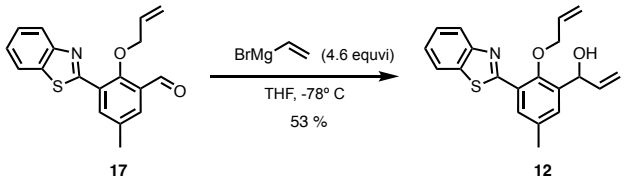

To a solution of 2-(allyloxy)-3-(benzo[d]thiazol-2-yl)-5-methylbenzaldehyde (**17**) (263 mg, 0.85 mmol, 1.0 equiv) in dry THF (4.0 mL) at - 78 ºC was added a solution of

1.0 M solution of vinylmagnesium bromide in THF (1.4 mL, 1.4 mmol 1.7 equiv). The reaction was kept at -78 ºC for 30 min. After the indicated time the reaction was allowed to reach room temperature and followed by TLC. The reaction was quenched with $NHCO_3$ (15 mL), extracted with EtOAc (3x10mL). The combined organic fractions were washed with water (10 mL), brine (10 mL), dried over $MgSO_4$, filtered and the solvent removed under reduced pressure.

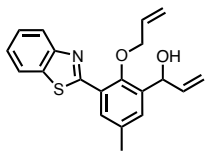

#t2

1-(2-(allyloxy)-3-(benzo[*d*]thiazol-2-yl)-5-methylphenyl)prop-2-en-1-ol (12). FCC in Hex:EtOAc (from 9:1 to 85:15). Isolated as white off solid. (153 mg, 0.28 mmol, 53%yield). **^{1}H NMR** (300 MHz, $CDCl_3$) δ 8.15 – 8.04 (m, 2H), 7.93 (d, *J* = 8.0 Hz, 1H), 7.60 – 7.45 (m, 1H), 7.46 – 7.33 (m, 2H), 6.23 – 6.01 (m, 2H), 5.63 (s, 1H), 5.51 – 5.38 (m, 2H), 5.35 – 5.22 (m, 2H), 4.49 – 4.31 (m, 2H), 2.41 (s, 3H).

Synthesis of the allylic alcohol HBT. 2-(benzo[*d*]thiazol-2-yl)-6-(1-hydroxyallyl)-4-methylphenol (15)

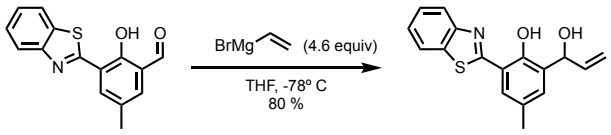

11 15

To a solution of 2-(allyloxy)-3-(benzo[d]thiazol-2-yl)-5-methylbenzaldehyde (**11**) (350 mg, 1.3 mmol, 1.0 equiv) in dry THF (6.5 mL) at - 78 ºC was added a solution of 1.0 M solution of vinylmagnesium bromide in THF (6.5 mL, 6.5 mmol 5.0 equiv). The reaction was kept at -78 ºC for 30 min. After the indicated time the reaction was allowed to reach room temperature and followed by TLC. The reaction was quenched with $NHCO_3$(15 mL), extracted with EtOAc (3x10mL). The combined organic fractions were washed with water (10 mL), brine (10 mL), dried over $MgSO_4$, filtered and the solvent removed under reduced pressure.

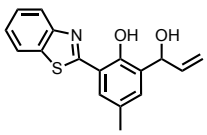

#t5

2-(benzo[*d*]thiazol-2-yl)-6-(1-hydroxyallyl)-4-methylphenol (15). FCC Hex:EtOAc (from 9:1 to 8:2). Isolated as yellow powder. (246 mg, 0.79 mmol, 72% yield). **^{1}H NMR** (300 MHz, $CDCl_3$) δ 7.99 (d, *J* = 7.6 Hz, 1H), 7.93 (d, *J* = 7.6 Hz, 1H), 7.59 – 7.49 (m, 1H), 7.49 – 7.39 (m, 2H), 7.31 – 7.23 (m, 1H), 6.26 (dddd, *J* = 17.2, 10.4, 5.5, 1.6 Hz, 1H), 5.55 – 5.38 (m, 2H), 5.26 (dq, *J* = 10.4, 1.7 Hz, 1H), 2.38 (s, 3H).

Acedan dual metal probe

Synthesis of intermediate 6-bromo-*N*-methylnaphthalen-2-amine (22)

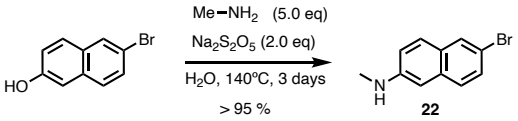

The synthesis of **22** was carried out according to a reported procedure:[2]

A mixture of N-methyl amine (4.0 mL 40% in H_2O, 43.5 mmol, 5.0 equiv), 6-bromo-2-naphtol (8.7 mmol, 2.0 g), $Na_2S_2O_5$ (17.4 mmol, 3.3 g, 2.0 equiv) and water (19.3 mL) in a sealed tube was stirred at 145 °C for 48 h. After being cooled to room temperature the reaction mixture was diluted with 20.0 mL of water and the product was extracted with CH_2Cl_2 (2 x 30.0 mL), dried over $MgSO_4$, filtered and the solvent removed under reduced pressure. No further purification was required.

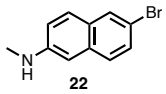

6-bromo-*N*-methylnaphthalen-2-amine (22). Isolated as white powder (2.0 g, 8.5 mmol, 97% yield). The NMR data is in accordance with that previously reported. **^{1}H NMR** (300 MHz, $CDCl_3$) δ 7.81 (d, *J* = 2.0 Hz, 1H), 7.51 (dd, *J* = 8.8, 6.3 Hz, 2H), 7.41 (dd, *J* = 8.8, 2.0 Hz, 1H), 6.88 (dd, *J* = 8.8, 2.4 Hz, 1H), 6.74 (d, *J* = 2.4 Hz, 1H), 2.93 (d, *J* = 3.5 Hz, 3H).

Synthesis of intermediate 6-(methylamino)-2-naphthaldehyde (23)

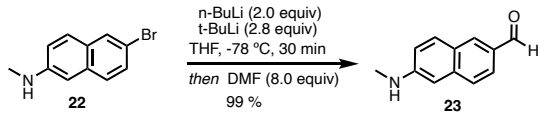

Aldehyde **23** was synthetized adapting a reported protocol: [3]

6-bromo-N-methylnaphthalen-2-amine (22) (680 mg, 2.88 mmol, 1.0 equiv) was dissolved in anhydrous THF (14 mL) in a heat gun dried round bottom flask, and the solution was cooled to -78 °C under nitrogen. Then, 2.5 M *n*-BuLi in hexane (2.3 mL, 5.76 mmol, 2.0 equiv) was added, followed by the addition of 1.9 M *t*-BuLi (4.2 mL, 8.1 mmol, 2.8 equiv). The reaction was stirred at -78 °C for 0.5 h and then treated with anhydrous DMF (1.8 mL, 23.0 mmol, 8.0 equiv). It was warm to -30 ºC and kept at that at that temperature for 1 h. After the indicated time the reaction mixture was quenched

[2] X. Gao, Y. Zhang, B. Wang, *Tetrahedron* **2005**, *61*, 9111–9117.
[3] M. T. Morgan, P. Bagchi, C. J. Fahrni, *Dalton Trans.* **2013**, *42*, 3240–3248.

with sat. NH_4Cl (5.0 mL). The product was extracted with EtOAc (2 x 30.0 mL). The organic fractions were collected, washed with brine, dried over $MgSO_4$, filtered and the solvent removed under reduced pressure. No further purification was required.

6-(methylamino)-2-naphthaldehyde (23). Isolated as white powder (530 mg, 2.87 mmol, 99%yield). The NMR data is in accordance with that previously reported.[4] **^{1}H NMR** (300 MHz, $CDCl_3$) δ 10.02 (s, 1H), 8.14 (s, 1H), 7.83 (dd, *J* = 8.5, 1.7 Hz, 1H), 7.75 (d, *J* = 8.8 Hz, 1H), 7.66 (d, *J* = 8.6 Hz, 1H), 6.93 (dd, *J* = 8.8, 2.3 Hz, 1H), 6.79 (d, *J* = 2.4 Hz, 1H), 2.98 (s, 3H).

Synthesis of intermediate allyl (6-formylnaphthalen-2-yl)(methyl)carbamate (24)

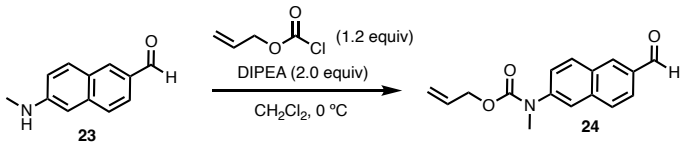

6-(methylamino)-2-naphthaldehyde **(23)** (100 mg, 0.54 mmol, 1.0 equiv) and DIPEA (188 µL, 1.08 mmol, 2.0 equiv) were dissolved in CH_2Cl_2 (1.1 mL) and cooled to 0 ºC in a water-ice bath for 10 min. Allyl chloroformate (70 µL, 0.65 mmol, 1.2 equiv) dissolved in CH_2Cl_2 (1.0 mL) was added dropwise over 1 h to the cooled reaction mixture. After the indicated time the reaction was allowed to warm to room temperature and stirred overnight. The reaction was diluted with CH_2Cl_2 (5 mL), and the organic phase washed with 1M HCl (5 mL), $Na2CO_3$ (5 mL), brine, dried over $MgSO_4$, filtered and the solvent removed under reduced pressure. No further purification required.

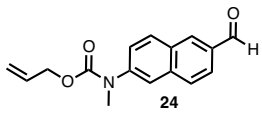

(6-formylnaphthalen-2-yl)(methyl)carbamate (24). Isolated as white powder (145 mg, 0.54 mmol, 99%). The. **^{1}H NMR** (300 MHz, $CDCl_3$) δ 10.07 (s, 1H), 8.23 (s, 1H), 7.95 – 7.76 (m, 3H), 7.69 (d, *J* = 2.2 Hz, 1H), 7.54 (dd, *J* = 8.7, 2.2 Hz, 1H), 5.90 (ddd, *J* = 22.3, 10.7, 5.4 Hz, 1H), 5.37 – 5.07 (m, 2H), 4.64 (dt, *J* = 5.5, 1.5 Hz, 2H), 3.41 (s, 3H). **^{13}C NMR** (75 MHz, $CDCl_3$) δ 191.9, 191.9, 155.1, 143.7, 136.7, 133.9, 133.9, 132.5, 130.4, 130.0, 128.7, 125.7, 123.3, 122.5, 117.7, 66.6, 37.5.

[4] H. M. Kim, B. H. Jeong, J.-Y. Hyon, M. J. An, M. S. Seo, J. H. Hong, K. J. Lee, C. H. Kim, T. Joo, S.-C. Hong, B. R. Cho, *J. Am. Chem. Soc.* **2008**, *130*, 4246–4247.

Synthesis of dual-metal Acedan probe. allyl (6-(1-hydroxyallyl)naphthalen-2-yl)(methyl)carbamate (18)

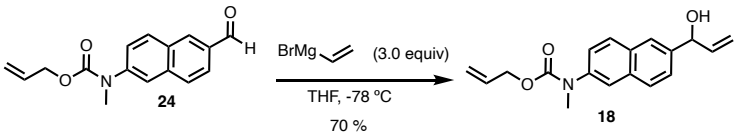

To a solution of (6-formylnaphthalen-2-yl)(methyl)carbamate **(24)** (140 mg, 0.52 mmol, 1.0 equiv) in dry THF (4.0 mL) at - 78 ºC was added a solution of 1.0 M solution of vinylmagnesium bromide in THF (0.55 mL, 0.55 mmol 1.05 equiv). The reaction was kept at -78 ºC for 30 min. After the indicated time the reaction was allowed to reach room temperature and followed by TLC. The reaction was quenched with $NHCO_3$ (15 mL), extracted with EtOAc (3x10mL). The combined organic fractions were washed with water (10 mL), brine (10 mL), dried over $MgSO_4$, filtered and the solvent removed under reduced pressure

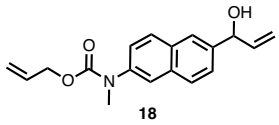

allyl (6-(1-hydroxyallyl)naphthalen-2-yl)(methyl) carbamate (**18**). **FCC** in Hex:EtOAc (from 8:2 to 7:3). Isolated as white powder (108 mg, 0.36 mmol, 70%). **^{1}H NMR** (300 MHz, $CDCl_3$) δ 7.83 – 7.72 (m, 3H), 7.64 (s, 1H), 7.47 (dd, *J* = 8.5, 1.7 Hz, 1H), 7.40 (dd, *J* = 8.8, 2.1 Hz, 1H), 6.19 – 6.00 (m, 1H), 5.89 (ddt, *J* = 16.2, 10.5, 5.4 Hz, 1H), 5.44 – 5.29 (m, 2H), 5.27 – 5.10 (m, 3H), 4.62 (dt, *J* = 5.4, 1.6 Hz, 2H), 3.40 (s, 3H), 2.57 (s, 1H). **^{13}C NMR** (75 MHz, $CDCl_3$) δ 155.6, 140.9, 140.4, 140.3, 133.1, 132.7, 131.6, 128.7, 128.2, 125.2, 124.7, 123.2, 117.5, 115.5, 75.3, 66.5, 38.0. **HRMS (ESI+)**: for $C_{18}H_{20}NO_3$ [M+H]+calc 214.1226 found 214.1231

Synthesis of Acedan fluorophore. 1-(6-(methylamino)naphthalen-2-yl)propan-1-one (19)

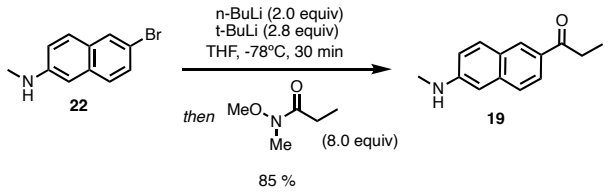

6-bromo-N-methylnaphthalen-2-amine (**22**) (1000 mg, 4.2 mmol, 1.0 equiv) was dissolved in anhydrous THF (21 mL) in a heat gun dried round bottom flask, and the solution was cooled to -78 °C under nitrogen. Then, 2.5 M *n*-BuLi in hexane (3.4 mL,

8.5 mmol, 2.0 equiv) was added, followed by the addition of 1.9 M *t*-BuLi (6.2 mL, 11.9 mmol, 2.8 equiv). The reaction was stirred at -78 °C for 0.5 h and then treated with *N*-methoxy-*N*-methyl propionamide (3.9 g, 33.9 mmol, 8.0 equiv). It was warm to -30 ºC and kept at that at that temperature for 1 h. After the indicated time the reaction mixture was quenched with sat. NH_4Cl (5.0 mL). The product was extracted with EtOAc (2 x 30.0 mL). The organic fractions were collected, washed with brine, dried over $MgSO_4$, filtered and the solvent removed under reduced pressure.

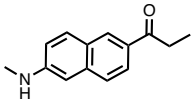

19

1-(6-(methylamino)naphthalen-2-yl)propan-1-one (**19**). FCC in CH_2Cl_2+0.1% *i*- PrOH. Isolated as white powder (770 mg, 3.61 mmol, 85%) **^{1}H NMR** (300 MHz, $CDCl_3$) δ 8.31 (s, 1H), 7.94 (dd, *J* = 8.6, 1.8 Hz, 1H), 7.70 (d, *J* = 8.9 Hz, 1H), 7.63 (d, *J* = 8.7 Hz, 1H), 6.90 (d, *J* = 8.4 Hz, 1H), 6.76 (s, 1H), 4.15 (s, 1H), 3.07 (q, *J* = 7.3 Hz, 2H), 2.96 (s, 4H), 1.27 (t, *J* = 7.3 Hz, 3H). **^{13}C NMR** (75 MHz, $CDCl_3$) δ 200.6, 149.2, 138.1, 130.8, 130.7, 129.8, 126.2, 126.1, 124.9, 118.5, 103.2, 31.6, 30.5, 8.8. **HRMS (ESI+)**: for $C_{14}H_{16}NO$ $[M+H]^+$calc 214.1226 found 214.1231.

Synthesis of Acedan probe intermediate 20. allyl methyl(6-propionylnaphthalen-2-yl)carbamate (20).

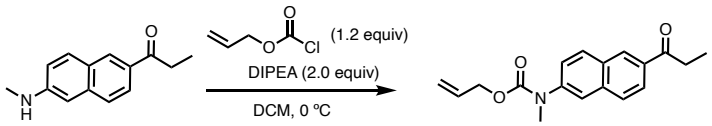

19 20

1-(6-(methylamino)naphthalen-2-yl)propan-1-one (**19**) (100 mg, 0.47 mmol, 1.0 equiv) and DIPEA (163 µL, 0.94 mmol, 2.0 equiv) were dissolved in CH_2Cl_2 (1.0 mL) and cooled to 0 ºC in a water-ice bath for 10 min. Allyl chloroformate (60 µL, 0.56 mmol, 1.2 equiv) dissolved in CH_2Cl_2 (1.0 mL) was added dropwise over 1 h to the cooled reaction mixture. After the indicated time the reaction was allowed to warm to room temperature and stirred overnight. The reaction was diluted with CH_2Cl_2 (5 mL), and the organic phase washed with 1M HCl (5 mL), Na_2CO_3 (5 mL), brine, dried over $MgSO_4$, filtered and the solvent removed under reduced pressure. No further purification required.

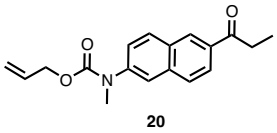

allyl methyl(6-propionylnaphthalen-2-yl)carbamate (20). Isolated as white powder (140 mg, 0.47 mmol, 99%). **^{1}H NMR** (300 MHz, $CDCl_3$) δ 8.45 (s, 1H), 8.04 (dd, *J* = 8.6, 1.8 Hz, 1H), 7.93 (d, *J* = 8.8 Hz, 1H), 7.84 (d, *J* = 8.6 Hz, 1H), 7.71 (d, *J* = 2.2 Hz, 1H), 7.53 (dd, *J* = 8.8, 2.2 Hz, 1H), 5.93 (ddt, *J* = 16.2, 10.7, 5.5 Hz, 1H), 5.32 – 5.14 (m, 2H), 4.66 (dt, *J* = 5.6, 1.5 Hz, 2H), 3.45 (s, 3H), 3.14 (q, *J* = 7.2 Hz, 2H), 1.29 (t, *J* = 7.3 Hz, 3H). **^{13}C NMR** (75 MHz, $CDCl_3$) δ 200.5, 155.2, 143.0, 135.7, 134.2, 132.5, 130.5, 130.1, 129.1, 128.1, 125.5, 124.5, 122.5, 117.6, 66.5, 37.6, 31.8, 8.4. **HRMS (ESI+)**: for $C_{18}H_{20}NO_3$ [M+H]+calc 214.1226 found 214.1231

Synthesis of Acedan probe intermediate 21. 1-(6-(methylamino)naphthalen-2-yl)prop-2-en-1-ol (21)

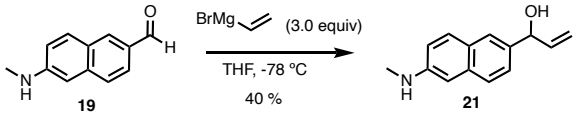

To a solution of allyl methyl(6-propionylnaphthalen-2-yl)carbamate (**19**). (140 mg, 0.52 mmol, 1.0 equiv) in dry THF (4.0 mL) at – 78 ºC was added a solution of 1.0 M solution of vinylmagnesium bromide in THF (0.55 mL, 0.55 mmol 1.05 equiv). The reaction was kept at -78 ºC for 30 min. After the indicated time the reaction was allowed to reach room temperature and followed by TLC. The reaction was quenched with $NHCO_3$ (15 mL), extracted with EtOAc (3x10mL). The combined organic fractions were washed with water (10 mL), brine (10 mL), dried over $MgSO_4$, filtered and the solvent removed under reduced pressure.

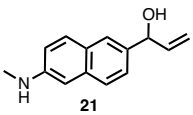

1-(6-(methylamino)naphthalen-2-yl)prop-2-en-1-ol (21). FCC in CH_2Cl_2:*i*- PrOH (99:1). Isolated as a white powder (110 mg, 0.52 mmol, 44% yield). **^{1}H NMR** (300 MHz, $CDCl_3$) δ 7.68 – 7.57 (m, 3H), 7.37 (d, *J* = 8.4 Hz, 1H), 6.93 – 6.81 (m, 1H), 6.79 (s, 1H), 6.13 (ddd, *J* = 16.6, 10.4, 5.8 Hz, 1H), 5.47 – 5.13 (m, 2H), 2.94 (s, 3H).

Synthesis of ALP-HBT probe. diallyl (2-(benzo[*d*]thiazol-2-yl)-6-formyl-4-methylphenyl) phosphate (25)

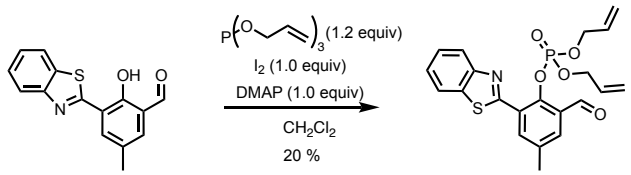

11 **25**

In a Schleck under N_2 the allylphosphate (737 µL, 3.57 mmol, 1.2 equiv) was dissolved in CH_2Cl_2 (7 mL), followed by the addition of I_2 (750 mg, 2.98 mmol, 1.0 equiv) at 0 ºC. After 10 min a solution of DMAP (360 mg, 2.98 mmol, 1.0 equiv) and 2-(benzo[*d*]thiazol-2-yl)-6-(1-hydroxyallyl)-4-methylphenol (**11**) (800 mg, 2.98 mmol, 1.0 equiv) dissolved in DCM (7 mL) was added dropwise to the solution at 0 ºC. After the addition the reaction was allowed to warm to room temperature and stirred overnight. The solution was then diluted with DCM (15 mL), washed with saturated $NaHSO_4$ (15 mL), saturated $NaHCO_3$ (15 mL), brine(15 mL), dried over $MgSO_4$, filtered and the solvent removed under reduced pressure.

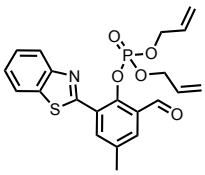

25

diallyl (2-(benzo[*d*]thiazol-2-yl)-6-formyl-4-methylphenyl) phosphate (25). FCC in Hex:EtOAc (75:25). Isolated as white powder (200 mg, 0.435 mmol, 15% yield) **^{1}H NMR** (300 MHz, $CDCl_3$) δ 10.4 (s, 1H), 8.2 (s, 1H), 8.1 (d, J = 8.1 Hz, 1H), 8.0 (d, J = 7.9 Hz, 1H), 7.8 (s, 1H), 7.5 (t, J = 7.7 Hz, 1H), 7.4 (t, J = 7.5 Hz, 1H), 5.8 – 5.6 (m, 2H), 5.2 – 5.0 (m, 4H), 4.6 – 4.3 (m, 4H), 2.5 (s, 3H). **^{13}C NMR** (75 MHz, $CDCl_3$) δ 188.26, 162.35, 152.76, 147.61, 136.99, 136.55, 135.97, 131.57, 131.48, 130.90, 129.54, 127.90, 126.40, 125.59, 123.37, 121.61, 119.12, 69.54, 69.47, 20.69. **^{31}P NMR** (202 MHz, $CDCl_3$) δ -5.81. **HRMS** (ESI+) Calculated for $C_{21}H_{21}NO_5PS$ [M+H]+ 430.0859 found 430.0871.

Synthesis of ALP-HBT intermediate 2-(benzo[*d*]thiazol-2-yl)-6-formyl-4-methylphenyl dihydrogen phosphate (28)

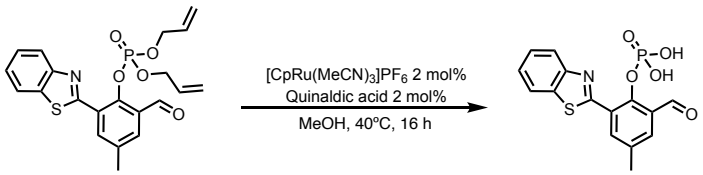

25 **28**

Diallyl (2-(benzo[d]thiazol-2-yl)-6-formyl-4-methylphenyl) phosphate (**25**) (50 mg, 0.116 mmol, 1.0 equiv) was dissolved in degassed MeOH (450 µL). 50 µL of a solution of $[CpRu(MeCN)_3]PF_6$ (5.0 mg, 11.5 µmol) and quinaldic acid (2.0 mg, 11.5 µmol) in degassed MeOH (500 µL) were added to the previous solution. The reaction mixture was stirred for 1 h. After the indicated time the solution was diluted with DCM and filtered through a florisil plug and the solvent removed under reduced pressure.

2-(benzo[*d*]thiazol-2-yl)-6-formyl-4-methylphenyl dihydrogen phosphate (28). Prep-HPLC reverse phase H_2O:MeCN from 70:30 to 25:75 in 15 min, 20 mL/min flow. **^{1}H NMR** (500 MHz, DMSO) δ 10.31 (s, 1H), 8.38 (d, J = 2.3 Hz, 1H), 8.18 (d, J = 7.9 Hz, 1H), 8.11 (d, J = 8.1 Hz, 1H), 7.75 (d, J = 2.4 Hz, 1H), 7.58 (ddd, J = 8.2, 7.1, 1.3 Hz, 1H), 7.50 (ddd, J = 8.2, 7.1, 1.2 Hz, 1H), 2.46 (s, 3H). **^{13}C NMR** (126 MHz, DMSO-d_6) δ 135.77, 133.63, 130.30, 127.44, 126.83, 126.32, 125.93, 123.29, 122.80, 122.77, 122.48, 40.60, 40.43, 40.26, 40.09, 39.93, 20.60, 20.22. **^{31}P NMR** (202 MHz, DMSO-d_6) δ -5.46. **HRMS-ESI:** Calc for $C_{15}H_{13}NO_5PS$ $[M+H]^+$: 350.0247; found: 350.0239.

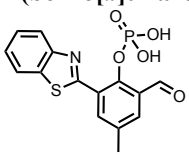

28

Bodipy dual deallylation-MAO probe

1,3-Dimethyl 4,4-Difluoro-4-bora-3a,4a-diaza-s-indacene (29)

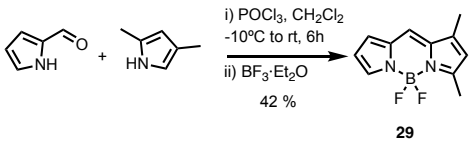

The synthesis of **29** was carried out according to a reported procedure:[5]

Pyrrole 2-carboxyaldehyde (1000 mg, 10.5 mmol, 1.0 equiv) was dissolved in CH_2Cl_2 (13 mL) and cooled down to 0 °C in a water-ice bath. 2,4-dimethylpyrrole (1080 µL, 10.5 mmol, 1.0 equiv) was added to the reaction mixture and stirred for 3 min, followed by slow dropwise addition of $POCl_3$ (960 µL, 10.5 mmol, 1.0 equiv). The reaction mixture was stirred at 0°C for 3h, then another 2h at rt. After the indicated time triethylamine (7.3 mL, 52.6 mmol, 5.0 equiv) and $BF_3{\cdot}OEt_2$ (6.6 mL, 52.6 mmol, 5.0 equiv) were added and stirred at room temperature for 3h. After the indicated time the reaction mixture was diluted with CH_2Cl_2 (200 mL), washed with water (200 mL×2), dried over $MgSO_4$, and the solvent removed under reduced pressure.

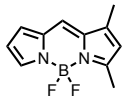

1,3-Dimethyl 4,4-Difluoro-4-bora-3a,4a-diaza-s-indacene (**29**). FCC in Hex:EtOAc (9:1 to 7:3). Isolated as shiny green powder (987 mg, 4.49 mmol, 43% yield). The NMR data is in accordance with that previously reported. **^{1}H NMR** (300 MHz, $CDCl_3$) δ 7.64 (s, 1H), 7.20 (s, 1H), 6.93 (s, 1H), 6.47 – 6.39 (m, 1H), 6.16 (s, 1H), 2.59 (s, 3H), 2.28 (s, 3H).

BODIPY fluorophore (30)

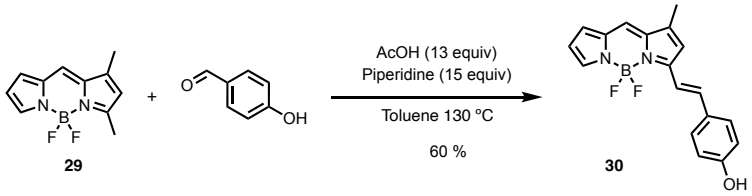

In a pressure tube **29** (30 mg, 0.136 mmol, 1.0 equiv) and 4-hydroxybenzaldehyde (25 mg, 0.205 mmol, 1.5 equiv) were dissolved in toluene (4 mL), followed by the addition of acetic acid (100 µL, 1.8 mmol, 13.0 equiv) and piperidine (200 µL, 2.1 mmol, 15.0 equiv). The tube was sealed, and the reaction mixture was heated to 130 ºC for 4 h.

[5] J.-S. Lee, N. Kang, Y. K. Kim, A. Samanta, S. Feng, H. K. Kim, M. Vendrell, J. H. Park, Y.-T. Chang, *J. Am. Chem. Soc.* **2009**, *131*, 10077–10082.

After the indicated time, the reaction was allowed to cool to room temperature. The solvent was removed under reduced pressure, and the residue redissolved in EtOAc, washed with $NaHCO_3$ (40 mL), 1M HCl (40 mL), brine (40 mL) and the organic phase dried over $MgSO_4$ and the solvent removed under reduced pressure.

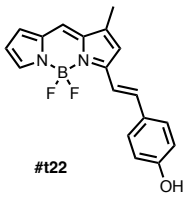

BODIPY fluorophore (30). FCC in Hex:EtOAC (6:4). Isolated as shiny red powder (5.0 mg, 0.015 mmol, 11% yield). The NMR data is in accordance with that previously reported. **^{1}H NMR** (300 MHz, $CDCl_3$) δ 7.65 (s, 1H), 7.56 – 7.44 (m, 3H), 7.36 (s, 1H), 7.14 (s, 1H), 6.94 – 6.79 (m, 3H), 6.74 (s, 1H), 6.45 (s, 1H), 2.32 (s, 3H).

BODIPY Ru-deallylation MAO probe (26)

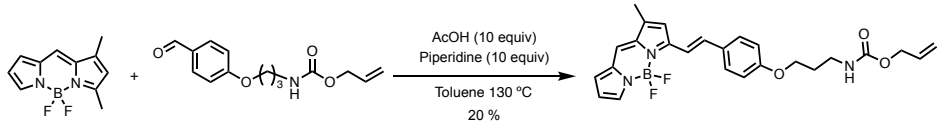

In a pressure tube **29** (150 mg, 0.68 mmol, 1.0 equiv) and allyl (3-(4-formylphenoxy)propyl)carbamate, **31** (180 mg, 0.68 mmol, 1.0 equiv) were dissolved in toluene (7 mL), followed by the addition of acetic acid (390 µL, 6.8 mmol, 10.0 equiv) and piperidine (670 µL, 6.8 mmol, 10.0 equiv). The tube was sealed, and the reaction mixture was heated to 130 ºC for 4 h. After the indicated time, the reaction was cooled to room temperature, the solvent was removed and the residue redissolved in EtOAc, washed with $NaHCO_3$ (40 mL), 1M HCl (40 mL), brine (40 mL) and the organic phase dried over $MgSO_4$, and the solvent removed under reduced pressure.

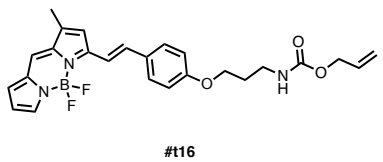

BODIPY Ru-deallylation MAO probe (**26**). FCC in Hex:EtOAC (6:4). Isolated as shiny red powder (85.0 mg, 0.183 mmol, 26.8% yield). **^{1}H NMR** (300 MHz, $CDCl_3$) δ 7.65 (s, 1H), 7.55 (d, J = 8.6 Hz, 2H), 7.48 (s, 1H), 7.39 – 7.20 (m, 2H), 7.13 (s, 1H), 6.95 – 6.86 (m, 2H), 6.73 (s, 1H), 6.48 – 6.40 (m, 1H), 5.92 (ddt, J = 16.4, 10.9, 5.6 Hz, 1H), 5.37 – 5.25 (m, 1H), 5.25 – 5.17 (m, 1H), 4.98 (s, 1H), 4.57 (d, J = 5.6 Hz, 2H), 4.07 (t, J = 5.9 Hz, 2H), 3.41 (q, J = 6.4 Hz, 2H), 2.30 (s, 3H), 2.08 – 1.98 (m, 2H). **^{13}C NMR** (75 MHz, $CDCl_3$) δ 160.38, 159.41, 156.32, 144.55, 140.01, 138.18, 137.98, 132.92, 129.69, 128.83, 125.29, 122.41, 117.67, 117.17, 116.47, 116.10, 114.91, 65.87, 65.55, 38.44, 29.69, 29.37, 11.48. **HRMS** (ESI^+) Calc for $C_{25}H_{26}BF_2N_3O_3Na^+$ $[M+Na]^+$: 488.1933, found 488.1930.

BODIPY MAO probe (32)

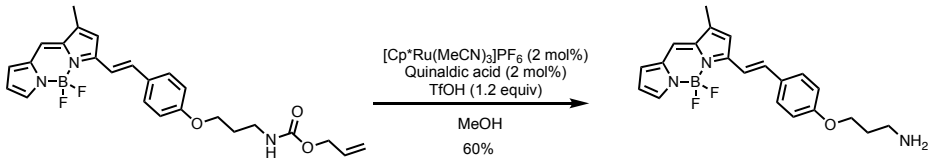

26 32

BODIPY probe (**26**) (35 mg, 75 µmol, 1.0 equiv) was dissolved in degassed MeOH (450 µL). 9µL of TfOH (98 mmol, 1.3 equiv) 50 µL of a solution of $[CpRu(MeCN)_3]PF_6$ (1.4 mg, 3.0 µmol) and quinaldic acid (0.7 mg, 3 µmol) in degassed MeOH (100 µL) were added to the previous solution. The reaction mixture was stirred for 1 h. After the indicated time the solution was diluted with DCM and filtered through a florisil plug and the solvent removed under reduced pressure.

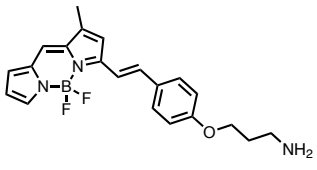

#t23

BODIPY MAO probe (**32**). Prep-HPLC reverse phase H_2O:MeCN from 70:30 to 25:75 in 15 min, 20 mL/min flow. **^{1}H NMR** (500 MHz, DMSO-d_6) δ 7.84 – 7.74 (m, 4H), 7.68 – 7.65 (m, 1H), 7.65 – 7.58 (m, 2H), 7.32 (d, J = 16.3 Hz, 1H), 7.13 (d, J = 1.2 Hz, 1H), 7.10 – 7.03 (m, 3H), 6.50 (dd, J = 3.9, 2.1 Hz, 1H), 4.14 (t, J = 6.1 Hz, 2H), 2.99 (q, J = 6.5 Hz, 2H), 2.34 (d, J = 1.0 Hz, 3H), 2.08 – 1.99 (m, 2H). **^{13}C NMR** (126 MHz, DMSO-d_6) δ 160.1, 158.9, 158.0, 157.7, 145.5, 140.9, 137.8, 137.5, 132.7, 129.5, 128.4, 125.8, 124.1, 117.7, 116.2, 115.3, 115.2, 64.8, 36.3, 26.8, 11.2. **HRMS** (ESI^+) Calc for $C_{21}H_{23}BF_2N_3O^+$ $[M+H]^+$: 382.1897, found 382.1892.

Synthesis of Ru-RGD

Synthesis of the Fmoc-K(alloc)-R(Pbf)-G-D(O*t*Bu)-CONH-Rink Amide

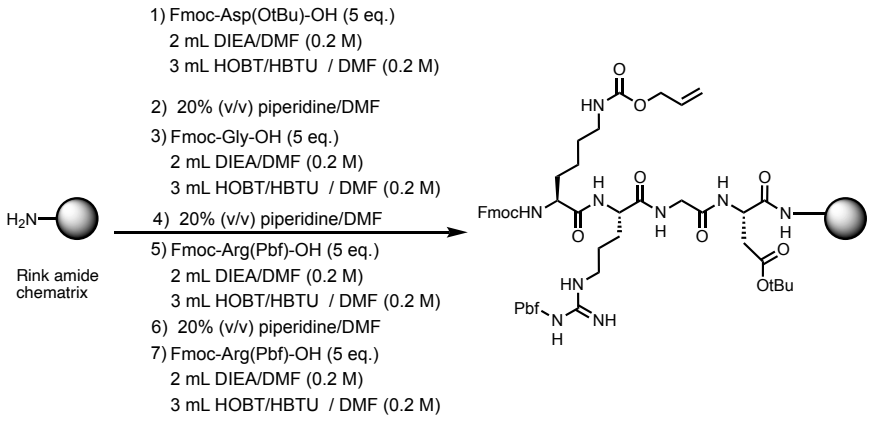

The peptide Fmoc-K(Alloc)-R(Pbf)-G-D(OtBu)-CONH-Resin was synthesized following the usual Solid Phase Peptide Synthesis (SPPS) protocol. Peptide syntheses was performed using Fmoc strategy on a Rink-amide-ChemMatrix (0.5 mmol/g) using DIC as activator, oxyma (ethyl(hydroxyimino)cyanoacetate) as base, and DMF as solvent. The removal of the temporal Fmoc protecting group was performed by treating the resin with 20% piperidine in DMF.

Deprotection of the alloc group of the lysine. Synthesis of the Fmoc-K(NH_2)-R(Pbf)-G-D(O*t*Bu)-CONH-Rink Amide

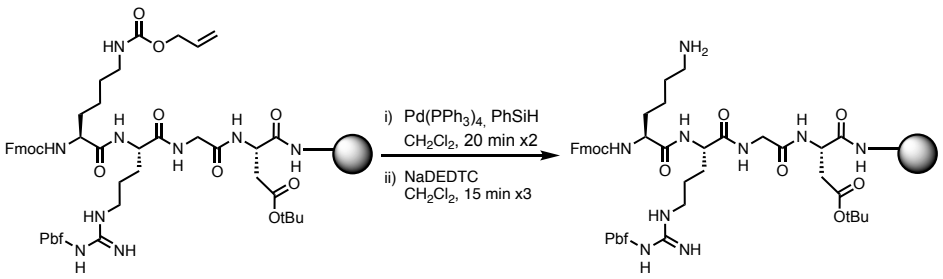

Following the procedure described by Imperiali [6] the resin-anchored peptide was suspended in dry DCM and the suspension kept bubbled for 5 min under N_2 stream. Next, $Pd(PPh_3)_4$ (11.6 mg, 0.01 mmol, 0.1 equiv) and phenylsilane (216.4 mg, 2 mmol, 20.0 equiv) are added and the suspension was kept bubbling with N_2 for 15 min. The resin was

[6] M. Sainlos, B. Imperiali, *Nat Protoc* **2007**, *2*, 3201–3209.

drained and washed with DCM. The process was repeated 3 times. Finally, residual palladium was removed by adding sodium diethyldithiocarbamate (DEDTC) while keeping the resin suspended in DCM bubbled for 5 min 3 times, obtaining product.

Coupling of the 8-allyl quinaldine ligand and deprotection of the N-terminus.

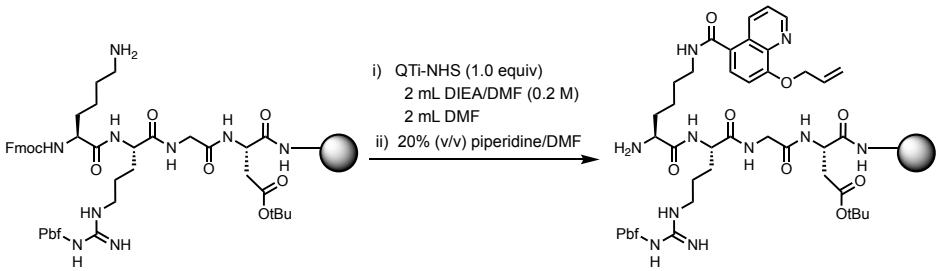

The 2,5-dioxopyrrolidin-1-yl 8-(allyloxy)quinoline-5-carboxylate, previously synthesized in the group, was dissolved in a solution of DIPEA (4 mL, 0.2 M in DMF) and added onto the resin with the anchored peptide. The mixture was kept in agitation on rotary disk stirrer for 1 h. The resin was drained and washed 3 times with DMF, maintaining bubbling with N_2.

For deprotection of the Fmoc group from the N-terminus, piperidine (5 mL, 20% in DMF) was added and the mixture was stirred by bubbling with N_2 for 10 min. The solution was drained and piperidine (5 mL, 20% in DMF) was added again, and the mixture was stirred again for 10 min. The mixture was washed 3 times with DMF keeping the mixture bubbling with N_2.

Coupling of 6-TAMRA-NHS and cleavage from the resin

N-succinimidyl-6-carboxytetramethylrhodamine ester (6-TAMRA-NHS) (63.4 mg, 0.12 mmol, 1.2 equiv) was dissolved in 4 mL of DIPEA (0.2 M in DMF). The solution was added over the resin and the mixture was stirred for 1 h. The resin was drained and washed 3 times with DMF under N_2 bubbling.

For cleavage of the peptide from the resin and deprotection of the side chains, 8 mL of deprotection cocktail (90:5:2.5:2.5:2.5 TFA:CH_2Cl_2:H2O:TIPS) were added and the mixture stirred for 2 h under N_2 bubbling. The solution was drained and collected, and the resin washed with 2 x 2 mL of the cocktail followed by 4 mL of CH_2Cl_2. The solvent was evaporated by N_2 stream to a final volume of 2-3 mL.

The crude peptide was precipitated by addition of 45 mL of cold Et_2O. The mixture was homogenized by vortexing, kept at 0 ºC for 10 min, centrifuged and the supernatant decanted. 45 mL of Et_2O were added again and the process repeated twice.

The solid was purified by preparative HPLC (from 20 to 75% MeCN in water in 15 min), yielding peptide RGD-PEPTIDE as a purple fluffy solid (15.5 mg, 0.014 mmol).

Name **RDG / Tmr-K(Qti)-R-G-D-CONH$_2$**

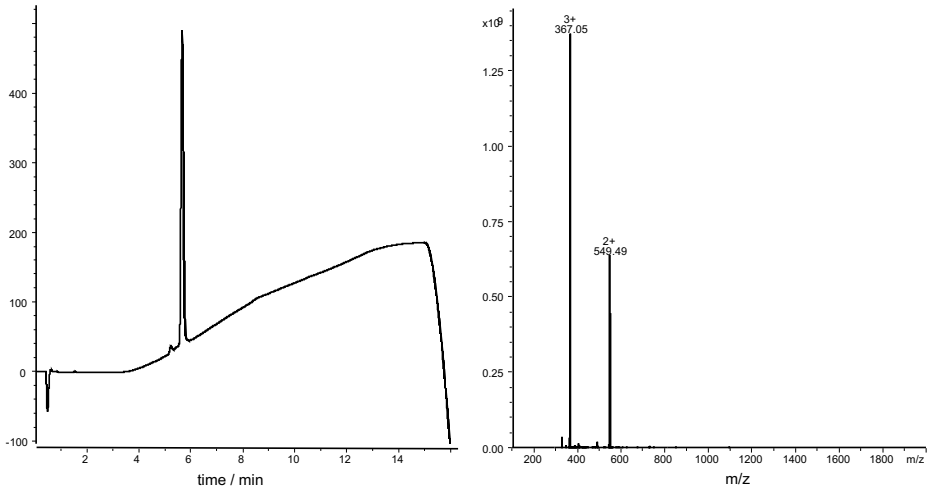

MS profile of **RDG / Tmr-K(Qti)-R-G-D-CONH$_2$** Calculated mass for $C_{56}H_{64}N_{12}O_{12}$ 549.49. Found: 549.48 $[M+2H]^{2+}$ and 367.05 [M+3H]3+.

Synthesis of Ru-RGD

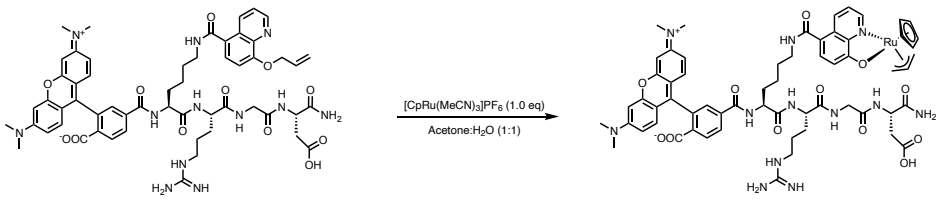

For the formation of the complex, H_2O Milli-Q grade and acetone were degassed in two vials under N_2 stream. In another vial, $[CpRu(MeCN)_3]PF_6$ (1.8 mg, 4.14 µmol) was transfer and subjected to 3 cycles of vacuum and N_2 and then dissolved in 300 µL of acetone.

In a fourth vial, **RGD** peptide (1.4 mg, 1.3 µmol, 1.0 equiv) was introduced and, after 3 cycles of vacuum and N_2, dissolved in 300 µL of degassed water. Over this solution 100 µL of the $[CpRu(MeCN)_3]PF_6$ ruthenium complex solution were added, and the

mixture stirred overnight. 5 µL of the obtained solution is dissolved in 300 µL of Milli-Q H_2O and analyzed by mass spectrometry. The signals obtained from mass spectrometric analysis are consistent with the expected isotopic pattern for product **Ru-RGD.**

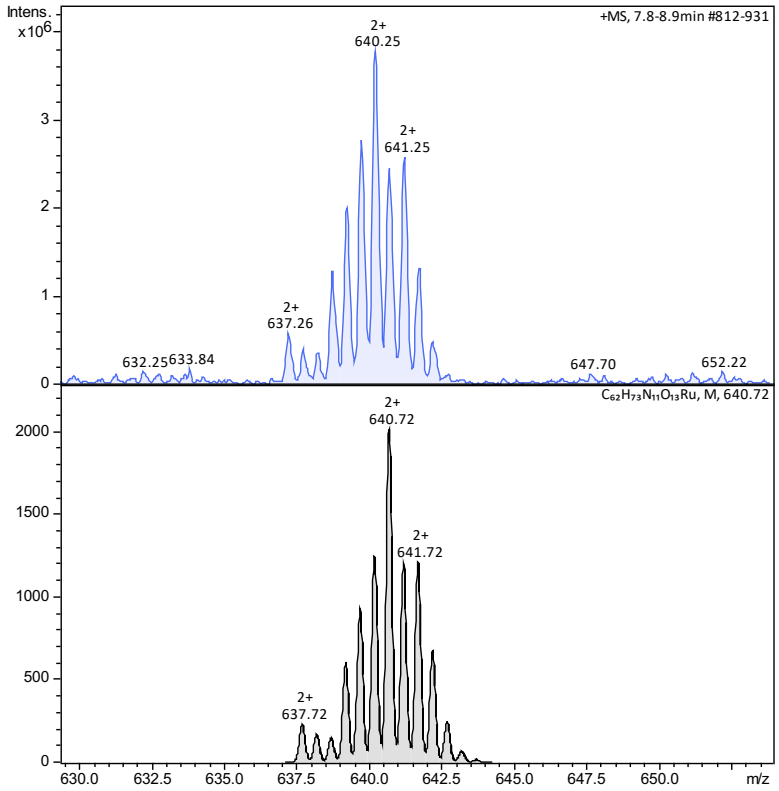

Figure S32. Comparison of the mass spectrum obtained (top) with the expected isotopic pattern (bottom) for the **Ru-RGD**.

In vitro experiments

Concurrent ruthenium promoted isomerization- ruthenium promoted deallylation reaction

Exemplified by a reaction of 1mM of **18** with 50 mol% of **Ru11** and **Ru13**:

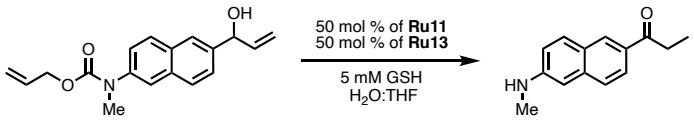

Fresh stock solutions of **Ru11** (25 mM in DMSO), **Ru13** (25 mM in DMSO), **18** (50 mM in DMSO) and GSH (5.0 mM in H_2O) were prepared.

In 500 µL Eppendorf vials were added 2 µL **18**, followed by a 80 µL of GSH (15 µL of THF, 2.5 µL of **Ru11** and 2.5 µL of **Ru13**. The reaction mixture was shaked at 700 rpm at 37 ºC for 4h. After the indicated time the reaction mixture was diluted with 300 µL of DMSO. 40 µL of the resulting solution were transfer to a 96 Flat Bottom Black Polystyrene well plate and diluted with 60 µL of DMSO and analyzed by fluorescence (λ_{exc} = 390 nM) in a plate reader Infinite 200Pro.

Tandem ruthenium promoted isomerization- ALP promoted hydrolysis reaction

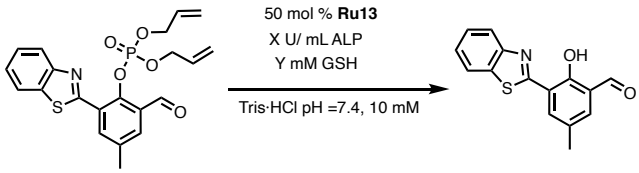

Fresh stock solutions of **Ru13** (10 mM in DMSO), **25** (10 mM in DMSO) ALP ($2.0 \cdot 10^4$ U/mL in Tris·HCl) and GSH (20 mM in Tris·HCl) were prepared.

To simplify the protocol serial dilutions were carried out for the ALP and the GSH in order to always add the same volume of each reagent:

- ALP : 0 U/mL, 2.0 U/mL, 20.0 U/mL, 200 U/mL and $2.0 \cdot 10^3$ U/mL
- GSH : 0 mM, 0.1 mM, 0.2mM, 0.5 mM and 5.0 mM

In a 96 Flat Bottom Black Polystyrene well plate were added 93.5 µL of the corresponding solution of GSH, 1µL of the **25** solution, followed by 5 µL of ALP solution and 0.5 µL of **Ru13** solution. The resulting solution was kept at 37 ºC covered with aluminum foil

for 4 h. After the indicated time the reaction was analyzed by fluorescence in a in a plate reader Infinite 200Pro.

RuRGD promoted deallylation of 17

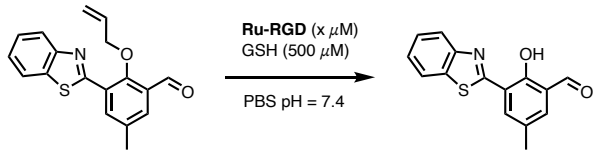

17
150 μM

11

Fresh stock solutions of **Ru-RGD** (5 mM in H_2O), **17** (10 mM in DMSO) and GSH (500 µM in PBS 1X) were prepared:

In 500 µL Eppendorf vials were added 1.5 µL **17**, followed by a 97 µL of GSH in PBS and 1.5 µL of **Ru-RGD**. The reaction mixture was shaked at 700 rpm at 37 ºC for 4h. After the indicated time the reaction mixture was diluted with 100 µL of DMSO. 100 µL of the resulting solution were transfer to a 96 Flat Bottom Black Polystyrene well plate analyzed by fluorescence (λ_{exc} = 360 nM) in a plate reader Infinite 200Pro.

Cell experiments

Protocol for the preparation of biological materials

Cell transfection with p-BLUESCRIPT CMV-SEAP plasmid:

In a 12-well plate, HEK-293 cells to be transfected are seeded 24 h in advance. At the time of transfection, as many eppendorfs are prepared as wells of the plate to be transfected. In a sterile eppendorf, 100 µL of D-MED Stock and 1 µg of p-BLUESCRIPT CMV SEAP plasmid (480 ng/µL) are added, homogenizing the mixture well by pipetting. Next, 3 µL of room temperature polyethylenimine (PEI) is added and pipetted again to ensure homogeneous mixing. The PEI mixture and plasmid in D-MED Stock are allowed to incubate for 30 min at room temperature. Finally, the contents of the eppendorfs are added dropwise to each well and the plate is shaken in gentle circular motions to promote good mixing. The cells are incubated for 24-72 h.

Biological experiments

Tandem Ruthenium deallylation ALP dephosphorylation with probe 25

In cell studies are performed in HEK-293 cells with physiological levels of ALP (untransfected) and with overexpressed ALP (transfected with plasmid p- BLUESCRIPT CMV-SEAP). For this purpose, HEK-293 cells are seeded in 24-well plates the day before transfection. The **Ru14** and **Ru15** catalysts are studied at 24 and 48 h post-transfection incubation times. Optimized reaction conditions are detailed below.

Cells are incubated with **Ru14** and **Ru15** complexes at a concentration of 25 μM for 30 min in DMEM. After two washing steps with DMEM (2 x 300 μL) to remove extracellular ruthenium complexes the cells were incubated with **25** (50 μM) in in fresh DMEM for 4-5 h. The live cells are then studied by fluorescence microscopy. Control experiments were performed in parallel. Digital pictures of the different samples were taken under identical conditions of gain and exposure under confocal and epifluorescence microscope.

Tandem Ruthenium deallylation MAO amine oxidation with probe 26

HeLa cells were seeded on 24 well plates two days before treatment. Cells were incubated with the ruthenium complexes (25 – 50 μM) for 30 min in fresh DMEM. After two washing steps with DMEM (2 x 300 μL) to remove extracellular ruthenium complexes, the resulting cells were incubated with **26** (75 – 100 μM) in fresh DMEM for 1.5 - 2 h. Control experiments were performed in parallel. Digital pictures of the different samples were taken under identical conditions of gain and exposure under confocal and epifluorescence microscope.

MAO amine oxidation with probe 32

HeLa cells were seeded on 24 well plates two days before treatment. Cells were incubated with the **32** (75 μM) for 20 min in fresh DMEM. After two washing steps with DMEM (2 x 300 μL) to remove extracellular **32**, picture were taken at 20 min and after 2 h Control experiments were performed in parallel. Digital pictures of the different samples were taken under identical conditions of gain and exposure under confocal and epifluorescence microscope.

Tandem Ruthenium deallylation MAO amine oxidation with probe 27

HeLa cells were seeded on 24 well plates two days before treatment. Cells were incubated with the ruthenium complexes (25 – 50 μM) for 30 min in fresh DMEM. After two washing steps with DMEM (2 x 300 μL) to remove extracellular ruthenium complexes, the resulting cells were incubated with **27** (75 – 100 μM) in fresh DMEM for 1.5 - 2 h. Control experiments were performed in parallel. Digital pictures of the different samples were taken under identical conditions of gain and exposure under confocal and epifluorescence microscope.

***In cellulo* studies of Ru-RGD.**

In cellulo assays were carried out by comparing two types of cell lines: HEK- 293 and MCF7. For this purpose, cells were seeded in 24-well plates 48 h prior to treatment. The optimized conditions under which these assays are carried out are shown below. Both cell types were incubated with **RuRGD** catalyst (15 μM) for 1 h 30 min in 300 μL of DMEM. Simultaneously, convenient control experiments are carried out. Finally, the results of the different assays are analyzed by fluorescence microscopy.

Selected NMR Spectra

allyl (6-(1-hydroxyallyl)naphthalen-2-yl)(methyl)carbamate (18)

^{1}H NMR (300 MHz, $CDCl_3$)

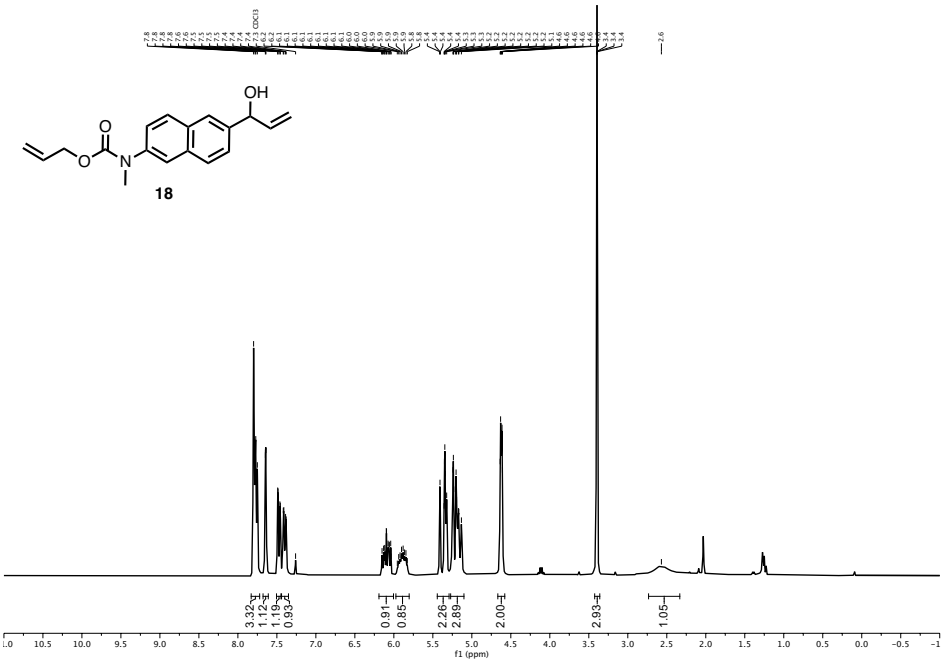

^{13}C NMR (75 MHz, $CDCl_3$)

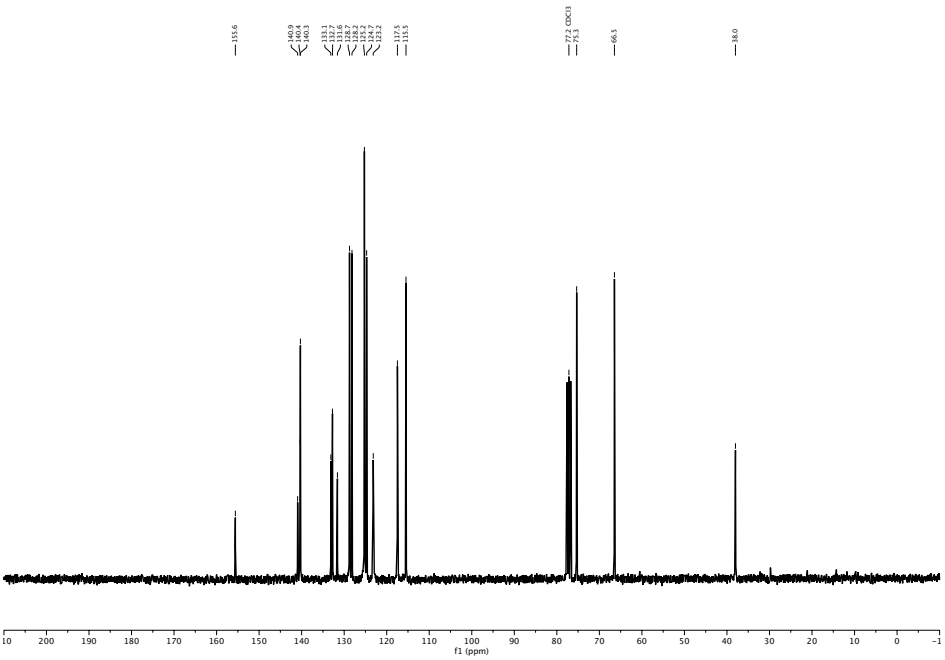

1-(6-(methylamino)naphthalen-2-yl)propan-1-one (19).

^{1}H NMR (300 MHz, $CDCl_3$)

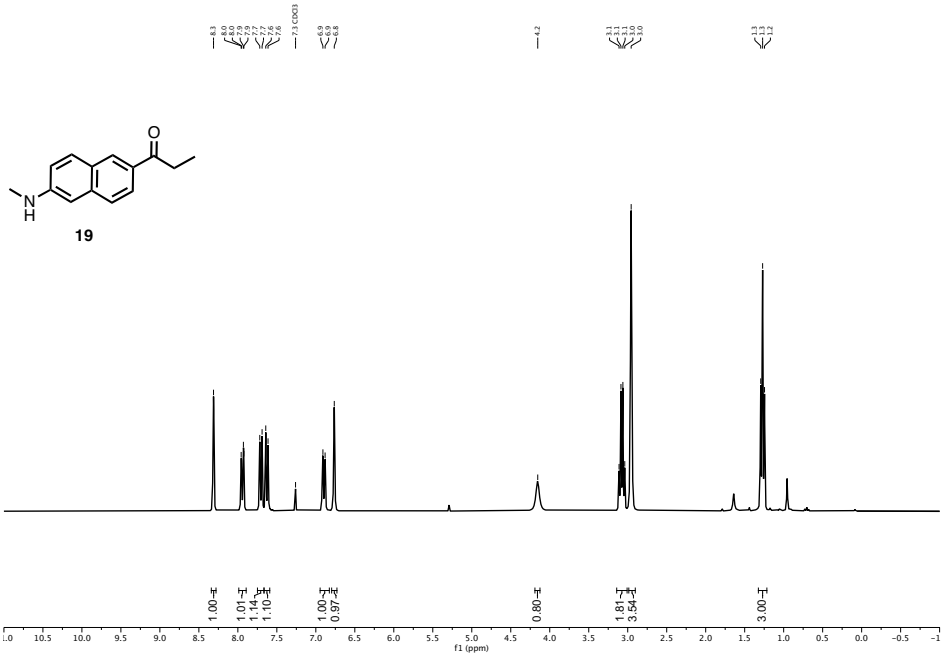

^{13}C NMR (75 MHz, $CDCl_3$)

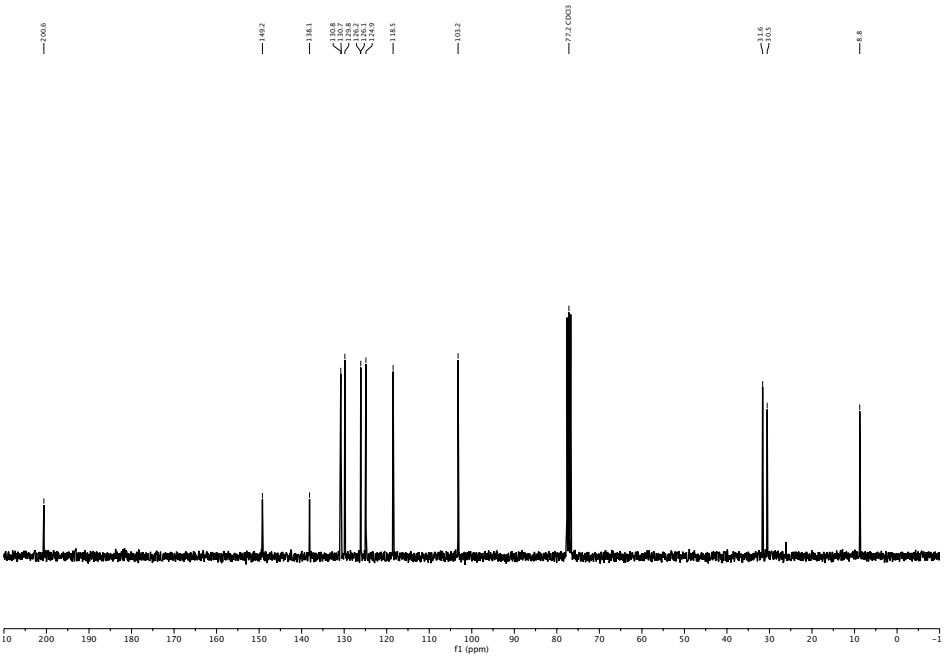

diallyl (2-(benzo[*d*]thiazol-2-yl)-6-formyl-4-methylphenyl) phosphate (25)

^{1}H NMR (300 MHz, $CDCl_3$)

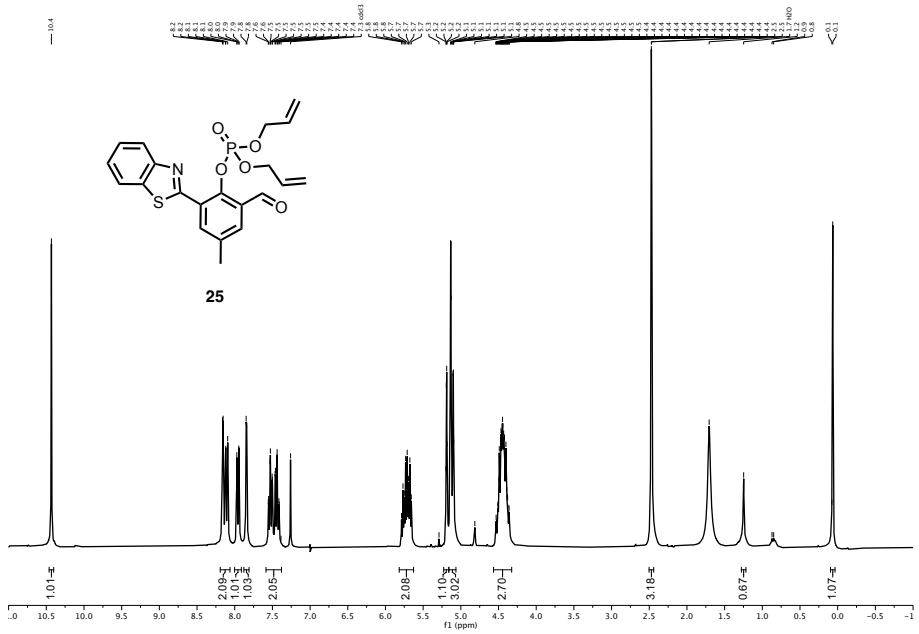

^{13}C NMR (75 MHz, $CDCl_3$)

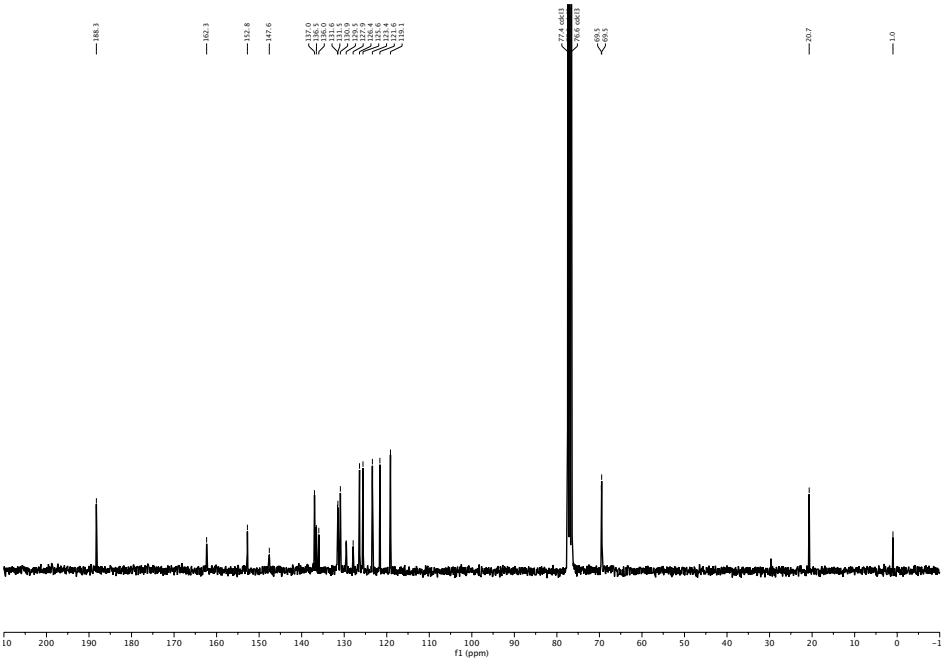

BODIPY Ru-deallylation MAO probe (26)

^{1}H NMR (300 MHz, $CDCl_3$)

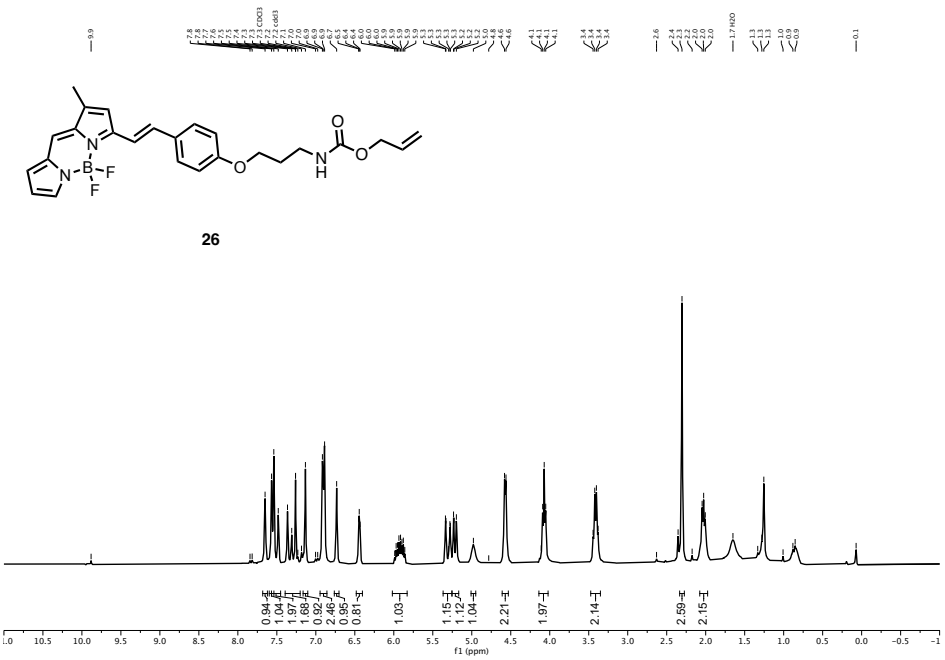

26

^{13}C NMR (75 MHz, $CDCl_3$)

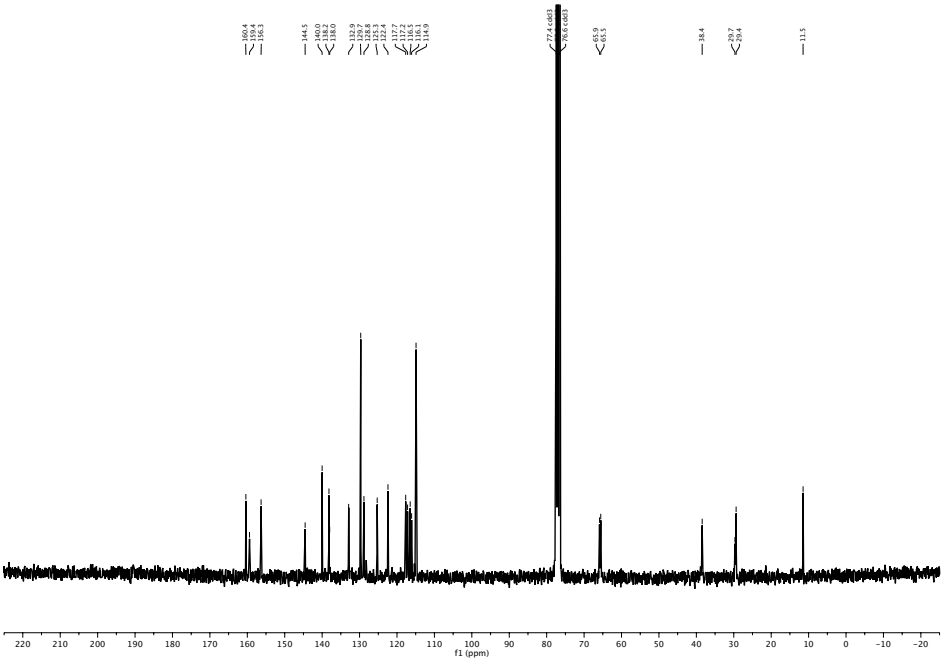

BODIPY MAO probe (32).

^{1}H NMR (500 MHz, DMSO-d_6)

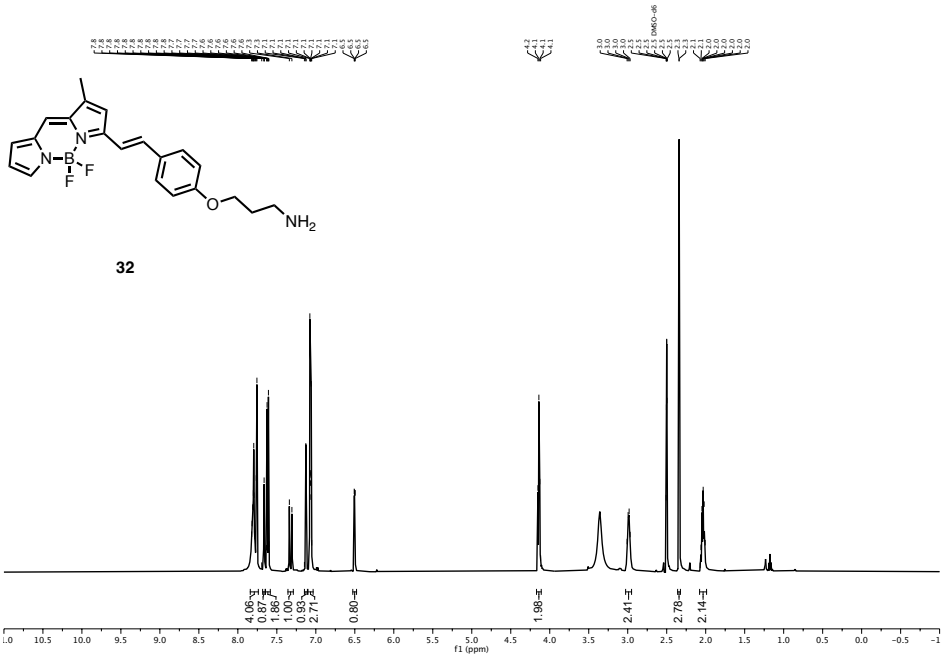

^{13}C NMR (126 MHz, DMSO-d_6)

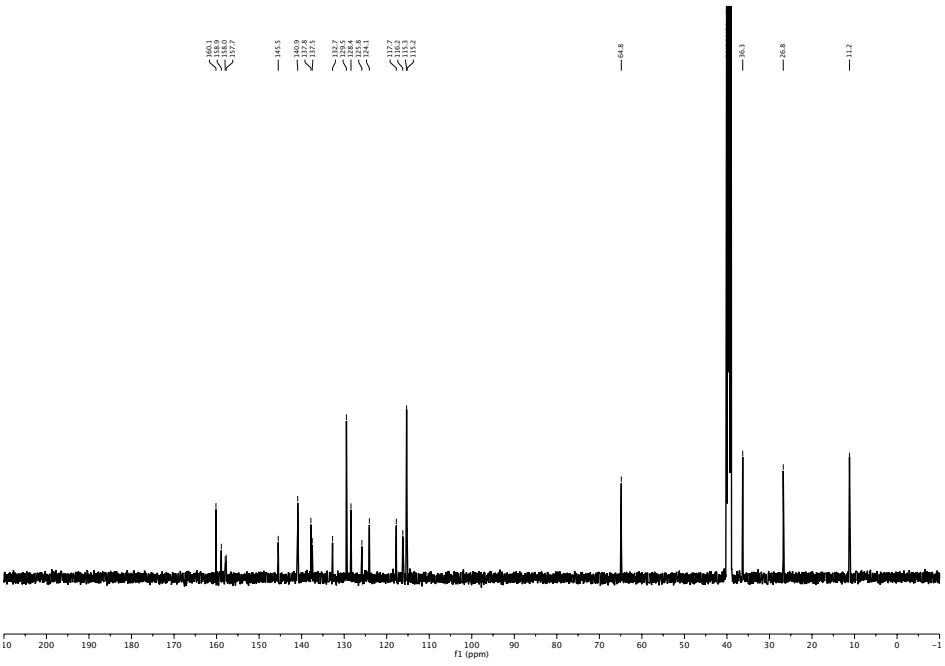

Relación de publicaciones derivadas de la tesis

Publicacion 1:

Título: *Bioorthogonal Azide-Thioalkyne Cycloadditions Catalyzed by Photoactivatable Ru(II) Complexes*

Autores: Alejandro Gutiérrez-González, Dr. Paolo Destito, Dr. José R. Couceiro, Dr. Cibrán Pérez-González, Dr. Fernando López, Prof. José L. Mascareñas.

Revista: *Angewandte Chemie International Edition* **Año:** 2021

DOI: 10.1002/anie.202103645 **Factor de impacto** (2021): 16,823

Categoría: *Multidisciplinary Chemistry* **Ranking categoría:** 15/179

Autorización: No necesaria. Publicación en abierto (*Open Access*) bajo licencia Creative Commons CC-BY

D. Alejandro Gutiérrez González estuvo involucrado en:

> Diseño, caracterización y síntesis de compuestos orgánicos y organometálicos. Ensayos in vitro. Experimentos mecanístico. Redacción y corrección del manuscrito.

Publicacion 2:

Título: *Ruthenium-catalyzed Redox Isomerizations inside Living Cells*

Autores: Cristian Vidal, María Tomás-Gamasa, Alejandro Gutiérrez-González, and José L. Mascareñas

Revista: *Journal of American Chemical Society* **Año:** 2020

DOI: 10.1021/jacs.9b00837 **Factor de impacto (2021):** 16.289

Categoría: *Multidisciplinary Chemistry* **Ranking categoría:** 16/179

Autorización: No necesaria. Publicación en abierto (*Open Access*) bajo licencia Creative Commons CC-BY-NC-ND

D. Alejandro Gutiérrez González estuvo involucrado en:

> Diseño, caracterización y síntesis de compuestos orgánicos y organometálicos. Ensayos in vitro. Experimentos mecanístico. Redacción y corrección del manuscrito.

Bioorthogonal chemistry has transformed cell research by providing new chemical tools. This thesis describes the development of novel ruthenium complexes that allow for efficient ruthenium-catalyzed azide-thioalkyne cycloadditions in the presence of cells. We adapted ruthenium-catalyzed alkene-alkyne coupling to aqueous and bioorthogonal conditions, enabling effective peptide modification. Additionally, we developed a ruthenium isomerization reaction capable of taking place within living cells, reducing natural cell levels of GSH. Lastly, we showed that a primitive artificial metabolic network can be established in living cells using discrete organometallic catalysts and natural enzymes.